CONF-890351--

# U.S. DEPARTMENT OF ENERGY THERMAL ENERGY STORAGE RESEARCH ACTIVITIES REVIEW 1989 PROCEEDINGS

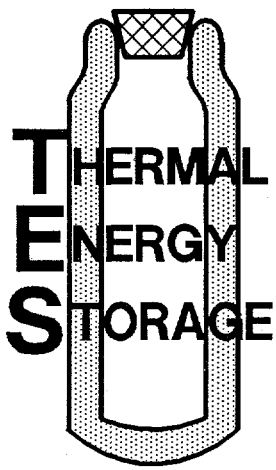


DIURNAL...INDUSTRIAL...SEASONAL

March 15-17, 1989
New Orleans, Louisiana

Co-Sponsored By
U.S. Department of Energy
Office of Energy Storage & Distribution
Battelle Pacific Northwest Laboratory
Oak Ridge National Laboratory

CONF-890351

# U.S. DEPARTMENT OF ENERGY THERMAL ENERGY STORAGE RESEARCH ACTIVITIES REVIEW 1989 PROCEEDINGS



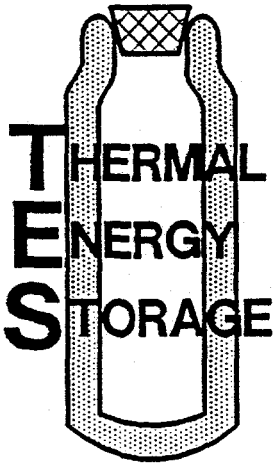


**DIURNAL...INDUSTRIAL...SEASONAL**

Editors

**Herbert W. Hoffman**
PAI Corporation

**John J. Tomlinson**
Oak Ridge National Laboratory



**March 1989**

# Table of Contents

## Table of Contents (continued)

## Foreword

Thermal Energy Storage (TES) offers the opportunity for the recovery and re-use of heat currently rejected to the ambient environment. Further, through the ability of TES to match an energy supply with a thermal energy demand, TES increases efficiencies of energy systems and improves capacity factors of power plants. The U.S. Department of Energy has been the leader in TES research, development, and demonstration since recognition in 1976 of the need for fostering energy conservation as a component of the national energy budget.

The federal program on TES R&D is the responsibility of the Office of Energy Storage and Distribution within the U.S. Department of Energy (DOE). The overall program (see keynote paper by E. Reimers) is organized into three program areas:

- Diurnal - relating primarily to lower temperature heat for use in residential and commercial buildings on a daily cycle.
- Industrial - relating primarily to higher temperature heat for use in industrial and utility processes on an hourly to daily cycle.
- Seasonal - relating primarily to lower temperature heat or chill for use in residential complexes (central supply as for apartments or housing developments), commercial (light manufacturing, processing, or retail), and industrial (space conditioning) on a seasonal to annual cycle.

The diurnal and industrial TES programs are managed for the U.S. DOE by the Oak Ridge National Laboratory (ORNL), Martin Marietta Energy Systems operating contractor; the seasonal TES program is managed by the Pacific Northwest Laboratory (PNL), Battelle Memorial Institute operating contractor.

The scope of the three program areas is described in overview papers by J. J. Tomlinson and L. Kannberg, while the research reports themselves reflect only currently funded projects. The reader is encouraged to contact the program area managers (Kannberg or Tomlinson) for information on the full range of TES activities since program inception, with suggestions for future R&D, and/or to inform them of studies underway outside of DOE auspices that may be relevant to the national mission.

It is intended that this volume, a record of papers presented at the 1989 annual TES Research Activities review, will not only document a set of interesting and challenging researches for the technical community but will also be of more than casual value to engineers, architects, builders, manufacturers, and utilities seeking energy conservation and efficiency in their structures and processes. We hope that, for this group of potential users, exposure to these project reports will both spark an interest in incorporating TES in their designs and encourage innovative applications.

We thank all of the authors for their efforts in preparing these papers on a very short time schedule and their acceptance of demands made under these circumstances by the editors. We also appreciate the work and accommodation of clerical staff, Cindy Eldridge and Charlotte Lawrence, PAI Corporation, Oak Ridge, Tennessee, in typing and formatting the papers.

*Oak Ridge, TN*
*March 1989*

# THERMAL ENERGY STORAGE PROGRAM DESCRIPTION

**E. Reimers**
U.S. Department of Energy
Office of Energy Storage and Distribution
Washington, DC

***Abstract***

*The U.S. Department of Energy (DOE) has sponsored applied research, development, and demonstration of technologies aimed at reducing energy consumption and encouraging replacement of premium fuels (notably oil) with renewable or abundant indigenous fuels. One of the technologies identified as being able to contribute to these goals is thermal energy storage (TES). Based on the potential for TES to contribute to the historic mission of the DOE and to address emerging energy issues related to the environment, a program to develop specific TES technologies for diurnal, industrial, and seasonal applications is underway. Currently, the program is directed toward three major application targets: (1) TES development for efficient off-peak building heating and cooling, (2) development of advanced TES building materials, and (3) TES development to reduce industrial energy consumption.*

## Introduction

Energy availability and utilization in the United States has undergone, and continues to undergo, substantial change. Instability in energy availability and cost triggered massive Federal and private action during the late 1970s and early 1980s. With the stabilization of petroleum prices in the late 1980s, the volatility of energy supply and cost has slipped into the background of national consciousness. However, factors less visible to the average American are at work that may yet raise his energy supply awareness and challenge our nation in new and profound ways.

The U.S. Department of Energy (DOE) has sponsored a substantial amount of research. development, and demonstration of technologies primarily aimed at reducing energy consumption and encouraging replacement of premium fuels (notably oil) with renewable or abundant indigenous fuels. One of the technologies identified as being able to contribute to these goals was thermal energy storage (TES) which functions to eliminate the temporal mismatch between thermal energy supply and demand. In this capacity, TES can assist to level energy demand reducing the need for peak energy supply or enable better utilization of intermittent energy sources. It can serve a broad spectrum of utility, industrial, commercial, and residential uses that contribute not only to the historic mission of the Department of Energy but help address emerging energy missions.

This document provides a brief description of the DOE Thermal Energy Storage Program as currently comprised. A short discussion of selected national energy and environmental trends is followed by a description of the TES Program mission, organizational structure, and technical activities. The paper closes with comments on a portion of the TES development occurring in other countries.

## National Energy and Environmental Trends

Energy consumption* in 1987 was 75.8 quads, a relatively modest increase (from 70.6 quads in 1975). However, the recent growth rate in energy consumption, particularly of oil, is alarming. Energy consumption by the year 2000 is expected to be approximately 85 quads, with a substantial portion of the increase coming from imported fuel. Total energy consumption per capita in the U.S. is 2.5 times that of Western Europe and Japan. Furthermore, U.S. consumption of oil per capita is equal to the total energy consumption in both Western Europe and Japan and is approximately twice their per capita oil consumption.

The U.S. transportation sector is consuming 20% more fuel today than in 1974 due to low fuel prices; five percent of the increased fuel consumption occurred in the last two years. The U.S. transportation sector uses a quarter of all oil consumed in the non-Communist world, more fuel than the U.S. produces. Despite record oil production in Alaska, U.S. oil output reached the lowest level in a decade at the end of 1987; production dropped a full 10% in the last year alone (late 1986 to late 1987). Oil imports have risen 29% in the last two years since OPEC effected price cuts. In 1987, the US imported oil costing aproximately $50 billion (equivalent to 25% of our foreign trade imbalance). Continued Free World consumption will most likely be met from the Middle East. The proportion of oil imported to the U.S. from the Middle East increased from 17% in 1986 to 22% in 1987. The Middle East holds 75% of the world's proven reserves, most of which can be produced at very low cost. It is estimated that by 1995 the U.S. will be importing 50% of its oil and over 60% by the year 2000.

Six quads of energy (8% of U.S. consumption) are obtained from renewable sources, half of which comes from hydroelectric power plants. Virtually all significant hydroelectric resources have been exploited. All other renewable resources (solar, wind, geothermal, biomass, ocean thermal energy conversion, etc.) comprise only a small part of current energy production. Only in very few market niches are these alternative sources economically viable. The implementation of alternative renewable sources will be strongly influenced by the pace of research-driven technological advances. Additional factors influencing implementation include the cost of competitive conventional technologies, unit scale, and uncertainties in performance and reliability that contribute to risk perception. Such factors make it very difficult to estimate the realistic contribution that renewables can make in the national energy picture over the next decade. However, in terms of the

---

* Energy supply/use data reported in this paper are those published by the United States Energy Association 1988, unless otherwise indicated.

TES technology contribution, assessment efforts are underway to more precisely gauge its impact; a contribution of 5 to 15 quads of renewable/displaced energy is technically possible.

The value of energy conservation has already been proven. During the eight-year period between 1978 and 1986, the economy grew 19% while energy consumption dropped 5% (78.1 quads to 74.3 quads). Had energy consumption grown with the economy, we would have required 93 quads in 1986. Energy consumption in residences has been reduced by 10% since 1973, while the number of households increased by 23%. Considerable additional energy savings are projected as Federal appliance energy efficiency standards begin to be applied and as more efficient space heating and cooling equipment and controls are employed. U.S. industry has also reduced energy consumption relative to product output. However, while oil consumption by the U.S. industry slightly increased in the period between 1974 and 1983, oil consumption by two of our major industrial competitors, Japan and West Germany, declined by more than 20%.

Electricity is a large and growing sector of our nation's energy infrastructure. During the period from 1973 to 1987, total energy consumption grew by 2%, while electric consumption grew by 42%. Electricity now comprises over half of the primary energy consumption in the U.S. outside of transportation. Growth in electricity has kept pace with growth in GNP and is a key element in making the U.S. industrial complex competitive in the global marketplace. In 1987, industrial use of electricity grew by 3.6%.

As electricity use has increased, the nature of its use has changed. Peak electrical demand has increased disproportionately with total electrical consumption. The U.S. annual electrical load factor (total electrical energy generated [kWh] divided by total generation capacity [kW x 8760 hr/yr]) has continued to drop from a peak value in the late 1950s of about 66% to about 61% in 1988 (Yu 1988). Much of this decrease has been attributed to growth in information and service sectors, which have load factors of about 0.65 while industrial load factors are about 0.85. Growth in the information and service sectors, requiring more office buildings, has combined with growing use of air conditioning to make most electric utilities "summer peakers."

A number of utilities have continued to experience load growth far in excess of expectations. While many electric utilities predicted growth rates of 1% to 2%, most have experienced growth rates above this value. Northeast utilities have been experiencing load growth at 4% to 5% annually. In the summer of 1988, two Northeast utilities experienced record loads with peak demands 10% greater than in 1987, prompting rolling brownouts (International Thermal Storage Advisory Council 1988). Many electric utilities have employed time-of-day and demand charge rate structures to encourage off-peak use. It is expected that most utilities will employ such rate structures within the next few years.

New electric supply strategies are being required. For a host of environmental, regulatory, and financial reasons, only one new coal-fired generating station and no nuclear plants have been ordered in the 1980s. Utilities are now relying on customer-side-of-the meter and non-utility generation to meet peak load requirements. In the near term, growth will be met by utility subsidized cogeneration companies, conser-

vation, installation of gas- and oil-fired turbines, and import from Canada. Over the last few years, imports of Canadian power have increased at an annual rate of 9.5%. It has been estimated that cogeneration and independent power production could meet 60% of the nation's capacity growth. At present, 4% (24,000 MW) of our generating capacity is independently owned and another 28,000 MW is under construction or planned. Half of the projects use cogeneration, and more than three-fourths of this is gas-fired.

Man's impact on the environment reached national attention in the late 1960s, prompting the establishment of the Environmental Protection Agency and the establishment of a regulatory steeplechase whose hurdles changed frequently causing confusion and conflict. The relative regulatory stability in the 1980s is, however, yielding to new environmental forces. Concern over the toxic waste dumps that stirred national action and establishment of the Superfund in the 1970s and early 1980s is now being focused on acid rain, global warming, and erosion of the ozone layer. These impacts are fundamentally different from those prompting earlier action because of their international consequences. The form and content of U.S. action to improve the environment as regards to these threats is yet to be determined. Congressional action in 1977 forced utilities to install $SO_2$ scrubbers (Leone 1988). This, combined with use of lower sulfur coal, resulted in a nearly 30% reduction in $SO_2$ emissions between 1973 and 1985, while coal consumption increased 42% (LaPier 1988). It is now estimated that over one-third of acid rain is caused by $NO_x$ emissions derived not only from coal combustion but from combustion of oil for transportation and natural gas.

Ozone depletion is attributed largely to release of chloroflourocarbons (CFC). CFC are commonly used in packaging materials, as refrigerants, propellants in spray cans, and insulation. DuPont, the primary manufacturer of CFC, has pledged to eliminate their production by the year 2000 and is spending $50 million to develop substitutes (LaPier 1988). Other organizations are also active in developing substitutes.

Global warming has been occurring for the last two centuries, but has accelerated in the last several decades. It is speculated that global warming is due to the "greenhouse effect" by which predominance of $CO_2$, $NO_x$, $CH_4$, and CFC gases in the atmosphere reduce thermal radiation to space. Carbon dioxide is the largest contributor. Man released 5.5 billion tons of $CO_2$ to the atmosphere in 1986, with 25% of this occurring in the U.S. (LaPier 1988). Carbon dioxide emissions are due primarily to combustion of fossil resources (coal, oil, and natural gas), although deforestation for fuel has the double effect of producing $CO_2$ while reducing natural means for decomposing $CO_2$. If $CO_2$ reduction becomes a significant issue for fossil fuel combustion, natural gas will become the preferred fuel because it produces about half the $CO_2$ per joule of energy released.

The widespread use of TES can have a beneficial impact on all three aspects of global climatic change. The use of less primary energy (i.e., greater use of renewable energy or improved energy efficiency) is a direct result of application of some TES technologies, notably waste heat TES in industry and for space heating, use of climate chill for industrial and space cooling, and improved utility and industrial energy

efficiency through diurnal TES and molten salt TES. Chloroflourocarbon refrigerants are eliminated or reduced through the use of seasonal winter chill TES, incorporation of advanced ammonia hydrate TES systems, and incorporation of some types of diurnal TES. Utilization of TES for load leveling at the power plant or at the customer contributes to wider use of some clean coal combustion technologies and reliance on other base-load plants, such as nuclear, that enable reduction of $SO_2$, $NO_x$, and $CO_2$ emissions.

## The DOE Thermal Energy Storage Program

The goal of the National Energy Policy Plan is to foster "an adequate supply of energy at reasonable costs." To accomplish this, a "balanced and mixed energy resource system", which will allow "producers and consumers to choose freely among a range of energy options", needs to be achieved. A key factor in providing such flexibility is the availability of energy storage technologies. The first legislative mandate for energy storage was the Solar Heating and Cooling Demonstration Act of 1974 (P.L. 93-409), which directed the development of thermal storage systems "for use in residential dwellings." The Non-Nuclear Research and Development Act of 1974 (P.L. 93-577. Section 6) complements this policy by mandating development of "storage systems to allow for efficient load following" by electric utilities. Further directives for thermal energy storage were given in the Solar Photovoltaic Energy Research, Development and Demonstration Act of 1978 (P.L. 94-413) and the Energy Security Act of 1980 (P.L. 96-294).

### Program Structure and Mission

The Thermal Energy Storage Program is managed within the Office of Energy Storage and Distribution (OESD), one of the offices reporting to the Deputy Assistant Secretary for Renewable Energy. The mission of OESD is to develop and advance energy conversion, storage. control, and delivery technologies that could benefit the nation by:

- increasing national security
- enhancing energy independence
- assuring public safety
- improving the quality of the environment
- enhancing U.S. competitiveness.

Consistent with this mission, the goal of the TES Program is to develop economically viable thermal energy storage systems that contribute to energy savings, fuel substitution, and environmental improvement. Particular emphasis is placed on developing TES technologies that:

- reduce peak electrical demand
- improve industrial. commercial. and residential energy efficiency
- facilitate the use of renewable resources and widely available domestic fuels, and
- reduce production of pollutants that contribute to global warming, acid rain, and ozone depletion.

The current DOE Program is organized to develop diurnal, industrial, and seasonal TES technologies. Selected research and development activities within each of these groups of technologies can be collected

within three program targets to meet four major applications, as shown in Figure 1. The TES Program is evolving to a new organizational structure that is more consistent with other OESD Programs. In the future, the Program will be classified according to two OESD elements: Materials and Systems, and Components. Over the last several years, the diurnal. industrial, and seasonal subprograms have used a common classification of projects consisting of the following topics:

- Heat Transfer Enhancement
- System/Component Studies
- Mathematical Modeling
- System Development
- Media (i.e., materials) Development
- Environmental/Institutional Studies.

The focus of studies within each subprogram varies among these topics. The present activities comprising each of these subprograms is briefly discussed in the subsequent section according to these elements. The discussions of the diurnal and industrial subprograms are combined because of the reduced size of these activities at this time. Concise statements of the objective, need. scope, status. and plans for these activities are described in the TES Project Summaries. To assist in addressing future OESD planning efforts, especially during the coming transition period, a matrix is given in Figure 2 that provides cross reference between the various projects within each subprogram (e.g., diurnal) with the new classification elements ("Materials" and "Systems and Components"). The appendix does not list the projects by the new classification elements, such revision will be made next year.

**Diurnal and Industrial TES Activities**

The current activities of the diurnal and industrial subprograms are identified and related to the TES Program targets as shown in Figures 3 and 4. Activities in each element are discussed below.

**Heat Transfer Enhancement.** Heat transfer is a critical issue in all thermal energy storage applications because it limits the rate at which thermal energy can be provided to or withdrawn from a source and delivered to an end use. In latent heat storage applications, fouling due to solids freezing to a heat exchanger surface during a charging cycle (as in the case of cool storage) or discharging cycle (as in the case of heat storage) is frequently the limiting heat transfer mechanisms. Conventional methods to accommodate this problem are provisions for large surface heat exchangers or systems that mechanically or thermally clean the heat exchange surface. Either technique results in increased costs.

In ice storage systems wherein ice is formed on an evaporator for later building cooling, work will continue to address the heat transfer issue. This work, initiated in FY 1988 and continuing through FY 1989, consists of an examination of methods whereby the evaporator surface can be made "selfcleaning," i.e., the ice that is formed floats or falls away from the surface thereby continuously refreshing the surface. The project scope will be extended to examine alternate means for defrosting the evaporator surface.

**Mathematical Modeling.** The thermodynamics of thermal storage systems based on sensible heat are generally described through equations that can be solved analytically. Solutions to most of the interesting

problems involving latent heat storage are found only through mathematical modeling using iterative techniques. Two modeling efforts are currently underway and will be continued. The objective of the first is the development of a thermodynamic description of a packed bed of thermal storage media immersed in a boiling or condensing heat transfer fluid. Upon completion and experimental verification, the model will be available for technical evaluation of storage heat pump systems with PCMs in packed beds, which are used as evaporators or condensers. The second project is the development of a packed bed TES system model for use in TES design optimization studies for brick plants. The packed bed being modeled consists of cylindrically shaped pellets of composite sensible/latent heat storage material that are charged with high-temperature industrial flue gas and discharged with air.

**Media Development.** Due to higher thermodynamic efficiency, smaller size, and the ability to store and deliver heat over a small temperature interval, PCMs are attractive as thermal storage media for building heating and cooling and industrial applications, as well. Thus, development of TES media where one or more components undergo a phase transition is a central element of the program. The first of five projects, incorporation of PCMs into building materials is directed toward comfort and efficiency improvements in building space conditioning. By imbibing paraffinic materials into (1) the interstices of gypsum concentrate or (2) pellets of crosslinked polyethylene that can then be cast into concrete, an effective PCM system for use in passive solar heating and cooling is possible. A determination of any tendency for PCM redistribution in gypsum wallboard that is thermally cycled is the principal FY 1989 objective for this project. As a supporting task to the PCM wallboard development, a simulation of PCMs suffused throughout a sensible heat matrix will be completed and used to study the effects of a distributed PCM in a wallboard.

Full-scale (4 ft x 8 ft) panels of wallboard containing the PCM will be fabricated and tested to determine bulk thermophysical properties above and below the phase-change temperature and to determine the dynamic response of the panel to a surface thermal flux or temperature profile.

Over the past four years, a major effort to develop high-temperature TES media for industrial applications has resulted in successful laboratory development of a sintered magnesium oxide (MgO) pellet with porosity suited for containment of a eutectic of carbonate salts. Capillary forces retain the PCM in the MgO interstices so that the pellet remains solid during thermal charging and discharging. During FY 1989, packed bed configurations of this media will undergo initial field testing in a brick plant to examine performance and lifetime issues when the media is used to extract thermal energy from the kiln flue gas. A test program will be conducted to measure and evaluate thermochemical and thermophysical properties of the media periodically during the field test.

**System Development.** Work will continue on two cool storage concepts for electrical load management. Development of a chill storage system based on ammoniated complexes for food processing and other low-temperature applications will be continued with industry cost-sharing. As a second project, an advanced direct-contact ice storage system for building cooling will be developed in a size suited for later field testing.

The system design uniquely solves oil and water carryover problems that have paralyzed early efforts to exploit the direct contact approach.

**System/Component Studies.** The objective of the first of six projects under this element is development of temperature-adjusted organic solid-state PCMs. Through the use of dopants to strain the crystal lattice, PCM alloys that undergo solid-solid phase transitions can be tailored for particular temperature applications (e.g., passive solar) with little effect on transition energetics.

The objective of a second project is to develop oil-water-refrigerant separation techniques and systems for use in ice storage system retrofit applications so that compressor replacement is unnecessary. This laboratory-scale effort will focus on thermo-mechanical separation techniques for the components at temperatures near saturation.

For reasons of high heat of fusion, little supercooling, and low vapor pressure, the PCMs being studied for incorporation into wallboard are organic compounds. As such, they are typically flammable, with smoke evolution perhaps of even greater concern. A project to address fire/smoke safety issues in the PCM wallboard development program will be initiated. This project will execute a safety testing program in accordance with accepted UL, ASTM, and NFPA standards.

A fourth project to determine the feasibility of using silicon carbide extrusions for containment of high-temperature PCMs will be initiated and completed in FY 1989. Methods for automatic extrusion, filling, and end sealing will be assessed and recommendations for further development of PCM systems based on new encapsulation techniques will be made.

An optimization study currently underway is aimed at determining the "best" (lowest ROI) high-temperature storage configuration for a two-kiln single dryer periodic brick plant. The study takes into account real-time uses for reject heat for which storage is not required. During FY 1989. this preliminary study will be completed and will be used as a basis for development of a procedure for analysis and TES design studies for a multikiln, multidryer plant.

A final project completes experimental verification of a model of an air/molten salt heat direct-contact heat exchanger. A range of molten salt temperatures will be used to validate the heat transfer model under conditions of various fluid properties and radiation heat transfer.

**Seasonal TES Activities**

Current activities of the seasonal subprogram are identified and related to TES Program targets, as shown in Figure 5. Activities in each element are discussed below. Because current work is focused on aquifers for which no heat transfer enhancement is economically reasonable, no activities are underway in that element. However, unlike diurnal and industrial TES, seasonal TES in aquifers will involve significant environmental and institutional concerns and research is underway to address those concerns.

**Mathematical Modeling.** Aquifer TES (ATES) weds geohydrology, thermal storage, and building heating and cooling technical fields not historically combined. As such, a merger in technical knowledge and application is necessary. One area for that merger is the development and application of numerical models

that serve as design aids in conceptual evaluation, detailed design, and design evaluation. Because of the variety of potential geohydrologic and end-use system configurations, a suite of models are under development. Models will span the range from feasibility assessment (using an expert system) through relatively simple tools that interrelate geohydrothermal and surface system arrangements for conceptual design and evaluation to complex and detailed geohydraulic (multidimensional) and geochemical codes. Work in FY 1989 is focused on development of an advanced version of the code ATESSS that includes interfaces with common equipment such as heat pumps, solar collectors, and winter chill cooling towers. ATESSS will also be applied at a site in Alabama to assist in conceptual design of a chill ATES system in an aquifer with high regional flow. Cooperatively, the U.S. Geological Survey will conduct three-dimensional simulations of the planned third long-term test cycle at the St. Paul Field Test Facility on the campus of the University of Minnesota. An expert system to assist heating, ventilation, and air conditioning (HVAC) engineers in determining site geotechnical feasibility will continue to be developed at a modest level, with initial testing planned in 1989. An assessment of CHARMI, a Dutch coupled geohydraulic-geochemical code developed through the International Energy Agency (IEA), is planned as part of the U.S. contribution but may be delayed while the Dutch resolve code performance problems.

**Media Development.** Two of the major issues in ATES are geochemical dynamics and water treatment. These issues affect not only the operation and performance of ATES but also its environmental and institutional acceptability. Efforts in 1989 are focused on continued development of the necessary knowledge of geochemical dynamics to enable reliable estimation of ATES geochemical behavior. The work being conducted includes both laboratory and modeling efforts and is closely linked with a major IEA activity as well as field testing at the University of Minnesota. Laboratory studies in the U.S. are combined with results of other IEA participants to develop a geochemical database (both equilibrium and kinetics) for classic aquifer groundwater and sediments at temperatures up to 300°C. This database will be validated with data from field tests including the field data from the University of Minnesota. Data from other geochemical environments will also be evaluated in support of the U.S. contribution to the IEA.

**System Development.** In the seasonal TES subprogram, system development involves developing and assessing STES as an entity within an energy supply and demand environment. Because development challenges are often encountered in the integration of STES in a field application, efforts in this element are focused on testing and/or evaluating performance of systems in the field.

The two primary system development activities involve field studies of ATES for heat at the University of Minnesota and chill storage at the University of Alabama. A third long-term test cycle will be conducted at the St. Paul Field Test Facility that is 50% longer than earlier tests and will involve use of the recovered heat in a campus building. This project is cofunded with the University of Minnesota and the U.S. Geological Survey, with DOE having the major portion. Data from the project will be used to validate geohydraulic and geochemical models, evaluate system performance, and provide information for potential integration into the campus heating system.

The second activity is monitoring of the University of Alabama (Tuscaloosa, Alabama) chill ATES system that provides cooling to the Student Recreation Building. Of special interest is the energy performance and assessment of measures taken to mitigate the negative impacts of regional flow at the site. Cooperative studies of the design of a chill ATES system for a local General Motors manufacturing facility will also be conducted. Finally, monitoring may be initiated at a recently installed chill ATES system at a Postal Service Mail Processing Center on Long Island, New York.

**System/Component Studies.** Identification and assessment of seasonal TES concepts and components, estimation of potential benefits, determination of early applications, and economic evaluation are essential to effective direction of research, development, and demonstration efforts. Activities of this nature to be conducted in 1989 include continued assessment of early application niches for chill ATES identification and assessment of heat pump/ATES systems and reevaluation of the cost goals for chill ATES. Other activities that have been postponed include solicitation for novel chill STES concepts, field characterization of heat pump/ATES systems, and award of site-specific feasibility study grants for seasonal TES.

**Environmental/Institutional Studies.** In most parts of the U.S., the environmental quality of our soil and groundwater resources is protected by law and regulated through state and local governmental agencies. Greater attention is rightly being focused on preservation of these resources. Any technology that uses these resources will be subject to close scrutiny, and potential degradation of these resources will have to be avoided or mitigated for net public benefit. Geochemical studies, both in the laboratory and field, is one topic previously addressed under Media Development. The focus of 1989 studies within this element is initiation of microbiologic concerns, especially those related to open cycle chill ATES systems. Specifically, field microbiologic monitoring of the chill ATES system at the University of Alabama is underway. Pathogenic organisms are being evaluated at the University of Alabama. Changes to other indigenous microorganisms are being determined at Pacific Northwest Laboratory. The U.S. is a subtask leader in an IEA Task (Annex VI) dealing with characterization and mitigation of water quality issues for ATES. The subtask deals explicitly with microbiologic issues, in terms of both hygiene and operations.

## International TES Development

The future economic health of the United States is closely tied to its ability to compete in the international marketplace. The U.S. was the world leader in international trade. However, over the last two decades, our market position has eroded dramatically. Foreign competitors have successfully implemented international business and technology strategies. Our international competitors have focused their resources on cooperative programs to develop and apply technology to the production of manufactured goods superior in quality and lower in cost than those produced in the U.S. Currently, the U.S. has a large balance of trade deficit with Japan, Canada, West Germany, Taiwan, the United Kingdom, Korea, Italy, and France.

The U.S. is now intensifying its effort to meet this challenge. These efforts cover many fronts ranging across many energy technologies. One of these technologies is TES.

TES can influence both the international competitiveness of our industries and balance of trade. In addition to improving the energy efficiency and economic competitiveness of various industries, TES systems themselves can be the topic of international trade. The benefits of employing TES in U.S. industry include improved product competitiveness, improved balance of trade, improved capital productivity, and enhanced energy security. Of course these same advantages exist for most countries and have been some of the reasons why TES development has been undertaken internationally. Another reason is that other nations see TES technology as exportable, with the U.S. being one of the largest target markets.

Unfortunately, U.S. energy research expenditures have reached a level that it is lower (per unit of GNP) than most developed nations including Japan, Italy, Canada, West Germany, the United Kingdom, and Switzerland [based on IEA documents, France is not in the IEA but is known to support a number of large TES projects] (International Energy Agency 1988). As is well known, U.S. energy research budgets have been substantially reduced over the last eight years. DOE TES budgets have diminished by a factor of about eight.

It is now apparent that TES concepts originally advanced and researched in the U.S. but set aside due to funding reductions, are approaching commercial introduction from foreign companies. For example, the advanced composite phase-change material (CPCM) originally proposed and examined in the U.S. is being pushed to commercialization by the West German government and industry. They have recently launched a $11 million, multiyear effort to complete development for application in their steel, chemical, glass, and ceramic industries. Under an IEA agreement, the U.S. was to jointly research this technology, but the agreement is in jeopardy because the U.S. has been unable to fund field tests in a U.S. brick plant of CPCM materials developed domestically.

Another example is the Japanese development of a combined heat pump/TES unit for off-peak heating. The system upgrades waste heat to higher temperatures for industrial uses for building heating and cooling. The system consists of a very high-performance compression heat pump and a TES system. The heat pump uses off-peak electricity to produce high-temperature heat; the high density TES system stores the heat for on-peak uses. The goal is to double existing heat pump/TES performance. TES systems being evaluated consist of clathrates and ammoniated complex compounds, both of which had been identified early in the U.S. as promising storage materials. DOE supported initial testing of clathrate TES but had to abandon it several years ago in the face of funding reductions. As noted in the above, R&D in the U.S. is being continued at necessarily low levels on ammoniated complex compound TES units. This is just one project in a Japanese energy storage R&D program that is twice the size of the U.S. DOE Program.

Similar trends are observable in seasonal TES. A 1985 IEA report identified a total of 62 large TES projects in IEA countries, most of which were seasonal systems (Lundin 1985). Of these 62 projects, 20 utilized aquifers, 17 used ground storage, 11 used tank storage, six used caverns, and five used pits. Projects were underway in nine IEA nations. Additional development is known to be underway in Japan, England, Italy, and China, and is suspected in the Soviet Union. Sweden alone invests more than $3.2 million

annually in building TES primarily for seasonal storage. The Swedes have developed an impressive array of large-scale, typically low-temperature pilot projects and full-scale demonstrations. They have utilized all types of storage configurations and have special expertise in use of boreholes in rock and clay and saturated earth storage types. Swedish experts have recently entered a bilateral agreement for development of artificial aquifer ATES at one of three locations in West Germany.

Considerable ATES development is underway in The Netherlands, Denmark, Switzerland, France, Canada, Finland, West Germany (artificial aquifers), and China. Chill ATES has been practiced in China for nearly 20 years and now is used in many large cities. ATES is used at over 32 textile mills in Shanghai and is estimated to conserve over 90,000 tons of coal annually. It is also used to cool at least 10 cinemas and the airport lounge in Shanghai (Sun 1986).

The U.S. is involved in Annex VI of the IEA Energy Conservation Through Energy Storage Programme, which deals with water quality issues of ATES. In this effort, cooperative R&D is conducted to define and resolve ATES water quality concerns.

## References


1. International Energy Agency, 1988. Energy Policies and Programmes of IEA Countries - 1987 Review. International Energy Agency, Paris, France.

2. International Thermal Storage Advisory Council, 1988. "Summer Heat Brings Record Peaks." An International Thermal Storage Advisory Council Thermal Storage Advisory, International Thermal Storage Advisory Council, 3769 Eagle Street. San Diego. California, October 1988.

3. LaPier, G. W., ed., 1988. "Energy Information for Mature Americans." Issue 39, G. W. LaPier (editor), 4027 Cape Code Drive. Pittsburgh, Pennsylvania, September/October 1988.

4. Leone, M., 1988. "Legislative Outlook. 1989: Environmental Issues Top Congressional Agenda." Power Magazine, December 1988.

5. Lundin, S. E., 1985. Large Scale Thermal Energy Storage Projects - In Operation or Under Construction. International Energy Agency. Executive Committee for the Energy Conservation through Energy Storage (available through the Swedish Council for Building Research), June 1985.

6. Sun, Y., 1986. "Aquifer Energy Storage Applications in China." STES Newsletter, C. F. Tsang ed., Volume VIII, No. 4, Lawrence Berkeley Laboratory, Berkeley, California, September 1986.

7. United States Energy Association, 1988. U.S. Energy 1988: Countdown to the Next Crisis, Second Annual Assessment of U.S. Energy Policy and Prospects. United States Energy Association, U.S. Member - Committee of the World Energy Conference, April 1988.

8. Yu, O. S., 1988. "The Potential Impact of Information on Automation Technologies and Load Factor." Presented at Information and Automation Technology: Serving Electric Utility Customers in the 1990s. (A Conference Sponsored by the Electric Power Research Institute, Palo Alto. California) December 5-7, 1988.

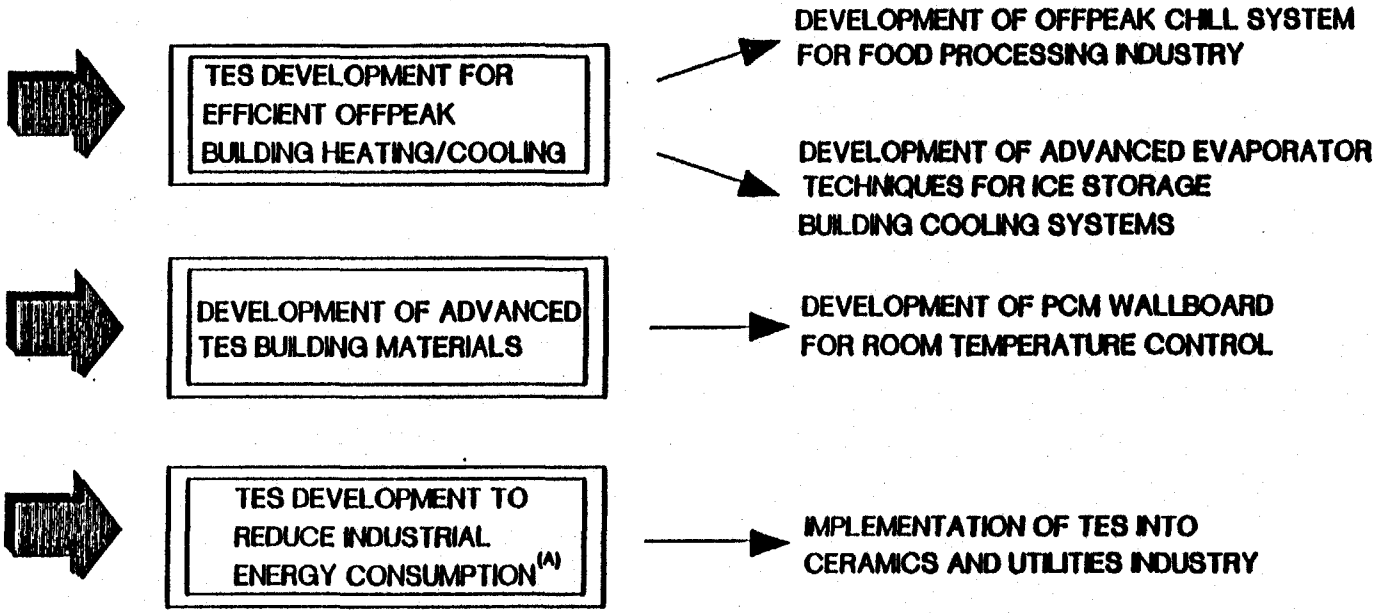


Figure 1. DOE TES Program development focus and application targets.

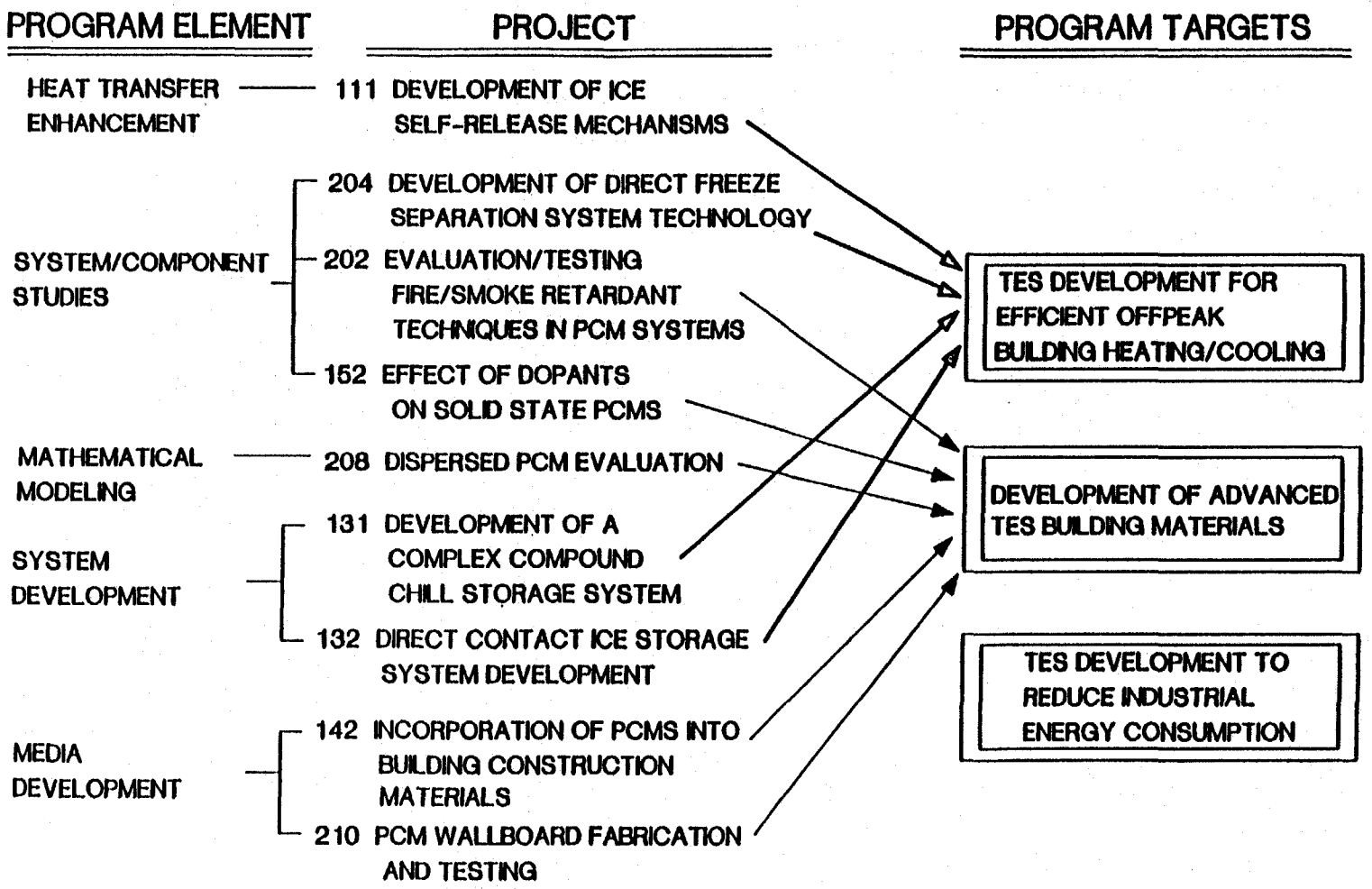


Figure 2. Diurnal TES Subprogram activities and relationship to development focus.

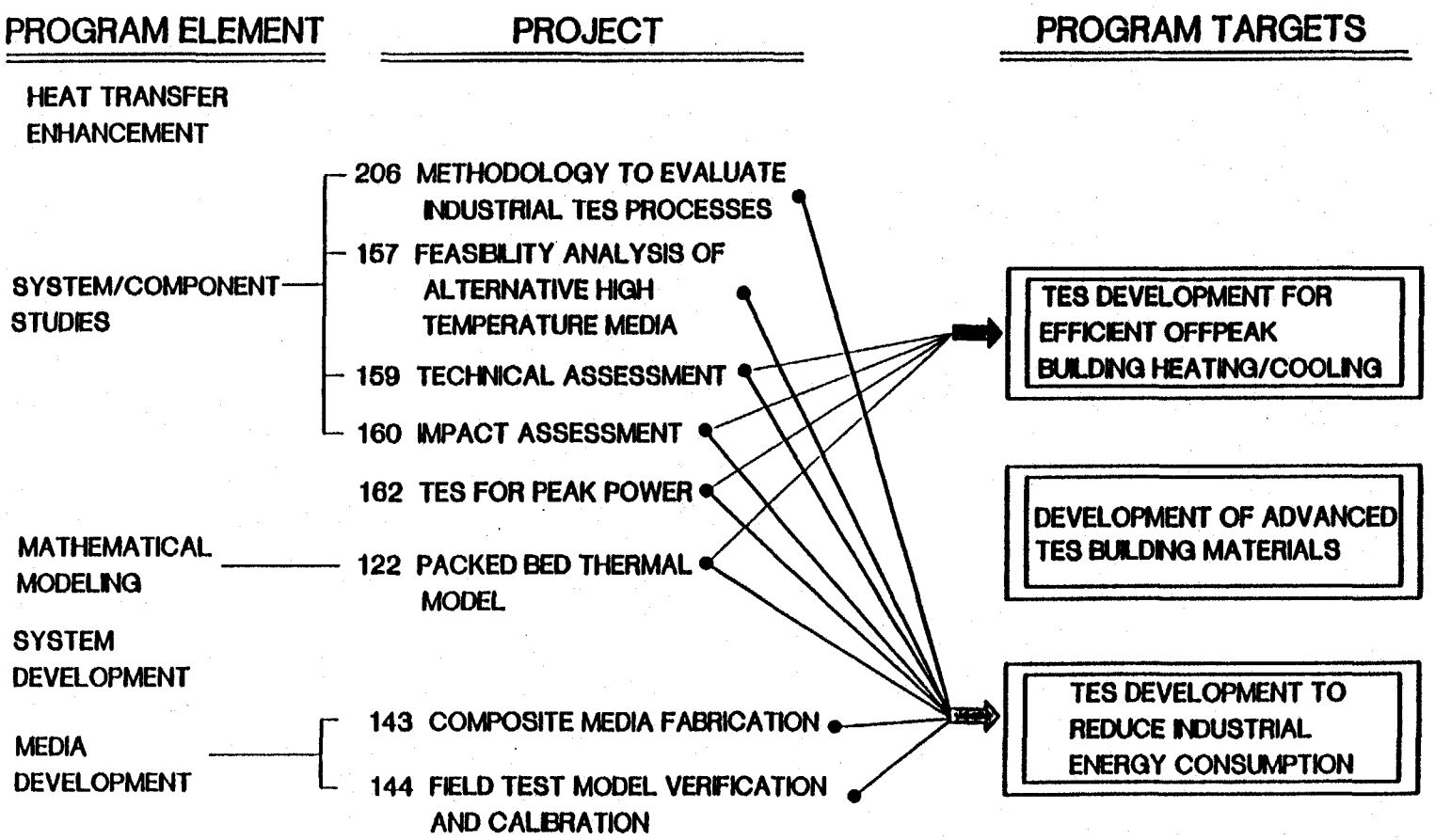


Figure 3. Industrial TES Subprogram activities and relationship to development focus.

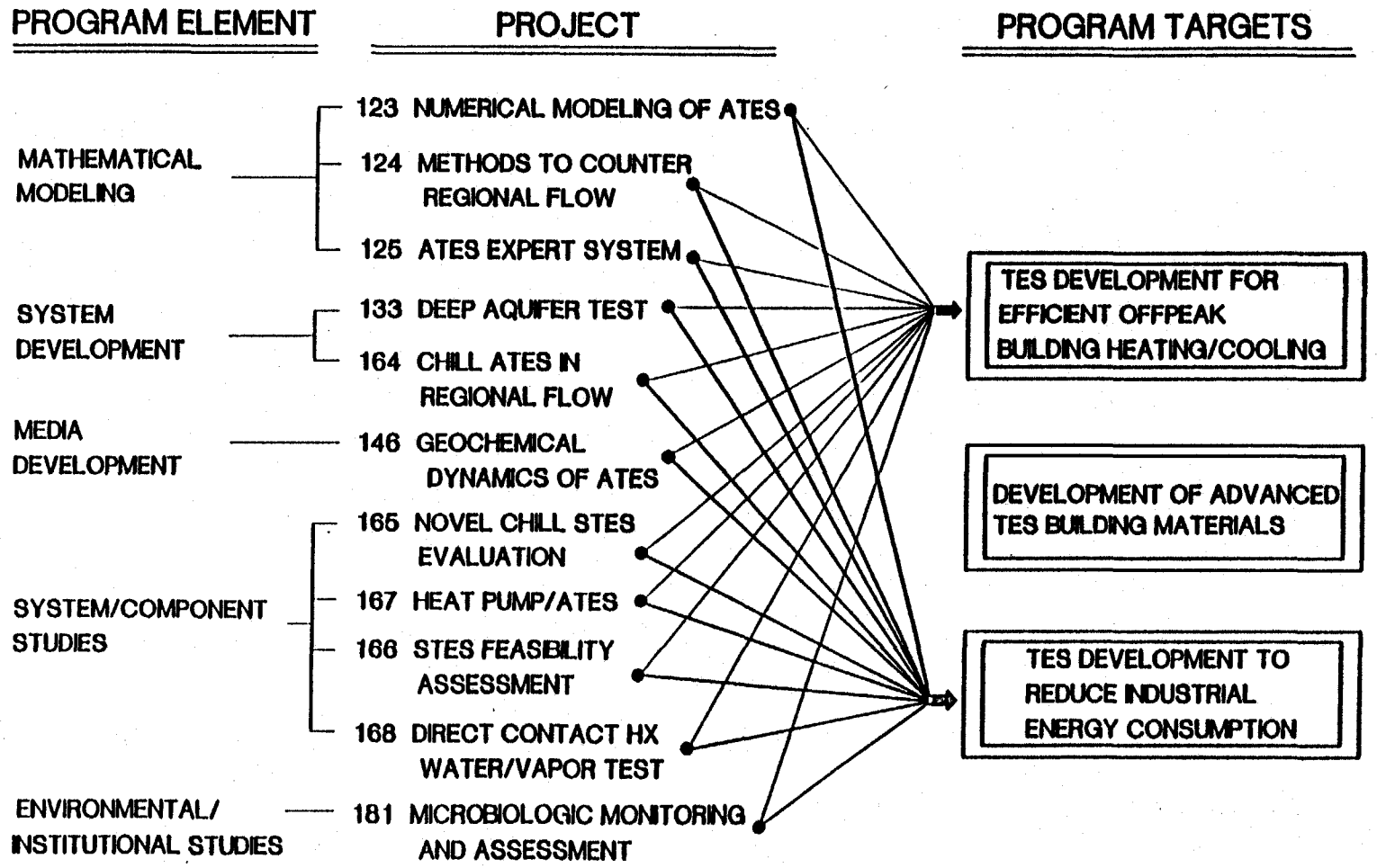


Figure 4. Seasonal TES Subprogram activities and relationship to development focus.

# DIURNAL THERMAL ENERGY STORAGE

# OVERVIEW OF THE DIURNAL AND INDUSTRIAL THERMAL ENERGY STORAGE PROGRAMS

**J. J. Tomlinson, Program Manager**
Thermal Energy Storage Program
Oak Ridge National Laboratory
Oak Ridge, Tennessee 37831

***Abstract***

*The U.S. Department of Energy (DOE) is charged with supporting development of technologies that improve the energy and environmental posture of the country in terms of increased energy efficiency and implementation of fuel switching strategies that emphasize greater reliance on indigenous energy resources. As an enabling technique for utilization of renewable energy resources and for improvement of utility load factors, thermal energy storage (TES) can play a vital role. Development of TES technologies by DOE for diurnal and industrial applications is continuing; current efforts are directed towards initiation of technology transfer activities in major application areas. This paper presents an overview of activities in the diurnal and industrial TES Subprograms and describes near term paths to the transfer of technology in specific application areas.*

## Introduction

Thermal energy storage covers a wide range of technologies that allow an energy supply to be coupled to a heating or cooling demand. In many cases, neither is the demand for heating or cooling constant (e.g., building space conditioning or an industrial drying operation) nor is the energy supply constant. In such cases of "temporal mismatch," TES acts as a buffer, storing energy when the supply exceeds the demand and supplementing the energy supply when the demand is higher. In this way, TES effectively couples the energy supply with demand.

Thermal energy storage is applied generally for reasons of equipment downsizing, capacity expansion, electric load management, waste heat utilization, or solar energy use.

**Equipment Downsizing.** In many applications, the demand for heating or cooling may vary greatly with time. Without TES, the energy source must be of such a size so to meet the peak demand requirement. Through use of TES, this peak demand can be met with a smaller energy supply system. Perhaps the most mentioned application of equipment downsizing is found in the diary industry where fresh milk must be chilled quickly to avoid spoilage. Without TES, a large chiller is needed to meet this peak cooling demand. However, with a cool storage system (ice) available, a small chiller builds ice over a long period; this ice can be quickly melted to meet the requisite cooling demand. This approach has also been used in buildings

**Capacity Expansion.** By lengthening the time over which a TES system is charged and shortening the time over which thermal energy is discharged, the effective capacity (power) of an existing system is increased. An example is a proposed expansion to building in which the additional heating or cooling load may be provided by the existing boiler or chiller running during periods of low demand to charge a TES system. During high demand periods, energy from storage supplements the baseline heating or cooling system to meet the load.

**Electric Load Management.** Thermal energy storage provides the ability to intentionally tailor the use of an energy supply to meet a given thermal load. One of the most interesting and useful applications of this TES capability may be found in electric power generation where excess baseload capacity is available at times that do not coincide with the demand for thermal energy. With storage, this baseload capacity can be exploited for heating and cooling during peak periods, reducing the need for peak electrical power generation. The result of electric load management of this type is an improvement in the capacity factor and overall efficiency of the electric utility through a reduction in peak electrical demand.

**Waste Heat Utilization.** In many industries, heat is generated as a by-product of a manufacturing process and exhausted into the atmosphere. Often in that same industry, heat is required in a process that does not coincide with the availability of waste heat. Thus, there is an opportunity for TES to be used, capturing heat that would normally be wasted for later reintroduction into the second process. The result is an overall reduction in the energy requirements of the industry.

**Use of Renewable Energy.** Examples of this application include utilization of solar energy available during the daytime for nighttime heating, or on a longer term, the use of "winter chill" from the ambient environment for cooling in summer.

## DOE TES Program

Every material whether solid, liquid, or gas changes its thermodynamic state with heat addition or removal; thus, every material can be considered as having a thermal storage capability. Yet, relatively few materials can be expected to meet cost, performance, safety, physical, and/or chemical constraints required for implementation as a working TES medium in specific applications. In addition, there are significant technical issues concerned with TES media containment, effective heat exchange between TES media and working fluid(s), and cost-effective means for incorporation of TES systems into these applications as well. The issues of greatest significance are to a large extent a function of the intended application. To maximize the return on TES R&D, the DOE TES Program is structured along three applications: diurnal, industrial, and seasonal. Technical cognizance over the diurnal and industrial subprograms is performed by the Oak Ridge National Laboratory. The method for performing research in both programs is primarily through subcontracts supplemented by complementary in-house R&D.

## Diurnal TES Subprogram

The application targets for the diurnal TES subprogram are development of TES for passive solar applications and for off-peak building heating and cooling systems. Projects have been classified into the

following technical areas:

1. Heat Transfer Enhancement
2. System/Component Studies
3. Mathematical Modeling
4. System Development
5. Media Development (i.e., materials)

These major technical areas, along with projects planned or currently underway in each of these areas, are shown in Figure 1.

**Heat Transfer Enhancement.** Heat transfer is a critical issue in all TES applications because it limits the rate at which thermal energy can be provided to or withdrawn from a source and delivered to an end use. In latent heat storage applications, fouling due to solids freezing to a heat exchanger surface during a charging cycle (as in the case of cool storage) or discharging cycle (as in the case of heat storage) is frequently the limiting heat transfer mechanism. Conventional methods to accommodate this problem are provisions for large surface heat exchangers or systems that mechanically or thermally clean the heat exchange surface; either technique results in increased costs.

In ice storage systems, wherein ice is formed on an evaporator for later building cooling, work will continue to address the heat transfer issue. Project 111, initiated in FY 1988 and continuing through FY 1989, consists of an examination of methods whereby the evaporator surface can be made "self-cleaning;" i.e., the ice that is formed floats or falls away from the surface, thereby continuously refreshing the surface. A second project in the heat transfer enhancement area to develop an electrochemical system for ice release is under consideration.

**System/Component Studies.** The objective of the first project (Project 204) is to study potential oil, water, refrigerant separation techniques and systems that facilitate use of conventional centrifugal compressors technology with a direct contact ice system. Development of such systems to the point of effecting adequate separation of moisture carryover from refrigerant exiting the evaporator and of separating lubricants in the refrigerant at the compressor discharge would facilitate retrofit applications of ice storage by eliminating the need for compressor replacement. This laboratory study is examining the potential of one thermomechanical technique as a means for separating components at temperatures near saturation.

A major project in the diurnal subprogram is the development of a wallboard material containing a phase change material (PCM). For reasons of high heat of fusion, little supercooling, and low vapor pressure, the PCMs being studied for incorporation into wallboard are organic compounds. As such, they are typically flammable, with smoke evolution perhaps of even greater concern. Project 202, addressing fire/smoke safety issues in the PCM wallboard development program, is to be initiated in FY 1989. This project will initiate a safety testing program on the PCM wallboard in accordance with accepted standards.

The objective of the third project under System/Component Studies is development of temperature-adjusted organic solid-state PCMs. Through the use of dopants to strain the crystal lattice, PCM alloys that

undergo solid-solid phase transitions can be tailored for particular temperature applications (e.g., passive solar) with only proportionate decreases in transition enthalpy.

**Mathematical Modeling.** Guidance in current research efforts to incorporate PCMs into building materials such as wallboard is being provided through development of a mathematical model of PCMs dispersed throughout a sensible heat matrix. This effort, contained in project 208, consists of a computer model of discrete PCM particles of arbitrary size which have been distributed either randomly or in an ordered fashion throughout a support matrix. The model will be validated experimentally and used later to quantify benefits of the PCM wallboard. Incorporation of this model as a subroutine in a larger building simulation code is under consideration.

**System Development.** Work will continue on two cool storage concepts for electrical load management. Development of a chill storage system based on ammoniated complexes for food processing and other low-temperature applications (Project 131) will be continued with industry cost-sharing. As a second project (Project 132), an advanced direct-contact ice storage system for building cooling is being developed in a size suited for later field testing. The system design is such that oil and water carryover problems that have paralyzed early efforts to exploit the direct contact approach have been resolved through use of a unique compressor technology.

**Media Development.** Due to their ability to store and release energy over small temperature ranges, PCMs are attractive as thermal storage media for space heating/cooling. Project 142 is a major initiative with a near term objective of developing a gypsum wallboard material containing a PCM. The advantage of this concept is that a significant amount of "thermal mass" can be provided to stud wall construction by using the PCM wallboard. The benefit to the occupant is increased thermal comfort and efficiency improvements in building space conditioning through greater utilization of passive solar energy. Due to higher thermodynamic efficiency, smaller size, and the ability to store and deliver heat over a small temperature interval, PCMs are attractive as thermal storage media for building heating and cooling and industrial applications as well. Thus, development of TES media where one or more components undergo a phase transition is a central element of the program. The first of five projects, incorporation of PCMs into building materials, is directed toward comfort and efficiency improvements in building space conditioning. By imbibing paraffinic materials into either the interstices of gypsum, or first into pellets of crosslinked high density polyethylene pellets which are then cast into gypsum during wallboard manufacture, an effective PCM system for use in passive solar heating and cooling is possible. A determination of any tendency for PCM redistribution in gypsum wallboard that is thermally cycled is the principal FY 1989 objective for this project. A supporting project (Project 210) is construction and use of a facility for preparing samples of wallboard that are imbibed with the PCM. Full-scale (4 ft x 8 ft) panels of wallboard containing the PCM will be fabricated and tested to determine bulk thermophysical properties above and below the phase-change temperature and to determine the dynamic response of the panel to a surface thermal flux or temperature profile.

## Industrial TES Subprogram

The scope of the industrial program is shown in Figure 2, indicating projects either underway or planned in four of the five program elements.

**Heat Transfer Enhancement.** The compactness and high heat transfer effectiveness of packed bed heat exchangers are of interest to the Industrial Subprogram. Direct contact heat exchange is particularly effective in applications of heat transfer between a gas and a liquid. Work initiated in prior years to develop a model of an air/molten salt heat exchanger is being continued to determine the effects of radiation heat transfer in the packed bed and to verify a heat transfer model under conditions wherein fluid properties are changed.

**System Component/Studies.** An optimization study currently underway is aimed at determining the "best" (highest ROI) high-temperature storage configuration for a two-kiln single dryer periodic brick plant. The study takes into account real-time uses for reject heat for which storage is not required. During FY 1989, this preliminary study will be completed and will be used as a basis for development of a procedure for analysis and TES design studies for a multikiln, multidryer plant.

**Media Development.** Over the past four years, a major effort to develop high-temperature TES media for industrial applications has resulted in successful laboratory development of a sintered magnesium oxide (MgO) pellet with porosity suited for containment of a eutectic of carbonate salts. Capillary forces retain the PCM in the MgO interstices so that the pellet remains solid during thermal charging and discharging. During FY 1989, packed bed configurations of this media will undergo initial field testing in a brick plant to examine performance and lifetime issues when the media is used to extract thermal energy from the kiln flue gas (Project 143, 144). A test program will be conducted to measure and evaluate thermochemical and thermophysical properties of the media periodically during the field test.

## Conclusion

The diurnal and industrial TES subprograms are continuing to show progress not only towards development of technologies, but their implementation as well. Of major emphasis is the development of the PCM wallboard which is being supported by several projects. This level of effort is commensurate with the high level of interest shown by manufacturers and the potential market size for the product. In addition, early transfer of the chill storage system to industry through a heavily cost-shared program is anticipated in FY 1990. These projects, in addition to the ones further back in the development stage, form a strong basis for addressing energy related issues that, through storage, can be successfully resolved.

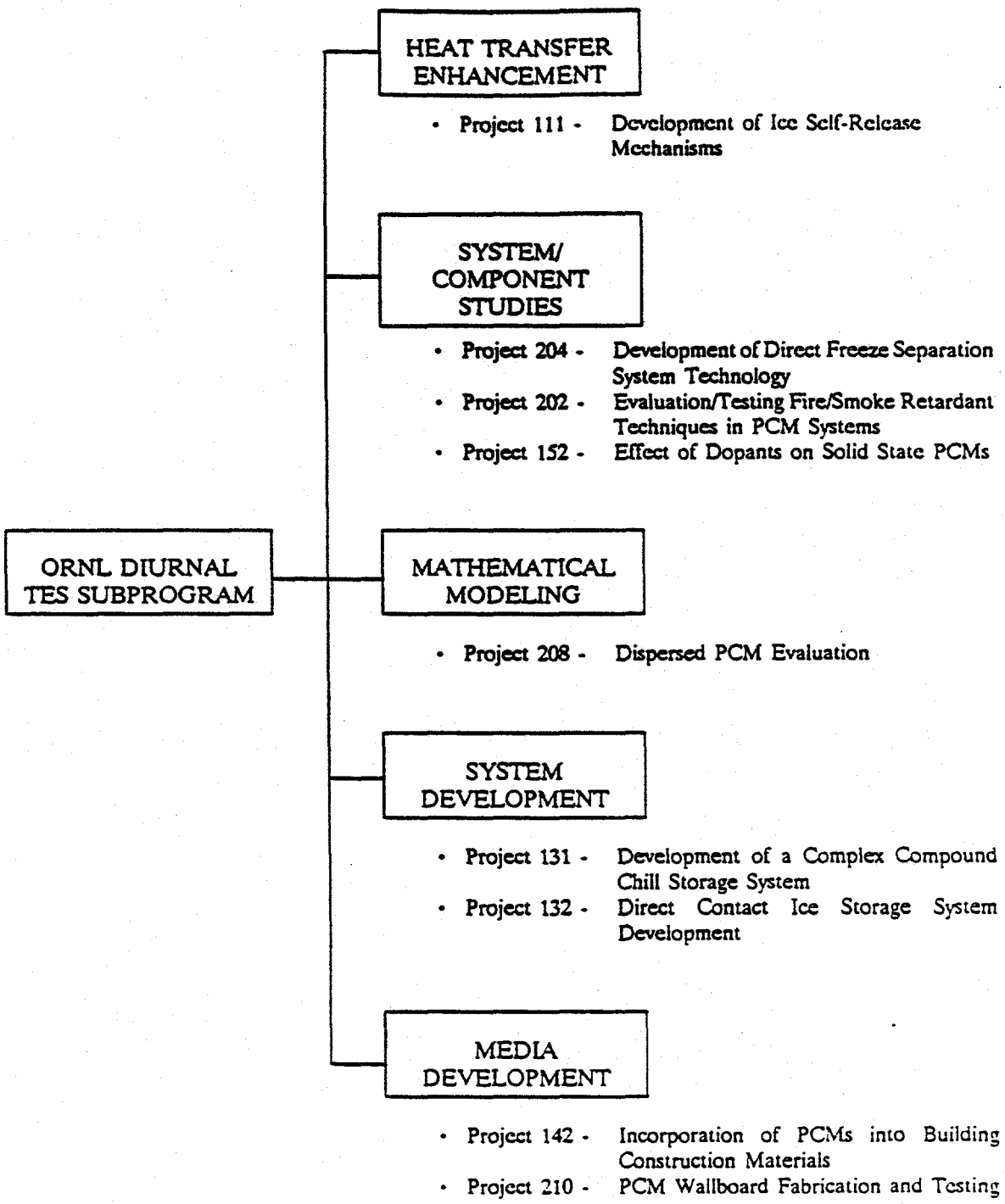


Figure 1. Diurnal TES subprogram structure.

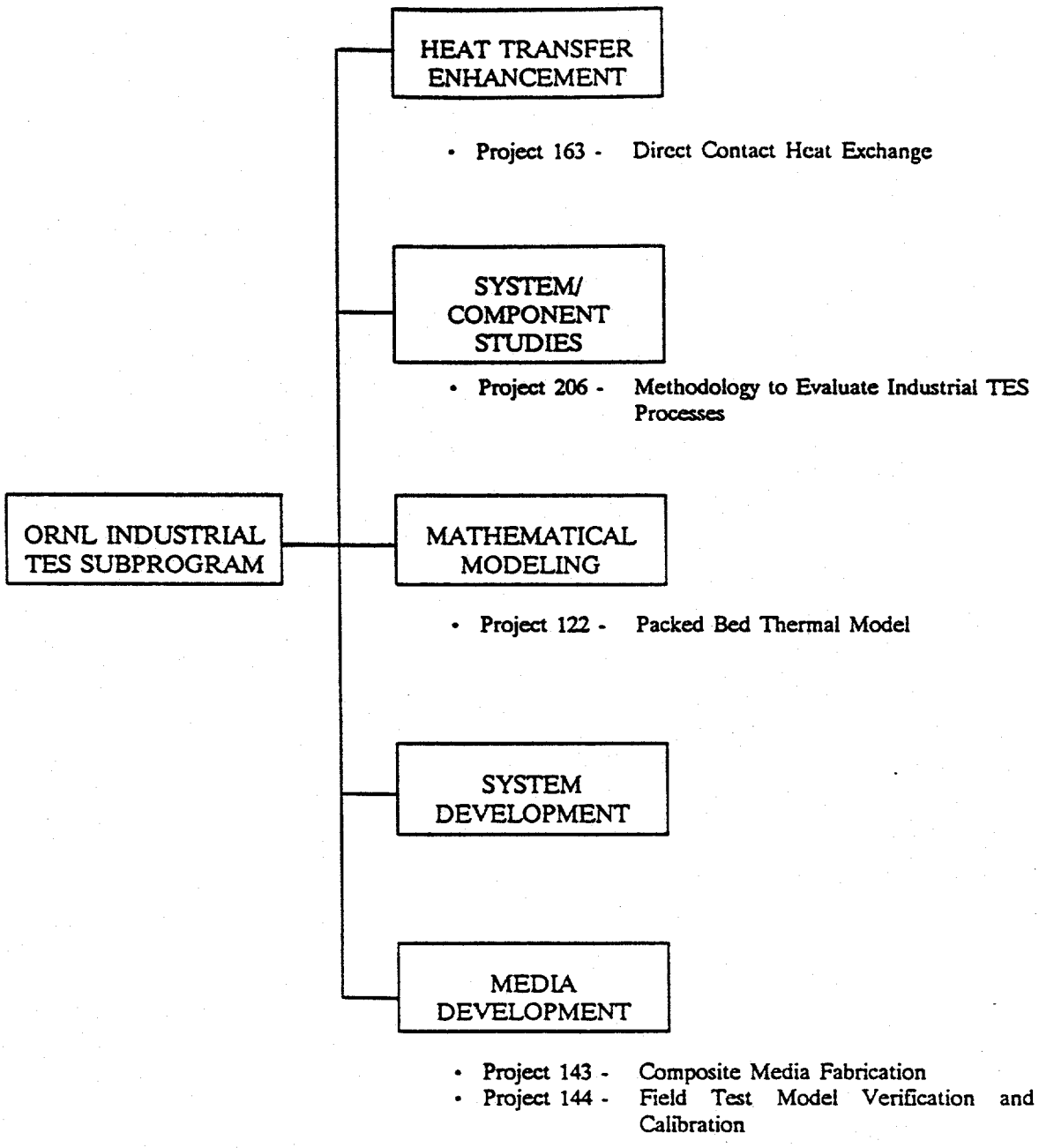


Figure 2. Industrial TES subprogram structure.

# EVAPORATIVE HEAT TRANSFER IN BEDS OF SENSIBLE HEAT PELLETS

**Rao V. Arimilli[*] and Carlos A. Moy[**]**
Department of Mechanical and Aerospace Engineering
The University of Tennessee
Knoxville, Tennessee 37996-2210

## *Abstract*

*An experimental study of boiling/evaporative heat transfer from heated spheres in vertical packed beds with downward liquid-vapor flow of Refrigerant-113 was conducted. Surface superheats of 1 to 50°C, mass flow rates of 1.7 to 5.6 Kg/min, sphere diameters of 1.59 and 2.54 cm, quality (i.e., mass fraction of vapor) of the inlet flow of 0.02 to 1.0, and two surface conditions were considered. Instrumented smooth and rough aluminum spheres were used to measure the heat transfer coefficients under steady state conditions. Heat transfer coefficients were independently determined for each sphere at three values of surface superheat.*

*The quantitative results of this extensive experimental study are successfully correlated. The correlation equation for the boiling heat transfer coefficients is presented in terms of a homogeneous model. The correlation may be used in the development of numerical models to simulate the transient thermal performance of packed bed thermal energy storage unit while operating as an evaporator.*

*The boiling of the liquid-vapor flow around the spheres in the packed bed was visually observed with a fiber-optic baroscope and recorded on a videotape. The visualization results showed qualitatively the presence of four distinct flow regimes. One of these occurs under subcooled inlet conditions and is referred as the Subcooled Regime. The other three occur under saturated inlet conditions and are referred to as the Low-quality, Medium-quality, and High-quality Regimes. The regimes are discussed in detail in this paper.*

## Introduction

Thermal energy storage may be used in heat pump cycles for shifting the electrical energy usage from "peak" to "off-peak" hours, thereby contributing to the load leveling of the local electrical utility. Packed beds of pelletized phase change materials can serve as thermal energy storage units at either of the two operating temperatures. In the energy recovery mode, the packed bed operates as an evaporator.

Previous work (Graves [1], and Arimilli and Graves [2]) on thermal energy storage in packed beds of encapsulated phase change materials was limited to the determination of convective heat transfer coefficients

---

[*] **Professor**
[**] **Graduate Student**

for the flow of fluids without any change of phase, such as boiling or condensation. There appear to be no published studies for the case when the working fluid is undergoing convective boiling or evaporation (also called flow boiling). Such would be the actual flow in a packed bed while it is operating as an evaporator within a heat pump cycle.

**Project Objective**

Numerical models have been developed for simulating packed bed thermal energy storage units having single phase flow of the working fluids. In the development of storage units for use with heat pumps, the working fluid boils within the evaporator, and the numerical models need input in the form of a correlation for the boiling heat transfer in such units. This project was undertaken to fill that need. Specifically, the objective is to determine the characteristics of boiling heat transfer from spherical particles in vertical packed bed thermal energy storage units while operating in the evaporator mode and to determine a correlation for the boiling heat transfer coefficients. Two sizes of spheres and two surface conditions are to be considered.

In this study, liquid-vapor Refrigerant-113 is used as the heat transfer fluid. A packed bed consisting of an aluminum cylinder packed with spheres is used in the present experimental investigation as the thermal energy storage unit. Two sizes of spheres having 1.59 and 2.54 cm diameters were used.

The heat transfer measurements are made with a series of instrumented-aluminum spheres positioned at one axial location of the packed bed. Heat transfer coefficients are determined from measurements for a range of mass flow rates, heat fluxes, inlet qualities, particle sizes, and particles surface conditions in order to conduct an extensive boiling heat transfer study.

**Project Accomplishments**

Based on the measurements, a correlation is developed for the boiling heat transfer coefficient for spherical particles as a function of the relevant parameters. These parameters include: diameter of the particles, inlet quality, mass flow rates, degree of superheat, particle size, and surface conditions. The results of this study may be used in the development of computer models to simulate the packed bed evaporators. Additionally, flow visualization studies of the liquid-vapor flow through the packed bed are conducted with the use of a fiber-optic baroscope (fiberscope). This technique is used to identify the boiling regimes occurring on the surfaces of the heated spheres within the packed bed. The project is now complete.

## Review of Literature

Boiling heat transfer from single spheres was studied extensively because of its importance to nuclear reactor operations under loss-of-coolant accident conditions. Such studies were used to simulate the behavior of molten fuel drops after ejection into coolant flow. Film boiling heat transfer from single spheres to saturated liquid in forced convection was studied by Witte [3], Bromley et al. [4], Kobayasi [5], Wilson [6], and Dhir and Purohit [7]. Pool boiling heat transfer from single spheres was studied by several investigators including Veres and Florschuetz [8], and Shoji et al. [9]. The literature pertinent to the present study is reviewed below.

**Pool Boiling Heat Transfer from Spheres in Porous Media**

Orozco et al. [10] investigated the problem of film boiling heat transfer from a sphere and a horizontal cylinder embedded in a liquid saturated porous medium. In their experiments the effect of surface roughness on the film boiling process in the porous media was studied. Refrigerant-113 was used as the working fluid. A stainless steel horizontal cylinder with an outside diameter of 12.7 mm was used to obtain experimental heat transfer data. The cylinder was machined to accommodate a high power cartridge heater. The porous media consisted of 3-mm glass beads. Their theoretical model for spheres was also compared with experimental data obtained by other investigators, including Tsung et al. [11], and the predictions were in excellent agreement with the experimental results.

Tsung et al. [11] experimentally studied boiling heat transfer from a sphere embedded in porous media composed of unheated glass particles. Measurements were made under steady state and transient quenching conditions. Refrigerant-113 under saturated conditions was used as the test fluid. Boiling heat fluxes on a 19 mm diameter stainless steel sphere were studied, while the particles forming the unheated porous media were varied from 19 to 2.9 mm. Induction heating was used as the mode of heating the stainless steel sphere. Three different surface conditions were considered for the stainless steel sphere. Results for all cases were presented by constructing typical pool boiling curves with the experimental data.

**Heat Transfer in Packed Beds with Liquid-Vapor Flow**

Orozco et al. [12] studied the problem of flow film boiling from bodies embedded in a liquid saturated porous medium. The problems of flow film boiling from both a sphere and a horizontal cylinder were modeled theoretically. Since the vapor film occupies a thin region near the cylinder and the sphere surface, the Brinkman-modified Darcy model is used to describe the flow inside the vapor film. Outside the vapor film, potential flow is assumed. The results reported in this paper document the effect of subcooling, incoming fluid flow velocity, and Darcy number on the heat and fluid flow characteristics.

A study on the transient thermal performance of an experimental packed bed of spheres was reported by Graves [1]. The investigation used a smooth horizontal cylinder, of the same diameter as the spheres in the bed, as the heat transfer geometry embedded in the packed bed. Liquid-vapor flow of R-113 was used for some of the experimental runs. Six different bed inlet qualities were used, ranging from 0.24 to 1.0. Two-phase flow R-113 was circulated through the bed until steady state conditions were obtained for each selected value of quality. For each two-phase flow run, data was recorded at three different heat flux levels to determine the influence of temperature superheat on heat transfer coefficient. The results were presented in the form of a correlation.

**The Present Study**

The present investigation uses a steady state approach to measure boiling heat transfer coefficients for solid aluminum spheres with liquid-vapor flow of Refrigerant-113 through a randomly packed bed. Bed inlet qualities ranged from 0.02 to 1.0. Three different power inputs to the aluminum spheres were used to determine the influence of superheat on heat transfer coefficient. An electrical resistance heater inserted

at the center of each of the spheres was used to heat the spheres. There appears to be no literature available on heat transfer from spheres with this type of heating or on heat transfer from spheres in packed beds having liquid-vapor flow of a working fluid.

## Experimental Facility

The two-phase flow test facility, temperature probes, heat transfer probes, and visualization tube were designed, fabricated, and installed in the laboratories of the Mechanical and Aerospace Engineering Department of The University of Tennessee-Knoxville.

### Two-Phase Flow Test Facility

The two-phase flow test loop used in this study is shown schematically in Figure 1. The nominal loop pressure can be adjusted by varying the amount of liquid in the loop and by contracting or expanding the stainless steel bellows in the pressurizer. The six-vane positive displacement pump can provide liquid flow rates up to 75.7 liters/min (20 gallons/min). Flow rate is measured with one of the two turbine flow meters; one for high-flow rates, and other for low-flow rates. The flow meters were calibrated in the laboratory. Three safety valves, each set at 10.2 atmospheres of pressure, relieve the system pressure should it exceed this value.

The working fluid can be heated in a vertical stainless steel resistant heating section, 3.05 meters (10 ft.) long, with a 25 KVA adjustable DC power supply. Also the distance between the electrodes is adjustable. This gives some additional capability for fine adjustment of the heater power. The system fluid is cooled by the building potable water in a single pass vertical shell and tube heat exchanger. The sight glass just downstream of the flow meters can be used to ensure that the flow out of the flow meters is always in the liquid phase. The sight glass upstream of the packed bed test section is used for visually monitoring the phase of the flow entering the test section.

Details of the vertical packed-bed test section and the arrangement of the probes used are shown in Figure 2. The test section, an aluminum cylinder 1.276 meters tall with an inside diameter of 12.7 cm (5 in) and a wall thickness of 1.27 cm (0.5 in), is lined on the inside with a 0.159 cm (1/16 in) thick Teflon liner bonded to the cylinder.

To provide access into the test section for instrumentation at the five stations along its length, five 0.95 cm (3/8 in) diameter radial holes were drilled, through the aluminum wall and teflon liner. These holes were positioned 26.67 cm (10.5~in) apart along the length of the test section and the axis of each is offset by 120 degrees from each other. This rotational offset is designed to reduce the influence of the wake of upstream probes on the downstream probes. On the outside of the cylinder, a 7.62 cm OD aluminum tube with flange was welded (view AA in Figure 2) concentric to each of the holes. An O-ring between the flange and its cover plate eliminates leakage of the refrigerant. Each cover plate is appropriately drilled and threaded for the installation of Conax bare wire sealing connectors for thermocouple wires, and insulated lead wire connectors for power supply to the heaters in the instrumented spheres. The Conax connectors prevent leakage of refrigerant around the thermocouple wires and the power leads. The packing

is confined at the top and bottom between two 0.16 cm thick stainless steel sheets stamped with 0.32 cm circular holes such that the hole area is about half that of the total area. The support screen at each end of the test section can be positioned within the slots of three small teflon tabs spaced 120 degrees apart and screwed to the inside of the test section. The flow area blocked by the teflon tabs in only 0.33 percent of the total and, therefore, would not influence the incoming flow pattern adversely.

**Temperature Probe**

In a packed bed the fluid temperature can be measured accurately with thermocouple when the thermocouple are in direct contact with the fluid, and not with the packing of the bed. To ensure this and to measure the radial variation of the temperature distribution in the bed, a thermocouple holder was fabricated to hold thirteen 36 gage type-T (copper-constantant) thermocouple at thirteen predetermined radial positions in the bed. This thermocouple holder will henceforth be referred to as the temperature probe and is shown in View AA in Figure 2 and Figure 3(a). Three temperature probes are located at stations one, two, and five.

**Heat Transfer Probes**

The heat transfer probes consist of aluminum spheres instrumented with a heater system and surface thermocouple. The installation of the heater system, surface thermocouple and surface conditions of the instrumented spheres are described next.

**Installation of the Heater System**

Each of the heater systems is composed of two lead wires and a heater element, all coated with a dielectric epoxy (OmegaBond 200). The heating element is made of a 25 gage (0.01 cm diameter) copel (55% Cu, 45% Ni alloy) wire having electrical resistivity of 60 ohms/meter. The length of the heater wire used is approximately 5 cm for the 1.59 cm aluminum spheres, and 8.9 cm for 2.54 cm aluminum spheres. To reduce the conduction heat loss through the 22 gage copper lead wires, two 20 gage constantan wires of 0.7 cm length are used, one at each end of the heater wire, to increase thermal resistance (by a factor of over 17 relative to copper) between the lead wires and the heater. The wires are butt-joined and soldered. The schematic of the heater system is shown in Detail at A in Figure 4.

One of the lead wires was first coated with epoxy over the constantan and part of the copper wire and cured at 204°C for two hours. After curing, the heater wire was coiled around the coated lead wire. Another coat of the epoxy was then applied over the entire coiled heater system and cured as before so that the entire system can be easily inserted as a single unit into the blind hole in the aluminum sphere as shown in Figure 4. This procedure reduced the heater system to a length of approximately 0.64 cm for the 1.59 cm spheres and 1.27 cm for the 2.54 cm spheres. The wire electrical resistance of each individual sphere was measured before the application of the epoxy and after it was cured to make sure that there was no shorting of the heater wire. Next the blind hole in the sphere was filled with the epoxy paste and the heater unit was inserted into the hole so that the heater unit is centered inside the sphere. The filling was stuffed repeatedly to eliminate trapped air bubbles and make good thermal contact. The epoxy was cured

again. The resistances used in the 1.59 cm spheres ranged between 4 and 5 ohms, and those in the 2.54 cm spheres ranged between 6 and 7 ohms, with an uncertainty of less than one percent.

**Surface Thermocouple**

For the surface temperature measurement two thermocouple were installed on each of the spheres as shown in Figure 4. Teflon insulated 36 gage (0.127 mm diameter) copper and constantan thermocouple wires were inserted through the 0.16 cm diameter holes in the sphere. The junction was first formed with two wires and then the wires were pulled back such that the active junction is flush with the surface of the sphere. At this position the countersunk portion of the hole was filled with soft solder as shown in Detail at B in Figure 4. Next the hole was filled with Omega Bond 200 from the back side of the hole and stuffed repeatedly to eliminate air bubbles and make good thermal contact. Later the soft solder part of the sphere was smoothed and polished.

**Surface Condition of Instrumented Spheres**

The instrumented spheres were uniformly polished using emery 400 sand paper. Throughout this report these spheres are referred as smooth spheres. After completing all the smooth-sphere runs, to determine the influence of roughness, the same spheres were roughened uniformly with emery 40 sand paper. These spheres are referred as the rough spheres.

**Visualization Tube**

A Lexan tube of 0.95 cm inside diameter and 1.27 cm outside diameter was used as a leak-proof path into the packed bed for the insertion of an Olympus IF-8D3/11D3 industrial fiberscope. The fiberscope consisted of a miniature lens system and light source which permitted flow visualization inside the packed bed at station two. The tube was sealed at one end to prevent leakage of Refrigerant-113. The other end of the tube was left open in order to insert the fiberscope. The Lexan tube was sealed from the outside using a compression fitting at the flange cover plate of station two; this is shown in Figure 5.

**Packing of the Bed**

The first bed was packed with 1.59 cm diameter smooth glass spheres up to station two. Seven instrumented aluminum spheres of the same size with their heater wires connected electrically in series, as shown in Figure 3(b), were first placed at seven radial positions in a random manner as shown in Figure 2, and later in a cluster configuration in which the heated spheres are in contact with each other. A temperature probe was inserted into position through the side port at station two, and the remaining length of the bed was filled with the smooth glass spheres. Another temperature probe was inserted through the port at station one. These two probes were used to determine the temperature distributions of the working fluid at the two stations. The visualization tube was also inserted through a side port at station two for some of the experimental runs. The void fraction obtained for this packing was 0.389. For the second packing, thirty eight centimeters of the bed length was packed with 2.54 cm diameter smooth Delrin spheres. The packing of the Delrin spheres was performed so that half the packing (19 cm) was above station two and half below station two. At station two, five 2.54 cm instrumented aluminum spheres

were placed first at five different radial positions and then in a cluster making contact with each other. The instrumented aluminum spheres were, as before, connected electrically in series. The rest of the bed was packed with 1.59 cm diameter smooth glass spheres. Temperature probes were arranged as before. The void fraction in the bed for the 2.54 cm sphere packing was 0.439.

The entire temperature measuring system composed of the thermocouple, the lead wires, and various connectors as used in the test set-up were calibrated in the laboratory. The maximum errors were found to occur at the higher temperatures. The maximum temperature encountered in this study is about 80°C, and the corresponding error for the surface temperature measurement system was found to be 0.3°C and for the fluid temperature measurement system 0.4°C.

All of the temperature measuring system composed of the thermocouples, the lead wires, and the various connectors as used in the test set-up were calibrated in the laboratory; and the maximum error was found to be 0.3°C for the surface temperature measurement system and 0.4°C for the fluid temperature measurement system. This maximum difference was present at high temperatures of about 80°C.

## Experimental Procedure

The total energy input to the instrumented aluminum sphere is balanced with the total energy output by (1) convection heat transfer to the two-phase working fluid and by (2) heat losses through the instrumented spheres lead wires was used to determine the heat transfer coefficient from each sphere individually. The energy balance was performed after the instrumented aluminum spheres had reached steady state.

The measurement of boiling heat transfer coefficients from the spherical particles in the packed bed was performed at one axial location of the bed, where the instrumented aluminum spheres (also referred to as heat transfer probes) were randomly placed in different radial positions, as shown in View A-A in Figure 2, and also placed in a cluster making contact with each other. At this axial location, a temperature probe consisting of thirteen thermocouple was installed for the measurement of the radial temperature distribution of the working fluid.

Refrigerant-113 was used as the heat transfer fluid in a recirculating mode in the test facility. For each experimental run a mass flow rate, the nominal pressure in the bed and the inlet quality of the boiling refrigerant are selected. The flow control valves, the power level to heat the stainless steel tube, and the amount of liquid in the loop are adjusted iteratively to arrive at the conditions selected. Typically 40 minutes are required to make these adjustments and reach steady state. In all of these boiling runs, the system was allowed to reach saturation state. This was ensured when the pressure in the bed matched the saturation pressure corresponding to the temperature of the liquid-vapor flow. Additionally, the temperature probes at station one and two indicated that the temperature is radially uniform. Then the power input to the instrumented spheres is turned on, and the scanning of the thermocouple in the temperature probes and on the heated spheres is initiated. Three different power inputs to the instrumented aluminum spheres were used for each quality setting. A Hewlett Packard 3447A Data Acquisition and Control Unit together

with a HP 9826 Desk top computer is used for scanning, acquiring, and storing data. The data acquisition was continued until steady state conditions are indicated by the surface thermocouple. The heat transfer coefficient is calculated separately for each sphere. In all of the runs considered, the variation of the temperature distribution was found to be under 0.2°C and is therefore essentially uniform.

**Validation of Sphere-Heat-Transfer Measurement System**

Natural convection, forced convection in the packed bed, and pool boiling tests were conducted with the instrumented spheres.

**Natural Convection Validation.** Both water and Refrigerant-113 were used as the fluid media. Aluminum spheres of 1.59 cm and 2.54 cm were used in separate tests covering Rayleigh number range of $10^5$ to $2x10^7$. The results were found to be within 10% of the correlation as given by equation 9.34 in Incropera and Dewitt [13].

**Forced Convection Validation in the Packed Bed.** With the 1.59 cm instrumented spheres located in the randomly packed bed a test for forced convection validation using unheated R-113 flow was conducted. For each particle Reynolds number more than one input power to the instrumented spheres was used to confirm, with the present instrumentation, that the Nusselt number correlation in single phase flow would be independent of the difference in temperature between the surface of the sphere and the ambient fluid. The present measurements as shown in Figure 6 clearly confirm this. The results are also compared with the general correlation of Baumeister and Bennett [14], and it can be seen that the agreement is good.

**Pool Boiling Validation.** Saturated Refrigerant-113 at atmospheric pressure was used as the heat transfer fluid in the pool boiling test. The heat flux to a single instrumented sphere and the temperature difference between the surface of the sphere and the R-113 were measured and plotted in a boiling curve. In Figure 7, the boiling curves of the 1.59 cm and 2.54 cm aluminum spheres are compared to results by Tsung et al. [11] for 1.9 cm stainless steel sphere and to results by Veres and Florschuetz [8] for 2.38 cm copper sphere. The present results fall between their results and indicate an acceptable degree of agreement for spheres in pool boiling of R-113 in the nucleate boiling region of the boiling curve.

It can be concluded from these three validation tests that the heat transfer probes used in the present investigation are dependable sensors for the measurement of heat transfer coefficients under natural convection, pool boiling, and forced convection conditions.

**Flow Boiling**

**Nearly in-line arrangement.** In the bed packed with 1.59 cm glass spheres, the 1.59 cm instrumented smooth spheres are positioned at 20 sphere diameters from the top of the bed in a nearly in-line arrangement so that the randomness of the packing is not significantly altered. In this arrangement, the instrumented spheres are in contact directly with the unheated spheres of the bed and not with each other.

A series of tests with constant mass flow rate were conducted with Refrigerant-113 under liquid-vapor flow conditions. For each mass flow rate, the inlet quality (x) was adjusted to a desired value; and the influence of the surface superheat on the heat transfer coefficient was investigated. Here surface superheat

is defined as the temperature difference between the two-phase fluid and the surface of the heated instrumented aluminum spheres. At each quality setting, this was accomplished by changing the power input to the spheres and allowing the temperatures indicated to reach steady state values. This procedure was repeated for a range of qualities between zero and one. These tests were repeated for a total of three mass flow rates.

Another series of tests were conducted with the rough 1.59 cm instrumented spheres.

The procedure used for the bed packed with 1.59 cm spheres is repeated with the bed repacked with 2.54 cm Delrin spheres and the 2.54 cm smooth instrumented aluminum spheres. The tests are also repeated with 2.54 cm rough instrumented spheres.

**Cluster arrangement.** In this arrangement all of the 1.59 cm smooth instrumented spheres are placed together in a cluster making direct contact with each other. The center of the cluster is positioned in the 1.59 cm sphere-packed bed at about the same location as the in-line arrangement. The packing procedure used for the in-line arrangement of 1.59 cm spheres was repeated for the cluster arrangement. These tests are also repeated with rough instrumented spheres in cluster arrangement.

The above procedure used for the bed packed with 1.59 cm spheres is repeated with the bed packed with 2.54 cm Delrin spheres and the 2.54 cm smooth instrumented aluminum spheres in the cluster arrangement. The tests are again repeated with the 2.54 cm rough instrumented spheres in the cluster arrangement.

The purpose of using the heated spheres in the cluster arrangement is to determined the influence, if any, on boiling heat transfer results from spheres in packed the bed when adjacent spheres are also heated. This configuration would be more representative of the situation in a packed bed evaporator.

**Boiling Heat Transfer Coefficients**

The boiling heat transfer coefficient for each sphere was calculated from the electrical power input to the sphere in the following manner:

1. The resistance of the heater in each of the instrumented spheres was measured. The current to the heaters when connected in series was also measured.

2. The average of the two-phase fluid temperature indicated by the thermocouple in the temperature probe (the variation between the thirteen thermocouples) was found to be within one standard deviation from the mean value and in no case exceeded 0.2°C and is denoted by $T_{sat}$. The average of the two surface temperatures of each of the spheres were determined and is denoted by $T_w$. The values indicated by the two surface thermocouple on each sphere were found to be within 0.4°C of each other. This large 0.4°C difference in the surface temperatures should be expected because some of the surface mounted thermocouples come in contact with the adjacent spheres in the randomly packed bed and therefore tend to indicate higher temperatures. When the results of all the spheres are taken into account, the final correlation should be considered as having effectively taken all of these factors into consideration. For example, measurements based on a single sphere would not be able to account for the differences in the flow fields around the different spheres as the local packing around the spheres is random not identical.

3. The heat transfer coefficient, $h_{2p}$, for each sphere was calculated from the following equation:

$$h_{2P} = \frac{I^2 R - Q_{losses}}{A(T_w - T_{sat})} \quad (1)$$

where

$I$ = current, amps

$R$ = resistance of heater, Ohms

$Q_{losses}$ = conduction heat loss to lead wires, Watts

$A$ = surface area of sphere, $m^2$

The maximum heat loss to the lead wires by conduction was estimated to be 2.8 percent of the total input power to the sphere. At this value is small, the $h_{2p}$ values reported in this paper are not corrected for the conduction heat losses.

**Uncertainty in $h_{2p}$ and x**

An uncertainty analysis is made of the various quantities derived from experimental measurements. The uncertainty in the determination of $h_{2p}$ was controlled predominantly by the uncertainty of the surface superheat ($T_w$-$T_{sat}$). As an example of one of the lower values of surface superheat reported in this study; namely, when ($T_w$-$T_{sat}$) = 3.1°C, the uncertainty in $h_{2p}$ is 11.5%. For higher values of surface superheat, the uncertainty would be lower. The uncertainty in the inlet quality of the liquid-vapor flow was determined to be 7.1%.

## Results and Discussion

A total of fourteen series of two-phase working fluid experimental runs were conducted. The instrumented spheres were used in two types of arrangements: (1) instrumented aluminum spheres in a cluster, and (2) instrumented spheres in-line. The results are discussed below.

**Instrumented Spheres in the Cluster Arrangement**

A series of twelve runs were conducted using the 1.59 cm and the 2.54 cm instrumented aluminum spheres. For each size, the instrumented spheres were packed together in the form of a cluster making contact with each other. In this arrangement of the instrumented spheres, the flow and the thermal boundary conditions around the center sphere would be similar to those occurring around individual spheres in a packed bed evaporator.

For each experimental run a range of qualities from zero to one was used. Results for these runs are shown in Figures 8 to 11. Figures 8 and 9 are for 1.59 cm diameter smooth and rough spheres, respectively. Figures 10 and 11 are for 2.54 cm diameter smooth and rough spheres, respectively. Within each of these figures, results for each mass flow rate are presented as three separate subplots and a fourth plot showing the results for the three different mass flow rates superposed for delineating the influence of mass flow rate on the boiling heat transfer coefficient. These figures show the influence of inlet quality, heat flux, and mass flow rate on boiling heat transfer from the center sphere in the cluster for the two sphere sizes used

and the two surface conditions. In these plots, the experimental boiling heat transfer coefficient, $h_{2P}$, has been plotted against x, the quality at the inlet to the bed. In general, at low inlet qualities, the two-phase heat transfer coefficient seems to increase very rapidly with x as x is increased from 0% to about 10 to 20%. For higher qualities, $h_{2P}$ remains almost constant until x approaches about 90%. For qualities higher than 90%, $h_{2P}$ tends to decrease with increasing x. This general trend is observed for all the cases presented in these figures. These figures also show that for the range of parameters used in this study, the surface roughness does not significantly influence the two-phase heat transfer coefficient. The apparent lack of dependence on surface roughness is attributable to the flow patterns observed around the spheres and discussed under flow visualization results.

**Instrumented Spheres in the In-Line Arrangement**

Two experimental runs were conducted placing the instrumented aluminum spheres in a single plane having no direct contact with each other. The tests were performed for each of the two sphere sizes and for one value of mass flow rate. Results for the 2.54 cm spheres are shown in Figure 12 and compared with the results of the cluster arrangement. It can be seen that under the same operating conditions the $h_{2P}$ for the center sphere within the cluster arrangement is higher than that for the spheres in the in-line arrangement.

**Visualization Results**

In this study the boiling phenomena occurring around heated spheres in a packed bed having downward liquid-vapor flow of R-113 was visualized. Such a flow situation is representative of the flow in a packed bed thermal energy storage unit while operating as an evaporator. The results presented in this section are based on the observations made with a mass flow rate of 5.6 Kg/min.

The flow regimes around the heated instrumented spheres under flow boiling conditions were observed using a fiberscope as described earlier and recorded on a video tape. A careful study was made of the recordings and the results are described below. Four distinct flow regimes were observed. One of these occurs under sub-cooled inlet conditions and is referred to as the Sub-cooled Regime; the other three occur under saturated inlet flow conditions and are referred to as the Low-quality, Medium-quality, and High-quality Regimes.

**Sub-cooled Regime.** This regime is observed when the inlet flow is sub-cooled. At low input fluxes no boiling occurs. For spheres in the in-line arrangement, at a high enough input flux small bubbles of vapor form, separate from the surface and stream upwards from a few nucleation sites on the surface of the heated sphere. Further increase in the flux increases the number of nucleation sites as well as the size of the bubbles streaming from the nucleation sites. The location of the nucleation sites is quite different when adjacent spheres are also heated as in the case of the cluster arrangement. For the center sphere in the cluster arrangement, the nucleation sites seem to occur predominantly at the points of contact with adjacent heated spheres. The point of contact between two heated spheres appears to provide favorable conditions for bubble formation because of the zero thickness of the liquid film at the point of contact and the heating

of the relatively thin film from both sides. Increasing the heat flux seems to increase the size of the bubbles streaming from the nucleation sites.

**Saturated Flow Boiling Regimes.** In general it was observed that under saturated boiling conditions, most of the liquid in the inlet flow impacts on the spheres in the bed within a short length of the bed (i.e., a few sphere diameters). Upon coming in contact with the spheres, the liquid adheres to the surface of the spheres because of surface tension. When sufficient liquid is available, a film of liquid forms; and the film continues to flow down the length of the bed by flowing down the spheres along the bed. In this process, downstream spheres receive the liquid from the spheres above at the points of contact with other spheres; and the vapor tends to flow through the voids between the spheres. In addition to the above general observation, three distinct saturated flow boiling regimes were observed. The occurrence of the flow regimes was seen to depend on the quality of the working fluid and the heat flux at the surface of the spheres. The flow boiling regimes are, in general, unsteady but appear to be approximately periodic. The flow pattern occurring in a roughly time-averaged sense corresponding to each regime is discussed below.

1. Low-quality Regime is observed at qualities between 0 and 10 to 20%. The surface of the heated sphere is completely covered with a blanket of liquid, as most of the liquid-vapor flow is composed of liquid at lower values of quality. The film thickness decreases with increasing quality of the working fluid. The liquid tends to wrap around the spheres as it makes its way down the vertical packed bed. At higher values of quality, the film thickness becomes sufficiently small; and the film breaks into streams of liquid flowing down the sphere. The path of the stream meanders down the surface of the sphere in a periodic manner. This regime is thus one of either liquid-film flow over the spheres at low qualities or of one having streams of meandering liquid flowing down the spheres at higher qualities. The flow pattern is essentially the same for in-line and the cluster arrangements of smooth spheres. For rough spheres, the break up of the liquid film into discrete streams is not observed. The heat transfer coefficient, $h_{2P}$, increases rapidly with quality in this regime, primarily as a consequence of decreasing film thickness, and reaches a maximum at a quality of about 10 to 20%. Further increases of quality results in the next regime.

2. The Medium-quality Regime starts at qualities as low as 10 to 20% and extends up to a quality of about 80 to 90%. This regime begins when the unwetted area (i.e., dry patches) on the sphere expands and contracts periodically. As the quality or the heat flux is increased, yet another periodic process occurs. In this process, the liquid film momentarily blankets the sphere surface then is followed by a complete vaporization of the liquid. This alternate wetting and drying of the heated sphere surface is observed to increase with increasing quality. As an example, for 1.59 cm smooth spheres in the in-line arrangement, the average frequency is about 40 cycles per minute at $x = 20\%$ and 60 cycles per minute at $x = 80\%$. The increase of heat flux to the heated spheres also increases the frequency of drying. The heat transfer coefficient, $h_{2P}$, practically remains constant in this regime. At the higher qualities, the entire surface of the heated sphere seems to dry up. When the amount of liquid available is insufficient to wet the entire surface, the High-quality Regime takes place.

3. The High-quality Regime occurs when the quality of the working fluid is high (80-90% or higher). There is little liquid coming in contact with the surface of the heated spheres. The surface of the heated sphere is dry most of the time, and an occasional drop of liquid R-113 impinges on the surface and evaporates almost immediately. The heat transfer coefficient, $h_{2P}$, decreases rapidly with quality in this regime.

The flow regimes described above are better defined for smooth spheres in the in-line as well as the cluster arrangement and less so for rough spheres in both arrangements.

**Correlation Based on Homogeneous Model**

The ratio of the heat transfer coefficient under boiling conditions, $h_{2P}$, to the corresponding heat transfer coefficient for the homogeneous model, $h_H$, is correlated with the dimensionless surface superheat $\Delta T^*$, the dimensionless heat flux to the instrumented spheres $q^*$, the liquid Reynolds number $Re_L$, and the inlet quality to the packed bed x. The heat transfer coefficient for the homogeneous model, $h_H$, is determined from the single-phase flow correlation of Baumeister and Bennett [14] as given by:

$$\frac{h_H D_P}{k_H} = 1.58\left(Re_H\right)^{0.60}\left(Pr_H\right)^{0.33} \qquad (2)$$

$$where \;\; Re_H = \frac{\rho_H V_s D_P}{\mu_H}, \;\; and \;\; Pr_H = \frac{c_{pH}\mu_H}{k_H}$$

The properties in the above equation are calculated using the homogeneous thermophysical properties of the flowing two-phase fluid as given by the following relations:

$$\begin{aligned} \rho_H &= x\rho_v + (1-x)\rho_L \\ \mu_H &= x\mu_v + (1-x)\mu_L \\ k_H &= xk_v + (1-x)k_L \\ c_{pH} &= xc_{pv} + (1-x)c_{pL} \\ V_s &= \frac{m}{\rho_H A_t} \end{aligned} \qquad (3)$$

The properties are evaluated at saturation temperature of the fluid, and m is the actual (experimental) mass flow rate. It was hoped that the homogeneous model would take into account all of the influence of (1) the quality via the use of homogeneous properties and (2) the mass flow rate and particle diameter via the Reynolds number $Re_H$. The results, however, indicate otherwise.

The correlation of the present results for the boiling heat transfer coefficients from spheres in packed beds is given below in dimensionless form:

$$\frac{h_{2P}}{h_H} = 0.2712 \quad \Delta T^{*-1.132} \quad q^{*1.103} \quad Re_L{}^{-0.604} \quad x^{0.175} \qquad (4a)$$

In physical variables, the correlation may also be written as:

$$\frac{h_{2P}}{h_H} = 0.2712 \left(\frac{(T_w - T_{sat})c_{pL}}{H_{Lv}}\right)^{-1.132} \left(\frac{qc_{pL}D_P}{k_L H_{Lv}}\right)^{1.103} \left(\frac{mD_P}{A_t\mu_L}\right)^{-0.604} x^{0.175} \qquad (4b)$$

The applicable range of the physical variables are:

$$0.40\ (\frac{Watts}{cm^2}) \leq \quad q \quad \leq 1.5\ (\frac{Watts}{cm^2})$$

$$0.50\ (°C) \quad \leq (T_w - T_{sat}) \leq \quad 50\ (°C)$$

$$1.7\ (\frac{Kg}{min}) \quad \leq \quad m \quad \leq \quad 5.6\ (\frac{kg}{min})$$

$$0.02 \quad \leq \quad x \quad \leq \quad 1.00$$

This correlation has an average absolute error of 12% in predicting $h_{2p}$, and the correlation coefficient is 0.978. In Figure 13 the correlation, Equation (4), is compared with the experimental results for the bed of 1.59 cm spheres, showing the variation of the heat transfer coefficient from spheres in a packed bed with the dimensionless temperature difference, $\Delta T^*$, as the independent variable. In Figures 14, similar comparison is made with the results for the bed of 2.54 cm spheres. Finally, in Figure 15 similar comparison is made with the results for these two beds. Figure 15 thus represents the composite of all the results for the cluster arrangement. The present correlation shows that the boiling heat transfer coefficient increases with increasing quality and decreases with increasing surface superheat. From Figures 13 to 15 it can be concluded that Equation (4) correlates very effectively with the dimensionless temperature difference. It can be seen from these figures that the results for smooth and rough spheres appear not to have any clearly distinctive trends. Therefore, it can be concluded that the surface roughness was not a significant parameter for the determination of $h_{2p}$ within the range of parameters used in this study. This conclusion is given further justification by the flow patterns observed. The above correlation may be used in the development of a numerical model to simulate the transient thermal performance of packed beds when the surface superheat, inlet quality to the bed, mass flow rate, and the total surface area of the particles are all known.

## Conclusions

Results of extensive experimental studies of boiling heat transfer from spheres in a packed bed with downward liquid-vapor flow of R-113 are presented. Surface superheats of 1 to 50°C, mass flow rates of 1.7 to 5.6 Kg/min, sphere diameters of 1.59 and 2.54 cm, quality of inlet flow of 2 to 100%, and two surface conditions are considered. The heat transfer coefficients around the heated spheres are measured as function of the various parameters.

**Correlation**

The quantitative results of this extensive experimental study are successfully correlated. The correlation for the boiling heat transfer coefficients based on a homogeneous model is presented. The correlation may be used in the development of numerical models to simulate the transient thermal performance of packed bed thermal energy storage unit while operating as an evaporator.

**Qualitative Results**

Flow visualization results of the boiling of the liquid-vapor flow around the spheres in the packed bed indicated the following:

Under sub-cooled inlet conditions the number of nucleation sites around the heated spheres when surrounded by unheated spheres increases with increasing heat flux and decreasing degree of subcooling. When adjacent spheres are also heated, the nucleation sites are mostly confined to the points of contact between the spheres.

Under saturated boiling conditions, in general, it was observed that the liquid flowing down the bed adheres to the surfaces of the spheres because of surface tension; and the vapor tends to flow through the voids between the spheres. Additionally, three distinct saturated flow boiling regimes are identified.

1. In the Low-quality Regime, the surface of the heated sphere is completely covered with a blanket of liquid. The film thickness decreases with increasing quality. At higher values of quality, the film breaks into streams of liquid flowing down the sphere. The path of the stream meanders down the surface of the sphere in a periodic manner. The pattern is essentially the same for in-line and the cluster arrangements of smooth spheres. For rough spheres the break up of the liquid film into discrete streams is not observed. The heat transfer coefficient, $h_{2P}$, increases rapidly with quality in this regime and reaches a maximum at a quality of about 10 to 20%.

2. In the Medium-quality Regime, the dry patch area on the sphere expands and contracts periodically. As the quality or the heat flux is increased, yet another periodic process occurs. In this process the liquid film momentarily blankets the sphere surface then is followed by a complete vaporization of the liquid. This alternate wetting and drying of the heated sphere surface is observed to increase with increasing quality. The increase of heat flux to the heated spheres also increases the frequency of drying. At the higher qualities, the entire surface of the heated sphere seems to dry up. The heat transfer coefficient, $h_{2P}$, practically remains constant in this regime.

3. In the High-quality Regime, there is little liquid coming in contact with the surface of the heated spheres. The surface is dry most of the time, and an occasional drop of liquid falls on the surface and evaporates almost immediately. The heat transfer coefficient, $h_{2P}$, decreases rapidly with quality in this regime.

The flow regimes described above are better defined for smooth spheres in the in-line as well as the cluster arrangement and less so for rough spheres in both arrangements.

## Acknowledgments

This study was conducted under Martin Marietta Subcontract No. 7685PA-Y21, funded by the U.S. DOE through the ORNL. The authors acknowledge the help of the project technical monitors, Mr. M. J. Taylor and Mr. J. J. Tomlinson, in arranging the loan of the fiber-optic baroscope from ORNL used in this study.

# Nomenclature

| | |
|---|---|
| $A_t$ | Cross-sectional area of bed $= \pi D_t^2/4$ |
| $c_p$ | Specific heat at constant pressure |
| $D_P$ | Sphere diameter |
| $D_t$ | Inside diameter of bed |
| $h$ | Heat transfer coefficient |
| $H$ | Specific enthalpy |
| $H_{Lv}$ | Latent heat of vaporization |
| $k$ | Thermal conductivity |
| $m$ | Mass flow rate |
| $q$ | Heat flux |
| $q^*$ | Dimensionless heat flux $= \frac{qD_p^2}{mH_{Lv}}$ |
| $Re$ | Reynolds Number based on particle diameter |
| $V_s$ | Superficial velocity in packed bed $= m/A_t$ |
| $x$ | Quality = (mass of vapor)/(total mass of liquid and vapor) |
| $\Delta T^*$ | Dimensionless temperature difference $= \frac{(T_w - T_{sat})c_{pL}}{H_{Lv}}$ |

## Greek Symbols

| | |
|---|---|
| $\rho$ | Density |
| $\mu$ | Dynamic viscosity |

## Subscripts

| | |
|---|---|
| $2P$ | Two-phase (boiling) fluid |
| $H$ | Homogeneous model |
| $L$ | Saturated liquid |
| $v$ | Saturated vapor |
| $sat$ | Saturation conditions |
| $w$ | Condition at the surface of the sphere |

## References


1. Graves, A. G., 1985, "Transient Thermal Performance of a Experimental Packed Bed," M. S. Thesis, University of Tennessee, Knoxville.

2. Arimilli, R. V., and Graves, A. G., 1984, "Single-Phase Liquid Flow Through a Packed Bed of PCM," Proc. Intersociety Conversion Engineering Conference, San Francisco, Vol. 2, pp 195-1200.

3. Witte, L. C., 1968, "Film Boiling From a Sphere," I. & E. C. Fundamentals, Vol. 7, pp 517-518.

4. Bromley, L. A., LeRoy, N. R., and Roberts, J. A., 1953, "Heat Transfer in Forced Convection Film Boiling," Ind. Eng. Chem., Vol. 45, pp 2639-2646.

5. Kobayasi, K., 1965, "Film Boiling Heat Transfer around a Sphere in Forced Convection," Journal of Nuclear Science and Technology, Vol. 2, pp 207-218.

6. Wilson, S. D. R., 1979, "Steady and Transient Film Boiling on a Sphere in Forced Convection," Int. Journal of Heat Mass Transfer, Vol. 2, No. 2, pp 207-218.

7. Dhir, V. K., and Purohit. G. P., 1978, "Subcooled Film-Boiling Heat Transfer From Spheres," Nuclear Engineering and Design, Vol. 47, pp 49-66.

8. Veres, D. R., and Florschuetz, L. W., 1971, "A Comparison of Transient and Steady State Pool-Boiling Data Obtained Using the Same Heating Surface," Journal of Heat Transfer, Vol. 93, No. 2, pp 229-232.

9. Shoji, M., Witte, L. C., and Sankaran, S., 1988, "The Effect of Liquid Subcooling and Surface Roughness on Film/Transition Boiling," Proceedings of the 1988 National Heat Transfer Conference, ASME HTD-96, Vol. 2, pp 667-673.

10. Orozco, J., Stellman, R., and Gutjahr, M., 1987, "Study of Film Boiling Heat Transfer from a Sphere a Horizontal Cylinder Embedded in a Liquid Saturated Porous Medium," Solar Energy Technology, ASME Sed-V. 4, pp 5-13.

11. Tsung, V. X., Dhir, V. K., and Singh, S., 1985, "Experimental Study of Boiling Heat Transfer from a Sphere Embedded in Liquid Saturated Porous Media," Heat Transfer in Porous Media and Particulate Flow, ASME HTD-Vol. 46, pp 127-134.

12. Orozco, J., Poulikakos, D., and Gutjahr, M., 1988, "Flow Film Boiling from a Sphere and a Horizontal Cylinder Embedded in Porous Medium," J. Thermophysics, Vol. 2, No. 4, pp 359-364.

13. Incropera, F. P., and DeWitt, D. P., 1985, Fundamentals of Heat and Mass Transfer, Second Edition, Wiley, New York.

14. Baumeister, E. B., and Bennett, C. O., 1958, "Fluid-Particle Heat in Packed Beds," AIChE Journal, Vol.4, No.1, pp. 69-74.

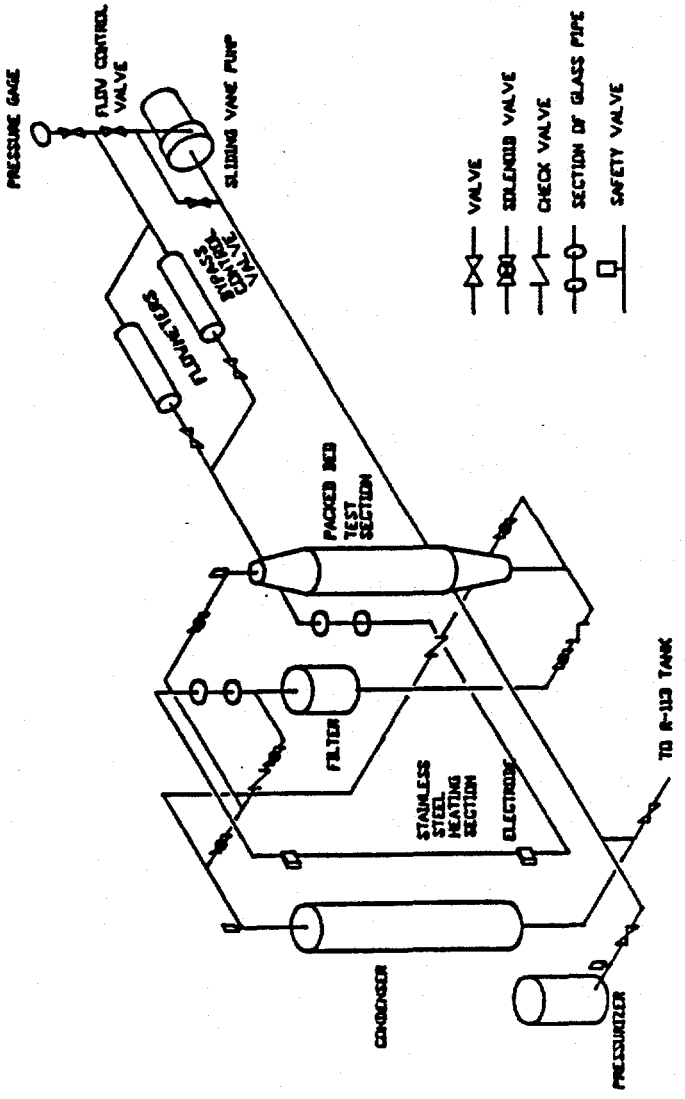


Figure 1. Schematic layout of test facility.

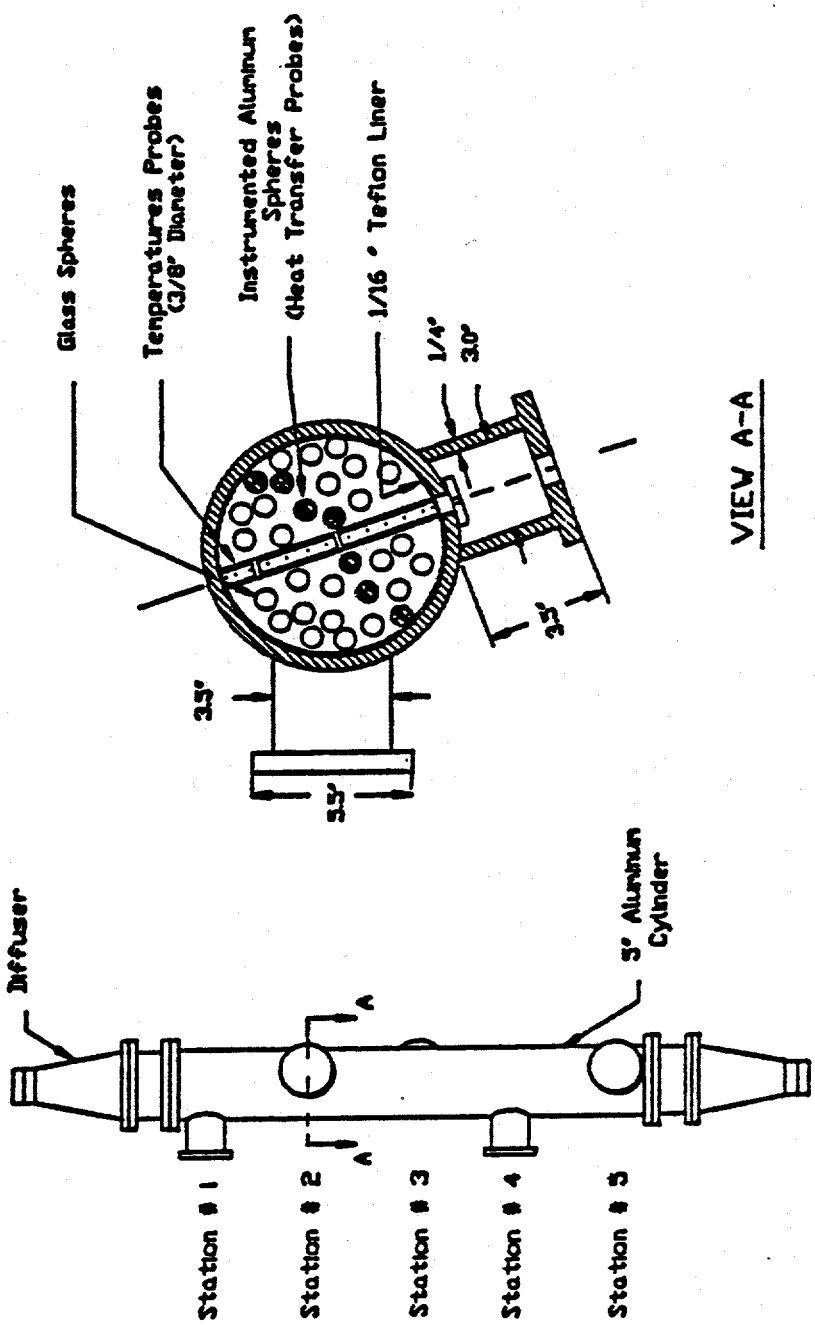


Figure 2. Vertical packed bed test section and probes.

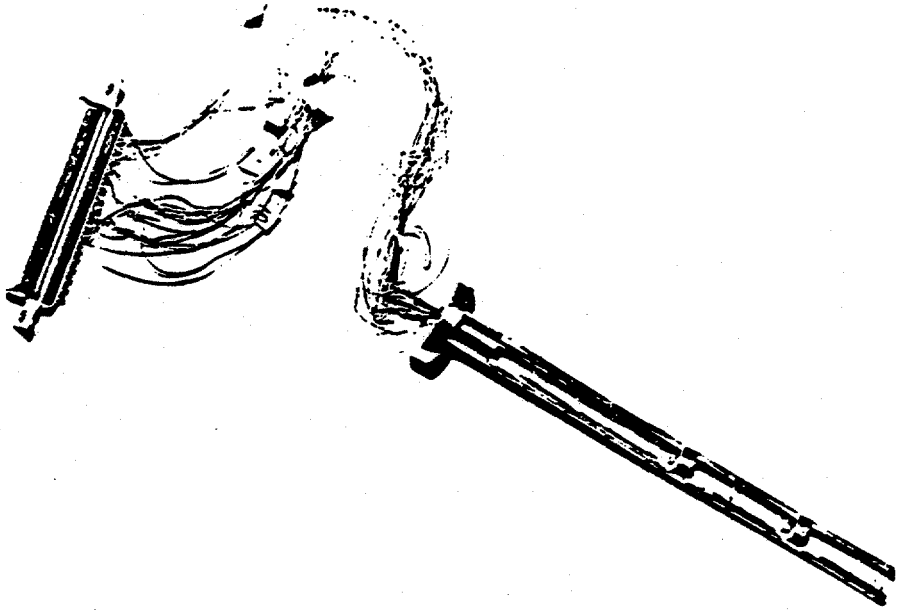

(a) Temperature probe

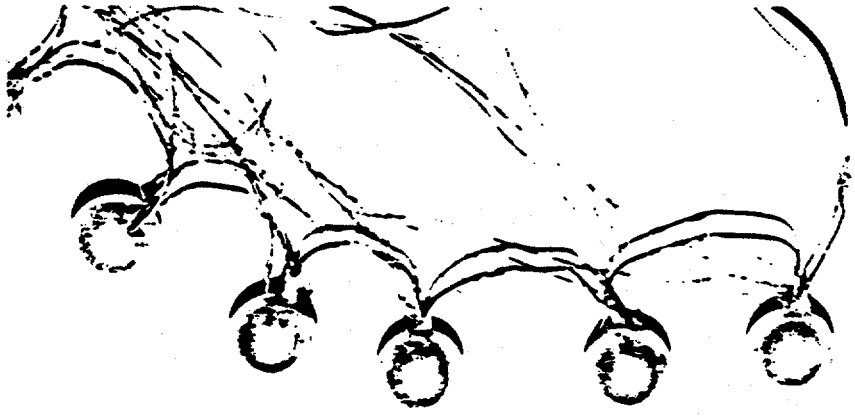

(b) Instrumented aluminum spheres

Figure 3. Thermometry system.

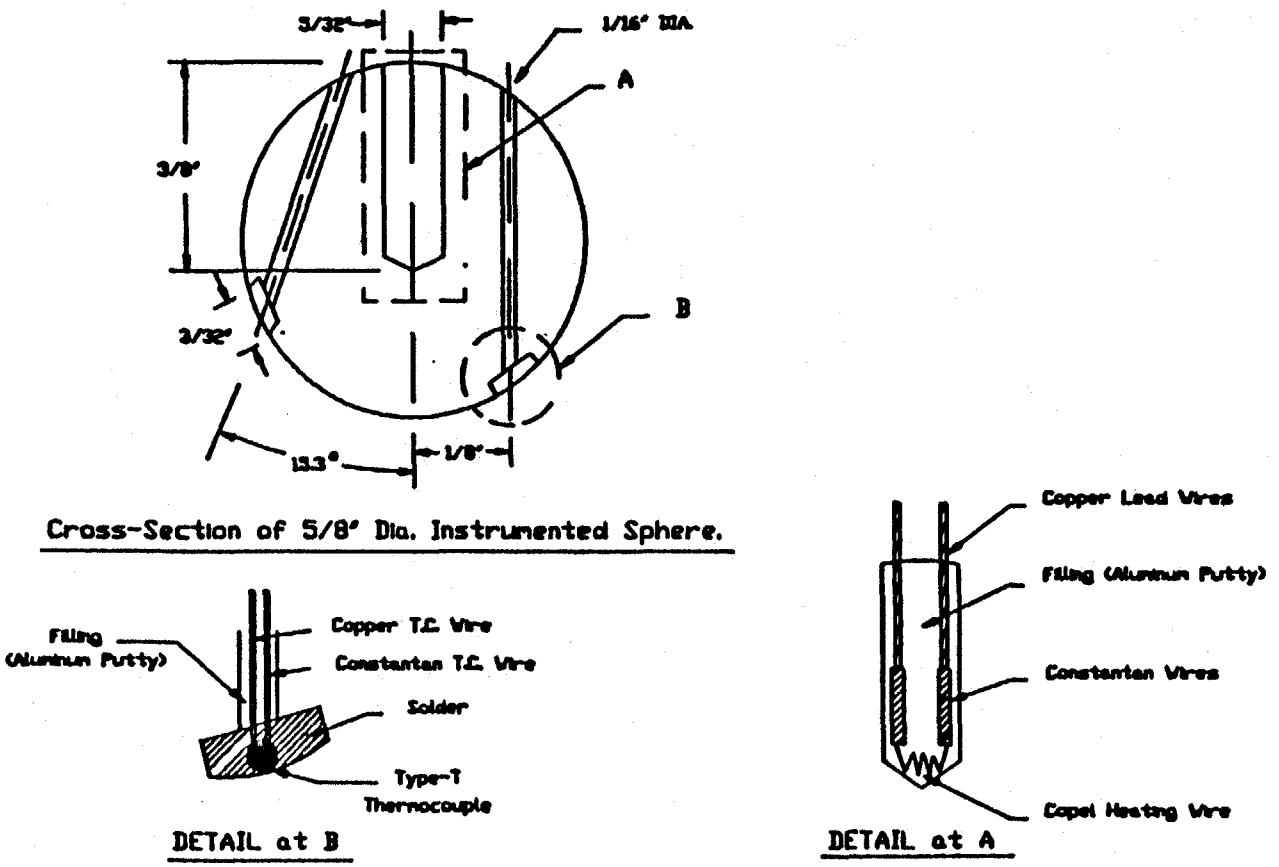


Figure 4. Heat transfer probe and details.

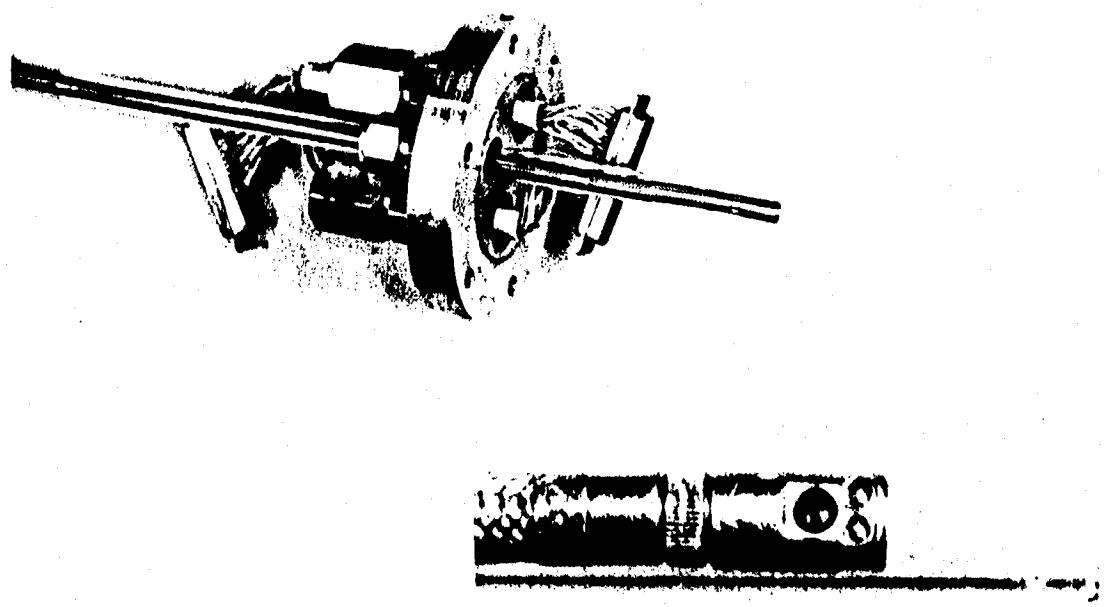

Figure 5. Photographs of visualization tube assembly and the fiberscope tip.

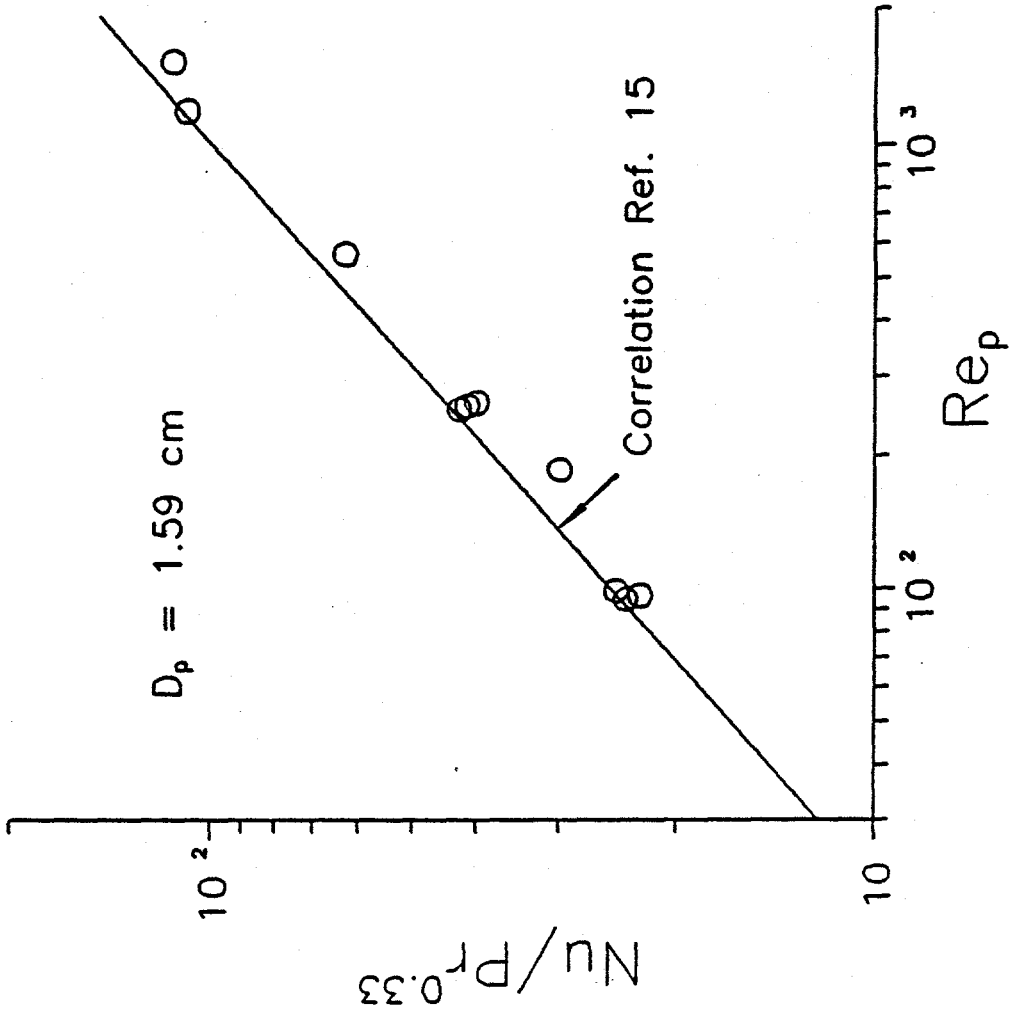


**Figure 6. Forced convection validation of heat transfer measurement system; 1.59 cm instrumented spheres in packed bed with liquid R-113 flow.**

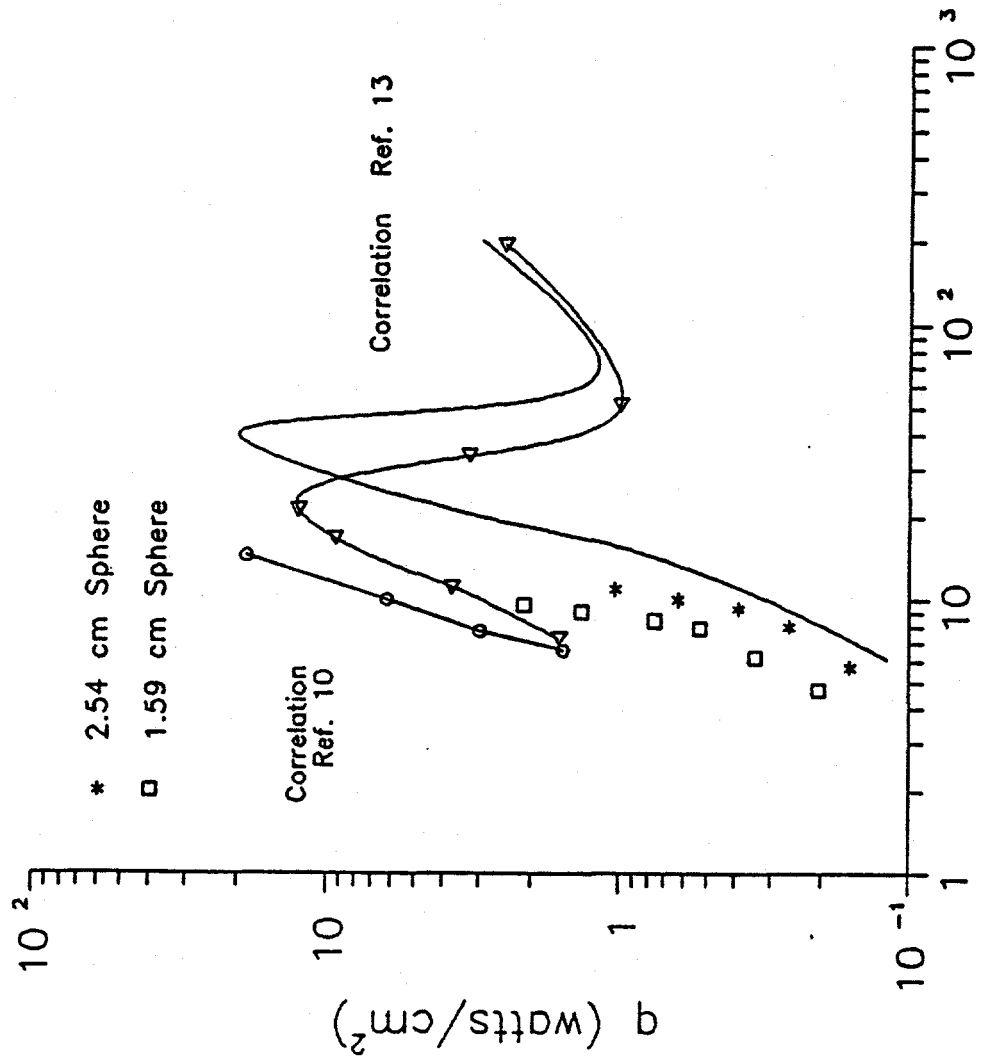


Figure 7. Pool boiling validation of heat transfer measurement system; 1.59 cm and 2.54 cm instrumented spheres in saturated liquid R-113.

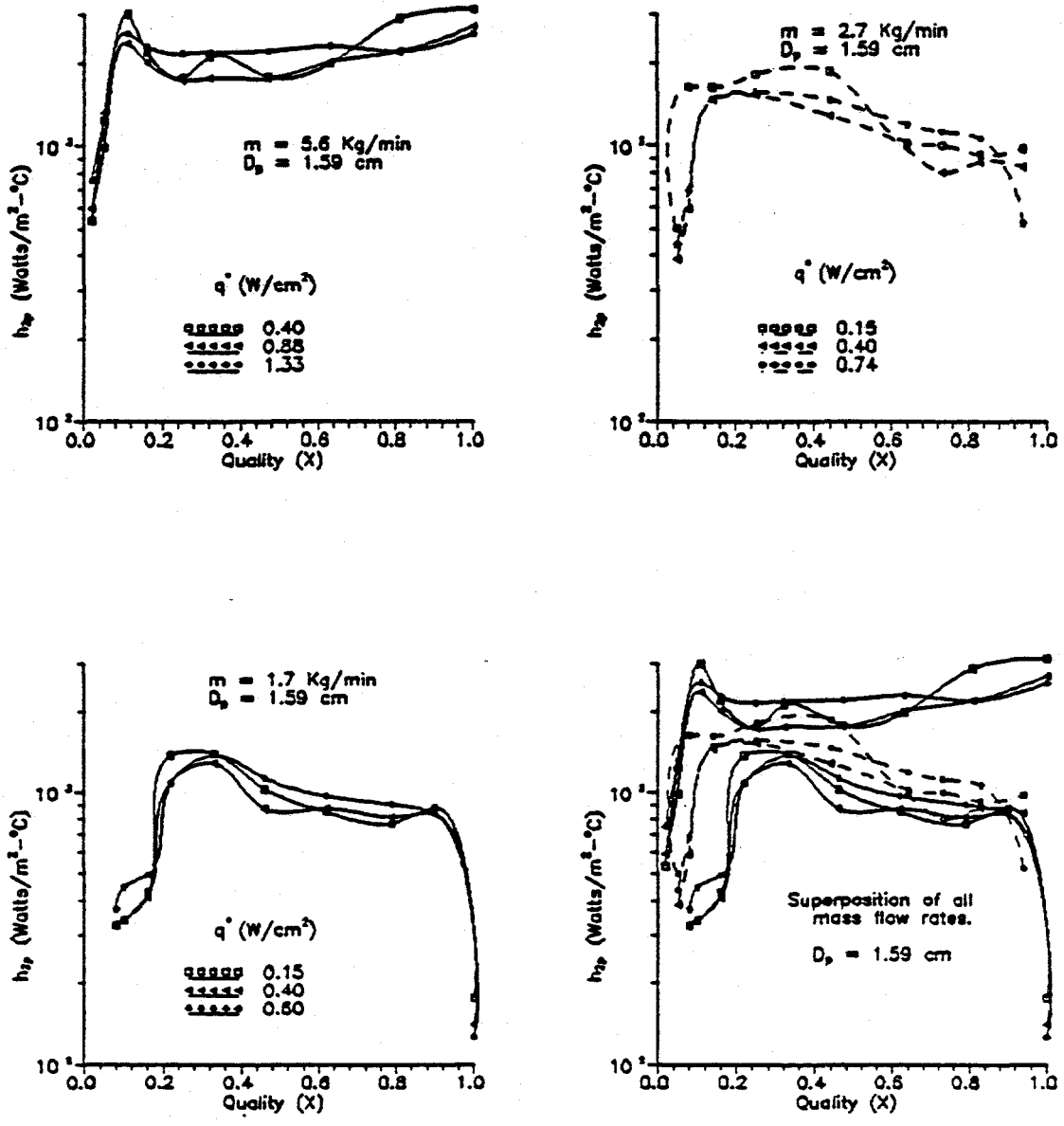


Figure 8. Influence of quality, heat flux, and mass flow rate on boiling heat transfer from center sphere in cluster; smooth 1.59 cm spheres in packed bed.

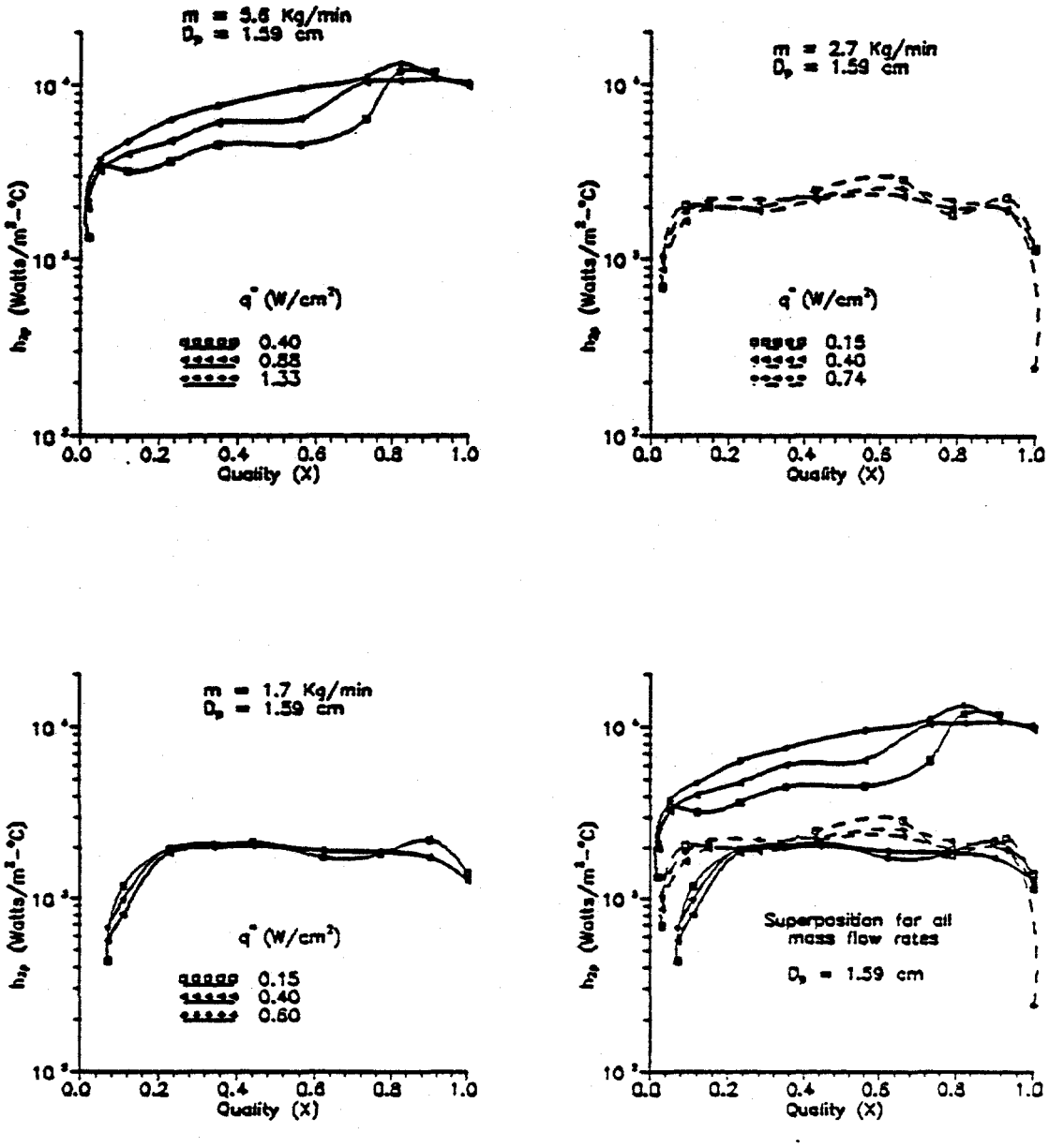


Figure 9. Influence of quality, heat flux, and mass flow rate on boiling heat transfer from center sphere in cluster; rough 1.59 cm spheres in packed bed.

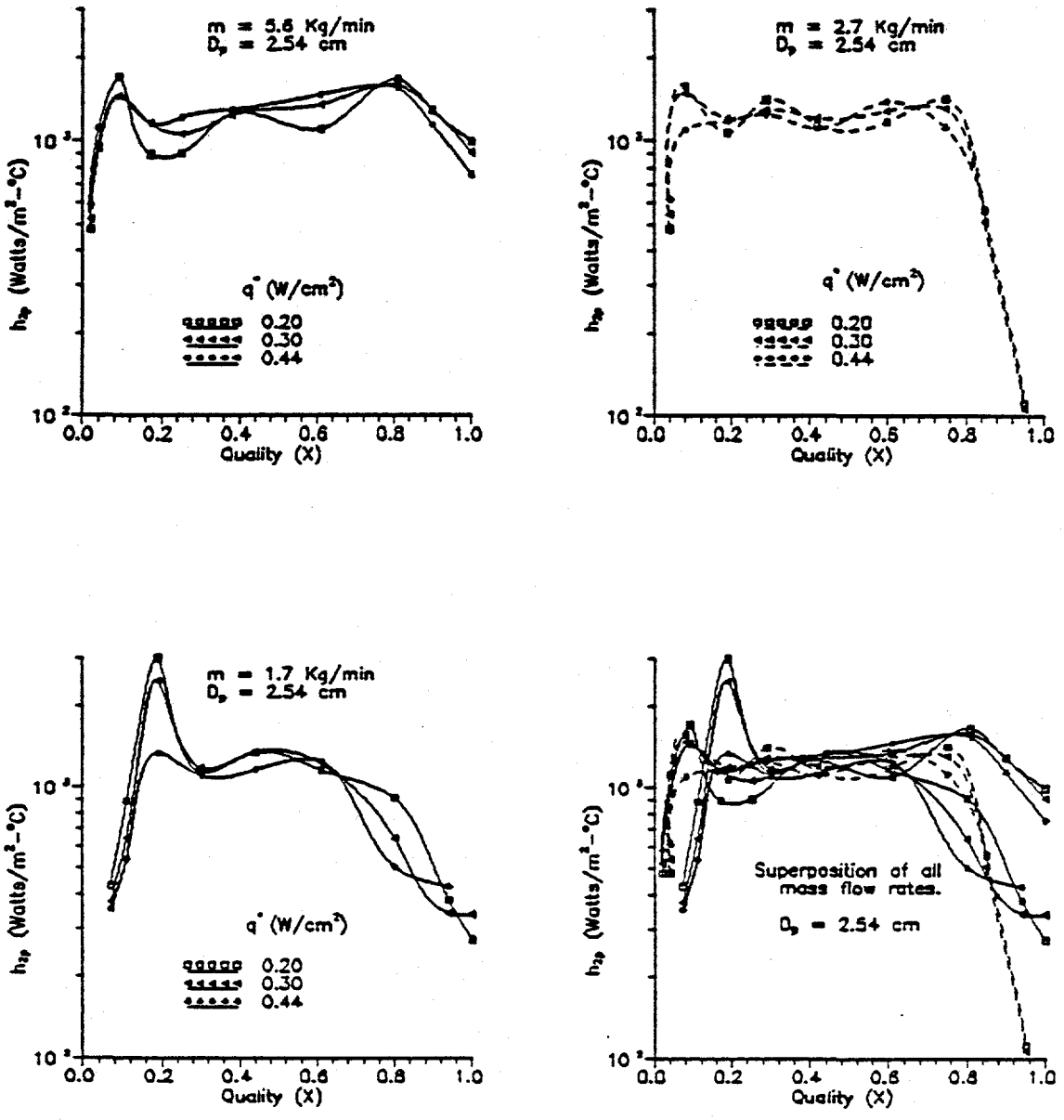


Figure 10. Influence of quality, heat flux, and mass flow rate on boiling heat transfer from center sphere in cluster; smooth 2.54 cm spheres in packed bed.

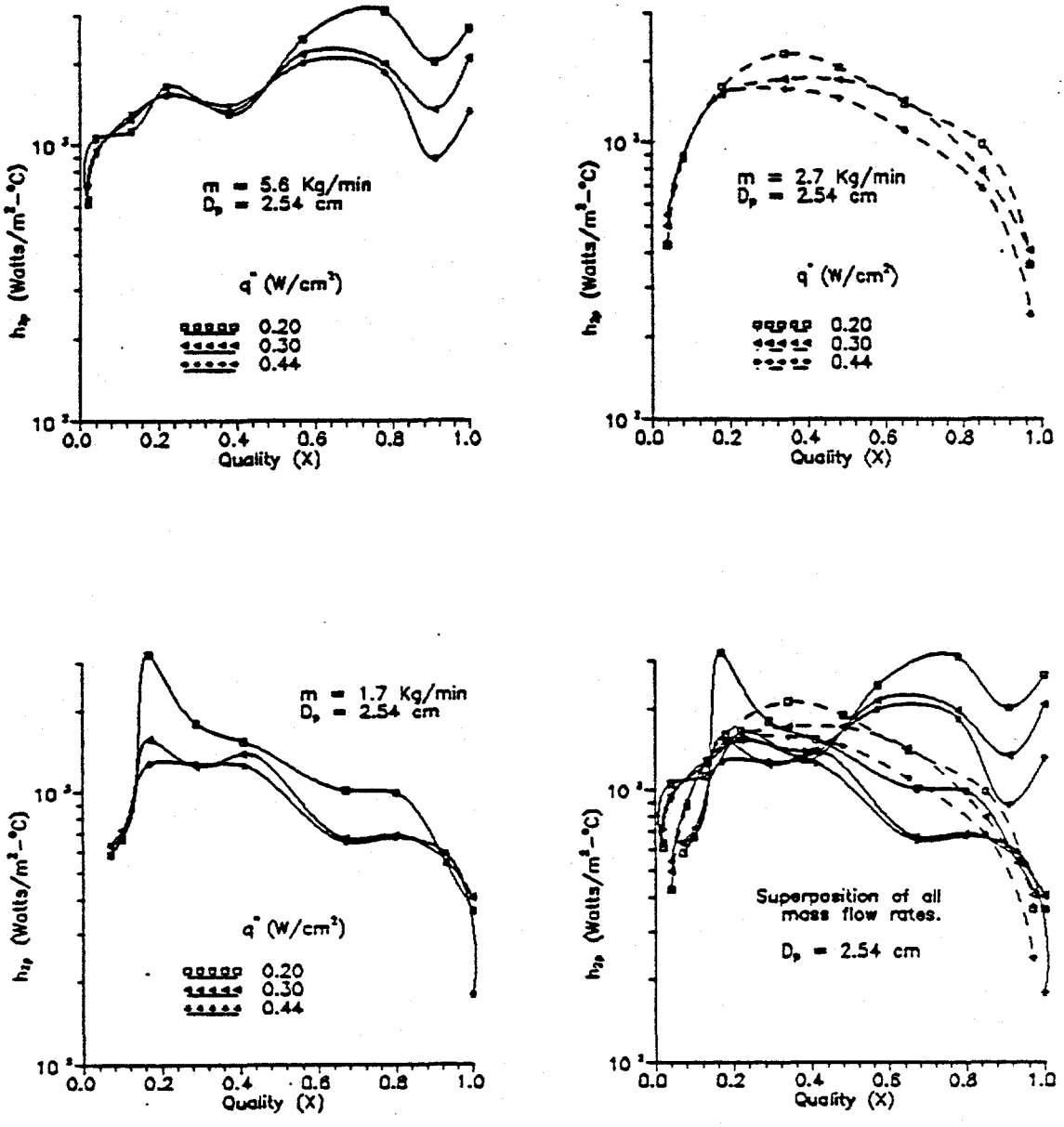


Figure 11. Influence of quality, heat flux, and mass flow rate on boiling heat transfer from center sphere in cluster; rough 2.54 cm spheres in packed bed.

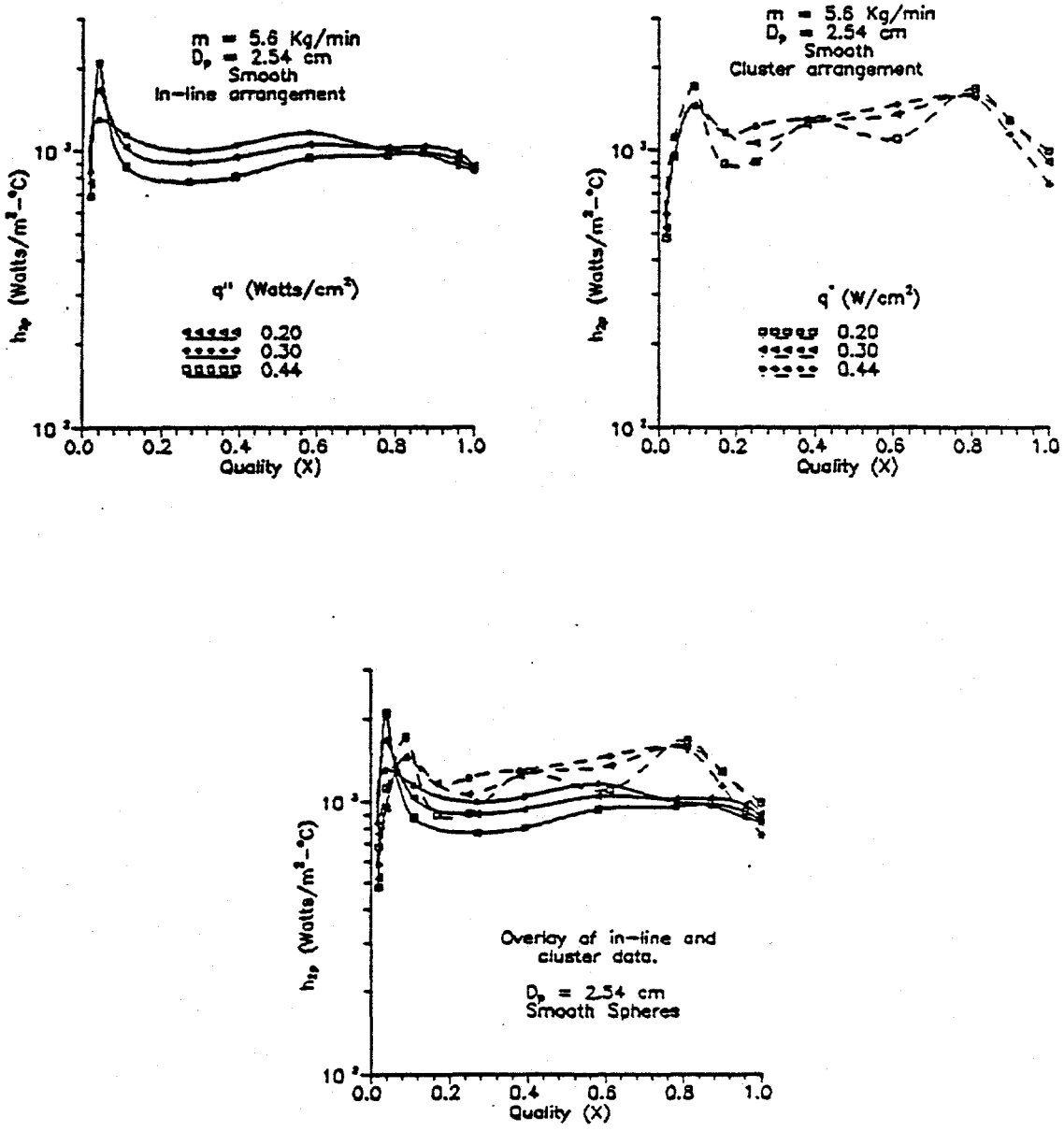


Figure 12. Influence of sphere arrangement, quality, and heat flux on boiling heat transfer; smooth 2.54 cm spheres in packed bed.

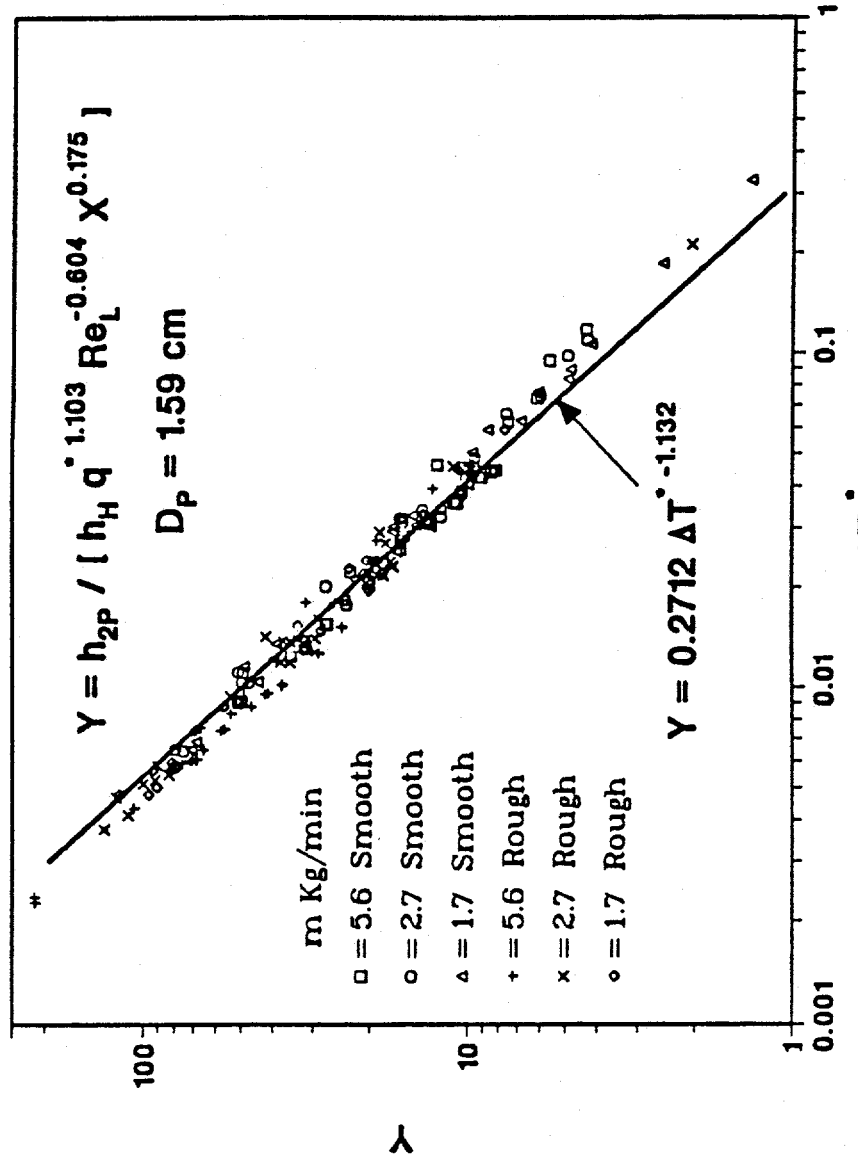


Figure 13. Variation of boiling results with ΔT* and comparison with present correlation; 1.59 cm spheres in cluster.

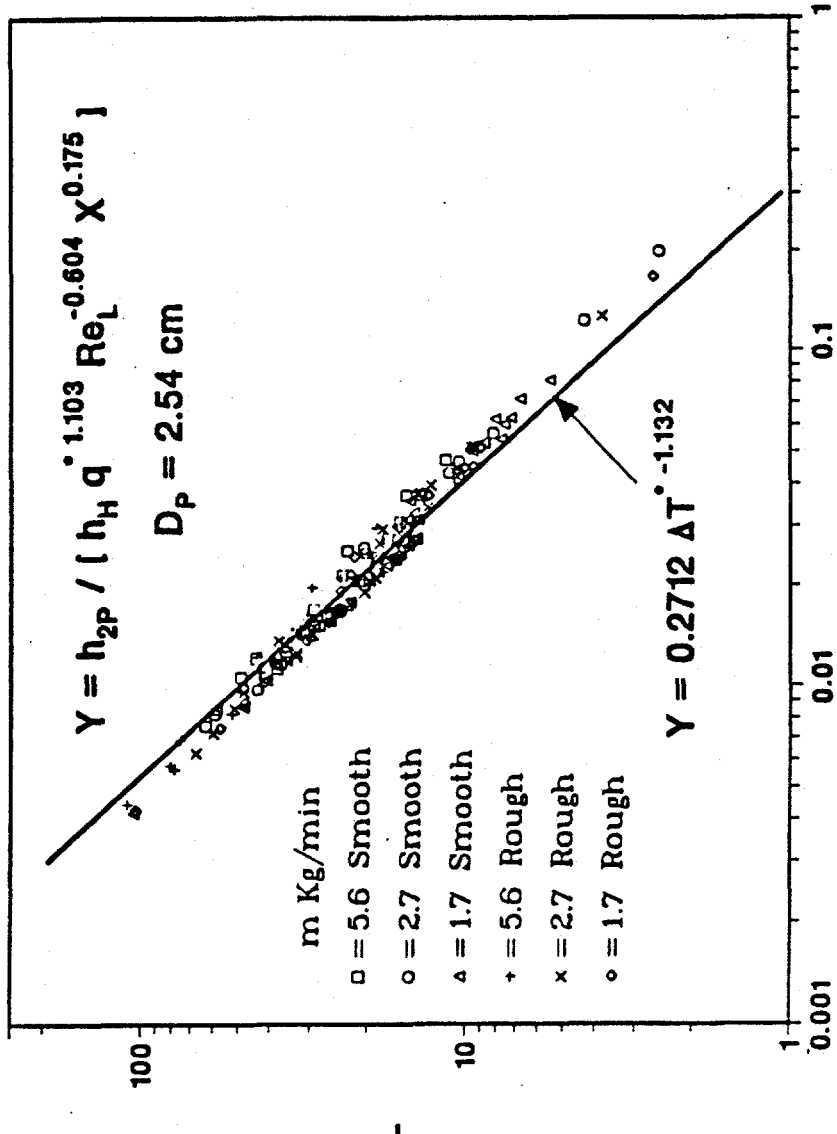


Figure 14. Variation of boiling results with ΔT* and comparison with present correlation; 2.54 cm spheres in cluster.

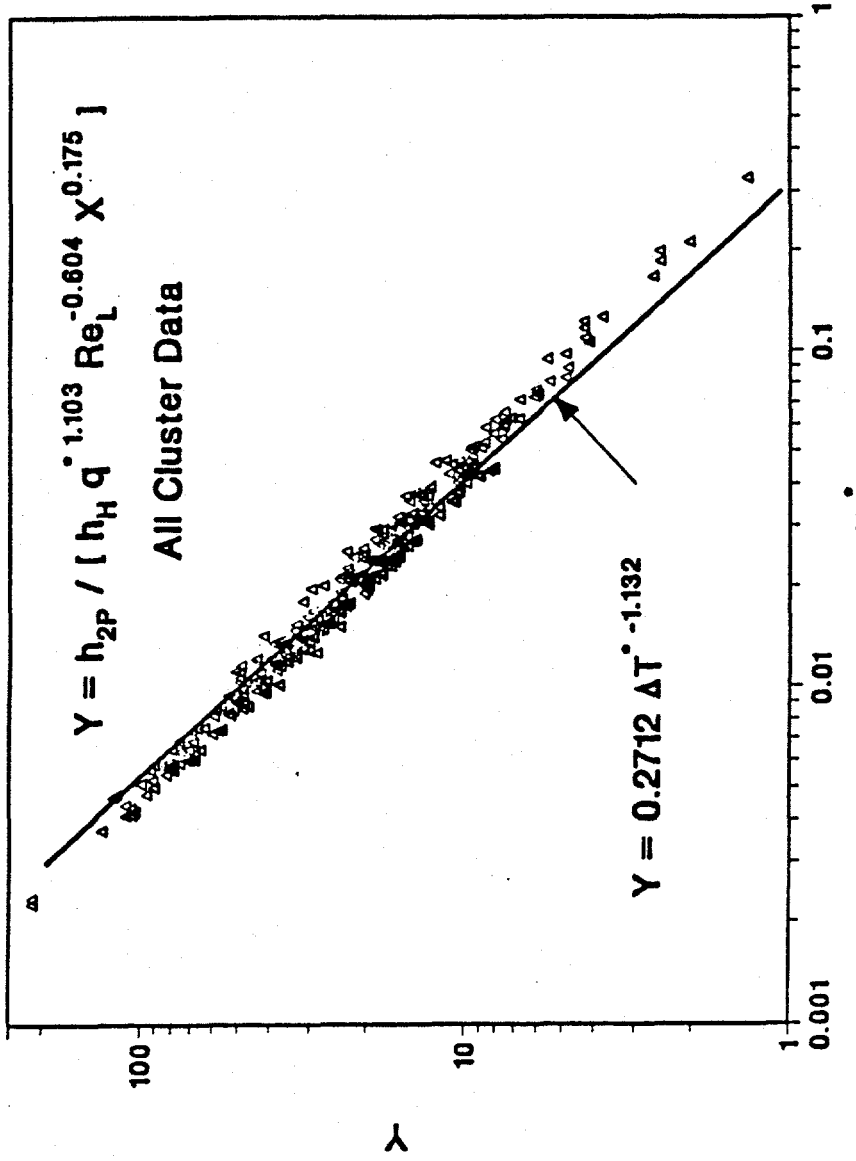


Figure 15. Variation of boiling results with $\Delta T^*$ and comparison with present correlation; all instrumented spheres.

# EFFECT OF DOPANTS ON CRYSTAL STRUCTURE AND THERMAL PROPERTIES OF PENTAGLYCERINE

**Dhanesh Chandra* and Wei Ding****
Department Of Chemical and Metallurgical Engineering
University Of Nevada-Reno
Reno, Nevada 89557

## *Abstract*

*The overall objective of this research program is to develop practical solid-state thermal energy storage materials. Research is focused on polyalcohol "Plastic Crystals" which undergo crystallographic changes at constant transition temperature absorbing or releasing large amounts of latent heat. The known pure polyalcohols have high transition temperatures; therefore, adjustment of transformation temperature is important to develop practical materials. The approach taken is to introduce substitutional and interstitial dopants so as to strain the lattice of the host crystal which results in lowering the transition temperature.*

*Current research is on temperature adjustment of pentaglycerine [PG] ($C_5H_{12}O_3$) initiated approximately four months ago. Results, so far, show that the substitutional dopants are more effective in reducing the transition temperature than interstitial dopants. The results in the first phase of this program show that the transition temperature of PG reduced significantly by using trimethylol propane [TMP] ($C_6H_{14}O_3$), 2-amino 2-methyl 1,3 propanediol [AMPL]($C_4H_{11}NO_2$) as dopants. It appears that some of these doped samples have near room temperature transitions; however, these results are not conclusive at this time. Recently, it was discovered that TMP has an additional solid-solid phase transformation, slightly below room temperature.*

*Crystal structure analyses showed some surprising results with regards to thermal expansion behavior of PG. Several sets of low as well as high temperature data were obtained from the pure and doped PG to characterize the structural changes, if any, and the thermal expansions. Research is in progress on crystal structure and thermal analyses.*

## Introduction

The overall objective of this research program is to develop solid state phase change materials for thermal energy storage. Current research involves investigations of organic polyalcohol materials which undergo solid-solid phase transformation storing large amounts of (latent) heat per unit mass at a constant transition temperature ($T_t$) well below their melting points. At this constant $T_t$ the energy is stored in the high temperature phase. The transition temperature of the known organic polyalcohols ($T_t$) is high and is not suitable for energy storage purposes; therefore, adjustment of the transition temperature to near room temperature is important.

---

* **Associate Professor**
** **Graduate Research Assistant**

These polyalcohols are also be referred to as "Plastic Crystals" implying plastically deformable behavior of the high temperature phase in which the energy is stored. There are four known important polyalcohols: pentaerythritol [PE] ($C_5H_{15}O_4$), pentaglycerine [PG] ($C_5H_{12}O_3$), neopentylglycol [NPG] ($C_5H_{12}O_2$), and neopentylalcohol ($C_5H_{12}O$). The first three are potential candidates and model materials for thermal energy storage. A few other related pure organic compounds, such as trimethylol propane [TMP] ($C_6H_{14}O_3$) and 2-amino 2-methyl 1,3 propanediol [AMPL] ($C_4H_{14}NO_2$), are of significance and are used as substitutional dopants.

Thermal applications of polyalcohols were first investigated by Murrill and Breed (1), in 1969 (under NASA contract) in order to evaluate the feasibility of passive temperature control of satellites. Because of the remarkable potential of solid-solid thermal energy storage in these polyalcohols, investigations were initiated for passive thermal energy storage in solar buildings by Benson et al.(2), under auspices of the DOE . They conducted thermal analyses and showed significant changes in the transition temperature by mixing PE/PG, PE/NPG, and PG/NPG to form solid-solutions. At that time, the details of the crystal structure were not known; and the thermal analyses by differential scanning calorimetry yielded broad peaks (endotherms) or multiple peaks for certain samples. This broadening of peaks was explained later by Chandra (3) and Chandra et al.(4) via crystal structure and phase diagram studies. The isomorphous replacement of the molecules by similar tetrahedral ones to form solid-solutions can substantially reduce the transitional enthalpy due to differences in the number of OH available for bonding between molecules. Chandra and Barrett (5) proposed the concept of use of non-tetrahedral type molecules as intersititial dopants in these polyalcohols. They reported significant decreases in the transition temperature of neopentylglycol [NPG] to near room temperature by the use of interstitial as well as substitutional dopants by taking into account the H-bonding sites for the dopants via crystal structure and thermal studies. In addition, drastic decreases in transition temperature in pentaerythritol [PE]( decreases up to 148°C ) with acceptable heats of solid-solid transition were reported with addition of dopants.

The designation of high temperature phase as "phase I" and the low temperature phase as "phase II", which was established by previous pioneering investigators such as Timmermans (6), Aston (7), Nitta (8) and others, has been recently modified by Chandra et al.(4) to take into account presence of additional phases in the case of binary or ternary systems. We have designated the high temperature phase for pure as well as solid solutions as "$\gamma$" phase replacing "phase I" which applied to pure polyalcohols. The change in nomenclature is more important in the low temperature phases which were designated as $\alpha$ and/or $\beta$ to cover the entire region in multicomponent systems.

The understanding of the molecular arrangement in the lattice of the polyalcohols is of great significance because this reveals the orientation of molecules and the possible interstitial sites for the insertion of the dopants. In addition, the nature of solid-solid phase transitions can be revealed by the structural studies. The structure of PE was well established by Lewellyn (9) and Nitta (10), approximately 50 years ago. More recently, in 1984, Chandra, Fitzpatrick and Jorgenson (11) determined thermal expansion coefficients in the

low $\alpha$ and high temperature $\gamma$ phases. Crystallographic relationships between the $\alpha$ and $\gamma$ phases were systematically determined. Models were proposed for the tetragonal to cubic transitions in which change of the rigid to non-rigid hydrogen bonds were predicted (10)(5). The energy is stored in the $\gamma$ phase above 188°C in which H-bonding is no longer rigid, as observed in the $\alpha$ layered structure. The structure of the two other important polyalcohols NPG and PG , from the thermal energy storage point of view, were not clearly defined in the literature. Recently, Chandra and Barrett(5) found that there were discrepancies in the reported structures of NPG (12); and research was undertaken to redetermine the structure by modern instrumentations. These studies revealed bimolecular chain formation in the lattice of NPG .

In this research program, research is underway to develop temperature adjusted pentaglycerine (PG) based energy storage materials which can store large amounts of energy during solid-solid transformations. The material has lower vapor pressure than the more commonly known NPG and potentially can store a larger amount of energy in temperature adjusted materials. We are focusing our research on adjustment of the transition temperature. Proper selection of sites of a dopant will involve detailed structural analyses. Eilerman et.al.(14) were the first ones to determine the structure of PG. Because of the problems with crystal growth, three possible low temperature $\alpha$ phases were listed: tetragonal (BCT) with lattice parameters of a=6.05Å and c=8.87Å, pseudo tetragonal with lattice parameters a=12.1Å and c=17.7Å , and finally an ordered monoclinic structure a=10Å, b=6.05 Å, c=8.87Å and B=124.3°. This is posing problems in indexing of the powder X-ray diffraction patterns, because some of the low intensity peaks could not be indexed by using I(4). Details of the structure will be discussed in the next section.

## Current Results

The solid-solid transition temperature of pentaglycerine(PG) has been adjusted by the addition of interstitial and substitutional dopants. The amount of dopant used varied depending on the size of the molecule and the type of bonding group. The effect of dopant on the thermal property of PG will be discussed first, and then the crystal structure of undoped and doped PG and the associated thermal expansions during the heating of the $\alpha$ phase and subsequent transformation to the $\gamma$ phase.

**Selection of Dopants**

The PG samples were made by using Aldrich synthesized (97% purity) powders. Several dopants of the interstitial and substitutional type were investigated. Trimethylol propane (TMP), 2-amino 2-methyl propanediol (AMPL) and PE were the primary substitutional tetrahedral type dopants used. In the case of TMP doped PG, solid solutions were made with 5%, 10%, 20%, 30%,40%, 50%, 60%, 70% and 80% TMP. Compositions ranging from 5% to 50% AMPL in PG were used for the experiments. Other dopants such as stearates with different molecular weights were also attempted which yielded approximately 30 °C transformations. The PG was also doped with interstitial dopants such as glycerol and xylitol ranging between 5% to 30%. The samples were prepared by melting the powders, mixing them in proper proportions in capped glass test tubes. Once solidification took place, these materials were melted again and poured into

shallow ceramic crucibles. These materials were then ground and used for the X-ray diffraction and thermal analyses research.

**Thermal Analyses**

Thermal analyses were first performed on a Perkin Elmer differential scanning calorimeter (DSC) using milligram range sample size. The heating rate used was 10°C/minute. Emphasis was on observing solid-solid transformations, and $\Delta H$ vs T°C plots were obtained for these transitions.

The sampling for the DSC work (4 to 10 mg) is very critical, where two phases may be present in the doped samples. Often the amount of each phase is not representative and therefore problems arise in interpretation of results. Therefore, we devised a simple bulk technique in which 6-10 grams of doped material is placed in the glass test tube with a thermocouple placed in the center of the tube. Temperature vs time output was obtained on a chart recorder; and the plots were later digitized, as shown in appendices (A) and (B). In this system, sampling errors are eliminated and a visual track can also be maintained to observe the phase changes, particularly for the solid-solid or solid-liquid type transformations. In fact, in most cases, one can distinguish between $\alpha$ and $\gamma$ phases. It has been found that these results are reproducible and can be used to check the $T_t$. The true enthalpies of the transformations are of course measured using the DSC, but rough estimations can be made by the bulk techniques also.

The thermal properties of pentaglycerine(PG) shown below suggest the lowering of the solid-solid transition temperature for use in thermal energy storage application.

| | | | Solid-Solid Transformation | |
|---|---|---|---|---|
| Name | Formula | Molecular Weight | Latent heat of Transistion | Transition Temperature |
| Pentagly-cerine | $C_5H_{12}O_3$ | 120.15 | 46 Cal/gm | 89°C |

Several substitutional dopants were used to lower the transition temperature($T_t$). The TMP and AMPL dopants were effective in reducing the transformation temperatures; while dopants, such as glycerine, xylitol and other stearates, were not effective in reducing the $T_t$. Table 1 shows a sample of the temperature adjusted polyalcohols. A solid solution series was made with PG/TMP, and DSC as well as the bulk thermal analyses methods were used to evaluate the phase transformation. The $T_t$ observed from the bulk experiment and DSC are listed . The discrepancies, in some cases, in the $T_t$ between the DSC and bulk sample data are attributed to the very small, milligram range sampling problems in the DSC analyses. The values of $T_t$ obtained from the bulk samples were reproducible. It is suspected that in some cases, perhaps in the case of phase separation, a very small amount(4 to 10 mg) of material may not have been representative. However, we are in the process of establishing new procedures to counter these effects. Table 1 shows the $\Delta H_y$ and the $T_t$ values for the doped materials. It can be seen that from the DSC's experimental results, the dopants xylitol and glycerol have limited effects on the $T_t$ of PG. While the bulk experiments

shows that TMP and AMPL can effectively reduce the $T_t$ of PG to room temperature, with the enthalpy still higher than 30 Cal/gm. In addition, TMP and AMPL can drastically reduce the melting point of PG.

We also discovered a near room temperature solid-solid phase transformation in pure TMP which was not reported earlier by the investigators. When pure TMP is cooled from a melt temperature of approximately 56°C down to 26°C, it retains high temperature $\gamma$ phase. The estimated $T_t$ is 18°C. The TMP appears to be a translucent solid in the $\gamma$ phase, which is typical of other polyalcohols and after $\gamma \rightarrow \alpha$ transition this solid appears like white powder. X-ray diffraction analyses confirmed the crystal structure changes; however, the exact structure of the ($\alpha$ phase) TMP is not known at this time. The pattern of the high temperature $\gamma$ phase is quite different from the other polyalcohols.

It has been observed that the interstitial dopants such as glycerol and xylitol which were effective in reducing the transformation temperature of NPG do not contribute to the reduction of $T_t$ in the case of PG. The maximum decrease in temperature $\Delta T_t$ was only 5.3°C for xylitol and 2.1°C for glycerol. It appears there was very little solubility of these two in the structure of PG. The AMPL dopant was effective with a maximum decrease in $\Delta T_t$ of 67°C, which is quite interesting. In fact, the sample with PG/AMPL 70%/30% decreased the $T_t$ from 85°C to 42°C with an estimated enthalpy of 35 cal/gm via bulk experiment. The sample with PG/AMPL 50/50 did not show any solid-state phase transformation; and yet the melting points decreased, perhaps indicating that the $T_t$ may be much below the room temperature or none at all. These low temperature studies have yet to be performed for these materials.

To summarize the thermal studies aspects, the research on pentaglycerine (PG) was initiated approximately four months ago. During this period, we performed thermal studies and have shown that the solid-solid phase transformation temperature could be reduced from ~85 to ~25°C. The enthalpy of temperature adjusted materials which have a transformation temperature of 42 to 43°C have a $\Delta H_t$ in the range of 30-35 cal/gm range. However, $\Delta H_t$ of the materials which have $T_t$ near room temperature ~ 25°C has not yet been evaluated. The thermal properties of the materials which have room temperature $T_t$ will be determined once a chiller is installed on the DSC; this is not currently available. Several other selected dopants were evaluated but not reported, since the transformation temperatures did not reduce substantially.

**Structural Analyses**

The crystallographic properties of polyalcohols are of great significance in order to understand the phase transition mechanisms. In this study, we have conducted X-ray diffraction analyses on the doped materials at room temperature as well as at elevated temperatures to determine the thermal expansion coefficients. Room temperature X-ray diffraction patterns were indexed as tetragonal (BCT) structure, although some very low intensity, low angle peaks appeared in the low temperature ($\alpha$ phase) of PG. The crystal structure analyses of PG has been initiated; but we encountered a single preparation problem, details of which are discussed in the following sections.

Two different types of X-ray systems were used for the structural analyses. For routine powder diffraction work, a Bragg- Brentano Phillips vertical diffractometer coupled to a Nicolet-Siemens Microvax II computer

was used. The d-spacings were calculated, and indexing of the pattern was performed manually. A least square program (ELST) was used for the calculation of the lattice parameters. In the case of the thermal expansion experiments, a Huber-Guinier high resolution diffraction system was used. Several sets of data were recorded on one film. The d-spacings were calculated and entered into the computer for the calculation of lattice parameters at each temperature. The alignment of the sample on the focusing circle and temperature calibration is rather difficult and time consuming. Details of this techniques are described in reference (11).

Room temperature X-ray diffraction powder data on the majority of the samples which were reported in the thermal analyses section was obtained on the Phillips diffractometer. The PG/TMP doped samples series were analyzed; and it was found that the original PG structure was retained up to 60% TMP, indicating complete solubility of the PG in TMP, in spite of the fact that the structures of PG and TMP appear different. The powder pattern of ($\alpha$ phase) pure TMP yielded a complex pattern which was not listed in the JCPDS files. The X-ray diffraction patterns of the PG/AMPL series showed that there was no significant difference in the structure of PG with addition of up to 20% AMPL, and we found decreases in the $T_t$ from 85°C to 61°C in the case of PG/AMPL 80/20. Further increase in the AMPL content to 30% decreased the $T_t$ to 42°C, broadened the X-ray peaks, and lowered the intensity. Detailed examination will be conducted in near future. It appears that there was little solubility of the xylitol, which is an interstitial dopant, in the structure of PG as indicated by the presence of additional peaks of low intensity whose peak positions correspond to that of xylitol's pattern. This explains why there were very little decreases in the transition temperatures even after adding 30 mole% to the host structure of PG. Similar low solubility problems occurred in the case of glycerol doped PG samples, and the transition temperatures were not lowered significantly.

**Thermal Expansion Experiments**

When thermal energy is applied to the polyalcohols such as PE and PG, with layered structures, it is expected that there will be anisotropic expansion of the lattice due to different types of bonding in the intra- and interlayers of these materials. Undoped Aldrich PG samples were placed in a 0.5mm quartz capillary and heated in a special furnace mounted on a Huber Guinier Camera with Seeman Bohlin focusing. Although we have a computer coupled Guinier diffractometer, we chose this film technique because it takes approximately 16 to 17 hours to obtain the data from the diffractometer as compared to 30-50 minutes in the case of the camera. Also many diffraction patterns can be collected on one film to allow us to evaluate thermal expansions or structural changes dynamically. X-ray diffraction film data for undoped PG was acquired at 14 different temperatures ranging from 32°C to 109°C as labeled in the photograph of the X-ray pattern in Figure 1. The phase transformation of PG occurred as expected from the tetragonal(BCT) to cubic (FCC), at approximately 84°C, rather than 85°C; this can be attributed to the temperature gradients of approximately (2°C). The changes in the lattice parameters of PG as a function of temperature are listed in Table 2. The thermal expansions in the $\alpha$ phases were low, 0.514% at 78°C in the a-direction, just below

the transition temperature, while the expansion in the c-direction of the crystal was 0.04% at 78°C. This result was rather surprising, because one expects a rather large expansion in the c-direction because of the layering. We compared the thermal expansion results of pentaerythritol, PE, whose crystal structure and layering is similar to that of PG from previous work [Chandra et al.(11)] and found that the expansion in the c-direction were quite large in the $\alpha$ phase of PE as illustrated in Figure 2 for comparison purposes. Note that there is preferential expansion between (002 )&(110) planes [2nd&3rd line] and (112)&(200) [3rd&4th lines] in the symmetric pattern from the center of the film. One can easily see the increased thermal expansion of the (002) with the increase in temperature. Now we compare the expansion in the PG and PE in Figure 1 and note that there is very little preferential expansion between (110) & (002) planes [2nd & 3rd line] and (200)&(112) planes [3rd&4th lines] in the symmetric pattern from the center of the film. This unexpected negligible expansion in the c-direction of the PG crystals is rather unusual and suggests perhaps that there may be a possible rotation between the layers as the temperature is increased. The thermal expansions which were calculated from the X-ray data are presented in Figure 2 for PG and PE, respectively. Although the thermal expansion results have been reproduced for PG, the reasons for very low expansion in the c-direction remain unresolved at this time. It can be noted that there is a very broad peak at low angles which disappears when the temperature is increased to above transformation temperature; we are concerned with whether the structure is truly BCT in the a phase. It is recommended that the structure of PG be re-evaluated.

In the $\gamma$ phase, one can see the characteristic (111) [1st line] and (200) [2nd line]of the FCC plastic phase in which the energy is stored. The reason for the absence or broadening of the peaks of the other reflections is not clear; perhaps, there is a synchronous molecular rotation of C-O bond around the C-C bonds of the PG molecules. In the $\gamma$ phase, the structure becomes isotropic with a sudden increase in thermal expansion of 4.2% from the $\alpha \rightarrow \gamma$ phase transformation. Thermal expansions in the doped PG/TMP (50%/50%), (40%/60%) samples have also been evaluated which show similar results as for the pure PG; but there were some sharp extra but low intensity lines in the $\alpha$ phase of these doped materials. The $\gamma$ phase structure becomes isotropic similar to that of pure PG with a sudden increase in thermal expansion of 5.4% from the $\alpha \rightarrow \gamma$ phase transformation. The thermal expansions in the $\gamma$ phase of the doped samples are slightly lower than those obtained for the pure PG. We plan to evaluate these high temperature X-ray diffraction patterns in detail once the structure of pure PG is well established.

**Molecular Arrangement in Pentaglycerine**

Although a body centered tetragonal structure has been assumed in this paper based on Eilerman et al (14), the molecular arrangement in PG is not clear. In an attempt to establish the arrangement of tetrahedral molecules in polyalcohol "Plastic Crystals", we may want to establish the possible molecular arrangement for the entire family of five polyalcohols; namely, neopentane (NP), neopentyl alcohol (NPA), neopentylglycol (NPG), PG, and PE with increasing number of hydrogen bonding sites. The structure of NP is not as important, because this polyalcohol crystallizes at -16.54°C. The low temperature $\alpha$ phase

structure of NPA has not been reported in the literature. The molecular arrangement in the $\alpha$ phase of PE has been well known and that of NPG has been recently reevaluated (4). Because the single crystal of PG are usually twinned, the molecular arrangement in the $\alpha$ phase structure of PG is not well established. In this research program, we have prepared a few batches of PG single crystals; but they were all twinned and a preliminary single crystal determination showed many extra weak reflections typically arising from the twinned structure. This may be because of the number of bonding -OH, available for linkage of the molecules as shown in the Table below. In the case of NPA, there is only one bonding -OH; and it is possible that it forms a square (O...H) bond with a group of four NPA molecules and several of these groups are van der Waal bonded in the lattice of the $\alpha$ phase NPA. The table following shows the five types of poly alchohols and the number of bonding -OH available in the low temperature ($\alpha$) phase.

| Polyalcohal | Formula | No. of (OH) Bonding Sites | Reported Structure |
|---|---|---|---|
| 1. Neopentane (NP) | $(CH_3)_2$-C-$(CH_3)_2$ | O | None |
| 2. Neopentyl- alcohol (NPA) | $(CH_3)_3$-C-$(CH_2OH)$ | 1 | None |
| 3. Neopentyl- glycol (NPG) | $(CH_3)_2$-C-$(CH_2OH)_2$ | 2 | Monoclinic (4) |
| 4. Penta- glycerine (PG) | $CH_3$-C-$(CH_2OH)_3$ | 3 | Tetragonal (14) |
| 5. Penta- erythritol (PE) | $(CH_2OH)_2$-C-$CH_2OH)_2$ | 4 | Tetragonal (11) |

In the case of structure of $\alpha$ phase NPG, two tetrahedral molecules join (via a square O...H bond) to form bimolecular double chains of indefinite extent producing a highly anisotropic structure. An ideal molecular arrangement is proposed in Figure 3 in which three oxygen in each tetrahedron are shared with adjacent tetrahedrons to form an extended flat sheet. This is the same as a double chain structure in NPG, but extended in two directions instead of one direction. The bimolecular linear chains of NPG form zig-zag alternating hydrogen bonds, and the chains themselves are van der Waal bonded. In the case of PG, one can extend these bimolecular chains in two directions, such that the adjacent PG molecules are connected with alternating H-bonds leaving behind non-hydrogen bonded sites in the layer plane. Since there are only three -OH's available, they link the PG molecules to form square (projected as rectangle) bonds; and the remaining bonds CH3 are clustered in the hole, marked H. . This was not a proposed study in this program, because there was a paper published already. We have prepared the single crystals of PG, but they were twinned.

## Conclusions

The solid-state phase transition temperature ($T_t$) of pentaglycerine (PG) has been reduced by the addition of dopants; up to 60°C decreases (from 85 to 25°C) have been observed. There are three temperature adjusted PG materials whose transition temperatures range between 25 to 42°C. The most effective dopants were the ones with tetrahedral type molecules such as TMP and AMPL. The non-tetrahedral alcohol molecules such as xylitol and glycerol, which are very effective in lowering the transition temperature of NPG, are ineffective in lowering of the transition temperature of PG because of low solubility in the host structure. It was discovered that TMP undergoes solid-solid phase transformation just below room temperature. The thermal expansion experiments on PG showed that there was very little expansion in the c-direction of the tetragonal layered crystals during heating. A sudden 4.8% increase in thermal expansion was observed at the transition temperature. In the case of TMP doped PG samples, structural data revealed extensive solubility of TMP in PG and no second phases were present. The crystal structure of the "Plastic" $\gamma$ phase of the doped as well as undoped PG samples was determined to be cubic (FCC). Research on crystal structure and thermal analyses of PG, TMP and AMPL are in progress.

## Acknowledgements

This research was conducted under a US Department of Energy contract No.OR21400 (Oak Ridge National Laboratory). The authors would like to thank Dr.Eberhart Reimers and Dr.John Tomlinson for their support of this research. We would also like to thank Renee Lynch of University of Nevada-Reno for her help in sample preparation.

## References


1. Murril, Eand Breed, L., Annual Summary Report No. 1 NASA Contract No. NAS 8-21452 (1969).

2. Benson, D. K., Webb, J. D., Burrows, R. W., McFadden, J. D. and Christianson, C., SERI Report, Task Nos. 1275.00 and 1464.00 WPA304 March 1985 (available through NTIS, SERI/TR 255-1828 Category 62e).

3. D. Chandra, Crystal Structure Changes in the Solid-Solutions of Pentaglycerine-Neopentylglycol, Final report to Solar Energy Research Institute, Midwest Research Institute, Golden CO, Contract number: CA-5-00491-01, September 10 (1986).

4. Benson, D. K. and Chandra, D., Journal of Electrochemical Society Aug. 1985. Extended Abstracts for October 1985 meeting, Electrochemical Society, Inc.

5. Chandra, D. and Barrett, C.S., Effect of interlayer ansd substitutional dopants on the thermophysical properties of the Solid-State Phase Change Materials, Final Report to the DOE Contract No. DE-ACO3-84SF12205, January 1986.

6. Timmermans, J., J.Phys. Chem. Solids, Pergamon Press, 1961, Vol.18, No.1, pp. 1-8 (1961).

7. Aston J. G., "Physics and Chemistry of Organic Solid State", Vol. 1, Chapter 9, Interscience Publishers Inc., New York, NY (1963).

8. Nitta, I. Z. Krist, 112,234 (1959).

9. Llewellyn, F. J., Cox, E. G., and Goodwin, T. H., J. Chem. Soc. 1883, (1937).

10. Nitta, I., and Watanabe T., Bull Chem. Soc. Japan, Vol.13, 28, (1938)

11. Chandra, D., Fitzpatrick, J. J, and Jorgenson, G., Adv. In X-ray Analyses, Vol. 28:353, Plenum Publishing, 1985.

12. Zannetti, R., Acta Cryst. Vol. 14, 203 (1961).

13. E. Nakano, K. Hirotsu, and A. Shimada, The Crystal Structure of Pentaglycerol and Neopentylglycol, Bull. Chem. Soc. of Japan, 42:3367, (1969).

14. Eilerman, D., Lippman, R., Rudman R., Acta. Cryst., B-39, 263-266 (1983).

Table 1. Thermal data on doped pentaglycerine samples.

| | Solid-Solid | | | Solid-Liquid |
|---|---|---|---|---|
| Materials | Transition Temperature $T_t$ (°C) | | $\Delta H_t$ | Melting Temperature (°C) |
| | Bulk | DSC | (cal/gm) | |
| 5% TMP | - | 84.02 | 40.58 | - |
| 10% TMP | 83.5 °C | 83.63 | 37.72 | 184 °C |
| 20% TMP | 80.5 °C | 83.92 | 38.11 | 167 °C |
| 30% TMP | 73 °C | 84.17 | 40.62 | 152 °C |
| 40% TMP | 70 °C | 81.78 | 37.65 | 138 °C |
| 50% TMP | 65 °C | 78.36 | 31.65 | 120 °C |
| 60% TMP | 52 °C | 52.01 | 31.52 | 103 °C |
| 70% TMP | 43 °C | - | 35.00 | 83 °C |
| 80% TMP | 25 °C | - | - | 68 °C |
| 5% AMPL | - | - | 36.54 | 192 °C |
| 20% AMPL | 61 °C | 76.10 | - | 192 °C |
| 30% AMPL | 42 °C | 85.00 | - | 183 °C |
| 40% AMPL | 18 °C | - | - | 177 °C |
| 50% AMPL | - | - | - | 170 °C |
| AMPL(PURE) | 78 °C | - | 37.04 | 120 °C |
| 5% XYLITOL | - | 84.04 | 36.34 | - |
| 10% XYLITOL | - | 84.22 | 25.50 | - |
| 20% XYLITOL | - | 84.27 | 23.28 | - |
| 30% XYLITOL | - | 79.70 | 49.75 | - |
| 5%GLYCEROL | - | 83.76 | 34.96 | - |
| 10%GLYCEROL | - | 83.88 | 34.51 | - |
| 20%GLYCEROL | - | 83.69 | 22.87 | - |
| 30%GLYCEROL | - | 82.82 | 13.69 | - |
| BRIJ52 | - | 84.66 | 32.10 | - |
| BRIJ78 | - | 85.17 | 30.10 | - |
| BRIJ102 | - | 85.10 | 31.68 | - |

Results from bulk and DSC data show decreases in transition temperature and enthalpies.

Table 2. Variation of lattice parameters in pentaglycerine with increase in temperature.

| T(°C) | a | Δa | c | Δc |
|---|---|---|---|---|
| 32 | 6.1672 | 0.0026 | 8.5477 | .0037 |
| 38 | 6.1634 | 0.0014 | 8.5542 | .0015 |
| 43 | 6.1708 | 0.0030 | 8.5524 | .0033 |
| 52 | 6.1681 | 0.0029 | 8.5600 | .0031 |
| 56 | 6.1693 | 0.0040 | 8.5547 | .0043 |
| 62 | 6.1678 | 0.0055 | 8.5619 | .0058 |
| 66 | 6.1790 | 0.0041 | 8.5553 | .0044 |
| 72 | 6.1740 | 0.0028 | 8.5614 | .0029 |
| 78 | 6.1790 | 0.0022 | 8.5638 | .0024 |
| 84 | 8.8656 | 0.0006 | | |
| 91 | 8.8772 | 0.0003 | | |
| 98 | 8.8800 | 0.0015 | | |
| 103 | 8.8937 | 0.0052 | | |
| 109 | 8.9090 | 0.0066 | | |

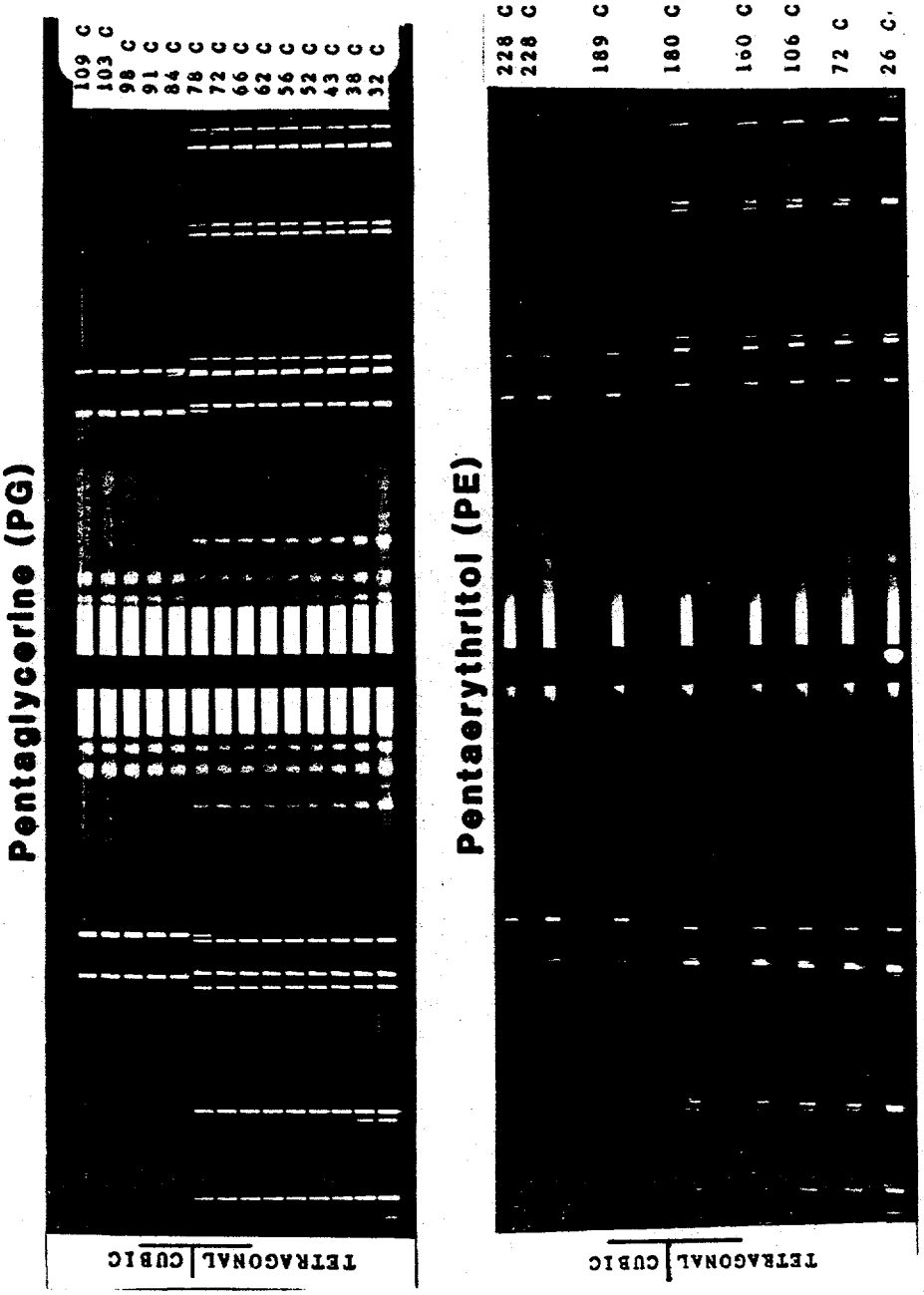


Figure 1. Photograph of X-ray diffraction patterns obtained by heating PG (top) at 14 temperatures over the internal from 32°C to 109°C. For comparison, similar patterns are shown for PE (bottom).

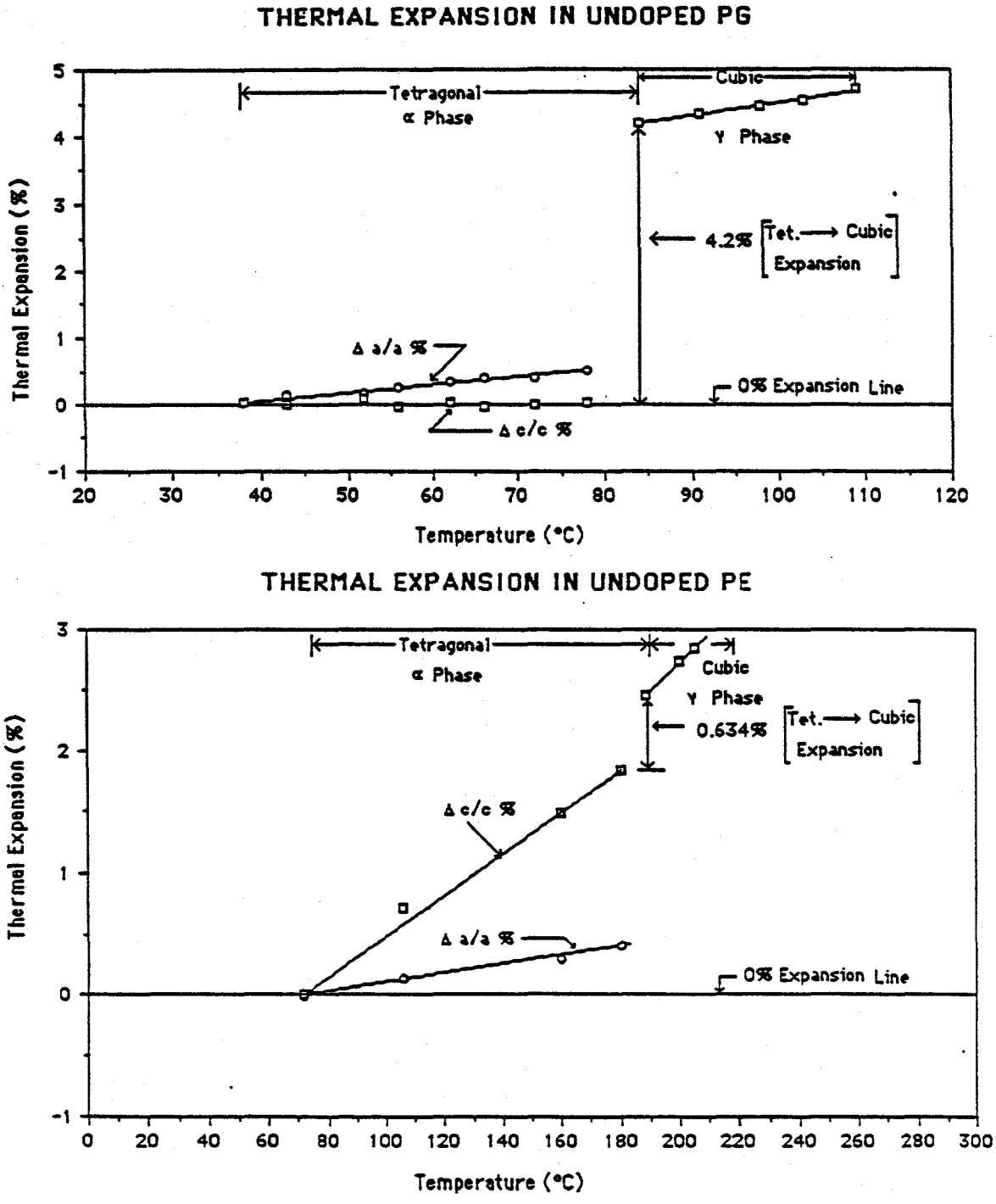


Figure 2. Thermal expansions in pentaglycerine (PG) and pentaerythritol (PE) in a- and c-directions.

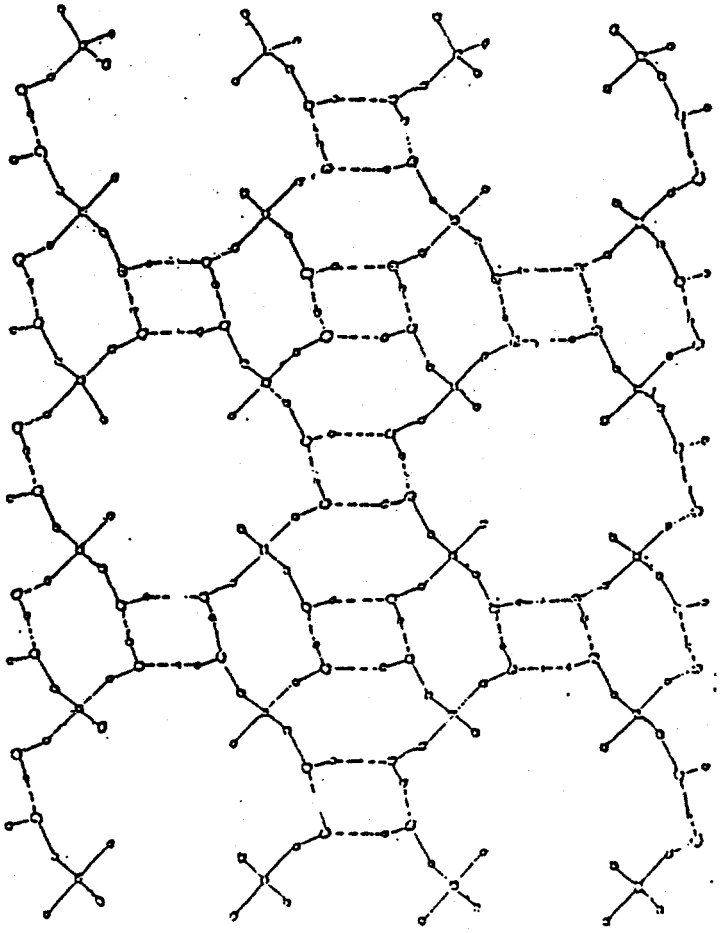

Figure 3. Proposed molecular linkage in PC projected on the a-c plane; bimolecular chains extend in two directions, forming a sheet structure with methyl groups residing in the cavity marked H.

## APPENDIX (A)

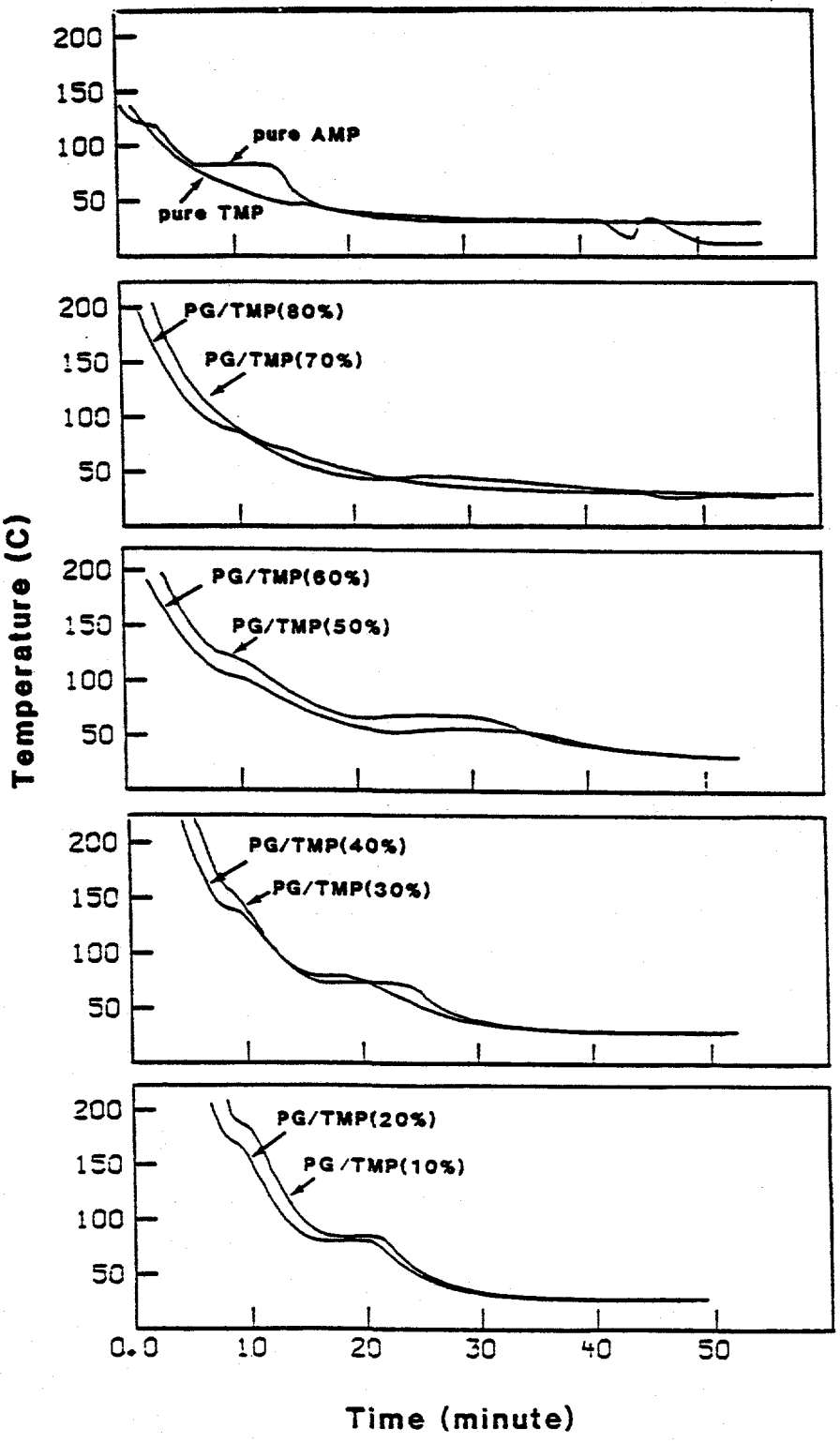


Figure A. Thermal data (temperature *vs* time diagrams) obtained with bulk samples for various concentrations of PG/TMP.

## APPENDIX (B)

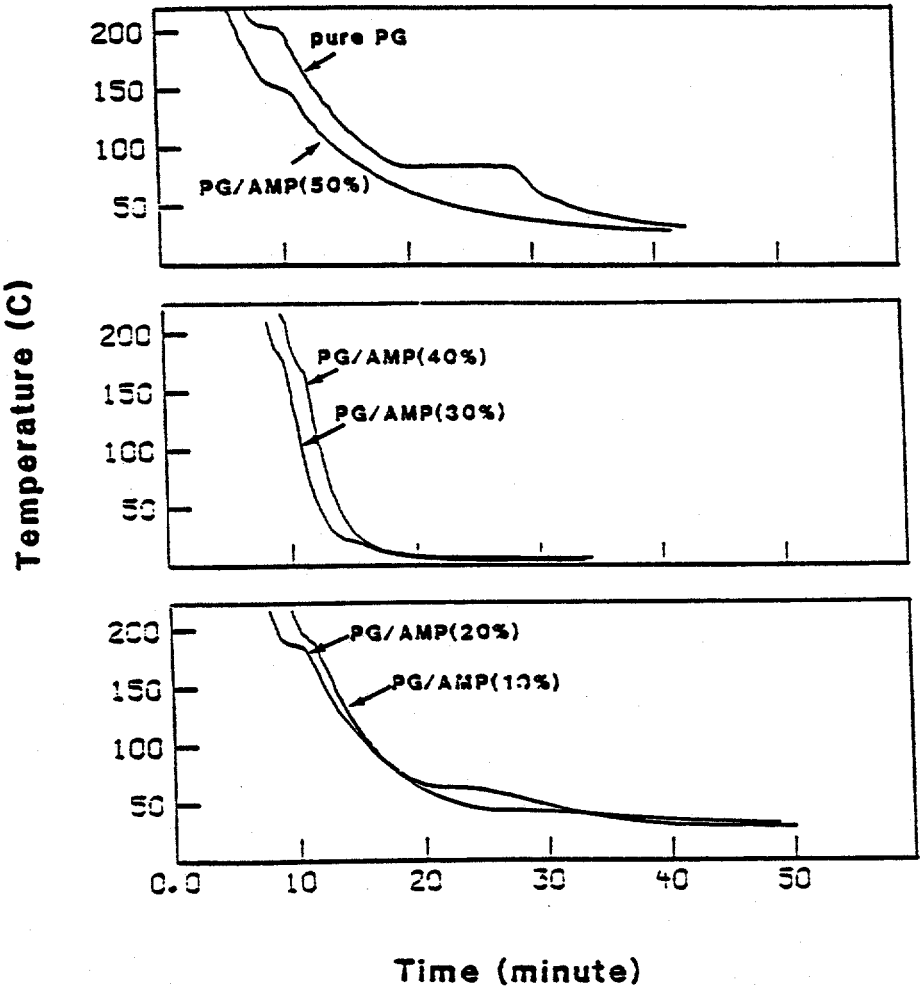


Figure B. Thermal data (temperature *vs* time diagrams) obtained with bulk sampled for various concentrations of PG/AMPL.

# ACTIVITIES IN SUPPORT OF THE WAX-IMPREGNATED WALLBOARD CONCEPT

**R. J. Kedl and T. K. Stovall**
Engineering Technology Division
Oak Ridge National Laboratory*
Oak Ridge, Tennessee

***Abstract***

*The concept of octadecane-wax impregnated wallboard for passive solar application is a major thrust of the Oak Ridge National Laboratory (ORNL) Thermal Energy Storage (TES) program. In support of this effort a number of internal efforts have been undertaken; results inlcude:*

- *The immersion process for filling wallboard with wax has been successfully scaled up from small samples to full-size sheets.*
- *Analysis shows that the immersion process has the potential for achieving higher storage capacity than adding wax-filled pellets to wallboard during its manufacture.*
- *Analysis indicates that 75°F is close to an optimum phase change temperature for the non-passive solar application.*
- *The thermal conductivity of wallboard without wax has been measured and will be measured for wax impregnated wallboard. In addition, efforts are underway to confirm an analytical model that handles phase change wallboard for the passive solar application.*

## Introduction

The concept of wax- (octadecane) impregnated wallboard for the passive solar application is a major thrust of the ORNL TES program, and several internal efforts have been initiated at ORNL in support of this concept. This paper will briefly report on these tasks, which are as follows:

Task 1: Scale-up of the immersion process, by which wallboard is filled with wax, from 1 ft x 1 ft samples to full-size sheets (4 ft x 8 ft).

Task 2: Analytical comparison of two concepts for incorporating wax into wallboard: wax absorbed by wallboard, or wax contained in pellets added to wallboard during manufacture.

---

*Operated by Martin Marietta Energy Systems, Inc. under contract DE-AC05-84OR21400 with the U.S. Department of Energy.

Task 3: Simplified analysis of the thermal coupling of phase change wallboard with adjacent air space.

Task 4: Measurement of thermal conductivity and heat capacity, and confirmation of analytical model for wallboard containing a phase change material (PCM).

Each task is considered separately in the section following.

## Scale-Up of Immersion Process

Concept development work thus far has been accomplished with small samples, typically 1 ft x 1 ft. It was necessary to extrapolate this process to full-size sheets of wallboard (4 ft x 8 ft) and to demonstrate that the amount of wax absorbed could be controlled and that it was distributed uniformly throughout the wallboard.

A heated pan large enough to accommodate a 4 ft x 8 ft sheet was fabricated and filled with molten wax. Wallboard was laid in a frame that featured a wire support bed for the wallboard. An overhead crane was used to lower and withdraw the sheets. Figure 1 shows a full-size sheet of wallboard being immersed in the wax. In all experiments reported here, the octadecane wax was maintained at 170-175°F for the immersion process. The sheetrock was supplied by U.S. Gypsum in three thicknesses (1/4, 1/2, and 5/8 inch) and came from the same factory run.

The wax immersion system was calibrated by dipping 1 ft x 1 ft squares of wallboard into the wax bath for different times and measuring the weight increase. These data are shown in Figure 2 for all three thicknesses. Also shown on these plots are the results of soaking full-size sheets of wallboard. Note the close proximity of the data points for samples and full-size sheets. The significance of this observation is that the wax must be absorbed by the wallboard through the flat surfaces, and edge effects on the absorption process are minimal.

The uniformity of wax distribution was also demonstrated by the following experiment. A 4 ft x 4 ft sheet of 1/2 inch wallboard was immersed in wax long enough to result in a concentration of 25.7 wt % wax in the product. The sheet was then cut into 1 ft x 1 ft squares, and each square weighed. Before immersion in the wax, each square would have weighed approximately 810 grams. After immersion, the average weight of the squares was 1090 grams with a standard deviation of only 12.1 grams. The conclusion was that the wax absorption was quite uniform over the flat surfaces of the wallboard.

Red dye (Oil Red O) was added to the wax. Thus, after immersion, the wallboard could be broken and the penetration of the wax could be observed visually. Immediately after immersion, the wax was observed to be concentrated near the surfaces. However, if the wallboard was maintained at a temperature above the wax melting point for a period of time, the wax diffused; and the concentration became uniform across the thickness.

After demonstrating that the amount of wax absorbed could be controlled by the time of immersion in wax and that the wax was distributed uniformly throughout the wallboard, a total of over 50 full-size sheets

were impregnated to achieve three concentrations (15%, 20%, and saturated). About half the wallboards were sent to the University of Dayton Research Institute for thermal tests, and about half were retained by ORNL for internal development activities. Before the wallboards were used for any purposes, they were maintained at a temperature of at least 125°F for a period of time (one or more days) in order for the concentration across the thickness to become uniform.

## Comparison of Wax Incorporation Concepts

Wax may be incorporated into gypsum wallboard using either of two methods. The first method uses 1/8-in. diameter pellets of high-density polyethylene (HDPE) to hold the wax. The gypsum wallboard material occupies the void space surrounding these pellets. The second method immerses conventional wallboard in melted wax so that the wax is taken up into the pores of the wallboard. One way to compare the potential performance of wallboards produced by these two methods is to compare their maximum energy storage capacity.

This capacity can be stated in terms of the volumetric storage capacity, i.e., the energy storage capacity per unit volume of wallboard. Under steady-state conditions, this capacity is affected by the density of the wallboard, the void fraction in the pellet wall, and the amount of wax imbibed into either the pellets or directly into the wallboard. Wallboard densities of 40, 50, 60, and 70 $lb/ft^3$ were considered in this analysis. The 40 $lb/ft^3$ density corresponds to wallboard commonly sold for residential use and is the lightest wallboard that can be successfully manufactured at this time. The 50 $lb/ft^3$ wallboard corresponds to commercially available fire-resistant wallboard. The higher densities are not in common use but could be made by reducing the amount of air infused during the manufacturing process.

The HDPE pellets were assumed to be approximately spherical in shape with a 1/8-in. diameter. Assuming that they are packed randomly in the wall, these spheres would produce a void fraction (the percent of the volume not occupied by the spheres) of approximately 0.406 in 5/8-in. wallboard and 0.415 in 1/2-in. wallboard(1).

The mass fraction (the mass of the wax divided by the total mass of the composite) of the wax in the HDPE pellets was varied from 0.50 to 0.70 for this analysis. The mass fraction of the wax in the imbibed wallboard was varied from 0.15 to 0.45. The upper bound for the mass fraction in the imbibed wallboard depends on the wall density. For this analysis, the upper limit was set equal to the amount of wax corresponding to a 0.45 mass fraction in 40 $lb/ft^3$ wallboard. This amount of wax absorption has been successfully achieved under laboratory conditions(2).

Figure 3 shows the range in energy storage that results from the application of these two approaches to standard 40 $lb/ft^3$ wallboard. The imbibed wallboard approach results in a higher storage capacity than the pellet wall, based on the parameters selected. The latent energy storage is shown by the energy storage that occurs at the melting temperature, $T_m$. This latent energy storage for the wax pellet wall varies from 1370 to 1880 $Btu/ft^3$ and is calculated using Eq. 1. The latent energy storage for the imbibed wax varies

from 610 to 2810 Btu/ft$^3$ and is calculated using Eq. 2. Both cases show similar sensible heat capacities, as reflected by the nearly parallel slopes of the lines in Figure 3.

$$\frac{Q_L}{V_T} = \frac{\rho_3 \Delta (1-\epsilon)}{(\rho_3/\rho_2)(1/f-1)+1} \quad (1)$$

$$\frac{Q_l}{V_T} = \frac{f_*}{1-f^*} \rho_1 \Delta h \quad (2)$$

where:

| | |
|---|---|
| f | = mass fraction of wax in pellet |
| f* | = mass fraction of wax in wallboard |
| $\Delta h$ | = latent heat of fusion |
| $Q_L/V_T$ | = latent energy storage per unit volume |
| $\epsilon$ | = void fraction |
| $\rho_1$ | = wallboard density (before imbibing process) |
| $\rho_2$ | = HDPE pellet density (before imbibing process) |
| $\rho_3$ | = wax density |

The sensitivity of the imbibed case to the various manufacturing parameters deserves discussion. Figure 4 shows the latent energy storage capacity increasing from 760 to 2810 Btu/ft$^3$ for 50 lb/ft$^3$ wallboard as the mass fraction of the wax increases from 0.15 to 0.40. If the mass fraction is held constant at 0.25 while the wall density is increased from 40 to 60 lb/ft$^3$, the latent energy storage increases from 1150 to 1720 Btu/ft$^3$ (see Figure 5). This increase is caused by the increasing amount of wax in the wall, shown by the increasing difference between the pre- and post-treatment densities, even though the ratio of wax mass to composite mass is held constant. The ability to achieve the same mass fraction for higher density wallboards has not been experimentally verified.

Wallboard density had no significant effect on the storage density for pellet walls, so all the results for this approach were based on 50 lb/ft$^3$ wallboard. Because the void fractions for 1/2-in. and 5/8-in. wallboard were so similar, this parameter also had no significant effect on the energy storage capacity. These void fractions were calculated to reflect the maximum amount of pellets that could be included in a wallboard. It would be possible to increase the void fraction by reducing the amount of pellets in the wall and thus decrease the energy storage capacity. As expected, increasing the mass fraction of the wax in the pellets improved the energy storage of the finished wall for 1/2 in. wallboard, as is shown in Fig. 6.

In the overall comparison, the imbibing approach to incorporating wax into wallboard demonstrates a higher potential for the energy storage capacity.

## Thermal Coupling of Wallboard and Air Space

It has been shown that energy storage can only reduce total energy usage in a building when there are alternating periods of net energy gain and loss(3) or when such storage can serve to capture solar energy that would otherwise have led to overheating. Therefore, questions have arisen regarding the usefulness of PCM wall energy storage in non-solar applications. That is, can a PCM wall usefully store energy without

direct solar radiation? How effectively can such a PCM wall serve to accept and store indirect solar energy (i.e., radiant energy converted to heat by other house elements and only available to the wall via natural convection from the air)? Can the wall serve to smooth out temperature swings within the house and perhaps reduce furnace cycling and its associated energy losses? Should the wall properties, such as melting temperature and total storage capacity, differ as a function of the wall's location in the house?

To address these questions, a simplified analysis of the charging cycle was performed to examine the relationship between the air and wall temperatures under conditions of 1) direct solar radiation, 2) air-heating (which could be supplied by either indirect solar gains or by a furnace) only, and 3) simultaneous solar and air-heating energy sources. The analysis assumed a single temperature for the wall, without consideration of temperature variations within the wall. The wall was assumed to be an interior wall so that heat loss through the wall was not a consideration. Under these assumptions, the basic relationships between the two temperatures are shown in Eqs. 3 and 4:

$$\rho_a V_a Cp_a \, dT_a/d\tau = Q_1 - h \, A_w \, (T_a - T_w) \tag{3}$$

$$\rho_w V_w Cp_w \, dT_w/d\tau = Q_2 + h \, A_w \, (T_a - T_w); \; T_w < T_m \text{ and } T_w > Tm \tag{4}$$

where:

| | |
|---|---|
| A | = area |
| Cp | = specific heat |
| h | = convective heat transfer coefficient |
| $Q_1$ | = constant heat source dispersed in air |
| $Q_2$ | = constant radiation heat source |
| T | = temperature |
| V | = volume |
| $\rho$ | = density |
| $\tau$ | = time |
| subscripts: | a = air; w = wall; m = melt |

The wall was chosen to be 8-ft tall and 12-ft wide. The associated air mass was chosen to be 288-$ft^3$, or 1/4 of the volume of a 12-ft x 12-ft room. Air heating and solar radiation incident on the wall were defined by constant values. Energy losses from the room were not considered during this analysis of the wall's behaviour during the charging cycle. The constant energy source in the air, $Q_1$, was chosen to be 250 Btu/hr. This value was selected by assuming an 80,000 Btu/hr furnace operating 1/4 of the time in a 2500-$ft^2$ house and taking a portion (based on floor area) of that heat for the wall's associated air mass. The solar radiation absorbed by the wall, $Q_2$, was set at 1600 Btu/hr, corresponding to an average value of 100 Btu/hr-$ft^2$ through a 16-$ft^2$ window. A convective heat transfer coefficient of 1 Btu/hr-$ft^2$-°F, appropriate for natural convection, was used. The latent storage capacity of the wall was set at 30 Btu/lb (97 Btu/$ft^2$ for 1/2 inch wallboard), based on a PCM heat of fusion of 86 Btu/lb in a wall with a mass fraction of 35%. The PCM melt temperature was specified to be 75°F.

This simplified analysis of the charging cycle shows PCM storage to be a useful moderator of room air temperature swings in both applications. Figures 7-9 show the relationship between room and wall

temperatures for a wall receiving direct solar radiation, one heated by convection from room air, and one receiving heat from both sources, respectively. These figures show that the air temperature was held near the PCM's melting temperature until all the PCM was melted.

Comparing the time axes of Figs. 7-9 shows that it would probably be appropriate to size the storage capacity (by varying the amount of PCM in the wall) according to the expected application. That is, walls that will receive significant amounts of direct sunshine will need a higher storage capacity than walls that are only receiving heat via convection from the room air.

On the other hand, it appears that there is no reason to change the melting temperature from one application to the next; because the air temperature is successfully controlled, under both applications, to a value very near the wall temperature.

This issue of the optimum melting temperature was considered in some detail by Drake(4). His analysis differed widely from the simplified model discussed here, but the conclusions are very similar. Drake's approach considered both charging and discharging behaviour, allowed for temperature variations throughout the wall, and specified day and night room temperatures. This analysis resulted in a desired melting temperature within about 3°F of the room's daytime temperature setpoint.

## Measure Conductivity and Confirm Analytical Model

An analytical model was developed to handle wallboard containing a PCM for the passive solar and other applications. In order to use this model, it is necessary to know the thermal conducitvity of wax impregnated wallboard (above and below melting point), and the model must be confirmed.

An existing faciltiy at ORNL was used to conduct these experiments. Figure 10 shows this facility, which was specifically designed to measure the thermal conductivity of building materials. It consists of a centrally located screen wire resistance heater, building materials being tested placed on both sides (two-directional heat flow), and a copper plate with cooling coils outside these on both sides. The screen wire heater has dimensions of 3 ft x 5 ft, and the 3 ft x 5 ft samples to be tested are framed with insulation. Thus, near the center of the assembly, heat flow is axial and edge effects may be neglected. The facility was built such that the minimum thickness that can be tested is approximately 1 1/2 inches. Therefore, when 1/2 in. wallboard is being tested, a stack of four sheets are required above and below the resistance heater.

To date, only the conductivity of wallboard without wax has been determined. The measured value of 1.22 Btu/hr $ft^{2o}F$/in. is in good agreement with the value reported in ASHRAE Fundamentals of 1.16 Btu/hr $ft^{2o}F$/in.

The analytical model will be confirmed by operating the facility under transient conditions. With the coolers on and no power going to the resistance heaters, the system will be allowed to approach a steady state temperature. Then, at time equal zero, the heater will be given a step change in power; the resulting temperature transient in the wallboard will be recorded.

## References

1. K. Ridgway, K. J. Tarbuck, "Voidage Fluctuations in Randomly-packed Beds of Spheres Adjacent to a Containing Wall," Chemical Engineering Science, 1968, Vol. 23, pp. 1147-1155, Pergamon Press, Printed in Great Britain.

2. I. Salyer, University of Dayton Research Institute, Dayton, OH.

3. K. W. Childs, G. E. Courville, E. L. Bales, "Thermal Mass Assessment - An Explanation of the Mechanisms by Which Building Mass Influences Heating and Cooling Energy Requirements," ORNL/COM-97, September 1983.

4. J. B. Drake, "A Study of the Optimal Transitoin Temperature of PCM-Wallboard for Solar Energy Storage," ORNL/TM-10210, September 1987, Oak Ridge National Laboratory, Oak Ridge, TN.

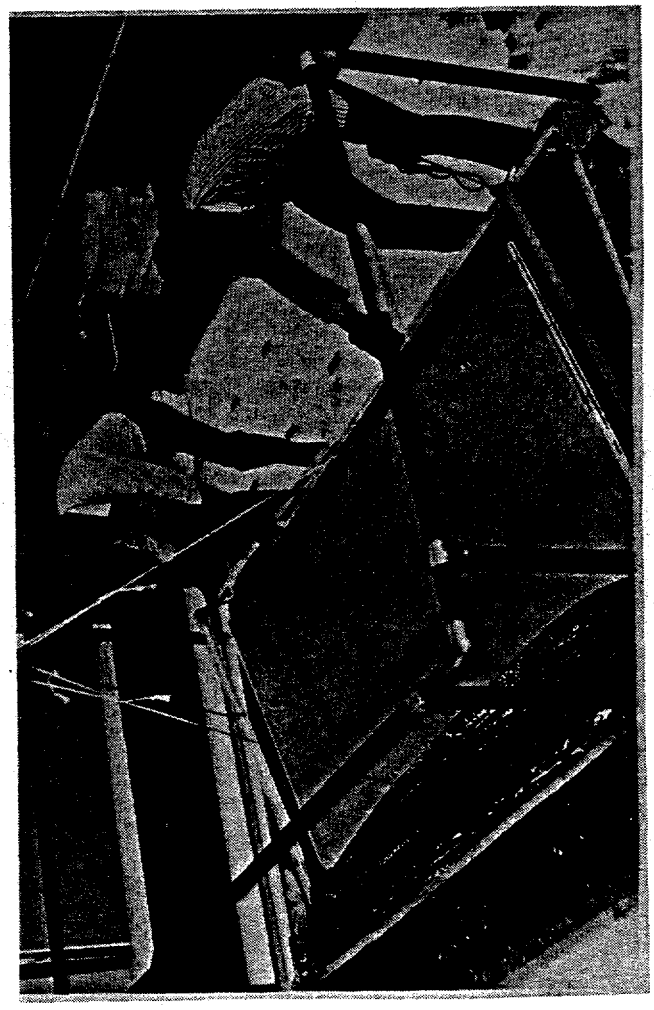

Figure 1. Immersing wall board in wax.

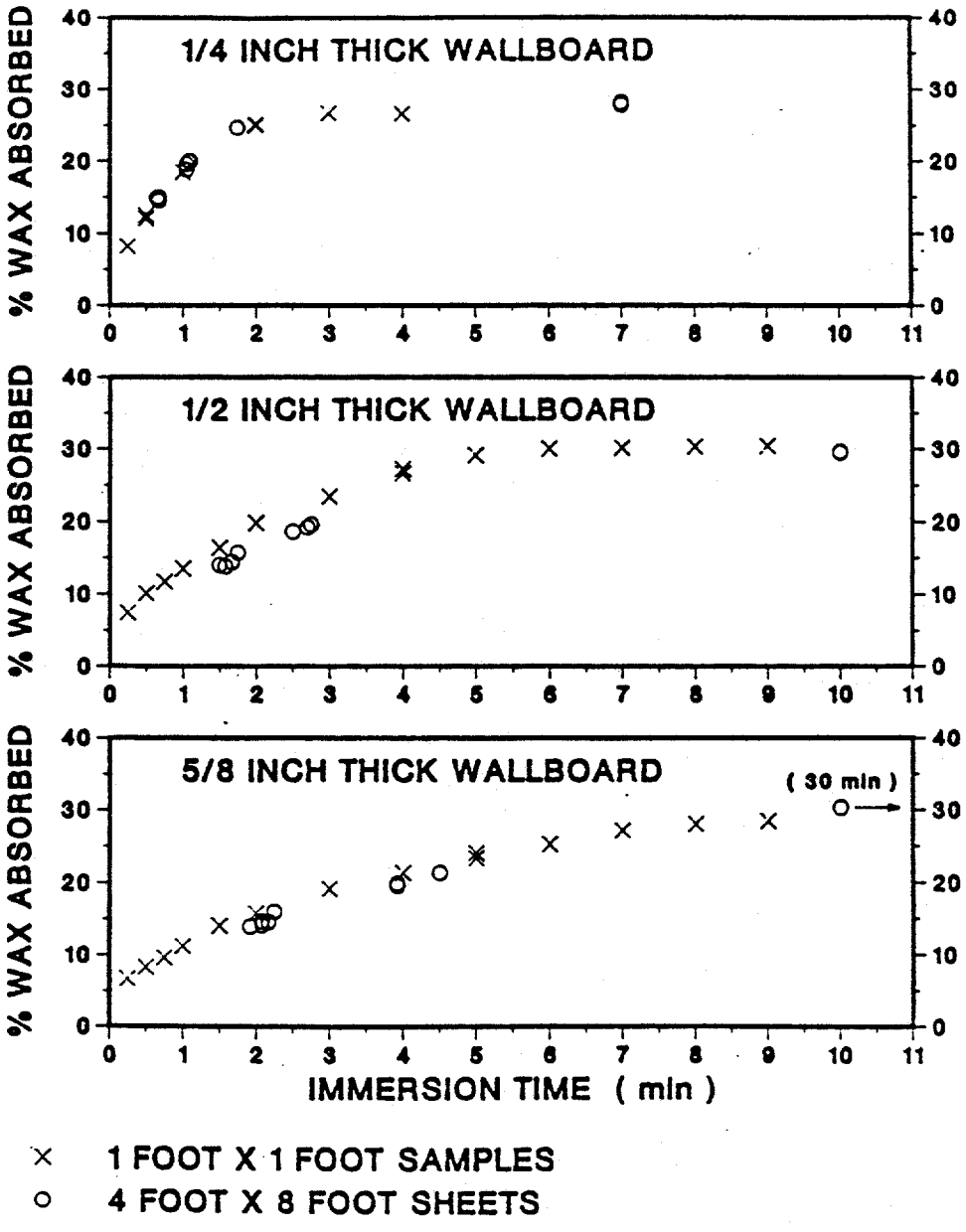


Figure 2. Wax absorbed by wallboard as function of immersion time.

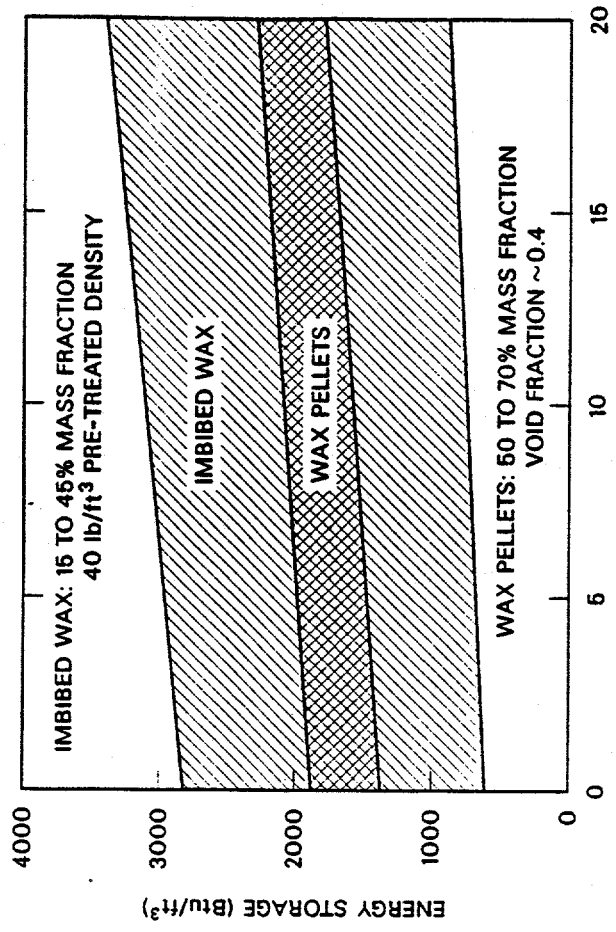


Figure 3. Comparison of pellet and imbibed cases.

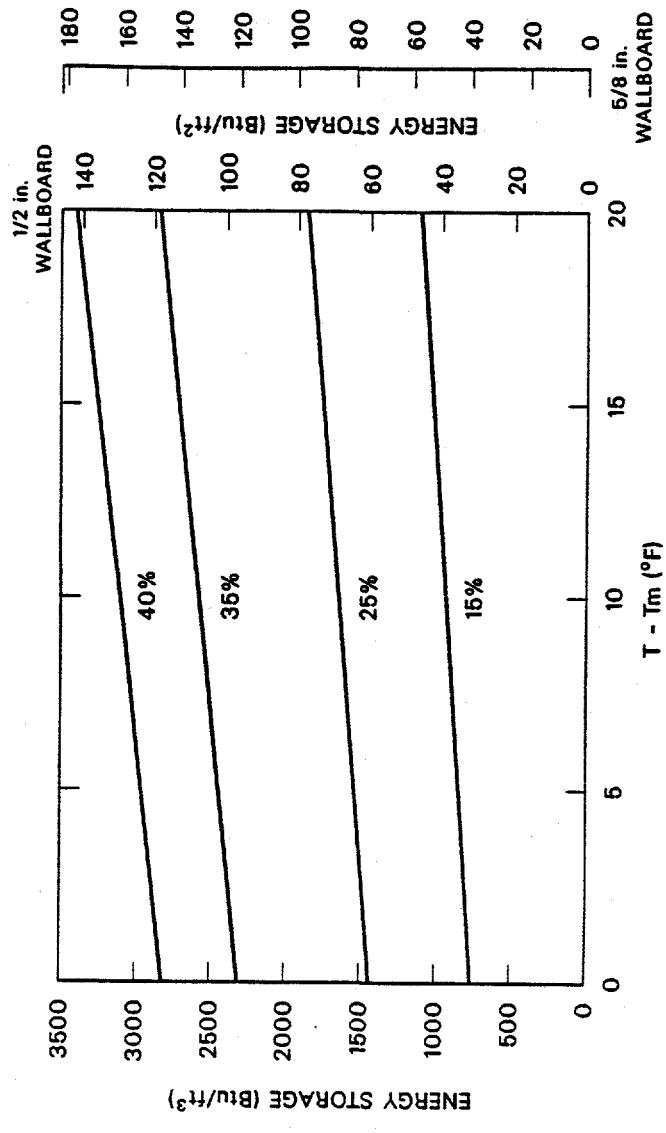


Figure 4. Energy storage increases with increasing PCM mass faction for imbibed case (wall density = 50 lb/ft³).

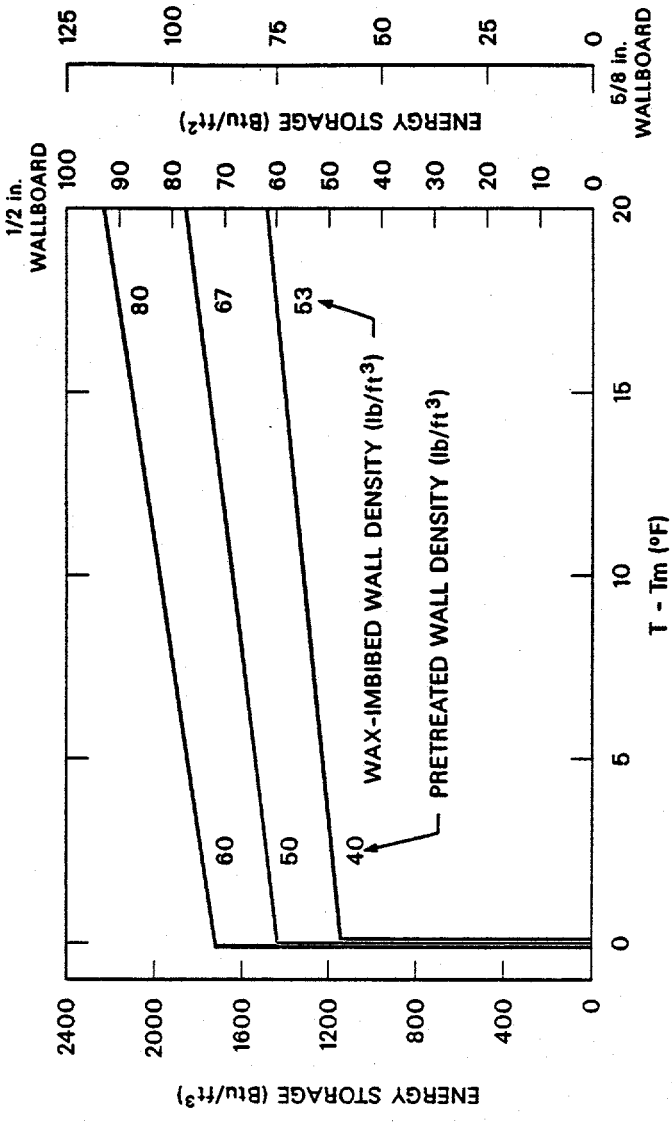


Figure 5. Energy storage in wax-imbedded wallboard increases with increasing density for constant mass fraction = 0.25.

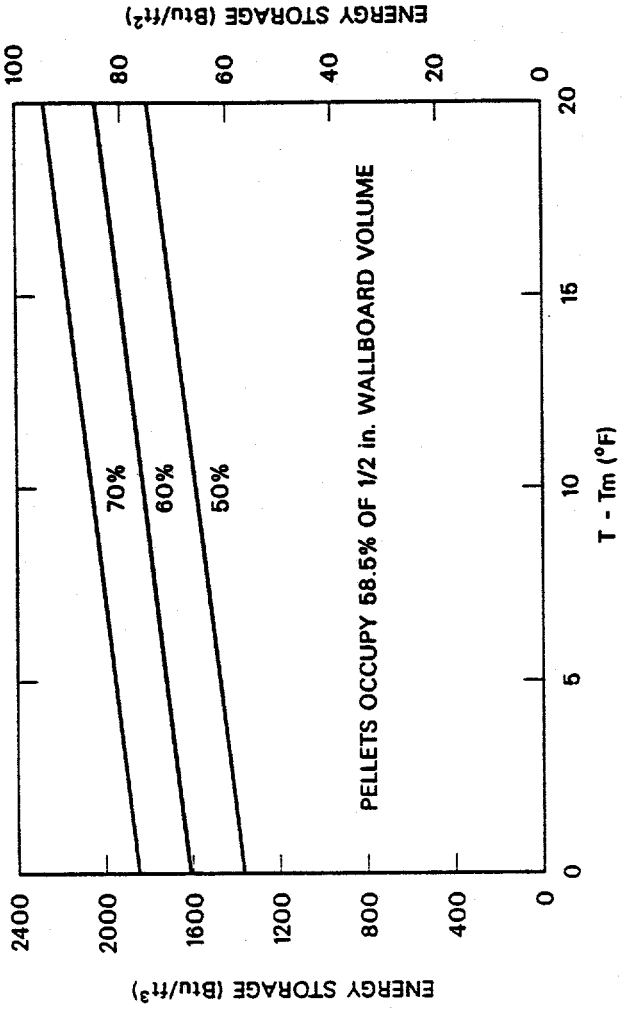


Figure 6. Increasing mass fraction of wax in pellet increases energy storage.

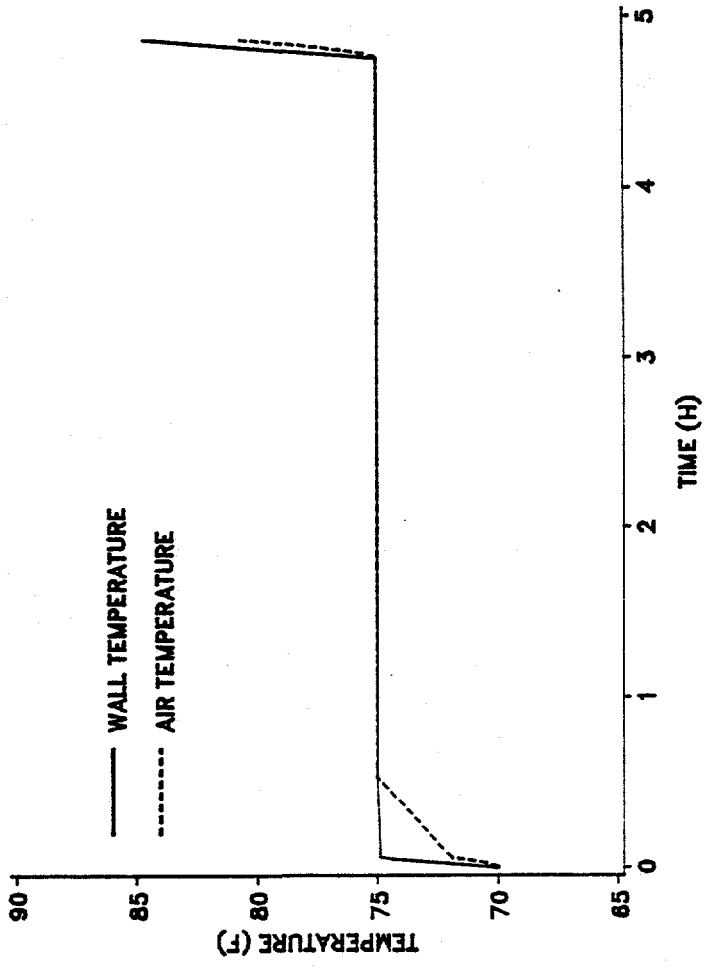


Figure 7. Coupled air and wall temperatures; direct solar radiation only.

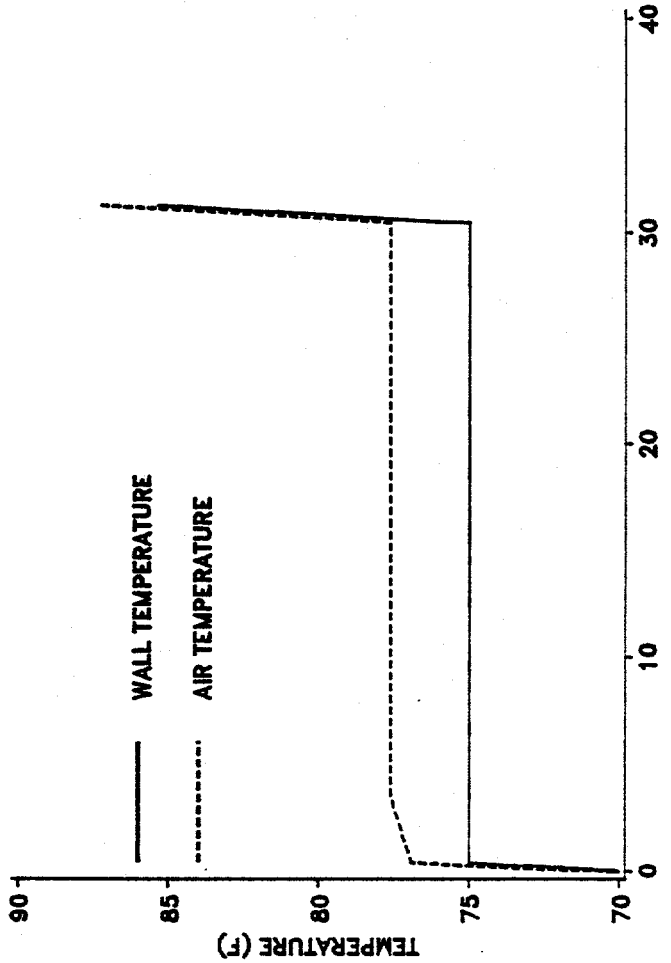


Figure 8. Coupled air wall temperatures; air heating only.

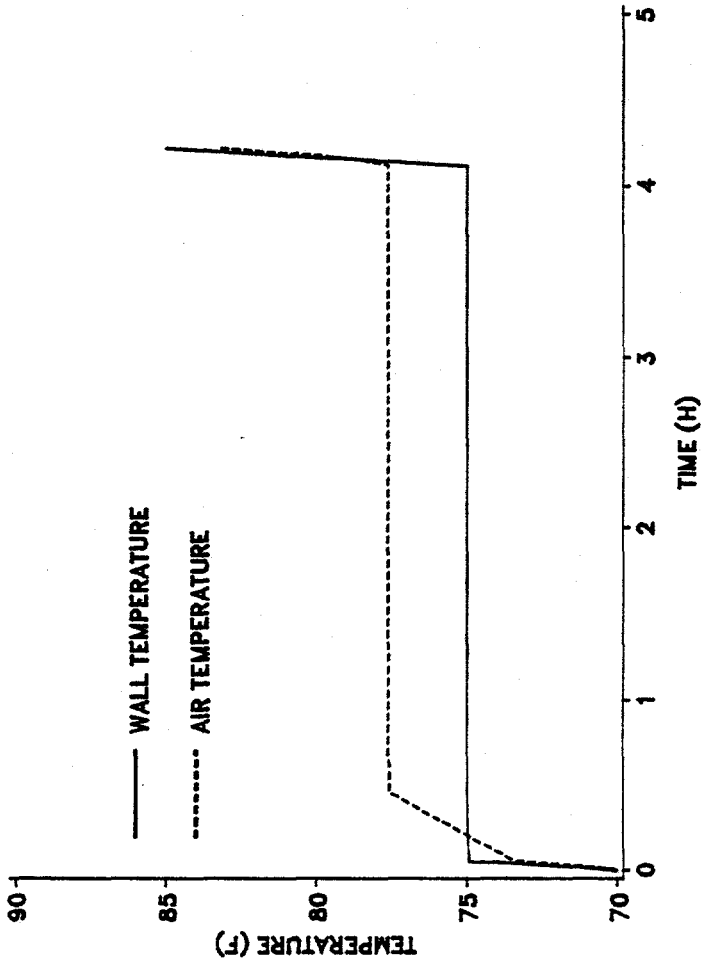


Figure 9. Coupled air and wall temperatures; direct solar radiation and air heating.

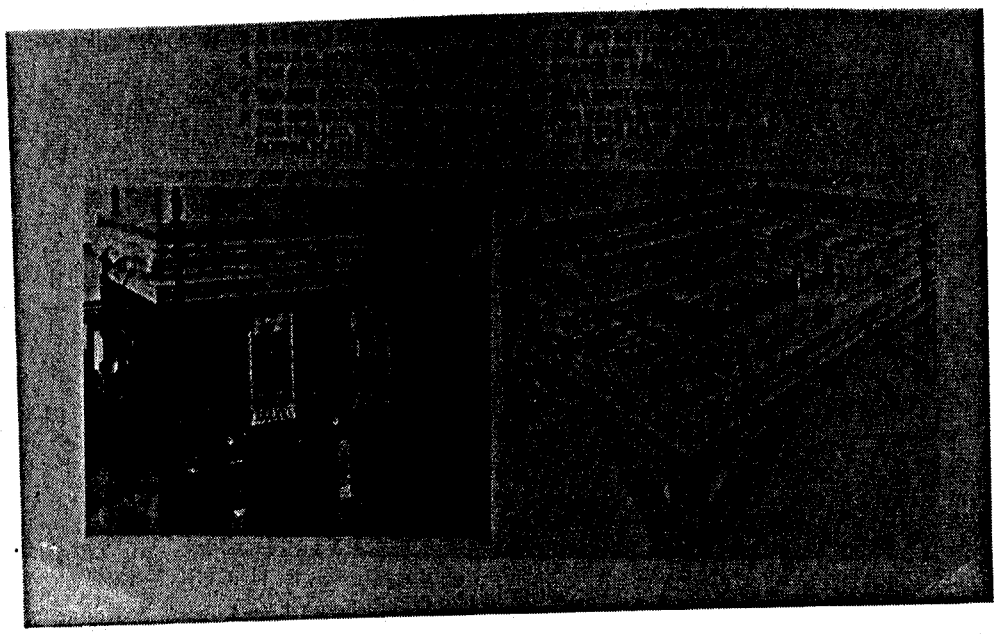

Figure 10. Assembled apparatus without perimeter insulation shows component positions to obtain one- or two-sided vertical heat flow to insulated copper plates.

# DEVELOPMENT OF SEPARATION TECHNIQUES FOR A DIRECT CONTACT THERMAL ENERGY STORAGE SYSTEM

**T.C. Min** and **J.J. Tomlinson**
North Carolina A&T State University
Greensboro, North Carolina 27411
Oak Ridge National Laboratory
Oak Ridge, Tennessee 37830

***Abstract***

*In direct contact ice-making processes, the refrigerant will pick up water vapor through direct percolation and oil from the compressor. The purpose of this project is to investigate methods for separating water vapor and oil from a mixture to complete a refrigeration cycle. In this paper, we report critical review on two separation techniques. From a literature search, we have identified a third technique; and plan to evaluate this method by bench-scale experiments. A recommendation for future work is included.*

**This paper was not received in time for inclusion in these bound proceedings, but is available separately.**

# DEVELOPMENT OF A DIRECT CONTACT ICE STORAGE SYSTEM

**R. Poirier**
Chicago Bridge & Iron Company
Plainfield, IL

***Abstract***

*The program described involves the design, construction, and performance testing of a Direct Freeze Thermal Energy Storage System. Task 1 (Design) has been completed; and Task 2 (construction) is in progress, with equipment procurements presently underway. Once constructed, the system will undergo extensive laboratory performance testing and analysis, followed by an assessment of the system's cost effectiveness. This study will advance the understanding and development of the direct freeze concept, which offers inherent benefits for thermal energy storage.*

## Introduction

This investigation[a] seeks to advance understanding and development of the Direct Freeze Thermal Energy Storage concept for comfort air conditioning applications. Phase I includes the design, construction, and laboratory testing of a 25 ton/300 ton-hr prototype unit; Phase II (presently not funded) includes field demonstration of the technology.

Figure 1 is a schematic of the Direct Freeze system. By direct contact heat transfer between refrigerant and water, the system produces an ice slurry which is capable of being pumped. Water is pumped from the bottom of a storage tank into a direct contact heat exchanger, where it is mixed with liquid refrigerant. Vaporized refrigerant is withdrawn to a condensing package, while the ice slurry is pumped to or sprayed into the storage tank. Stored refrigeration is later recovered by withdrawing water from the bottom of the storage tank and pumping it to the thermal load. The returning warm water is sprayed into the storage tank and rechilled by melting ice crystals.

Benefits of the Direct Freeze technology include:

Constant High Efficiency. The direct contact heat transfer between the refrigerant and water minimizes the temperature differential required to make ice. Unlike other ice systems, the resulting high efficiency does not degrade as ice is generated and stored.

No Defrost Cycle. The Direct Freeze system produces ice continuously without any buildup of ice on the Direct Freeze heat exchanger. No expensive and inefficient defrost cycle equipment is required.

---

[a] Work performed for the Oak Ridge National Laboratory, Thermal Energy Storage Program, under Contract No. 86X-SA942V.

**Simple Operation**. The Direct Freeze system has few moving parts and operates automatically using simple, conventional controls. The system uses no oil and requires minimal maintenance. During initial cooldown, the system operates as a water chiller until icemaking begins. The thermal storage capacity allows the compressor to run at full load, further maximizing efficiency and reliability.

**Low Cost Heat Exchanger**. The Direct Freeze heat exchanger is a simple, compact, low cost unit which contains no moving parts. There is no costly shell-and-tube or plate heat transfer surface. The compact heat exchanger also minimizes the amount and cost of the system refrigerant charge.

**Pumpable Ice Slurry**. The Direct Freeze system produces ice crystals which can be easily pumped with water as an ice slurry. For district cooling applications, a Direct Freeze ice slurry can significantly reduce the distribution system pipe size. In addition, the Direct Freeze slurry exhibits up to a 40% reduction in pressure drop compared to water at the same velocity.

The Direct Freeze system development work to date has included concept innovation, evaluation, initial laboratory work, operation of refrigeration units (2.5, 10 and 25 tons), and ice slurry pumping tests.

## Current Results

The following Task 1 and Task 2 elements have been completed:

1. Results of prior design and test work on the Direct Freeze system were reviewed.
2. System design calculations were performed; per the contract requirements, the system size will be 25 tons ice-making capacity with 300 ton-hours of storage.
3. The process flow sheet was completed.
4. The piping and instrumentation diagram was completed.
5. The preliminary layout drawings were completed.
6. The major equipment specifications were prepared and sent to vendors.

The work currently being executed includes the selection of major equipment suppliers in preparation for completion of Task 2: Construction of the Skid. Additional work to be performed includes a review of alternate refrigerants for the Direct Freeze system, including non-CFC refrigerants.

Future work will include the following Phase I tasks:

- **Task 3: Startup and Testing at CBI R&D Center**

  The system will be commissioned and operated for a six week test period. The tests will analyze the maximum storage capacity, discharge characteristics, component performance, and materials corrosion.

- **Task 4: Technology Assessment**

  The results of Task 3 will be used to develop costs and performance for a commercial sized Direct Contact Thermal Energy Storage (DCTES) system. Installation paybacks shall be calculated for two geographic locations (i.e., utility rate structures) in order to assess the DCTES technology.

- **Task 5: Field Test Justification**

  Candidate sites for field installation of the 25 ton DCTES will be identified and evaluated.

- **Task 6: Documentation and Deliverables**

  Documentation and deliverables will be submitted in accordance with the contract requirements.

The potential exists for installing the 25 ton DCTES at the field site identified in Task 5 (presently not funded). Details will be finalized after successful completion of Phase I.

## Conclusions

This contract will advance the development of the Direct Freeze Thermal Energy Storage System by designing, constructing and testing a 25 ton/300 ton-hr prototype unit. The Direct Freeze System offers a number of inherent benefits for thermal energy storage.

The contract execution is proceeding on schedule with Task 1 (Design) work items complete and Task 2 (Construction) work items in progress.

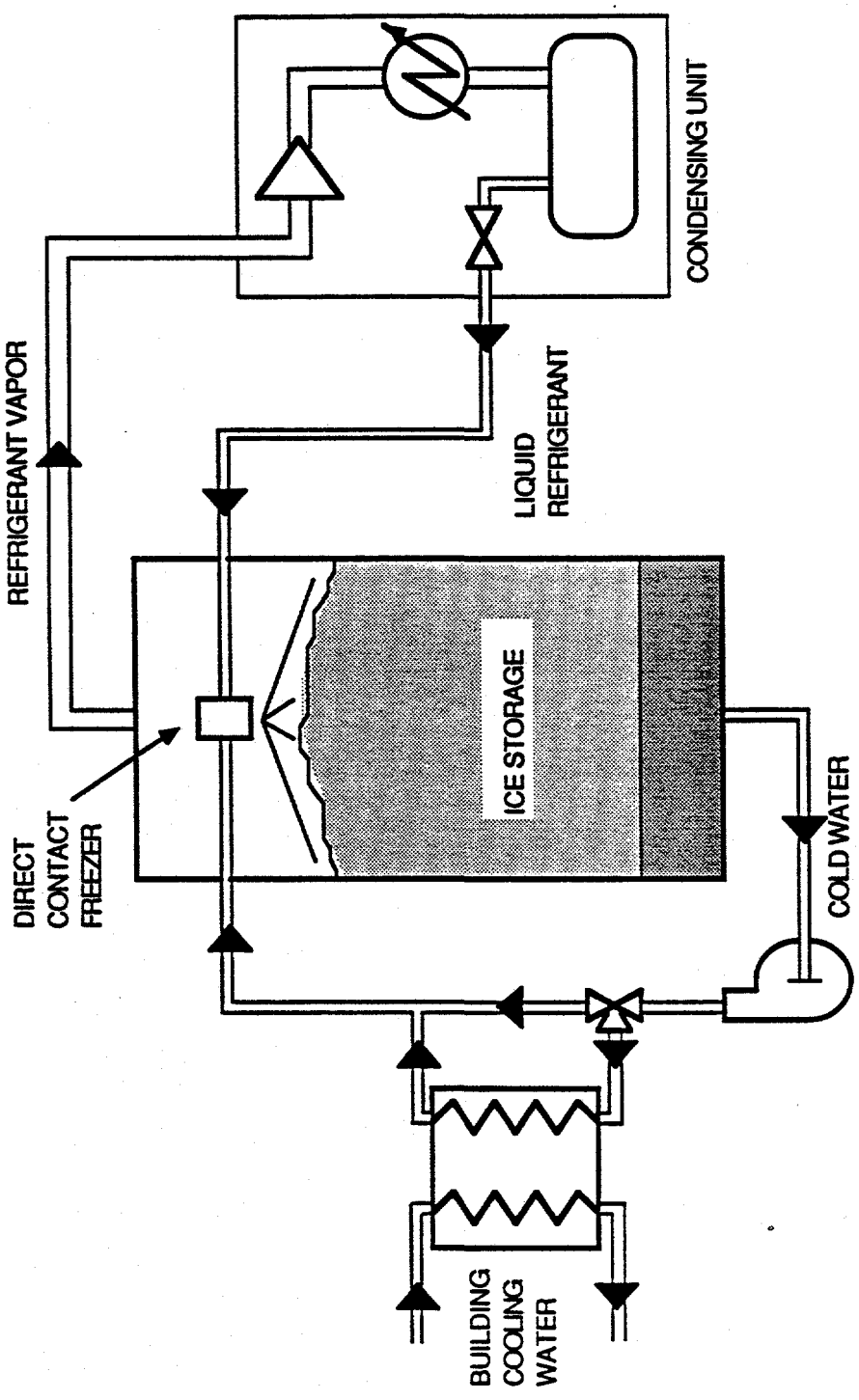


Figure 1. Deep Freeze System flow schematic.

# DEVELOPMENT OF PCM WALLBOARD FOR HEATING AND COOLING OF RESIDENTIAL BUILDINGS

**Ival O. Salyer and Anil K. Sircar**
The University of Dayton Research Institute
Dayton, Ohio

## *Abstract*

*This research was initially sponsored by the Solar Passive Division of the Department of Energy under a contract that started in 1983. The program, with several funding hiatuses, has continued to the present. The original goals of the project were to find, test, and develop an effective phase change material (PCM) for heating and cooling of residential buildings. Specifications for the PCM included thermal storage of at least 30 cal/gm, congruent melting and freezing, at 25°C, nontoxic, noncorrosive, nonhygroscopic, low-cost, and commercially available in quantity. Additionally, the PCM must be able to be incorporated into ordinary building materials (plasterboard, concrete, floor tile) by processes adaptable to commercial manufacture. The goals of the original program have been substantially achieved by identifying a series of linear crystalline alkyl hydrocarbon PCM that are commercially available from petroleum refining (lower cost, lower "purity"), and from polymerization of ethylene (higher cost, higher "purity"). Four alternate processes have been developed whereby these PCM can be incorporated into plasterboard and concrete building materials. Two of the processes have been successfully demonstrated in the laboratories of the two largest U.S. manufacturers of plasterboard, and collaborative development leading toward commercialization is still ongoing.*

*Problem areas remaining to be resolved include: establishing unequivocably the economic viability of the system, developing environmentally acceptable fire retarding procedures, scale up of the manufacturing processes and evaluating effects of long-term thermocycling.*

*In the current study,* we are scaling up the immersion process to include imbibing and testing 4-ft x 8-ft plasterboard panels. Successful completion is expected to encourage a plasterboard manufacturer to commercialize the technology.*

*Five U.S. patents have been issued. Additional U.S. and foreign patents are pending. One foreign license has been negotiated. Spin-offs of the technology likely to be commercialized soon in the U.S. include tableware, hot and cold medical wraps, and wraps to prevent the overnight freezing of citrus tree trunks.*

## Introduction

During the last six years under the sponsorship of the DOE Solar Passive Division, The University of Dayton Research Institute (UDRI) has investigated several phase change material (PCM) systems for utility

---

* Work performed under Oak Ridge National Laboratory subcontract 19X-SC-542V.

in thermal energy storage for solar passive heating and cooling applications. From this research on the basis of cost, performance, containment, and environmental acceptability, we have selected as our current and most promising candidate phase change materials, the series of C-15 to C-24 linear crystalline alkyl hydrocarbons. Ultrapure C-18 alkyl hydrocarbons (PCM) from ethylene polymerization that melt and freeze sharply in the 25°C temperature range desired for solar passive applications are available from Humphrey Chemical at a premium price of $1.86/lb (technical grade) and $9.68/lb (98% pure grade). These alkyl hydrocarbons have heats of fusion of 50-60 cal/gm, are self-nucleating, and exhibit little or no supercooling. The lower melting members of this family of commercial alkyl hydrocarbons have been evaluated, "neat" and in "blends."

However, a series of crystalline paraffin waxes that can provide acceptable thermal energy storage are commercially available at the much lower cost of $0.26/lb to $0.50/lb from petroleum refining (Witco, Shell, Exxon, Union). These petroleum-based paraffins have melting points ranging from 15-80°C, depending on carbon chain length, and a quoted price of $0.26/lb to $0.50/lb for tank-car quantities.

Containment costs and attendant problems have been the bane of many of the PCM systems developed in the past. We have defined four economic and effective methods of packaging the candidate PCM in common construction materials. Importantly, the containment methods appear to also provide means for adequate heat transfer, and the processes are of the type that could be rapidly implemented by commercial manufacturers of building materials.

The four processes are as follows:

1. Direct incorporation of PCM into the wet mix of building materials;
2. Direct incorporation into rubber or plastics medium for floor and wall tiles;
3. Indirect incorporation by first swelling the PCM into crosslinked polyethylene pellets or powder which are then incorporated into building materials;
4. Direct incorporation by imbibing (percolating) the melted PCM into the open spaces in porous building materials.

As is well known, all organic PCM after ignition will continue to burn in a normal air atmosphere. In the processes where the PCM is completely encapsulated in a non-burning matrix of plaster or concrete (processes 1 and 3), the building material is less likely to burn. However, in process 4, where the PCM is percolated into plasterboard (in high concentrations), the plasterboard after ignition will continue to burn slowly until the PCM is exhausted. In process 2, where the PCM is compounded into rubbers and plastics, the resulting composite will also burn, unless the polymer matrix is made fire retardant with effective additives.

We have preliminarily addressed the flammability problem in these four processes by incorporating a state-of-the-art fire retardant system consisting of chlorinated paraffin and antimony oxide into the PCM to thereby render it self-extinguishing. However, there are difficulties in applying this fire retarding

technology effectively in process 4 (percolation). Accordingly, more research on this specific process and on the whole area of fire retardance was carried out. This was a subject of major emphasis in the last year's research, and further work is required to scale-up and optimize the processes developed.

However, other areas were also intensively investigated. We completed laboratory tests of both pure and lower cost commercially available linear alkyl hydrocarbon PCM to define materials that could provide the most cost-effective performance for solar passive applications. We carried out extensive thermocycling tests (1,000 times) of small-scale samples of building materials containing PCM but have not completed analysis of the results. We continued our efforts towards commercializing the results for home heating and cooling through demonstrations of processes 3 and 4 in the laboratories of two major U.S. manufacturers of plasterboard, and aggressive marketing of the technology elsewhere in the U.S. and abroad.

In separate research, we have developed several promising spin-offs of the PCM technology that may reach commercial fruition considerably sooner than the application in building materials. These spin-off applications include use in tableware for keeping food and drinks hot or cold, citrus tree wraps to prevent overnight freezing, and hot and cold packs for medical therapeutical uses.

Several patent applications have been filed in the United States and abroad on the technology developed in the research. Five U.S. patents have been issued and others are pending. One license agreement has been negotiated with a major Japanese company that is exclusive for Japan. Three option/ license agreements are in the active state of negotiation in the United States, and at least one will be completed within the next two to three months.

On an overall basis, the research to date can be said to constitute a major breakthrough in thermal energy storage technology that can in the near future become commercialized in a variety of applications. Successful commercialization in building materials for residential heating and cooling can affect substantial energy conservation, and perhaps, thereby minimize the "greenhouse effect" as well.

A chronological history of this research program can be found in the list of publications contained in the Section entitled "References."

## Current Results

The major part of the research during this contract period was directed toward the following three objectives.

- Find, test, and develop low-cost effective phase change materials (PCM) that melt and freeze sharply in the comfort temperature range of 73-77°F for use in solar passive heating and cooling of buildings.
- Define practical materials and processes for fire retarding plasterboard/PCM building products.
- Develop cost-effective methods for incorporating PCM into building construction materials (concrete, plasterboard, etc.) which will lead to the commercial manufacture and sale of PCM-containing products resulting in significant energy conservation.

**Phase Change Materials Development**

**Basic Studies of Pure Linear Alkyl Hydrocarbon PCM.** Humphrey Chemical Company has for some time marketed a series of 99% pure alkyl hydrocarbons having carbon chain lengths from C-6 through C-44. The even carbon atom members of this series are obtained primarily from ethylene polymerization to 1-olefins that are then hydrogenated and distilled to obtain the high-purity products. The ultra-pure PCM are prohibitively expensive ($10.00 to $20.00/lb) for use as PCM in residential heating and cooling. Nevertheless, it was of both theoretical and practical interest to determine their thermal energy storage characteristics for comparison with the less pure Humphrey Technical Grades and the commercial paraffin blends from petroleum refining.

Small samples of 99% pure C-6 through C-44 furnished gratis by Humphrey were analyzed by differential scanning calorimetry (DSC) at a heating and cooling rate of 10°C/min. Data obtained on a portion of the series, C-9 through C-22, are summarized in Table 1. This table also shows the pronounced solid-state transition in these PCM that starts early (C-9) in the odd carbon atom species, but only at C-22 and higher in even carbon atom species. DSC graphs are shown for 99% pure octadecane (Figure 1) and nonadecane (Figure 2).

Using these same pure samples, synthetic blends were prepared to simulate the type of distribution of carbon chain lengths present in linear alkyl hydrocarbons from petroleum refining. DSC analysis of these blends showed sharp melting and freezing at the temperature predicted for pure PCM of the same average chain length with only minimum concurrent reduction in latent storage capacity. This finding was important, since it confirmed earlier indications that blending could be used to "tailor" a PCM for intermediate temperature ranges.

The effect of the rate of heating and cooling in the DSC analysis was investigated using 99% pure hexadecane and rates of heating and cooling of 10, 5, and 2°C/minute. The temperature of melting and freezing and the thermal distance between melting and freezing were plotted as a function of the rate of heating and cooling in Figure 3. The difference between the measured melting and freezing temperature decreases rapidly as the rate of temperature change decreases. These data indicate clearly that little or no supercooling would be encountered at the slow rates expected in actual use of PCM for residential heating and cooling.

**Evaluation of Technical Grades of Linear Alkyl Hydrocarbons.** The Humphrey Technical Grades are available in chain lengths of 14 to 24 carbon atom lengths. Because of the absence of solid-state transitions due to odd carbon chain length compositions, the technical grades tend to have significantly higher heats of fusion and crystallization than the lower cost products from petroleum refining. For this reason, we conducted a thorough evaluation of the Humphrey C-18 Technical Grades of PCM, since it was believed they could be cost effective at the selling price of about $0.70/lb (projected about two years ago), with even lower prices foreseen as possible for large-scale production quantities.

Differential Scanning Calorimeter (DSC) analysis at 2°C/minute rate of heating and cooling showed that Humphrey Tech Grade C-18 has a melting and freezing temperature near the comfort temperature range of 73-77°F and stores and releases about 50 cal/gm heat of fusion and crystallization. The effect of the rate of heating and cooling on the measured melting and freezing temperature is shown in Figure 4.

However, during the last two years, the cost of the ethylene monomer starting raw material has escalated rapidly to more than double its earlier price. Accordingly, the selling price of all products made from ethylene has also risen dramatically resulting in Humphrey Tech Grade C-18 now selling for about $1.86/lb, a figure that would require prohibitively long pay-back times through energy savings in home heating and cooling.

Therefore, much emphasis, in the last year, has been placed on cooperative research with petroleum refiners, such as Witco, with the objective of defining a more cost-effective PCM for home heating and cooling applications.

**Improved PCM for Residential Heating and Cooling From Petroleum Refining Operations.** As pointed out earlier, the "purer" alkyl hydrocarbons from ethylene polymerization are considerably more expensive than the corresponding by-products of normal petroleum refining. Accordingly, one of our projects of emphasis during the project period was collaborating with Witco Chemical Company to develop lower cost PCM in the C-16 to C-18 range which are not now commercially available.

We participated with Witco in developing an effective process for commercial manufacture of K-61, a PCM that is a likely candidate to be used for solar heating and cooling of buildings because of its transitions near the comfort range. DSC and gas chromatographic analyses of different fractions from distillation versus solvent crystallization temperature were carried out. It was observed that fractions from crystallization precipitates mostly the higher molecular weight linear hydrocarbons leaving the lower and branched homologues in solution. This is reflected in higher heats of fusion and crystallization (46-48 cal/gm) as compared to the unfractionated products (35-44 cal/gm).

A five-gallon supply from a larger lot of solvent fractionated K-61 (prepared by Chevron for Witco) was found to compare favorably with regard to thermal energy storage characteristics with that of small laboratory samples of K-61 previously obtained from Witco. This is important in indicating that scale-up of the solvent fractionation process for eventual commercial production is feasible.

Importantly, in January 1989, Witco made their first plant production manufacture of a 7000-gallon quantity of their K-61 PCM. The plant run was very successful in that they were able to duplicate on a larger scale the results obtained in their laboratory experiments and in Chevron five-gallon pilot plant production. DSC analysis of a sample of the plant production, Table 2 and Figure 5, show very sharp melting and freezing in the desired temperature range of 25°C with little or no supercooling. Witco has set a selling price of $0.50/lb for this initial lot, and they project a lower selling price of about $0.30 for later production in large order sizes.

The success achieved in this first plant production is a major milestone since it makes available for the first time a PCM of good quality at a price that will provide an acceptable pay-back time to the homeowner.

**Evaluation of Fatty Acid Ester PCM for Solar Passive Applications.** In the event of a major crisis in the Mideast that could curtail the supply and escalate the price of petroleum, a renewable indigenous source, such as the fatty acid esters, could become of interest. For this reason, as well as to obtain background data on research elsewhere (e.g., Canadian Mines and Resources), we have determined the chemical composition and thermal energy storage properties of U.S. commercial grades of butyl stearate.

The chemical composition of the butyl stearate was determined by chromatographic analysis to be butyl stearate/butyl palmitate (67/33). The thermal energy storage properties were analyzed by DSC at several rates of heating and cooling. The butyl stearate was found to melt and freeze near 20°C and to store and release about 35 cal/gm. Esters with shorter side chains melt at somewhat higher temperatures (e.g., methyl ester, approximately 38°C).

To obtain an evaluation of the rate of temperature change effects in butyl stearate, we ran DSC measurements at 10, 5, 1, and 0.1°C/min rate of heating and cooling. The results were interesting in showing that like the alkyl hydrocarbon PCM, butyl stearate melting and freezing temperatures closely approach the same temperature (congruent) at slower rates of heating and cooling (e.g., 1.0 and 0.1°C/min). See Figure 6 for DSC graph and Figure 7 for rate of heating and cooling effects.

The "impure" grade of butyl stearate is projected to sell in the United States for about $0.70/lb. A purer grade obtained by distillation of the mixed esters is projected to sell for $1.10/lb. The fatty acid esters could undergo hydrolysis with long-term exposure in cementitious building materials, and they may also support mold growth. Further, the products can only cover a very limited range of temperatures. Thus, on the basis of overall cost/performance, the fatty acid esters are less desirable than the alkyl hydrocarbon PCM, unless petroleum should suddenly become less available and less competitive in price.

We have done, for the same reason as above, DSC analysis on three commercially available fatty acid esters from Japan that are derived from palm oil. These esters (Thermotops) can store and release thermal energy in the same limited range of temperatures as the esters from animal fats. However, because of their higher palmitic ester content, their thermal energy storage capacity is significantly lower.

**Fire Retardance of PCM Containing Materials.** Most of these experiments were directed at making PCM-imbibed plasterboards fire retardant. Chlorowax 70S and antimony oxide, the cheapest and most common fire retardants, are not soluble in hydrocarbon PCM and so cannot be used to fire retard plasterboard during incorporation of PCM by percolation. After examining a number of halogenated organic compounds from Ethyl Corporation and Great Lakes Corporation, Ethyl's BCL-462 (dibromoethyldibromocyclohexane) was found to be soluble with the hydrocarbon PCM in all proportions. This was considered a breakthrough; since, in combination with submicron particle-size antimony pentoxide, this has the potential of fire retarding plasterboards simultaneously with percolation of the PCM. Several

plasterboard samples percolated with Witco 45A/BCL-462 in the ratio of 75/25 showed improved fire retardance in laboratory experiments.

Encouraging fire retardance in imbibed plasterboard was also obtained using a soluble halogenated alkyl hydrocarbon from Ferro Chemical Company. Ferro's Bromochlor 50 was soluble in our PCM at room temperature, and their Bromochlor 70 at the standard 80°C percolation temperature. Further comparison experiments are planned to determine whether the Bromochlor fire retardants in combination with antimony oxide are equal or better than the BCL-462 with which we have more extensive experience. In follow-up experiments with the soluble fire retardant, BCL-462, it was found that up to 49% Witco 45A/BCL-462 combination can be incorporated in plasterboards by sequential percolation in PCM and BCL-462. By varying the duration and order of immersion, different ratios of these components can be incorporated in plasterboard. A number of these combinations showed potential for improved fire retardance.

In very recent experiments, we found that solubility of the fire retardant in the PCM is not a requirement if the sequential percolation method referred to above is used to adjust the amount of PCM absorbed as well as to preferentially locate the fire retardant on the surface.

From the Dow Chemical Company, we have obtained two phosphate ester fire retardant compounds, FYROL CPF (trichloroisopropyl phosphate) and FYROL CEF (trichloroethyl phosphate). Neither of these compounds are soluble in alkyl hydrocarbon PCM. In sequential percolation experiments, we found that we could control the PCM uptake by varying the PCM and FYROL percolation time. Best results were obtained with the FYROL CEF in that we obtained excellent resistance to initial ignition, quick extinction after the flame was removed, and little smoke or fumes emitted.

Experiments were also carried out to fire retard plasterboard by in-situ incorporation of insoluble (and cheaper) fire retardants during the manufacturing process.

In order to introduce fire retardants by the in-situ process, it was necessary to duplicate the commercial process to prepare low-density plasterboards. Preliminary experiments showed that it was possible to match the density of commercial plasterboards by adjusting the amount of foaming agent in the plaster formulation.

In parallel experiments, it was considered that it may be possible to fire retard plasterboards by lowering the amount of PCM absorption by using PCM diluted in a solvent as the imbibing medium. Accordingly, samples with varying PCM content from 2%-23% by weight were prepared by percolation of PCM in heptane or methylene chloride solvents. The samples containing 18% PCM extinguished in five seconds. This is a very encouraging development, since plasterboards with significant thermal energy storage and reduced flammability can be made by varying the solvent/PCM ratio to reduce the PCM content.

Subsequently, it was found that use of solvent diluent to limit PCM uptake could be avoided entirely. The plasterboard was first percolated for a very short time (e.g., one minute) to obtain about 20% composite weight PCM uptake, then followed by post heating to equilibrate the surface concentrated PCM throughout the interior of the board. Thereby, we obtained a lower and non-wicking average concentration

of PCM throughout the board. This is a very promising approach which should be followed up if there is continuing commercial interest in developing the percolation process.

Importantly, the approach of limiting the total quantity of PCM to below the critical level required to support combustion has also been investigated by our Japanese licensee using HDPE/PCM pellets incorporated into the wet mix of the plasterboard. They have evaluated the burning characteristics of plasterboard containing 20% and 40% wt of the PCM in the HDPE/PCM pellets with very encouraging results. At the lower PCM concentration, the plasterboards would not ignite. At the 40% PCM level, the plasterboard burned slower than plywood. Off-gas products were also monitored in their tests. Data obtained in their surface burning test is summarized in Table 3 and results of their box test in Table 4.

Another method of fire retarding plasterboard containing either imbibed or in-situ incorporated PCM was briefly investigated during the last quarter of the current contract period. We investigated the thermal energy storage properties of halogenated alkyl hydrocarbons (1-bromo octadecane and 1-bromo hexadecane) supplied by Humphrey Chemical Company. DSC analysis at 2°C/min showed the 1-bromo octadecane to melt and freeze at about 23°C and to have a heat of fusion and crystallization of about 42 cal/gram. This approach is interesting since the PCM would be composed entirely of an inherently fire retardant chemical. Unfortunately, this Humphrey chemical is also expensive and sells for about $3.08/lb, a price that would require an excessively long energy pay-back time if used for home heating and cooling applications.

In any continuing research, we therefore plan to place most emphasis on obtaining lower-but-useful concentrations of PCM in plasterboard, preferably by the in-situ HDPE/PCM pellet approach. However, we would also continue to develop the solvent-free imbibing of lower-but-useful PCM concentrations into plasterboard that can provide non-wicking fire retardant products.

We would continue to devote some effort to the sequential imbibing of PCM followed by imbibing of a fire retardant. In this approach, we would use sequential percolation in a second immersion bath consisting of the combination of a soluble halogenated fire retardant plus the submicron particle-size antimony oxide or an immersion bath of FYROL CEF (trichloroethyl phosphate).

**Further Developments on Containment Methods**

In further studies on permeation, it was possible to swell about 90% K-61 PCM and about 81% NP-15 in Marlex 6006 (10 m-rad). NP-15 melts and freezes below room temperature and can be potentially useful for cool storage and bridge deck deicing.

In the above experiments with NP-15 and HDPE pellets, it was observed that washing with poorer solvents (MEK > ethanol > methanol) increased the ultimate weight retained in the swelled pellets. This indicates that washing removes the swelled wax from the top layer of the pellets. This has been confirmed by DSC experiments from different layers of the swelled pellets.

The above observation about the removal of swelled wax by washing with MEK is of minor consequence for the pellets, but it has a major impact for the HDPE powders. We would like to imbibe HDPE powders with PCM since the small particle size of the powder would be less detrimental to the strength of the

building material. However, earlier work showed no PCM retained for HDPE powder swelled in Witco 45A at 150°C for two hours and washed with MEK. Followup work during this period with methanol rinsing showed substantially higher PCM weight retained for 45A imbibed into Marlex 6006 powder. Only minor effect of the level of gamma irradiation between 4-8 m-rad was noted on imbibed weight or DSC determination of PCM (provided the samples were washed with methanol). This conclusively proves that because of the smaller size, a good solvent like MEK washes away most of the imbibed PCM in powders. Further research is necessary to develop an effective gamma irradiation crosslinking process for HDPE powders that can subsequently be swelled to approximately 80% wt PCM.

The second method attempted is crosslinking of HDPE by chemical methods (e.g., peroxide and vinyl triethoxy silane). Some samples of LDPE, HDPE and polypropylene prepared by one or the other of these methods, and subsequently swelled in paraffinic hydrocarbon, have been tested by us for thermal energy storage and were found to contain up to 85% PCM hydrocarbon, an amount comparable to HDPE pellets crosslinked by gamma irradiation.

Prior work shows, potentially, the peroxide method will be cheaper than gamma irradiation. Accordingly, a series of samples were recently made by extrusion crosslinking with dicumyl peroxide at different concentration levels at Springborn Laboratories. Some of these also contained antimony pentoxide to simultaneously fire retard the pellets (after they are subsequently permeated with PCM/BCL-462 solution). Pellet sizes can also be adjusted to obtain smaller sizes. Further research on swelling of these pellets, analysis of thermal energy storage, and subsequent incorporation into building materials is planned.

In further efforts aimed at reducing the cost of the crosslinked HDPE/PCM pellets, we evaluated incorporating the PCM into the liquid melt of HDPE. By simply mixing the PCM into the molten HDPE at a temperature of about 150°C, we were able to incorporate up to 85% of composite weight of PCM. The melts were manually cut into pellets and later extruded to obtain small hard pellets that are apparently stable to room temperature thermocycling.

Significant cost savings can be realized in this process since the irradiation crosslinking is eliminated. This modification is claimed in patent applications, and should be further investigated in the continuing research.

The work was also directed to alternatives to the containment methods already described. One of the methods evaluated was microencapsulation. Preliminary data showed good encapsulation and thermal energy storage, but projected encapsulation costs are very high ($5.00-$10.00/lb).

**Stability of PCM to Melt/Free Cycling**

One of the most important criteria of PCM for use in Solar Passive heating and cooling of buildings is the ability to undergo many repeated cycles (e.g., 1000 times) of melting and freezing without degradation of thermal energy storage properties. To test the stability of the alkyl hydrocarbon PCM to such thermocycling, samples of the PCM, PCM in HDPE pellets, and PCM in building materials were placed in small glass vials in an automated oven and cycled between -20°C and +80°C for 1000 cycles.

This thermocycling portion of this experiment has been completed. The preliminary results were very encouraging, since there was no visually apparent degradation of the PCM themselves or the building products containing them. The HDPE/PCM pellets showed little or no oozing out of the pellets. There was no visible PCM "running out" of imbibed (percolated) plasterboard samples. DSC analysis of the products was scheduled but not completed due to unavailability of contract funds. The samples are stored, and therefore could still be analyzed if the necessary funds become available.

**Technology Transfer to Industry**

Transfer of the PCM technology to the building products industry was continued throughout the current contract period. A technical presentation made at the 20th Intersociety Energy Conversion Engineering Conference (IECEC) in August 1985 led to many subsequent inquiries. We have placed our principal (almost entire) effort on interesting the large manufacturers of plasterboard here in the United States. The potential for use of the PCM in concrete was also evaluated to some extent and should be further investigated.

We did demonstrations of the wet mix HDPE/PCM pellet process and imbibing "percolation" process in the laboratories of United States Gypsum Corporation (USG) and the National Gypsum Company (NGC).

We received an option offer from USG that we did not accept. The offer was later withdrawn after USG went through extensive restructuring and cutbacks in personnel and research funding.

During the last year, we have had an active research program with NGC to work with them in a joint program to evaluate the HDPE/PCM pellets incorporation into the wet mix of plasterboard and imbibing (percolation) into finished plasterboard. This work is still continuing and is nearing a decision that will be determined by the projected economics (energy saving pay-back time). The work was supported entirely by NGC and details are therefore proprietary. However, NGC's Senior Vice President, Joe Keller, has expressed stronger interest in the HDPE/pellet process for many reasons (little added capital equipment, easier to fire retard, etc.).

During the last quarter of 1988 under a new DOE initiative funded through ORNL and monitored by Mr. John Tomlinson, we have begun a new research program to scale-up the immersion imbibing process. Facilities were set up at ORNL for imbibing full-size 4-ft x 8-ft plasterboard sheets in three thicknesses (1/4-in, 1/2-in, and 5/8-in), and to three levels of PCM concentrations of 30, 20, and 15% composite weight. The imbibing was successfully completed on January 19 and 20 at ORNL. See Table 5 for representative data. The imbibed plasterboards were received at UDRI on January 24, and the specified aging stability tests are now in progress. The tests will be completed in the second quarter of 1989. There have been no unanticipated problems in the project to date. The objective of the research is to determine whether there will be any running out of the PCM from the eight-foot sheets stored vertically at 100°F and to determine whether there is any redistribution or other changes in the imbibed PCM in thermocycling under conditons that simulate diurnal temperature cycling of the PCM-containing plasterboard in use. Successful completion

of the series of tests is expected to encourage a plasterboard manufacturer to pick up and commercialize this technology.

**Spin-off Applications of the PCM Technology**

During the current contract period, we have also investigated with separate funding the potential of the alkyl hydrocarbon PCM for applications other than for heating and cooling of houses.

The use of the PCM in tableware for keeping hot foods and drinks at the correct temperature, cold foods cold, is of strong interest to two separate industrial organizations. An option/license agreement is anticipated to be finalized in the very near future.

Another application for the alkyl hydrocarbon PCM technology is in medical therapy (hot packs and cold packs). Four companies are currently interested in this technology.

A combination of an insulative PCM "wrap" for citrus tree trunks to prevent overnight freezing is also of current interest to a large Florida manufacturer of frost protection products.

Other potential applications include preventing overnight freezing of bridge decks, PCM-containing textiles, and waterproofing of cementitious materials (concrete, plasterboard, etc.).

We have negotiated a license for the phase change technology with a large Japanese enterprise that is exclusive for Japan and excludes the North American continent. They expect to have their first products on the market early in 1989.

## Conclusions

Taken together with the prior DOE/UDRI sponsored research, the linear alkyl hydrocarbon phase change materials (PCM) defined in this program constitute a major breakthrough in thermal energy storage materials for the human comfort temperature range (e.g., 73-77°F) and for temperatures immediately above and below this.

It is unlikely that PCM which are more cost-effective than the linear alkyl hydrocarbons derived from petroleum refining ($0.50/lb, 35 cal/gm) for home heating and cooling applications can be found. Importantly, these PCM are non-toxic and stable to hydrolysis, thermocycling, and prolonged storage.

It is also unlikely that PCM having equal or higher thermal energy storage than the ultra pure C-18 linear alkyl hydrocarbons derived from polymerization of ethylene ($1.86 to $10.00/lb, 50-60 cal/gm) for the near ambient temperatures can be found at any price.

To anticipate the future possibility of an acute petroleum shortage, alternate PCM from renewable resources (e.g., fatty acid esters) have also been evaluated and methods of "containment" developed for them. Until such a shortage of petroleum raw material develops, the fatty acid esters are second best to the alkyl hydrocarbon PCM by a considerable margin because of their higher cost, lower storage capacity, susceptability to hydrolysis, limited temperature range and limited adaptability to blending to achieve exact melting and freezing temperatures.

Of both theoretical and practical interest, we have obtained differential scanning calorimeter data on an extensive series of ultrapure (98% to 99%) alkyl hydrocarbons and on synthesized blends of these pure

PCM. We found pronounced secondary solid-state transitions early in odd-number carbon chains (e.g., C-9) and later (e.g., C-22) in even-number carbon atom chains. We have also determined the effect of rate of heating and cooling on the measured melting and freezing temperatures of pure alkyl hydrocarbons, commercial products (which are blends), and fatty acid esters. Importantly, these data establish clearly that the alkyl hydrocarbon PCM melt and freeze congruently at rates of heating and cooling that are well within the range of temperature change that would be encountered in actual applications. Additionally, it was found that commercial paraffins that are blends of up to four chain lengths nonetheless melt and freeze sharply at the temperature predicted from their average chain length, provided the blends are nearest "neighbors" in the homologous series. This single melting temperature is of critical importance to the use of the lower cost commercial alkyl hydrocarbon PCM blends derived from petroleum refining.

Practical processes have been defined and demonstrated whereby these PCM can be incorporated into building construction materials including plasterboard and concrete. Currently, incorporating PCM in the form of HDPE/PCM pellets into the wet mix of plaster is preferred over the imbibing (percolating) into finished plasterboard. If either PCM process technology can be successfully commercialized in the United States, major energy conservation should result with significant attendant benefits including reducing U.S dependence on imported oil and diminishing the $CO_2$ "greenhouse" effect. Commercialization of the technology for home heating and other applications now appears certain to occur this year (1989) in Japan but will occur later in the United States.

The problem of fire retardance in plasterboards containing the alkyl hydrocarbon PCM has been addressed effectively, but much further research remains to be done. Regulating the PCM content to a level that will not support combustion (about 20% composite weight) appears to be the most practical solution but may require use of thicker plasterboards (e.g., 5/8" or 3/4") to supply adequate storage. However, effective fire retardant additives were also defined, as well as processes for incorporating them into plasterboard.

There have been several important potential spin-offs of the technology for other applications including tableware, medical hot and cold wraps, and insulative wraps to prevent overnight freezing of citrus tree trunks. These applications can and probably will be commercialized in the United States soon, and well before the use of the PCM for heating and cooling of residential buildings.

Other spin-offs of the technology that are further from commercialization include preventing the overnight freezing of highway bridge decks, textile wearing apparel, and waterproofing of concrete.

Comprehensive patent applications covering important aspects of the phase change technology have been filed in both the United States and abroad. There are five issued U.S. patents and several more pending. One foreign license has been negotiated, and several U.S. licenses are in the negotiation stage.

## Recommendations for Future Research

**Phase Change Material Containment**

As described in the Introduction, we have developed four different methods or processes for containing linear alkyl hydrocarbon phase change materials (PCM) in cementitious products for solar passive heating and cooling of residential buildings. The process of greatest current interest for commercialization in plasterboard is the one wherein HDPE/PCM pellets are incorporated into the wet mix of plaster and concrete. The process of continuing but secondary interest is where the PCM is incorporated into the plasterboard or concrete by immersion into liquid PCM (imbibing, percolation). We believe further research and development on both processes, in collaboration with plasterboard and concrete building materials manufacturers, is necessary.

**Chemical Crosslinking**

We have in prior research evaluated the use of vinyl triethoxy silane (VTES) coupling agent as a method to crosslink high-density polyethylene and polypropylene. This modification, after hydrolysis crosslinking, should result in Si-O crosslinks that could provide strong adhesive bonding to plaster and concrete, and thereby significantly enhance the physical properties of the product. We recommend that this alternate crosslinking be reevaluated to determine its relative merit and cost effectiveness compared to electron-beam or gamma-irradiation crosslinking.

**PCM In Uncrosslinked Polyethylene**

We have in recent research found that it may be possible to incorporate the PCM into uncrosslinked HDPE pellets with significant reductions in raw material costs effected thereby. We recommend further investigation of this lower cost process be undertaken in any continuing research.

**Fire Retardance**

Another important issue that requires continuing research is that of fire retardance. The relative merit of the two approaches (reducing the PCM content below that which will support combustion and fire retardant additives) needs significant further research and development, including large-scale fire tests.

**PCM in Concrete Building Materials**

Primarily at the direction of our DOE Contract Monitor, the principal and almost exclusive emphasis in the research during the last two contract periods was placed on developing methods (processes) for incorporating the alkyl hydrocarbon PCM into plasterboard. Concrete and hollow-core concrete blocks are also major building materials for use in residential housing. Due to the mass of concrete building materials, a small percentage of PCM by weight (e.g., 5%) can achieve equivalent or greater storage than 35% wt in plasterboard. Additionally, depending on the process used, the concrete can be simultaneously waterproofed as in plasterboard.

In view of the above, we recommend that further investigation of the use of alkyl hydrocarbon PCM in various forms of concrete building materials, especially hollow-core concrete blocks, be included in continuing DOE-sponsored research.

**Alternative to PCM From Petroleum**

Whether they are obtained from petroleum refining operations or the polymerization of ethylene, the ultimate source of the current alkyl hydrocarbon PCM is fossil fuels (petroleum and natural gas). There is no question, at the present rate of consumption, these resources will gradually become depleted. The question is exactly when will the total world demand exceed the total world supply by a significant amount. There is also no doubt when this occurs, the resulting crisis will be an order of magnitude greater than the short-lived OPEC-generated shortage in 1977. At that future time, the price of hydrocarbon raw materials will rapidly escalate toward the selling price of more-valuable-than-fuel products made from them.

Since the above scenario is certain to occur, it is strongly recommended that the study of alternate PCM from non-fossil fuel resources, we have already briefly investigated, be continued and expanded. The fatty acid esters, alcohols, and saturated hydrocarbons which can be derived from these indigenous renewable resources should receive intensive effort in continuing DOE-sponsored research to develop the most cost-effective systems.

**Technology Transfer and Commercialization**

The PCM technology is at a critical state of development insofar as transfer of the technology to U.S. industry for heating and cooling of buildings is concerned. The principal issue to be resolved is economic pay-back time in energy cost savings.

Government assistance would materially speed transfer of the PCM technology through demonstrating unequivocably the energy savings and added comfort of the PCM installed in one or more houses. Theoretical analysis now scheduled will not convince the homeowner to undergo the added expense of the PCM system. Preferably, two identical houses should be built in two or three selected climate zones in the United States in which families can live for a two-year cycle, interchanging after the first year; all energy costs would be monitored and the added "comfort" features evaluated. With these data, the economic pay-back time can be accurately determined and cost effectiveness established with certainty.

Upon completion, most of the government's investment could be recovered through sale of the houses.

## References


1. Salyer, Ival O. and Donovan S. Duvall, "Passive Phase Change Materials for Use in Passive and Hybrid Solar Heating and Cooling Systems," Proceedings of the Passive and Hybrid Solar Energy Storage Update, Washington D.C., September 26-28, 1983.

2. Salyer, Ival O. and Donovan S. Duvall, "Phase Change Materials for Use in Passive and Hybrid Solar Heating and Cooling," Interim Report DOE Contract DE-ACOZ-82-CE-30755, November 1983.

3. Salyer, Ival O., Donovan S. Duvall, Charles W. Griffen, Steven P. Molnar, Richard P. Chartoff, and Daniel E. Miller, "Advanced Phase Change Materials for Passive Solar Storage Applications," Proceedings of the Passive and Hybrid Solar Energy Update, September 5-7, 1984.

4. Salyer, Ival O., Anil K. Sircar, Richard P. Chartoff, "Advanced Phase Change Materials for Passive Solar Storage Applications," Proceedings of the Solar Buildings Conference, Washington D.C., March 18-20, 1985.

5. Salyer, Ival O., Anil K. Sircar, Richard P. Chartoff, and Daniel E. Miller, "Advanced Phase Change Materials for Passive Solar Storage Applications, Proceedings of the 20th Intersociety Energy Conversion, Engineering Conference, Miami Beach, Florida, August 18-23, 1985.

6. Salyer, Ival O., Anil K. Sircar, and Richard P. Chartoff, "Analysis of Paraffinic Hydrocarbons for Thermal Energy Storage," Proceedings of the 15th North American Thermal Analysis Society Conference, Cincinnati, Ohio, September 12-14, 1986.

Table 1. DSC analysis of thermal energy storage of paraffinic hydrocarbons (Humphrey Chemical Company).

| Sample Identification and Composition | $T_m$ (°C) | $T_c$ (°C) | $T_m - T_c$ (°C) | $\Delta H_f$ (cal/gm) | $\Delta H_c$ (cal/gm) |
|---|---|---|---|---|---|
| n-Nonane $C_9H_{20}$ | | | | | |
| Primary | -50.4 | -57.4 | 7.0 | 33.1 | 31.5 |
| Secondary | -53.8 | -60.3 | 6.5 | 11.0 | 11.4 |
| n-Decane $C_{10}H_{22}$ | -25.8 | -36.0 | 10.2 | 50.2 | 47.8 |
| n-Undecane $C_{11}H_{24}$ | | | | | |
| Primary | -21.5 | -30.2 | 8.7 | 36.0 | 35.8 |
| Secondary | -35.3 | -40.3 | 5.0 | 11.1 | 9.9 |
| n-Dodecane $C_{12}H_{26}$ | -6.9 | -15.5 | 8.6 | 52.4 | 51.3 |
| n-Tridecane $C_{13}H_{28}$ | | | | | |
| Primary | -5.0 | -8.8 | 3.8 | 38.7 | 38.5 |
| Secondary | -18.5 | -21.7 | 3.2 | 9.5 | 9.8 |
| n-Tetradecane $C_{14}H_{30}$ | 9.0 | -0.2 | 9.2 | 55.6 | 55.6 |
| n-Pentadecane $C_{15}H_{32}$ | | | | | |
| Primary | 12.5 | 4.8 | 7.7 | 38.6 | 42.7 |
| Secondary | -1.1 | -6.5 | 5.4 | 13.2 | 9.6 |
| n-Hexadecane $C_{16}H_{34}$ | 21.1 | 12.2 | 8.9 | 56.5 | 56.5 |
| n-Heptadecane $C_{17}H_{36}$ | | | | | |
| Primary | 25.0 | 16.5 | 8.5 | 42.3 | 43.8 |
| Secondary | 12.7 | 6.9 | 5.8 | 13.7 | 12.3 |
| n-Octadecane $C_{18}H_{38}$ | 31.2 | 22.0 | 9.2 | 59.1 | 58.7 |
| n-Nonadecane $C_{19}H_{40}$ | | | | | |
| Primary | 34.4 | 26.4 | 8.0 | 42.6 | 43.8 |
| Secondary | 23.9 | 18.3 | 5.6 | 14.9 | 13.7 |
| n-Eicosane $C_{20}H_{42}$ | | | | | |
| Primary | 39.0 | 31.3 | 7.7 | 60.8 | 60.8 |
| Secondary | None | 29.9 | --- | None | Small |
| n-Heneicosane $C_{21}H_{44}$ | | | | | |
| Primary | 42.3 | 35.9 | 6.4 | 39.9 | 45.5 |
| Secondary | 31.4 | 29.7 | 1.7 | 19.0 | 13.6 |
| n-Docosane $C_{22}H_{46}$ | | | | | |
| Primary | 45.9 | 38.8 | 7.1 | 56.0 | 55.6 |
| Secondary | None | 35.6 | --- | | |

Table 2. DSC analysis of K-61 Kenwax 18 at 2°C/min (Witco Chemical Company).

| RUN NO. | $T_m$ (°C) | $T_c$ (°C) | $T_m - T_c$ (°C) | $\Delta H_f$ (cal/gm) | $\Delta H_c$ (cal/gm) |
|---|---|---|---|---|---|
| 1. Primary | -1.82 | -5.22 | 3.40 | 4.24 | 4.22 |
| Secondary | 26.50 | 23.94 | 2.56 | 35.91 | 38.71 |
| 2. Primary | -2.44 | -5.51 | 3.07 | 4.61 | 4.04 |
| Secondary | 26.60 | 23.63 | 2.97 | 38.92 | 37.75 |
| 3. Primary | -2.80 | -5.70 | 2.90 | 4.34 | 4.08 |
| Secondary | 25.66 | 23.44 | 2.22 | 36.03 | 38.33 |
| Average | | | | | |
| Primary | -2.35 | -5.48 | 3.12 | 4.40 | 4.11 |
| Secondary | 26.25 | 23.67 | 2.58 | 36.95 | 38.26 |

Table 3. Results of surface test.

| ITEM | Test Piece A | B | C | D |
|---|---|---|---|---|
| Ignitability (min) | 1.1 | 2.2 | 6< | 6< |
| Exothem (°C min) | 659 | 310 | 0 | 0 |
| Extinguish time (sec) | 120 < | 120 < | 0 | 0 |
| $CO_2$ Concentration (%) | 0.234 | 0.147 | 0.119 | 0.106 |

A Plywood.....12mm
B PCM Board No. 1 (Contains 40% PCM pellets).....12mm
C PCM Board No. 2 (Contains 20% PCM pellets).....12mm
D Gypsum Board.....12mm

Table 4. Results of box test.

| ITEM | | Test Piece E | F | G |
|---|---|---|---|---|
| Max Temp | (min) | 680 | 700 | 355 |
| Max Exotherm Rate | (kj sec) | 119.5 | 75.8 | 110.0 |
| Total Exotherm Heat | (kj) | 67700 | 53100 | 39900 |
| $CO_2$ Concentration | (%) | 0.681 | 0.326 | 0.412 |
| CO Concentration | (%) | 0.00243 | 0.00142 | 0.00028 |

E Plywood.....12mm
F PCM Board No. 1 (contains 40% PCM pellets.....12mm
G Gypsum Board.....12mm

Table 5. USG plasterboards imbibed with C-18; Oak Ridge National Laboratory, January 19-20, 1989.

| Plasterboard No. | Thickness (in) | Immersion Bath Temp. (°F) | Immersion Time (min) | (sec) | Initial Board Wt. (lbs) | Final Board Wt. (lbs) | Weight PCM In Board (lbs) | Composite Weight (%) | Plasterboard BTU/ft$^2$ |
|---|---|---|---|---|---|---|---|---|---|
| A-1 | 1/4 | 178 | 7 | 0 | 37.00 | 51.500 | 14.500 | 28.2 | 36.70 |
| A-5 | 1/4 | 177 | 1 | 5 | 37.00 | 46.250 | 9.250 | 20.0 | 23.40 |
| A-7 | 1/4 | 176 | 0 | 40 | 37.00 | 43.500 | 6.500 | 14.9 | 16.45 |
| B-1 | 1/2 | 175 | 10 | 0 | 58.25 | 83.000 | 24.750 | 29.8 | 62.64 |
| B-6 | 1/2 | 174 | 2 | 42 | 58.25 | 72.500 | 14.250 | 19.4 | 36.07 |
| B-12 | 1/2 | 173 | 1 | 38 | 57.00 | 67.125 | 10.125 | 15.0 | 25.62 |
| C-1 | 5/8 | 175 | 30 | 0 | 73.75 | 106.230 | 32.500 | 30.6 | 82.26 |
| C-5 | 5/8 | 174 | 3 | 55 | 74.00 | 92.000 | 18.000 | 19.6 | 45.56 |
| C-9 | 5/8 | 175 | 2 | 5 | 74.00 | 86.750 | 12.750 | 14.7 | 32.27 |

1. Calculation based on thermal energy storage of C-18 = 45cal/gm x 1.8 = 81 BTU/lb.

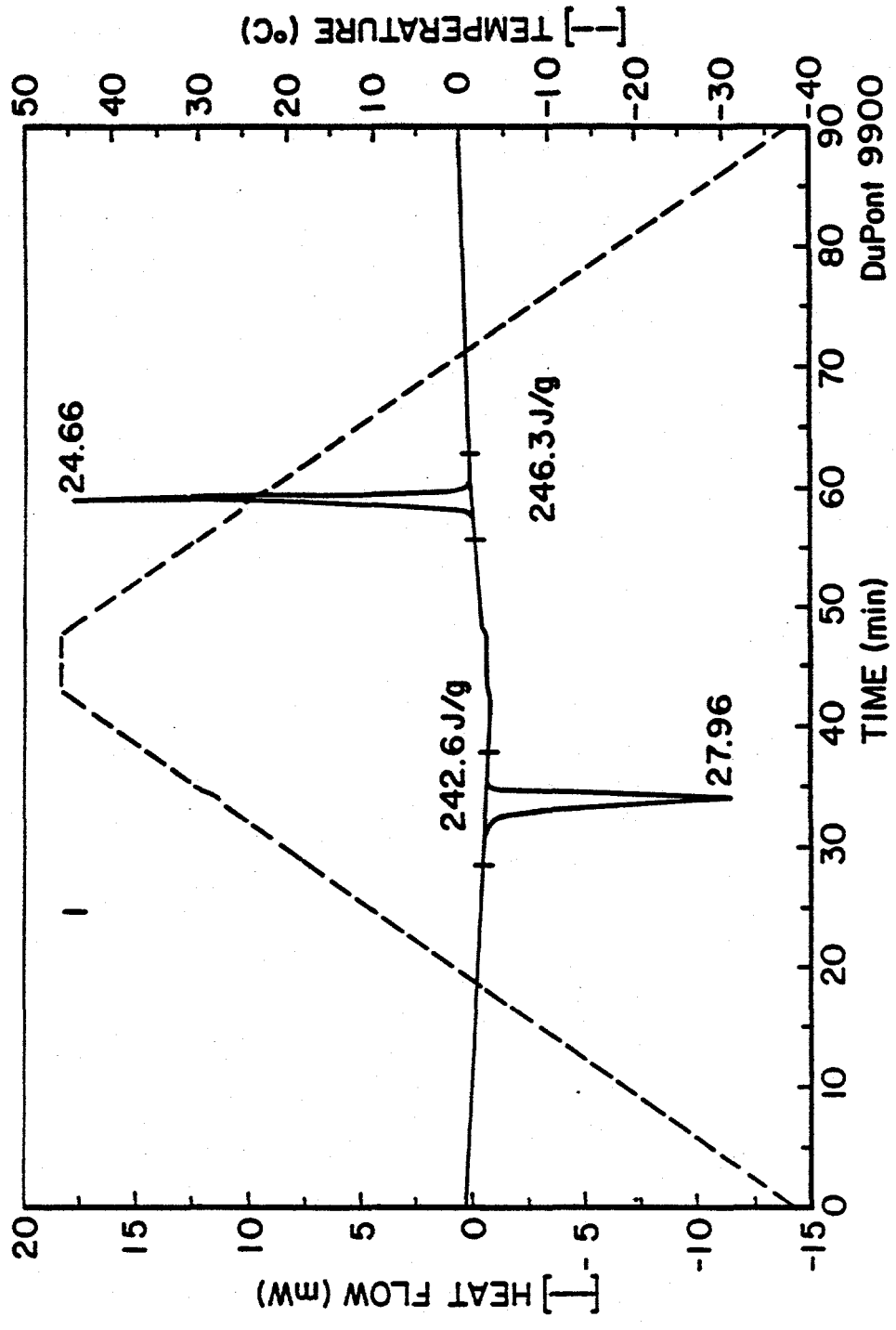


Figure 1. DSC analysis of n-octadecane at 2°C/min.

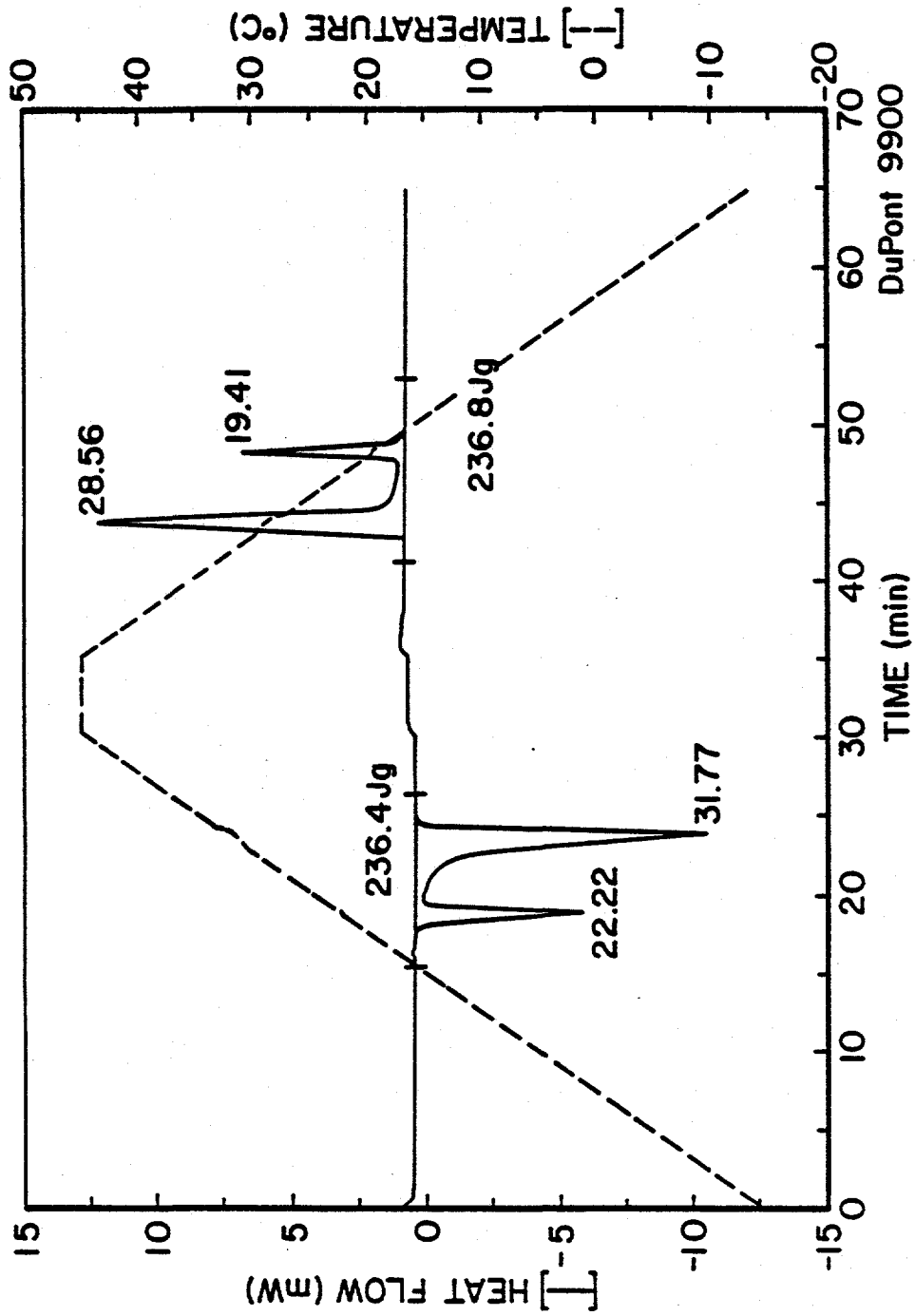


Figure 2. DSC analysis of n-nonadecane at 2°C/min.

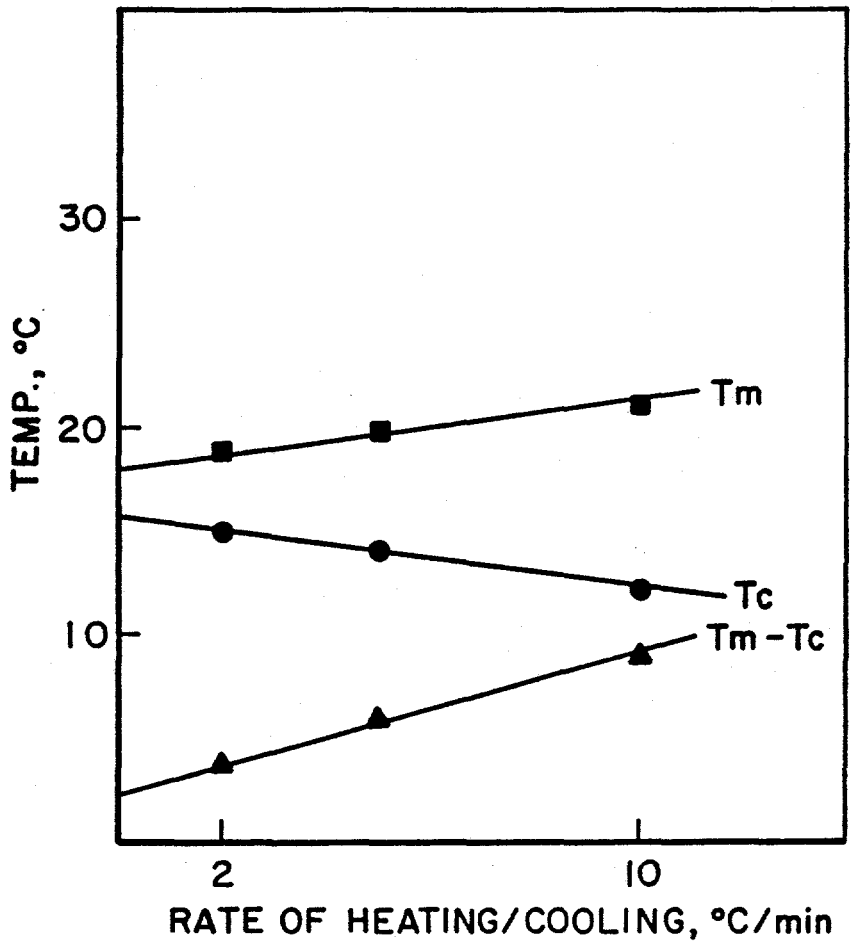


Figure 3. Effect of rate of temperature change *vs* melting and crystallization temperature of n-hexadecane.

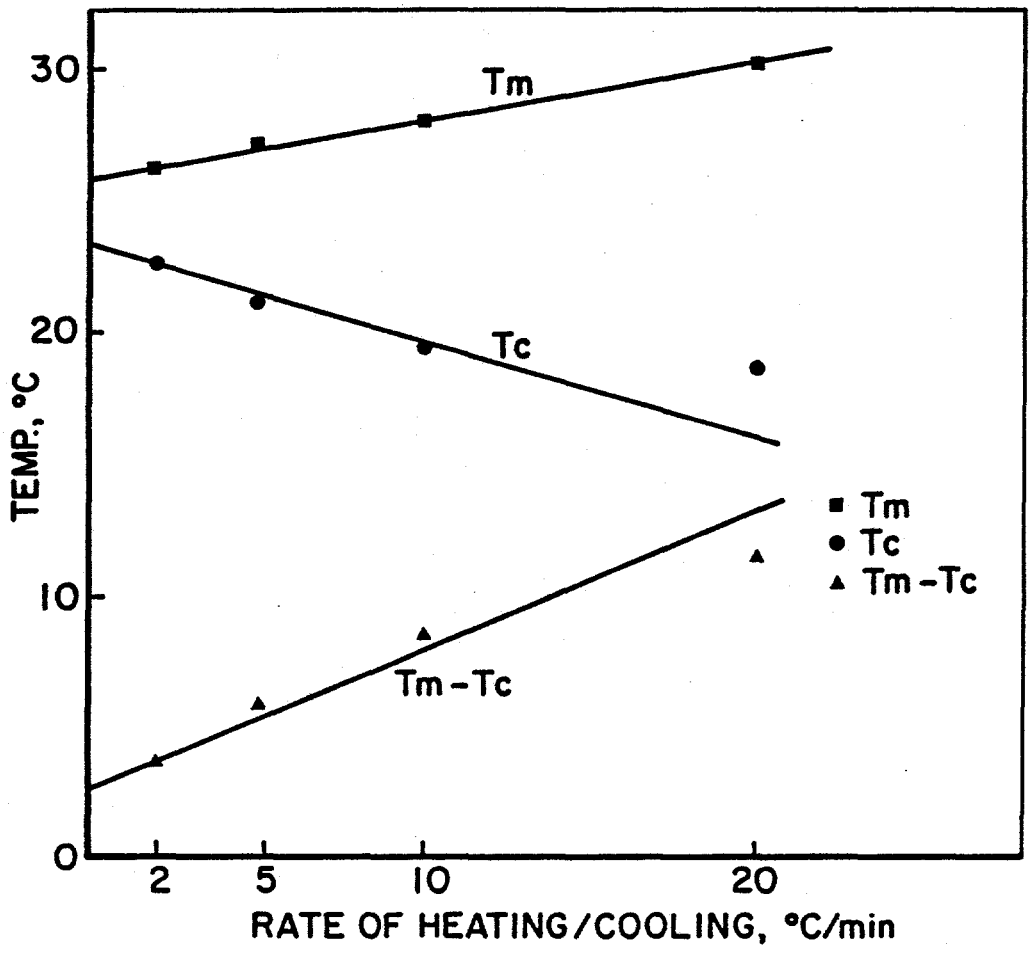


Figure 4. Effect of rate of temperature change *vs* melting and crystallization temperature of Humphrey technical grade n-octadecane.

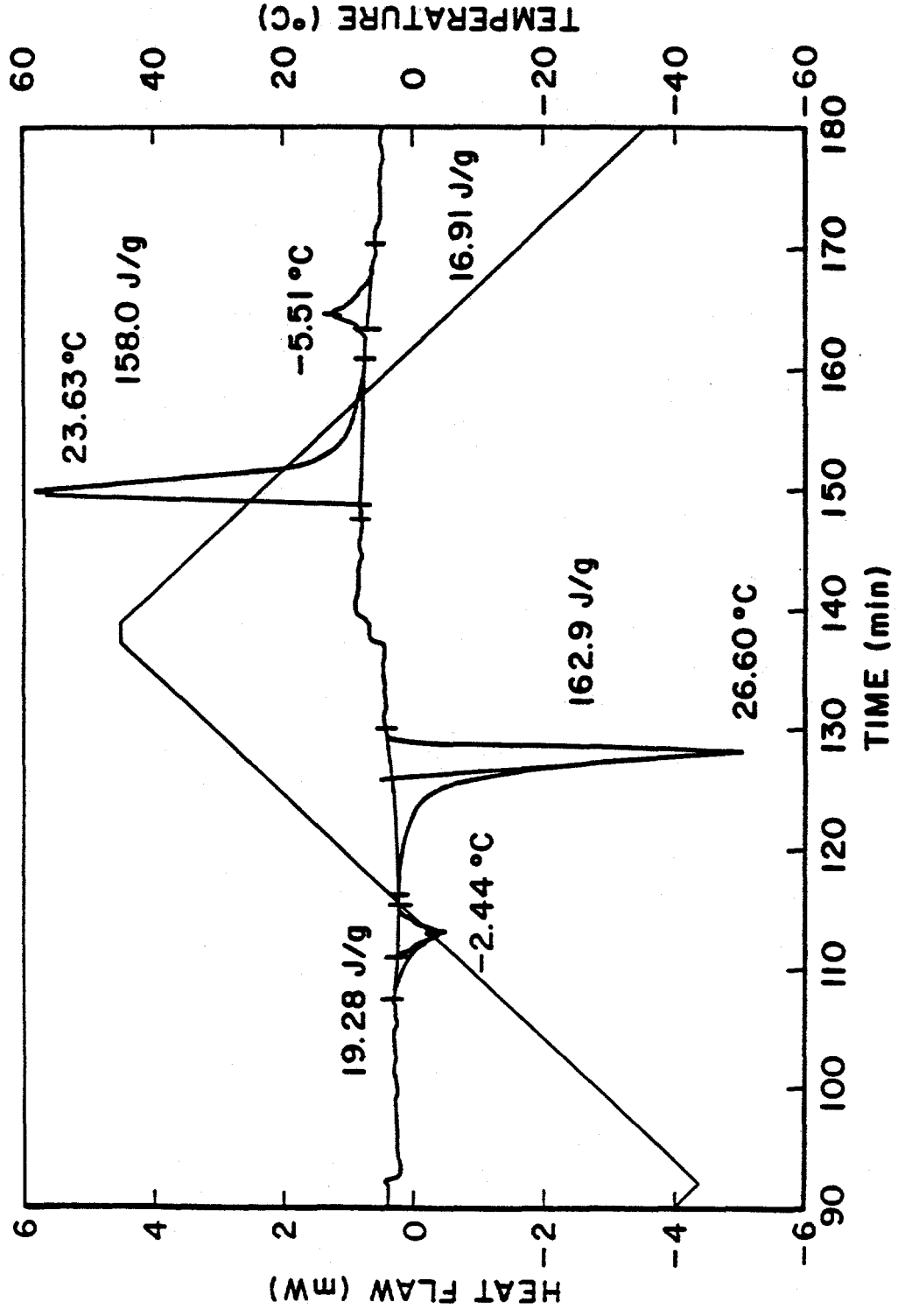


Figure 5. DSC analysis of Witco K-61 at heating and cooling rate of 2°C/min.

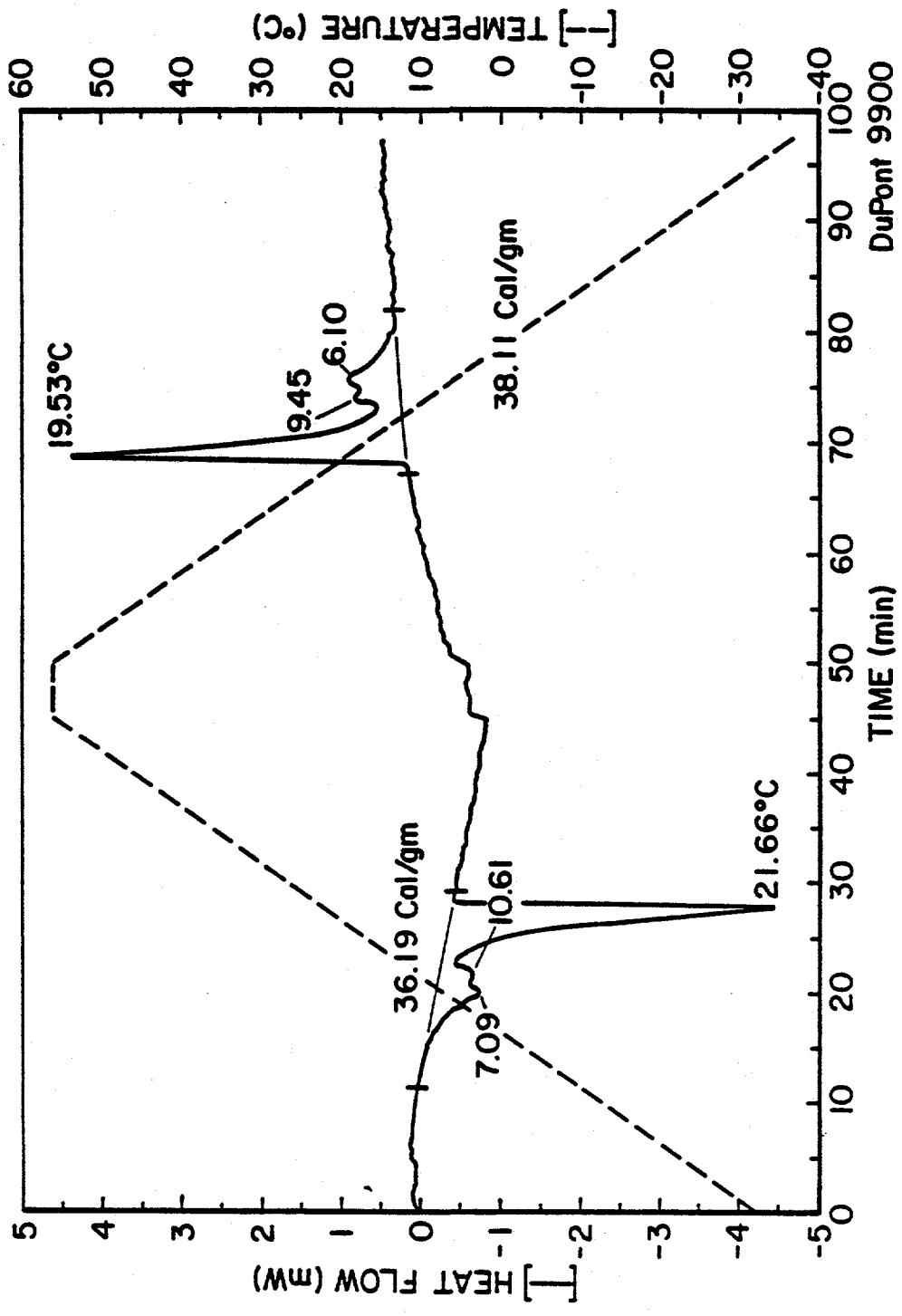


Figure 6. DSC analysis of butyl stearate at 2°C/min heating and cooling rate.

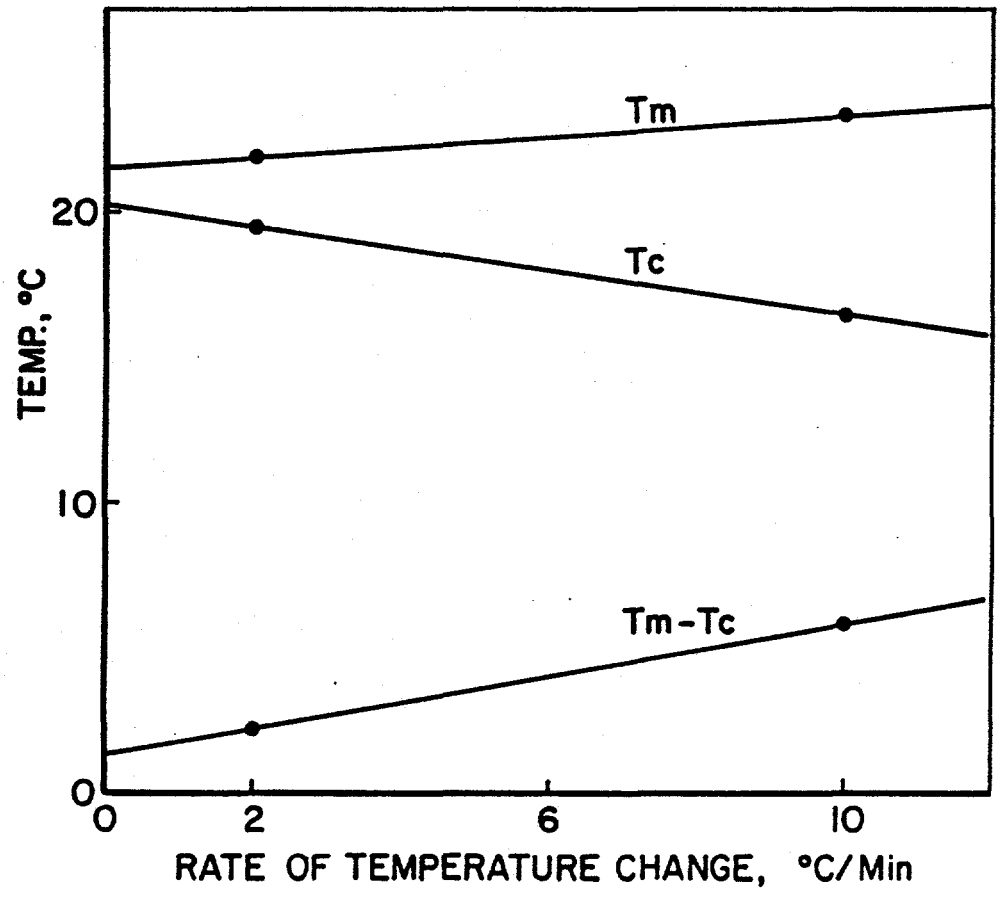


Figure 7. Rate of heating and cooling *vs* melting and crystallization temperature of butyl stearate.

# COMPUTER AND GRAPHICS MODELING OF HEAT TRANSFER AND PHASE CHANGE IN A WALL WITH RANDOMLY IMBIBED PCM

**Alan D. Solomon**
Consultant
Omer, Israel

***Abstract***

*We describe the theoretical basis and computer implementation of a simulation code for heat transfer and phase change in a rectangular 2-dimensional region in which PCM has been randomly placed with a preassigned volume fraction.*

## Introduction

Phase change and heat transfer processes in phase change materials (PCM's) can be modeled, in certain cases, by explicitly known expressions for temperature distribution and phase change front location with time [1]. For a broader class of processes analytical approximations are available [1]; however, these methods must be used cautiously for they are capable of yielding physically unrealistic predictions of thermal behavior [2]. Moreover, explicit solutions and analytical approximations are of only very limited help for more general boundary conditions, resulting in cycling of phase change states as it is seen in typical thermal storage situations [3]. Hence, numerical simulation is called for as the "ultimate" mathematical tool for analyzing the possible performance of a PCM-based thermal storage system, buttressed of course, by a parallel experimental effort.

The most effective means for numerical simulation of heat transfer and phase change processes in a PCM, for general boundary conditions and arbitrary (1-3) space dimensionality, is the so-called weak solution or enthalpy method [4,1]. This approach eliminates the need to pay explicit attention to the location of the front(s) separating liquid and solid regions and is based on local energy balances for control volumes into which the region of interest is subdivided. The thermal state of each control volume is "updated" through successive time steps enabling us to predict the evolution of the region beginning with some user-input initial state. Previous applications of this approach to storage situations include space station power system storage [3,6], passive thermal storage for a building structure [5], binary alloy solidification processes [7], solidification of super-cooled liquid [8] and pulsed laser annealing of silicon [9].

In recent years, significant progress in storage methodologies has resulted in our being able to impregnate certain matrix materials with phase change materials [10]. This progress has made it reasonable to raise the question of how a PCM-imbibed matrix structure would perform thermally in a passive storage

environment. If the PCM is uniformly mixed with the matrix material, then the simulation of thermal performance can be performed via an enthalpy method applied to an imaginary material whose thermo-physical properties are mass averaged values of those of the components, with some allowance taken for thermal conductivity. For a PCM-imbibed material this is no longer reasonable, for the PCM now appears in the form of "lumps" of relatively large size, distributed randomly amidst the matrix. For a wallboard, the PCM might be thought of as occupying the voids and having an average relatively large minimum size. Modeling such a body cannot be done by the above methods, for these would not account, for example, for the possible streaming of heat around the finite, isolated PCM lumps. Similarly, the PCM lumps are not small enough for us to be able to ignore the time-dependent phase change processes occurring in them.

The present project arose from our wish to develop an enthalpy approach to the numerical simulation of a body consisting of randomly located "lumps" of PCM in a sensible heat matrix. With the wallboard application in mind, the code WALL89 was prepared for a two-dimensional rectangular region. Boundary conditions were to be sufficiently general time-dependent conditions, and an initial user assigned PCM volume fraction was to be included. With the aim of making a tool whose use would be attractive to workers in the field, the code was designed to have "user-friendly" input and execution and is available on floppy disks in executable form. Similarly an executable, BASIC-language version was prepared with graphics output. In the next section, we describe the use of the code and its capabilities; while a fuller description of the code mechanics is found in the Appendix.

## Current Results

Consider a rectangular region containing a sensible heat "matrix" material (SHM). Such a region might represent a wallboard with gypsum serving as the matrix material. Into the rectangle, we randomly place a phase change material (PCM), in such a way that in its final configuration the wall appears with the SHM containing interspersed "lumps" of the PCM. At each of the four faces of the region, we are able to assign time dependent boundary conditions of the form,

$$\text{flux in} = \text{convective flux} + \text{direct gain},$$

where convective flux is defined by time varying heat transfer coefficient and ambient temperature, and direct gain is defined by a time-varying flux function. An imposed face temperature is described by setting the heat transfer coefficient equal to infinity (its reciprocal equal to zero).

WALL89 operates in two steps. The first is to distribute the PCM randomly in the rectangle according to user supplied values of PCM volume fraction and "minimal" PCM lump size. Then, for a given uniform initial temperature and phase state WALL89 will calculate the temperature and phase state distribution of the rectangle as they vary over a user-input time interval, beginning with the initial state. Thus, at all future times, the code can output the temperature at every point of the rectangle, the phase state of the PCM at every point at which PCM is located, the surface temperature, surface heat fluxes, and global energy

balances. Distinct runs for the same PCM volume fraction will produce different PCM distributions, enabling us to determine statistical properties of the wallboard performance.

WALL88 is available on diskettes in both source and executable forms, in both FORTRAN and Microsoft BASIC language versions. The BASIC language version includes graphics capabilities making it possible to visually track temperature profiles and PCM states with passing time during a program "run". The executable codes have been prepared for an IBM compatible computer.

## Conclusions

WALL88 is a tool enabling us to examine the possible performance of a rectangular region of a SHM with imbibed PCM. It is the first heat transfer code having this capability and as such can serve as a test bed for examining a number of extremely fascinating questions related to the thermal performance of such a body. Among such questions the following are currently under study:

1. What is the effect of "lump size" and PCM volume fraction on the thermo-physical properties of such a SHM/PCM combination? In particular, is there a "critical" volume fraction demarcating a PCM-like behavior and a SHM-like behavior? Preliminary studies for the case of a one-phase melting or freezing problem in a dimensionless form have led us to believe that there is.

2. What is the "equivalent insulation value" of a wallboard with imbibed PCM for various PCM volume fraction values? This question goes to the heart of the ultimate utility of such a wallboard in building passive thermal control.

## References

1. A. Solomon, V. Alexiades and D.G. Wilson, The mathematical modeling of melting and freezing processes, Hemisphere Press (to appear, 1989).

2. A. Solomon, On the limitations of analytical approximations for phase change problems with large Biot numbers, Letters in Heat and Mass Transfer 8 (1981), 475-482.

3. A. Solomon, M. Morris, M. Olszewski and J. Martin, The development of a simulation code for a latent heat thermal energy storage system in a space station, ORNL-6213, 1986.

4. A. Solomon, Some remarks on the Stefan problem, Mathematics of Computation 20 (1966), 347-360.

5. A. Solomon, G. Geist and C. Serbin, PCMSOL-1, A computer simulation code for a direct gain passive solar structure, Parts I, II, ORNL/CSD-127, 1984.

6. R. Wichner, J. Drake, G. Giles and A. Solomon, Thermal analysis of heat storage canisters for a solar dynamic space power system, Proceedings of the ASME Solar Energy Division Conference, April 1988.

7. V. Alexiades, A. Solomon and D.G. Wilson, Macroscopic global modeling of binary alloy solidification processes, Quarterly of Applied Mathematics 43 (1985), 143-158.

8. A. Solomon, D.G. Wilson and J. Kerper, An enthalpy method for the solidification of a supercooled liquid, ORNL-6217, 1986.

9. R. Woods, et al, Modeling of undercooling, nucleation, and multiple phase front formation in pulsed-laser melted amorphous silicon, pp. 159-168 in Materials Research Society Symposium Proceedings 35, 1985.

10. I. Salyer, Development of PCM-imbibed wallboard, these proceedings.

## Appendix

WALL89 is based on a subdivision of the rectangular region into small rectangular "control volumes." The control volume size is to be equal to or less than the "minimal lump size" of the PCM. The code begins by randomly distributing "lumps" among the control volumes in such a way that the final PCM volume fraction is equal to the desired user-input volume fraction value. This is done by an iteration procedure linked to a bisection method for volume fraction. The randomness of the method is based on the use of the computer random number generator, whose seed is linked to the real time clock of the system, guaranteeing that for the same volume fraction different PCM distributions will be generated for different runs. Each control volume consists either of PCM or SHM.

Heat transfer and phase change processes are simulated by using the enthalpy (specific internal energy) as the key state variable to be updated. The enthalpy-temperature relations are different for SHM and PCM. However temperature is continuous, with temperature gradients driving heat transfer. Thus, internal energy is used to keep track of the thermal state of each control volume, while temperatures of control volumes drive internal energy changes. In updating the system state over a time interval, the boundary conditions drive heat into or out of the region, and conduction within the region alters the internal energy in each control volume. The enthalpy-temperature relation is then used to update the temperature in each control volume, whereupon we are able to update the system again.

The numerical method used in WALL89 is a variant of an implicit numerical scheme due to Ockendon and Elliott [1]. The scheme is unconditionally stable for all time/space step combinations, but for high levels of accuracy requires small control volume sizes. Actual "runs" of the code may take anywhere from minutes to hours depending on the desired accuracy and run duration. The code contains a "rerun" feature that allows the user to continue an earlier run from the point at which it ended, with its final state as the initial state for a subsequent run.

# SELF-RELEASING SUBMERGED ICE MAKER

**W.E. Stewart, Jr., M.E. Greer, and L.A. Stickler**
Energy Research Laboratory
Mechanical and Aerospace Engineering Dept.
University of Missouri-Columbia/Kansas City
Truman Campus
Independence, MO 64050

***Abstract***

*This study reports the results of a series of experiments which investigated a thermal storage technology whereby slush ice is grown on a submerged cold surface and the resultant growth of slush ice releases without auxiliary thermal or mechanical means. The process investigated consists of growing slush ice from an electrolyte solution of low molarity. The cold surface (substrate) upon which the slush ice forms is submerged in the bulk solution. As the buoyancy force on the ice crystals exceeds the adhesion to the cold surface, the slush ice is forced from the substrate and floats away, to the top of the solution. The results of this study reveal the relative insensitivity of the growth rate of ice crystals to solution initial bulk concentration over the range of values tested and to concentration of electrolyte during accumulation of ice crystals. The critical parameter appears to be substrate temperature, which generally cannot be less than approximately 2°C below the freezing point temperature of the solution, as apparent adhesion increases rapidly with decreasing substrate temperature.*

## Introduction

The project described in this report concerns the testing of a submerged cold plate type of ice-maker, where the water being frozen to ice is actually an electrolytic solution. The electrolytic solution, when frozen by the submerged cold plate surface, has the characteristic of reduced adhesion/cohesion between the cold plate surface and the resulting "ice".

The reduced adhesion/cohesion between the "ice", in slush form, and the cold surface (substrate) eliminates the need for any type of ice harvesting technique. The harvesting technique usually employed in ice-makers, utilized for thermal energy storage purposes, is that of hot gas defrost. Hot gas defrost entails directing refrigerant gas from the compressor outlet to the evaporator, upon which ice has formed. The hot refrigerant gas then warms the evaporator, melting the ice at the ice/evaporator surface interface, allowing the ice to be removed, such as by gravity and fall into a holding tank below the evaporators. A similar harvesting technique would be required if the evaporator or other cold surface was submerged in the water.

If the adhesion/cohesion of the ice is reduced such that the slush "ice" mass self-releases due to gravity, buoyancy, or other forces (or a combination of forces), the energy cost of harvesting the ice is eliminated.

The energy cost of harvesting typically amounts to 10-20% of operating costs for a commercial ice-maker. This process whereby adhesion/cohesion is reduced has been employed for both suspended cold surfaces and evaporators where the solution is allowed to flow over the surface and for submerged cold surfaces (patent pending).

For the situation of concern here, a submerged cold surface (substrate) is used to grow an "ice" mass; and the buoyancy forces on the "ice" mass overcome the apparent adhesion forces and hence forces the mass from the cold surface, accomplishing a cyclic, periodic growth and self-release process. The "ice" mass is physically a mixture of essentially pure ice and concentrated electrolytic solution contained in the grain boundaries of the ice crystal, though some ions may be incorporated into the ice crystals' structure, replacing water molecules. There is also a strong attraction between the small ice crystals formed and the rejected solution, since the resulting "ice" mass is an interconnected mass of ice crystals and concentrated solution. When a sample of "ice" mass is removed from the bulk solution used to form the "ice", drainage of part of the solution surrounding ice crystals occurs; but the "ice" mass retains liquid, similar in appearance to partly melted crushed ice.

The obvious explanations of reduced adhesion include the rejection of solute, which forms concentrated solution between and adjoining the ice crystals and the substrate. This thereby reduces the effective area of contact between ice and the substrate and the adhesion and/or cohesion between the ice and substrate. Several other mechanisms could be responsible, in part, for the greatly reduced adhesion/cohesion.

This project involved an effort to characterize the rate of ice production as a function of solute concentration, substrate material, and rate of heat removal (heat flux) through the substrate. Also the ability of the technique to generate a reservoir full of "ice" was tested. The experiments used in the testing of self-releasing ice from a cold plate submerged under approximately four feet of solution include:

1. Determining the effect on ice release/production characteristics of:

   - different $Ca(NO_3)_2$ concentrations,
   - different cooling rates, and
   - different substrate material; and

2. Determining the concentration of solute throughout the solution column and in the "ice" while:

   - completely filling the column with ice,
   - melting a full tank of ice, and
   - melting ice at the same rate as it is formed.

One series of tests, Series A, included experiments completed in the laboratory at room temperature. A stainless steel plate was used as the substrate during the course of this set of experiments. The second series of tests, Series B, were conducted with the test column in an environmental chamber operated at a temperature of 5°C or less. The substrate used during these experiments consisted of a stainless steel plate with a nylon based coating approximately 0.1mm thick. A total of 15 runs were completed under Series A test conditions, and 13 under Series B.

The test apparatus, shown in Figure 1, was constructed of Lexan. The inner column held solution, while the outer column served to insulate the solution. A thin, two-sided vertical plate arrangement, which was situated in the center of the inner column, was devised for the tests. Two different plates were used during the course of the tests, these were sheet metal bent into the configuration shown in Figure 2.

The inside surface of the substrates was cooled by pumping either an alcohol-water mixture (50/50 by volume) or ethylene glycol and water mixture (50/50 by volume) through piping extending from the bottom of the plates up into the interior. A cooled alcohol-water mixture was pumped through the outer box surrounding the test column to act as an insulate.

Those tests designated as Series B were conducted with the test column in an environmental chamber at a temperature below 5°C. This test system is shown in Figure 3, the guard coolant was replaced with styrofoam beads. During initial runs, ice grew across and adhered to the mounting screws at the plate edges. To counter this problem, a strip heater consisting of nichrome wire inside Tygon tubing was attached to the sides of the plate and the bottom edge of the plate. The wire was connected to a power supply which allowed the current and voltage in the heater to be monitored. A flow meter was installed in the coolant line to monitor the rate of heat removal through the plate. Thermocouples were positioned near the bottom, middle, and top of the solution in the test column, in the coolant lines at the plate, and in the guard coolant box and environmental chamber.

A calorimetric analysis was performed on the "ice" in the column by the following procedure. After a predetermined test period, the "ice" that had accumulated at the top of the column from self-release was removed with the aid of a strainer; and the ice, along with solution present in the ice, placed in a chilled beaker. The total ice mass sample was weighed and placed in a vacuum bottle. An amount of hot water, close in weight to that of the ice removed, had previously been weighed, its temperature measured with a thermometer and recorded, and placed in the vacuum bottle. The mixture of ice and hot water was magnetically stirred until the ice melted. The temperatures of the melt and of the solution at the top of the column at the time the ice was extracted were recorded using the same device. This procedure was conducted in the laboratory at room temperature for Series A tests and in the environmental chamber for Series B tests.

The "ice" mass was calculated from

$$m_i h_{if} + m_s C_{pw} (T_m - T_s) = m_{hw} C_{pw} (T_{hw} - T_m) \quad (1)$$

The use of this equation assumes the solution to have the same specific heat and heat of fusion as pure water. Tap water was used to melt the ice in the first three tests; deionized water was used in the remainder.

In most cases, the total amount of "ice" mass collected from the column was melted to determine the amount of solid ice present. In the others, only a portion of the ice collected was melted. The amount of solid ice, $m_i$, present in that portion of "ice" that was melted was calculated using Eq. (1). This amount was divided by the "ice" mass melted, $m_s$, to obtain the fraction of solid ice. The total amount of solid ice

was then found by multiplying this mass fraction by the total amount of ice that had been collected and weighed.

The amount of heat removed form the solution by the substrate to produce ice is

$$Q_{ice} = \frac{m_i h_{if}}{(t)} \tag{2}$$

The total mass of solid ice, $m_i$, is found from Eq. (1) or Eq. (2); the latent heat of fusion of the ice is represented by $h_{if}$, and the run time used in the equation is in seconds.

The rate of ice production is calculated as

$$\text{Ice production} = \frac{m_i\ (0.0022046\ \text{lb/g})}{(A)(t)} \tag{3}$$

The heat removed by the substrate was determined from the measured temperature increase across the plate and the flow rate to the plate.

Heat gains to the system are calculated as

$$Q_{gain} = Q_{sub} - Q_{ice} - Q_{htr} \tag{4}$$

Where $Q_{htr}$ pertains only to those runs of Series B and represents the heat input from the strip heater on the plate.

The concentration of electrolyte in the ice of the "ice" mass was calculated from a mass concentration balance on the "ice" mass removed from the column and melted in a vacuum bottle,

$$m_m C_m = m_i C_i + (m_s - m_i)\ C_{sol} \tag{5}$$

The concentration of solution in the ice was assumed as the average concentration of the solution at the top of the column. A conductivity reading of the melt yielded its concentration, $C_m$.

In the three runs in which tap water was used to melt the ice instead of deionized water (which yields a conductivity reading of zero), the concentration of ice was calculated from

$$m_m C_m = m_i C_i + (m_s - m_i)\ C_{sol} + m_{tw}\ C_{tw} \tag{6}$$

This equation accounts for the impurities in the water.

In runs 10-12 of Series B, conductivity readings of ice were taken with a probe immersed in a sample of melted ice. This small sample was taken from the total amount collected from the column after it had been weighed. The concentration of electrolyte in the ice was calculated from

$$C_s = \frac{m_i}{m_s} C_i + \frac{(m_s - M_i)}{m_s} \cdot C_{sol} \tag{7}$$

The amount of real ice, $m_i$ as found from Eq. (1), was based on the mass of the sample left after the portion to be used in making a conductivity measurement was subtracted from the total mass removed from the column.

The efforts extended in this research have resulted in the confirmation that the process and method of producing self-releasing ice works over an extended period of time. Also the production of ice appears to be somewhat independent of the substrate material, somewhat dependent upon the solvent (tap or distilled

water), apparently independent of the heat removal rate, strongly dependent upon substrate temperature, and somewhat independent of solute concentration.

Due to the limitations of a very small experimental fixture, test results as a function of the independent parameters are not clearly definitive.

## Current Results

The experiments performed allowed the observation of the ice production processes, the establishment of the long term ability of the process to effect periodic self-releasing ice, and the measurement of ice production rates for varying solute concentration, heat removal rate, and the use of tap or deionized water as the solvent. Other parameters investigated include solute concentration (conductivity), stratification in the test solution column, and the concentration of solute in "ice" mass samples.

Tabulated lists of all the experimental conditions and data obtained from the experiments in Series A and B tests are given in Tables I, II, and III. Also shown in the tables are calculated data based upon measured data. All three tables include data for the 23 runs, indicating different data in the three tables. The measured amount of "ice" produced is given in the fifth column of Table II as $Q_{ice}$. The amount of ice produced should, of course, be a linear function of the heat removed through the cold surface (substrate), given as $Q_{sub}$ in Table II, less the guard heater energy ($Q_{htr}$) and extraneous heat gains ($Q_{gain}$).

Of course, all of the heat removed at the plate does not contribute to the final mass of "ice" produced. After a steady-state condition of periodic ice growth and self-release cycle is established, part of the heat removed at the plate can be attributed to cooling the solution to the freezing (melting) point temperature, the removal of heat gains through the contact of the plate (substrate) to the test fixture, heat gains to the test solution at the top, bottom, and sides of the test solution column, and replacing an amount of ice that may have melted during the period of the test run.

Several attempts were made to calculate $Q_{gain}$ from heat balances on the test fixture. Calculating the heat transfer between the guard solution and test solution in the Series A experiments and the heat transfer through the insulation at the top and bottom of the test column revealed a wide disparity in comparison to the value of $Q_{gain}$ in Table II. Hence, reliable calculated values of $Q_{gain}$ are not given; and the value of $Q_{gain}$ in Table II is essentially only a deduced value from measured values, or $Q_{sub}$-$Q_{ice}$-$Q_{htr}$. Since there was little variation in the guard solution and test solution temperatures during the Series A experiments, there does not appear to be an explanation for the wide variation in $Q_{gain}$. This discrepancy, especially between runs of Series A, appears to more directly related to the larger temperature differential and a lower flow rate of substrate coolant across the substrate. This large heat gain for Runs1 through 15 of Series A may indicate a large heat gain at the bottom of the test column, though this area was insulated in the same manner as Runs 5 through 10. This effect is shown in the much greater values of $Q_{sub}$ for Runs 11 through 15 but with ice production greatly decreased. As a result, the net heat flux through the substrate available to produce ice is unknown; and as shown in Fig. 4, there is little apparent correlation between measured ice production and the net heat removed from the substrate plate ($Q_{sub}$). These large discrepancies are due

to the large variations in heat gains to the test solution and substrate coolant, due in part to the relatively small substrate surface area in comparison to the test fixture.

The discrepancy of $Q_{ice}$ between runs inside and outside of the environmental chamber are seen in Figure 5. The group of 6 data in the upper left and the group of 5 on the right are for runs outside of the environmental chamber, while the group in the lower center are for the runs in the chamber.

It was observed during the experiments that the adhesion of the "ice" mass appears to be a strong function of the substrate temperature. Lower substrate temperatures should increase ice production but also increase adhesion. The lower substrate temperature increases the adhesion/cohesion forces to such an extent as to be greater than the buoyancy forces that effect self-release of the "ice" mass. The substrate temperature hence governs the balance between growth rate of the "ice" mass to a certain size and the sufficiently low adhesion to effect self-release. It may be possible to grow very small crystals that continuously release (noticed in most runs at the edges of the substrate or on the outer surface of the "ice" mass) rather than a large "ice" mass.

As shown in Fig. 6, the highest ice production was achieved at the smaller temperature differentials of the substrate coolant. Though there is not a consistent trend in this regard, lower temperature differentials imply a more nearly uniform temperature across the substrate which probably has more effect upon the release of ice than the actual temperature differential. The smaller temperature differentials also, of course, make it much more prone to errors in measurement of the differentials.

The typical growth characteristic during these tests of the "ice" mass was such that the "ice" mass will grow to approximately 5mm in thickness and then self-release. From this behavior it is apparent that as the "ice" mass increases in thickness, the percentage volume of ice in the "ice" mass increases, otherwise individual ice crystals or very small "ice" masses should release almost instantaneously upon formation. This increase in percent volume of ice in the "ice" mass increases with increasing thickness of the "ice" mass, which increases the buoyancy forces until self-release occurs. On the other hand, if the substrate temperature is lowered below some critical value, the adhesion at the substrate and/or the cohesion between crystals increases as to exceed the buoyancy force. For these cases, at the relatively cool substrate temperatures, the "ice" mass will grow but not self-release and eventually reaches a "steady-state" ice thickness, on the order of 12mm for the range of experimental conditions investigated. Within the temperature limitations of the physical processes affecting the apparent adhesion and/or cohesion of the "ice" mass at the "ice" mass/substrate interface, the production of ice and self-release has been shown to perform on a continuous basis. Two tests were performed where the column was substantially filled with ice; and the increase in concentration of electrolyte did not appear to appreciably affect the self-release process.

As suspected and confirmed in this study, the most critical parameter governing the self-release of "ice" is the temperature of the cold substrate surface. The secondary effects of extraneous heat gains, test solution temperature, solution concentrations, and parallel temperature gradients on the substrate (to prevent edge effects) control the overall rate of ice production.

The apparent (active) area of the cold substrate used in these experiments is relatively small in area in relation to the total area of the substrate. Extraneous heat gains were sometimes as large or larger than the heat removed to actually produce ice. This disparity in magnitudes of heat fluxes, of course, allows for substantial uncertainty in the measurement of efficiency of ice production. Also, as the "ice" mass floats to the top of the solution column, an unknown amount of melting can occur, with corresponding change in the percentage of mass of ice crystals in the "ice" mass.

As the "ice" mass forms, rejection of the electrolyte occurs. Due to the measured differences in solute concentration in samples of the "ice" mass and the bulk solution, diffusive and convective mass transfer from the "ice" mass to the bulk solution of the electrolyte is also probable, especially as the "ice" mass floats to the top of the column, These processes would be very difficult to account for with the apparatus used in these experiments.

The requirement for a closely controlled, nearly constant substrate temperature over a very narrow range, prescribes limitations on the methods of cooling the substrate. In order to achieve reliable self-release, the temperature gradient across the substrate surface should be as negligible as possible. To achieve this near zero gradient, a refrigerant evaporator that would be nearly completely flooded may be required to achieve a near zero temperature gradient in the refrigerant. The height of the evaporator may have to be limited such that there are no temperature (pressure) gradients within the liquid refrigerant.

The alternative of using a secondary liquid to cool the substrate, as used in these experiments, may be the most easily controlled method. It would be relatively easy to control the entering substrate coolant temperature, but flow rates would need to be large so that decreases in liquid temperature from inlet to outlet of the substrate were not substantial.

## Conclusions

The mechanisms governing the growth and self-release of the "ice" mass appear to be quite complex and probably involve, in part, temperature and concentration gradients between the substrate and the bulk solution, electrochemical potentials at the ice/substrate interface and between the ice and surrounding solution, differential mass transfer of the electrolyte, differential incorporation of ions into the ice crystals, and other interdependent mechanisms.

The "macro" effect of all these underlying mechanisms is though, that under certain restrictions, self-release of ice occurs; and the periodic self-release process performs reliably (pat. pend.). For ice-harvesting types of ice-makers for thermal energy storage applications, both experiments essentially filled the test solution column indicating the practical, long-term ability and usefulness of the self-release method and process. The density of ice crystals in the "filled" column was estimated to be approximately 25%, as opposed to some reported commercially obtainable densities for harvesting types of ice-makers on the order of 40 to 50%. The trade-off between the decrease in operating costs due to the increase in thermal efficiency (higher low-side temperature and no harvest energy) would necessarily have to be balanced against larger storage volumes. Also the requirement of increased total substrate surface area, due to lower

temperature differentials and decreased ice production rates per unit area, would result in higher initial equipment cost and would have to be balanced against lower operating costs.

## Reference

1. Jellinek, H.H.G., (1975), "Adhesion of Ice Frozen from Dilute Electrolyte Solutions," ACSSymposium Series, Vol. 8, pp. 248-260.

## Nomenclature

| | |
|---|---|
| $A$ | area of substrate covered by "ice" - $cm^2$ |
| $A_d$ | adhesive force of "ice" - $N/m^2$ |
| $c_{pw}$ | specific heat of water - J/g°C |
| $C_{hw}$ | concentration of hot water - M |
| $C_i$ | concentration of solid ice - M |
| $C_m$ | concentration of melted "ice"" and hot water - M |
| $C_s$ | concentration of melted "ice" sample - M |
| $C_{sol}$ | concentration of solution in "ice" sample - M |
| $\varepsilon$ | fraction of solution in "ice" sample - g/g |
| $F_B$ | buoyant force on "ice" - N |
| $h_{if}$ | latent heat of fusion of ice - J/g |
| $m_{hw}$ | mass of hot water - g |
| $m_m$ | mass of mixed melted "ice" and hot water - g |
| $m_s$ | mass of melted "ice" sample - g |
| $m_{TOT}$ | total mass of "ice" sample collected - g |
| $m$ | mass flow rate of coolant - kg/min |
| $Q_{htr}$ | heat input from strip heater - W |
| $Q_{ice}$ | heat value of ice produced - W |
| $Q_{gain}$ | heat gain to the system - W |
| $Q_{sub}$ | heat removed by substrate - W |
| $T$ | run time duration - sec |
| $T_{hw}$ | temperature of hot water - °C |
| $T_m$ | mixed temperature of melted "ice" and hot water - °C |
| $T_s$ | temperature of "ice" mass - °C |
| $\rho_{ice}$ | density of ice at 0°C - $g/cm^3$ |
| $\rho_{sol}$ | density of solution at 0°C - $g/cm^3$ |
| $\Delta T$ | substrate coolant temperature differential - °C |

## Appendix A - Estimates of Adhesion Forces

As the buoyancy forces on the "ice" mass are very small, measurement of the force required to release ice growth would be difficult, especially at the substrate near the bottom of the solution column. The apparent surface area of the "ice" mass on the substrate changed form one run to another as did the volume of the "ice" mass from run to run. This was primarily due to changing plates, coolants, and ambient conditions.

An indication of the adhesion/cohesion forces at the substrate/ice interface can be found from the approximate measurement of the apparent surface area of the "ice" in contact with the substrate, the volume of the "ice" mass at release, and the percent by volume of ice crystals in the "ice" mass.

The buoyancy force on the "ice" mass will be approximately

$$F_B = (\rho_{ice} - \rho_{sol})Vg\varepsilon$$

where $\rho_{ice}$ and $\rho_{sol}$ are the densities of pure ice and solution, respectively; V is the volume of the "ice" mass; g acceleration of gravity; and $\varepsilon$ the fraction of ice crystals by volume in the "ice" mass.

The adhesion force is $F_B$ divided by the apparent area of contact, A, between the substrate (plate) and the "ice" mass,

$$A_d = F_B/A$$

These calculations were performed based upon, in part, the data in Table 3, for values of $\varepsilon$. Since the precise values of $\varepsilon$ were difficult to determine experimentally, calculated values were used. The values of $\varepsilon$, typically 0.23 to 0.50 may be up to 50% larger than actually existed at the plate surface, due to drainage of the ice sample before the mass of ice crystals in the sample was determined. Also it was assumed, though the "ice" mass is typically convex lens shaped, that the average thickness was approximately 0.3175 cm (1/8-inch).

The results are shown in Table IV. The calculated adhesion forces, $A_d$, though not uniform throughout the runs, are fairly consistent. Most importantly, the values of $A_d$ reveal the relative magnitude of the adhesion, ~1 N/m$^2$. This compares to the adhesion of pure ice on clean aluminum of ~800,000 N/M$^2$ and ~425,000 N/m$^2$ on wax-treated aluminum (Jellinek, 1975).

Table 1. Experimental data.

| | | MEASURED TEMPERATURES (°C) | | | | | | | | | | |
|---|---|---|---|---|---|---|---|---|---|---|---|---|
| | | SUBSTRATE | | GUARD COLUMN | | | | TEST COLUMN | | | | |
| DATE | RUN | COOLANT INLET | COOLANT OUTLET | COOLANT CHILLER | UPPER AVG. | LOWER AVG. | AVG. | BOTTOM AVG. | MIDDLE AVG. | TOP AVG. | AVG. | SUBSTRATE MATL* |
| SERIES A | | | | | | | | | | | | |
| 6/14 | 5 | | | -2.9 | -2.11 | -2.15 | -2.13 | -1.63 | -1.10 | -0.97 | -1.23 | S.S. |
| 6/15 | 6 | | | -3.0 | -1.56 | -1.58 | -1.57 | -1.33 | -1.19 | -0.99 | -1.17 | " |
| 6/16 | 7 | | | -3.0 | -1.53 | -1.58 | -1.56 | -1.48 | -1.12 | -0.91 | -1.17 | " |
| 6/29 | 8 | | | -3.0 | -1.21 | -1.22 | -1.22 | -1.18 | -0.80 | -0.82 | -0.93 | " |
| 7/1 | 9 | | | -3.0 | -1.54 | -1.50 | -1.52 | -1.36 | -1.18 | -1.15 | -1.23 | " |
| 7/3 | 10 | | | | -1.02 | -1.08 | -1.05 | -0.92 | -0.83 | -0.79 | -0.85 | " |
| 7/8 | 11 | | | -2.7 | -1.32 | -1.32 | -1.32 | -1.06 | -1.13 | -1.04 | -1.08 | " |
| 7/12 | 12 | | | -2.7 | -1.28 | -1.28 | -1.28 | -1.18 | -1.13 | -1.11 | -1.14 | " |
| 7/15 | 13 | | | -2.7 | -1.32 | -1.29 | -1.31 | -1.08 | -1.09 | -1.07 | -1.08 | " |
| 7/16 | 14 | | | -2.7 | -1.37 | -1.34 | -1.36 | -1.22 | -1.17 | -1.16 | -1.18 | " |
| 7/18 | 15 | | | -2.5 | -1.39 | -1.35 | -1.37 | -0.98 | -1.08 | -1.15 | -1.07 | " |
| SERIES B | | | | | | | | | | | | |
| 8/17 | 1 | -2.46 | -2.41 | -2.7 | | | | -0.69 | -0.52 | -0.80 | -0.67 | R |
| 8/18 | 2 | -2.48 | -2.43 | -2.7 | | | | -0.95 | -0.82 | -0.98 | -0.91 | " |
| 8/18 | 3 | -2.47 | -2.42 | -2.7 | | | | -0.86 | -1.00 | -0.99 | -0.95 | " |
| 8/19 | 4 | -2.47 | -2.43 | -2.7 | | | | -0.90 | -1.01 | -1.03 | -0.98 | " |
| 8/19 | 5 | -2.52 | -2.48 | -2.9 | | | | -0.93 | -0.98 | -1.00 | -0.97 | " |
| 8/24 | 6 | -2.44 | -2.36 | -2.9 | | | | -1.04 | -0.82 | -0.81 | -0.89 | " |
| 8/25 | 7 | -2.46 | -2.40 | -2.9 | | | | -1.12 | -0.98 | -1.00 | -1.03 | " |
| 8/26 | 8 | -2.66 | -2.59 | -2.9 | | | | -1.40 | -1.19 | -1.27 | -1.29 | " |
| 10/28 | 9 | -2.08 | -2.00 | -2.5 | | | | -0.40 | -0.33 | -0.78 | -0.50 | " |
| 11/7 | 10 | -2.02 | -1.94 | -2.4 | | | | -0.48 | -0.39 | -0.84 | -0.57 | " |
| 11/10 | 11 | -2.31 | -2.23 | -2.6 | | | | -0.91 | -0.84 | -1.19 | -0.96 | " |
| 11/11 | 12 | -2.31 | -2.25 | -2.6 | | | | -0.99 | -0.99 | -1.20 | -1.06 | " |

*S.S. - stainless steel substrate
R - Rilsan coated stainles steel substrate

Table 2. Experimental and calculated data; Part 1.

| DATE | RUN | ICE PRODUCTION ($kg/m^2$-hr) | $q_{ice}$ (W) | $q_{sub}$ (W) | $q_{htr}$ (W) | SUBSTRATE $q_{gain}$ MEAS. (W) | SUBSTRATE SOLID ICE (%) | SUBSTRATE COOLANT FLOWRATE (l/min) | SUBSTRATE T AVG. (°C) | RUN TIME (hrs) | INITIAL TEST SOLUTION CONC* (M) |
|---|---|---|---|---|---|---|---|---|---|---|---|
| SERIES A | | | | | | | | | | | |
| 6/14 | 5 | 1.75 | 6.90 | 5.96 | NA | -0.94 | 23.6 | 5.75 | 0.017 | 2.0 | 0.25 T |
| 6/15 | 6 | 1.09 | 4.15 | 4.27 | NA | -0.12 | 25.4 | 2.80 | 0.025 | 2.0 | 0.25 T |
| 6/16 | 7 | 1.14 | 4.51 | 6.57 | NA | 2.06 | 43.3 | 4.31 | 0.025 | 2.0 | 0.25 T |
| 6/29 | 8 | 1.23 | 4.83 | 8.82 | NA | 3.99 | 37.6 | 5.79 | 0.025 | 2.0 | 0.25 D |
| 7/1 | 9 | 1.59 | 6.25 | 8.65 | NA | 2.40 | 26.9 | 5.79 | 0.025 | 2.0 | 0.30 D |
| 7/3 | 10 | 1.17 | 4.62 | 3.02 | NA | -1.60 | 37.0 | 5.83 | 0.013 | 2.0 | 0.20 D |
| 7/8 | 11 | 0.67 | 2.66 | 18.50 | NA | 15.85 | 29.7 | 2.23 | 0.136 | 3.0 | 0.25 D |
| 7/12 | 12 | 0.47 | 0.98 | 16.30 | NA | 15.32 | 23.0 | 2.04 | 0.130 | 4.0 | 0.25 D |
| 7/15 | 13 | 0.71 | 1.49 | 16.30 | NA | 14.81 | 29.4 | 2.12 | 0.130 | 6.5 | 0.25 D |
| 7/16 | 14 | 0.67 | 1.40 | 13.40 | NA | 12.00 | 42.0 | 2.08 | 0.110 | 23.0 | 0.25 D |
| 7/18 | 15 | 0.38 | 0.80 | 14.70 | NA | 13.90 | 21.8 | 2.12 | 0.120 | 7.0 | 0.25 D |
| SERIES B | | | | | | | | | | | |
| 8/17 | 1 | 0.79 | 0.85 | 12.00 | 4.88 | 6.27 | 37.1 | 4.84 | 0.043 | 4.0 | 0.25 D |
| 8/18 | 2 | 1.22 | 1.31 | 14.40 | 4.23 | 8.86 | 26.3 | 4.84 | 0.051 | 15.3 | 0.25 D |
| 8/18 | 3 | 1.15 | 1.24 | 14.40 | 3.50 | 9.66 | 28.3 | 4.84 | 0.051 | 3.3 | 0.25 D |
| 8/19 | 4 | 1.72 | 1.85 | 12.00 | 2.60 | 7.55 | 39.5 | 4.84 | 0.043 | 15.0 | 0.25 D |
| 8/19 | 5 | 1.10 | 1.20 | 14.40 | 2.70 | 10.50 | 28.5 | 3.22 | 0.077 | 3.5 | 0.25 D |
| 8/24 | 6 | 1.83 | 2.00 | 11.30 | 1.25 | 8.05 | 36.5 | 2.54 | 0.076 | 3.5 | 0.25 D |
| 8/25 | 7 | 2.29 | 2.50 | 9.40 | 3.10 | 3.80 | 52.8 | 2.54 | 0.064 | 16.0 | 0.25 D |
| 8/26 | 8 | 1.45 | 1.60 | 11.30 | 1.80 | 7.90 | 36.1 | 2.54 | 0.076 | 3.0 | 0.25 D |
| 10/28 | 9 | 1.03 | 1.10 | 11.60 | 3.68 | 6.82 | 36.8 | 2.61 | 0.076 | 3.5 | 0.20 T |
| 11/7 | 10 | 1.01 | 1.08 | 10.41 | 4.68 | 4.65 | 58.1 | 2.35 | 0.076 | 4.8 | 0.20 T |
| 11/10 | 11 | 1.28 | 1.37 | 11.93 | 4.16 | 6.40 | 45.8 | 2.69 | 0.076 | 4.0 | 0.30 T |
| 11/11 | 12 | 1.63 | 1.75 | 12.07 | 4.16 | 6.16 | 61.9 | 3.26 | 0.069 | 15.8 | 0.30 T |

*D - deionized water as solvent
T - tap water as solvent

Table 3. Experimental and calculated data; Part 2.

| DATE | RUN | ENVIRONMENTAL CHAMBER TEMP.(°C) | TEST SOLUTION CONDUCTIVITY (ms/cm) BOTTOM AVG. | MIDDLE AVG. | TOP AVG. | TEST SOLUTION CONCENTRATION (M) BOTTOM AVG. | MIDDLE AVG. | TOP AVG. | AVG. | CALC CONC OF ICE (M) |
|---|---|---|---|---|---|---|---|---|---|---|
| SERIES A | | | | | | | | | | |
| 6/14 | 5 | NA | 39.8 | 39.4 | 37.3 | 0.290 | 0.283 | 0.265 | 0.28 | 0.048 |
| 6/15 | 6 | NA | 39.9 | 39.3 | 35.1 | 0.290 | 0.283 | 0.243 | 0.27 | 0.021 |
| 6/16 | 7 | NA | 39.0 | 38.2 | 33.8 | 0.285 | 0.273 | 0.235 | 0.26 | 0.046 |
| 6/29 | 8 | NA | 37.1 | 35.6 | 31.5 | 0.260 | 0.250 | 0.215 | 0.24 | 0.067 |
| 7/1 | 9 | NA | 40.3 | 38.8 | 37.4 | 0.293 | 0.280 | 0.265 | 0.28 | 0.018 |
| 7/3 | 10 | NA | 29.3 | 29.5 | 26.8 | 0.193 | 0.195 | 0.175 | 0.19 | 0.040 |
| 7/8 | 11 | NA | 36.3 | 35.5 | 32.7 | 0.255 | 0.250 | 0.223 | 0.24 | -0.058 |
| 7/12 | 12 | NA | 38.0 | 37.7 | 36.6 | 0.271 | 0.267 | 0.255 | 0.26 | -0.068 |
| 7/15 | 13 | NA | 37.5 | 37.4 | 36.2 | 0.265 | 0.264 | 0.255 | 0.26 | -0.062 |
| 7/16 | 14 | NA | 39.0 | 38.6 | 38.0 | 0.280 | 0.275 | 0.271 | 0.28 | -0.070 |
| 7/18 | 15 | NA | 40.7 | 38.2 | 37.4 | 0.298 | 0.273 | 0.264 | 0.29 | -0.132 |
| SERIES B | | | | | | | | | | |
| 8/17 | 1 | 1.6 | 39.1 | 38.0 | 36.8 | 0.280 | 0.271 | 0.259 | 0.27 | |
| 8/18 | 2 | 0.7 | 40.6 | 37.9 | 37.2 | 0.295 | 0.270 | 0.263 | 0.28 | -0.310 |
| 8/18 | 3 | 3.5 | 38.3 | 37.2 | 37.1 | 0.274 | 0.265 | 0.264 | 0.27 | -0.076 |
| 8/19 | 4 | 2.5 | 40.2 | 38.6 | 38.3 | 0.293 | 0.275 | 0.273 | 0.28 | -0.040 |
| 8/19 | 5 | 4.1 | | | | | -0.086 | | | |
| 8/24 | 6 | 1.1 | 45.3 | 39.6 | 38.4 | 0.343 | 0.288 | 0.274 | 0.30 | 0.060 |
| 8/25 | 7 | 0.5 | 44.5 | 38.1 | 37.5 | 0.335 | 0.273 | 0.266 | 0.29 | 0.010 |
| 8/26 | 8 | 1.2 | 45.2 | 38.7 | 38.6 | 0.343 | 0.275 | 0.275 | 0.30 | -0.060 |
| 10/28 | 9 | 0.2 | 35.2 | 33.1 | 32.7 | 0.245 | 0.227 | 0.222 | 0.23 | |
| 11/7 | 10 | -1.1 | 31.9 | 31.5 | 31.3 | 0.217 | 0.213 | 0.210 | 0.21 | 0.055 |
| 11/10 | 11 | -0.4 | 42.4 | 41.8 | 41.7 | 0.314 | 0.308 | 0.307 | 0.31 | -0.127 |
| 11/11 | 12 | -0.7 | 45.7 | 44.0 | 43.9 | 0.329 | 0.330 | 0.349 | 0.34 | -0.020 |

NA - not applicable

Table 4. Approximate adhesion forces.

| Run | Initial Conc. (M) | $A_d$(N//m2) |
|---|---|---|
| 1 | 0.25 | 0.6089 |
| 2 | " | 1.1172 |
| 3 | " | 0.6554 |
| 4 | " | 0.6953 |
| 5 | 0.30 | 0.6953 |
| 6 | 0.20 | 0.9547 |
| 7 | 0.25 | 0.7740 |
| 8 | " | 0.5934 |
| 9 | " | 0.7586 |
| 10 | " | 1.0837 |
| 11 | " | 0.5676 |
| 12 | " | 0.9547 |
| 13 | " | 0.6786 |
| 14 | " | 0.7302 |
| 15 | " | 1.0063 |
| 16 | " | 0.7353 |
| 17 | " | 0.9418 |
| 18 | " | 1.3623 |
| 19 | " | 0.9289 |
| 20 | 0.20 | 0.9495 |
| 21 | 0.20 | 1.4991 |
| 22 | 0.30 | 1.1817 |
| 23 | " | 1.5971 |

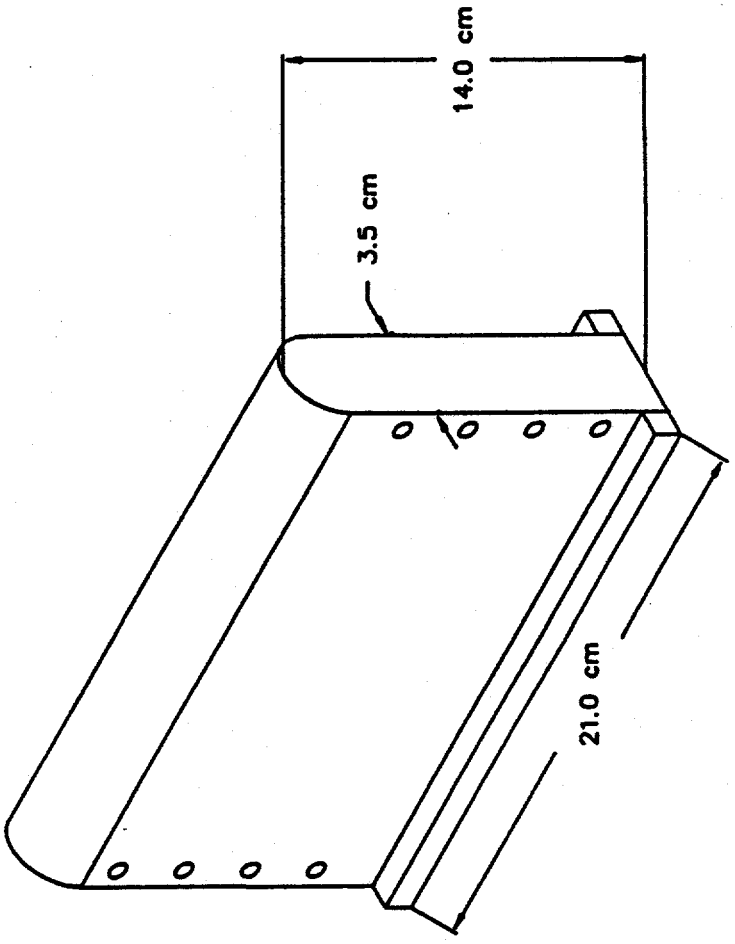


Figure 2. Dimensions of the substrate.

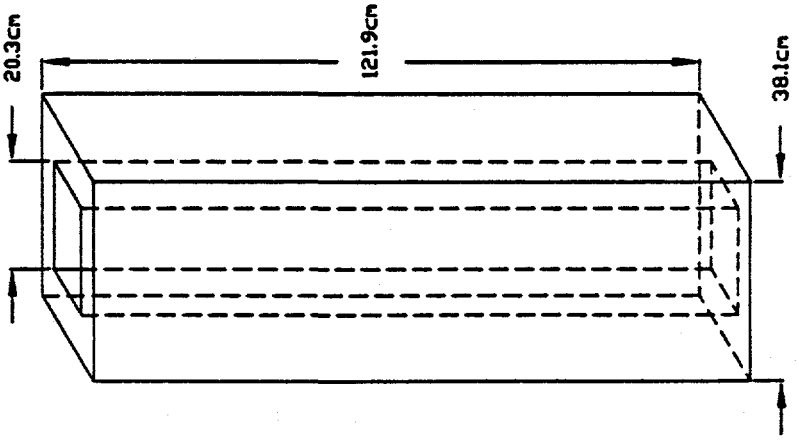


Figure 1. Schematic of solution column with inner and outer columns.

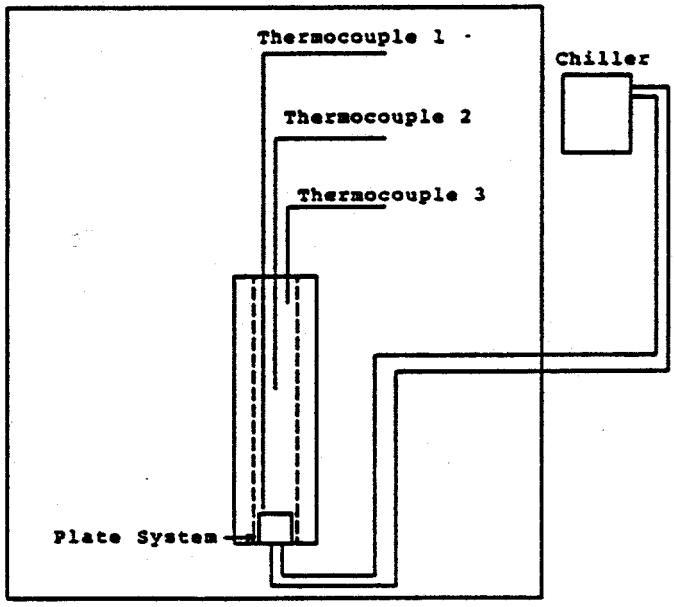


Figure 3. Schematic of test equipment in environmental chamber.

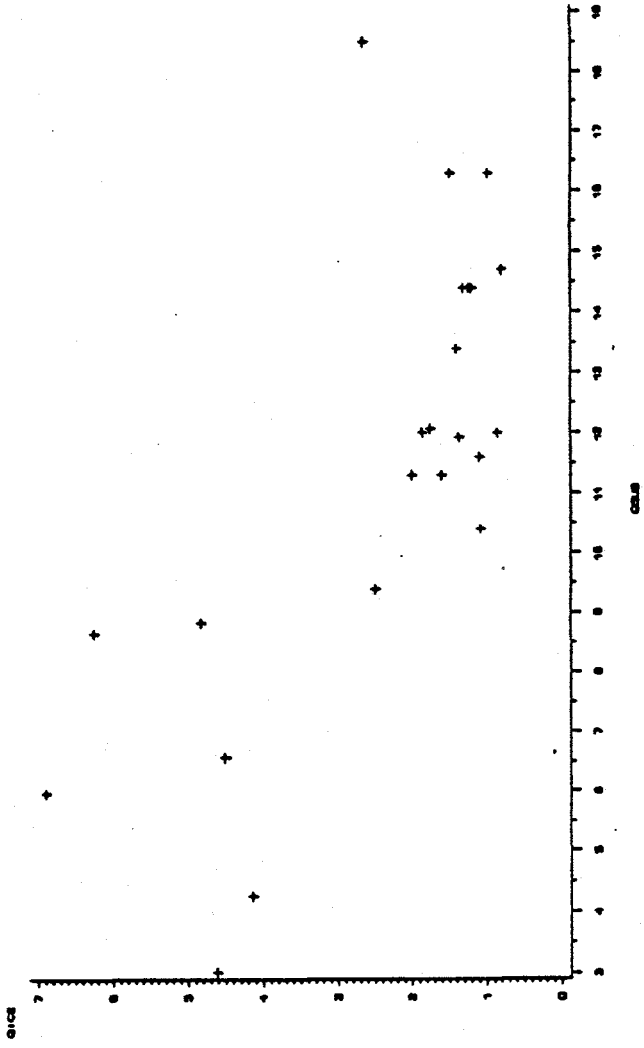

Figure 4. Ice production ($Q_{ice}$) *vs* heat removed by substrate ($Q_{sub}$) for all runs.

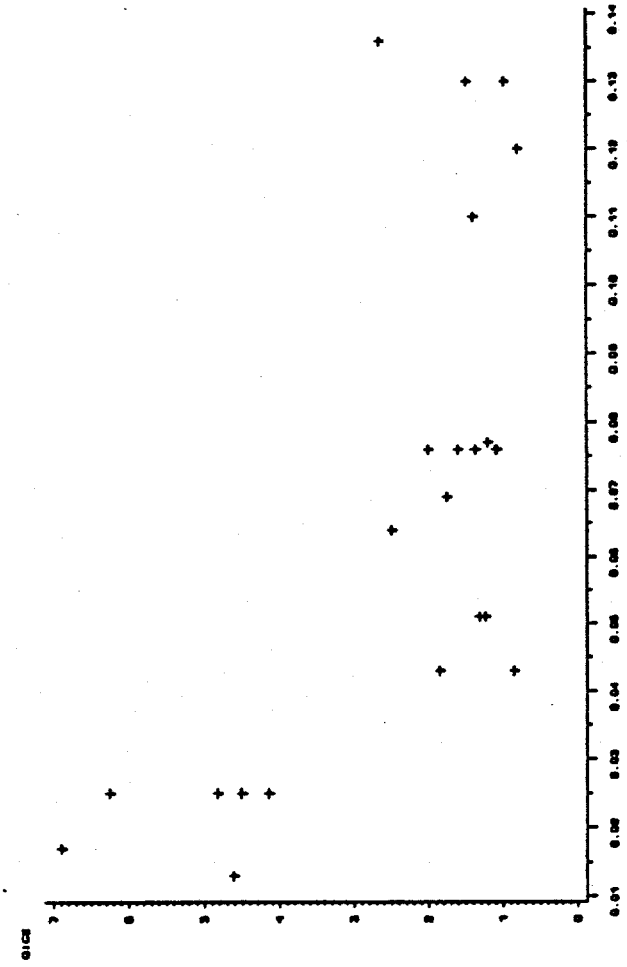

Figure 5. Ice production ($Q_{ice}$) *vs* substrate coolant temperature differential ($\Delta T$) for all runs.

# THERMAL ENERGY STORAGE WITH LIQUID-LIQUID SYSTEMS

**Elizabeth A. Santana and Leonard I. Stiel**
Polytechnic University
Brooklyn, New York 11201

***Abstract***

*The use of liquid-liquid mixtures for heat and cool storage applications has been investigated. Suitable mixtures exhibit large changes in the heat of mixing above and below the critical solution temperature of the system. Analytical procedures have been utilized to determine potential energy storage capabilities of systems with upper or lower critical solution temperatures.*

*It has been found that aqueous systems with lower critical solution temperatures in a suitable range can result in large increases in the effective heat capacity in the critical region. For cool storage with a system of this type, the cooling process results in a transformation from two liquid phases to a single phase. Heats of mixing have been measured with a flow calorimeter system for a number of potential mixtures, and the results are summarized.*

## Introduction

Several investigators (1,2) have suggested the use of liquids with limited miscibility to store thermal energy through temperature differences in the heats of mixing in the critical region of the system. A project has been conducted to identify aqueous systems with potential for heat or cool storage applications. Experimental heat of mixing data have been obtained with a flow calorimeter system for a number of mixtures identified to be promising for this application.

Liquid-liquid systems can have lower or upper critical solution temperatures (LCST OR UCST) which separate the two-liquid phase region from the region of complete miscibility. For a system with an UCST, the heat of mixing is positive at the critical point and increases with increasing temperature. For systems with LCSTs, the excess enthalpy is negative, becoming more positive with increasing temperature.

For liquid-liquid systems, the heat of mixing varies linearly with composition over the range of immiscibility. For these compositions, the heats of mixing for the two phase system is determined by the relative amount of the coexisting phases and can be expressed as:

$$H^E = a + bx_1 \qquad (1)$$

The enthalpy difference between two temperatures $T_2$ and $T_1$, above and below an upper critical solution temperature, is given as:

$$\Delta H = C_P^\circ(T_2-T_1) + H^E_{T2} - H^E_{T1} \qquad (2)$$

where,

$$C_{Po} = x_1 C_P^\circ{}_1 + x_2 C_P^\circ{}_2 , \quad (3)$$

and $C_P^\circ{}_1$ and $C_P^\circ{}_2$ are average heat capacities of components 1 and 2. Equation (2) can also be expressed as:

$$\Delta H = C_P M (T_2 - T_1), \quad (4)$$

where $C_P$ and M are the mean heat capacity and molecular weight of the mixture. From Equations (3) and (4):

$$C_P = C_P^\circ/M + (H^E_{T2} - H^E_{T1})/ M (T_2 - T_1). \quad (5)$$

It can be seen from Equation (5) that, for a high effective heat capacity, large differences in $H^E_{T2}$-$H^E_{T1}$ are required for a small temperature change, $T_2$-$T_1$. The molecular weight M of the mixture should also be as low as possible. For the triethyl amine (1) - water (2) system with a composition $x_1 = 0.13$, the experimental heats of mixing of Chand et. al. (3) show a difference of 500 J/mole between the temperatures 15 and 20°C, which are slightly below and above the LCST of the system. This difference in the heat of mixing corresponds to an effective heat capacity of 7.45 J/g, or an increase of almost 80% over the heat capacity of water.

For heat storage, a mixture with an UCST is heated from the two liquid phase region to above the critical point to form a single phase solution. For a system with a LCST, the heating process results in a transformation from a single phase to two liquid phases. Heat is then provided to the building space by cooling the solution to the original condition. The system can also exhibit a solid-liquid phase change at different conditions to aid in the storage capabilities. For cool storage, an aqueous system can be used with a critical solution temperature of approximately 5°C. This system would then form a solution of ice and the liquid component below 0°C. The cool energy can be recovered by heating the liquid to its initial condition. A conceptual diagram illustrating the use of a liquid-liquid system with an LCST for cool storage is shown in Figure 1. In the charging step, heat is provided to a heat pump by cooling the two phase liquid to below its LCST to form a single phase solution. The cool energy is then recovered for the bulding space by heating the liquid to its initial condition. In Figure 2, the charging and discharging steps above and below the LCST correspond to path 1-2 and 2-1 respectively.

## Analytical Studies

Models for the excess Gibbs free energy can be utilized to estimate heats of mixing in the single liquid phase region through the relationship:

$$H^E/R = \partial (G^E/RT)/ \partial (1/T) \quad (6)$$

Most of the models have two adjustable constants for binary mixtures, which can be calculated from phase equilibrium data.

In the first phase of this investigation (4,5), the use of several activity coefficient models was examined for the calculation of heats of mixing from Equation (6) for liquid-liquid systems. For systems with UCST's, mutual solubilities and heat of mixing data were utilized to evaluate these procedures. Most

reliable results were obtained with the Van Laar model and the relationship $A_{ij}$=Cij/T for the temperature variation of the constants of the model. For several aqueous systems considered, close agreement with the experimental values resulted with the Uniquac relationships (6) with parameters $a_{ij}$ varying linearly with 1/T. For systems with LCST's, more complex relationships for the temperature variation of the constants of the model were found to be required. For several aqueous systems with LCST's, the Uniquac procedure with quadratic relationships for the variation of the constants $a_{ij}$ with 1/T was found to result in good agreement with experimental heats of mixing.

These analytical procedures were used to evaluate potential aqueous systems with UCST's or LCST's of approximately 50°C for combined heat and cool energy storage applications. It was found that larger increases in the heat of mixing with temperature were possible for systems with LCST's. Several systems with LCST's in this range were identified to be promising for further study for this application, including mixtures of water with methyl diethyl amine, 2-6 dimethyl pyridine, dimethyl-tert-butyl amine and tri- methyl pyridine. For cool storage applications, large temperature variations in the heat of mixing at low temperatures were indicated for dipropyl amine-water (LCST=-5°C) by the quadratic Uniquac procedure with available liquid-liquid phase equilibrium data.

For thermal energy storage in other temperature ranges similar aqueous systems with LCST's were suggested. Davison et al (7) found that aqueous mixtures of secondary and tertiary amines have LCST's in the range 10-80°C depending on the degree of branching of the molecules. Similar ranges of LCST's are indicated by Malcolm and Rowlinson (8) for aqueous mixtures of polyethylene and polypropylene glycols of varying molecular weights.

## Experimental Measurements

In order to accurately determine the heats of mixing and thermal energy storage capabilities of potential systems, an isothermal flow calorimeter system has been developed. The calorimeter is capable of measurement of $H^E$ to within about 1% for temperatures from 0-150°C and pressures to 2000 psi.

The principal components of the calorimeter system used to measure the heat of mixing are the isothermal flow reaction vessel, the constant temperature water bath,the isothermal control unit,the calibration system, and the flow circuit utilizing two syringe pumps. A schematic diagram of the system is shown in Figure 3.

The reaction vessel, Hart Scientific Model 501, consists of a mixing coil wrapped around an isothermal cylinder. Inside the cylinder are a control heater, calibration heater, and a Peltier thermoelectric cooler. A thermistor inside the cylinder serves to monitor isothermal operation, which is maintained by balancing the heat withdrawn by the cooler and the heat of mixing with the heating rate of the control heater by the use of the Hart Model 3704 temperature controller. The control heater rate varies from 0.05 to 20 Joules/pulse, and the heat pulse frequency varies from 0 to 100,000 pulses/sec.

The variation of the heat pulse frequency serves to maintain the isothermal operation of the calorimeter. The calibration heater inside the cylinder is used to calibrate the control energy change by

simulating heat that would be generated in the flow tube. The temperature of the mixing vessel is monitored by the use of the Hart Model 1701 measuring unit that also serves to calibrate the control heater settings.

The flow cell of the calorimeter is submerged in a well-stirred constant temperature bath (Hart Scientific Model 5004). A Hart Model 3002 Temperature controller maintains the bath temperature constant to within +/- 0.0005°C of the set point. For operation at low temperatures, an additional 7.5 gallon refrigerant bath (Forma Scientific Model 2095), is used to circulate ethylene glycol as cooling fluid through the 5004 constant temperature bath.

The two liquids to be mixed are pumped through 1/16 inch stainless steel lines by ISCO Model LC-2600 high precision syringe pumps. The flow rates of the pumps were accurately calibrated by timing the flow of water through a 5 ml buret.

Before entering the calorimeter each liquid passes through lengths of tubing submerged in the 5004 water bath to provide sufficient time for thermal equilibration before the fluids reach the reaction vessel. The mixing occurs at the union of the two inlet lines.

A stable baseline for the control heater pulse frequency is initially established with one of the pure components pumped through the calorimeter system. The flow through the calorimeter of the second component is then initiated. When a new stable baseline is attained for the mixture, the heat of mixing is calculated as:

$$H^E \text{ (J/mole)} = \frac{Q\,(P)}{M} \tag{7}$$

where Q is the calibrated heater rate (J/pulse), P is the increase or decrease in the pulse frequency (pulses/sec), and M (moles/sec) is the combined calibrated flow rate through the pumps, which is calculated as:

$$M = \frac{V_1 \rho_1}{MW_1} + \frac{V_2 \rho_2}{MW_2} \tag{8}$$

where $V_1$ and $V_2$ are the calibrated pump flow rates and $\rho_1$ and $\rho_2$ are the liquid densities of the components at room temperature.

For combined heat and cool storage applications, the propylene carbonate-water system (UCST = 60-70°C) was recommended in a preliminary phase of this investigation. Therefore, heats of mixing were measured for this system for temperatures in the range 50-70°C and are presented in Figure 4. The experimental heats of mixing are essentially consistent with values calculated by analytical procedures (5). Possible dissociation of propylene carbonate was indicated at 70°C and low compositions of this component, which is close to the critical region of the system. The heat of mixing of the propylene carbonate system is unusually high for aqueous mixtures with upper critical solution temperatures. However, the thermal energy storage capabilities of this system at low propylene carbonate compositions appear to be limited, due to the high percentage of water in the propylene carbonate phase. These experimental results are consistent with one of the conclusions of the first phase of this investigation, that aqueous systems with UCST's are

unlikely to exhibit large increases in $H^E$ in the critical region. Therefore, systems with LCST's have been emphasized in the subsequent experimental studies.

In Figure 5, experimental heats of mixing are presented for methyl diethyl amine-water in the range 45-55°C. This system has a LCST approximately equal to 49°C and is suitable for heat storage applications. At a mole fraction $X_1 = 0.1$, $H^E$ for this system varies by about 340 J/mole over the temperature range 48-55°C, coresponding to an effective heat capacity about 30% higher than that of pure water. The experimental heats of mixing for this system are consistent with those predicted by analytical procedures (5).

Polypropylene glycol with a molecular weight of 425 has an LCST of about 48°C, in a suitable range for heat storage. The experimental values of $H^E$ for this system in the range 45-60°C are shown in Figure 6. At a weight fraction of the glycol $w_1 = 0.4$, this system exhibits an effective heat capacity about 15% higher than that of water in this temperature range. Heat of mixing measurements were also conducted for this system in the range 10-27°C. At 27°C, the experimental values from this study are in good agreement with those of previous investigators (9,10) for similar polypropylene glycol-water systems. Although this system is miscible at all compositions in this temperature range, the effective heat capacity in this range is only slightly lower than that of water.

For potential cool storage applications, heats of mixing were also measured for the dipropylamine-water system in the range 5-25°C. The experimental results are presented in Figure 7. The experimental values of $H^E$ change less rapidly with temperature in the range 5-15°C than the values predicted by the quadratic Uniquac procedure. These differences are due to the fact that the equilibrium phase compositions indicated by the linear portions of the experimental $H^E$ isotherms change slightly less rapidly than the previous experimental phase values (11).

A polypropylene glycol with a higher molecular weight is required for cool storage applications. Therefore, heats of mixing were measured for the polypropylene glycol (MW =725)-water system, which has a LCST in the range 5-10°C. In Figure 8, values of the heat of mixing for this system are presented for temperatures from 5-25°C. It can be seen that for a weight fraction of the glycol $w_1 = 0.4$, the heat of mixing increases about 10 J/g in the range 10-15°C. This corresponds to an increase in the heat capacity of about 20% over that of water in this temperature interval.

## Current Results

During this period, heat of mixing measurements were conducted for additional aqueous systems evaluated to have potential for cool storage applications. Because of their low toxicity compared to other organic fluids such as amines and pyridines, aqueous mixtures containing glycol or glycol derivatives have been primarily considered. Because the polypropylene glycols previously investigated were of high molecular weight, further enhancement in the effective heat capacity could possibly be obtained by the use of a lower molecular weight glycol derivative with suitable phase behavior for cool storage applications. A list of some ethylene, diethylene, and propylene glycol ethers along with their molecular weights is presented in Table 1.

Phase equilibrium tests were conducted in order to estimate approximate LCST's for these glycol ethers. Samples of different mole fractions of the glycol ethers were prepared and were cooled or heated as necessary in order to visually obtain the separation temperatures. The approximate LCST's resulting from these phase data experiments (or from literature values when available) are included in Table 1.

Diethylene glycol monomethyl ether (methylcarbitol)-water mixtures were recommended for thermal energy storage applications (1,2). Heats of mixing presented by Pathak et al (12) for this system exhibit substantial variation with temperature in the range 25-45°C. Experimental measurements of heats of mixing were conducted in the range 10-35°C, and the values are shown in Figure 9. The experimental values of $H^E$ for this study are in agreement with those of Pathak only at low compositions of the carbitol and exhibit smaller changes with temperature. Liquid-liquid behavior could not be observed for this system in this temperature range.

Further substitution of the diethylene glycol molecule should lower the value of the lower critical solution temperature to the suitable range. Heat of mixing measurements were also conducted for the diethylene glycol diethyl ether-water system for temperatures from 10-35°C. The lower critical solution temperature for this system was found to be about 25°C. Nakayama and Shinoda (13) measured heats of mixing for this system at 25°C and indicated liquid-liquid behavior for compositions $0.01<x_1<0.1$. In the present study, at 35°C a narrow two-liquid phase region was observed in the composition range $0.06<x_1<0.11$. The new data for this system are in general agreement with those from the previous study as is shown in Figure 10.

Experimental heats of mixing for the diethylene glycol dibutyl ether-water system were also determined in the range 10-25°C. The LCST for this system was found to be below 0°C. Small changes in the heats of mixing were found in this temperature range.

It can be seen from Table 1 that substituted ethylene glycols have lower values of LCST's than the corresponding substituted diethylene glycol ethers. It was found that the commercially-available substituted ethylene glycols have either higher or lower LCST's than the optimum range for cool storage, as shown in Table I. Based on these analyses, ethylene glycol diethyl ether was considered to be most suitable for further study. Heat of mixing isotherms in the range 5-25°C are presented in Figure 11 for ethylene glycol diethyl ether-water. This system has a LCST less than -5°C. At a mole fraction of the glycol of about 0.074, an increase in the heat of mixing of 185 J/mole was obtained between 5-10°C. This increase represents an enhancement of about 15% over the heat capacity of water in the same temperature interval.

Experimental heats of mixing were also determined for the propylene glycol dimethyl ether-water and the dipropylene glycol dimethyl ether-water systems. These systems have LCST's below 0°C. Moderate changes in the heats of mixing resulted for these systems.

## Heats of Mixing for Three-Component Systems

Lower critical solution temperatures of aqueous systems containing mixtures of glycols are determined primarily by the phase behavior of the high molecular weight glycol constituent (14). Because the binary

aqueous mixtures studied with lower molecular weight glycols have LCST values either higher or lower than the desired range (5-10°C), ternary systems with blends of glycols were used in order to attempt to obtain optimum properties.

Heats of mixing are more difficult to obtain for multicomponent mixtures than for binary systems. In several studies (15,16), procedures have been developed to calculate heats of mixing for multicomponent systems. In order to evaluate the contributions of the heat of mixing of the glycol blends, values of $H^E$ were measured for the ethylene glycol diethyl ether -polypropylene glycol (MW=725) system. The heats of mixing for this system were found to be small and exhibited no variation with temperature. Therefore, in this study the ternary mixtures were approximately treated as effective binary systems, neglecting the small contributions to the heats of mixing for the glycol components. Heats of mixing measurements for ternary systems were conducted by mixing the two glycol components in the desired ratio and charging the mixture into one of the pumps. Distilled water was then charged into the other pump, and the measurements were initiated.

A list of the blends used in this study, the ratios of the glycol components by volume, and their molecular weights are included in Table 2. Approximate values of the LCST's for the ternary systems were obtained by phase equilibrium tests and are included in Table 2. The addition of diethylene glycol diethyl ether to ethylene glycol diethyl ether - water raised the LCST to about 2°C, but the ternary system did not exhibit as large variations in $H^E$ as the original binary system. In order to reduce the molecular weight of the polypropylene glycol (MW=725) - water system, ternary mixtures were formed by adding respectively ethylene glycol diethyl ether, diethylene glycol diethyl ether, and polypropylene glycol (MW=425). The resulting ternary mixtures did not exhibit as large inreases in the effective heat capacity between 5 and 10°C as the higher molecular weight binary system.

Alternate three - component systems were also investigated. It has been found that the addition of a third component to a mixture can increase or decrease the phase separation temperatures (17). Third components which are soluble in both components increase the separation temperatures, while third components which are only soluble in one of the mixture components decrease the separation temperatures (17).

Since the triethyl amine-water system (LCST ~ 18°C) exhibits large increases in the effective heat capacity in the critical region, the effect of the addition of small amounts of dipropyl amine, sodium chloride, and urea to this system was investigated. It was found that the largest decreases in the phase separation temperatures were obtained by the addition of sodium chloride, but the shape of the resulting phase curve would not be similar to that of the triethyl amine-water system. However, it was also found from these experiments that the addition of urea resulted in a phase curve with close to the optimum shape shown by triethyl amine -water. Based on these analyses, heats of mixing were measured for the ternary triethyl amine-ure water system.

It was found through phase equilibrium experiments that optimum results were obtained for initial mole fractions of urea in water, $x'_u$, in the range 0.077-0.1. The value of the LCST for this system is about 5°C. Experimental heats of mixing for the ternary system with $x_u' = 0.077$ are shown in Figure 12. It can be seen that the heats of mixing of this system decrease dramatically in the range 5-25°C, with the largest decrease occurring between 10 and 15°C. At a mole fraction of triethyl amine $x_1 = 0.122$, the experimental heats of mixing show an increase of 602 J/mole (19.413 J/g) between 10 and 15°C. This increase corresponds to an effective heat capacity of 7.231 J/g°C, and represents an enhancement of about 70% over the heat capacity of water in this temperature range. The effective heat capacity for the ternary system was calculated from Equation (8), assuming no changes in the heat of solution of urea-water for the temperature range.

Additional heats of mixing were measured for this mixture with $x_u = 0.1$. The LCST for this system is about 3°C. The experimental heats of mixing are shown in Figure 13. It can be seen that substantial changes occur in the range 5-12°C. For a mole fraction of triethylamine $x_T = 0.2$ in the three-component system, an increase in the heat capacity of about 50% over that of water is indicated for this temperature range.

For a system that does not show optimum phase behavior as a binary mixture, the addition of a third component could improve the temperature variations of the heats of mixing. In order to obtain a system with a suitable critical solution temperature and improved phase curve, the effect of the addition of sodium chloride to the diethylene glycol diethyl ether-water system was investigated. The critical solution temperature for the binary system was found to be about 25°C, and it exhibited small changes in the heats of mixing in the critical region. For an initial mole fraction of salt in water $x'=0.011$, close to the largest variations in the equilibrium phase compositions resulted between 5 and 10°C. For this ternary system, the LCST is about 0°C.

Experimental heats of mixing for the three-component system are shown in Figure 14 for 5 and 15°C. It can be seen that improved variations in the heat of mixing, compared to the binary mixture, occur for a glycol mole fraction of about 0.1. Although the effective heat capacity of the ternary system is slightly lower than that of water, it is improved compared to that of the binary diethylene glycol diethyl ether-water system for a comparable temperature range in the critical region. The important implication indicated by the results for this system is that the phase behavior of binary systems with LCST's can be altered and improved for energy storage applications by the addition of small amounts of a salt or similar compound.

## Conclusions

The heat of mixing data obtained in this study enabled the evaluation of potential systems for heat or cool storage applications. For several systems, the magnitudes and temperature trends of the experimental values were consistent with those predicted in the first phase of this investigation through

analytical procedures (4,5). Highly accurate liquid-liquid phase equilibrium data are required to obtain reliable predictions of heats of mixing by these methods.

For heat storage, several systems with LCST's of about 50°C exhibited moderate changes of the heats of mixing in the critical region, including methyl diethyl amine-water and polypropylene glycol (MW=425)-water. Of the systems containing glycols or glycol derivatives which were considered for cool storage applications, largest variations in the heat of mixing at low temperatures resulted for aqueous mixtures with ethylene glycol diethyl ether and polypropylene glycol (MW=725). The experiments were only conducted with commercially-available materials, and other glycol derivatives could possibly be synthesized which have improved phase behavior with water for cool storage. Although aqueous systems containing blends of glycol derivatives resulted in reduced molecular weights and altered phase behavior, the ternary systems of this type considered did not exhibit higher effective heat capacities at low temperatures than the optimum binary glycol systems.

The addition of small quantities of a salt or similar compound to binary liquid-liquid systems appears to be promising for further study. It was found that the ternary triethyl amine-urea-water system exhibited similar phase behavior as the nearly optimum triethyl amine-water binary system, with LCST's and effective heat capacities suitable for cool storage applications. It has also been found that the addition of a salt to a binary mixture with non-optimum phase behavior can decrease the LCST and improve the thermal energy storage capabilities of the system.

## Acknowledgement

This work was conducted under Subcontract No. 19X -27470V for Oak Ridge National Laboratory, operated by Martin Marietta Energy Systems, Inc. for the U.S. Department of Energy. The authors appreciate the help of John Tomlinson as Technical Monitor and of James Martin in the first phase of this investigation.

## Literature Cited

1. Fraser, M., Report EPRIEM-3159-SR, p 35-1 (JULY 1983).

2. Grodzka, P. G., Lockheed Report LMSC-HREC-TR (AUGUST 1983).

3. Chand, A., A.R. McQuillan, and P.V. Fenby, Fluid Phase Equilibria, 2, 263 (1979).

4. Stiel,L.I., ORNL Report /Sub/ 86-2747011 (July, 1987).

5. Rastogi,S., M.S. Thesis, Polytechnic University, (1987).

6. Prausnitz,J.M., R.N. Lichtenthaler, and E.G. de Azevedo, "Molecular Thermodynamics of Fluid-Phase Equilibria", Second Edition, Prentice Hall (1986).

7. Davison R.R., W.H. Smith, and D.W. Hood, J. Chem. Eng. Data 5, 420(1960).

8. Malcolm, G. N. and J. S. Rowlinson, Trans. Far. Soc., 53, 921 (1957).

9. Cunninghame, R. B., and G. W. Malcolm, J, Phys. Chem. 65, 1454 (1961).

10. Lakhanphal, M. L., Singh, H. G., Singh, H., and Sharma, S. C., Ind. J. Chem., 6,95 (1968).

11. Sorensen, J. M. and W. Arlt, "Liquid-Liquid Equilibrium Data Collection", Dechema Chem. Chemistry Series, Vol V, Pt.1 (1979). 12. Nakayama, H. and K. Shinoda, J. Chem. Thermodynamics, 3, 401 (1971).

12. Bilimova, Y.S., G. A. Gladkouskii, V. M. Golubev, and Z. N. Medved, Polymer Science USSR, 22, 2456 (1980).

13. Tsao, C. C. and J. M. Smith, Chem. Eng. Prog. Symp. Ser. 49, 107 (1953).

14. Battler J.R., W.M. Clark, and R.L. Rowley, J. Chem. Eng. Data, 30, 254 (1985).

15. Hales, B. J., G.L. Bertrand, and L.G. Hepler, J. Phys. Chem. 70, 3970 (1966).

Table 1. Potential glycols for cool storage applications.

| SUBSTANCE | MW | LCSTS (°C) |
|---|---|---|
| Ethylene Glycol Methyl Ether | 76.1 | >>25 |
| Ethylene Glycol Dimethyl Ether | 90.1 | >20 |
| Ethylene Glycol Ethyl Ether | 90.1 | >25 |
| Ethylene Glycol Diethyl Ether | 118.2 | <-5 |
| Ethylene Glycol Methyl-tert-Butyl Ether | 132.2 | <25 |
| Ethylene Glycol Butyl Ether | 118.0 | 49 |
| Ethylene Glycol is-Butyl Ether | 109.0 | 25 |
| Diethylene Glycol Monomethyl Ether | 120.2 | >25 |
| Diethylene Glycol Dimethyl Ether | 134.2 | >25 |
| Diethylene Glycol Methyl tert-Butyl Ether | 176.3 | <25 |
| Diethylene Glycol Monoethyl Ether | 134.2 | >25 |
| Diethylene Glycol Diethyl Ether | 162.2 | 25 |
| Diethylene Glycol mono-Butyl | 162.2 | >20 |
| Diethylene GlycolDibutyl Ether | 218.3 | ~ 0 |
| Propylene Glycol Monomethyl Ether | 90.1 | >32 |
| Propylene Glycol Dimethyl Ether | 104.2 | < 0 |
| Propylene Glycol Monoethyl Ether | 104.0 | >32 |
| Propylene Glycol Diethyl Ether | 118.0 | > 0 |
| Propylene Glycol Dipropyl Ether | 160.0 | <<25 |
| Dipropylene Glycol Methyl Ether | 148.2 | >20 |
| Dipropylene Glycol Dimethyl Ether | 162.2 | < 0 |
| Tripropylene Glycol n-Propyl Ether | 160.0 | <25 |
| Tripropylene Glycol Methyl Ether | 190.2 | <25 |
| Tripropylene Glycol Dimethyl Ether | 204.2 | < 0 |
| Tripropylene Glycol n-Propyl Ether | 201.0 | <<25 |

Table 2. Aqueous systems with glycol mixtures.

| Glycols Mixture | Ratio | Molecular Weight | LCST°C |
|---|---|---|---|
| Ethylene Glycol Diethyl Ether-Diethylene Glycol Diethyl Ether | 1:6 | 154.51 | 2 |
| Ethylene Glycol Diethyl Ether-Polypropylene Glycol (MW 725) | 1:5 | 417.71 | <0 |
| Polypropylene Glycol (MW 725)-Diethylene Glycol Diethyl Ether | 1:3 | 205.18 | 8 |
| Polypropylene Glycol (MW 725)-Polypropylene Glycol (MW 425) | 1:3 | 474.16 | 15 |

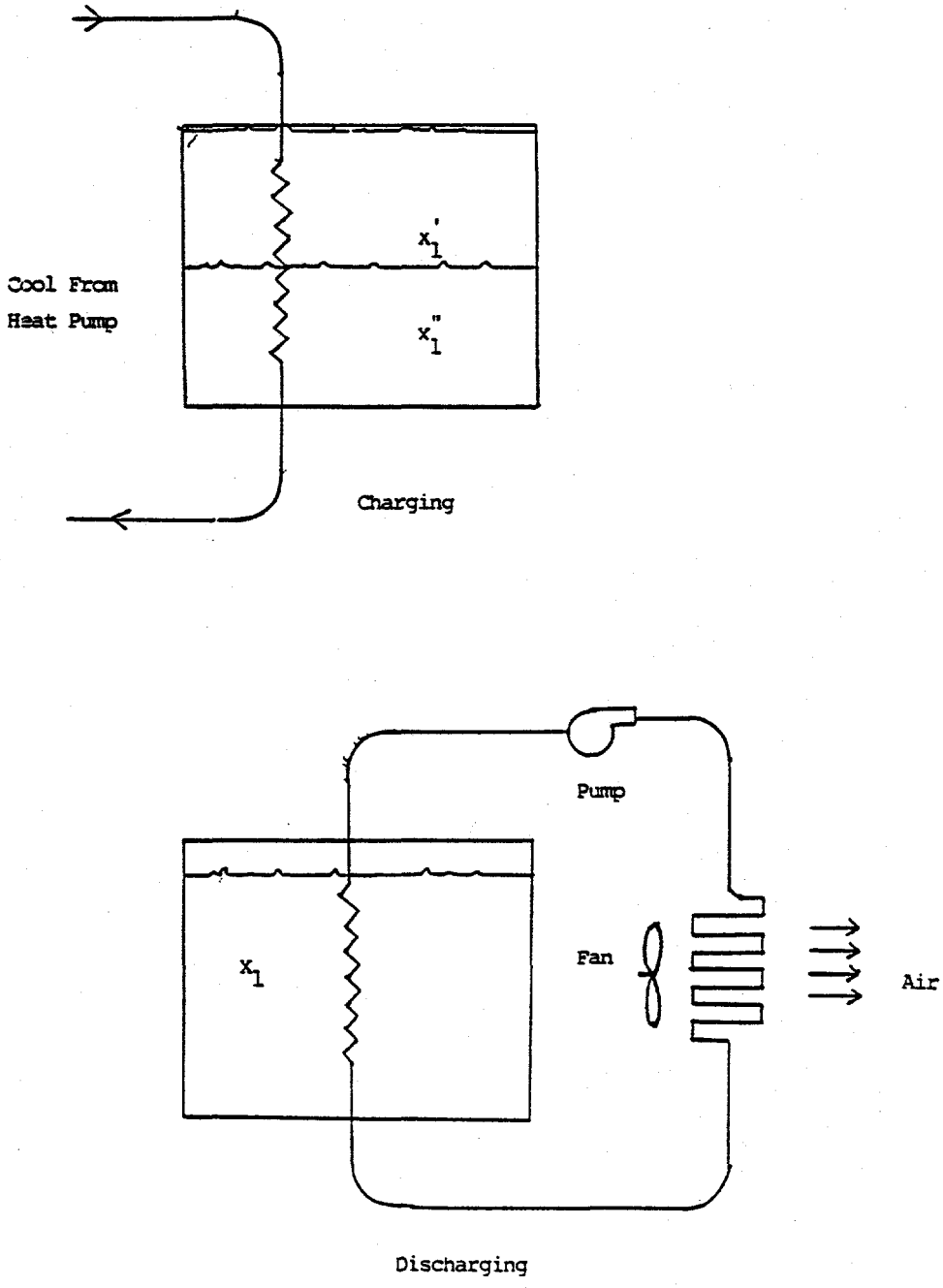


Figure 1. Conceptual cool storage system.

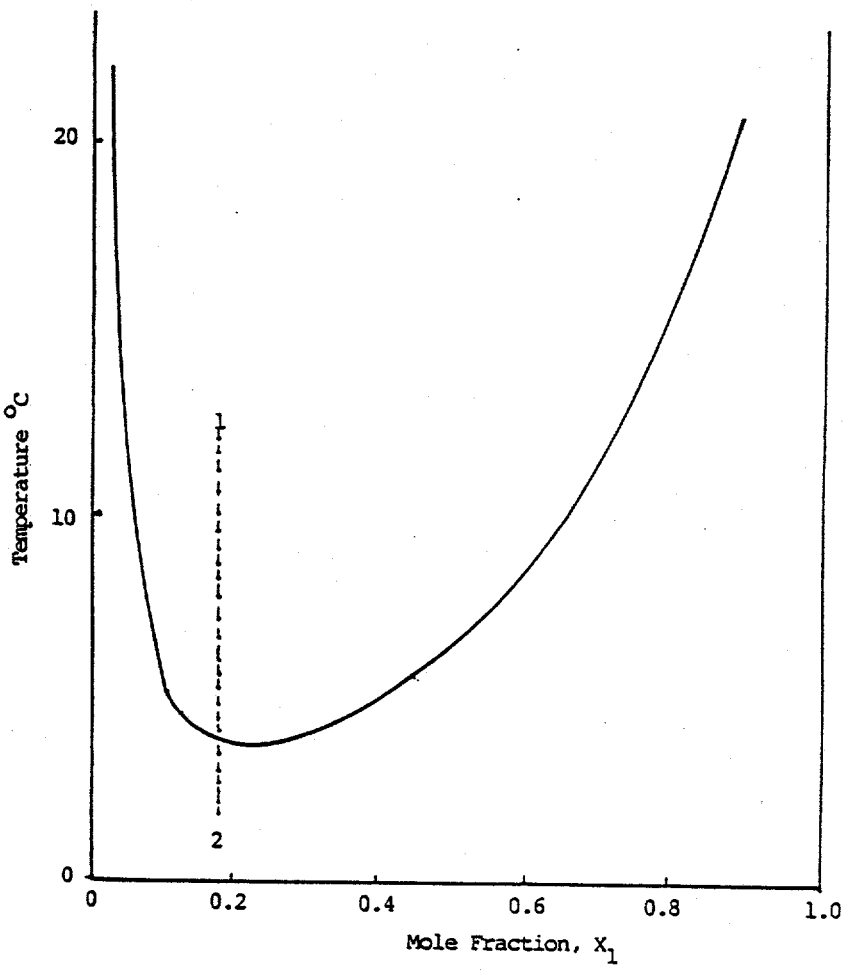


Figure 2. Cool storage with LCST system.

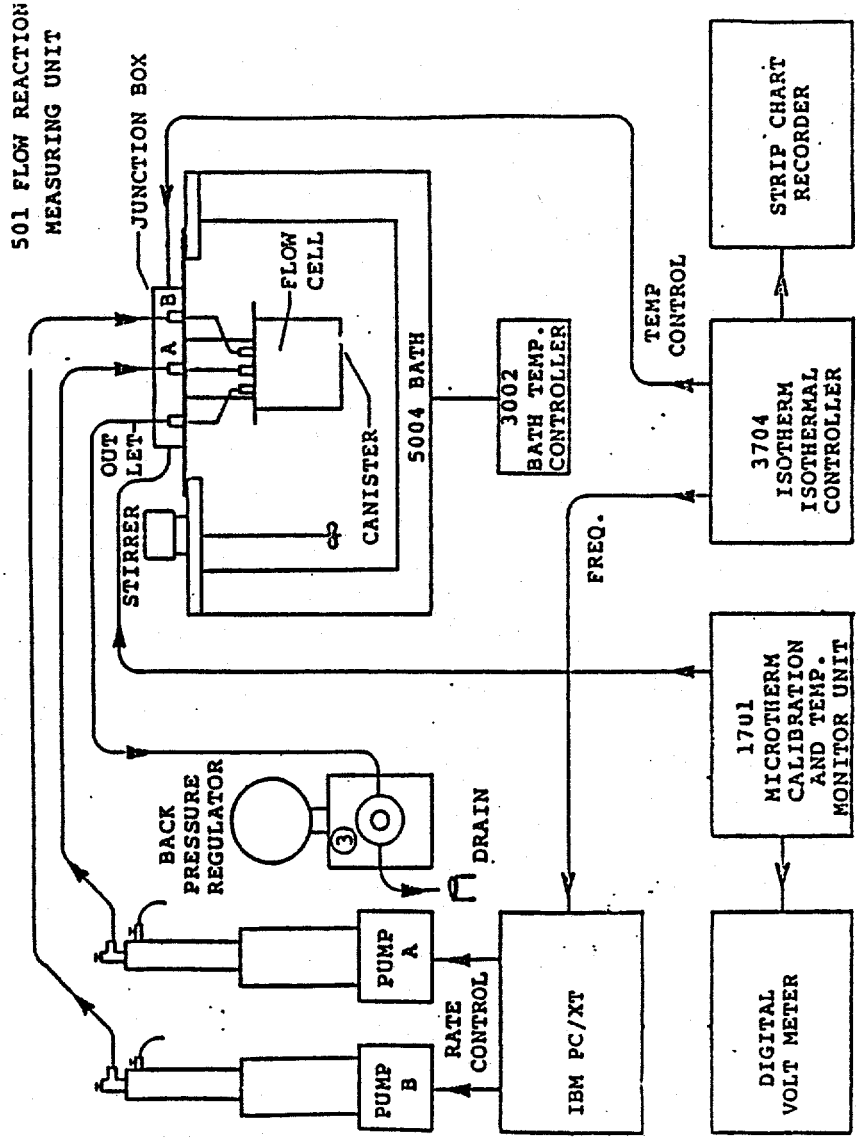


Figure 3. Flow calorimetry schematic.

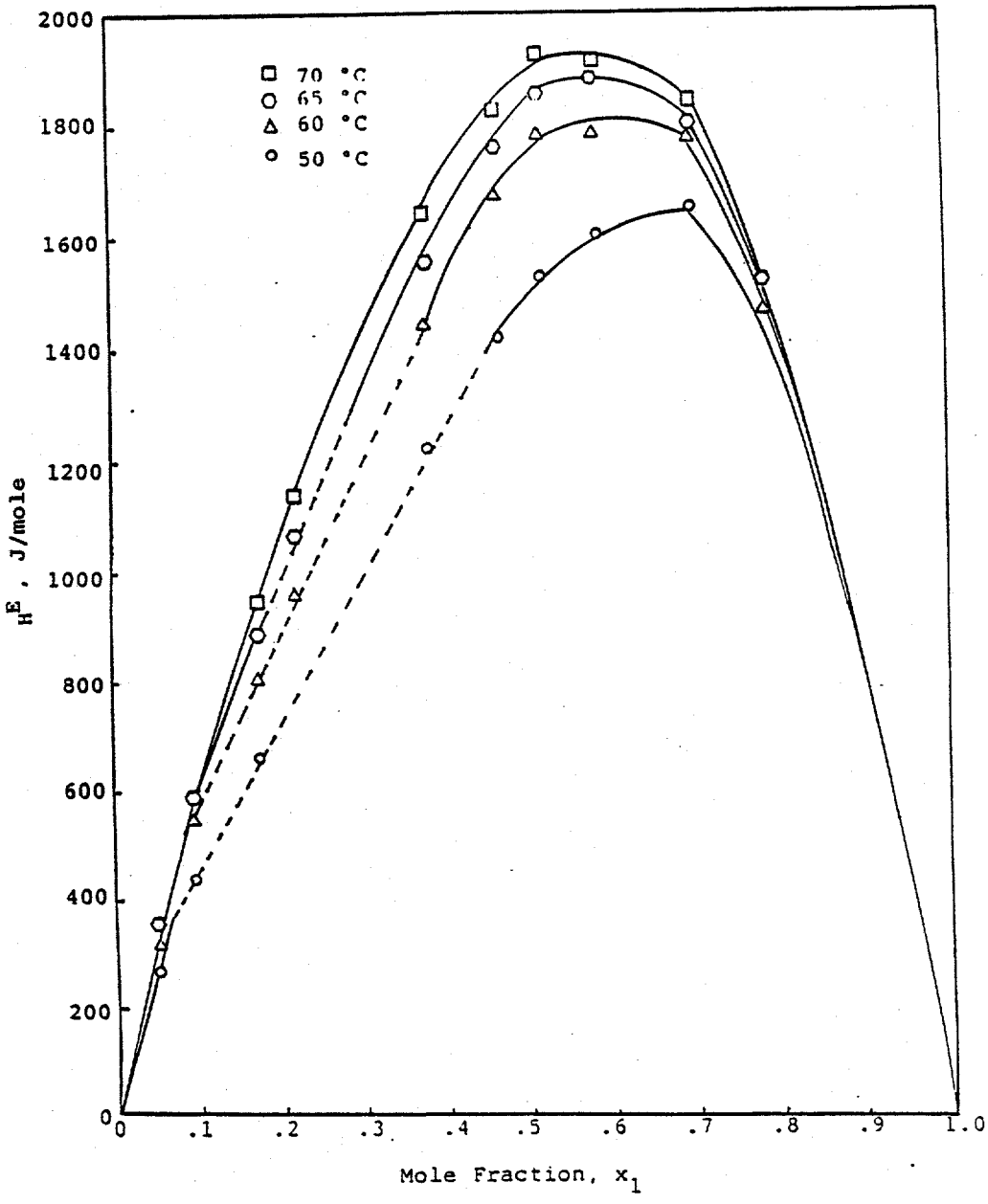


Figure 4. Heats of mixing for propylene carbonate (1) - water (2).

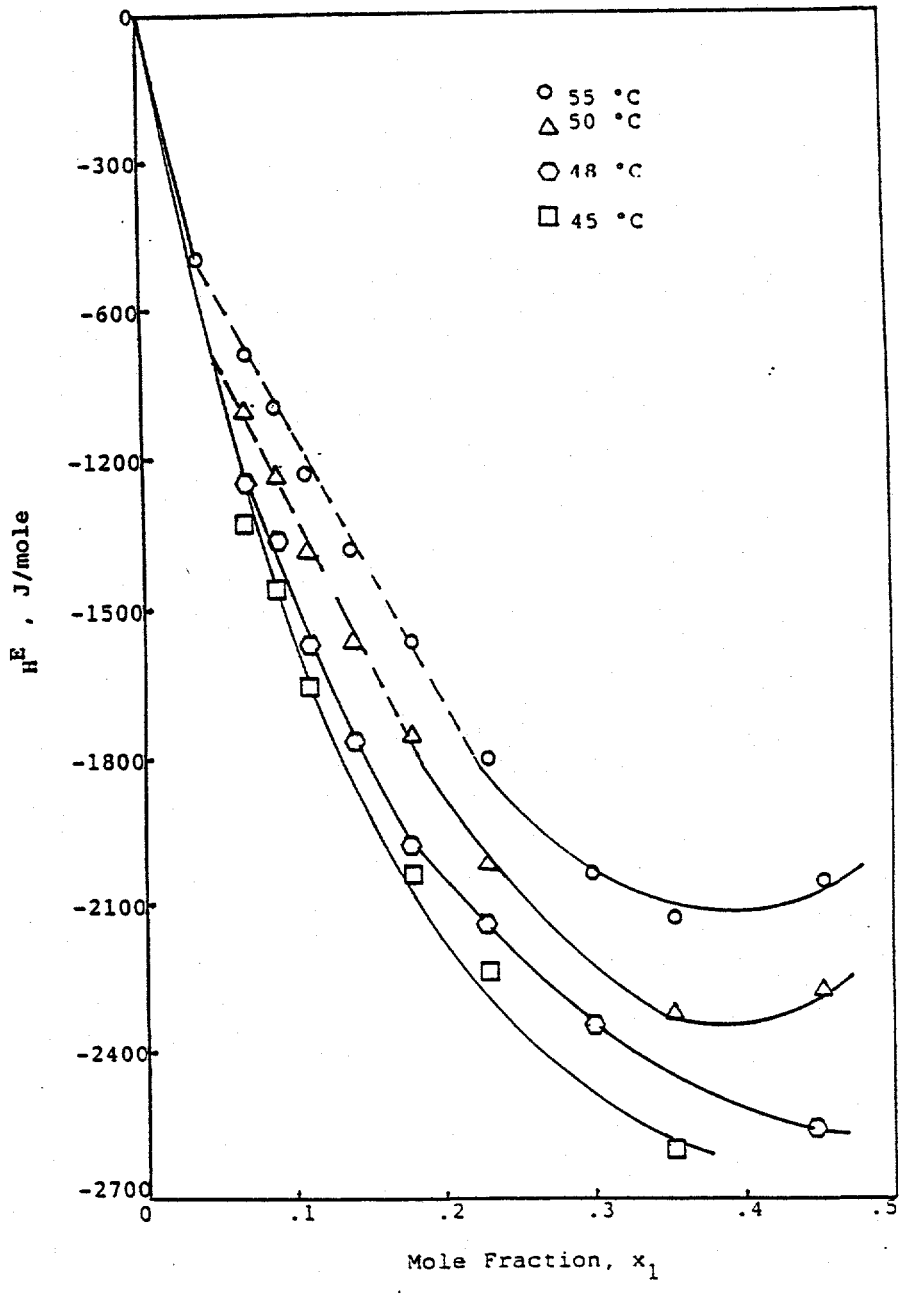


Figure 5. Heats of mixing for methyl diethyl amine (1) - water (2).

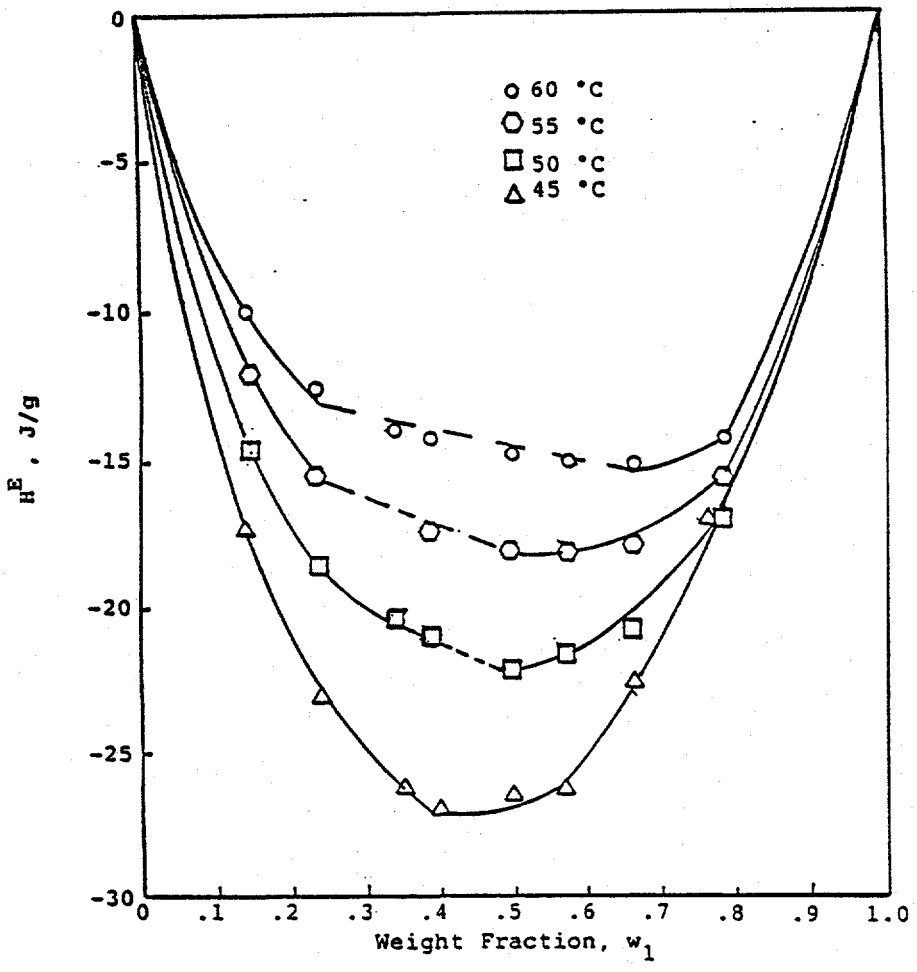


Figure 6. Heats of mixing for polypropylene glycol (1) - water (2); MW=425.

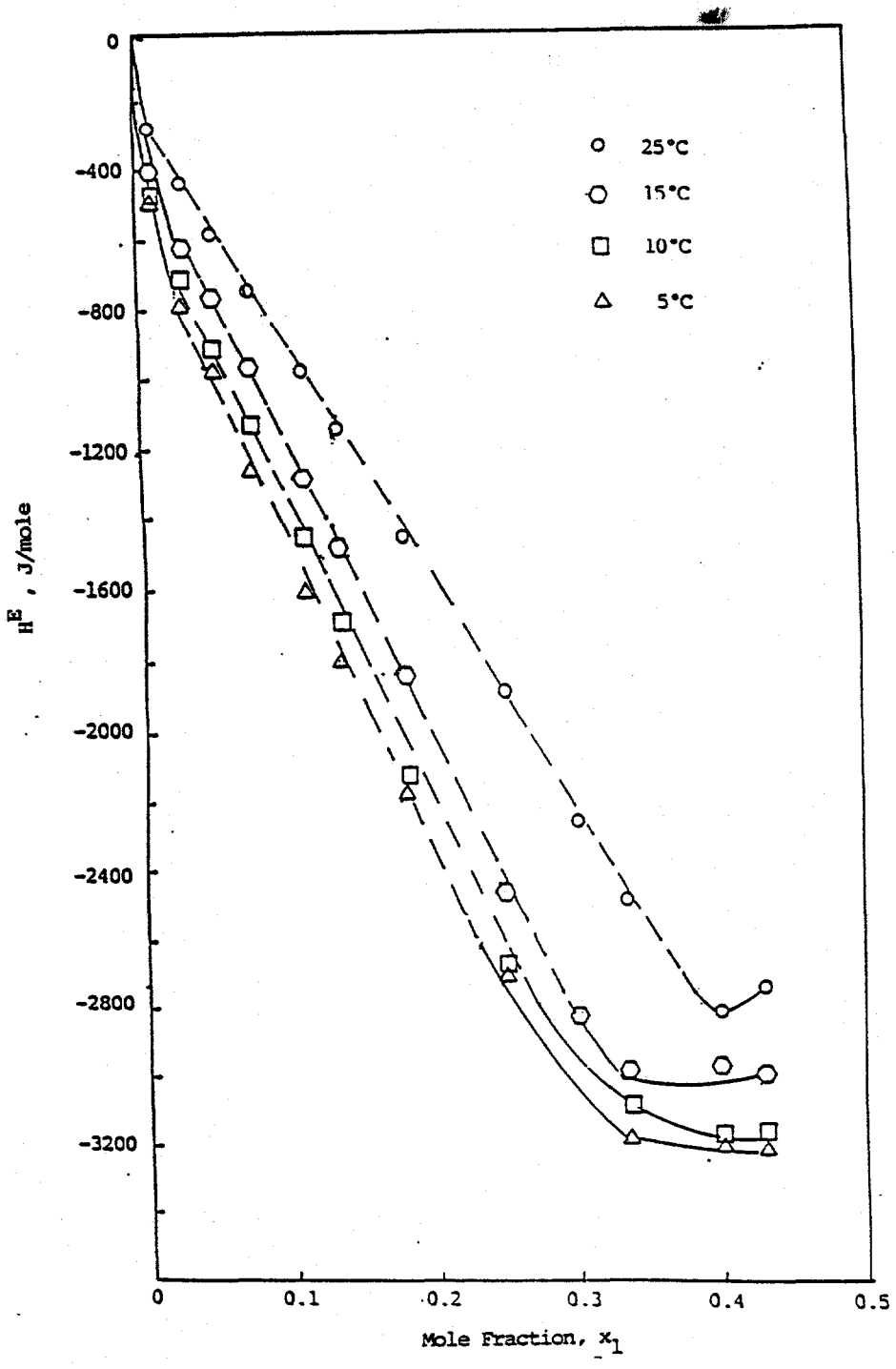


Figure 7. Heats of mixing for dipropylamine (1) - water (2).

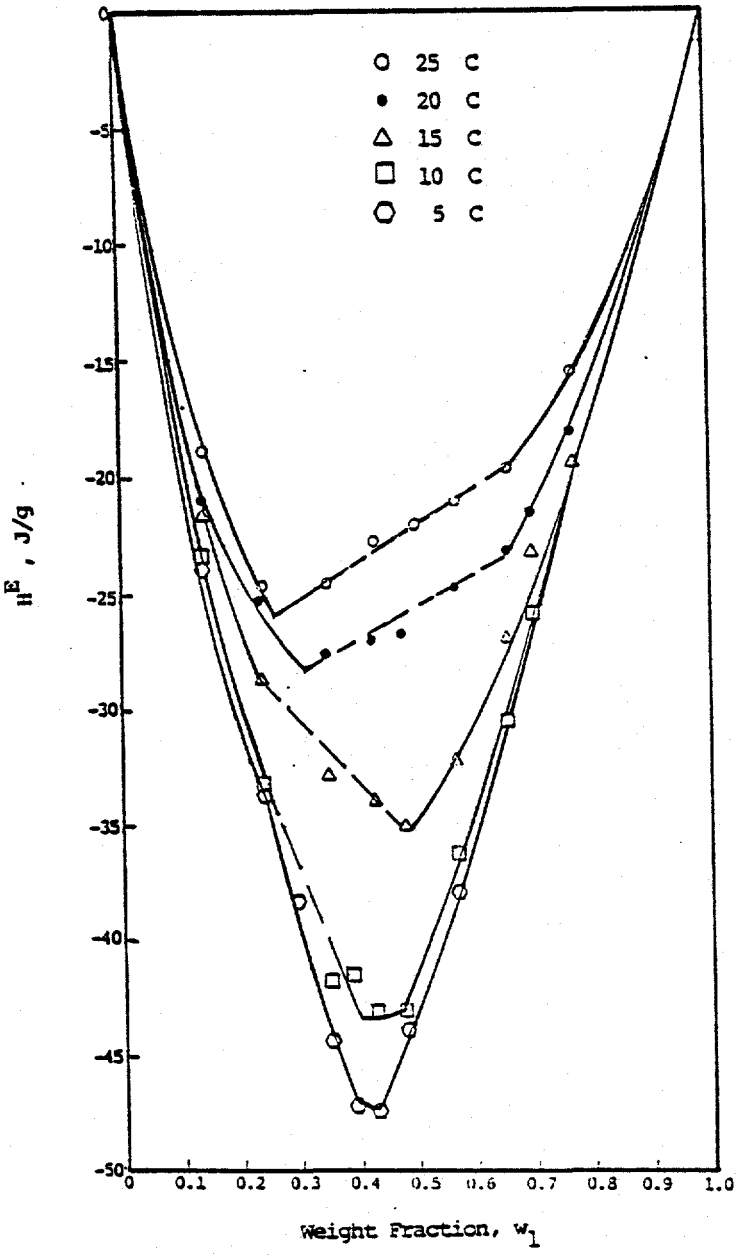


Figure 8. Heats of mixing for polypropylene glycol (1) - water (2); MW=725.

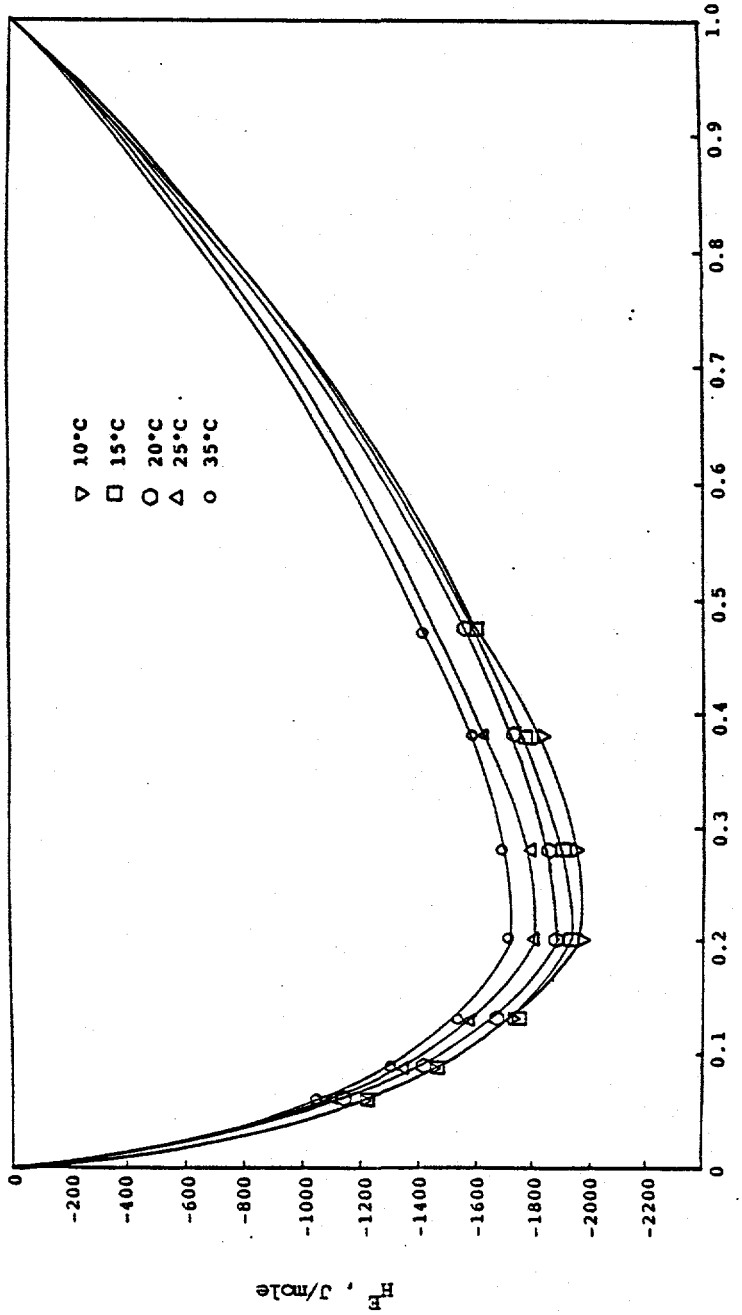


Figure 9. Heats of mixing for methyl carbitol (1) - water (2).

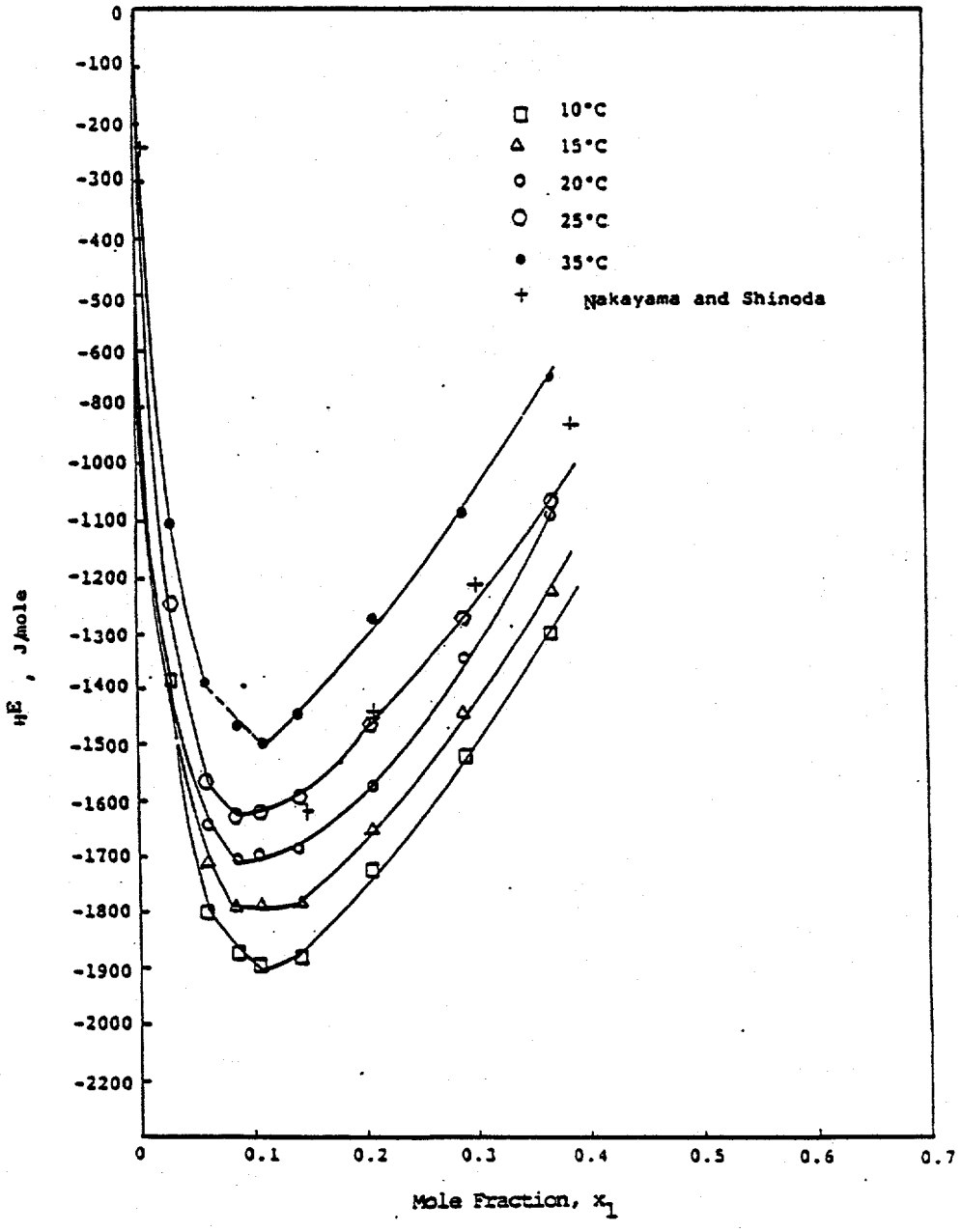


Figure 10. Heats of mixing for diethylene glycol diethyl ether (1) - water (2).

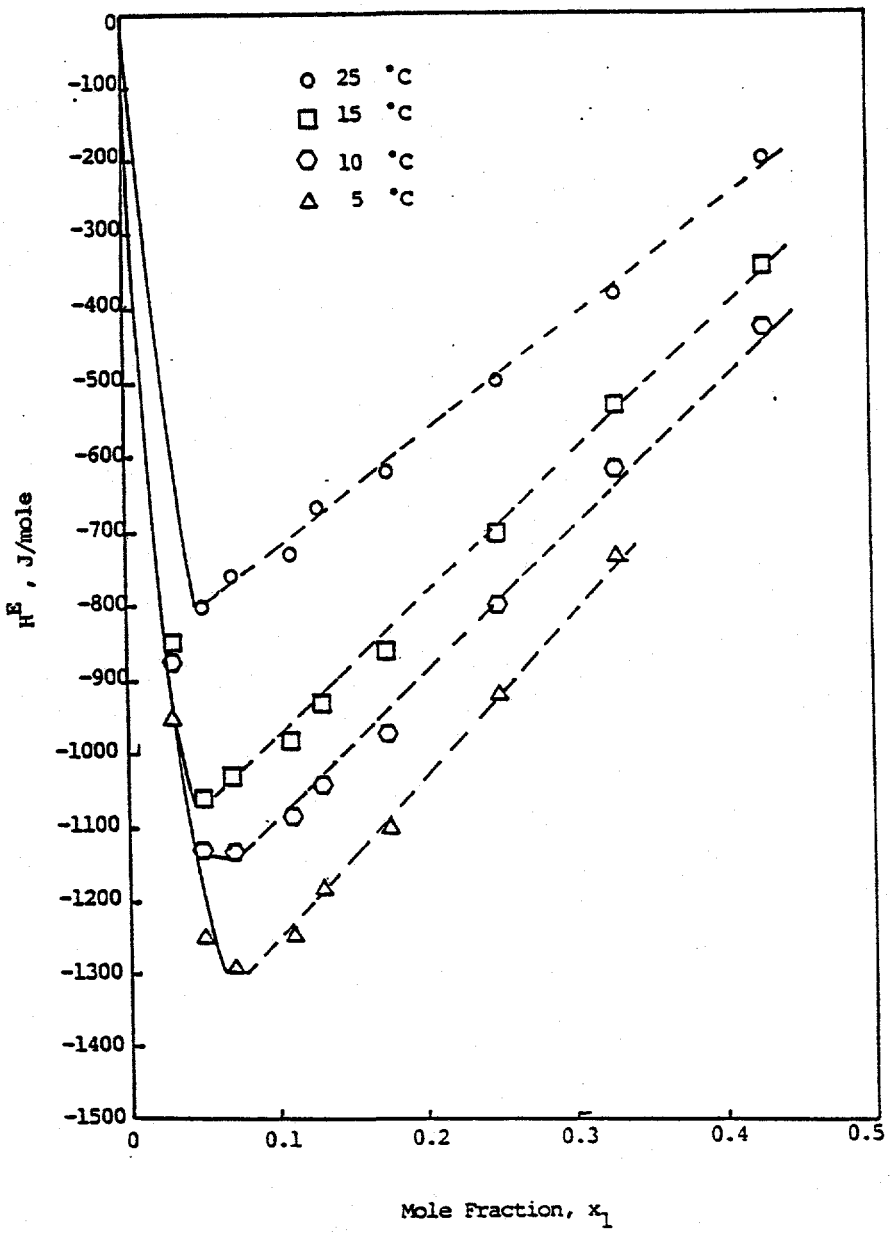


Figure 11. Heats of mixing for ethylene glycol diethyl ether (1) - water (2).

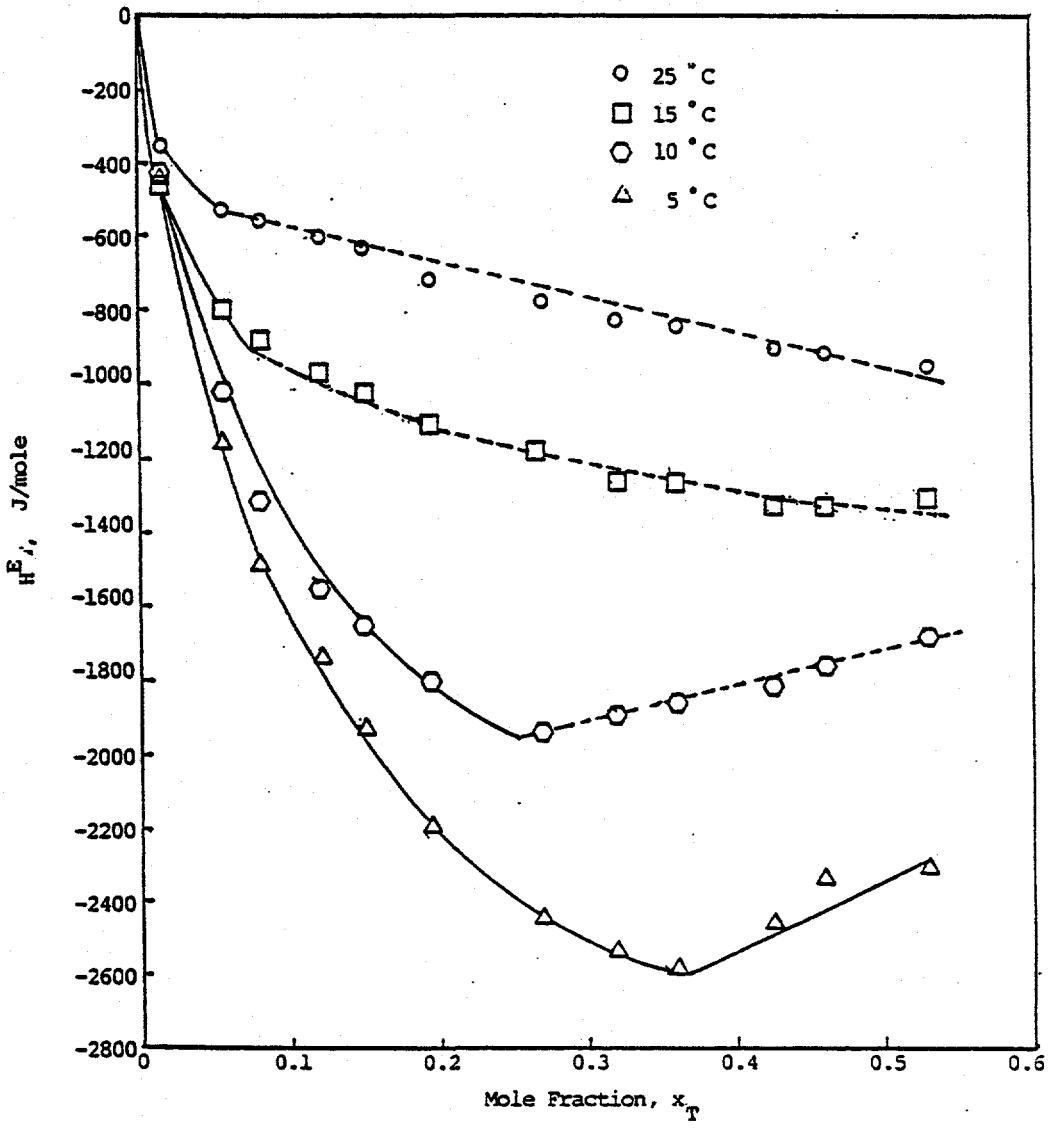


Figure 12. Heats of mixing for triethylamine-urea-water; $x_u^i = 0.077$.

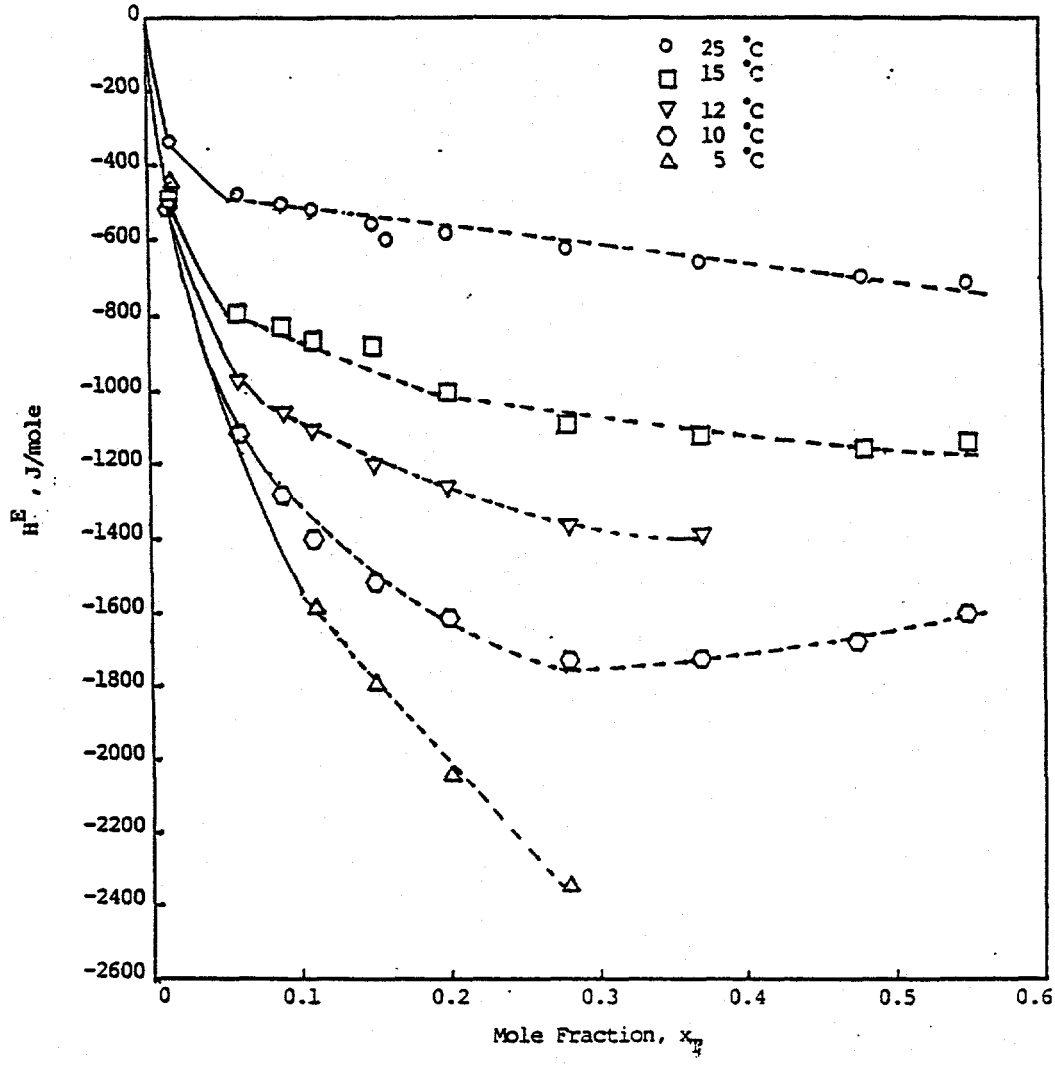


Figure 13. Heats of mixing for triethylamine-urea-water; $x_u^i = 0.1$.

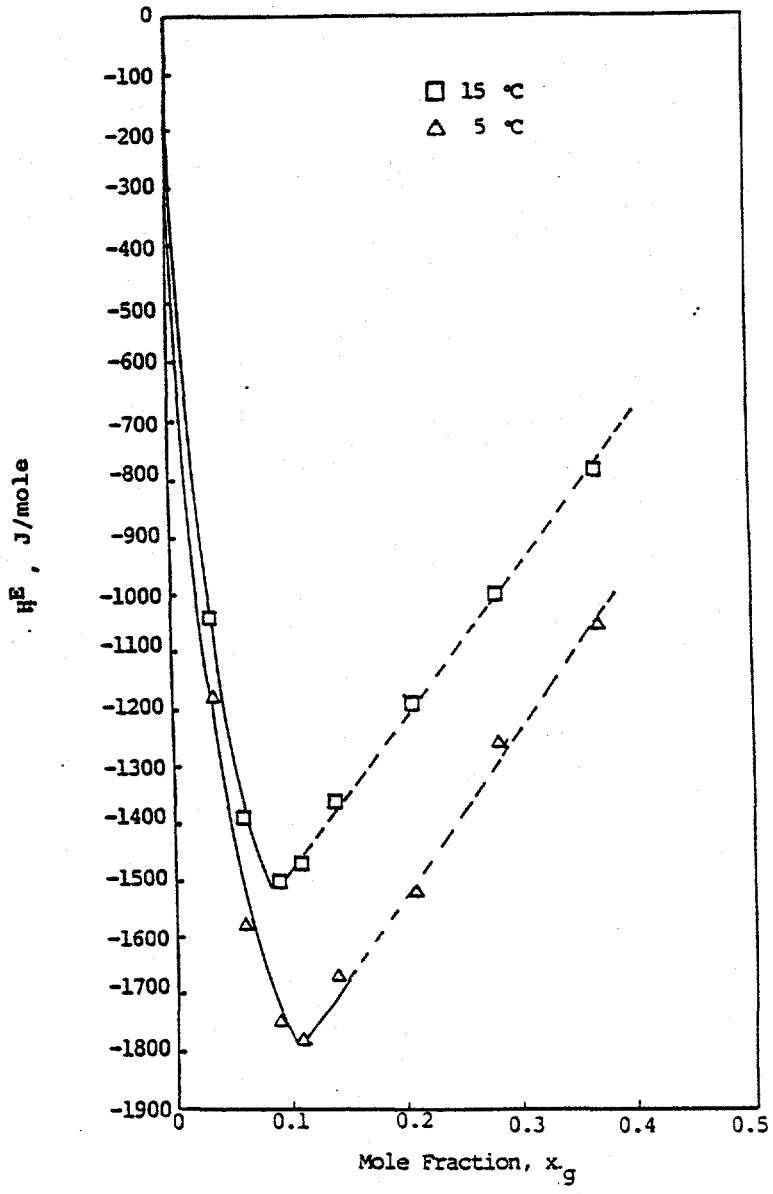


Figure 14. Heats of mixing for diethylene glycol diethyl ether (1)-NaCl-water; $x^i_{NaCl} = 0.0113$.

# INDUSTRIAL THERMAL ENERGY STORAGE

# SIMULATION OF A HIGH TEMPERATURE THERMAL ENERGY STORAGE SYSTEM EMPLOYING SEVERAL FAMILIES OF PHASE-CHANGE STORAGE MATERIAL

**George A. Adebiyi**
Mechanical and Nuclear Engineering Department
Mississippi State University
Mississippi State, Mississippi 39762

***Abstract***

*Previous work by the author entailed modeling of the Packed Bed Thermal Energy Storage System, utilizing Phase-Change Materials, and a performance evaluation of the system based on the Second Law of thermodynamics. A principal conclusion reached is that the use of a single family of phase-change storage material may not in fact produce a thermodynamically superior system relative to one utilizing sensible heat storage material. This prompted us to modify our model so that we could investigate whether or not a significantly improved performance may be achieved via the use of multiple families of phase-change materials instead.*

*Other factors investigated in the present work include the effect on system performance due to the thermal mass of the containment vessel wall, varying temperature and mass flow rate of the flue gas entering the packed bed during the storage process, and thermal radiation which could be a significant factor at high temperature levels. The resulting model is intended to serve as an integral part of a real-time simulation of the application of a high temperature regenerator in a periodic brick plant.*

*This paper describes the more comprehensive model of the high temperature thermal energy storage system and presents results indicating that improved system performance could be achieved via a judicious choice of multiple families of phase-change materials.*

## Introduction

Research previously performed by Mississippi State University on the High Temperature Thermal Energy Storage (TES) system is part of a project whose primary goal has been described as the development of a cost-effective latent heat storage system for the periodic brick kiln and an appropriate analytical capability for optimum system design. Specifically, our research was aimed at supplying the analytical capability for thermal energy storage systems utilizing cylindrical, encapsulated phase change storage material. The work is documented (see Adebiyi, 1988a and 1988b); and it should, therefore, be sufficient for us to merely restate the scope of that work and reiterate the principal conclusions reached.

**Previous Work**

The original work statement required the construction, validation, and utilization of a mathematical model for the packed bed. We developed a computer program, based on our approximate model of the packed bed TES system. The program can be modified and further refined as improved data becomes available, leading to more accurate thermal models for the packed bed. In other words, we envisage the validation process to be one which involves successive iteration between design, based on our model, testing of an experimental unit, and further refinement of the model on the basis of the experimental data obtained.

The computer program is in FORTRAN 77 and we extensively exercised it on a Harris Computer main frame for the conduct of generic first- and second-law studies on the packed bed storage system utilizing phase change storage material. We investigated a variety of design and operational variables which included:

(i) whether or not a TES system utilizing a phase change material (PCM) would necessarily always perform better than one employing sensible heat storage material;

(ii) the influence of PCM characteristics (such as phase-change temperature) on performance of the TES system;

(iii) the dependence of performance on packed bed dimensions (for example, the bed length);

(iv) system performance as a function of starting and stopping scenarios for the storage and removal processes;

(v) constant and ramp hot fluid entry temperature-time profile, respectively, applied to the packed bed storage system.

Our study clearly demonstrated the extreme usefulness of a second-law analysis in the characterization and optimization study of the packed bed thermal energy storage system. We were able, with the aid of a second-law analysis, to identify which stages of operation resulted in the most significant dissipation of exergy and consequent loss in efficiency. Thus, we found, for example, that subjecting a packed bed, utilizing a PCM with a high phase-change temperature, to a ramp hot fluid entry temperature-time profile would result in a poor level of performance due to excessive loss of exergy associated with the charging fluid leaving the packed bed at a high temperature for a disproportionately long time period. In our view, the situation could be remedied or improved somewhat by using a range of PCMs in series such that the PCM with the highest melting point is at the hot fluid entry to the bed, while that with the lowest melting point is positioned towards the exit to the bed.

We noted another unfavorable trend in our studies, this time in relation to the relative time periods for the storage and removal processes. The removal period turned out to be typically disproportionately short compared with the storage period. Again, the proposed use of a multiple set of PCMs may turn this unfavorable trend around.

For a TES system utilizing a single family of PCM, our studies seemed to indicate that the principal advantage in the use of phase change storage material is in respect to an enhanced storage capacity,

compared with the same size of packed bed utilizing a sensible heat storage material. Thermodynamically, it was not apparent that a system employing a single family of phase-change storage material would always, or necessarily, be superior to that using a sensible heat storage material.

**Current Research**

The extension to our previous work was prompted, in part, by some of the conclusions reached in the study. In addition, certain refinements to the computer program were needed to enhance the analytical capability for proposed design optimization studies which would use a periodic brick plant simulation model that definitively marks out the windows of opportunity, on a real-time basis, for waste heat storage and subsequent cost-effective utilization. The prescribed modifications are such that the new model will be capable of accomodating the following:

(i) a gas inlet stream with time varying mass flow rates, temperatures, and chemical compositions;

(ii) gas-to-pellet radiation heat transfer and pellet-to-pellet conduction during periods of no flow;

(iii) any number of different PCMs distibuted vertically within the bed;

(iv) thermal effects of the packed bed containment vessel wall; and,

(v) the effect of temperature-dependent properties of the TES system inlet stream on heat transfer and pressure drop.

## Project Implementation and Results

We have already reconstructed our model of the packed bed such that the above-listed prescribed features are incorporated into the new model. A computer program for the improved model has been written in FORTRAN 77 with a version for the IBM-PC, based on the WATFOR 77 version of FORTRAN. (Program execution on the PC does take a rather long time period, however.) We provide an outline, later in this paper, on the modifications we made to the previous computer model in our construction of the new program.

We have exercised the new program quite extensively; and this paper will provide results we obtained on the transient response of the bed during periods of flow and no flow, the effect on performance of the bed due to the thermal mass of the containment vessel wall, and the use of a few families of PCMs in place of just one.

In its present form, the new program does not include routines for a second-law analysis. A proper evaluation of any thermodynamic process does require a second-law, study and it is our intention to include this in the final package.

The final version of the program will also be such that data generated on flue gas flow rates and inlet temperatures, on a real time basis, from the brick kiln simulation model can be fed directly to the new computer model of the TES packed bed, while the output of our program can be used in an optimization package for the entire brick plant storage system design.

**Modifications to the Previous Packed Bed Model**

The fundamental equations for the improved model are given in Appendix A for both the flow and no flow situations. The equations for the flow situation are basically the same as those for the storage and removal processes in the previous model except that account is now taken of the thermal effects associated with the thermal mass of the containment vessel wall. The corresponding set of equations for the stagnant bed is based on the general equations derived for the packed bed.

The inclusion of fluid-container wall heat transfer and the container wall-ambient air heat transfer requires us to solve an additional equation for the transient conduction through the containment vessel wall. We have assumed that temperature variations in the containment vessel wall will be important only in two space dimensions, radial (R) and along the length of the bed (x).

The governing equations for the fluid medium, the PCM storage media, and containment vessel wall are all, essentially, parabolic partial differential equations. This fact dictates the use of the implicit method for the finite-difference scheme, if an unconditionally stable procedure is to be achieved. Our problem is further complicated by two factors, however. The two space dimensions for the vessel wall region makes the use of the Implicit Alternating-Direction (I.A.D.) method necessary if the procedure is to be unconditionally stable without a serious loss of computational efficiency.

Secondly, the non-linearity in the enthalpy-temperature relationship for the PCMs tends to render an implicit scheme not-so-unconditionally stable after all, when conditions are in the region of the phase-change temperature. Thus far, we have been constrained to work with small time increments in order to achieve a stable scheme. Our method is basically that suggested by Shamsundar and Sparrow (1975) which uses the conduction equation written with the thermal energy storage term explicit in enthalpy rather than temperature. We are exploring other approaches such as one which uses an artificially high specific heat capacity, $c_p$, for a phase change material in the region of the phase-change temperature. Our expectation is that so long as we can avoid introducing a sharp discontinuity into the transient conduction equation for the phase change process, we may be able to have an implicit scheme which will be a lot less sensitive to the size of time increment employed.

Distribution of different PCMs (to a maximum of 5) within the bed is accomodated by characterizing the properties for each family of PCM as a function of their axial location in the bed. This characterization is effected at the start of the program, and the computational schemes employed are based on this characterization.

The heat transfer and pressure drop correlations assumed in the new and previous models are tenuous but can easily be replaced as more reliable and accurate data (for improved correlations) becomes available.

Our program uses the governing equations for the packed bed reduced to a dimensionless form. Appendix B gives the dimensionless form of the fundamental equations, as well as a set of similarity criteria which may be employed in scaling between a sub-scale test unit and a full-sized bed design.

**Sample Results Obtained with the New Program**

Preliminary results obtained with the new program are presented in Figures 1 to 7.

**Step Input Inlet Gas Temperature.** The results shown on Figures 1 to 4 are for runs having a step input for the inlet gas temperature in both the storage and removal periods. There is a dwell period separating the storage and removal processes.

Figures 1-3 are for a packed bed utilizing 5 PCMs with phase-change temperatures of 1000 K, 900 K, 800 K, 700 K, 500 K, respectively. All other thermophysical properties (including the latent heat of fusion) for the different PCMs are assumed identical.

In Figure 4, on the other hand, we are comparing the fluid outlet temperatures versus time response for three cases:

(i) One case corresponds to the transient response shown on Figure 1 for a bed utilizing 5 PCMs.

(ii) A second case uses 5 PCMs as before but assumes the containment vessel wall to be thermally isolated from the gas stream through the bed, in other words, this solution ignores the effect of the thermal mass of the containment vessel wall and the thermal conduction through it to the ambient air.

(iii) The third case includes the containment vessel wall effect but uses only one PCM family with a phase-change temperature of 1000 K.

No far-reaching conclusions should be read into the results at this stage since no conscious effort was made to optimize performance for any particular operational mode. It should be noted, however, that unless care is taken about the choice of operational mode, there may be little or no advantage derived by using multiple PCMs rather than a single PCM family.

We may note also that the inclusion of the thermal response of the containment vessel wall does significantly affect the predicted performance of the bed.

**Ramp Fluid Inlet Temperature-time Profile.** Figures 5 to 7 show results obtained when the fluid inlet temperature-time profile is a ramp.

Figure 5 corresponds to the case when a single PCM family is employed with a phase-change temperature ($T_{pb}$) of 1000 K and a dimensionless latent heat of fusion of 0.06.

The packed bed uses 5 PCMs in the cases shown on Figures 6 and 7. The phase-change temperatures are 1000 K, 900 K, 800 K, 700 K, 500 K, respectively. For the case shown on Figure 6, the dimensionless latent heat of fusion is 0.06 for each of the 5 sets of PCM, while all the other thermophysical properties are assumed identical for the different PCMs.

The 5 PCMs in the case shown on Figure 7, on the other hand, have dimensionless latent heats of fusion of 0.06, 0.3, 0.4, 0.5 and 0.6, respectively.

All the figures indicate relatively small differences in temperature between the fluid and the pellet surface at each axial location in the bed. However, the loss of exergy (or availability), due to the hot fluid exiting the packed bed hot during the storage process, becomes less as we position PCMs with a

combination of lower phase-change temperature and higher latent heat of fusion towards the exit to the packed bed. The condition described is also found to lead to a more favorable recovery time period (relative to the storage period) as compared to the other cases shown on Figures 5 and 6.

In all the cases shown on Figures 5 to 7, the storage process was terminated immediately all the PCMs had melted; the removal process was stopped when all the PCMs are completely solid again.

## Conclusions

We now have a computer model of the packed bed TES system with the kind of capabilities prescribed in the latest statement of work by the Oak Ridge National Laboratory (ORNL). Preliminary studies conducted with the new computer program lead to the following tentative conclusions:

(i) The effect of the thermal masss of the containment vessel wall on the bed performance appears significant; this factor should not be ignored in a realistic model of the bed.

(ii) Improved bed performance of the packed bed TES system is likely when multiple PCMs (rather than a single PCM family) are utilized with properties that are judiciously selected.

The final version of our computer programs will include subroutines for a second-law evaluation of the packed bed TES system and features which will facilitate the incorporation of the program to the more comprehensive TES system design package for a periodic brick plant. We are working also on a review of the numerical schemes currently employed by our program with the expectation that the computational efficiency would be improved, thus significantly reducing the program execution time.

## References

1. Adebiyi, G. A.,1988a, "Development of PCM Packed Bed Thermal Model for Industrial Applications,"Proceedings USDOE Diurnal/Industrial Thermal Energy Storage Research Activities Review (March 9-10, 1988), pp.328-379.

2. Adebiyi, G. A., 1988b, "First and Second Law Studies on Packed Bed Energy Storage Systems Utilizing Phase-Change Materials," Proceedings ASME's Winter Annual Meeting, AES-Vol. 6/HTD-Vol. 97, pp. 9-18.

3. Shamsundar, N. and Sparrow, E. M., 1975, "Analysis of Multidimensional Conduction Phase Change Via the Enthalpy Model," Journal of Heat Transfer, pp. 333-340.

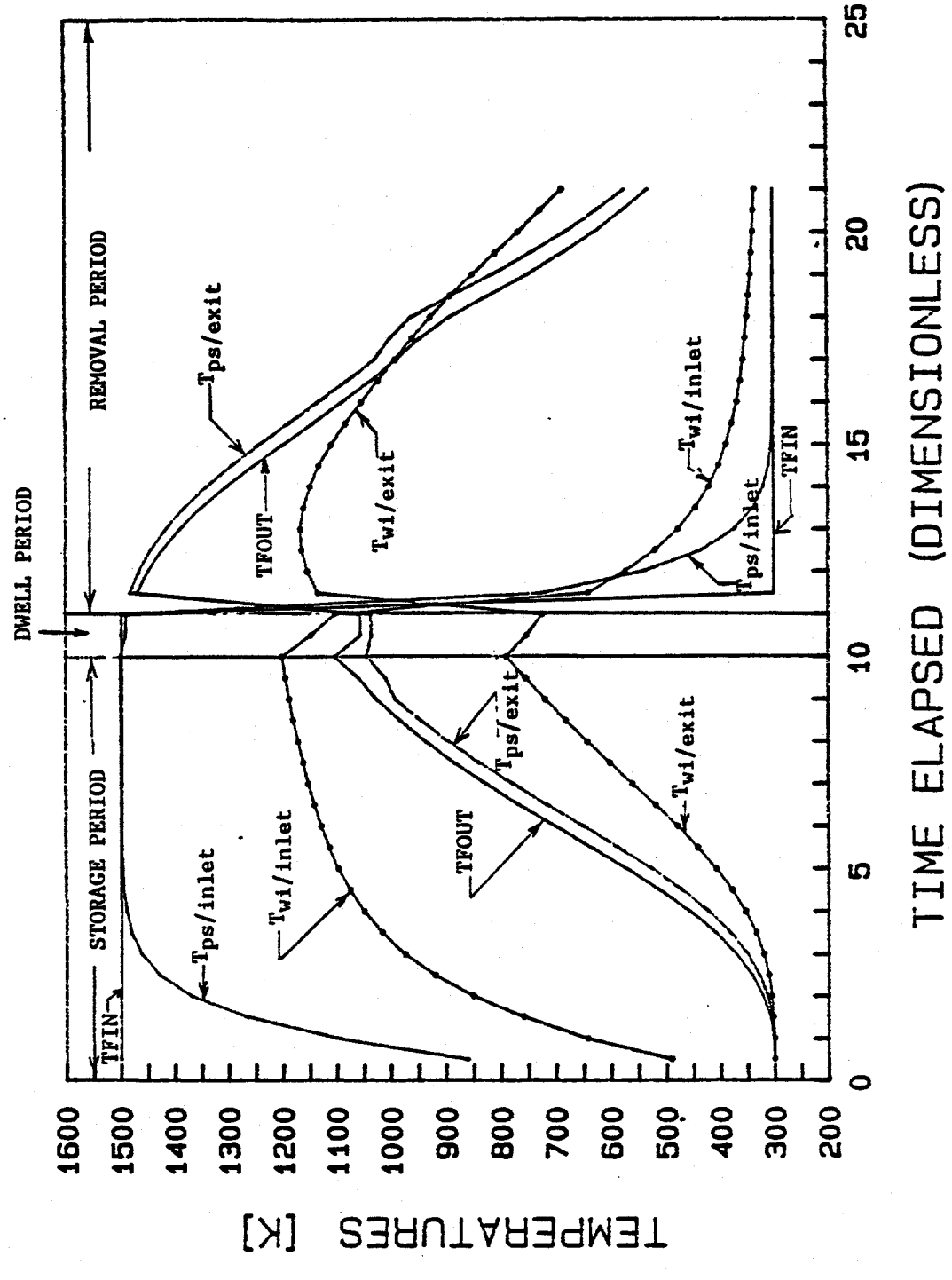


Figure 1. Transient response over a complete cycle (storage, dwell, and removal) for a packed bed utilizing five different PCMs; $G_c = G_n = 0.5$ Kg/m$^2$.s.

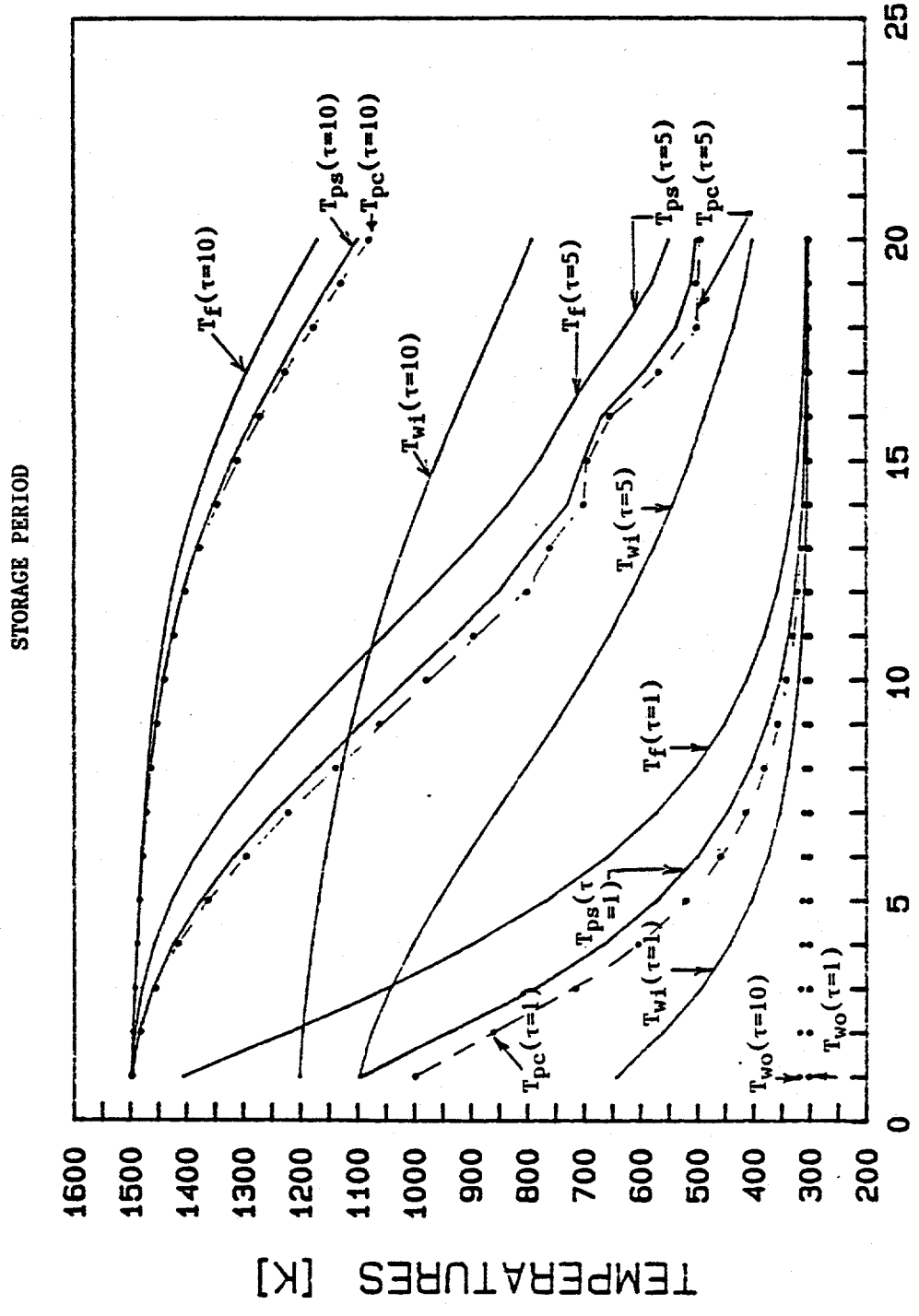


Figure 2. Temperature-axial position profiles for the packed bed utilizing five families of PCM; storage period.

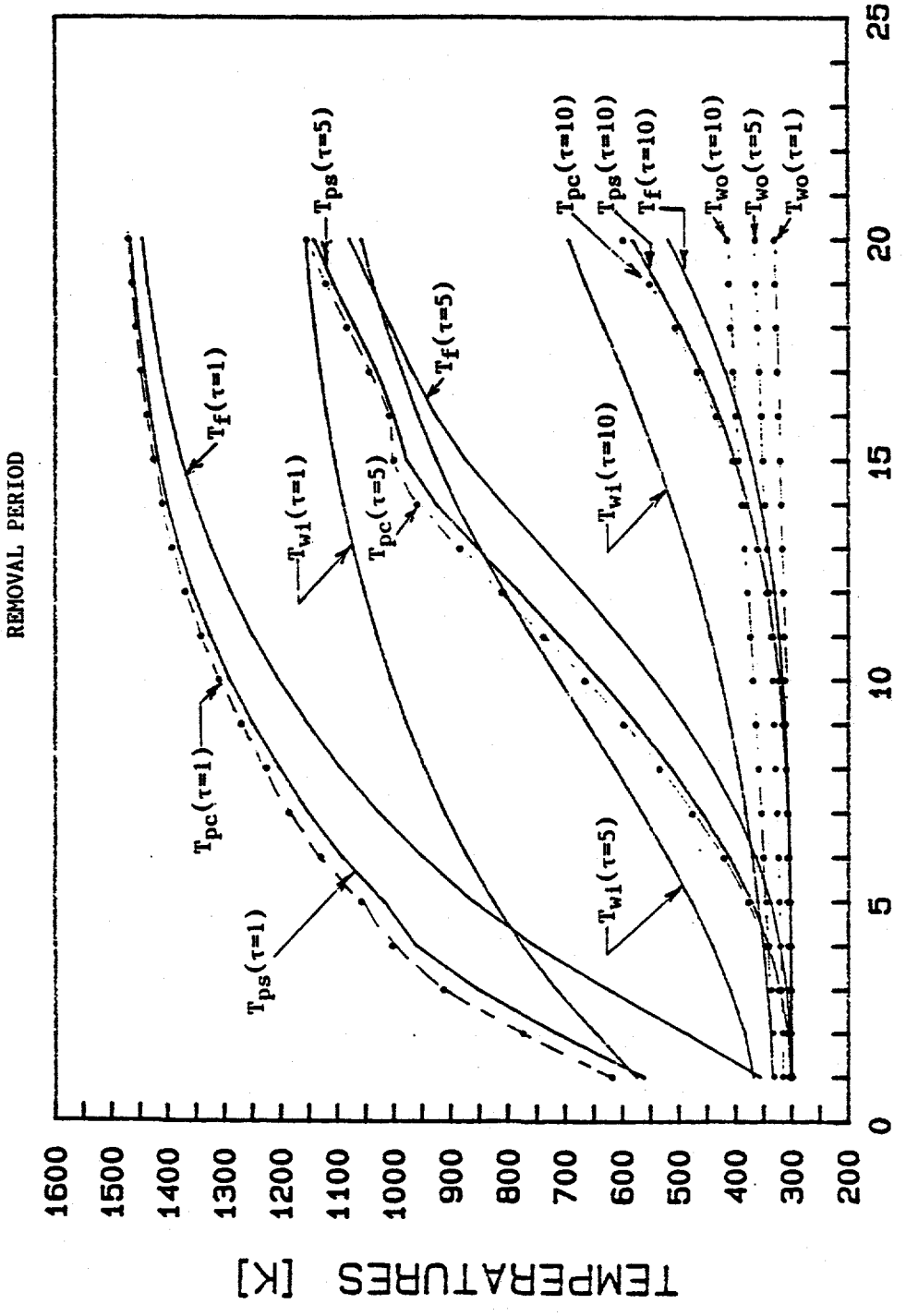


Figure 3. Temperature-axial position profiles for the packed bed utilizing five families of PCM; removal period.

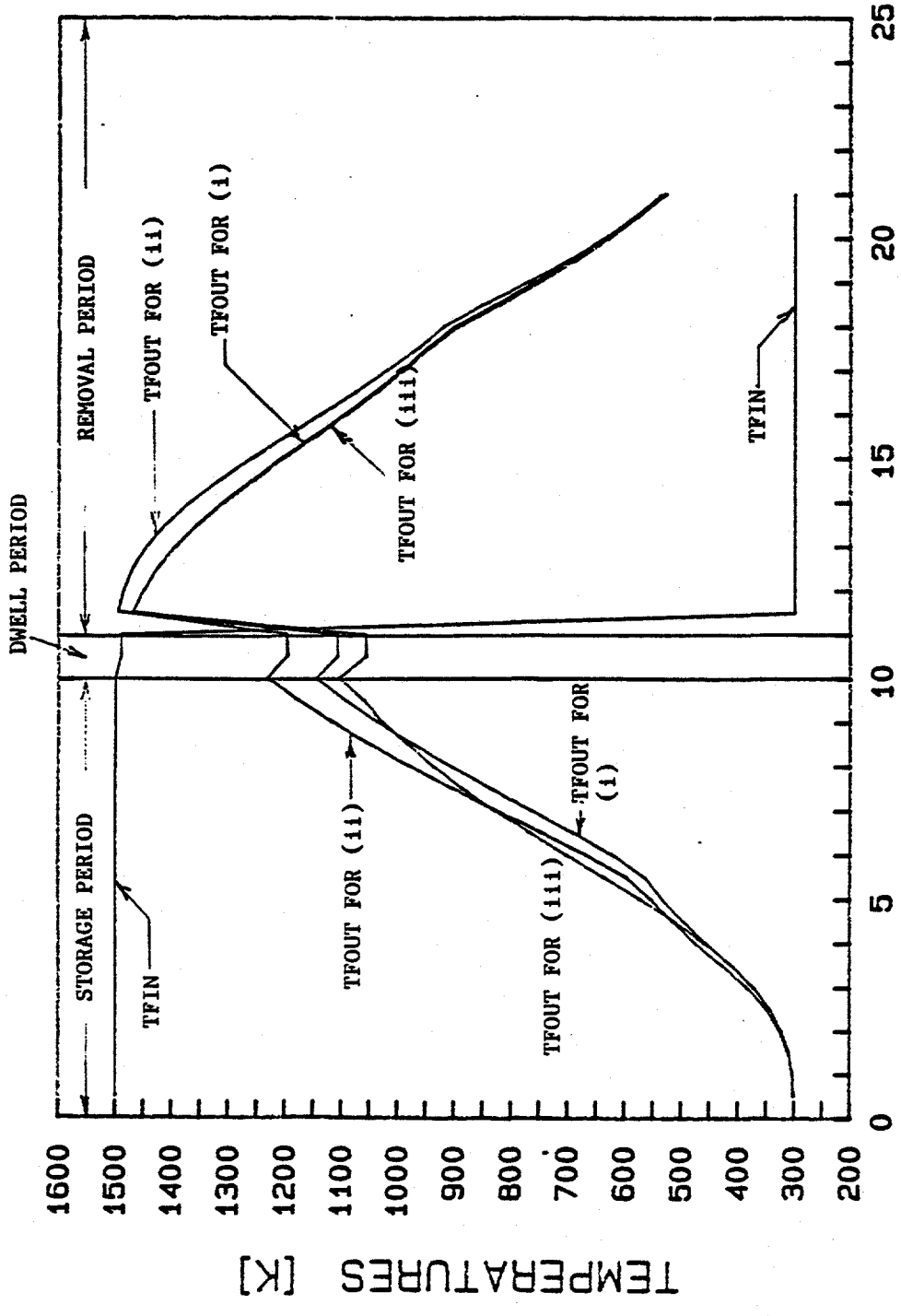


Figure 4. Comparison of the transient performance for the packed bed; (i) utilizing five PCM sets, (ii) utilizing five PCM sets with wall effect neglected, and (iii) utilizing one PCM family.

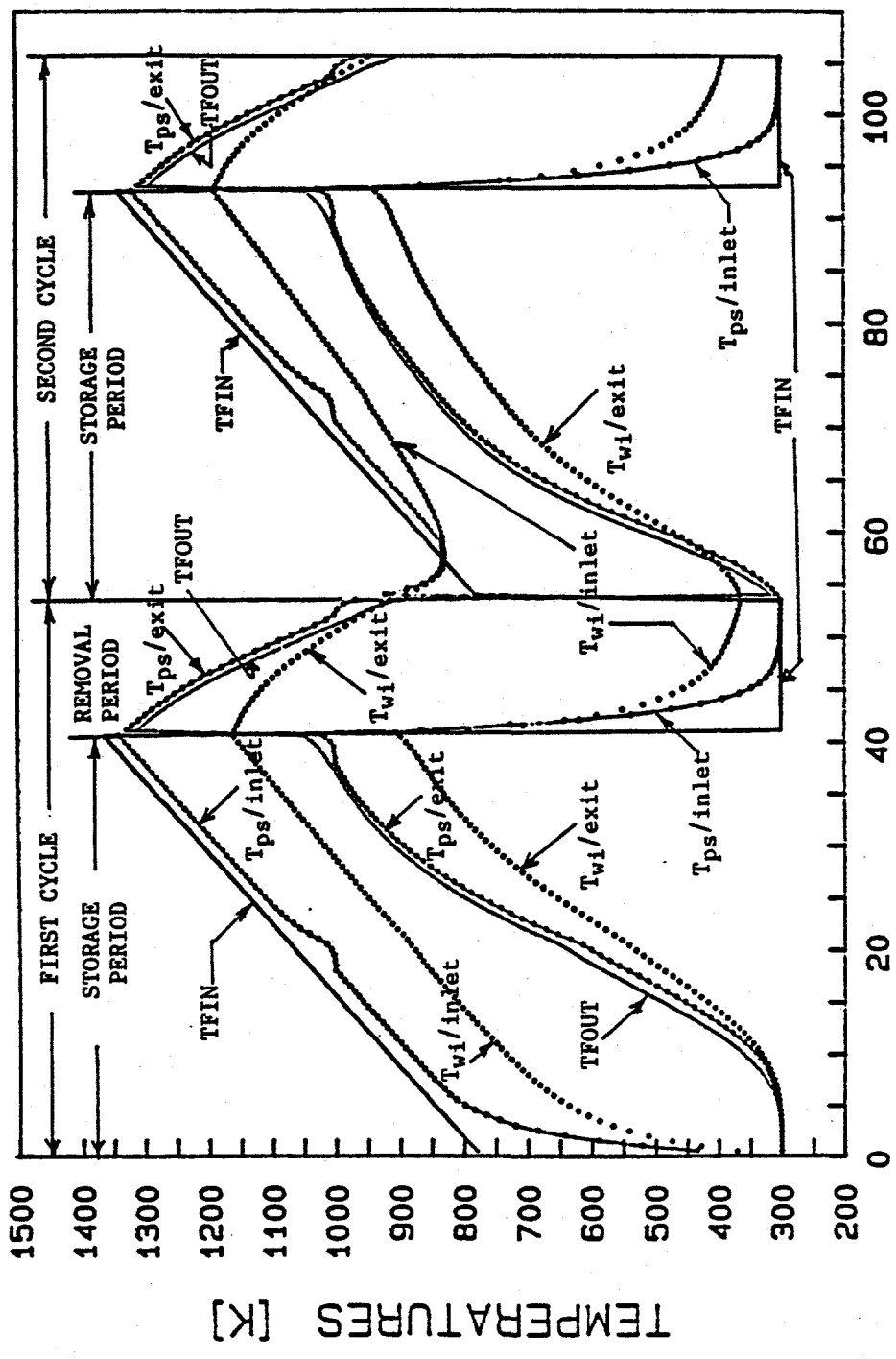


Figure 5. Transient performance of the packed bed TES unit utilizing one PCM family; $T_{ph}$ = 1,000K, $i_{ph}/C_s.\Delta T_o$ = 0.06.

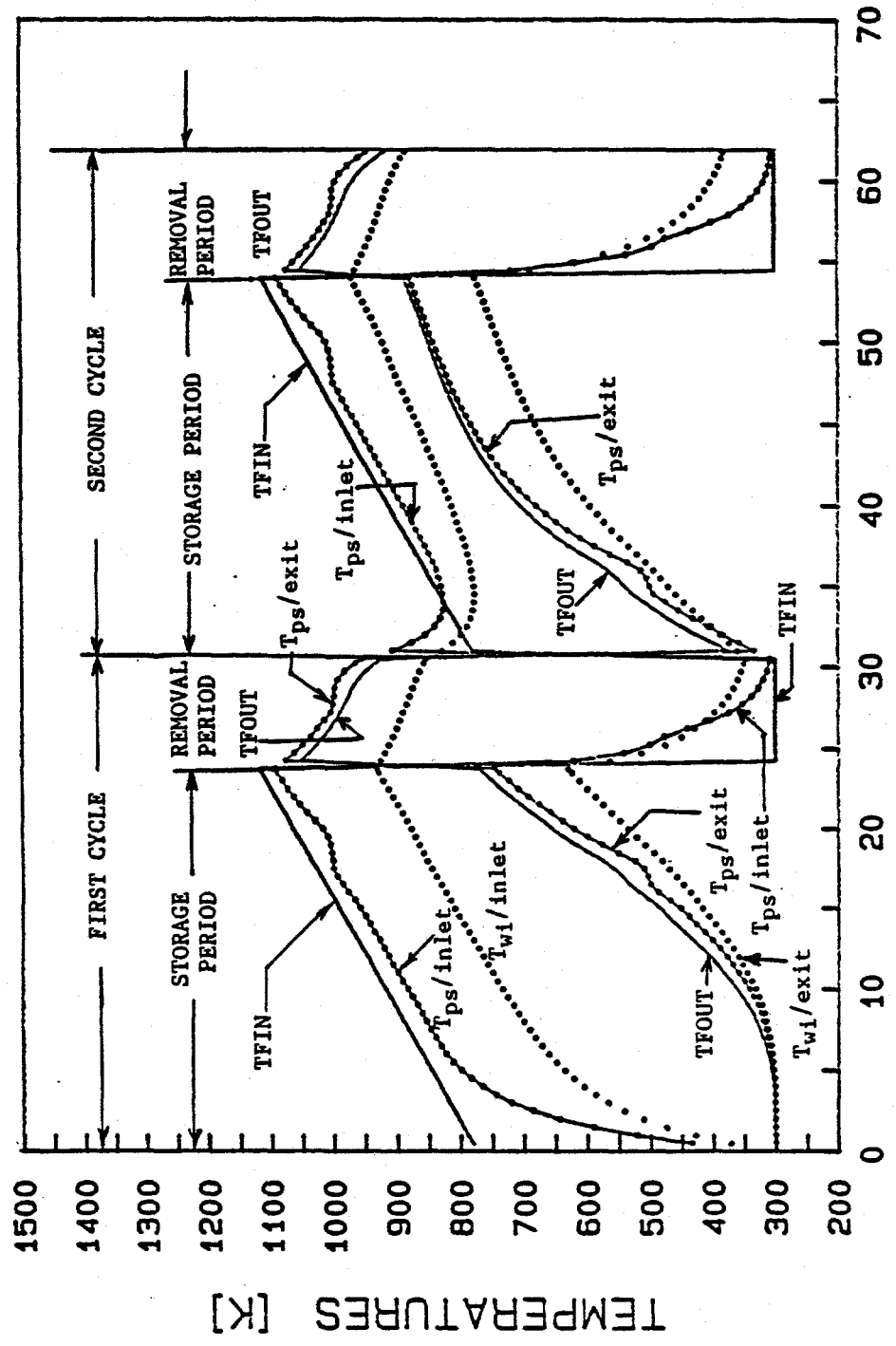


Figure 6. Transient performance of the packed bed TES unit utilizing five PCM families; $T_{ph}$ = 1,000K, 900K, 800K, 700K, and 500K and $i_{ph}/C_s.\Delta T_o$ = 0.06.

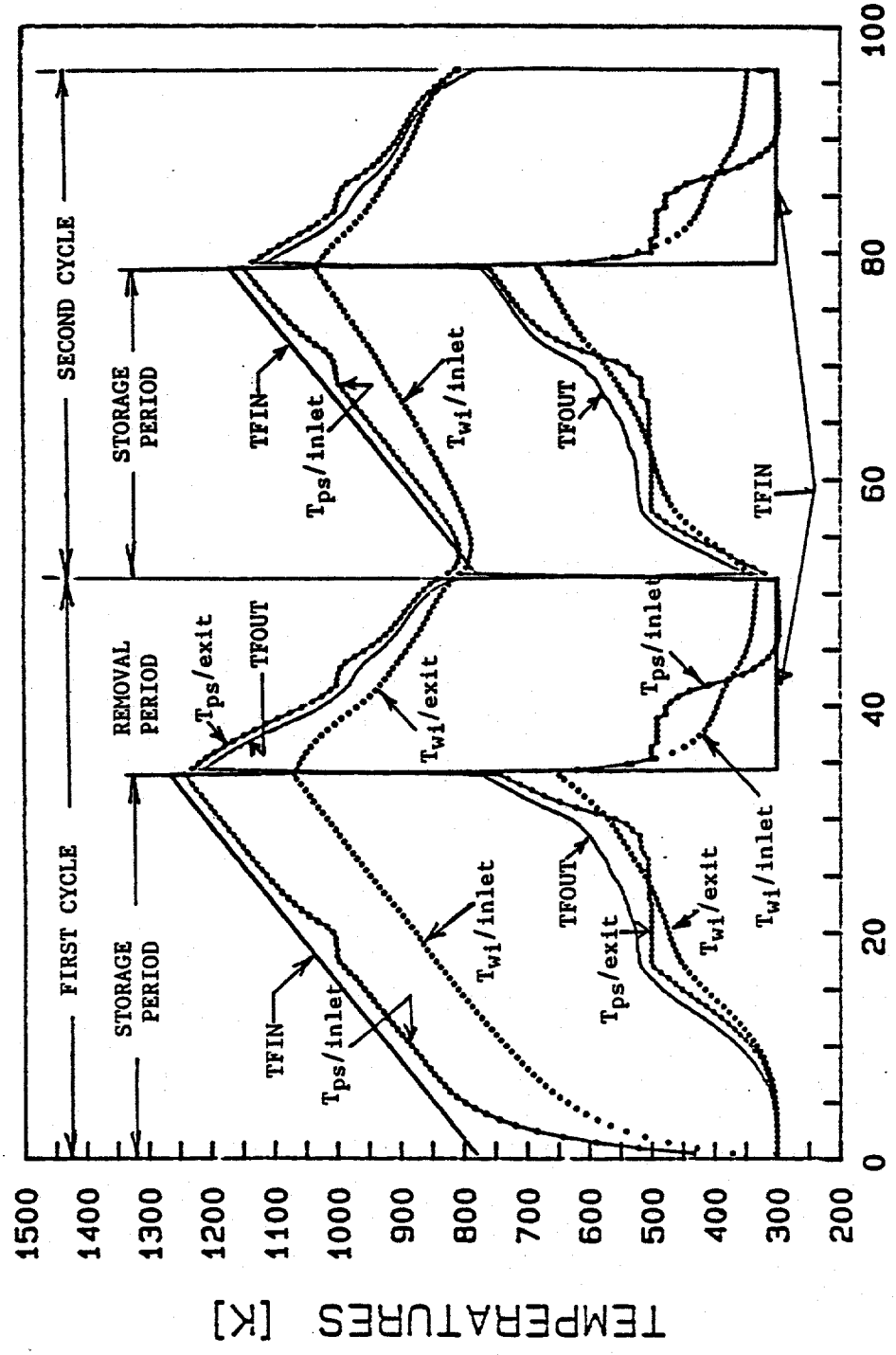


Figure 7. Transient performance of the packed bed TES unit utilizing five PCM families; $T_{ph}$ = 1,000K, 900K, 800K, 700K, and 500K and corresponding $i_{ph}/C_s.\Delta T_o$ = 0.06, 0.3, 0.4, 0.5, and 0.6.

# APPENDIX A

## THE FUNDAMENTAL EQUATIONS FOR THE PACKED BED IN THE STORAGE, REMOVAL AND DWELL PERIODS

Figures 1(a), 1(b) and 1(c) show the coordinate systems for the packed bed and the cylindrical bed particle. The approximate model is shown in Fig. 2 with the bed particles effectively reduced to longitudinal elements somewhat resembling "linked sausages." The fluid flow through the bed voids is then taken, essentially, as slug or plug flow.

The containment vessel is assumed cylindrical with inner and outer radii of $R_{wi}$ and $R_{wo}$, respectively. The ambient environment is at a temperature $T_0$[K] and the convective heat transfer coefficient on the outside of the cylindrical containment vessel is $h_{wo}$[kW/m$^2$ - K].

Relative to the coordinate systems and the model defined in Figs. 1 and 2, we may write comprehensive energy balance equations for the fluid medium, the bed particles and the containment vessel wall as follows:

**Fluid medium:**

$$\frac{\epsilon}{(c_p/c_v)_f} \cdot \frac{1}{\alpha_f}\frac{\partial T_f}{\partial t} + \frac{u_o}{\alpha_f}\frac{\partial T_f}{\partial x} = \frac{ha}{k_f}(T_{ps} - T_f) + \frac{h_{wi}(2/R_{wi})}{k_f}(T_{wi} - T_f) +$$

$$\frac{k_{e,f}^{(x)}}{k_f}\frac{\partial^2 T_f}{\partial x^2} + \frac{k_{e,f}^{(R)}}{k_f} \cdot \frac{2}{(2R + D_e)}\left[\frac{\partial T_f}{\partial R} + (R + D_e)\frac{\partial^2 T_f}{\partial R^2}\right] \qquad (A1)$$

In general, $R >> D_e$ (especially as we move away from the core region of the bed) and, hence, to a good approximation (A1) may be rewritten as:

$$\frac{\epsilon}{(c_p/c_v)_f} \cdot \frac{1}{\alpha_f}\frac{\partial T_f}{\partial t} + \frac{u_o}{\alpha_f}\frac{\partial T_f}{\partial x} = \frac{ha}{k_f}(T_{ps} - T_f) + \frac{h_{wi}(2/R_{wi})}{k_f}(T_{wi} - T_f)$$

$$+ \frac{k_{e,f}^{(x)}}{k_f}\frac{\partial^2 T_f}{\partial x^2} + \frac{k_{e,f}^{(R)}}{k_f}\left[\frac{1}{R}\frac{\partial T_f}{\partial R} + \frac{\partial^2 T_f}{\partial R^2}\right] \qquad (A2)$$

The parameter a is given by

$$a = 6(1 - \epsilon)/D_{e,c} \qquad (A3)$$

We have established approximate criteria governing when some of the terms in equations (A1) and (A2) may be negligible. The summary is as follows:

(i) The accumulation (or storage) terms may be neglected if

$$V_H(\text{heat capacity ratio}) = \frac{(1-\epsilon)}{\epsilon}\frac{\rho_s c_s}{\rho_f c_f} \gg 1 \qquad \text{(A4)}$$

(ii) The axial dispersion term may be neglected if

$$Re_o \cdot Pr_f > 50 \qquad \text{(A5)}$$

with

$$Re_o = \rho_f u_o D_p/\mu_f \qquad \text{(A6)}$$

(iii) The radial dispersion term may be neglected if

$$R_{wi}/D_e > 10 \qquad \text{(A7)}$$

(iv) For the term involving fluid stream-containment vessel wall heat transfer, the criterion works out as

$$(h_{wi}/h) \ll 3(1-\epsilon)\, R_{wi}/D_{e,c} \qquad \text{(A8)}$$

if this factor is to be negligible.

In the present study, we shall assume that (A7) still applied but we shall now include the axial dispersion effect, especially for the no-flow situation. Suitable empirical correlations for $k_{e,f}^{(x)}/k_f$ are given by Yagi[1] et al and Yagi and Kunii[2].

The heat transfer coefficients defined should include radiation effects at the high temepratures. McAdams[3] gives a formula, due to Damkohler, for the inclusion of radiation effects in a thermal model for the packed bed.

**Storage medium:**

The transient conduction in each cylindrical particle is modeled as a quasi-one-dimensional problem. We make use of a dimensionless parameter w given by the following:

---

[1]Yagi, S., Kunii, D. and Wakao, N., "Studies on Axial Effective Thermal Conductivities in Packed Beds," A.I.Ch.E. Jl, Vol. 6, No. 4, 1960, pp. 543-546.

[2]Yagi, S. and Kunii, D., "Studies on Effective Thermal Conductivities in Packed Beds," A.I.Ch.E. Jl, Vol. 3, No. 3, 1957, pp. 373-381.

[3]McAdams, W. H., Heat Transmission, 3rd Ed., McGraw-Hill Koga Kusha, London, 1954, p. 290.

$$\frac{A_p \cdot b}{V_p} = 1 + w \tag{A9}$$

The transient conduction equation for a cylindrical phase change storage material may be written:

$$\rho_s \frac{\partial e}{\partial t} = \frac{1}{y^w} \frac{\partial}{\partial y} \left[ y^w \cdot k_s \frac{\partial Tp}{\partial y} \right] \tag{A10}$$

Since the storage material can undergo a phase change, we shall have need to specify a non-linear e-$T_p$ relationship for each PCM employed:

$$T_p = T_p(e) = \begin{cases} (e - e_s)/c_s + T_{ph}, & \text{when } e \leq e_s \\ T_{ph}, & \text{when } e_s \leq e \leq e_\ell \\ (e - e_\ell)/c_\ell + T_{ph}, & \text{when } e \geq e_\ell \end{cases} \tag{A11}$$

For the boundary condition, we can show that if $\bar{e}_p$ is the total energy per unit mass of a bed particle,

$$\rho_s \frac{\partial \bar{e}_p}{\partial t} = \frac{6h}{D_{e,c}} (T_f - T_{ps}) \tag{A12}$$

$\bar{e}_p$ [kJ/kg] in turn is obtained from

$$\bar{e}_p = \int_{V_p} e \frac{dV}{V_p} \tag{A13}$$

In addition, we have for the storage medium-fluid boundary

$$\frac{\partial T_p}{\partial y} \Big|_{y=b} = \frac{h}{k_s} (T_f - T_{ps}) \tag{A14}$$

The equations (A9) - (A14) will be employed in turn to families of PCM's each characterized by the equation (A11).

**Containment Vessel Wall:**

If the containment vessel wall is thick, we would need to solve the two-dimensional transient conduction equation:

$$\frac{1}{\alpha_w}\frac{\partial T_w}{\partial t} = \frac{\partial^2 T}{\partial x^2} + \frac{1}{R}\frac{\partial}{\partial R}\left[R\frac{\partial T}{\partial R}\right] \tag{A15}$$

subject to the following equations for the boundary condition:

$$\left[\frac{\partial T_w}{\partial R}\right]_{R=R_{wi}} = \frac{h_{wi}}{k_w}(T_{wi} - T_f) \tag{A16}$$

and

$$\left[\frac{\partial T_w}{\partial R}\right]_{R=R_{wo}} = \frac{h_{wo}}{k_w}(T_o - T_{wo}) \tag{A17}$$

More realistically, the vessel wall thickness will be small compared with either $R_{wi}$ or $R_{wo}$ in which case we may treat conduction in the vessel wall as essentially two-dimensional conduction in a slab or plane wall:

$$\frac{1}{\alpha_w}\frac{\partial T_w}{\partial t} = \frac{\partial^2 T_w}{\partial x^2} + \frac{\partial^2 T_w}{\partial z^2} \tag{A18}$$

with $z = R - R_{wi}$.

# APPENDIX B
# THE FUNDAMENTAL EQUATIONS FOR THE PACKED BED REDUCED TO A DIMENSIONLESS FORM

The fundamental equations for the packed bed are given in Appendix A; they are equations (A2), (A10) and (A18) for the fluid medium, the storage medium and the containment vessel wall, respectively. These equations may be reduced to a dimensionless form based on the following:

$\ell_o$ = characteristic length dimension for the bed.

(For linear dimensions within each bed particle, b will be taken as the characteristic length.)

$\Delta T_o$ = a temperature difference which is to serve, essentially, as a scaling factor for the media temperatures. Typically, $\Delta T_o$ may be taken as 1000 K.

$u_o$ = characteristic velocity which is also the superficial velocity of the fluid stream through the bed.

$c_{so}$ = characteristics specific heat for the storage medium; its value may be chosen as that for the solid phase of any of the PCMs.

$k_{so}$ = characteristic thermal conductivity for the storage medium.

$\rho_{so}$ = characteristic density for the storage medium.

$\alpha_{so} = k_{so}/(\rho_{so} \cdot c_{so})$ is a characteristic thermal diffusivity for the storage medium.

Thus, we may define:

$$X = x/\ell_o,\ Z = z/\ell_o,\ R^* = R/\ell_o \text{ and } Y = y/b$$

$$\tau = \alpha_w t/\ell_o^2,\ t^* = \alpha_{so} t/b^2$$

$\tau$ and $t^*$ are related according to

$$\tau/t^* = (\alpha_w/\alpha_{so})(b/\ell_o)^2 .$$

$$T_f^* = T_f/\Delta T_o,\ T_p^* = T_p/\Delta T_o,\ T_w^* = T_w/\Delta T_o$$

$$e^* = e/(c_{so} \cdot \Delta T_o)$$

$$u^* = u/u_o$$

We now use the above dimensionless parameters to convert the fundamental equations to the following dimensionless form.

Fluid Medium (Equation A2):

$$A_1 \frac{\partial T_f^*}{\partial \tau} + C_1 u^* \frac{\partial T_f^*}{\partial X} = C_p(T_p^*|_{Y=1} - T_f^*) + C_w(T_w^*|_{Z=0} - T_f^*) + D_X \frac{\partial^2 T_f^*}{\partial X^2} + D_R\left[\frac{1}{R^*}\frac{\partial T_f^*}{\partial R^*} + \frac{\partial^2 T_f^*}{\partial R^{*2}}\right] \quad \text{(B1)}$$

where

$$A_1 = \frac{1}{(c_p/c_v)_f}\left[\frac{a_w}{a_f}\right]\left[\frac{\epsilon}{6(1-\epsilon)}\right]\cdot\left[\frac{D_{e,c}}{\ell_o}\right]^2 \quad \text{(B2)}$$

$$C_1 = \epsilon\left[\frac{D_{e,c}}{\ell_o}\right]\cdot Re_{D_c}\cdot Pr_f \quad \text{(B3)}$$

$$C_p = h\cdot D_{e,c}/k_f \quad \text{(B4)}$$

$$C_w = \frac{2(D_{e,c}/D_{bed})}{3(1-\epsilon)} \cdot \left[\frac{h_{wi}\cdot D_{e,c}}{k_f}\right] \quad \text{(B5)}$$

$$D_X = \left[\frac{D_{e,c}}{\ell_o}\right]^2 \left[\frac{\epsilon}{6(1-\epsilon)}\right]\cdot\left[\frac{k_{e,f}^{(x)}}{\epsilon k_f}\right] \quad \text{(B6)}$$

$$D_R = \left[\frac{D_{e,c}}{\ell_o}\right]^2 \left[\frac{\epsilon}{6(1-\epsilon)}\right]\cdot\left[\frac{k_{e,f}^{(R)}}{\epsilon k_f}\right] \quad \text{(B7)}$$

$D_{bed}$ is the inside diameter of the packed bed. $Re_{D_c}$ and $Pr_f$ are defined as:

$$Re_{D_c} = \frac{G_o D_{e,c}}{6(1-\epsilon)\mu_f} \quad \text{(B8)}$$

$$Pr_f = \mu_f c_{pf}/k_f \quad \text{(B9)}$$

From Yagi, S. et al[1], we can surmise the following for the effective axial and radial thermal conductivities:

---

[1]Yagi, S., Kunii, D. and Wakao, N., "Studies on Axial Effective Thermal Conductivities in Packed Beds," A.I.Ch.E.Jl., Vol. 6, No. 4, 1960, pp. 543-546.

$$\frac{1}{\epsilon}\frac{k_{e,f}^{(x)}}{k_f} = \frac{1}{\epsilon}\frac{k_{e,x}^{(o)}}{k_f} + 6(1-\epsilon)\delta Re_{D_c} Pr_f \qquad (B10)$$

$$\frac{1}{\epsilon}\frac{k_{e,f}^{(R)}}{k_f} = \frac{1}{\epsilon}\frac{k_{e,x}^{(o)}}{k_f} + 6(1-\epsilon)(\alpha\beta)Re_{D_c} Pr_f \qquad (B11)$$

$\delta$ = 0.7 (for metallic particles) and 0.8 (for non-metals).

$\alpha\beta$ ~ 0.1 - 0.3

$\frac{1}{\epsilon}\frac{k_{e,x}^{(o)}}{k_f}$ is the axial effective thermal conductivity for stagnant bed (typical value is in the range 7 to 13).

$\frac{1}{\epsilon}\frac{k_{e,R}^{(o)}}{k_f}$ is the axial effective thermal conductivity for stagnant bed with values varying typically between 8 and 19.

Storage Medium (Equation (A10))

The transient conduction equation, in dimensionless form, for the storage medium is

$$\frac{\partial e^*}{\partial t^*} = \left[\frac{\rho_{so}}{\rho_s}\right]\left[\frac{k_s}{K_{so}}\right]\left[\frac{\partial^2 T_p^*}{\partial Y^2} + \frac{\omega}{Y}\frac{\partial T_p^*}{\partial Y}\right] \qquad (B12)$$

The storage medium-fluid boundary condition (equation (A14)) may, likewise, be written in dimensionless form:

$$\left.\frac{\partial T_p^*}{\partial Y}\right|_{Y=1} = \left[\frac{hb}{k_{so}}\right]\left[\frac{k_{so}}{k_s|_{Y=1}}\right]\left[T_f^* - T_p^*|_{Y=1}\right] \qquad (B13)$$

The e-$T_p$ relationship, given by (A11) becomes:

$$T_p^* = T_p^*(e^*) = \begin{cases} (c_{so}/c_s)(e^*-e_s^*) + T_{ph}^*, & \text{when } e^* \leq e_s^* \\ T_{ph}^*, & \text{when } e_s^* \leq e^* \leq e_\ell^* \\ (c_{so}/c_\ell)(e^*-e_\ell^*) + T_{ph}^*, & \text{when } e^* \geq e_\ell^* \end{cases} \qquad (B14)$$

(B14) may be simplified somewhat if we only have a single PCM family for the storage medium. We could use $T_o$ as the datum for the specific internal energy for the bed particles. Thus, $e_s$ and $e_\ell$ may be written:

$$e_s = c_s(T_{ph} - T_o) \tag{B15}$$

and

$$e_\ell = e_s + i_{ph} \tag{B16}$$

where $i_{ph}$ is the specific heat of fusion for the PCM bed particle. $T_p^*$ and $\Delta T_o$ may be redefined such that

$$T_p^+ = (T_p - T_o)/\Delta T_o \tag{B17}$$

replaces $T_p^*$ in (B12) and (B13) while

$$\Delta T_o = T_{ph} - T_o \tag{B18}$$

$T_f^*$, $T_w^*$ should likewise be redefined as

$$T_f^+ = (T_f - T_o)/\Delta T_o \tag{B19}$$

and

$$T_w^+ = (T_w - T_o)/\Delta T_o \tag{B20}$$

With the above listed redefinitions, we only need to replace $T_p^*$, $T_f^*$, $T_w^*$, with $T_p^+$, $T_f^+$ and $T_w^+$ respectively, in the earlier dimensionless equations.

We can further rewrite the e-$T_p$ relationship in the following alternative form:

$$T_p^+ = T_p^+(e^*) = \begin{cases} (c_{so}/c_s)e^*, \text{ when } e^* \leq e_s^* \\ 1, \text{ when } e_s^* \leq e^* \leq e_\ell^* \\ (c_{so}/c_\ell)e^* + (1 - c_s/c_\ell) - (c_{so}/c_\ell)(i_{ph}/c_{so}\cdot\Delta T_o), \\ \quad \text{when } e^* \geq e_\ell^* \end{cases} \tag{B21}$$

with

$$e_s^* = (c_s/c_{so}) \tag{B22}$$

$$e_\ell^* = (c_s/c_{so}) + i_{ph}/(c_{so}\cdot\Delta T_o) \tag{B23}$$

If we have a single PCM family, we can choose $c_{so} = c_s$. Also, quite often $c_s$ and $c_\ell$ are approximately the same. In such cases, (B21) reduces to

$$T_p^+ = T_p^+(e^*) = \begin{cases} e^*, \text{ when } e^* \leq 1 \\ 1, \text{ when } 1 \leq e^* < 1 + i_{ph}/c_{so}\cdot\Delta T_o \\ e^* - i_{ph}/c_{so}\cdot\Delta T_o, \text{ when } e^* \geq 1 + i_{ph}/c_{so}\cdot\Delta T_o \end{cases} \tag{B24}$$

Containment Vessel Wall (Equation (A18))

The transient conduction equation for the containment vessel wall may be written:

$$\frac{\partial T_w^*}{\partial \tau} = \frac{\partial^2 T_w^*}{\partial X^2} + \frac{\partial^2 T_w^*}{\partial Z^2} \qquad \text{(B25)}$$

in the region $0 \leq X \leq L_{bed}/\ell_o$

and $0 \leq Z \leq (R_{wo} - R_{wi})/\ell_o (= Z_o)$

The boundary conditions, in dimensionless form, are:

$$\left.\frac{\partial T_w^*}{\partial Z}\right|_{Z=Z_o} = \left[\frac{h_{wi} D_{e,c}}{k_w}\right]\left[\frac{\ell_o}{D_{e,c}}\right]\left[T_w^*|_{Z=0} - T_f^*\right] \qquad \text{(B26)}$$

and

$$\left.\frac{\partial T_w^*}{\partial Z}\right|_{Z=Z_o} = \left[\frac{h_{wo} D_{e,c}}{k_w}\right]\left[\frac{\ell_o}{D_{e,c}}\right]\left[T_o^* - T_w^*|_{Z=Z_o}\right] \qquad \text{(B27)}$$

We could replace $T_w^*$ and $T_f^*$ in the above equations with $T_w^+$ and $T_f^+$, respectively. (B25) and (B26) are unchanged. (B27) becomes:

$$\left.\frac{\partial T_w^+}{\partial Z}\right|_{Z=Z_o} = -\left[\frac{h_{wo} D_{e,c}}{k_w}\right]\left[\frac{\ell_o}{D_{e,c}}\right] T_w^+|_{Z=Z_o} \qquad \text{(B28)}$$

Numerical Estimates

PCM Characteristics

The approximate characteristics of the high-temperature PCM developed by IGT are given as follows:

$c_s (\approx c_\ell) \approx 1200$ J/kg-K (0.287 Btu/lb-°R)

$\rho_s (\approx \rho_\ell) \approx 3400$ kg/m$^3$ (212 lb/ft$^3$)

$k_s (\approx k_\ell) \approx 4.5$ W/m-K (2.6 Btu/ft h R)

Thus, $\alpha_s \approx 11.10^{-7}$ m$^2$/s.

Fusion temperature, $T_{ph} = 983$ K (1310°F)

Specific heat of fusion, $i_{ph} = 71.6$ kJ/kg (30.8 Btu/lb)

The bed particles are cylindrical and, in the proposed full-scale design, their sizes would be 25.4 mm (1") x 25.4 mm (1") or 50.8 mm (2") x 50.8 mm (2").

## Bed Size and Flow Rate

Typical TES application previously envisaged for the Brookhaven brick plant uses a bed of 1.31 m (4.3') diameter and approximately the same height.

The volume flow rate envisaged is in the region of 1.77 $m^3/s$ (28,050 gal/min) which translates to a superficial velocity, $u_o$, of 1.31 m/s (4.3 ft/s).

The voidage, $\epsilon$, may be taken as 0.3.

## Containment Vessel Wall

An operating TES unit will probably use fire-clay brick for the containment vessel wall. The following approximate thermophysical properties may be assumed for such a brick wall material:

$$k_w = 1.3 \text{ W/m-K}$$

$$\rho_w = 2400 \text{ kg/m}^3$$

$$c_w = 960 \text{ J/kg-K}$$

Thus, $\alpha_w = 5.64 \cdot 10^{-7} \text{ m}^2/\text{s}$.

## Fluid Medium

We shall initially assume that the thermophysical properties of the gas stream are approximately those for dry air at atmospehric pressure. Later, this assumption can be relaxed and we can employ property values appropriate to the actual chemical composition of the gas stream.

During the storage period, an average temperature of 800 K may be assumed for the hot fluid stream. The corresponding thermophysical properties are:

$$\nu_f = 8.2 \cdot 10^{-5} \text{ m}^2/\text{s}$$

$$k_f = 0.058 \text{ W/m-K}$$

$$\rho_f = 0.44 \text{ kg/m}^3$$

$$c_{pf} = 1100 \text{ J/kg-K}$$

Thus, $\alpha_f \approx 1200 \cdot 10^{-7} \text{ m}^2/\text{s}$

$((c_p/c_v)_f \sim 1.4.)$

## Similarity Criteria

A careful examination of the dimensionless equations for the packed bed TES utilizing a single family of PCM reveals the following as the dimensionless groups on the basis of which similarity may be established between a sub-scale test unit and the full-sized bed:

$(\alpha_w/\alpha_f)$, $(\alpha_w/\alpha_{PCM})$, $(k_{PCM}/k_f)$, $(k_w/k_f)$, $i_{ph}/c_s(T_{ph} - T_o)$

$\epsilon$, $Re_{D_C}$, $Pr_f$

$(b/D_{e,c})$, $(D_{bed}/D_{e,c})$, $(L_{bed}/D_{e,c})$, $(R_{wo} - R_{wi})/D_{e,c}$

Further to these, we should include $D_{e,c}$ in view of the fact that typical pressure drop correlations[2] for packed beds utilizing cylindrical pellets do indicate a dependence on the particle diameter.

Also, if the containment vessel is not properly insulated, additional dimensionless groups must be recognized which are dependent on the outer physical dimensions and surface characteristics (if radiative loss is important) of the container as well as the characteristics of ambient air.

We can, via a judicious choice of containment vessel material, the PCM employed and the fluid streams for the storage and removal processes, ensure nearly identical values of $(\alpha_w/\alpha_f)$, $(\alpha_w/\alpha_{PCM})$, $(k_{PCM}/k_f)$, $(k_w/k_f)$, $i_{ph}/c_s(T_{ph} - T_o)$ and $Pr_f$ for both the sub-scale test unit(s) and the full-size bed. It is commonly assumed that the thermal and hydraulic behavior of the packed bed are uncoupled so that similarity

---

[2]Schmidt, F. W. and Willmott, A. J., Thermal Energy Storage and Regeneration, Hemisphere Publishing Corporation, New York, NY, 1981, pp. 342-344.

in respect of thermal performance between the test unit(s) and the full-sized bed will be achieved if the following dimensionless groups have the same values:

$$\epsilon,\ Re_{D_C},\ (b/D_{e,c}),\ (D_{bed}/D_{d,c}),\ (L_{bed}/D_{e,c}),\ (R_{wo} - R_{wi})/D_{e,c}$$

$\epsilon$ is determined principally by the manner in which the bed particles are loaded into the packed bed. Thus, if cylindrical pellets are randomly packed, and if $(D_{bed}/D_{e,c})$ is larger than about 30[3], the voidage will be effectively the same for both the sub-scale unit(s) and the full-size bed, regardless of the actual pellet diameter.

$(b/D_{e,c})$ is identical for cylindrical pellets having an aspect ratio of unity.

If we select a small diameter pellet (e.g., 1/4"-dia.) for the sub-scale test, the original bed diameter and length which were both to be 1.31 m (4.3') when utilizing 1"-dia. pellets, should now be reduced to 0.33 m (~ 1') to retain the original $(D_{bed}/D_{e,c})$ and $(L_{bed}/D_{e,c})$.

The Reynolds number, $Re_{D_C}$, will be identical also if the mass velocity in the test case is four times that intended in the original unit.

The wall thickness of the containment vessel in the proposed tests needs only be one-fourth that for the full-sized bed.

---

[3]Schwartz, C. E. and Smith, J. M., "Flow Distribution in Packed Beds," Industrial and Engineering Chemistry, Vol. 45, No. 6, 1953, pp. 1209-1218.

Nationally, the brick and structural clay industry accounted for about 30% of the SIC 32 (Stone, Clay and Glass) energy requirements in 1975. This represents an energy consumption of 0.12 quads annually. Most of this is provided by natural gas and oil for drying and kiln firing. As an example of the energy use level, the energy consumption of a behive kiln averages 1.18 billion BTU's per firing.

**Process Description**

The operation of drying reduces the moisture content of the wet ware from as much as 30% moisture content to less than 3%. This typically requires days in the dryer, and possibly stages of drying to ensure the surface is not dehydrated while the interior mass remains moist. Initial drying air is nearly saturated to allow even heating of the ware before evaporation occurs. Once the major shrinkage has taken place, a second phase of the drying is entered. In this phase, the temperature is raised slightly above the vaporization temperature of water (e.g., to 230 F); and the remaining moisture is removed by diffusion through the ware as vapor.

In the kiln firing stage, the product goes through four distinct thermal conditions. These are dehydration, densification, vitrification, and finally recrystallization and cooling. A typical material, the common clay kaolinite, enters the densification phase at a temperature of 1025 F. The "soaking" portion of the kiln cycle is achieved at at a maximum temperature which depends on the material and the process and at at rate which is highly plant specific. A typical heating rate is 74 F per hour and cooling at 172 F per hour. The maximum product temperature ranges from 1900 F to 2800 F. By way of a typical example, the firing kiln temperature profile would be (Figure 15, p.37 [1]) as shown in the table:

| Process Phase | Length (hr) | Temperature Range (°F) |
|---|---|---|
| dehydration | 75 | 100-1000 |
| densification | 40 | 1000-1800 |
| crystalization | 25 | 1800-2000 |
| cool | 12 | 2000-100 |

**TES Role**

The definition study [1] recommended a centrally located TES unit that would store heat from the kiln and reuse to preheat combustion air for other kiln runs or to provide heat to the dryer. The need for storage is seen most strongly when supplying the dryer. The dryer demands less energy than the kiln but over a long period. In fact, a rough energy balance indicates that all the fuel currently used for product drying might be eliminated if a well designed TES system were in place.

The use of energy storage for preheating combustion air and in kiln preheating may also have a big effect. There is an upper limit of 1000 F on preheating combustion air; but with this preheating, the fuel available heat factor increases from an average of 0.56 to 0.71 producing a fuel savings near 25%. Typical air flow rates are 6000-24000 cubic feet per min.

The breakdown of energy sources and requirements in a periodic plant cycle is as follows (Table 16, [1]):

| Energy Source | Temperature (°F) | Energy Uses | Temperature Requirements (°F) |
|---|---|---|---|
| Kiln Firing | 1600 | Kiln Preheat | 70-1000 |
| Cooling | 2000-70 | Combustion Air | |
| Preheat | 500-1000 | | |

## Optimization

There are many aspects of the design and operation of a brick plant that might be optimized. We have endeavored to develop a general model that allows for optimization of plant layout and operation. The duct connections between devices and the mass flow rates of these ducts during the operating cycle provide the focus of the optimization study.

**An Example Plant**

To fix ideas we will consider a two-kiln periodic plant with a single dryer. Two heat exchangers and a single TES unit will be added to the plant to provide capability for the reuse of waste heat.

The plant will follow a kiln operating schedule as shown in Figure 1. Each kiln will operate for a period of one week out of the month. A twelve hour heating time and cooling time are assumed with a maximum operating temperature of 2000 F. A week's time is required between kiln runs to load and unload kilns. The dryer will operate continuously with a maximum temperature of 230 F.

Depending on duct diameter, length, insulation and blower efficiency, it is possible to predict significant savings of fuel cost over an extended time period arising from the incorporation of TES into the waste heat reuse system.

It has been a common practice to have recycling of waste heat between simultaneously operating devices [2]. Storage, however, opens the possibility of significantly expanding this capability. As we see in Figure 1, if efficient redistribution of waste heat from kilns one and two is possible, we can predict significant amounts of heat being stored and then being available for use by the dryer during weeks 1-4 and kiln two during week 3.

In the desire to make these speculations precise, we have developed a computer code REUSE1, which simulates all relevant aspects of the storage, heat transfer, and flue-gas-derived waste heat redistribution in the system. For the plant of Figures 1 and 2, this involves 31 possible connections between devices, together with the addition of the heat exchangers and storage device. Also accounted for are the electricity costs involved in operating blowers for pumping the various gasses through the system, fuel costs, and mixing of various air and gas streams in the system. The system is optimized for maximum "return on investment" over a typical operating cycle. Optimization is carried out in two stages: an "outer" stage, involving possible physical configurations of the system including ducts, pumps, etc.; and an "inner" stage

involving redistribution of heated gasses. The outer loop optimization is carried out using top-down and bottom-up searches; while the inner loop is done via a simple method (linear programming) approach, based on the linear system of constraints and conservation relations. Similarly, an inner "iteration" is carried out involving alternative iterations of temperatures in ducts and mass flow rates through them. The code is now being debugged and exercised, and results for the system shown will be available shortly.

We must also make some assumptions about plant layout, as the cost of piping enters the performance and the cost functions for the plant. We will assume that the storage unit is located at an equal distance between the kilns and the dryer. The heat exchangers are physically near the kilns. With these concrete but somewhat arbitrary assumptions on the plant and the operating schedule, we now consider the cost of the plant.

**Cost Functions: Return on Investment**

The cost of the plant can be divided into the capital and operating costs. The capital costs include the cost of the kilns and dryer, as well as the incremental capital costs of extra ducting, blowers, heat exchangers, and the TES unit. For example, the cost of a connection between the two kilns allowing for possible heating of one with the waste heat of the other is proportional to the length of duct required. Since we are primarily interested in the retrofitting of existing plants, we will not include kiln and dryer cost and consider only the incremental capital costs.

The operating costs include fuel and electricity and depend on the daily operation of the plant in a direct way. The fuel requirement can be influenced in two ways.

1. Preheating air adds heat directly to the kiln or dryer reducing the energy requirements.

2. Preheating combustion air increases the efficiency of the burn also reducing energy requirements.

From a practical point of view, these are accomplished by controlling the mass flow rates of waste heat streams to and from the devices. The electric cost depends on the flow rates required and also on pressure drops in the system. In our preliminary model, only the direct addition of heat from storage or from an operating device is considered.

**Independent Variables**

Three classes of independent variables affect the cost of the brick plant. First are the geometric or configuration variables, these specify which connections between devices obtain. The second class is operational and consists of the mass flow rates under control of the plant operator. The gas mass flow rate and the combustion air flow rates are determined by the burn requirements. But the flow rates of the clean air streams directly into each device may be adjusted. By adjusting the flow rates the amount of waste heat going into storage or into immediate use by a device can be controlled. The third class of independent variables are sizing and device variables. This class includes the size of the storage and the physical parameters that govern its performance such as the critical temperature and the specific heat. The heat exchanger efficiency as a function of actual geometry or heat transfer coefficient is also of this class. The

size of the pipes between devices may also be considered in this class.

The primary impact of the operational variables is on the fuel costs, while the geometric variables impact the capital costs primarily. The sizing variables enter in a much more complicated fashion, in fact many enter the cost function as nonlinear terms. For example, the size of the ducts effects the cost of fan operation and the size of the fans. The size of the pipes enters the cost function in both the capital and the operating portions. The size influences the electric requirements necessary to drive given mass flow rates.

**Plant Model**

Underlying any optimization must be a model of the plant. This consists primarily of a network model giving connections between devices and a set of equations relating the state of each device and the output from each device to the input of the device. The model allows us to examine the effect of changes in say mass flow rate of one device on the other devices in the plant.

The basic connectivity for the example plant is shown in Figure 2. Here we have included all allowable connections, and part of the optimization problem will be to determine which ones are cost effective.

The equations relating the states of devices can be very complicated and thorough, but for our purposes simple approximations have been used when possible. The plant model must conserve mass and energy in the simplest statement. Since the fuel costs are integral to the cost analysis of the plant and the preheated combustion air can significantly effect the fuel needed, we have also included combustion equations. These equations provide a balance of basic chemical components of air and fuel, so that the performance of various fuels can also be analyzed. The equations describing the plant model are given elsewhere.

**Optimization Strategy**

Finding the optimal plant design and operation is the ultimate goal of the project. In pursuit of this goal, we have identified three layers of the optimization. First, the daily or hourly operation of the plant can be optimized with respect to operating costs. Second, the plant connections can be optimized to allow the maximum return on investment for operation over a specified period. And third, the size and characteristics of each device can be optimized in the context of the optimal plant. These layers define optimization problems that must be done one within another.

Our current work optimizes the first two layers simultaneously. This resembles certain operations research problems but has additional complications that make this problem unique and very difficult. The first complication is the time dependence of the mass flow rates. At each hour, or some appropriate time interval, the optimal mass flow rates must be found. With the addition of storage, the possibility exists for the instantaneous (1 hour interval) optimals to no longer give the optimal solution over the entire plant schedule.

The optimization without storage can be described as a search on connections and device sizes coupled with the simplex algorithm to optimize the time interval mass flow rates. The optimization of the first two layers is accomplished in the following steps:

Geometric optimization

Downwards Search

1. Beginning with a fully connected plant, find the optimal mass flow rates for each time interval of the simulation.

2. Assign a cost to each link, and remove the most costly connection to the lowest fuel consuming device.

Upwards Search

1. Beginning with an unconnected plant, find the energy costs of each device at each hour of the simulation.

2. Add one connection between the device having the highest cost and the source with the least connection cost.

The two searches provide a good heuristic for finding a near optimal plant configuration. We will refer to the plant as a network.

**Operational Optimization**

Apply the simplex method, with constraints, to the plant at each hour of the simulation. For each configuration, we find the mass flow rates resulting in the least total operating cost.

**Complication of Storage**

With a thermal storage unit included in the brick plant, the inner operational optimization is no longer the desired optimum. The operational optimization will always favor immediate reuse of heat to storage, since it has a limited time interval over which to optimize. With storage, the future operation of the plant effects the optimal strategy for reuse of waste heat. Rather than immediate reuse of waste heat, it may be the case that storage for a demand at a future time is more cost effective.

The time dependent storage problem resembles some inventory and production scheduling problems familiar to the operations research community. We have taken a dynamic programming approach to the problem and believe that fruitful results will follow.

The method can be described by considering a grid of time values and permissible storage states at each of these time points. For illustration, suppose that storage can be filled, by simply dumping excess heat at a prescribed rate, in increments of 1/4 of the storage medium's capacity. There are then five storage levels that the plant can have, empty, 1/4, 1/2, 3/4, and full. If we require that storage be filled or emptied during a time interval by one of these increments, then the other mass flow rates can be found optimally along with a cost associated with the plants operation over this time interval.

Suppose now that the cost of operation is given (computed by the simplex algorithm) for each point of the time-storage grid and for each possible increment of the state of the storage. This defines a directed graph with costs associated to each storage increment option. An example of such a graph is given in Figure 3. The graph edges a,b,c,d, and e have costs associated with each of them. The dotted lines which

move from less in storage to more over the time interval indicate an infeasible solution. There is no heat available from the kiln during this period and thus storage can only discharge. Each x would have similar edges and costs associated with possible storage paths.

To find the optimal schedule, we must find the optimal path through this graph. A simple search technique suffices for this. The search proceeds by finding the cheapest path from one of the first nodes to each node at a time level say i. To find the cheapest paths from this first node to each of the nodes at time level i+1 requires comparison of five paths for each of the five nodes. When we get to the end of the network in this forward marching algorithm, the cheapest path from the first node to any ending node is known. In the figure, a periodic "optimal" path is shown, which would indicate the best use of storage. (This is an example and is not the result of any computation.)

The inclusion of storage and heat exchangers also requires that the temperatures be known for each connection in the network. Unfortunately, the temperatures interact non-linearly with the mass flow rates, so that they cannot be determined by the simplex algorithm. Some of the constraints coming from the devices are given in terms of maximum temperatures. To incorporate the temperature considerations, we have used an iterative technique where the best temperature guess is used to define constraints and costs for the simplex method. Once the mass flow rates which minimize the cost function are found, the temperatures of the network can be calculated. These newly calculated temperatures are then feed back into the simplex method, and the mass flow rates are recalculated. This procedure repeats until convergence of the mass flow rates and temperatures is obtained.

**Non-linear Sizing Optimization**

The final level of optimization has not been integrated with the other two. This level requires a non-linear constrained optimization. Our approach is to first define the near optimal connection and use pattern and then use this to optimize the performance of individual components. It was felt that the additional complexity of this last layer was not justified until the operating requirements of each device could be clearly established.

## Results

The output from the computer program consists of return on investment values for each possible step of the dynamic programming algorithm. The periodic schedule that maximizes ROI for the duct configuration is found and output.

The results for the example plant will be reported along with details of the costs used and computation of the ROI in a forthcoming report.

## References

1. Thermal Energy Storage System Definition Study and Industry Characterization for the Brick, Clay and Ceramic Industry, Institute of Gas Technology, Chicago, June 1982

2. Brick and Tile Engineering, Harry C. Plummer, Structural Clay Products Institute, Washington D.C., 1950

3. Drying - Principles and Practice, R. B. Keey, Pergamon Press, 1972

4. Physical Ceramics for Engineers, Lawrence H. Van Vlack, Addison Wesley Publishing Co., 1964

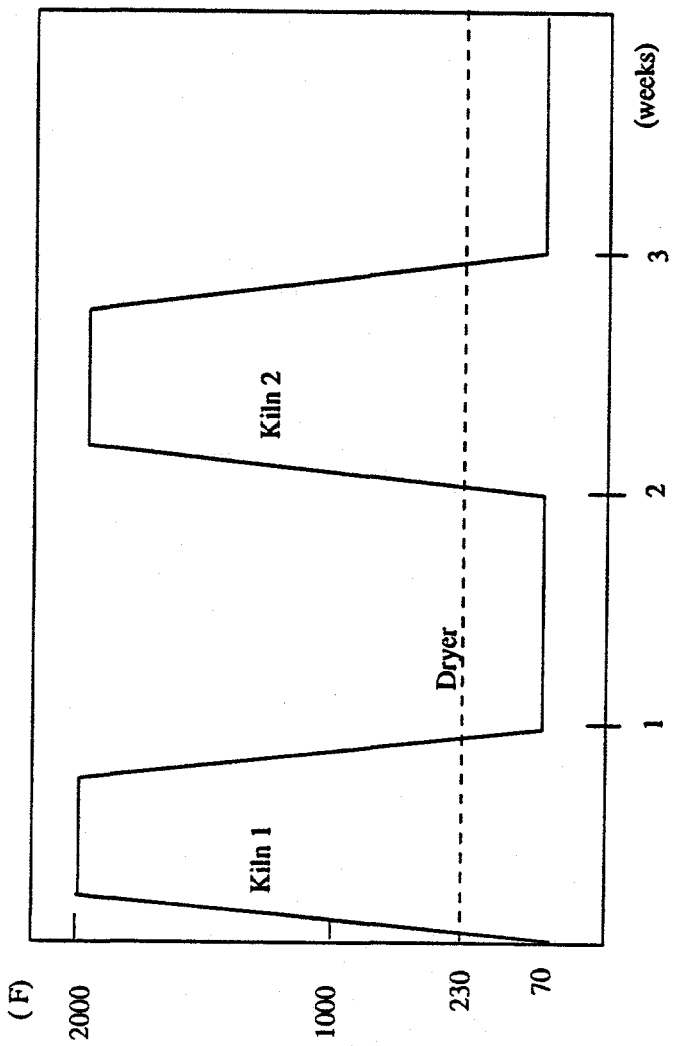


Figure 1. Example Plant Schedule

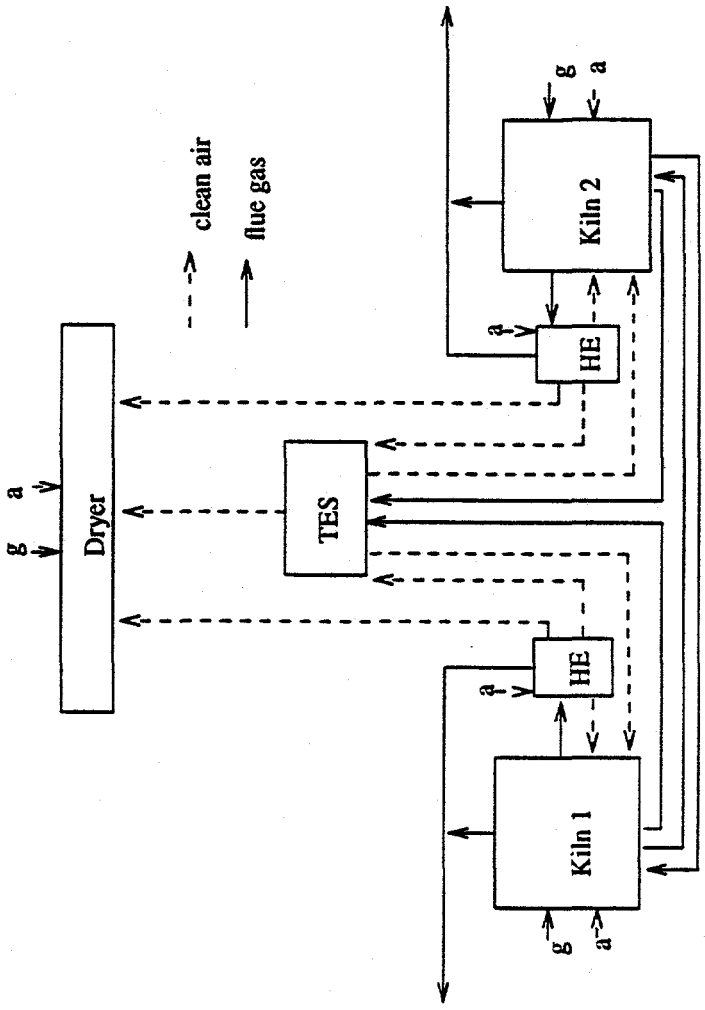


Figure 2. Example Brick Plant

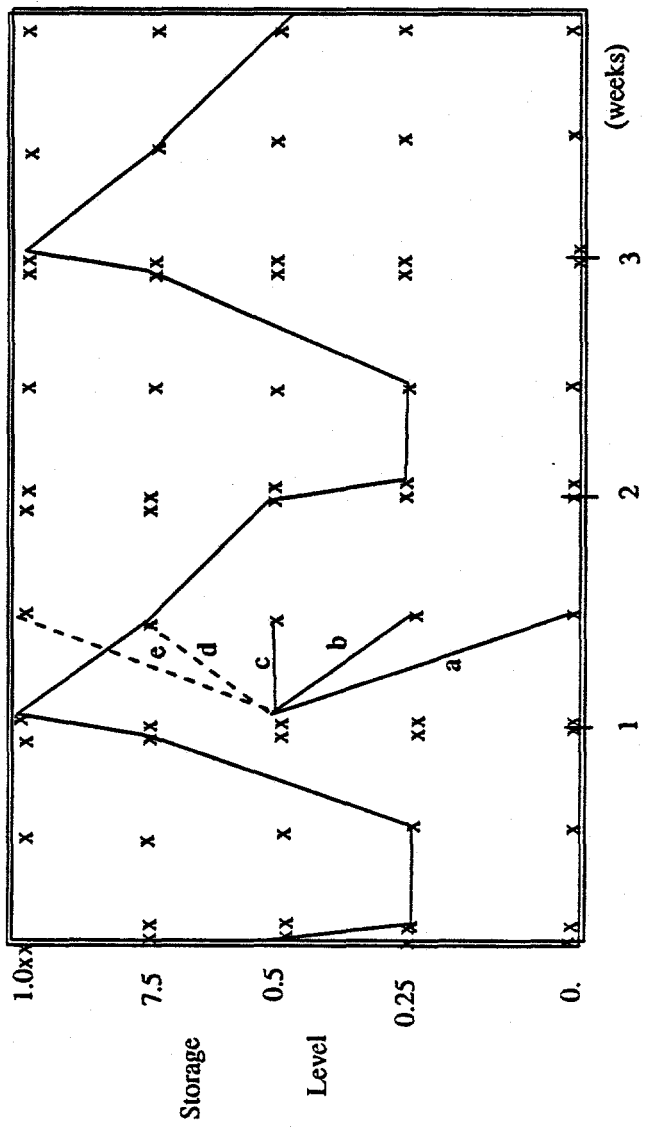


Figure 3. Dynamic Storage Optimization

# THERMAL ENERGY STORAGE FOR POWER GENERATION

M. K. Drost
Pacific Northwest Laboratory[a]
Richland, Washington 99352

## *Abstract*

*This study investigated the technical and economic feasibility of using molten nitrate salt thermal energy storage (TES) in a coal-fired power plant to provide peak and intermediate loads. The use of thermal energy storage allows the continuous operation of the coal-firing equipment while allowing the plant to produce peaking and intermediate load power. Continuous operation of the coal-firing equipment avoids cycling these systems and allows the use of smaller and less expensive components. The study concluded that coal-fired nitrate salt heating using conventional pulverized coal-firing technology and nitrate salt TES was technically feasible. An economic evaluation concluded that a plant with molten nitrate salt TES produced lower cost power than a conventional cycling coal-fired power plant for a range of operating schedules. The study also concluded that the concept has other important advantages and may have attractive applications with clean coal combustion technologies.*

## Introduction

There are increasingly strong indications that the United States will face wide-spread electrical power generation capacity constraints in the 1990s with most regions of the country experiencing capacity shortages by the year 2000. Using the National Electricity Reliability Council's base case predictions, the mid-Atlantic, Northeast, and Southeast regions of the country will experience generating capacity constraints by the year 2000. In many cases, the demand for increased power will occur during peak demand periods. If the country is to avoid further dependence on petroleum fuels, alternatives to oil- and gas-fired turbines and combined-cycle plants need to be developed.

A number of demand-side and system-wide energy options exist but when new generation is unavoidable, the only non-petroleum option is a cycling coal-fired power plant. A preliminary evaluation of an alternative method of using coal to generate peak and intermediate load power was conducted by the Pacific Northwest Laboratory (PNL). The approach uses a continuously operating coal-fired salt heater to heat molten nitrate salt, which is then stored. During peak demand periods, the hot salt is used as a heat source for a conventional steam/Rankine power plant.

---

[a] Operated for the U.S. Department of Energy by Battelle Memorial Institute under Contract No. DE-AC06-76RLO 1830.

## Concept Description

There are a number of ways to integrate thermal energy storage (TES) with conventional and advanced coal technologies. This study focused on using conventional pulverized coal combustion technology. Alternative arrangements, using advanced coal technologies, are briefly described in the Section on other characteristics.

The concept evaluated in this study, uses a pulverized coal-fired salt heater to heat cold molten nitrate salt [280°C (536°F)]. The hot molten salt [560°C (1040°F)] is returned to a hot salt tank and stored. During peak demand periods, hot salt is withdrawn from the hot salt tank and used as a heat source for the steam generator. The molten salt is then returned to the cold molten salt storage tank. The steam generator produces steam for a conventional steam cycle. Turbine inlet conditions are 538°C (1000°F) and 16,500 kPa (2400 psi). The concept is shown in Figure 1.

The coal-fired salt heater operates continuously, charging storage. The steam generator and turbine only operate during intermediate and peak demand periods. This allows the steam generator to be approximately 1/3 the size of coal-fired steam generator in a conventional cycling coal-fired power plant. In addition, the salt heater would not be cycled, avoiding the difficulties associated with cycling a coal-fired steam generator. The general impact of the concept is to decouple the generation of thermal energy storage and its conversion to electricity.

The storage media is a mixture of sodium nitrate (60 wt%) and potassium nitrate (40 wt%). Thermal energy is stored as sensible heat in the molten salt. The salt freezes at a temperature near 240°C (464°F). Consequently precautions must be taken to ensure that the temperature of the molten salt never drops below the freezing point.

While not commercially available, nitrate salt thermal energy storage has been extensively investigated as part of the U.S. Department of Energy's (DOE) Solar Thermal Program. The concept has been the subject of bench-scale experimental investigations, several detailed design studies, and a small-scale field demonstration (Weber 1980; Martin Marietta 1984, 1985). While significant problems remain, the balance of opinion is that nitrate molten salt thermal energy storage is technically feasible (Delameter 1987).

## METHODOLOGY

The general approach used in this study consisted of developing a preconceptual design and cost estimate for a coal-fired plant with thermal energy storage and comparing the results to the costs for a conventional pulverized coal-fired plant operated during peak and intermediate demand periods. The comparison was made for a range of plant operating schedules. Table 1 summarizes the operating schedules and gives several key design features of the thermal storage concept.

*Table 1. Plant Operating Schedules*

| Days of Operation per Week | Hours of Operation per Day | Aproximate Capacity Factor, % | Aproximate Size of Storage MWHt | Equivalent Size of Coal Firing Equipment for TES System, MWE |
|---|---|---|---|---|
| 5 | 8 | 20 | 6,763 | 167 |
| 5 | 12 | 30 | 7,591 | 250 |
| 5 | 16 | 40 | 6,591 | 330 |
| 7 | 6 | 20 | 5,698 | 125 |
| 7 | 9 | 30 | 7,139 | 188 |
| 7 | 12 | 40 | 7,591 | 250 |

In all cases the plant net output was assumed to be 500 MWe for both the conventional plant and the coal-fired plant with TES. The significant design variations occurred in the coal-firing equipment. As the capacity factor decreases, the size and cost of the coal-firing equipment in the thermal energy storage option will decrease while the size and cost of the thermal energy storage subsystem will increase.

In many cases, the conventional plant and the plant using TES will have similar equipment. Examples include the coal handling equipment, pollution control equipment, the turbine/generator, and the switchyard. The design study concentrated on subsystems that were impacted by the addition of molten salt TES. These include the coal-fired salt heater, salt transport piping, salt storage, and the salt-heated steam generators.

The coal-fired salt heater was a new component and design data was not available. The component was characterized by using data developed for molten salt heating solar central receivers and conventional coal-fired steam generators to size major heat exchanger surfaces. The coal-handling equipment, combustion air handling equipment, flue gas handling equipment, pollution control equipment, and structural design were assumed to be similar to a conventional coal-fired steam generator.

The molten salt TES and steam generator subsystems were characterized by using design information developed as part of several design studies conducted for the Department of Energy's Solar Central Receiver Program [Martin Marietta 1978, Arizona Public Service Company (APS) 1988].

The economic evaluation was conducted by calculating and comparing the levelized energy cost (LEC) of a conventional cycling coal-fired to a coal-fired plant with molten salt TES. Levelized cost analysis combined initial cost, annually recurring cost, and system performance characteristics with financial parameters to produce a single figure-of-merit that is economically correct and can be used to compare the projected energy costs of alternative power plants.

Initial capital costs were identified for a conventional 500-MWe coal-fired power plant at a relatively detailed level. Individual cost elements were then aggregated into coal-handling, boiler, emissions-handling, power generation, and balance-of-plant components. Equations estimating the cost of each of these

components as a function of power-generation or coal-firing capacity were derived from power plant economy-of-scale studies described in the literature.

Molten salt storage and steam generator costs were obtained from research reports investigating solar thermal power systems (APS 1988). Molten salt heater costs were scaled from conventional boiler costs based on their different heat transfer tubing designs. Finally, molten salt piping designs and costs were prepared by PNL.

## Current Results

The preconceptual design consisted of two activities: an engineering design evaluation and a cost evaluation. The engineering design evaluation focused on defining the characteristics of the subsystems unique to a plant using molten salt TES. The cost evaluation used the results of the engineering study to develop levelized energy costs for a conventional coal-fired power plant and the plant using molten salt TES.

Unlike other molten salt TES components, the direct use of a coal-fired salt heater has not previously been studied. The evaluation of the coal-fired salt heater concluded that the component was technically feasible and had several advantages when compared to a coal-fired boiler. The heat transfer in a molten salt heater is comparable to a conventional boiler for most heat transfer surfaces and superior to a conventional boiler for superheaters and reheaters. The pressure of the molten salt (which does not undergo a phase change in the boiler) is low compared to water. This allows the use of thin-walled tubes with the resulting savings in tube cost. One negative impact is increased flow rate. Calculations showed that molten salt requires a substantial increase in the mass and volume flow rate than for a conventional boiler. This results in an increase in pumping power consumption.

The storage subsystem design is based on designs developed for solar thermal power applications and uses a two-tank concept with separate hot and cold molten salt storage tanks (APS 1988).

The steam generation subsystem consists of four separate heat exchangers including a preheater, evaporator, superheater, and reheater. The heat exchanger designs were based on designs developed for solar thermal power applications (Martin Marietta 1978).

The salt transport subsystem was characterized by developing a preconceptual layout for the nitrate salt storage tanks, hot salt piping, cold salt piping, and pumps. The major components of the transport subsystem were sized and the thermal and pumping requirements were calculated. The design of the transport subsystem was subsequently used to develop a capital cost estimate.

The performance evaluation involved two issues: the heat rate of the plant with thermal energy storage relative to the conventional cycling plant and the availability of a plant with thermal energy storage relative to the conventional cycling plant.

The determination of plant heat rates involved taking a heat rate for a base load coal-fired power plant and then adjusting the heat rate to account for special features of the conventional cycling plant and the plant with thermal energy storage. The heat rate for the conventional cycling plant was adjusted for startup losses, and the resulting annual heat rate was 10,192 Btu/kW [Electric Power Research Institute (EPRI)

1986]. The annual plant heat rate for the plant with a thermal energy storage unit after accounting for TES parasitics was 10,224 Btu/kW. Given the accuracy of the study, the conclusion was that the two designs have essentially similar heat rates.

Historically, smaller coal-fired power plants have had a higher availability than larger plants. This observation is in agreement with the plant availabilities reported in EPRI's Technical Assessment Guide (EPRI 1986). The outage rate for the coal-firing equipment in the TES plant was adjusted for the smaller size of the equipment. The resulting plant availability is higher than that for a conventional cycling coal-fired power plant. This result is based on the assumption that a non-cycling, coal-fired salt heater will have the same unplanned outage rate as a conventional cycling, coal-fired steam generator of the same size.

Levelized energy costs for the conventional cycling coal-fired power plant and the plant with TES are summarized on Figure 2. The results are presented for the six operating schedules. The results show the coal-fired plant with TES to have an LEC lower than the corresponding coal plant for all of the plant operating schedules. The coal-fired plant with TES looks most attractive at lower plant capacity factors where the size of coal-firing equipment has been most sharply reduced and, hence, the benefits of incorporating TES are the greatest. The key factors contributing to the reduction in LEC for the coal-fired plant with TES are a decrease in initial capital cost and an increase in plant availability.

## Other Characteristics

The possible applications of molten salt TES in utility power generation extend beyond conventional coal combustion technologies to advanced concepts, such as fluid bed combustion and gasification combined cycle options. In addition, the use of thermal energy storage can have other benefits that were not captured in the cost comparison.

The use of multiple, small (200 MWt to 400 MWt) modular salt heaters for charging storage would allow the phased construction of a power plant with variable operating characteristics. The modular plant arrangement would have a number of advantages including: higher plant availability, convenient phased construction, and attractiveness for advanced coal combustion technologies. A modular power plant using TES may allow a utility to initially install a small plant that can subsequently be expanded and modified to meet the utility's power generation needs.

The use of TES allows the continuous warming of the steam generator and turbine, keeping these components at a temperature near to their operating temperature. This will permit the rapid startup of the steam turbine assuming that the power plant includes provisions to deal with silica buildup after major reductions in load.

Advance coal combustion technologies, such as slagging combustors, bubbling bed, and circulating fluidized bed combustors, will benefit from the development of TES for utility power generation applications. In all cases, the use of a TES system will allow the advanced coal combustion technology to meet intermediate and peak loads without having to cycle the coal combustion equipment. This is

particularly important for fluid bed combustion and coal gasification technologies that have high turn-down ratios or are difficult to cycle.

Molten salt thermal energy storage has the potential for substantial improvements in cost and performance. Two approaches have been proposed to improve the cost effectiveness of molten salt TES. The first approach involves innovative design of the high-temperature storage tank while the second considers alternative molten salts (Kohl, Newcomb and Castle 1987; Bradshaw and Tyner 1988).

Molten nitrate salt TES has been extensively investigated and field tested. The results indicated that molten nitrate salt TES is technically feasible but problems related to freeze protection and component reliability need to be resolved (Delameter 1987).

A variety of molten salts have been considered for TES. The freezing point for these salts range between 185°C (365°F) and 285°C (545°F). In all cases, the salts freeze at temperatures well above ambient. This can create a problem when a component is out of service because the salt will cool and eventually freeze.

Pumps and valves associated with salt transport have also proved to be problem areas. Sandia National Laboratory is currently conducting a technology development program in molten salt handling and the balance of expert opinion is that the problems can be solved.

## Conclusions

The significant conclusions from this evaluation of thermal energy storage for utility power generation are summarized below.

- **Molten Nitrate Salt TES is Technically Feasible.** While acknowledging that problems exist with certain aspects of salt handling, these appear to be resolvable. The overall judgement, both of this study and similar evaluations in the solar thermal area, is that molten nitrate salt TES is technically feasible and it is reasonable to assume that the technology can be successfully commercialized.

- **A Coal-Fired Power Plant Using Thermal Energy Storage Produces Lower Cost Power Than a Conventional Cycling Coal-Fired Power Plant For a Range of Operating Conditions.** The results of this study show that a coal-fired power plant with molten salt TES produces substantially lower cost power than a conventional cycling coal plant over a range of operating schedules.

- **Molten Salt TES May Have Attractive Applications With Advanced Coal Combustion Technologies.** The use of TES with advanced coal combustion technologies, such as a coal gasification combined cycle plant and fluid bed combustion, improves the flexibility of these technologies by letting them provide peak and intermediate load power. If technically feasible, direct-contact salt heating would be particularly attractive for applications with coal gasification combined cycle plant.

## References


1. Arizona Public Service. 1988. Utility Solar Central Receiver Study. DOE/AL/38741-1, Arizona Public Service Company, Phoenix, Arizona.

2. Bradshaw, R. W., and C. E. Tyner. 1988. Chemical and Engineering Factors Affecting Solar Central Receiver Applications of Ternary Molten Salts. SAND88-8686, Sandia National Laboratory, Albuquerque, New Mexico.

3. Delameter, W. R. 1987. "The Molten Salt Electric Experience: A Project Overview." In Proceedings of the ASME-JSME-JSES Solar Energy Conference, eds. D. Y. Goswami, K. Watanabe, and H. M. Healey. American Society of Mechanical Engineers, New York, New York.

4. Electric Power Research Institute. 1986. Technical Assessment Guide. EPRI P-4463-SR, Electric Power Research Institute, Palo Alto, California.

5. Kohl, A. L., J. C. Newcomb and W. R. Castle. 1987. Evaluation of a Conical Tank for High Temperature Molten Salt Containment. SERI/STR-231-3193, Solar Energy Research Institute, Golden, Colorado.

6. Martin Marietta Corporation. 1978. Conceptual Design of Advanced Central Receiver Power System. DOE/ET/20314-1/2, National Technical Information Center, Springfield, Virginia.

7. Martin Marietta Corporation. 1984. Alternative Central Receiver Power System, Phase II Volume II - Molten Salt Receiver. SAND81-8192/2, Sandia National Laboratory, Albuquerque, New Mexico.

8. Martin Marietta Corporation. 1985. Volume 1 - Molten Salt Thermal Energy Storage Subsystem Research Experiment. SAND80-8192, Sandia National Laboratory, Albuquerque, New Mexico.

9. Weber, E. R. 1980. Saguaro Power Plant Solar Repowering Project. DOE/SF/10739-1, National Technical Information Center, Springfield, Virginia.

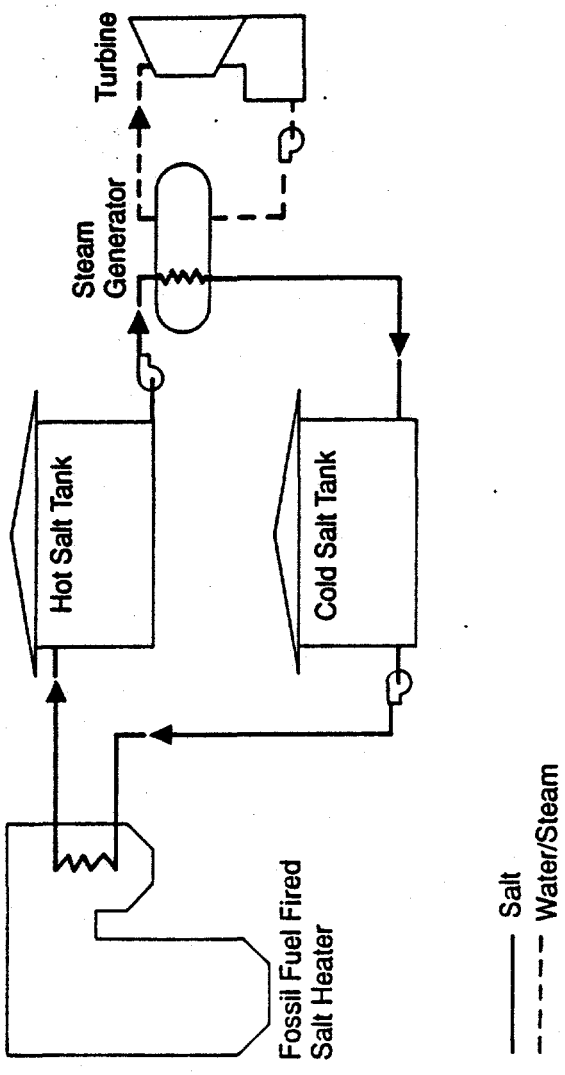


Figure 1. Schematic arrangement of a coal-fired power plant with thermal energy storage.

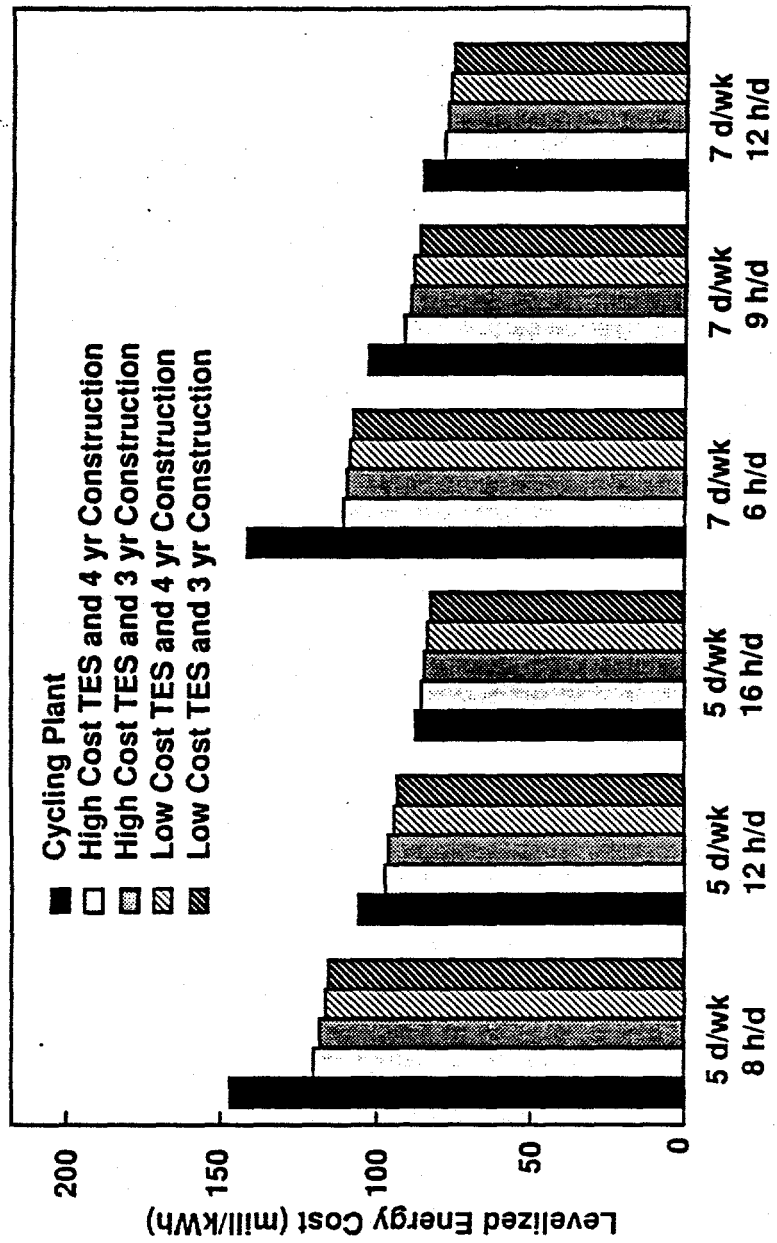


Figure 2. Levelized energy costs.

# COMPLEX-COMPOUND LOW-TEMPERATURE TES SYSTEM

**U. Rockenfeller**
Rocky Research
Boulder City, NV 89005

***Abstract***

*Development of a complex-compound low-temperature TES system is described herein from basic chemical principles through current bench scale system development. Important application engineering issues and an economic outlook are addressed as well.*

*The system described uses adsorption reactions between solid metal inorganic salts and ammonia refrigerant. It is the coordinative nature of these reactions that allows for storage of ammonia refrigerant within the solid salt crystals that function as a chemical compressor during on peak periods (substituting the mechanical compressor) and release ammonia during off peak periods while a mechanical vapor compression system provides the necessary reactor pressure and heat.*

## Introduction

Thermal storage has long been recognized as an economically viable method of peak load shifting and shaving. The economics are driven primarily by utilities' programs that offer installation incentives, off-peak power rates, and demand charge-free operating hours. Other advantages to the end user are potential capacity reduction of vapor compression equipment and back-up capacity availability. The major drawbacks of thermal storage are an uncertain future for utility incentive programs and increased electric power consumption because of thermodynamic heat transfer losses inherent to thermal storage equipment.

Thermal storage systems developed and marketed in the past enjoy their most significant market penetration in commercial air conditioning. Most systems offered today provide a 20 to 50% return on investment in utility areas with active incentive programs for commercial installations. The residential air conditioning market, which has tougher economic requirements than the commercial market due to shorter operation seasons and diverse resale issues, constitutes a multibillion dollar market opportunity with substantial load shifting opportunities for electric utilities; however, currently available technology does not offer the economics required for a broad-based in-road to the HVAC market.

Today's commercially available thermal storage products are almost exclusively applicable to commercial and industrial air conditioning. The refrigeration industry of the United States, which operates refrigeration equipment at evaporation temperatures between -50°F and 20°F, has not been successfully approached with thermal storage products. This is primarily because all mature thermal storage systems are based on phase change materials or sensible heat systems operating at or above 32°F. Low temperature brine and salt

augmented ice storage systems do not provide satisfactory operating characteristics or economics. In particular, successful thermal storage systems operating below 20°F have not been developed.

The refrigeration industry, however, is an attractive customer for thermal storage because such plants operate typically 365 d/yr and are of 200 to 500 tons refrigeration capacity per installation. Refrigeration warehouses alone account for several hundred thousand tons of refrigeration capacity. The typical operating temperatures (-40°F for flash freezing, and -20°F and 20°F for product storage) result in much lower equipment performances than obtainable in HVAC applications, in turn leading to higher electrical power demand.

Development of complex-compound low-temperature thermal storage systems is geared toward the refrigeration market. To provide a successful product, several requirements must be fulfilled; these criteria, however, cannot be met with today's commercially available technology.

The refrigeration market is not a single-temperature target as encountered in the HVAC industry. As a minimum, three temperature levels (20°F, -20°F, and -40°F) must be addressed. Since capacity and efficiency of vapor compression equipment are very sensitive to suction pressures at low temperature levels, excessive approach temperatures dictated by specific phase change materials must be avoided. Finally, the technology must be simple enough to allow for easy system integration, minimum maintenance, and a return on investment exceeding 25 to 33% depending on the particular application(1).

Use of coordinative complex compounds based on ammonia as the refrigerant (liquid) makes it possible to develop hardware that can be operated at several temperatures in the above range by merely exchanging the adsorbing salt substrate. Thus, one hardware design could be used for an entire line of thermal storage products. Ninety percent of U.S. refrigeration warehouses operate with ammonia refrigerant. This makes it possible to design a direct-contact complex-compound thermal storage system for this industry.

The thermal storage reactions operate on a chemisorption process requiring no moving parts other than control valves; thus, maintenance efforts are minimized. A recent breakthrough in complex compound packaging and heat exchanger development allows for average approach temperatures of 7°F to 9°F. The first systems, currently under development, focus on large capacity markets using 20°F and -20°F thermal storage temperatures. Initial economic analyses, performed by independent refrigeration engineering specialists, show returns on investment between 30 and 60% depending on the utility area(2).

## Background of Complex Compound Chemistry

### Complex Compound Equilibria

The complex compounds considered consist of metal inorganic salts (absorbents) and ammonia refrigerant (ligand). These complexes are held together by coordinative covalent bonds between the ligand and the adsorbent salt. Ammines and hydrates are the most common representatives of inorganic complex compounds.

The coordination number of a complex is defined as the total number of ligand molecules or ions bound to a central molecule or ion. The central particle of a complex compound bonds more particles (ligand

molecules) than is expected from its charge or position in the table of elements. This is because the coordinating central adsorbent molecule does not necessarily have an unbalanced charge. Many complex formations are obtained by mere electron displacement, as is the case with diammine zinc chloride.

The dissociation energy of a complex compound depends largely on the ligand. For heat pump and thermal storage applications, it is important to achieve a high energy density per unit mass of ligand. Ligands with one lone pair usually have lower bond energies than those with two lone pairs. For energetic density per unit mass, however, the number of lone pairs must be related to the mole mass of the ligand. Therefore, the ratio of the number of lone pairs to the mole mass of the ligand is a useful measure for the energy density of the bond energies regardless of the central molecule. Applying the above ratio rule leads to $NH_3$ and $H_2O$ as the most promising ligands.(3)

For solid-vapor metal inorganic complex compounds such as hydrates and ammines, the ligand vapor pressure is a function of the complex temperature. However, within one coordination polyhedron, the vapor pressure is independent of the molar ratio of adsorbent to adsorbate (salt to refrigerant). Barium chloride, for example, can complex up to eight moles of ammonia in one coordination step; the complexing reaction for this pair is:

$$BaCl_2 \cdot n\ NH_3 \leftrightarrow BaCl_2 + n\ NH_3 \quad \text{with} \quad 0 \leq n \leq 8 \tag{1}$$

The phase diagram is shown in Figure 1.

The equilibrium constant for this reaction can be expressed in terms of the activities of the reactants and products.

$$K_{eq} = \frac{(a(BaCl_2)^{1/8})\ \ (a(NH_3))}{a\ (BaCl_2 \cdot 8\ NH_3)^{1/8}} \tag{2}$$

The activity is a function that correlates changes in the chemical potential associated with changes in quantities such as concentrations or partial pressures. For one-step mechanisms, the equilibrium constant can be expressed with the reaction constants of the forward and reverse reaction:

$$K_{eq} = \frac{k_f}{k_b} \tag{3}$$

Equation (2) is known as the law of mass action. Gas activities are often approximated by concentrations or partial pressures; and the activities of solids are taken to be unity. Thus:

$$k_p = p(NH_3) \tag{4}$$

The activities of salts and ammoniates in liquid solutions depend on the molar ratio of absorbent to absorbate and are therefore not constant. Hence, those activity constants cannot be taken to be unity. Even for solid coordinative adsorbents and complexes, this can only be considered an approximation; because

the change in chemical potential with ligand concentration, due to the shielding effect and interaction of the ligand molecules, is omitted in this consideration.

The maximum amount of energy released in an isobaric and isothermal process that is free to produce useful work is $\Delta G$; the quantity G is called the Gibb's free energy. In the equilibrium state, both reactants and products possess the same free energy; therefore, $\Delta G = 0$. Because of irreversibilities of real processes, work obtained from spontaneous processes is always less than predicted by $\Delta G$.

Gibb's free energy is defined as:

$$G = H - TS. \tag{5}$$

For constant T and p, this can be transformed to:

$$\Delta G = \Delta H - T\Delta S. \tag{6}$$

Although $\Delta G$ may predict if a process is spontaneous, no information on reaction rates can be derived. The criterion for a chemical equilibrium in ideal gas phases can be expressed as

$$\ln K = - \frac{G°(T)}{R_m T} \tag{7}$$

where $\Delta G°$ is the standard free energy of the reaction. Equations (6) and (7) lead to

$$\ln K = \frac{\Delta S°}{R_m} - \frac{\Delta H°}{R_m T} \tag{8}$$

With Equation (4), the relationship of the equilibrium pressure to the absolute temperature is

$$\ln p(lig) = \frac{\Delta S°}{R_m} - \frac{\Delta H°}{R_m T}, \tag{9}$$

where $\Delta S°$ and $\Delta H°$ are the standard entropy and enthalpy changes of the reaction, respectively, and $R_m$ is the universal gas constant.

Analyses of complex compounds in the 1930s and 1940s were based mainly on the New Heat Theorem from Nernst. The Nernst approximation formula is a first approach to predict the vapor pressure of a complex by means of heat evolution and vice versa(4).

$$\log p(lig) = \frac{(Q_o)}{(2.303\ R_m T)} + 1.75 \log T - aT + C \tag{10}$$

$Q_o$ represents heat evolution in Joules, $R_m$ is the universal gas constant, "a" is a constant for the coordination step, and C is a constant for the ligand.

The "a" value has been approximated with a formula by Biltz and Huettig. They derived a direct linear function between "a" and the coordination number for ammoniated complex compounds.(5) This useful approximation proved to be a simple tool to predict the heat evolution with an accuracy of approximately

±7%. However, the equations are only valid for pressures well below the critical pressure of the ligand; because they are based on ideal gas law assumptions.

**Heat and Mass Transfer in Complex Compounds**

Sorption rates in porous sorbents are controlled more by sorbate transport within the pore network rather than by kinetics of surface sorption. Bulk flow through the pores is generally negligible such that the intraparticle transport must be considered a diffusive process. Such processes are described by Fick's first equation, which correlates the sorbate flux J with the diffusivity D(c) and the concentration gradient:

$$J = -D(c) \frac{\partial c}{\partial x} \tag{11}$$

Pore diffusion may occur via several mechanisms depending on the pore size, the sorbate concentration, and other conditions.(6,7)

Transport in intracrystalline pores usually is referred to as micropore diffusion. Molecules diffusing in micropores never escape the adsorbent surface's force field; transport requires an activated process involving jumps between sorbent sites. Diffusion in larger pores, such that the diffusing molecule escapes from the surface field, is referred to as macropore diffusion. Since actual reactions always use an assemblage of microparticles rather than one single isolated particle, the additional diffusional resistance associated with sorbate transport through the crystal bed must also be considered in a micropore diffusion analysis. This particular macropore diffusivity is often referred to as bed diffusivity.

In an adsorbate layer or pellet assumed to have isothermal behavior, the sorption rate may be controlled by micropore diffusion, macropore diffusion, or a combination thereof. If the micropore resistance is dominant, the concentration gradient must appear in the microparticle rather than in the layer or pellet, and the layer thickness or gross particle size should have only a minor influence on the sorption rate. If macropore resistance is the rate limiting mechanism, the concentration with the microparticle must be uniform; and the adsorption rate depends on the layer thickness or gross particle size.

Experiments performed with several different salts as the adsorbent and ammonia as the adsorbate revealed a strong dependence of the adsorption rate on the layer thickness; this leads to the conclusion that, for this case, macropore diffusion is the rate limiting diffusion mechanism.

## Technical Approach

The technical approach toward development of low temperature chill storage equipment can be divided into several steps. Initially, complex compounds with suitable vapor pressure equilibria for the thermal storage temperatures of interest were identified. An experimental investigation of media stability and the maximum possible refrigerant density was then conducted. After completing equilibrium property analyses, the dynamic reactivity properties were investigated as a function of various operating parameters. Once the most appropriate heat and mass transfer method was selected, the development of cost effective hardware and system integration strategies, currently underway, began.

**Equilibrium Properties**

Screening of Rocky Research's complex compound database led to identification of numerous ammoniated complex compounds with vapor pressure equilibria that allow for ammonia adsorption processes at pressures between 0.4 bar and 4 bar (6 psia and 60 psia) resulting in evaporator temperatures between -40°C and 0°C (-40°F and 32°F). Of this group, two complex compounds showed particular promise because of their capability to provide refrigeration around 20°F and -20°F, the most prevalent temperatures in the refrigeration market. The vapor pressure equilibria are depicted in Figures 2 and 3.

Storage density is determined by the refrigerant density of the complex compound, i.e., the mass fraction of the renegerable ammonia refrigerant contained in a unit mass of complex compound. Therefore, refrigerant uptake at constant pressure and temperature was measured. Figures 4 and 5 show the tension curves of the two candidate complex compounds. Only the refrigerant concentration range of constant pressure is available to the thermal storage process.

In order to verify the stability of the selected complex compounds, the media were adsorbed and desorbed in consecutive cycles for a duration of one month. No chemical breakdown was observed. In addition, the media were exposed to temperatures much higher than expected during normal thermal storage operation. Both complex compounds were heated to 75°C (107°F) for several hours. No instabilities were observed.

**Reactivity Analysis**

Solid-gas chemisorption or adsorption reactions are limited by heat and mass diffusion. Subcooling of the solid adsorbent leads to adsorption reactions, and superheating results in the corresponding desorption reaction. For an energy efficient thermal storage system, however, the degree of subcooling and superheating is important. Therefore, heat and mass transfer resulting from thermal and mass diffusivities is an important process characteristic requiring significant attention in the development process. Heat and mass transfer limitation is one of the traditional problems of solid-vapor thermal processes which has prevented commercial success of most thermal equipment developments until today.

Three different approaches toward effective heat and mass transfer have been pursued in parallel. Since it was well known that heat and mass transfer rates of fixed bed reactions are largely dependent on bed thickness and resulting diffusion paths, the first attempt to improve heat and mass transfer properties was made by means of generating a slurry consisting of an ammonia permeable liquid and an adsorbent salt that could be pumped across heat transfer surfaces. Several liquids were tested and significant increases in reaction rates were observed. Figure 6 shows a reaction rate comparison between a conventional dry bed reactor and agitated slurry reactor. Further experimental tests revealed that pumpability of the candidate complex compounds can be maintained throughout the entire sorption process, if 35% wt carrier liquid or more was used with the adsorbent salts. The major reduction in heat transfer area due to the increased reactivities led to promising economics. The technical problem to be solved centered around slurry conditioning and proper agitation.

Analysis of achievements made after four months development led to the general conclusion that to resolve slurry distribution, agitation, and vapor carryover issues, about 1,500 engineering hours and 2,500 technician hours would be required. Such an effort was beyond the scope of funding for new thermal equipment, so an alternative solution avoiding slurry mixing problems was prepared.

Diffusivity can be enhanced by mechanically moving the solid adsorbent (as with the slurry concept) or by mechanically forcing a carrier liquid through a fixed bed of adsorbent, thereby enhancing heat transfer and ammonia transport. Transport is effective if the carrier liquid has a high ammonia absorption capacity such that the ammonia refrigerant can be absorbed in a conventional liquid-vapor absorber and then released to the coordinative complex compound as the liquid is pushed through the solid bed.

Since the improvement was aimed at simplified fluid mechanics, a hardware loop was designed and operated to verify ease of liquid pumping through fixed beds of complex compound. While mechanical pumping and separation led to promising results, identification of suitable liquids proved difficult.

In order for a liquid to qualify as a refrigerant carrier fluid, it must perform as an ammonia absorbent and therefore be soluble in ammonia; at the same time it may not dissolve any significant amount of adsorbent salt, i.e., be inert to the adsorbent. Several organics that fulfill the above criterion were identified. Sorption power of the carrier liquids for ammonia refrigerant, however, was limited such that reasonable ammonia uptake and transport could only be achieved at ammonia equilibrium temperatures of 30°F or higher. Lower temperatures resulted either in low ammonia transport and excessive parasitic pump power requirements for the carrier liquid, or, for liquids that showed high sorption capacity at low temperatures, the salt dissolved in the carrier liquid as it desorbed ammonia and was carried into the liquid vapor absorber. Since the technical approach using a liquid carrier fluid as the ammonia transport mechanism does not address the refrigeration target market with its typical operating temperatures at or below 20°F, investigation of this particular approach was discontinued.

The third approach to optimize heat and mass transfer in solid-vapor complex compounds was investigated in parallel to the liquid- and slurry-based approaches. The approach was based on a breakthrough in complex compound reactor development for industrial heat pumps achieved a few months prior to initiation of the thermal storage project. New records in solid-vapor reactivities had been achieved reaching energy densities of 2 kW/kg and higher at approach temperatures (deviation from equilibrium) of only 8 K to 11 K (14.5°F to 20°F). While these approach temperatures and reactivities were a significant breakthrough for solid-vapor heat pumps, applicability to boundary conditions suitable for thermal storage required verification. Discharge and charge periods of thermal storage systems are typically a duration of several hours and therefore, one order of magnitude larger than heat pump cycles. This eases the reaction rate requirement accordingly by about one order of magnitude. The allowable approach temperatures for a cost effective thermal storage system, however, are much lower than those tolerable in heat activated heat pumps.

Therefore, the dry bed complex compound density control technique, which led to extremely promising heat pump reactor performances, was adapted to thermal storage conditions of lower reaction rates and much lower approach temperatures. Both candidate complexes were investigated with respect to their desorption and adsorption reactions. Reaction rates of 0.7 mol/mol-h to 1.2 mol/mol-h constitute the desired range of reactivity. Figure 7 shows the results obtained with the candidate complex compounds. Complex CC180-1580 can maintain a desorption rate of 1.5 mol/mol-h for a period of 220 minutes at approach temperatures of 4 K (7.2°F). This corresponds to a mole number change of 5.5, which is 75% of theoretical coordination sphere for this complex compound. Greater approach temperatures permit higher rates or slightly larger mole number utilization. Results for adsorption are nearly identical.

**Cycle Operation**

Ammoniated, hydrated, alcohol or ammine complex compounds consisting of a solid metal salt and a gaseous refrigerant ligand are ideal reaction fluids for heat, cool, and chill storage systems. The multitude of salt adsorbents and refrigerant adsorbates makes it possible to cover a temperature range from approximately -60°F to 600°F. Storage operation is possible by either pairing two single complex compounds or by using one complex and the plain ligand refrigerant.

The systems can be designed as direct refrigerant contact or indirect thermally coupled systems. The direct contact design uses the refrigerant of the vapor compression cycle as the ligand gas in the storage medium. This has the advantage of low heat transfer gradients but requires an almost oil-free refrigerant for the system. The indirect contact system is coupled to the refrigeration unit and/or a waste heat source across heat exchanger walls. This causes an additional temperature gradient, but it yields the safest integration of the storage system with existing chiller or refrigeration units.

Chill storage systems can also be designed as indirect coupled heat actuated chiller/storage systems, but most envisioned applications use a compressor to compress the ligand refrigerant which is in direct contact with the complex. The most relevant refrigerant ligand for direct contact systems is ammonia, since it is used commonly as refrigerant in compressor units and as ligand in complex compound formation.

Figure 8 shows the schematic of a compressor actuated chill storage system. The system operates with one complex compound and the plain ligand refrigerant. Dual complex systems can be developed on the same basis.

During discharge, the liquid ammonia ligand evaporates in the evaporator providing chill to the user process. The vapor pressure of the ammonia at the low evaporator temperature, however, is still higher than the complex compound vapor pressure at the high heat rejection temperature maintained by an evaporative condenser or cooling tower. Therefore, the ammonia leaves the ligand storage tank, evaporates, and undergoes an exothermic adsorption reaction with the complex compound. Figure 9 shows the discharge process in the phase diagram.

In order to charge the system, the ammonia gas flow must be reversed. This can be obtained by either raising the ammonia pressure of the complex compound sufficiently high or to cool the condenser

sufficiently low to condense the ammonia and ultimately lead the liquid back into the ligand storage tank. In any case, the pressure gradient must be reversed such that a positive flow of ammonia from the complex to the condenser can be maintained.

If an existing vapor compression refrigeration system is used to charge the system, the ammonia is drawn out of the complex and fed into the low temperature receiver where it is picked up by the compressor. In order to maintain the design suction pressures, the complex must be heated with the chiller reject heat such that the low pressure receiver pressure is in approximate equilibrium with the complex compound ammonia pressure.

The most promising chill storage integration concept for an initial installation and field test is achieved by directly coupling with the low pressure receiver. Figure 10 shows a schematic of a directly coupled thermal storage system. During the charge process, the compressor is active; and ammonia gas leaves the complex compound reactor. The condenser heat is used to maintain the complex compound temperature around 95°F. During the discharge process, the compressor is not operating and ammonia vapor is drawn from the receiver into the complex compound reactor. The complex compound temperature is maintained by means of the evaporative condenser or cooling tower.

## Economics

Exact data on complex compound thermal storage systems are not available, since the reactor systems are still under development. Cost predictions, however, can be made based on the current development status. If no further performance improvement is obtained, costs for a -10°F to -20°F thermal storage system, based on a 1000 ton-h capacity system, are:

- Adsorbent mass CC180-1580
  24 kg/ton-h at $2.60/kg = $62.40/ton-h
- Heat exchange surface
  $3.50/kg adsorbent = $84.00/ton-h
- Vessels and enclosures
  $2.25/kg adsorbent = $54.00/ton-h.

The above costs are based on vendor quotes for technical grade salts, heat exchange surface, and ASME pressure vessels. This leads to a total of approximately $200/ton-h component cost. Installation and packaging costs were ascertained from manufacturers and application engineers(8,9). For a simple system integration, as envisioned for the thermal storage system, a mark up factor of 1.5 to 1.65 is to be expected. This leads to an estimated installed cost of $300 to $330/ton-h.

The return on investment is largely dependent on electric utility rates. The extremely low consumption of additional electric power during the charge process is one of the major advantages of complex compound thermal storage systems, which also simplifies the economic trade-off calculations. In utility areas with purchase incentives, returns on investment exceeding 50% can be achieved. Where no purchase incentives

exist, returns are lower but typically not below 30%. Extensive economic analyses have been performed by Kohlenberger Associates(10). The study shows that systems with much higher electrical parasitic penalties save about $100/yr and ton-h in utility expenses. Buying incentives are typically restricted to $100,000. Applying these numbers leads to the above mentioned return on investment of 30% in areas with no buying incentives and of 45 to 50% in areas with active buying incentive programs.

A detailed analysis of economics will be performed once equipment development is in the final design stage. At this point in development, a more accurate cost prediction attempt would only result in academic exercises which are not part of the project. Third party analyses of the complex compound TES concept, however, led to optimistic projections by manufacturers, application engineers, and end users.

## Conclusions

Ammoniated complex compounds are attractive as media for reactive thermal storage at low temperatures. Research and development has led to reactor hardware with promising operational features, possibilities simple integration for into existing refrigeration plants, and attractive low cost.

The major tasks of the final developments are long term media stability investigations, optimization of the reactor hardware, development of controls, construction of scaled-up systems, and the prototype field test. An operational field test unit can be expected within 24 to 30 months.

## References


1. C. Kohlenberger, private communication, Kohlenberger Associates Consulting Engineers, Inc., Fullerton, CA, October 1988.

2. R. Stamm, private communication, Industrial Refrigeration, Inc., Chicago, IL, October 1988.

3. U. Rockenfeller, Development of Dual Temperature Ammines for Heat Pump Latent Storage Application - Final Report, ORNL/Sub/84-47999/1, March 1986, available from National Technical Information Service, Springfield, VA.

4. W. Nernst, The New Heat Theorem, New York: Dover Publications, 1969.

5. W. Biltz and G. Huettig, "Ueber Ammoniakverbindungen der Halogenide," Zeitschrift f. anorg. Chemie., 109, S. 89, 1919.

6. F. A. L. Dullien, Porous Media, Fluid Transport, and Pore Structure, New York: Academic Press, 1979; Chap III.

7. M.D. Ruthven, "Zeolites as Selective Adsorbents," Chemical Engineering Progress, February 1988, pp.42-50.

8. R. Vig, private communication, Vilter Manufacturing Corporation, Milwaukee, WI, July 1988.

9. R. Stamm, private communication, Industrial Refrigeration, Inc., Chicago, IL, October 1988.

10. Kohlenberger Associates Consulting Engineers, Inc., An Investigation into Low-Temperature Thermal Energy Storage Technologies, Fullerton, CA, September 1987.

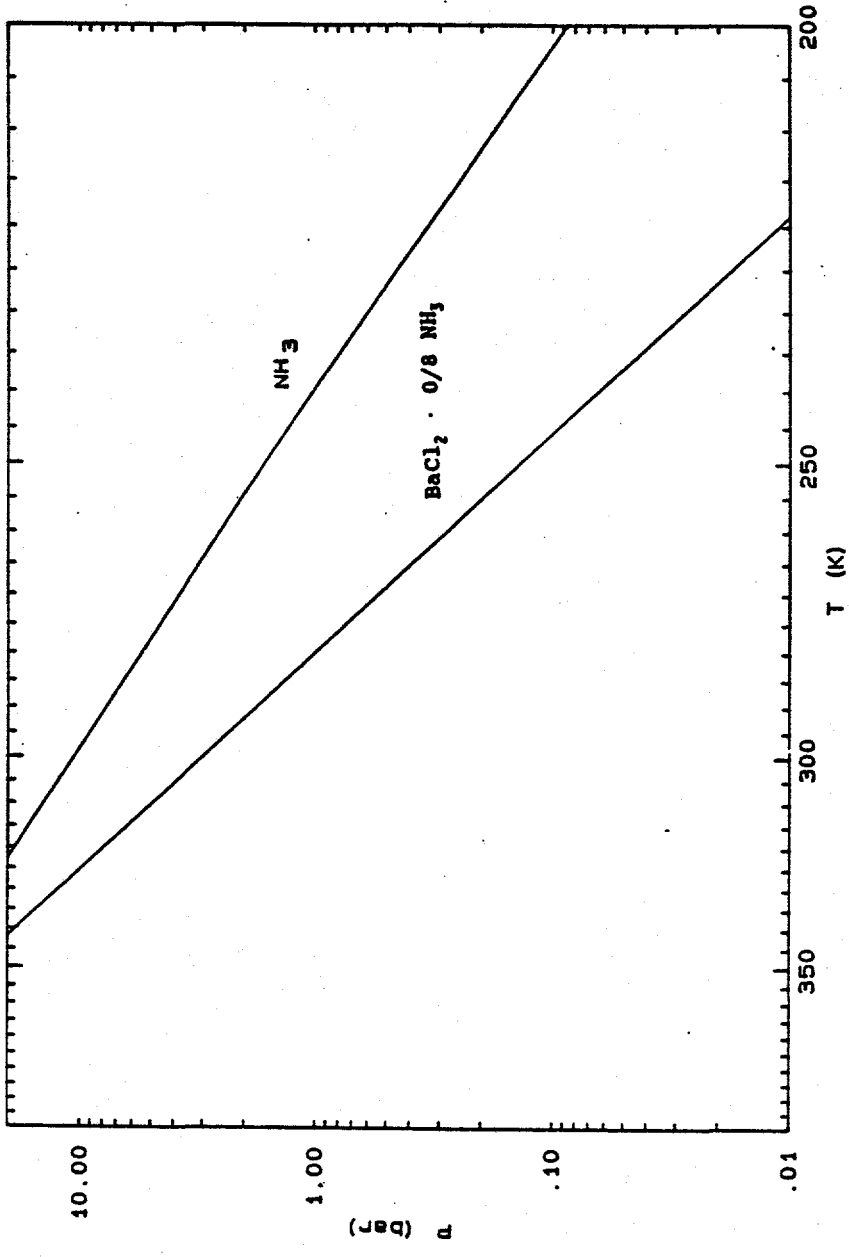


Figure 1. Phase diagram for $BaCl_2 \cdot 0/8\ NH_3$.

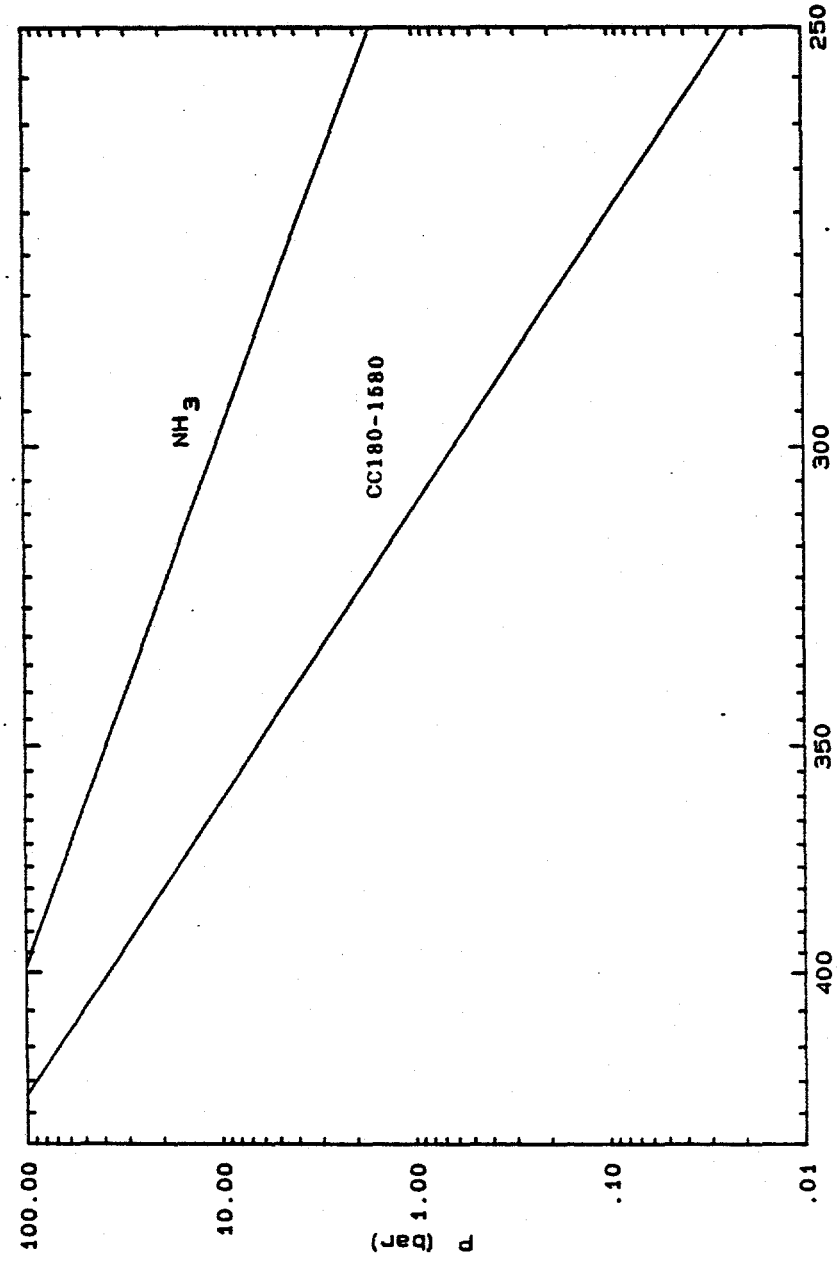


Figure 2. Vapor pressure-temperature relation for CC480-1110.

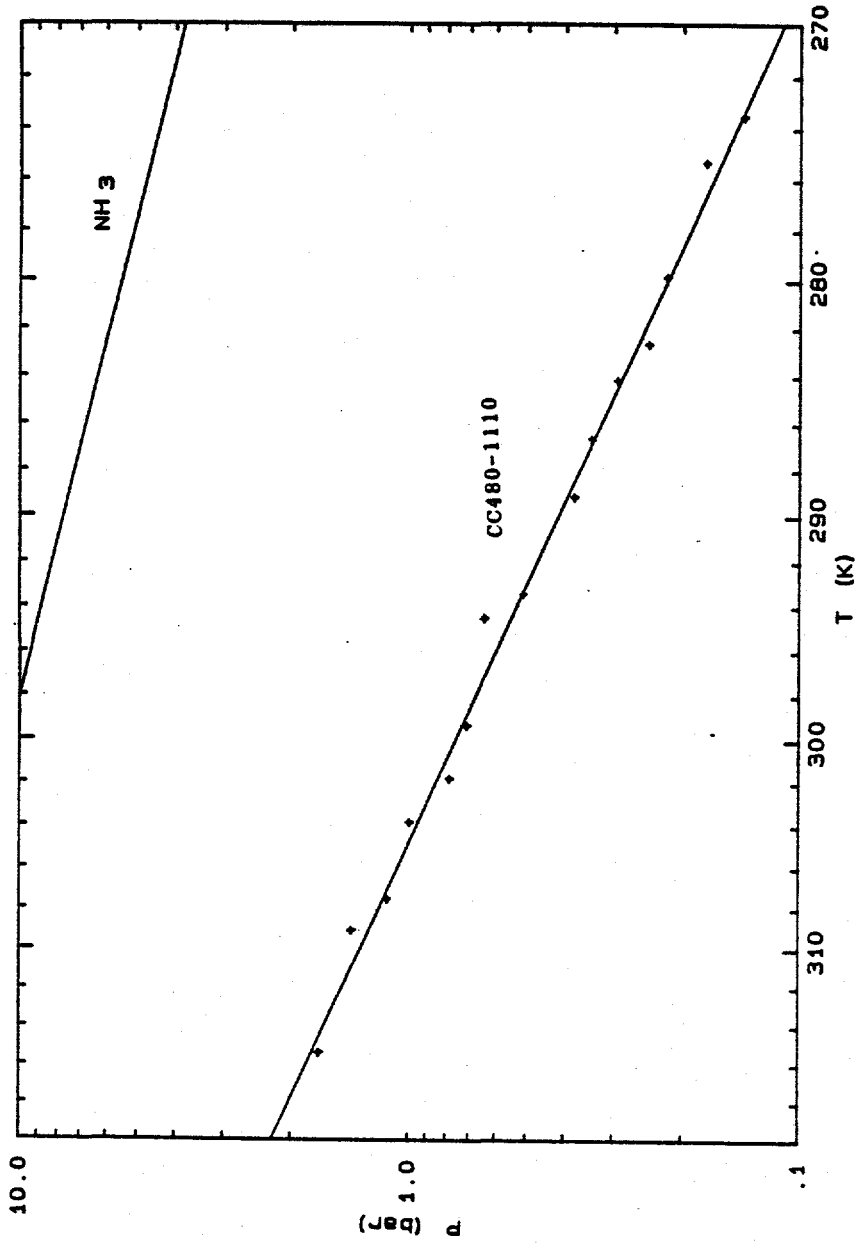


Figure 3. Vapor pressure-temperature relation for CC180-1580.

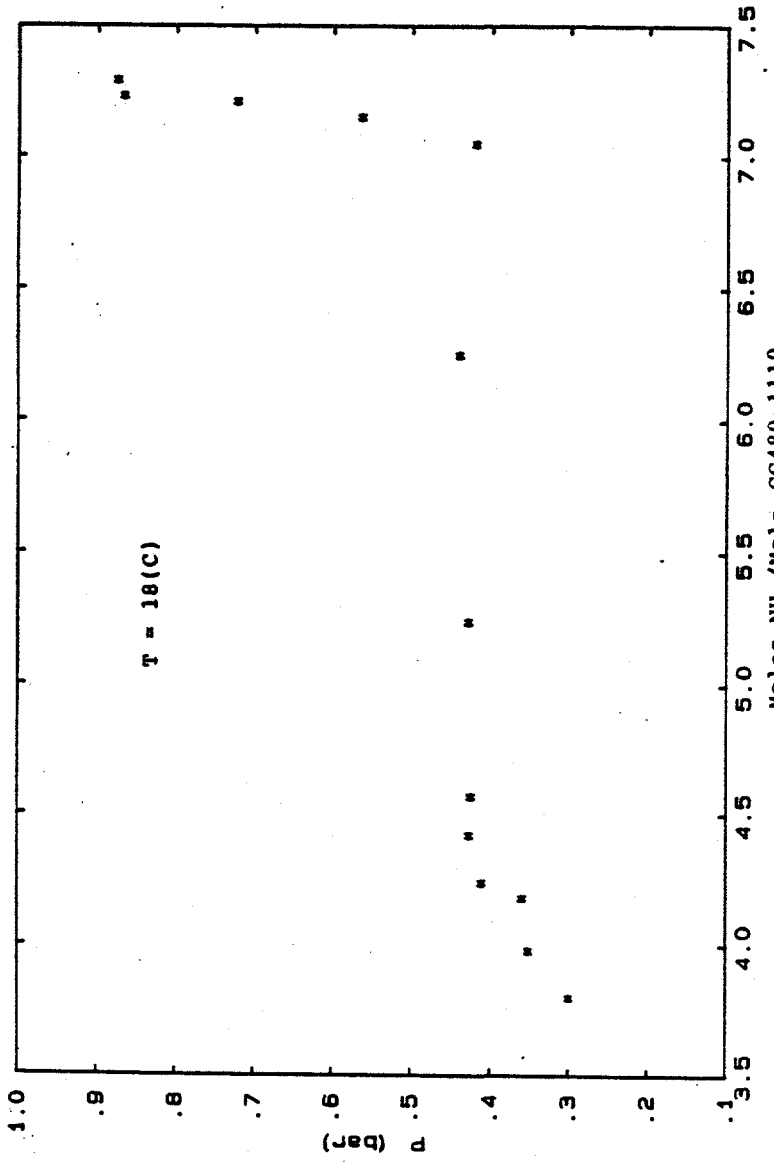


Figure 4. Tension curve for CC480-1110.

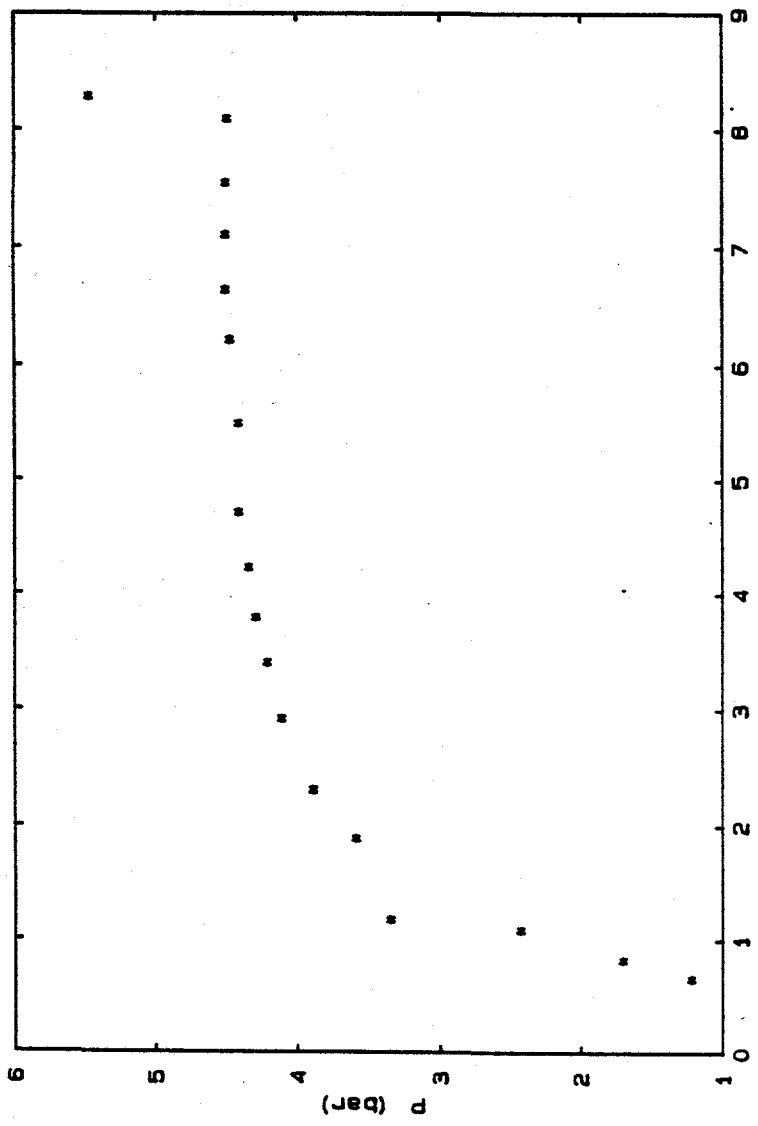


Figure 5. Tension curve for CC180-1580.

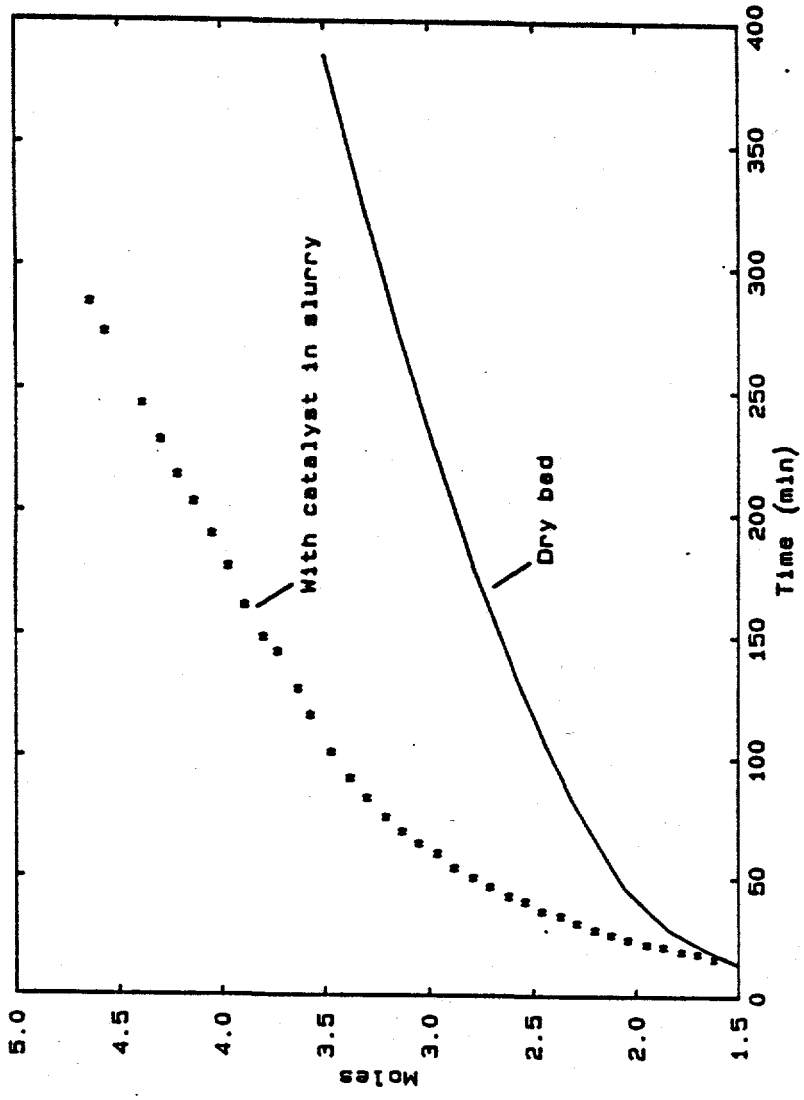


Figure 6. Adsorption uptake curve for CC480-1110.

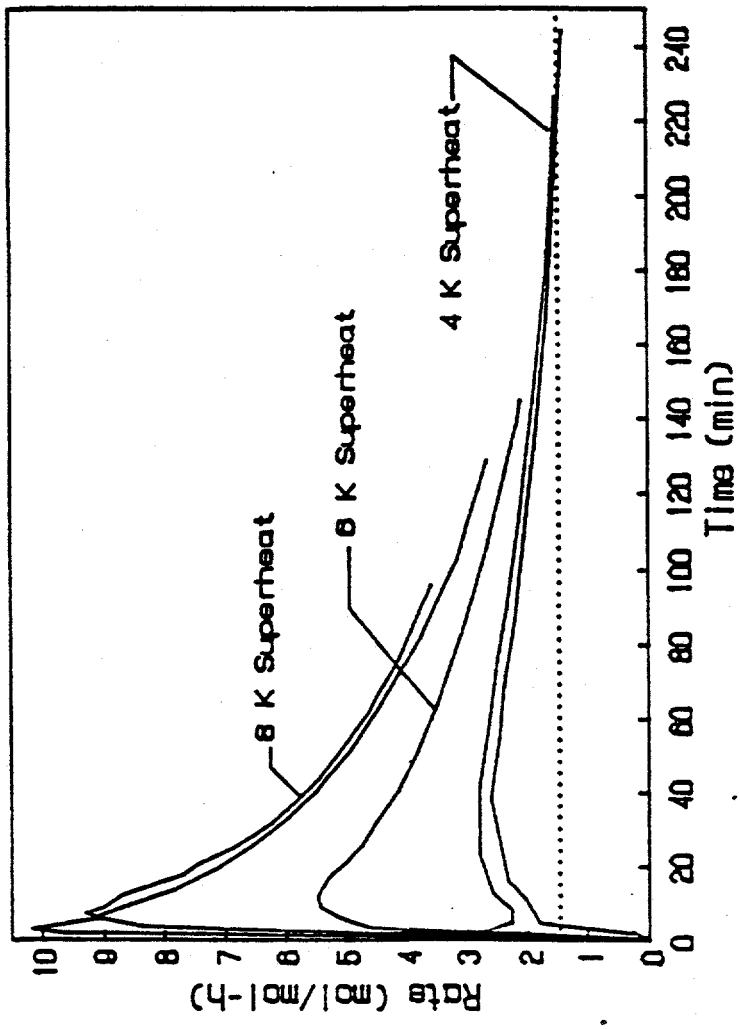


Figure 7. Reactivity of CC180-1580.

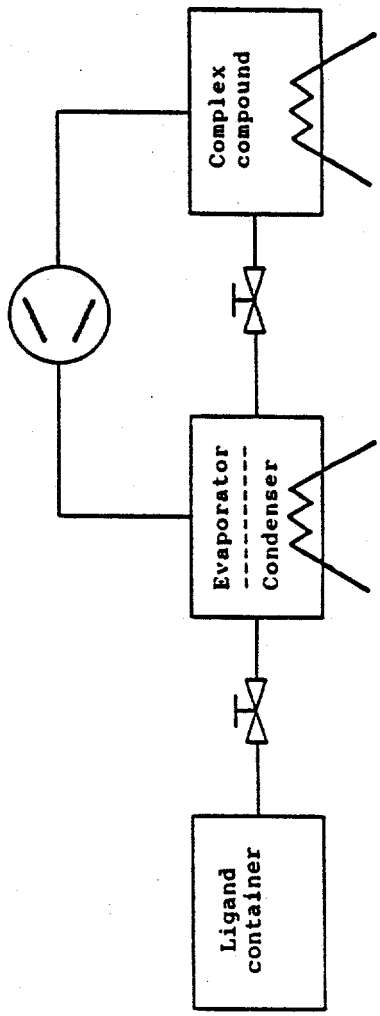


Figure 8. Cool storage concept using compressor.

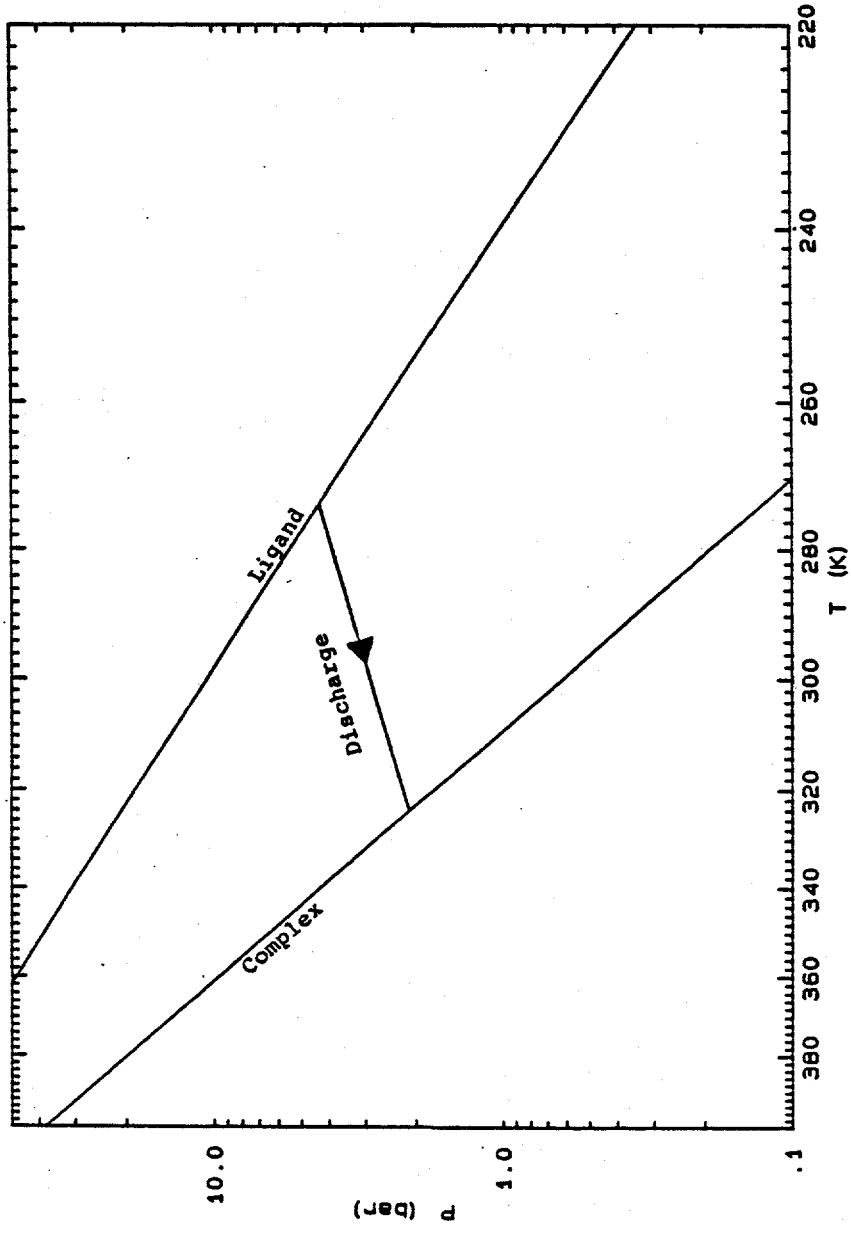


Figure 9. Discharge of complex compound chill storage system.

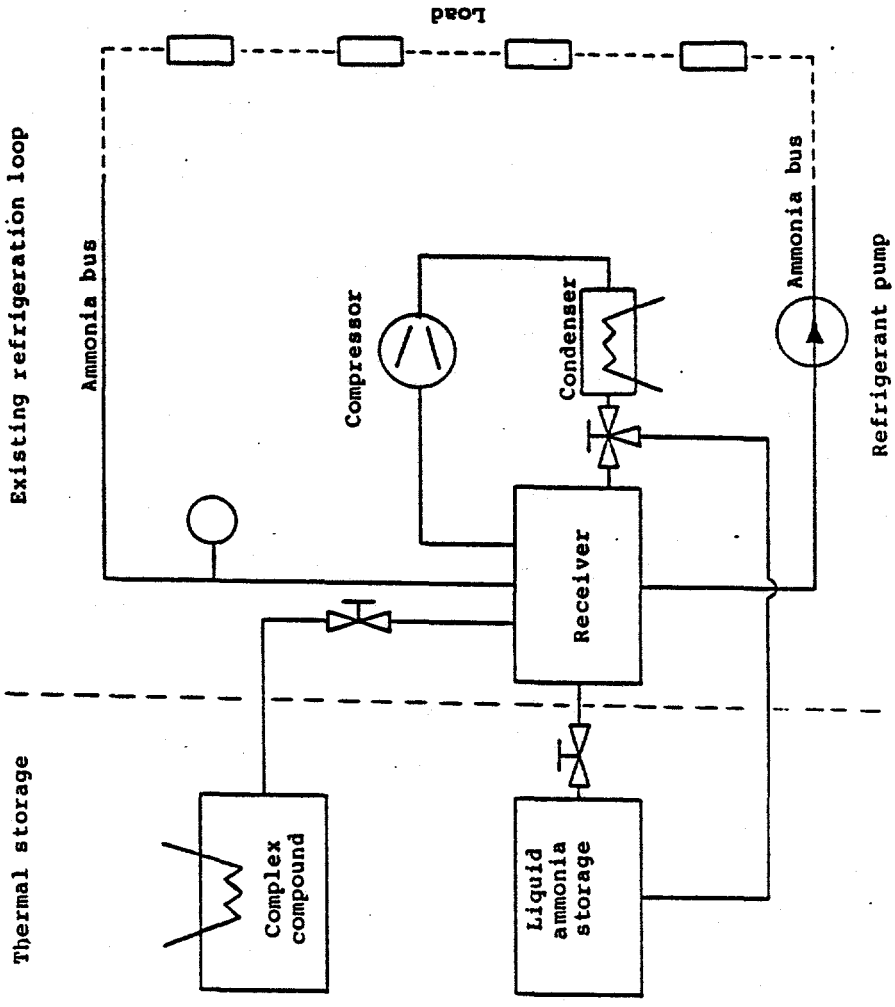


Figure 10. Refrigeration loop with complex compound TES system.

# SEASONAL THERMAL ENERGY STORAGE

# OVERVIEW OF THE SEASONAL THERMAL ENERGY STORAGE PROGRAM

**L. D. Kannberg, Program Manager**
Pacific Northwest Laboratory[a]
Richland, Washington 99352

## *ABSTRACT*

*Seasonal thermal energy storage (STES) has the potential to provide storage for large-scale industrial and building heating and cooling at many sites in the United States. It is one of a number of technologies required to help meet national energy needs to reduce peak electrical demand, improve energy utilization efficiency, facilitate use of renewable and domestic energy sources, as well reduce emissions causing global climate changes. The U.S. Department of Energy (DOE) is conducting a research and development program to develop STES technologies. Development of aquifer thermal energy storage (ATES) is currently emphasized because of its wide applicability and relatively low cost. Current efforts are focussed on developing the necessary knowledge base to design and operate ATES systems. This knowledge base includes geohydraulic, geochemical, and geomicrobiologic features affecting design, performance, and institutional acceptability of ATES systems. The scope of activities includes numerical model development and application, laboratory geochemical and microbiologic evaluation, and field performance testing and monitoring. Additional efforts are underway to identify the best ways to integrate ATES with end uses. Future plans follow three primary thrusts: 1) complete investigation of fundamental ATES phenomena and development of design aids (such as computer models), 2) begin assertive technology transfer and assist implementation by cost-shared feasibility studies and pilot-scale field tests/demonstrations, and 3) begin investigations of other promising STES technologies, such as ice storage, rock borehole, and earth STES.*

## Introduction

How often have you wished that you could have some of that winter cold as you sweltered in the summer heat? How often have you wished for some of that summer heat as you've struggled through another bitter winter?

While these may have seemed just wistful daydreams, efforts are underway to make this a reality for some applications. Furthermore, energy trends in the U.S. indicate that this technology, along with many others, are needed to satisfy our future energy needs.

As a result of record high summer temperatures, continued growth in the use of air conditioning, and greater use of electricity in service and industrial sectors, electric utilities set record peak electrical demand

---

[a] Operated for the U.S. Department of Energy by Battelle Memorial Institute under contract No. DE-AC06-76RLO 1830.

and sales figures in 1988. In some locations, available reserves were nearly exhausted and rolling brownouts were necessary. Electric generation load factor continues to drop, with values now approaching 60%. The number of utilities using load management techniques, such as chill storage incentives, demand charges, and time-of-day rates, continues to increase. Utilities are placing greater reliance on independent power producers, development of cogeneration, conservation efforts, and installation of combustion turbines to meet future load growth.

Low petroleum prices have encouraged greater use of foreign oil (5% more in the last 2 years and are projected to increase from the current 40% to over 50% by 1995) with an ever larger share coming from the Middle East. The proportion of foreign oil coming from the Middle East increased from 17% to 22% in the last 2 years alone. Furthermore, only one new coal plant, and no nuclear plants, were ordered in the 1980s. Finally, we are confronting new environmental issues. Concern over acid rain, global warming, depletion of the ozone layer, and solid waste disposal could have a profound effect on how we provide and utilize energy.

Seasonal thermal energy storage (STES) can contribute to meeting these challenges. In particular, STES can reduce energy consumption for space heating and cooling, substantially reduce peak electrical requirements, and facilitate incorporation of large-scale solar heating. For these reasons, the U.S. Department of Energy has sponsored research and development to advance these technologies. This paper describes the DOE STES Program, managed by Pacific Northwest Laboratory (PNL); its past, present, and future.

## DOE STES Program

The mission of the DOE's Office of Energy Storage and Distribution (OESD) is to develop and advance energy conversion, storage, control, and delivery technologies that benefit the nation by:

- increasing national security
- enhancing energy independence
- assuring public safety
- improving the quality of the environment, and
- enhancing U.S. competitiveness.

Consistent with this mission the goal of the DOE TES Program is to develop economically viable thermal energy storage systems that contribute to energy savings, fuel substitution, and environmental improvement. Particular emphasis is now placed on developing TES technologies that

- reduce peak electrical demand and improve industrial, commercial, and residential energy efficiency
- facilitate the use of renewable resources and widely available domestic fuels, and
- reduce production of pollutants that contribute to global warming, acid rain, and ozone depletion.

Seasonal thermal energy storage technologies are among those being advanced because they can substantially reduce total energy consumption, leading to greater energy independence and improved environmental quality. Once technical and economic risks have been reduced through proven performance, STES is expected to be a highly economical option that will contribute to U.S. competitiveness by reducing energy costs in industrial and commercial operations.

It has been estimated that STES is technically suitable to provide up to 10% of the nation's energy needs (Anderson and Weijo, 1988). Residential and commercial building heating, cooling, and domestic water heating consumed 15 quads of energy[b] in the U.S. in 1983, primarily as natural gas and petroleum distillates (U.S. Department of Energy 1986). It has been estimated that over 2 quads of energy are available as industrial waste heat. A substantial portion of this is well suited for STES. Furthermore, use of climate energy from renewable sources (i.e., solar heat and winter chill) provides additional potential for meeting building heating and cooling needs using STES. It has been estimated that over 2 quads of residential and commercial cooling exist, a portion of which could potentially be integrated with winter chill STES. A 1979 study (TRW 1979) estimated that, if aggressively pursued, STES could be expected to supply 2 quads of building heating and cooling by the end of the century. While energy economic conditions have changed in the last few years, the enormous potential for STES remains.[c]

Developing STES technologies requires a focussed program based on STES technology development needs and priorities and a correct perception of the Federal role in energy technology development. Therefore, STES Program efforts are focussed on acquiring and transferring knowledge to those seeking to use STES for industrial, commercial, and residential heating and cooling.

**STES Program Objectives**

The objectives of the STES Program are:

- Establish a technical and economic knowledge base for private and public sector development and implementation of STES technologies.
- Transfer this knowledge base to industrial and commercial developers for implementation.
- Ensure the adequacy of the knowledge base by monitoring and assisting early STES implementation.

The knowledge base includes an understanding of geotechnical processes, STES system interactions, and relevant engineering features. The characterization of STES geotechnical behavior and the development of sound engineering guidelines for satisfactory long-term storage require detailed numerical analyses, laboratory experimentation, and field testing. Likewise, the analysis of alternate or more-advanced storage concepts

---

[b] 1 quad = 1015 Btu, ≈1018 Joules, or ≈3 x 1014 kWh.

[c] One quad of energy was worth approximately $11 billion at fuel prices available to commercial building owners in 1985.

requires technical and economic characterization and screening, development of testing procedures for critical high-risk components or subsystems, proof-of-principle testing, and field performance monitoring.

Transfer of the knowledge gained through targeted research and development (R&D) and field testing is vital if the OESD mission is to be accomplished. Mechanisms for this transfer include involvement of groups seeking to implement the technology in R&D activities, cost-shared implementation of STES systems in pilot projects, assembly and publication of R&D results, and preparation of guidelines for analysis, design, and construction of STES systems.

Feedback on field performance of STES systems, particularly prototype commercial installations, is essential to identifying real-world challenges that may not have been apparent during research and development and for validating the knowledge base. Such feedback can only be obtained if researchers remain active throughout the technology-transfer phase and are involved in early application and monitoring of STES systems.

**STES Program Scope**

The program scope encompasses concepts that seasonally store heat or chill from waste or other surplus sources to reduce peak period energy demand, reduce electric utility peaking requirements, or contribute to the establishment of favorable economics for district heating and cooling systems. Aquifers, ponds, earth, lakes, and engineered structures (e.g., tanks, excavated caverns, and artificial aquifers) are examples of physical systems with potential for seasonal storage.

Achievement of significant private and public development of STES will require research and development to establish technical and economic feasibility and institutional acceptability of a variety of STES concepts. Seasonal thermal energy storage in aquifers has been determined to have the greatest potential due to its low cost and the existence of suitable aquifers underlying more than 60% of the nation. Therefore, emphasis has been placed on aquifer thermal energy storage (ATES). Consequently, research programs have been initiated to characterize the technical features of ATES and identify and resolve the technical issues that increase risk beyond that acceptable to entrepreneurs. These risks involve virtually all aspects of ATES, including both technical as well as institutional issues. The various ATES issues are listed in Table 2.1 along with the factors they influence, their relative importance, relative state-of-knowledge, and research ranking. The various rankings are subjective, based primarily upon the experience to-date at operational ATES systems around the world.

**STES Development Strategy**

The STES Program employs a sequence of activities to acquire and transfer the knowledge necessary to implement STES technologies. The sequence generally progresses from conceptual investigations through pilot tests depending on the promise and technical risks associated with the concept. The successive steps include:

- identify and rank promising STES technologies
- identify and prioritize the technical, economic, and institutional issues facing technology implementation
- establish cohesive programs to characterize and resolve the issues
- transfer research and development results (including findings, methodologies, tools, guidelines, design aids, new concepts, and other knowledge) to STES implementors
- verify and augment this knowledge by assisting and monitoring implementation of pilot, and early commercial, STES systems

The limits of the DOE role in STES development influence the nature of research and development conducted as part of the program. Most STES technologies use or can influence groundwater resources that are the subject of state and local environmental quality statutes. This fact increases the institutional risk associated with implementation and cannot be overlooked in our efforts to establish an adequate knowledge base for STES implementation. Program involvement in implementation of STES technologies is limited to instances where technical knowledge is insufficient or unreliable or where a unique opportunity exists to extend or validate the existing knowledge base.

Program research and development generally concentrates on knowledge necessary to design STES systems or address state or Federal regulatory concerns. To the extent possible, field R&D is done at sites in regions that are early candidates for commercial development of STES technologies. In this manner, appropriate research and development is obtained in regions of the country where it will be most applicable and where early technology experience will be most beneficial.

## Past STES Development

The historical STES Program activities are illustrated in Figure 1. Evaluation of ATES began in 1975 at the Mobile field test site near Mobile, Alabama. A number of other STES development and evaluation efforts have been conducted over the years ranging from field studies and demonstration projects (subsequently discontinued) to studies of regulatory issues. Most program activity occurred in the late 1970s and early 1980s when energy conservation research and development was of high priority and correspondingly high budgets were available. Beginning in 1982, funding levels dropped dramatically and the scope of research and development abruptly shifted away from demonstration projects. Recent funding levels have stabilized, allowing consideration of program long-term goals and activities. The organization of the STES Program has changed as the direction and scope of DOE funded efforts have changed. In 1987, all DOE-OESD thermal energy storage (TES) efforts were reorganized. Six project classifications were developed within which various projects were collected. The classifications include:

- System Development - system evaluation or development in the field (i.e., pilot or commercial-scale systems).

- Mathematical Modeling - development of tools to simulate important physical and chemical processes affecting system performance and behavior.

- Media Investigation and Development - characterizing the physical and chemical behavior of thermal storage media and its confinement.

- System and Component Studies - preliminary investigation of TES systems and components, especially concept feasibility assessments and bench or field characterization of a major TES component.

- Heat Transfer Enhancement - development of means to improve heat transfer to and from TES elements (includes heat exchange to and from the media, container, or ancillary equipment, such as indirect heat exchangers).

- Environmental and Institutional Studies - characterization and resolution of TES issues affecting environmental or institutional acceptability.

## Current STES Development Activities

The current organization of STES projects within the classification system described above is shown in Figure 2. Several of the projects serve multiple classifications. This is especially true of field projects where the information concerning several fundamental scientific issues is obtained along with data on operational behavior from testing in a realistic environment. Other projects are single-purpose studies.

Two large field projects are underway that provide information on many of these issues and provide field data to corroborate laboratory and numerical modeling efforts. University of Minnesota researchers at the St. Paul field test facility completed the second long-term test cycle in 1987. This test used a higher temperature (120°C) than any previous aquifer field test and was completed according to schedule. A thermal energy recovery factor of 0.62 was computed based on actual source water temperature. The recovery factor would be 0.69 if the source water had been at normal groundwater temperature (11°C). Scaling of calcium carbonate in the heat exchanger was controlled with the use of ion-exchange water softening. Although softened prior to injection, the recovered groundwater was nearly at equilibrium with the minerals present in the aquifer, with the exception of the sodium introduced to the aquifer through water treatment. Only 80% of the injected sodium was recovered, although sodium was expected to be a conserved substance. Uncertainty exists whether mixing or chemical reactions account for the unrecovered sodium. Aquifer thermal behavior during the second long-term test was consistent with earlier testing. High permeability zones were evident by their rapid thermal rise (as hot groundwater flowed through these zones). Less permeable layers were heated by conduction from adjacent zones having higher permeability. Zones distant from the permeable layers were unaffected during the test.

The chill ATES system at the Student Recreation Center at the University of Alabama continues to be monitored by University researchers. Steps were recently taken to improve the performance of the system. The steps included revising the operating strategy to counteract the negative effects of regional groundwater flow at the site. The system has met all the sensible cooling loads of the Recreation Center since

its initial operation. During 1986-87 approximately 80% of the injected chill was recovered. However, nearly 2.5 times as much groundwater was pumped during recovery as during injection to meet the cooling load. Part of the reason for this is the severe weather during the year (warm winter and hot summer). But an equally significant problem is the loss of stored chill; being swept away by regional groundwater flow. Based on first results, the revised operating strategy, implemented in 1987-88, appears to be having a beneficial effect. During 1986-87, the system posted an annual coefficient-of-performance of 5.0 and reduced summer peak electrical consumption for cooling by an estimated factor of 20 compared with conventional technology. This results in an estimated annual savings of approximately $17,000. The projected 1988 COP is 3.7.

ATES-specific numerical models are necessary to design and assess ATES systems. A suite of codes was identified for ATES simulation. The codes are applicable to a spectrum of potential ATES simulation. The mainstay of the suite is the ATESSS (Aquifer Thermal Energy Storage System Simulator) code, developed for initial site screening and design optimization. Other codes have been, or are being, collected to deal with specific design issues at various levels of sophistication. ATESSS has been used recently to assess various design options for mitigating regional flow effects at the Student Recreation Center and a planned chill ATES system at a General Motors Plant in Tuscaloosa, Alabama. These simulations indicated that a well field that is collinear with the hydraulic gradient may provide good thermal recovery at a smaller cost than designs that use up-gradient pumping to control regional flow. ATESSS was also used to assess the role of impermeable layers in aquifers. Nomographs for assessing the importance of impermeable layers were developed. It was determined, for instance, that for a seasonal cycle an aquifer composed of many alternating layers of permeable and impermeable media will have first-cycle thermal recovery efficiencies of 93% for layers 0.25-m thick, 62% for layers 5.0-m thick, and 85% for layers 25-m thick.

All remaining models identified for the suite are available in the U.S. except for CHARM1, the first version of a geochemical/transport code being developed by The Netherlands as part of its contribution to International Energy Agency (IEA) Annex VI of the Energy Conservation Through Energy Storage Programme. The U.S. is contributing to this Annex in several ways including providing an up-to-date geochemistry model database, providing experimental data on fundamental geochemical reactions and their kinetics for sandstones, and leading a subtask to assess microbiologic issues.

Geochemical laboratory testing is underway to determine fundamental geochemical behavior for sandstones, primarily those from the St. Paul field test facility site. This testing increases the knowledge of groundwater geochemistry, contributes to our understanding of geochemical behavior at the St. Paul site, and helps satisfy Department of Energy (DOE) IEA agreements. Results of the testing to-date indicate the influence of fines (small particles in the sandstone) on geochemical reactions and their rates. The fines appear to be a source of calcium for dissolution during storage, despite the inability to identify any calcium mineral forms in the sandstone samples. The laboratory results are consistent with those of earlier field tests and explain some of the ambiguities. Increased sulfate concentrations were observed during storage

for both field and laboratory tests. Laboratory tests explained that feldspar dissolution was the source of potassium in recovered groundwater. Finally, dissolved silicon is controlled by dissolution of, and equilibrium with, quartz. This last finding is important because 1) it reduces the number of geochemical constituents of interest for ATES site characterization and 2) if silica scaling becomes a problem at the site, additional water treatment will be required because the aquifer can serve as a nearly inexhaustible supply of silica. One nagging question remains. What is the role of mixing in the aquifer on geochemical dynamics?

Two new environmental studies were recently initiated. An assessment of ATES effects on microbiota was conducted; and as a result, a field monitoring program was initiated at the chill ATES site on the University of Alabama. Aquifers are habitat to an abundant and diverse microbial population. Unfortunately, little information is available on these organisms. It is known that indigenous organisms are subject to environmental factors including: aquifer porosity, nutrient availability, oxidation-reduction conditions, pH, temperature, and adsorption on aquifer rock matrix. While impacts on indigenous organisms are of concern, immediate interest is focussed on pathogenic microorganisms, especially Legionella. Monitoring for coliform bacteria at the St. Paul field test facility site has determined that no coliform bacteria were introduced or survived during high-temperature testing at that site. However, it is expected that groundwater utilized at the Student Recreation Center at the University of Alabama will interact with a verdant microbiologic community. Therefore, monitoring for both indigenous and pathogenic organisms has been initiated. The results of the preliminary assessment has been provided to fellow IEA participants in Annex VI and results are being provided at this conference and will be provided semiannually to IEA participants and more widely through timely topical reports.

International activity in ATES has increased, with pilot projects underway at many sites. European and Scandinavian countries are the most active at this time (primarily in heat storage), although China has many chill ATES systems in service. As noted earlier, the U.S. Department of Energy is active in an International Energy Agency activity (Annex VI of the Energy Conservation through Energy Storage Program) dealing with defining and resolving ATES water quality issues.

## Future STES Development

The long-term plans for STES research are shown in Figure 3. Planned activities are shown according to the classification identified above for the next 5 years. The schedule for performance of these activities is aggressive; they can only be completed if sufficient resources are available.

The major thrusts for the next 5 years are threefold: 1) complete investigation of fundamental ATES phenomena and development of design aids (such as computer models), 2) begin assertive technology transfer and assist implementation by cost-shared feasibility studies and pilot-scale field tests/demonstrations, and 3) begin investigation of other promising STES technologies, such as ice storage, rock borehole, and earth STES. The first two thrusts are required to commercialize ATES technology. The investigation of other STES technologies is directed at providing STES alternatives for locations at which ATES is not viable or is not the most economic option.

## References

1. Anderson, M. R., and R. O. Weijo. 1988. Potential Energy Savings From Aquifer Thermal Energy Storage. PNL-6588, Pacific Northwest Laboratory, Richland, Washington.

2. TRW. 1979. Thermal Energy Storage Application Areas. McLean, Virginia.

3. U.S. Department of Energy. 1986. FY 1988 Energy Conservation Multiyear Plan. Washington, D.C.

Table 1. Relative ranking of issues affecting ATES development.

| Issue | Influences | Rating[a] Importance | Rating[a] State of Knowledge[b] | Ranking |
|---|---|---|---|---|
| Fundamental knowledge | | | | |
| Geohydrology | Energy recovery (economics, viability) | 5 | 3.5 | 3.5 SS[c] |
| | Well field design (performance/economics) | | | |
| Geochemistry | Injectability (well performance) | 4 | 1.5 | 5.0 SS |
| | Water quality (environmental) | | | |
| | Water treatment (economics) | | | |
| Microbiology | Water quality (environmental) | 3 | 1 | 4.0 |
| | Water treatment (economic) | | | |
| | Injectability (performance) | | | |
| Design knowledge | | | | |
| Source/load integration | Performance (economics, viability) | 4.5 | 1.5 | 4.5 SS |
| System optimization | Performance (economics, viability) | 4.0 | 2.0 | 4.0 |
| Well field design | Energy recovery (economics, viability) | 5.0 | 3.0 | 3.5 |
| Water treatment | Water quality (environmental) | 4.5 | 3.0 | 3.5 |
| | Performance (economics, viability) | | | |
| Institutional factors | | | | |
| Environmental acceptability | Permitting (viability) | 4 | 2 | 3.5 SS |
| Legal ownership | Risk perception | 3.5[d] | 1 | 3.5 |

(a) 1-5 from low to high.
(b) Inverse of risk
(c) "showstopper" - A factor capable of solely determining the viability of a project.
(d) Difficult to assess at present

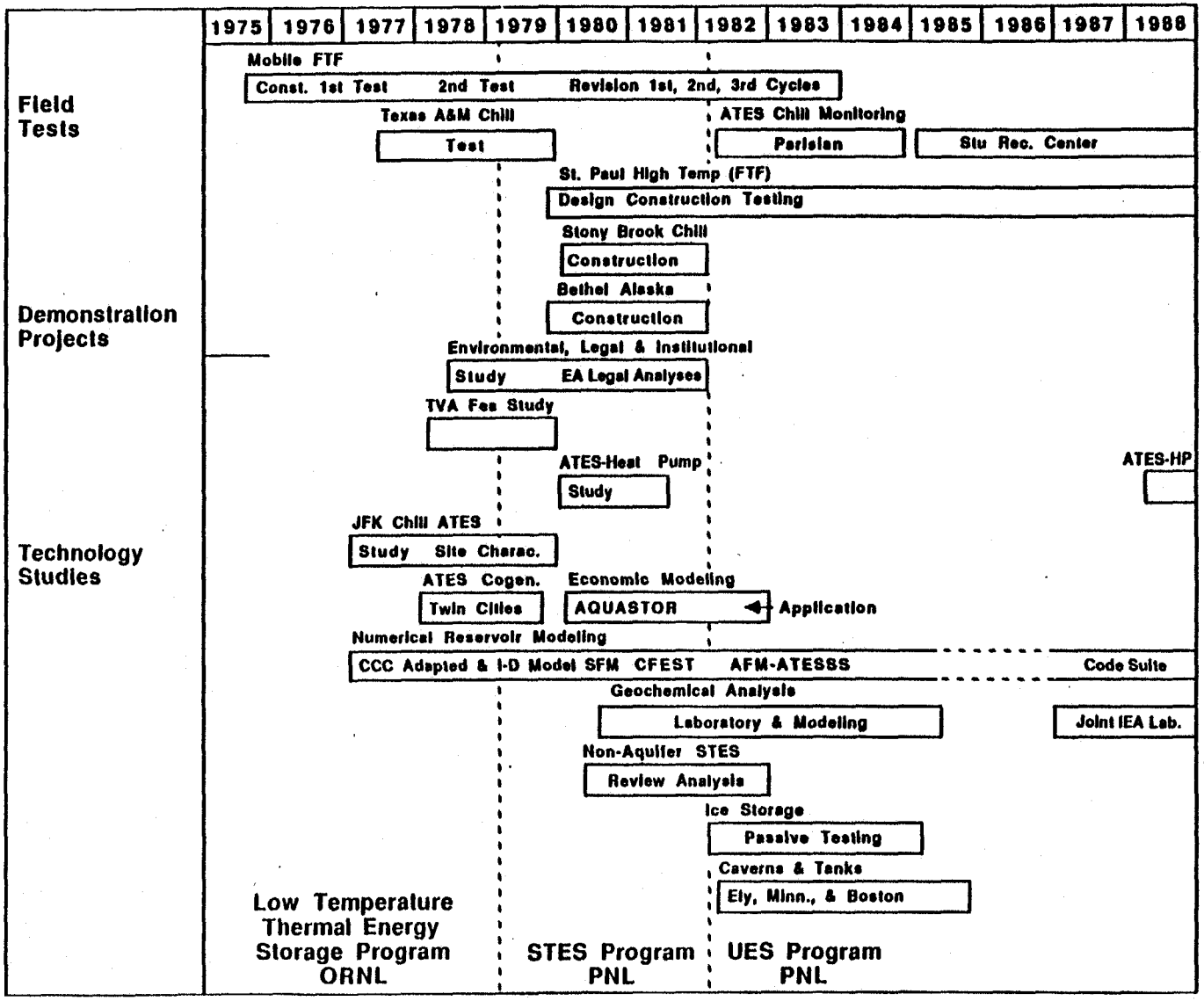


Figure 1. Department of Energy seasonal thermal energy storage program history.

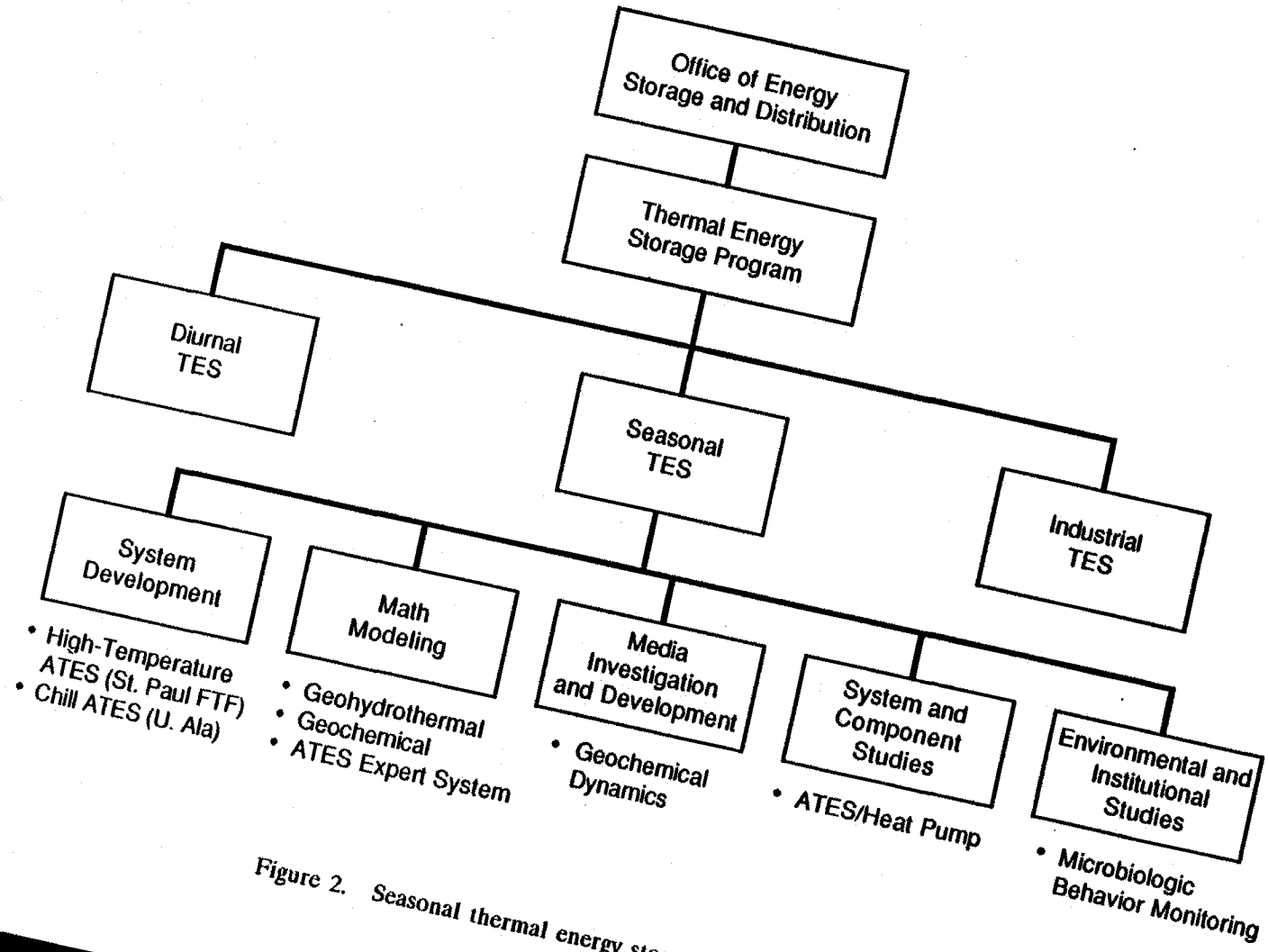


Figure 2. Seasonal thermal energy storage project organization.

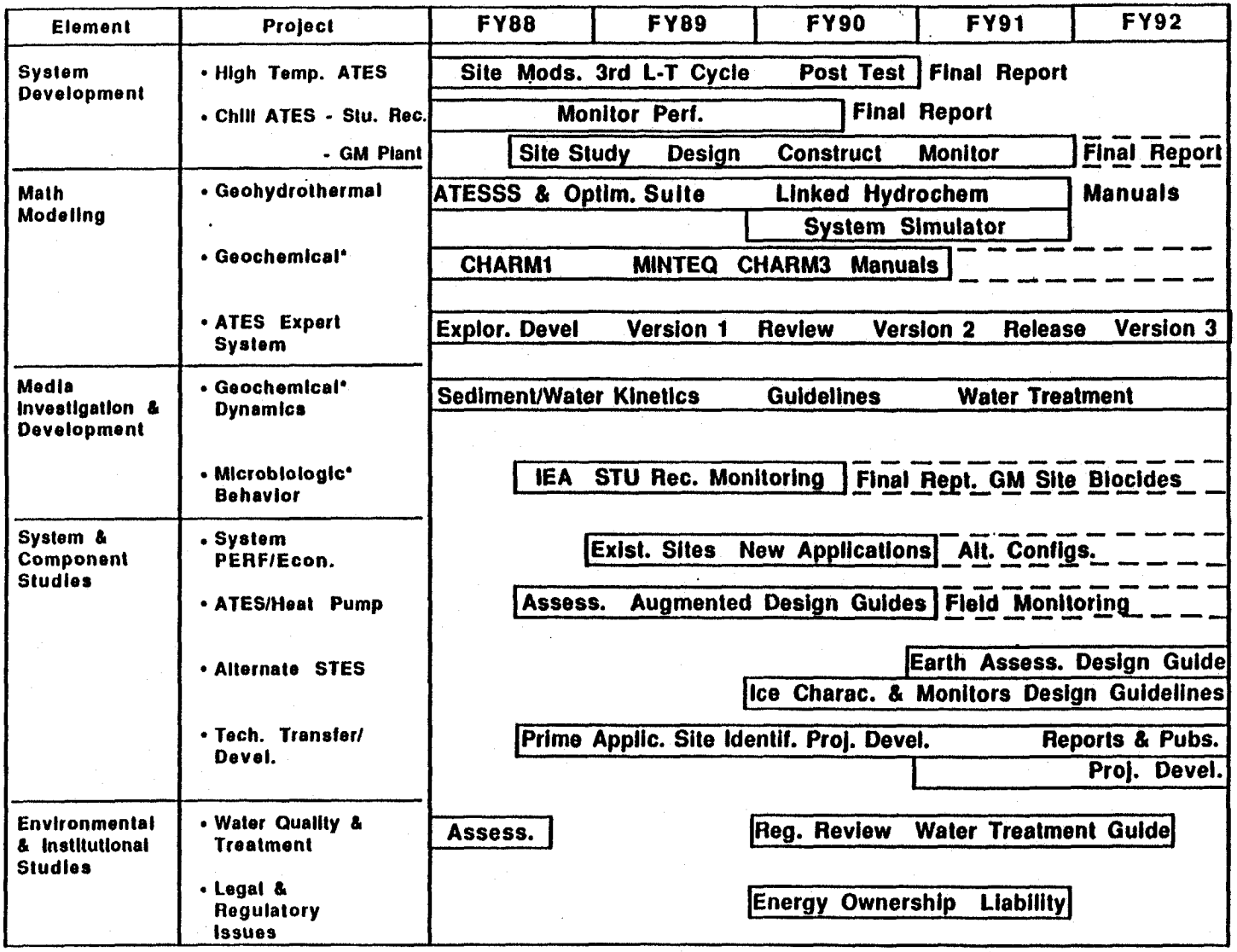


Figure 3. Seasonal thermal energy storage program from FY 1988 through FY 1993.

# CENTRAL SOLAR HEATING PLANTS WITH SEASONAL STORAGE

**Dwayne S. Breger and J. Edward Sunderland**
Department of Mechanical Engineering
University of Massachusetts

***Abstract***

*The University of Massachusetts has recently started a two year effort to identify and design a significant Central Solar Heating Plant with Seasonal Storage (CSHPSS) in Massachusetts. The work is closely associated with the U.S. participation in the International Energy Agency (IEA) Task on CSHPSS. The University is working closely with the Commonwealth of Massachusetts to assist in identifying State facilities as potential sites and to explore and secure State support which will be essential for project development after this design phase. Currently, the primary site is the University of Massachusetts, Amherst campus with particular interest in several large buildings which are funded for construction over the next 4-5 years. Seasonal thermal energy storage will utilize one of several geological formations.*

## Introduction

The use of solar energy to serve the space heating demands of buildings represents an important opportunity to reduce the use of non-renewable energy resources. However, the solar availability and space heating demand are out of phase over the annual cycle. In many geographical regions (particularly Northern latitudes), poor winter insolation makes a significant solar contribution to space heating demand particularly difficult. The concept of the Central Solar Heating Plant with Seasonal Storage (CSHPSS) is the unconstrained collection and storage of solar energy during the entire year to prepare a sufficient heat source to meet winter heating loads. CSHPSS are therefore designed to meet essentially the entire space heating and hot water load of a site.

The conceptual difference between the CSHPSS approach and the conventional solar (diurnal storage) systems is illustrated in Figure 1. A schematic configuration of a CSHPSS system is not different from diurnal storage solar systems. The difference lies in the relative and absolute size of the components and in the technologies employed to make the system cost-effective. The capacity of the seasonal storage sub-system must be large enough to absorb all or most of the solar collector summer output without overheating. Thus, the ratio of storage volume to collector area is much higher in a seasonal storage system. Seasonal storage systems must also be large in an absolute sense to be efficient and cost-effective. It is necessary to resort to large scale construction techniques, rather than manufacturing techniques, to achieve acceptable performance and economies.

Seasonal thermal energy storage can be accomplished in several ways. Heat can be stored in water in a tank constructed above or below ground, in an excavated rock cavern, or an earth pit. Heated water can be stored in aquifers through displacement of ambient aquifer water. Heat can also be stored directly in earth or rock of suitable characteristics with heat exchange consisting of a matrix of bore-holes through which hot water is circulated. For large systems, the storage volume may be uninsulated or partially insulated. An illustration of these seasonal storage techniques is shown in Figure 2.

Since 1979, a focus of work on seasonal solar thermal energy storage has been within the International Energy Agency (IEA), Solar Heating and Cooling Program, Task VII on CSHPSS [1,2]. To date over 30 projects internationally can be classified to some degree as CSHPSS. The current IEA effort is focused on the evaluation of some of the operating plants and in the design of advanced systems. The status of the technology is most advanced in Sweden [3] where the largest project (Lykebo) successfully serves the demand of 500 houses using high efficiency flat plate collectors and a 100,000 $m^3$ water-filled rock cavern. A new project is now planned which is about four times the size of Lykebo. The experience in Sweden and other countries has proven the technical feasibility of CSHPSS and the commercial development of future projects in Sweden is now very likely.

Several CSHPSS analysis and design activities in the U.S. have been performed [4,5]. A small project with seasonal solar thermal energy storage in a shallow earth layer was built in Massachusetts in 1983 [6]. A design for a small project for a school in Franklin, Massachusetts is currently in progress and will be compared with other system alternatives.

## Current Activities

### Project Description

The CSHPSS project at the University of Massachusetts, Amherst was started in September 1988. The project is scheduled for a duration of two years and is closely associated with the U.S. participation in the IEA Task. The purpose of the project is to initiate the development of a significant CSHPSS in Massachusetts and to develop the circumstances under which the project can be constructed. The objectives include both the technical analysis, evaluation, and design of the CSHPSS and the formation of State interest and commitment to support further project development and construction. Due to limitations in DOE budget and program scope, the State will need to assume the central role of project support for development to continue past this two year study.

The technical tasks contained in the project work plan are outlined in Table 1. Phase I will be completed in 9-12 months and will result in a site selection and preliminary CSHPSS feasibility design study. Phase II will concentrate on detailed design and analysis of system performance and cost for the selected site.

### Current Status

Site Identification. A primary site under consideration is the University of Massachusetts campus. The large campus is served by a steam distribution network fed by a central coal-fired boiler plant. Of particular

interest are the heat loads of the few large buildings which centrally exchange the steam source to hot water or forced hot air for building distribution, and the several planned large buildings funded for construction over the next four years. The geological conditions for thermal energy storage on the campus include a 100 foot clay deposit, an aquifer, and bedrock. The characteristics of the aquifer and bedrock are not well known at this time. The clay is soft and includes varied layers (1/16 to 1/4 inch thickness) of sand, silt, and clay. Heat exchange pipes may be readily pushed or driven through the 100 foot clay at low cost. The use of the clay for high temperature storage (up to 70-80 °C), so that the load can be met without a heat pump, is uncertain and will be investigated.

Two other sites near Amherst have been identified. These are a small private college campus and a planned commercial and research office development. The heating load of the college campus is attractive due to its low temperature demand (nominally 50 °C). The planned development is near a cogeneration wood-chips plant which currently operates only in winter to produce steam for greenhouse heating. Operation of the plant during summer could provide a heat source to charge the seasonal store.

Due to the necessary State participation in project development, other State facilities (in addition to the University) are of particular interest. Assistance is being provided by the Massachusetts Executive Office of Administration and Finance, Division of Capital Planning and Operations (DCPO), in identifying other suitable State facilities. A DCPO data base and audits of the energy characteristics of all State facilities are being used in conjunction with specific criteria for the CSHPSS project. The major criteria and useful guidelines are: 1) large load size (10,000 MWh), 2) low temperature demand (55/35 °C nominal supply/return), and 3) open land area available for the collector array. Possible other State sites include colleges, hospitals, and two planned prisons.

Site Evaluations. Evaluation of the sites identified is underway. The MINSUN program [7] is used for analysis of system performance over a range of sub-system options. Cost data are applied to these results to provide an economic optimization. MINSUN is used with one of three storage models as appropriate for the site: SST for stratified water storage in a pit or cavern, DST for duct (bore-hole) storage in earth or rock, and AST for aquifer storage.

Cost and technical data for the construction of the large water and duct thermal energy storage facilities are not well developed for U.S. conditions. Data based on Swedish experience is useful but may not be applicable to specific U.S. sites or construction industry. Investigations will be made into current cost and technical experience for the construction requirements of the sites under evaluation.

Development of State Support. The effort at the University of Massachusetts to initiate a CSHPSS project in Massachusetts is funded by the U.S. DOE. However, it is clearly the intention of DOE that the State government must accept the central role of support for the project to proceed after the current identification and design effort. The scope of this support and strategies for securing it are being explored in the current project phase.

A meeting with DCPO initiated this effort. Ideas for developing a network of State interest were suggested and additional meetings were recommended. The identification of a State (versus privately owned) facility is thought to have significant advantages in terms of attracting State participation.

## Conclusions

The activity at the University of Massachusetts represents an excellent opportunity to initiate the awareness and development of CSHPSS technology in the U.S. Through the on-going IEA efforts, the U.S. can build directly on the experiences of the participating countries and their operating systems. The Commonwealth of Massachusetts and the New England region exhibit the climate and economic conditions which make the CSHPSS solar approach attractive and past support and interest by the State is encouraging.

Sites for evaluation have been identified and others will be added using a data base of energy characteristics of all State facilities. Opportunities for a project at the University of Massachusetts campus are currently of primary interest though final evaluation results are not yet available.

## References

1. Bankston, C. A., Central Solar Heating Plants with Seasonal Storage - Evaluation of Concepts, IEA, Solar Heating and Cooling Program, Task VII, Report #T.7.2.B., November 1986.

2. Proceedings of the Workshop CSHPSS - Towards Better Cost-Effectiveness, (held at ISES World Congress, Hamburg, Germany, September 1987), edited by N. Fisch, IEA, Solar Heating and Cooling Program, Task VII, May 1988.

3. Dalenback, J-O., Large-Scale Swedish Solar Heating Technology - System Design and Rating, Swedish Council for Building Research, D6:1988, ISBN 91-540-4859-1, 1988.

4. Breger, D.S. and Michaels, A.I., A Seasonal Storage Solar Energy Heating System for the Charlestown, Boston Navy Yard National Historic Park - Phase II. Analysis with Heat Pump, Argonne National Laboratory, ANL-83-58, June 1983.

5. Breger, D.S. and Michaels, A.I., An Assessment of Solar Heating Systems with Seasonal Storage in New England - Systems Using Duct Storage in Rock and a Heat Pump, Argonne National Laboratory, ANL/EES-TM-279, January 1985.

6. Sunderland, J.E., et al., "Seasonal Storage of Solar Energy Using Insulated Earth", Proceedings, Congress of International Solar Energy Society, Montreal, Pergamon Press, June 1985.

7. Chant, V.G. and Hakansson, R., Central Solar Heating Plants with Seasonal Storage - The MINSUN Simulation and Optimization Program, Application and User's Guide, IEA, Solar Heating and Cooling Program, Task VII, September 1985.

Table 1. Project work plan.

Phase I: Site Identification and Evaluation

1. Site Identification
   State Facilities, Private Facilities
2. Site Data Collection
   Heat Load Characteristics, Site Layout, Geology
3. Industry Participation
   Technical Expertise, Cost Data
4. Site CSHPSS Evaluations
   Performance/Cost Analysis and Optimization
   Other Evaluation Criteria
5. Comparative Evaluation and Site Recommendation

Phase II: Detailed Design and Analysis of CSHPSS Project

1. Detailed Design of Sub-Systems
   Collector Array, Storage, Distribution
2. Geological Investigation of Storage Site
3. Detailed Analysis of System Performance and Cost
4. Recommendations for Project Development

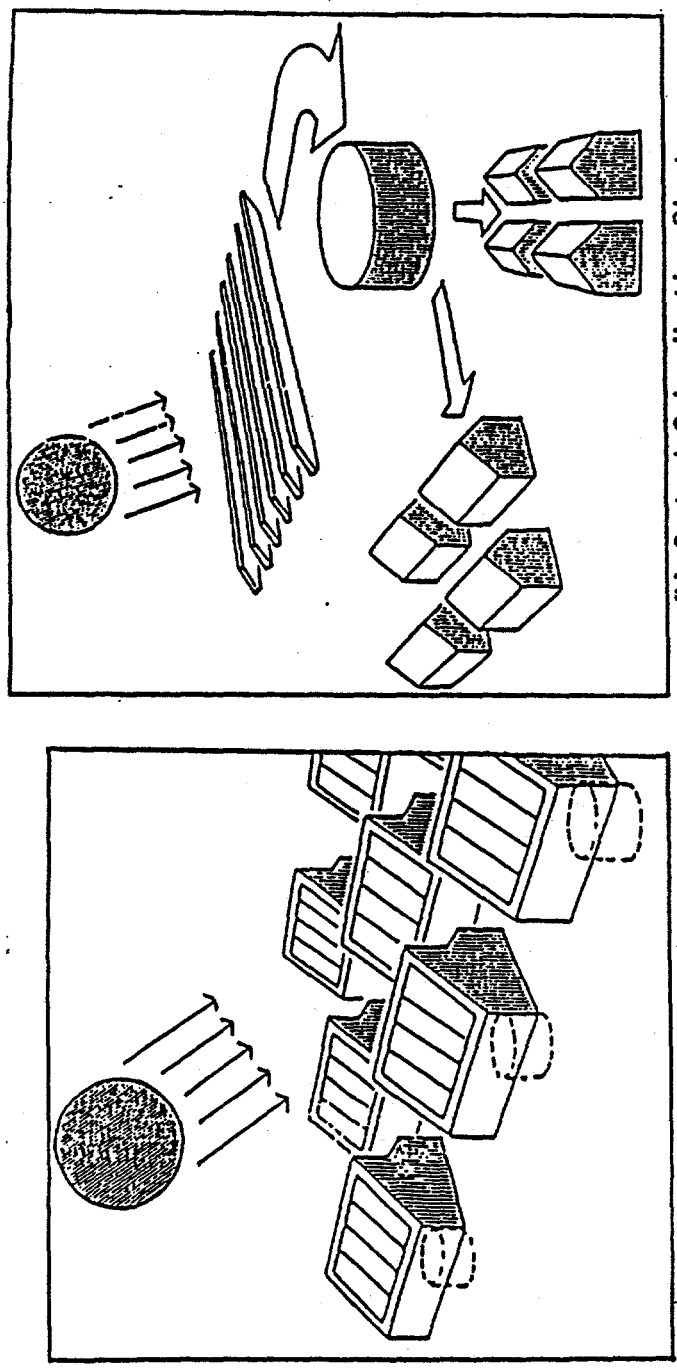


Figure 1. Conceptual comparison: CSHPSS *vs* distributed solar approach.

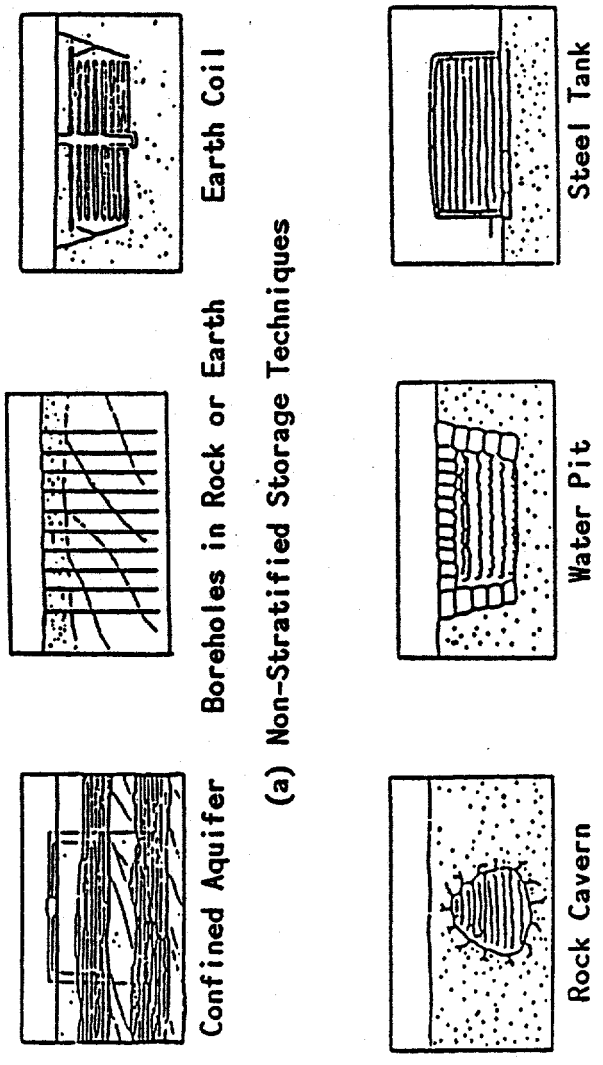


Figure 2. Options for large-scale seasonal thermal energy storage.

# ATES/HEAT PUMP SYSTEMS FOR COMMERCIAL OFFICE BUILDINGS

**D. R. Brown and G. E. Spanner**
Pacific Northwest Laboratory[a]
Richland, Washington 99352

***Abstract***

*An aquifer thermal energy storage (ATES) system can be coupled with ground water heat pumps to recover thermal energy that is wasted in conventional ground water heat pump systems. The cost, performance, and overall system economics of three ground water heat pump systems (two conventional systems and one ATES-augmented system) were evaluated for two commercial office building sizes in two cities. Aquifer simulation predicted that relatively warm and cool wells were created by alternating the supply and rejection of water from one well to the other when switching from heating to cooling modes. However, the insensitivity of conventional water source heat pump coefficient-of-performance to water source temperature resulted in a performance improvement of 3% or less compared to the conventional systems. Overall, the improvement in performance and resulting reduction in annual electrical costs was not enough to pay for the additional costs of the ATES system.*

## Introduction

Many potential applications and configurations of ATES technology exist. This paper reports on an assessment of an ATES system coupled with ground water or water source heat pumps for the heating and cooling of commercial office buildings. The work was conducted by the Pacific Northwest Laboratory (PNL) for the U.S. Department of Energy's Office of Energy Storage and Distribution.

Ground water heat pumps reject relatively cool water when in the heating mode and relatively warm water when in the cooling mode. An ATES system provides a means of recovering the relatively cool and warm water for reinjection into the aquifer. The result is a higher heating source temperature and a lower cooling reject temperature for the ground water heat pump, thus improving the heat pump's overall performance. Of course, the additional wells, piping, and pumps will increase the ATES-coupled system's capital and operating costs.

The objective of this study was to determine the benefit of incorporating an ATES system with ground water heat pumps for heating and cooling commercial office buildings. The benefit was determined by

---

[a] Operated for the U.S. Department of Energy by Battelle Memorial Institute under Contract No. DE-AC06-76RLO 1830.

comparing the levelized cost ($/MMBtu) of delivering heat and chill by the following three heat pump systems: 1) water/air heat pumps with a single supply well and rejection to sewer, 2) water/air heat pumps with nonreversing supply and rejection wells, and 3) water/air heat pumps with reversing (ATES configuration) supply and rejection wells. Each of the heat pump systems was evaluated for two different commercial building sizes and two different locations to examine the effect of load size, climate, and utility rate structure on the comparison.

## Site and System Description

Spokane, Washington and Rapid City, South Dakota were selected as the reference locations from a list of candidate sites across the U.S. The principal site screening criteria were a climate that would yield relatively balanced annual heating and cooling loads for the two building sizes being evaluated (54,000 and 180,000 $ft^2$) and electric rates that would generally allow heat pumps to be economically employed. The large internally-generated cooling loads for the two buildings require a cool climate to result in an overall balance between annual heating and cooling loads. Prospective locations were limited to those with electric rates that would make heat pumps competitive with fossil-fired systems. The applicable commercial electric rates include both demand and energy charges in the two cites. Demand charges were $4.50/kW-month in Rapid City and $2.00/kW-month in Spokane. Energy charges were $0.0305/kWh in Rapid City and $0.03692/kWh in Spokane (CSA Energy Consultants 1986).

In addition to the heat pumps, each of the ground water systems has a water piping system within the building and a supply well and pump. Reject water from the single well heat pump system is presumed to be sent to the sewer. Depending on local regulations, either dumping to sewer or rejection to the aquifer may be required. Rejection requires an additional well (but no additional pump) plus piping separating the supply and rejection wells. Operation as an ATES system requires an additional pump in the second well.

## Performance Assessment

A performance assessment was completed for each of the heat pump systems evaluated to determine the electrical consumption required to meet the building's heating and cooling loads. The performance assessment includes four distinct elements: heating and cooling loads, heat pump performance, aquifer modeling, and water supply system. The analytical approach and performance results for these four elements are summarized in the following sections.

### Heating and Cooling Loads

A building energy simulation model known as DOE-2 (version DOE-2.1C) was used to calculate heating and cooling loads for the two offices and two locations evaluated in this study (Lawrence Berkeley Laboratory 1985). Summary heating and cooling load results for the four combinations of office size and location modeled are shown in Table 1. The heating and cooling loads in Rapid City are slightly greater

Table 1. Heating and cooling load summary.

| City | Building Size, $ft^2$ | Annual Cooling Load, $10^6$ Btu | Annual Heating Load, $10^6$ Btu |
|---|---|---|---|
| Rapid City | 54,000 | 398.728 | 976.487 |
| Rapid City | 180,000 | 2342.012 | 1465.652 |
| Spokane | 54,000 | 377.312 | 877.146 |
| Spokane | 180,000 | 2189.736 | 1333.242 |

than in Spokane, because its climate is slightly more extreme. Both heating and cooling loads for the large buildings are greater than for the small buildings, but the relative size of the heating and cooling loads changes. Heating dominates the total annual load for the small buildings, while cooling dominates the total annual load for the large buildings. Thus, the site selection process succeeded in identifying locations that would result in relatively balanced heating and cooling loads for the two building sizes evaluated.

**Heat Pump Performance**

Heat pump performance data are combined with the simulated heating and cooling loads to estimate the annual electrical requirements. Heat pump performance was characterized as a function of source temperature and water flow rate per ton of heat pump capacity, with corrections for cyclic operation, in both heating and cooling modes.

Heat pump performance was based on data reported in a study completed at Oak Ridge National Laboratory (ORNL) (Mei 1984). The ORNL study measured the full-load coefficient-of-performance (COP) for water source heat pumps over a range of source temperatures at several different water flow rates per ton of heat pump capacity. In general, heat pump performance improves at higher source water flow rates; but pumping energy also increases. The optimum flow rate depends on the pumping head that must be overcome in the water supply system. A flow rate of 3 gpm/ton of heat pump capacity was chosen as the reference design assumption, and a flow rate of 1.5 gpm/ton was investigated as a sensitivity case.

The heat pump performance reported in Mei (1984) was for new equipment. The COP data were reduced by 15% to account for expected fouling from the ground water source. The resulting equations used for modeling full-load water source heat pump performance are shown below:

Source Flow Rate = 3 gpm/ton

$$\text{Heating Mode COP} = 2.550 + 0.0190\,[T(°F) - 45] \quad (1)$$
$$\text{Cooling Mode COP} = 3.245 - 0.0278\,[T(°F) - 45] \quad (2)$$

Source Flow Rate = 1.5 gpm/ton

$$\text{Heating Mode COP} = 2.489 + 0.0160\,[T(°F) - 45] \quad (3)$$
$$\text{Cooling Mode COP} = 3.014 - 0.0309\,[T(°F) - 45] \quad (4)$$

**Aquifer Modeling**

Simulation of the fluid and energy flows within the aquifer was conducted with the Aquifer Thermal Energy Storage System Simulator (ATESSS) model developed at PNL (Vail 1989). ATESSS was specifically developed to assist with the design and evaluation of ATES systems. The simulations were run with aquifer modeling parameters that were largely based on a general knowledge of aquifer formations rather than the specific conditions that exist in either Spokane or Rapid City. The natural ground water temperature in Spokane and Rapid City (about 50°F) was employed, however. Key aquifer modeling assumptions are summarized in Table 2.

Table 2. Aquifer modeling parameters

| | |
|---|---|
| Depth | 150 ft |
| Thickness | 30 ft |
| Porosity | 35% |
| Thermal conductivity | 2.10 W/mC |
| Ambient temperature | 50°F |

Aquifer conditions were simulated for a 3-year period. By the end of the first year, thermal conditioning of the aquifer was essentially complete. Simulation results for the third year changed by less than 1% from the second year. A summary of the average cool and warm well temperatures from the third year of operation is presented in Table 3 for each of the cases evaluated in this study.

Table 3. Summary aquifer modeling results.

| Case Description | Average Temperature From Cool Well, °F | Average Temperature From Warm Well, °F |
|---|---|---|
| Rapid City, 54,000 ft$^2$ building, 3 gpm/ton | 46.18 | 50.59 |
| Rapid City, 180,000 ft$^2$ building, 3 gpm/ton | 49.62 | 54.39 |
| Spokane, 54,000 ft$^2$ building, 3 gpm/ton | 46.17 | 50.65 |
| Spokane, 180,000 ft$^2$ building, 3 gpm/ton | 49.62 | 54.37 |
| Rapid City, 54,000 ft$^2$ building, 1.5 gpm/ton | 42.48 | 51.17 |
| Rapid City, 180,000 ft$^2$ building, 1.5 gpm/ton | 49.05 | 58.30 |

The values in Table 3 indicate that enhanced water source temperatures were achieved in all of the cases; i.e., the average temperatures from the cool wells were all below 50°F and the average temperatures from the warm wells were all above 50°F. The smaller buildings achieved greater enhancement of the cool well temperatures than the warm well temperatures. Much more cold water is injected into the cool well during the heating cycle than is withdrawn during the cooling cycle for the small buildings because the heating loads are greater than the cooling loads. Little temperature enhancement is seen in the warm wells of the smaller buildings where more water is withdrawn than injected on an annual basis. The larger buildings, with annual cooling loads greater than annual heating loads, have the exact opposite effect, resulting in a greater enhancement of the warm well temperatures than the cool well temperatures. Lowering the flow rate per ton of heat pump capacity from 3.0 gpm to 1.5 gpm approximately doubles the temperature enhancement seen for hot and cold wells in both building sizes.

Heat pump electrical loads are presented in Table 4 for ATES and non-ATES water source heat pump systems. Overall, the incorporation of ATES reduced the heat pump electrical load by 1.3 to 1.5% for systems with a water flow rate of 3.0 gpm/ton of heat pump capacity. Reducing the water flow rate to 1.5 gpm/ton increased electrical consumption for both ATES and non-ATES systems but increased the performance advantage of ATES systems over non-ATES systems to 2.6 to 2.8%. Although lowering the flow rate per ton of heat pump capacity from 3.0 gpm to 1.5 gpm approximately doubles the temperature enhancement seen for hot and cold wells, heat pump energy consumption increases by about 5% for the 1.5 gpm cases, because the lower flow rate results in an overall decrease (increase) in the average water temperature in the heat pump evaporator (condenser) while in the heating (cooling) mode.

Table 4. Annual heat pump electrical loads.

| Case Description | ATES Heat Pump Energy, kWh | Non-ATES Heat Pump Energy, kWh |
|---|---|---|
| Rapid City, 54,000 ft$^2$ building, 3 gpm/ton | 183,796 | 186,217 |
| Rapid City, 180,000 ft$^2$ building, 3 gpm/ton | 575,404 | 584,166 |
| Spokane, 54,000 ft$^2$ building, 3 gpm/ton | 166,049 | 168,236 |
| Spokane, 180,000 ft$^2$ building, 3 gpm/ton | 523,058 | 531,023 |
| Rapid City, 54,000 ft$^2$ building, 1.5 gpm/ton | 189,010 | 194,411 |
| Rapid City, 180,000 ft$^2$ building, 1.5 gpm/ton | 604,028 | 620,384 |

**Water Supply System**

The water supply system is the key feature distinguishing each of the heat pump systems evaluated in this study. Supply system components include the supply and return piping within the building, well(s), pump(s), and well separation piping. Water supply system equipment requirements were developed from a preliminary design analysis of each component. Building piping lengths were estimated from piping layouts prepared for a typical floor. Well separation piping lengths were calculated from engineering rules of thumb relating adequate spacing to the height of the aquifer and the total water injected. Pipe diameters were established based on a design water velocity of 7 ft/second. Well depth was assumed to be 150 ft, with a 100-ft thick aquifer. The maximum well flow rates were established based on an assumed supply rate of either 3.0 or 1.5 gpm/ton of heating or cooling capacity and the peak heating or cooling load determined from the DOE-2 modeling. Pump sizes and pumping energy were based on the supply flow requirement and the pressure drop calculated for the systems. The resulting pumping energy requirements are summarized in Table 5.

Table 5. Pumping energy requirements.

| Case Description | Annual Pumping Energy, kWh | | |
|---|---|---|---|
| | Cooling | Heating | Total |
| Rapid City, 54,000 ft$^2$ building, 3 gpm/ton | 4,414 | 7,889 | 12,303 |
| Rapid City, 54,000 ft$^2$ building, 1.5 gpm/ton | 1,726 | 3,086 | 4,812 |
| Rapid City, 180,000 ft$^2$ building, 3 gpm/ton | 29,474 | 19,049 | 48,523 |
| Rapid City, 180,000 ft$^2$ building, 1.5 gpm/ton | 13,609 | 8,795 | 22,404 |
| Spokane, 54,000 ft$^2$ building, 3 gpm/ton | 3,689 | 7,378 | 11,067 |
| Spokane, 180,000 ft$^2$ building, 3 gpm/ton | 27,442 | 32,457 | 59,899 |

In general, pumping energy is proportional to building load and the cooling, heating, and total pumping energies calculated for each of the cases correlates with their respective thermal loads. An exception is the heating-related pumping energy for the 180,000 ft$^2$ Spokane building. Pump performance suffers in the heating mode for this case because the pump operates at a low efficiency at the design heating mode flow

rate. Pumping energy was reduced by 55 to 60% for the two Rapid City cases, when the water flow rate to the heat pumps was reduced from 3.0 to 1.5 gpm/ton of thermal load. The pump sizes were reduced in this sensitivity analysis, but head losses were based on the same building and well separation piping diameters.

## Economic Assessment

The levelized cost of heating and cooling ($/MMBtu) was calculated for each of the 16 heat pump systems evaluated to determine the relative economic attractiveness of the alternative design and operating conditions. Each of the heat pump systems represents a unique combination of water supply system design, building size, location, and assumed water flow rate per ton of heat pump capacity.

Estimates were prepared for the initial capital, interim capital, maintenance, and electricity costs associated with each of the 16 heat pump systems evaluated. Initial capital items were heat pumps, building supply and return water system, wells, pumps, and well separation piping. The lone interim capital item was the pumps, which were replaced after 10 years. The balance of the equipment had a design life of 20 years. Maintenance was included for each of the initial capital and interim capital items. The cost estimates were developed by applying unit cost data from published reports, cost estimating handbooks, and PNL's own cost data files to the design requirements developed for the performance assessment.

Levelized, life-cycle cost estimates were calculated using the methodology and economic assumptions specified in Brown et al. (1987) for a commercial business. Estimates of initial capital, interim capital, maintenance, and electricity costs and the economic assumptions were input to the economic methodology to produce an estimate of the life-cycle cost of heating and cooling, expressed in $/MMBtu. The resultant total life-cycle costs are shown in Table 6.

Overall, relatively little variation in the life-cycle cost was seen among all of the cases evaluated. The most expensive system was only 20% more costly than the least expensive system. When comparisons are limited to the same combination of building size and city, the difference between most expensive and least expensive is even less. The similarity in life-cycle cost can be partly attributed to heat pump and building piping capital-related costs, which remain constant for each city/building size combination and account for 50 to 60% of the total life-cycle cost. The balance of the system costs vary by more than 40% when these fixed costs are removed from the total life-cycle cost.

The life-cycle cost results indicate that the cost for each of the ATES heat pump systems was higher than the cost for either the single-well or two-well non-ATES heat pump systems. In short, the performance improvement gained by the ATES configuration was not enough to pay for the incremental costs. The ATES system requires an additional pump compared to the two-well system and an additional pump, well, and well separation piping compared to the single-well system. The performance is the same for both of the non-ATES systems; the result is lower life-cycle costs for the single-well systems.

Table 6. Life-cycle cost results.

| City | Building Size, $ft^2$ | Flow/Ton, gpm | # Wells | ATES | 1987 $/MMBtu |
|---|---|---|---|---|---|
| Rapid City | 54,000 | 3.0 | 1 | no | 22.56 |
| Rapid City | 180,000 | 3.0 | 1 | no | 24.28 |
| Spokane | 54,000 | 3.0 | 1 | no | 21.82 |
| Spokane | 180,000 | 3.0 | 1 | no | 23.92 |
| Rapid City | 54,000 | 3.0 | 2 | no | 24.27 |
| Rapid City | 180,000 | 3.0 | 2 | no | 25.59 |
| Spokane | 54,000 | 3.0 | 2 | no | 23.38 |
| Spokane | 180,000 | 3.0 | 2 | no | 25.30 |
| Rapid City | 54,000 | 3.0 | 2 | yes | 25.97 |
| Rapid City | 180,000 | 3.0 | 2 | yes | 26.37 |
| Spokane | 54,000 | 3.0 | 2 | yes | 25.10 |
| Spokane | 180,000 | 3.0 | 2 | yes | 26.19 |
| Rapid City | 54,000 | 1.5 | 2 | yes | 24.19 |
| Rapid City | 54,000 | 1.5 | 2 | no | 23.01 |
| Rapid City | 180,000 | 1.5 | 2 | yes | 25.23 |
| Rapid City | 180,000 | 1.5 | 2 | no | 24.73 |

Site-specific factors had a small effect on life-cycle costs. The Rapid City and Spokane climates were similar enough to produce nearly the same annual heating and cooling loads for the same building sizes. The lower life-cycle costs seen for Spokane can be attributed to its slightly lower electric rates. Building size was not a strong differentiating factor because the distributed nature of the majority of the equipment does not allow for potential economies of scale for cost or performance. In fact, the life-cycle cost was always lower for the smaller, building when all other design factors were the same. This advantage can be attributed to the better performance of the heat pumps in the smaller buildings, where each zone tends to operate at a higher annual capacity factor than in the larger buildings, i.e., cycling losses are lower. The advantage for the smaller buildings declines as the complexity of the water supply system increases; because of large economies of scale in wells, pumps, and piping. Note that the cost difference between the two building sizes is the least for the ATES systems.

Operation at a water flow rate of 1.5 gpm/ton of heat pump capacity lowered the life-cycle cost of each system operated in this manner, relative to operation at 3 gpm/ton. Lowering the flow rate to the water source heat pump decreases its efficiency by effectively increasing (decreasing) the average source temperature available to the heat pump when in the cooling (heating) mode, but this is more than offset

by reduced capital and operating expenses associated with pumping. Reducing the flow rate results in a greater cost reduction for the ATES systems, because the negative impact of increasing the source temperature range experienced by the heat pump is mitigated by a greater enhancement of the natural aquifer temperature.

## Conclusions

Analysis of ATES/ground water heat pump systems indicated that the natural aquifer temperature would be enhanced by rejecting the waste heat from the heat pump to one well and rejecting the waste chill from the heat pump to another well. Simulation of the ATES system predicted that hot and cold well temperatures would stabilize within the first 3 years of operation, even with unbalanced annual heating and cooling loads. The magnitude of the temperature enhancement varied from less than 0.5°F to nearly 8°F depending on the relative size of the annual cooling and heating loads and the source water flow rate per ton of heat pump capacity. Unbalanced annual heating and cooling loads resulted in greater temperature enhancement for the well supplying water to the smaller of the two loads and less temperature enhancement for the well supplying water to the larger of the two loads. Lowering the source water flow rate per ton of heat pump capacity increased the temperature enhancement of both wells.

Changing the source water flow rate per ton of heat pump capacity has several effects on the cost and performance of the heat pump system. Heat pump performance is affected in two counteracting ways. For example, lowering the flow rate per ton of heat pump capacity reduces the COP for a given source temperature, but operation of the ATES system counteracts this effect by enhancing the source temperature. The results of this study indicated that these two effects combined to reduce heat pump performance. However, lowering the flow rate per ton of heat pump capacity reduces capital and operating expenses associated with the water supply system. The net effect seen in this study was an overall benefit of operating at the lower flow rate per ton of heat pump capacity.

Although the natural temperature of the aquifer was enhanced by several degrees, negligible performance improvement was obtained due to the insensitivity of conventional ground water heat pump COPs to the source water temperature. Incorporation of ATES improved annual heat pump performance by 1.3 to 1.5% relative to the non-ATES systems when operating with a source water flow rate of 3 gpm/ton of heat pump capacity. Reducing the source water flow rate to 1.5 gpm/ton of heat pump capacity resulted in a 2.6 to 2.8% improvement in annual heat pump performance for the ATES system relative to the non-ATES system operating under the same flow conditions.

The ATES system requires an additional pump compared to the two-well non-ATES system and an additional well and pump compared to the single-well non-ATES system. Additional initial costs and annual maintenance costs are associated with both of these components. Overall, the improvement in performance and resulting reduction in annual electrical bills was not enough to pay for the additional ATES system costs.

The ATES system evaluated in this study represents only one potential application of ATES technology for building heating and cooling. No general conclusion should be drawn about the potential feasibility of other ATES system configurations. Alternative system configurations and/or alternative operating conditions should be identified and investigated.

## References

1. Brown, D. R., J. A. Dirks, M. K. Drost, G. E. Spanner, and T. A. Williams. 1987. An Assessment Methodology for Thermal Energy Storage Evaluations. PNL-6372, Pacific Northwest Laboratory, Richland, Washington.

2. CSA Energy Consultants. 1986. Electric Rate Book. CSA Energy Consultants, Arlington, Virginia.

3. Lawrence Berkeley Laboratory. 1985. Overview of the DOE-2 Building Energy Analysis Program. LBL-19735, Lawrence Berkeley Laboratory, Berkeley, California.

4. Mei, V. C. 1984. Laboratory Test of a Residential Low-Temperature Water Source Heat Pump. ORNL/CON-100, Oak Ridge National Laboratory, Oak Ridge, Tennessee.

5. Vail, L. W. 1989. "ATES/Heat Pump Simulations Performed with ATESSS Code." PNL-SA-16541, Pacific Northwest Laboratory, Richland, Washington.

# TARGETS FOR EARLY COMMERCIALIZATION OF AQUIFER THERMAL ENERGY STORAGE TECHNOLOGY

**M. P. Hattrup and R. O. Weijo**
Pacific Northwest Laboratory[a]
Richland, Washington 99352

## *Abstract*

*This study generated and then screened a list of potential entry market applications for aquifer thermal energy storage (ATES). Several screening criteria were used to identify promising ATES applications. An in-depth analysis was conducted of the four most promising applications.*

*The application that best met the criteria for early ATES commercialization is the cooling of large industrial structures that are currently not being air conditioned. Storage of certain types of fruits and vegetables also appears to be an attractive application for ATES. Shopping malls do not represent a good initial entry market application. Heating, ventilation, and air conditioning (HVAC) systems in shopping malls must be very reliable and extremely sensitive to small changes in temperature.*

## Introduction

Since 1979, the Pacific Northwest Laboratory (PNL) has managed the Seasonal Thermal Energy Storage Program for the U.S. Department of Energy. A primary goal of the program is to develop the aquifer thermal storage concept into a viable technology for deployment to the private sector.

In support of the Seasonal Thermal Energy Storage Program, a study was conducted to guide research and development leading to eventual commercialization of ATES by the private sector. The private sector is typically very risk-averse and will not adopt a new technology unless the benefits associated with a technology clearly outweigh its costs. One strategy to help foster the adoption of a new technology is to identify promising market applications. The applications may not be in the most lucrative markets in the long term nor provide significant energy savings initially. However, initial applications of a technology are often intended to demonstrate the technology's potential marketability. This successful demonstration then becomes the platform or springboard into other profitable market applications.

[a] Operated for the U.S. Department of Energy by Battelle Memorial Institute under Contract No. DE-AC06-76RLO 1830.

This study generated and screened a list of potential entry market applications for ATES. The initial goal is the eventual identification of up to four commercial sites interested in ATES and willing to share the cost of a detailed technical study of its potential application. A further goal is to identify a site on which to demonstrate a commercial application of this technology.

## Identification and Screening of ATES Applications

This section discusses the methodology employed to generate and screen applications of ATES. This includes the development of an initial list of potential ATES applications, development of initial screening criteria, identification of secondary screening criteria, and finally, contacting industry representatives to help evaluate each promising application.

The initial list of potential ATES applications was developed from literature reviews, contacts with experts in the field, and two brainstorming sessions. The brainstorming sessions involved PNL research staff of various technical backgrounds and knowledge levels about ATES. An initial list of 58 potential ATES applications was generated.

Seven criteria were developed to winnow the list of 58 ATES applications to a more manageable number. The initial screening phase allowed for subjectivity in evaluating the applications. If a purely objective measure were used, a more detailed analysis of each application would be required. Such a detailed analysis was beyond the scope of this study. The seven criteria used to subjectively evaluate the ATES applications were:

- Is there a mismatch between the availability and usage of energy?
- Does the application represent a large market?
- Is the application able to utilize proven technology?
- Is the location of the application usually remote (i.e., will the site have enough surface area property rights to cover the region of the aquifer)?
- Is the application located in a growing or stable market rather than a declining market?
- Is the investment capital requirement going to be relatively small and easily accessible?
- Will the developer be dealing with a small number of decision makers?

An application was considered a viable entry market candidate if it met all seven of the initial screening criteria. Although some of the applications dropped from consideration may eventually prove to be viable, those that survived the screening process are thought to represent the best initial applications of ATES. This does not mean that excellent candidates do not exist in applications discarded as part of the screening process. Rather, it means that an unusually favorable combination of site factors must be present to encourage their pursuit.

The 26 ideas still under consideration following the first screening appeared to have potential as possible entry markets for the ATES technology. However, contacting representatives in 26 industries was beyond the scope of this study. Thus, a secondary screening procedure was developed.

In the secondary screening procedure, each remaining application was segregated by market sector and by probable ATES system configuration. An assessment was then conducted to determine which of the market sectors and system configurations had the fewest and least significant barriers to adoption.

The application that appeared to face the fewest barriers to adoption consisted of using ATES chill storage to space condition a single building in a remote location. It appears that such an application faces fewer legal and regulatory barriers and is less likely to experience technical problems than would a heat ATES system, a complex process cooling application, or a concept including an extensive distribution system. The idea that free winter chill is available from the environment may be attractive to potential users. Those applications that use the single-building space conditioning configuration (and may also be a future candidate for a heat ATES application) were particularly emphasized. Successful application of chill storage to these facilities would ultimately benefit the acceptance of ATES heat storage.

The candidates that best met the secondary screening criteria included 1) fresh produce storage industry, 2) large manufacturing plants (i.e., auto assembly plants), 3) breweries, and 4) shopping centers. With the selection of these four applications, the in-depth analysis of each began.

## The In-Depth Analysis of ATES Market Potential of Four Promising Applications

The in-depth analysis of each of the four remaining applications determined if an idea actually represented a possible entry market for ATES. This phase of the analysis involved contacting knowledgeable professionals in relevant trade associations, institutions, and industries. The following sections discuss the results of the in-depth analysis of each of the promising ideas.

### Cool Storage Warehouses

Several sources were contacted to obtain information on the viability of using ATES in warehouses. This search identified information on storage temperature requirements for various foods. This information was found in The Packer (Leahy 1988), which was used to identify produce items with temperature requirements within the range of ATES technology. Table 1 includes a list of produce items identified in the review. The best applications of ATES require temperatures of about 45°F and above.

Table 1. Fruits and Vegetables with Minimum Storage Temperature Requirements of 45°F or Higher

| | | |
|---|---|---|
| Avocados | Grapefruit | Pineapples |
| Bananas | Lemons | Potatoes |
| Beans | Limes | Pumpkins |
| Cantaloupe | Mangoes | Squash |
| Cucumbers | Melons | Sweet Potatoes |
| Dates and raisins | Okra | Tangerines |
| Eggplant | Oranges | Tomatoes |
| | Peppers | |

Several produce items (with temperature requirements of 45°F or higher) and the meat packing industry received specific attention. Selection was based to some extent on the size of the annual shipments given in Leahy, and the length of time the items could be held in storage. Produce selected for further study include potatoes, tomatoes, lemons, and grapefruit. The meat packing industry was chosen in an effort to diversify, with attention to warehouse size, temperature requirements, period of storage, and the type of site under consideration.

**Potatoes.** According to Leahy (1988), the ideal storage temperature for potatoes is between 38°F and 45°F, which is slightly below the ideal temperature range of ATES. The potato was selected for consideration because the volume of potatoes being shipped is much greater than for any other produce item. The structures used to store potatoes ranged in capacity from 2000 to 8000 tons. A building with an 8000-ton capacity might be 60 x 300 x 20 to 22 ft, generally 50 $ft^3$/ton of potatoes. In Washington State, there are approximately 200 individual storage facilities; most are in the 5000-ton range. One popular design uses a common air plenum running between two quonset huts. This design usually has 3000-ton capacity on each side.

At harvest time, potatoes come out of the ground at 65+°F. It is important to cool them to 45°F to 50°F as quickly as possible. This enhances storage life considerably. Potatoes can be stored as long as 18 months; however, this is not typical. It was estimated that 20% to 25% of a typical year's Washington crop was still in storage after April. The harvest typically starts around the middle of September and is over by early November; thus, 20% to 25% of the crop is in storage for more than 7 or 8 months. The crop in Washington has averaged about 64,000 [1,000 cwt][2] for 1986, 1987, and 1988. It is apparent that a significant portion of the crop is stored for several months. Most of the potatoes from Washington are used for processed products, i.e., frozen french fries.

The Idaho Potato Commission and the Idaho Crop Reporting Service were also contacted for information. The Commission said about 23% of the Idaho crop is sold as fresh pack, while 60% goes to

[2]cwt = 1 hundredweight

processing. The Idaho Crop Reporting Service indicated that Idaho's crop averaged nearly 96,500 (1000 cwt) for 1986, 1987, and 1988 [U.S. Department of Agriculture (USDA) 1988]. The total potato production figure for the United States, for all four seasons, totals 352 million cwt.

**Tomatoes.** Tomatoes require temperatures in the 60° to 70°F range for ripening. This is done in a degreening room. Once a tomato has attained its color (ripens), it can be stored at temperatures as low as 52°F. Most packers typically will store tomatoes at or slightly above 55°F. Tomatoes are usually not stored for more than 1 week, including the time spent in the degreening process. The rooms used to degreen tomatoes often double as storage rooms.

In Florida, there are about 5000 degreening rooms, most with a two-car capacity (about four semi-truck loads). There are about 75 packing houses in Florida, but about 30 houses do 90% of the business. In the northern parts of Florida, tomatoes are being stored in large single-room warehouses, formerly used as tobacco warehouses. These facilities are typically cooled with patchwork/retrofit systems. An ATES system may be appropriate for such a facility, because performance expectations may be lower than for a newly constructed warehouse. California is second to Florida in tomato production, but ships most of its crop from June through November. Thus, packers in California face warmer temperatures than those in Florida. Because Florida is a fall/winter harvester, California may be a better location for an ATES application.

In general, the warm temperatures of Florida and southern California may make it difficult to obtain sufficient winter chill to cool the warehousing facilities to the desired temperature, or to provide adequate aquifer chill charging time.

**Lemons.** Lemons were selected for the study because they can be stored from 1 to 5 months, and the crop averages about 45 to 50 thousand carloads[3]. Over 90% of this crop comes from California and Arizona, according to the Lemon Administration Committee. Storage facilities vary through the industry; between 40 and 50 packing operations specialize in lemons only. In southern California, lemons are handled 12 months out of the year. Storage is an integral part of the business (lemons are typically stored for 90 to 120 days).

Some degreening is done at temperatures from 60°F to 70°F with ethylene gas added to the room. Usually, lemons are picked at different stages of ripeness, based on the intended use. For example, ripe or yellow fruit is picked for quick packing, whereas green fruit is picked and put into storage where the natural ethylene gas is vented to slow down the ripening process. The fruit in storage is to be packed at a later date in an effort to provide a supply of lemons over a longer period of time. Degreening is done in response to an unexpected demand for the fruit.

One large processor contacted in California has several separate packing facilities that occupy between 5 and 9 acres each. Because of concern with rising energy costs, especially the summer peak electric rates, this processor has experimented with modifying system operation; he has turned off the system during peak

---

[3]One carload is equivalent to 1000 38-lb cartons.

period rates. This processor was interested in the possibility of a more in-depth analysis of the feasibility of ATES for this particular application. Based on the combination of temperature requirements, ownership of a relatively large surface area, and concern over energy costs, the lemon industry in general seems to be a good candidate for more detailed analysis.

**Grapefruit.** Grapefruit was selected because of the volume of fruit that is shipped. The Packer (Leahy 1988) showed that grapefruit from California, Arizona, and Texas can be stored as long as 3 months.

The Florida Citrus Packers Association and other industry sources indicated that the vast majority of grapefruit from both Florida and Texas are not stored for any length of time. Because Florida produces most of the U.S. grapefruit crop, storage of this product does not appear to be a good entry market for ATES when compared to the market for lemons. In the future, cool storage capacities may expand among the grapefruit packers and become a viable application for ATES.

**Meat Packing/Processing Industry**

In an attempt to determine whether or not the meat packing/processing industry could utilize a temperature of 45°F or higher, several contacts were made. The USDA has been attempting to persuade the meat packing industry to use outside air (during winter) to maintain coolers. However, the industry seems unwilling to change its practice of using chillers. ATES would probably meet similar resistance.

The USDA inspectors specify maximum temperatures of about 50°F in processing plants and 40°F or less for stored products. Based on these findings, ATES does not have a direct application for cooling stored meat. However, the industry uses water sprayed on the carcasses for pre-cooling to take the body heat out of the carcass. The carcasses are sprayed to drop the temperature down from approximately 105°F to about 34°F.

Based on industry contacts, storage facilities in the meat packing industry are not a good match for ATES. However, there appears to be at least a possibility that ATES could be used in the industry's pre-cooling process. ATES could be used to reduce the temperature of the source water coming out of the well, reducing the amount of latent heat the chillers have to remove from the water. The chillers would use less energy in reducing the water temperature to 33°F from 45°F than from 65°F. Based on the findings, ATES may have an application in this cooling process; the meat packing industry should receive a more detailed analysis.

**Shopping Centers**

In the effort to determine whether shopping centers represented a viable entry market for ATES, several information sources were contacted. The International Council of Shopping Centers provided information on the heating, ventilation and air conditioning (HVAC) operating and maintenance costs for shopping centers, and information on some new technologies. A few underlying themes became apparent in the four articles they provided (Chain Store Age Executive 1987; Nichol 1986, 1987, and undated): 1) retailers are very concerned about maintaining the comfort of the customer; and 2) an HVAC system must be very dependable and not require repeated maintenance, which could result in customers' discomfort.

Shopping centers may be an appropriate market in the future. However, demonstrations of ATES should first show that it is a dependable technology that does not require much maintenance. Currently, ATES does not have an established record that would convince a developer or contractor of a new shopping center that it is a proven technology. Those involved in the shopping center industry may be more concerned with temperature variation and system failure than those involved in the cool storage/warehouse industry. Because of this, the warehousing industry may be a more appropriate entry market, and large manufacturing plants with no air conditioning are definitely more appropriate.

**Auto Manufacturing Plants**

Plant walkouts during the summer of 1988 provided the incentive for the in-depth analysis conducted on auto manufacturing plants. Two articles describing plant walkouts that appeared in the St. Louis Post-Dispatch on June 22 and 23 highlight this problem. These articles suggest that a potential ATES application for space conditioning in auto manufacturing plants exists. The articles contain the following comments: "The plant, like most its size, has no air conditioning" and "It's hot in there, and there's no fresh air coming through to give us relief." A manager of public relations-manufacturing for Chrysler said he didn't know of any assembly plant that is air conditioned, but the plants are ventilated and the workers are given ice. Comments such as these suggest that the potential for space conditioning may be large.

**Brewery Storage Facilities**

Several industry professionals were contacted in the in-depth analysis of brewery storage facilities. They suggested that use of ATES in brewery storage facilities is unlikely. The brewing industry typically does not cool their packaged products in the warehouse. However, a different application for ATES in the brewing industry exists. The following is what was learned in this analysis.

A brewery in Georgia had commissioned several studies to identify an economical cooling system for the production facility itself. Temperatures inside this facility during the summer are very uncomfortable. Management would like to drop the indoor temperature between 5° and 15°F during those months. However, every solution they have explored has been too expensive. They have been primarily concerned with a high concentration of workers in one particular area of the facility. They felt it might be possible to set up a demonstration on this high population area only. This organization provided the most positive reaction to the concept to date.

## Summary and Recommendations

This in-depth analyses identified several possible entry market applications for aquifer thermal energy storage, and presented important criteria to consider when selecting an entry market application that had gone unrecognized. These include required system reliability, application sensitivity to temperature variation, and the required temperature range. The best entry market for ATES would be one where reliability is not important, wide temperature variations are acceptable, and relatively high temperatures are allowable.

The application that best meets these criteria is the cooling of a large industrial structure that currently has no air conditioning system. Two of the potential applications, auto assembly plants and a brewery, fit

the requirements. Two articles appearing in the St. Louis Post-Dispatch in June 1988 stated that temperatures in the paint shop of an auto assembly plant can reach 110°F. Temperatures at the brewery reach into the 90s, which prompted management to try to identify an economical cooling system to cool plant workers. In both instances, no cooling is currently offered to workers; and any level of cooling will improve their current situation. Thus, cooling of large industrial plants meets the above listed criteria.

Storage of a variety of fruits and vegetables may prove to be equally attractive applications for ATES. For example, potatoes are stored between 40°F to 45°F. Lemons are typically stored between 60°F and 70°F. Thus, an opportunity may exist to use ATES in storage facilities for fruits or vegetables that require temperatures within its range.

Evaluation of shopping malls against the above criteria shows that malls are not a good entry market application of ATES. An article supplied by the International Council of Shopping Centers indicated that, keeping the customer happy in a not-too-hot, not-too cold environment is very important. The article stated, "A manager can tell, because you can see the fluctuation in business; and you can see the customers walk in and walk right out when the temperature is off." HVAC systems in this environment must be very reliable and extremely sensitive to small changes in temperature. An ATES system would be considered a very risky technology to adopt in such an environment. Though it has long-term potential, this is not a good entry market for ATES.

## Future Directions

With the in-depth analysis of the four ideas complete, two avenues were identified on how this research could proceed. The first avenue, a broadening effort, would require further application exploration to identify additional entry market applications for ATES. The second avenue involved selecting the best existing applications for further in-depth (i.e., plant-specific) analysis.

The second avenue requires additional in-depth analysis on a plant-specific basis. This analysis will require a crude technical assessment of an application of ATES at an actual site within one of the targeted industries. This assessment would attempt to determine if ATES technology could be installed cost effectively and used in an actual plant. It would locate plants considered typical of the industry in geographic regions previously identified as appropriate for ATES.

## References


1. Barksdale, C. June 23, 1988. "Chrysler Worker Dies; Hundreds Leave Auto Plants, Protesting Heat." St. Louis Post-Dispatch, St. Louis, Missouri.

2. Chain Store Age Executive. July 1987. "Pre-Cooling: Cutting Down On HVAC Costs -- Test At Millers Outpost Lowers Temperatures As Well As Energy Bills." Lebhar-Friedman, Inc., New York, New York.

3. Leahy, L., ed. 1988. "1988 Produce Availability and Merchandising Guide." The Packer. Vance Publishing Corporation, Shawnee Mission, Kansas.

4. Nichol, F. March 1986. "HVAC Operations Use Computers to Solve Problems Of Old and New." Shopping Center World. Communication Channels Inc., Atlanta, Georgia.

5. Nichol, F. August 1987. "Today's HVAC Is Flexible, Efficient -- Making Replacement Easier Is One Of The Major Thrusts Behind Improved HVAC Products." Shopping Center World. Communication Channels Inc., Atlanta, Georgia.

6. Nichol, F. Undated. "HVAC Technology Proves Energy-Wise -- Recent Technological Advances In HVAC Systems Make The Products More Efficient And Cost Effective." Shopping Center World. Communication Channels Inc. Atlanta, Georgia.

7. St. Louis Post-Dispatch. June 22, 1988. "Workers Cite Heat Walk Out At Chrysler." St. Louis, Missouri.

8. United States Department of Agriculture. 1988. Idaho Potatoes, Production -1986 and 1987. Idaho Crop and Livestock Reporting Service, Agricultural Statistics Service, Boise, Idaho.

# MICROBIOLOGICAL FEATURES OF AQUIFER THERMAL ENERGY STORAGE SYSTEMS

**R. J. Hicks**
Pacific Northwest Laboratory[a]
Richland, Washington 99352

**T. E. Thompson, C. E. Brett, F. S. Allison, J. A. Neville, C. Shea, and A. L. Winters**
University of Alabama
Tuscaloosa, Alabama

## *Abstract*

*A study was initiated to determine the environmental effects of aquifer thermal energy storage (ATES) technology pertaining to microbial communities indigenous to ATES aquifers and the propagation, movement, and release of pathogenic microorganisms within ATES systems. Six water samples from various locations within a chill ATES system in Tuscaloosa, Alabama, were obtained to develop a microbial profile. In addition, two head wells were sampled using glass slides/solid support device (SSD) to assess the importance of adhering microbial populations. Bacteria were observed in all water samples collected. Heterotrophic bacteria represented the largest group observed. In addition, coliforms and pseudomonad (bacteria that may be opportunistic human pathogens) were observed in many of the samples. However, no true human pathogens were observed in the water or solid support samples. Although preliminary, the data suggests that chill ATES does not increase the level of pathogenic microorganisms in aquifers.*

## Introduction

The acceptability of ATES technology depends, in part, on the impact aquifer storage systems have on the environment. That is, the sum total of positive effects must outweigh the sum of the negative effects and no one negative environmental effect may be intolerable (Reilly 1980). Previous assessments of ATES systems indicate that these technologies will have a net positive effect on the environment, primarily due to a reduced national demand for fossil fuels and the resultant reduction in pollution from the extraction, refining, and combustion of those fuels (Reilly 1980). Some potentially negative effects (such as thermal pollution of aquifers, chemical contamination, changes in regional groundwater flow, and stimulation of

[a] Operated for the U.S. Department of Energy by Battelle Memorial Institute under Contract No. DE-AC06-76RLO 1830.

seismic activity) have been evaluated (Reilly 1980) and deemed to be unimportant or avoidable with proper engineering design, careful operation, and continuous monitoring.

However, the effect ATES systems may have on aquifer biological systems including changes in the indigenous microbial populations and/or on the propagation and release of pathogenic microorganisms has not been carefully examined. Therefore, a project was undertaken to determine the environmental effects (both adverse and beneficial) of aquifer thermal energy storage (ATES) technology pertaining to microbial communities indigenous to subsurface environments (i.e., aquifers) and the propagation, movement, and release of pathogenic microorganisms (specifically, Legionella) within ATES systems.

Groundwaters are habitat to an abundant and diverse microbial population (Ghiorse and Wilson 1988; Fredrickson and Hicks 1987; Ghiorse and Balkwill 1984; Balkwill and Ghiorse 1985; Wilson et al. 1983; Hirsch and Rades-Rohkol 1984; White et al. 1984; Harvey, Smith and George 1984; Ehrlich et al. 1984). Indigenous microorganisms have been shown to have a major role in cycling of elements (e.g., carbon, sulfur, nitrogen, iron) and governing the behavior of organic contaminants entering groundwater aquifers (Hicks et al. 1989; Ghiorse and Wilson 1988; Fredrickson and Hicks 1987; Wilson et al. 1983; Harvey, Smith and George 1984). In addition to indigenous microbial populations, allochthonous organisms (i.e., organisms foreign to that environment) can survive and grow in aquifers. Allochthonous microorganisms detrimental to human health (i.e., pathogens) are of particular concern. The large number of disease outbreaks caused by microbially contaminated groundwater demonstrate that the subsurface can frequently harbor pathogenic organisms and that the environmental conditions within the subsurface can be conducive to the propagation of these allochthonous populations (Keswick 1984).

The growth and activity of microorganisms, both indigenous and allochthonous, is governed by a variety of environmental factors including: 1) the porosity of the aquifer, 2) nutrient availability, 3) oxidation-reduction conditions, 4) pH, 5) temperature, and 6) the adsorption of microorganisms to subsurface particles. Perturbations, caused by the implementation of ATES technology, may alter these physciochemical factors that, in turn, can affect the growth and activities of microorganisms inhabiting groundwater aquifers, as well as help to propagate and release pathogenic organisms that enter these environments.

Hicks and Stewart (1988) performed a literature review to determine the potential effect ATES systems have on microorganism inhabiting groundwater aquifers. The organisms of interest included both those microorganisms indigenous to aquifers, as well as those microorganisms that enter aquifers (i.e., allochthonous) and are able to survive there. The allochthonous microorganisms of particular concern were the Legionella bacteria. These organisms are ubiquitous in aquatic environments and can cause serious infections in humans. Their review suggested that of the previously mentioned environmental factors influencing the types and activities of microorganisms in aquifers, temperature changes caused by the use of ATES systems have the greatest potential for influencing microbial growth. They found:

- Heat systems (particularly at temperatures over 100°C) may prohibit both the indigenous microbiota and pathogenic organisms from entering the aquifer. While the suppression of pathogenic organisms is favored, the loss of important cycling activities of indigenous microbiota would adversely effect the environmental quality of the groundwater.

- Chill systems do not appear to inhibit the survival of indigenous microorganisms, although their activities would probably be suppressed. An issue of greater importance is the possibility of increased pathogen survival in these systems, especially of Legionella spp. These organisms are often associated with cooling towers and cold waters, such as those found in chill ATES systems, and their survival is favored with decreasing temperatures.

To assess further the importance of ATES system operation on microorganisms in groundwaters, a monitoring program was initiated in November 1988 at the University of Alabama. The 18-month monitoring effort is to assess the indigenous and allochthonous microorganisms populating the chill ATES system, as well as other selected campus HVAC systems that employ cooling towers. The findings of the first 3 months of this effort are reported here.

## Experimental Studies

### Sample Collection

Six water samples from various locations (Figure 1, A-F) within the ATES system were obtained to develop a microbial profile. In addition, two wells (H4E AND H1W, Figure 1) were sampled using glass slides/solid support device (SSD) to assess the importance of adhering microbial populations. Well H4E is outside the zone affected by the ATES system. The rationale for sampling at each of the specific sites is provided in Table 1 (see end of paper).

Water samples are collected from sites A, B, and C during pumping of the warm water production wells (wells 1-3; Figure 1), while water samples are collected from sites D and E when water is pumped from the cool wells (wells #4-6; Figure 1). Sampling at site F (sand filter) is performed when the sand filter is backflushed. To collect water samples, sterile Nalgene silicone tubing is attached to spigots located at each sampling site. The spigot is then opened and water is allowed to flow until pH, conductivity, and temperatures stabilize and water has flowed for at least 15 minutes. Eight liters of free-flowing water are collected into a sterile polycarbonate bottle for microbiological assessment [7 liters are processed at the University of Alabama and 1 liter of water is collected and shipped on ice to Pacific Northwest Laboratory (PNL) for microbiological assessment of heterotrophic organisms]. In addition, water (750 mL) is also collected for chemical analysis by Tuscaloosa Testing, Tuscaloosa, Alabama.

Samples were collected at the two head wells (H1W and H4E) by lowering a sterile SSD into the well. The sampling apparatus is raised 3 ft above the bottom of the well by a sterile nylon line and remained suspended for 5 to 30 days. At the end of the sampling period, the device is raised from the well and placed into a sterile container for transport to The University of Alabama's, microbiology laboratory and analyzed for adherent microbial populations.

Finally, water from four conventional cooling towers, operating at The University of Alabama and in close proximity to the ATES system, was collected to compare and contrast differences between the microbial populations of these cooling towers and the ATES cooling tower.

**Microbiological and Chemical Analysis**

Water samples processed at The University of Alabama were analyzed for indicator organisms of fecal contamination and human pathogens with potential for occurrence in the operating ATES system. The microbiological groups examined in the water samples and SSD, along with the media used and incubation conditions, are shown in Table 2.

Table 2. Bacterial groups assayed in water and SSD sample collected from ATES site in Alabama.

| Bacterial Groups | Culture Media | Incubation Conditions |
|---|---|---|
| Total heterotrophs | R2A | 25°C and 35°C, 5 to 7 days |
| Coliforms | m-Endo LES | 35°C, 24 to 48 hr |
| Pseudomonas | M-PA | 42°C, 48 hr |
| Yersinia | YSA | 25°C, 48 hr |
| Campylobacter | Campy thio | 42°C in Campy-Pak Plus, 48 hr |
| Mycobacteria | Middlebrook 7H10 OADC | 30°C, 14 days |
| Legionella | BCYE and GPAV | 35°C in 2,5% $CO_2$, 7 days |
| Vibrio | TCBS | 35°C, 48 hr |
| Salmonella/ Shigella | XLD | 35°C, 48 hr |

Water samples shipped to PNL were examined for total heterotrophs by direct counting procedures, denitrifying bacteria, sulfate reducers, and sulfur oxidizers.

Chemical characterization of the water samples collected at the ATES site included total organic and inorganic carbon, ammonium, nitrate, nitrite, and sulfate.

**Results**

Water samples from sampling sites A-C were processed according to the methods described above. Bacterial isolates obtained from these water samples collected between November 1988 and January 1989 are shown in Table 3. Heterotrophic bacteria represented the largest group observed. While coliforms were

Table 3. Microbiological analysis of ATES water samples collected between November 1988 and January 1989.

| Bacterial Groups | Site A | Site B | Site C |
|---|---|---|---|
| Heterotroph counts | 30 to 160 cfu[(a)]/ml | 30 to 180 cfu/ml | 60 to 140 cfu/ml |
| Coliforms | Citrobacter<br>Enterobacter<br>Serratia<br>Serratia | Enterobacter<br>Klebsiella<br>Morganella | Enterobacter<br>Morganella<br>Serratia |
| Pseudomonas | P. aeruginosa<br>P. acidovorans<br>P. maltophila | P. aeruginosa<br>P. acidovorans | P. aeruginosa<br>P. acidovorans |

(a) cfu = colony forming units

observed in the water samples, their densities ($<3 \times 10^{-3}$ cfu/ml) were much less than the densities of total heterotrophs (30 to 180 cfu/ml). In addition, their concentration was far below the maximum allowable concentration for primary drinking waters (0.01 cfu/ml) set by the U. S. Environmental Protection Agency (Lehr, Mielson and Montgomery 1984). Three Psuedomonas species were observed in the water sample (Table 3); however, as with the coliforms, their densities (<1 cfu/ml) was much less than the densities of total heterotrophs. Bacterial species from the remaining genera (i.e., Yersinia, Campylobacter, Mycobacteria, Vibrio, Salmonella, Shigella, and Legionella) were not isolated from the water samples as of this date.

Bacterial analysis of SSD samples collected from the two head wells showed similar results to those obtained in the water samples (i.e., the presence of coliforms and pseudomonas, the absence of human pathogens). However, a greater variety of microorganisms were isolated from the SSD samples than from the water samples (Table 4). In addition, the population densities for these organisms appeared to be greater than the population densities observed in the water samples (Table 5).

Table 4. Comparison of isolates obtained by attachment sampling (SSD)[a] to those obtained from aquifer water samples

| Bacterial Species | Site A | Site B | Site C | Control Well H4E | Field Well H1W |
|---|---|---|---|---|---|
| Citrobacter freundii | +[b] | -[c] | - | + | - |
| Enterobacter cloacae | + | + | + | + | + |
| Kledsiella pneumoniae | - | - | - | + | + |
| Klebsiella oxytoca | - | + | - | - | - |
| Morganella morganii | - | + | + | - | - |
| Pseudomonas acidovorans | + | + | + | + | + |
| Pseudomonas aeruginosa | + | + | + | + | + |
| Pseudomonas fluorescens | - | - | - | + | + |
| Pseudomonas maltophila | - | + | - | + | + |
| Serratia marcescens | - | + | + | + | + |

(a) SSD = solid support device, consisting of a microscope slide + 1 in. x 2 in. nylon planktonic net bag
(b) + = organism is present
(c) - = organism is absent

Table 5. Bacterial Analysis of SSD[a] Specimens Obtained from Head Wells H1W and H4E during December 1988

| Head Well | Date | Bacterial Isolate Density[b,c] A | B | C | D | E | F | G |
|---|---|---|---|---|---|---|---|---|
| H1W | 12/2 to 12/7 | 190 | ND[d] | ND | ND | 30 | ND | ND |
| | 12/7 to 12/12 | ND | 3 | ND | ND | 17 | ND | ND |
| | 12/14 to 12/19 | 1 | ND | 20 | 4 | ND | ND | ND |
| H4E | 12/2 to 12/7 | 1000 | 4000 | ND | ND | 70 | 30 | ND |
| | 12/7 to 12/12 | ND | 200 | ND | ND | 25 | 13 | 8 |
| | 12/14 to 12/19 | 200 | ND | 200 | ND | 9 | 5 | ND |

(a) SSD = solid support device, consisting of a microscope slide + 1 in. x 2 in. nylon planktonic net bag
(b) Density measured in colony forming units (cfu)
(c) Bacterial isolates: A = Pseudomonas aeruginosa, B = Pseudomonas spp., C = Pseudomonas acidovorans, D = Pseudomonas fluorescens, E = Serratia marcescens, F = Citrobacter freundii, G = Klebsiella pneumoniae
(d) ND = not detected Microbiological analysis of the water samples to determine the population densities of denitrifiers, sulfate reducers, and sulfur oxidizers are not complete at this time.

## Findings

Results to date represent only 5 sampling periods at most; therefore, it is impossible to reach any conclusions concerning the effect of ATES systems on indigenous and allochthonous microbial populations. In general, the data collected to date suggests that human pathogens may not be a problem in the ATES system or associated aquifer water. Coliforms and pseudomonads, many of which can be considered opportunistic pathogens, were observed in the ATES waters. Their presence in the samples, however, does not necessarily indicate that the ATES system is contributing to the level of pathogens in the aquifer. The species identified are also common to soils and water (Starr et al. 1981) and, therefore, may be indigenous to the aquifer. The observation (Table 4) of these organisms in head well H4E (that lies outside the ATES system) seems to support this hypothesis. Interestingly, a greater number and variety of these coliform and pseudomonads were observed in the non-ATES head well (H4E) than in the ATES head well (H1W; Table 5). This suggests that the ATES system may actually reduce the level of pathogens in the aquifer, possibly because of temperature reduction within the aquifer (data not shown). However, the data are too sparse to fully support this conclusion.

Legionella were not detected in any of the water or SSD samples. This important human pathogen is commonly found in cooling towers (Hicks and Stewart 1988) and its absence in water specimens taken from site B (post-cooling tower) contrasts with the observation of Legionella in conventional cooling towers located at the University of Alabama (data not shown). The ability of Legionella to become established in the conventional cooling towers but not in the ATES cooling tower may be due to two factors. First, the ATES cooling tower has a lower mean temperature than the conventional cooling towers. This lower temperature may suppress Legionella growth and, therefore, its establishment in the ATES cooling tower. Second, the residence time of water passing through the ATES cooling tower is lower than the residence time of water passing through the conventional cooling towers. This should also suppress Legionella establishment in the ATES cooling tower.

Although preliminary in nature, these data suggest that chill ATES systems do not contribute to the propagation and release of pathogenic bacteria and may actually reduce their survival. However, the present project is just beginning and the final conclusions must wait until the project is completed. Sampling at the other sites (D and E, Figure 1) to be done in the summer may demonstrate that pathogens are important. In addition, the effect of ATES systems on indigenous organisms, important to geochemical cycling, has not been established. Nor have the microbiologic effects of heat ATES at modest temperatures been established. Results to date suggest that bacterial populations are important parameters that need to be accounted for in the design and implementation of future ATES systems.

## References


1. Balkwill, D. L., and W. C. Ghiorse. 1985. "Characterization of Subsurface Bacteria Associated with Two Shallow Aquifers in Oklahoma." Appl. Environ. Microbiol. 50:580-588.

2. Ehrlich, G. G., E. M. Godsey, D. F. Goerlitz and M. F. Hult. 1984. "Microbial Ecology of a Creosote-Contaminated Aquifer at St. Louis Park, Minnesota." Dev. Ind. Microbiol. 25:235-245.

3. Fredrickson, J. K., and R. J. Hicks. 1987. "DOE's Deep Subsurface Probe: A Microbiological Profile." ASM News 53:78-79.

4. Ghiorse, W. C. and D. L. Balkwill. 1984. "Enumeration and Morphological Characterization of Bacteria Indigenous to Subsurface Environments." Dev. Ind. Microbiol. 25:213-224.

5. Ghiorse, W. C., and J. T. Wilson. 1988. "Microbial Ecology of the Terrestrial Subsurface." Adv. Appl. Microbiol. 33:107-172.

6. Harvey, R. W., R. L. Smith and L. George. 1984. "Effect of Organic Contamination upon Microbial Distributions and Heterotrophic Uptake in a Cape Cod, Massachusetts Aquifer." Appl. Environ. Microbiol. 25:183-200.

7. Hicks, R. J., B. A. Denovan and J. K. Fredrickson. 1989. "Aerobic and Anaerobic Biodegraqdation of Selected Nitrogen-Containing Aromatic Compounds in Deep Subsurface Sediments." Appl. Environ. Microbiol. (in review).

8. Hicks, R. J., and D. L. Stewart. 1988. Environmental Assessment of the Potential Effects of Aquifer Thermal Energy Storage Systems on Microorganisms in Groundwater. PNL-6492, Pacific Northwest Laboratory, Richland, Washington.

9. Hirsch, P., and E. Rades-Rohkol. 1984. "Microbial Diversity in a Groundwater Aquifer in Northern Germany." Dev. Ind. Microbiol. 25:183-200.

10. Keswick, B. H. 1984. "Sources of Groundwater Pollution." In Groundwater Pollution Microbiology, eds. G. Bitton and C. P. Gerba, pp. 39-64. John Wiley and Sons, New York, New York.

11. Lehr, J. A., D. M. Mielson and J. J. Montgomery. 1984. "U.S. Federal Legislation Pertaining to Groundwater Protection." In Groundwater Pollution Microbiology, eds. G. Bitton and C. P. Gerba, pp. 353-371. John Wiley and Sons, New York, New York.

12. Reilly, R. W. 1980. A Descriptive Analysis of Aquifer Thermal Energy Storage Systems. PNL-3298, Pacific Northwest Laboratory, Richland, Washington.

13. Starr, M. P., H. Stolp, H. G. Trupper, A. Balows and H. G. Schlegel. 1981. The Prokaryotes: a Handbook on Habitats, Isolation, and Identification of Bacteria, Vol. 2.n. Springer-Verlag, New York, New York.

14. White, D. C., G. A. Smith, M. J. Gehron, J. H. Parker, R. H. Findlay, R. F. Martz and H. L. Frederickson. 1984. "The Groundwater Microbiota: Biomass, Community Structure and Nutritional Status." Dev. Ind. Microbiol. 25:201-211.

15. Wilson, J. T., J. F. McNabb, D. L. Balkwill and W. C. Ghiorse. 1983. "Enumeration and Characterization of Bacteria Indigenous to a Shallow Water-Table Aquifer." Ground Water 21:134-142.

Table 1. Sampling site description and rationale for sampling.

| Specimen | Sampling Site | Notes on Sample | Rationale | Assessment |
|---|---|---|---|---|
| A (Fig. 1) | Pre-cooling tower (warm water wells) | Microbiota may be affected by drawdown on the aquifer exposing aquifer matrix. This sample will provide only a partial spectrum of adherent microorganisms in the aquifer. | Ideally, a "baseline" of the microbiological spectrum should be obtained from a production well that pumps approximately 200 gpm and is "upstream" from the ATES system well field. However, this type of well has not been drilled because of financial constraints. Although the warm water wells were used for the injection of warm water during the 1985-1986 and 1986-1987 seasons, time, substantial pumpage, and the natural aquifer movement should have returned this site to near equilibrium. Therefore, the microbiological spectrum identified in this sample will be used as the "baseline" for the aquifer. | The microbiological spectrum will probably be dynamic during the periods where the pumping cycles on and off frequently. It is expected that microbial populations will stabilize with consistent pumping. Numbers, confidence intervals, and colony types will be established for comparative purposes. Data from this site will be compared to previous data from this site. |
| B (Fig. 1) | Post-cooling tower (warm water wells) | The aerobic environment and exposure to airborne microorganisms suggests a potential for modulating the water microbiota. Aerosols created by the cooling tower may provide a source of human pathogens (respiratory route). | Modulation of microbiota by the cooling tower environment should be reflected and can be compared with non-ATES cooling towers on campus. | Numbers, confidence intervals, and colony types will be established for comparative purposes. Data from this site will be compared to sample A and to previous data from this site. Perceived modulation of the microbiota will be confirmed by performing statistical tests on data from the three microbial populations. |
| C (Fig. 1) | Post-sand-filter (pre-cooling water wells) | A build-up of microorganisms on the matrix of the sand-filter may occur. As these colonies enlarge, microorganisms may be released into the water by the pumping action. | Modulation of microbiota by the sand-filter environment should be reflected. The microbiological spectrum identified in this sample will be used as the "baseline" for microorganisms that will be injected into the aquifer. | Numbers, confidence intervals, and colony types will be established for comparative purposes. Data from this site will be compared to samples A and B and to previous data from this site. Perceived modulation of the microbiota will be confirmed by performing statistical tests on data from the three microbial populations. |

Table 1. (Continued)

| Specimen | Sampling Site | Notes on Sample | Rationale | Assessment |
|---|---|---|---|---|
| D (Fig. 1) | Post-cool water wells (pre-air-handling units) | Microbiota may be affected by drawdown on the aquifer exposing aquifer matrix. This sample will provide only a partial spectrum of adherent microorganisms in the aquifer. | Comparison of the spectrum of microorganisms in this sample with the "baseline" water and water being injected into the aquifer will indicate whether the ATES system is modifying the aquifer. | Numbers, confidence intervals, and colony types will be established for comparative purposes. Data from this site will be compared to samples A and C and to previous data from this site. Perceived modulation of the microbiota will be confirmed by performing statistical tests on data from the three microbial populations. |
| E (Fig. 1) | Post-air-handling units (water applied to playing fields) | Increased water temperatures from the air-handling unit may affect the microbiota. This water may provide a source of human pathogens (enteric and respiratory route). | Modulation of microbiota by the air-handling unit should be reflected. | Numbers, confidence intervals, and colony types will be established for comparative purposes. Data from this site will be compared to samples A and D and to previous data from this site. Perceived modulation of the microbiota will be confirmed by performing statistical tests on data from the three microbial populations. |
| F (Fig. 1) | Backflush of sand filter | The sample should be enriched with adherent microorganisms. | This sample should confirm the microbiological spectrum of sample C and will provide a potential concentration step that would detect very low concentrations of culturable microorganisms. | Numbers, confidence intervals, and colony types will be established for comparative purposes. Data from this site will be compared to sample C and to previous data from this site. Perceived modulation of the microbiota will be confirmed by performing statistical tests on data from the three microbial populations. |
| SSD #1 | Head well H4E | The site is "upstream" from the ATES system. | This sample will provide the "background" of the spectrum of adherent microorganisms in the aquifer independent of the ATES system. | Numbers, confidence intervals, and colony types will be established for comparative purposes. Data from this site will be compared to previous data from this site. |
| SSD #2 | Head well H1W | Site is within the pool of injected cool water. | This sample should reflect modulation of adherent microorganisms by injection of water processed through the cooling tower. | Numbers, confidence intervals, and colony types will be established for comparative purposes. Data from this site will be compared to SSD specimen #1 and to previous data from this site. |

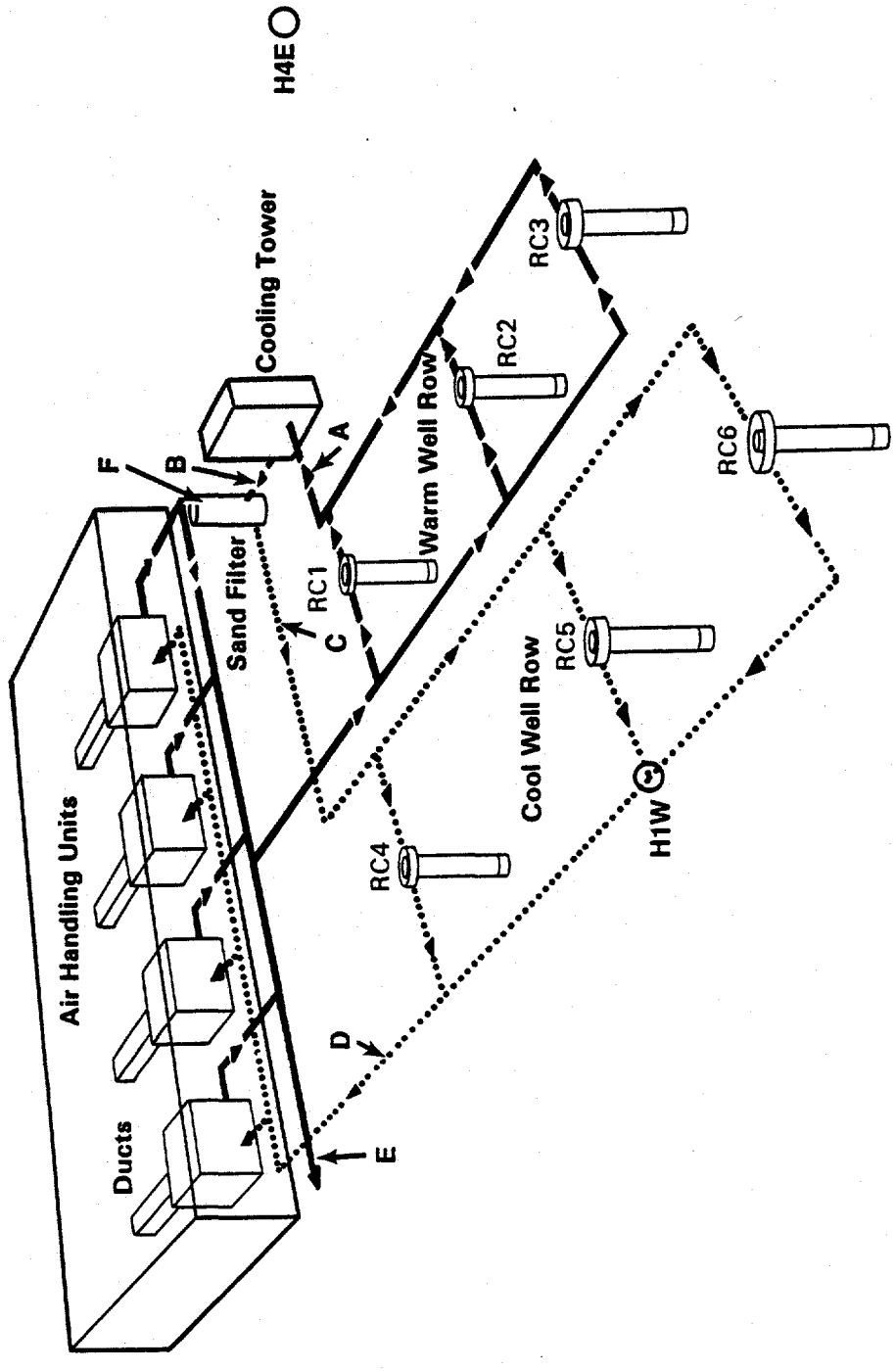


Figure 1. Sampling locations for water and SSD specimens (A-F, H1W, H4E) obtained at the University of Alabama.

# GEOCHEMICAL RESEARCH FOR HIGH-TEMPERATURE AQUIFER THERMAL ENERGY STORAGE

**Everett A. Jenne, James P. McKinley, and Robert W. Smith**
Pacific Northwest Laboratory[a]
Richland, Washington 99352

***Abstract***

*The goal of these investigations is to develop the capability to predict and thereby avoid the geochemical problems that have plagued most aquifer thermal energy storage (ATES) systems. The experimental work focuses on the DOE-funded Field Test Facility (FTF) at St. Paul, Minnesota. Samples from the storage aquifer (Galesville Sandstone) are being used in closed-system (hydrothermal) laboratory experiments at 60°, 90°, and 120°C. These results are being used to improve the reliability of speciation and solubility calculations made with the MINTEQ geochemical model (GCM) in high-temperature ATES systems. A "reaction" model is being constructed of minerals important in regulating those dissolved constituents that form scale and cause clogging. A mixing model is being developed to permit calculation of the extent of mixing thermally treated water with native ground water to facilitate interpreting of composition of the withdrawn water. The CGM improvements, reaction model, and reconciliation of laboratory and St. Paul FTF data are designed to permit assessment of potential geochemical problems at future ATES sites as well as to reduce capital investment and the start-up and operating costs.*

## Introduction

The heating and injection of heated water into an aquifer results in chemical reactions that adversely affect the performance of ATES systems. Such reactions include the precipitation of carbonate and silica scale during heat addition and extraction, respectively, and a potential reduction in aquifer permeability. The Pacific Northwest Laboratory (PNL) is studying the geochemical problems identified by participants of Annex VI[b] of the International Energy Agency (IEA) and of the DOE-funded Field Testing Facility (FTF) at the St. Paul campus of the University of Minnesota. The goal of the Geochemical Dynamics Project

---

[a] Pacific Northwest Laboratory is operated for the U.S. Department of Energy under Contract DE-AC06-76RLO 1830 by the Battelle Memorial Institute.

[b] "Environmental and Chemical Aspects of Thermal Energy Storage in Aquifers and Research and Development of Water Treatment Methods."

research is to develop the capability to interpret, predict, and quantify the important geochemical reactions, including those causing scaling and potential permeability reductions at the St. Paul FTF and other ATES ground water systems. Research objectives are 1) to add selected geochemical modeling (GCM) capabilities via code modifications and database additions (i.e., thermodynamic data for temperature and solid solution competence and rate data for mineral dissolution), 2) to develop a site-specific "reaction" model, 3) to investigate selected water treatment processes, 4) to carry out cooperative geochemical studies with other IEA participants, and 5) to demonstrate GCM capability at the St. Paul FTF.

## Geochemical Model and Database Development

### Temperature Competence

The database of most GCMs, including the MINTEQ code, were originally developed to model water/rock equilibria at near-ambient temperatures. To obtain the necessary reliability of MINTEQ calculations for high-temperature (up to 300°C) ATES systems, equations and coefficients were derived for calculating mineral hydrolysis constants, solubility products, and formation constants for 60 minerals and 57 aqueous species in the 13-component thermodynamic system, $K_2O$-$Na_2O$-CaO-MgO-FeO-$Al_2O_3$-$SiO_2$-$CO_2$-$H_2O$-HF-HCl-$H_2S$-$H_2S$-$H_2SO_4$ (Smith 1988). In addition, an option that allows more accurate activity coefficients to be calculated was added to MINTEQ. For certain solute species (e.g., $CO^{2-}_3$, $Fe^{2+}$, $SO^{2-}_4$, $Mg^{2+}$) the effect of the added temperature competence is quite significant, as shown in Figure 1.

### Solid Solution

Coprecipitation of minor ions with calcium carbonate to form a solid solution results in potential misinterpretation of Saturation Index (SI)[a] calculations for carbonates. Magnesium coprecipitation has a major effect on the solubility of the resultant magnesium-calcite. In order to correctly interpret the SI of calcite, the stoichiometric solubility product must be known. Literature data is being evaluated and algorithms developed to allow the calculation of stoichiometric solubility products using MINTEQ. The incorporation of code modifications and addition of an appropriate database will provide more accurate interpretation and prediction of dissolved constituent concentrations and carbonate precipitation in ATES systems.

## "Reaction" Model Development

Prediction of the extent of scaling and clogging requires that the dissolved concentration of important constituents be estimated. This requires that the important dissolution and precipitation reactions be identified and quantified. Thus, the hydrothermal laboratory research is focused on the development of a "reaction model" using aquifer samples (i.e., Galesville Sandstone) from the St. Paul FTF. Experimental details (preparation of synthetic ground water, aquifer sediment selection, sample preparation, reaction

---

[a] The Saturation Index is defined as log IAP - log $K_T$, were IAP is the ion activity product for the reaction and $K_T$ is the solubility value at temperature T. An SI value of zero indicates saturation of the modelled solution with respect to the solid phase. Positive and negative values indicate supersaturation and under saturation, respectively.

vessels used, and analyses) are given by McKinley, Jenne, and Smith (1988). Experiments are being carried out at temperatures of 60°, 90°, and 120°C. The results at 120°C are presented here for illustrative purposes.

Neither pH nor inorganic carbon varied systematically with time, whereas dissolved Ca, $SO_4$, Si, and other constituents show temporal increases during individual experiments (Figure 2). The parallel increase in Ca and $SO_4$ suggests that these two solutes have a common source such as gypsum. Since gypsum has not been identified by x-ray diffraction or casual thin-section examination, detailed thin-section examination is planned to resolve its presence or absence. Silica concentration increased with time, approaching a limiting concentration of nearly 1 mM. Potassium concentration increased with time at all temperatures and was strongly covariant with silica. Quartz and feldspar were identified by x-ray diffraction in the bulk sample.

An SEM examination of crushed sandstone showed a marked reduction in surface roughness (but not of angularity) of quartz and potassium feldspar clasts following reaction at 120°C. Quartz grains developed etch pits indicative of dissolution (Knauss and Wolery 1988), and feldspar grains developed a terraced appearance. Thus, both quartz and feldspar contribute important constituents to the heated water.

The version of MINTEQ computer code (Felmy, Girvin, and Jenne 1984) containing the thermodynamic data for elevated temperature, called IMINTEQP3, was used to calculate the 1) pH at experimental temperature from ambient temperature measurements, 2) equilibrium distribution of aqueous species, and 3) degree of saturation with minerals for the results of the hydrothermal laboratory experiments. The at-temperature pH values were estimated by running MINTEQ at fixed pH and an as-measured temperature of 25°C to obtain the calculated molar concentration of total H; then, MINTEQ was rerun at the experimental temperature with fixed total H and model-dependent Ph. The at-tempertaure calculation resulted in an increase of 0.1 to 0.2 pH units (Table 1). The temporal variation of SI for calcite and quartz are given, with and without increased temperature competence, in Figures 3 and 4. The scatter is the result the combined errors of sampling and of analyses (e.g., measurement of pH)j. These data indicated that at 120°C calcite equilibria limits the dissolved Ca concentrations and the quartz controls aqueous silica concentrations. However, at 60°C quartz is oversaturated (data not shown). This may be explained by the high activation energy for quartz precipitation below about 100°C (Rimstidt and Barnes 1980).

Calcite, quartz, and feldspar have been identified as solids controlling the dissolved constituents of thermally treated water at the St. Paul FTF. Additional minerals that might be significant sources of important dissolved constituents include gypsum, dolomite, glauconite, and amorphic silica. Other minerals, which are calculated to be in equilibrium in some of the experimental systems, include magnetite and sepiolite. Research is under way to determine which of these minerals need to be included in the "reaction model."

Table 1. At-Temperature pH Values Calculated for 120°C Sandstone-Ground Water Experiments Using Previous (MINTEQP2) and Temperature-Enhanced (MINTEQP3) Versions of MINTEQ

| Sample No. | 25°C Measured pH | 120°C Calculated pH | |
|---|---|---|---|
| | | MINTEQP2 | MINTEQP3 |
| 164.5 | 6.41 | 6.65 | 6.54 |
| 600.0 | 6.54 | 6.79 | 6.66 |

## Comparison of Laboratory and Field Test Results

There are similarities in overall temporal variations in solution chemistry between the field and laboratory tests. Alkalinity of injection waters varied by 0.8 meq/L over the course of the long-term test, but alkalinity during withdrawal of the same water varied by only about 0.2 meq/L. Variation in pH was also relatively small during withdrawal (perlinger et al. 1987). The small experimental variation of these parameters in the laboratory studies parallels observations in the field. Sulfate increased in ground water over the course of each test and, on average, from test to test (Walton et al. 1984). This trend toward increased concentration was also found in laboratory experiments. Holm et al. (1987) suggested that K was controlled either by dissolution of feldspar or by cation exchange; careful examination of the temporal variation of K and Si data are under way to estimate the contribution of K from dissolution processes.

A major problem in the use and interpretation of the chemical composition of water withdrawn from ATES storage is the generally unknown extent of mixing of the thermally treated water with native ground water. Preliminary results indicated that mixing may occur to a significant extent at the FTF. A reliable calculation of the extent of mixing will improve the accuracy of estimates of the magnitude of dissolution of primary minerals and precipitation of secondary minerals. The mixing issue is being addressed in a current project study using laboratory and FTF data in conjunction with GCM and information about the solids present to estimate the elemental fluxes and develop a mass-balance model for Si, Na, and Cl for the ATES system. This model may be useful in predicting scaling and in evaluating water treatment and post-ATES water quality problems.

## Conclusions

The results of a systematic examination of temperature (60°C to 120°C) and temporal variations in dissolved constituents for a key sample have allowed the development of a tentative "reaction" model for this site and the testing of model and database improvements. These studies, combining experimental studies with GCM simulations, demonstrate that the approach being used will allow the development of an experimental plan for future ATES systems that will allow geochemical problems to be anticipated and alternative designs or water treatment methods evaluated before start-up of an ATES system.

Further studies are needed to resolve questions of possible additional minerals that need to be included in the "reaction" model for predicting dissolved concentration of important constituents at this site. Although this "reaction" model is site-specific, cooperative studies with other IEA Annex-VI participants indicate that it is likely that there are limited number of minerals that have a significant effect on the major element composition of heated ground water. Therefore, the "reaction" model developed for St. Paul is expected to be applicable to other sites with the addition of a minimum number of additional minerals.

## References[a]


1. Felmy, A. R., D. C. Girvin, and E. A. Jenne. 1984. MINTEQ: a Computer Program for Calculating Aqueous Geochemical Equilibria. EPA-600/3-84-032, National Technical Information Service, Springfield, Virginia.

2. Holm, T. R., S. J. Eisenreich, H. L. Rosenberg, and N. P. Holm. 1987. "Ground Geochemistry of Short-Term Aquifer Thermal Energy Storage Test Cycles." Water Resources Research 23:1005-1029.

3. Knauss, K. G. and T. J. Wolery. 1988. "The Dissolution Kinetics of Quartz as a Function of pH and Time at 70°C." Geochim. Cosmochim. Acta 52:43-53.

4. *McKinley, J. P., E. A. Jenne, and R. W. Smith. 1988. Experimental Investigation of Interaction Between Heated Ground Water and Sandstone. JIGASTOCK88, Versailles, France.

5. Perlinger, J. A., J. E. Almendinger, N. R. Urban, and S. J. Eisenreich. 1987. "Groundwater Geochemistry of Aquifer Thermal Energy Storage: Long-Term Test Cycle." Water Resources Research 23:2215-2226.

6. Rimstidt, J. D. and H. L. Barnes. 1980. "The Kinetics of Silica-Water Reactions." Geochim. Cosmochim. Acta. 44:1683-1699.

7. *Smith, R. W. 1988. Calculation of Equilibria at Elevated Temperatures Using the MINTEQ Geochemical Code. PNL-6700, Pacific Northwest Laboratory, Richland, Washington.

8. Walton, M. W., S. J. Eisenreich, N. L. Holm, T. R. Holm, M. C. Hoyer, R. Kanivetsky, J. Lauer, H. C. Lee, R. T. Miller, and H. Runke. 1984. Aquifer Characterization Report for the University of Minnesota's Aquifer Thermal Energy Storage (ATES) Project Short-Term Test Cycles. Minnesota Geological Survey, University of Minnesota, St. Paul Minnesota.


---

[a] Publications of the Geochemical Dynamics Project are marked with an asterisk.

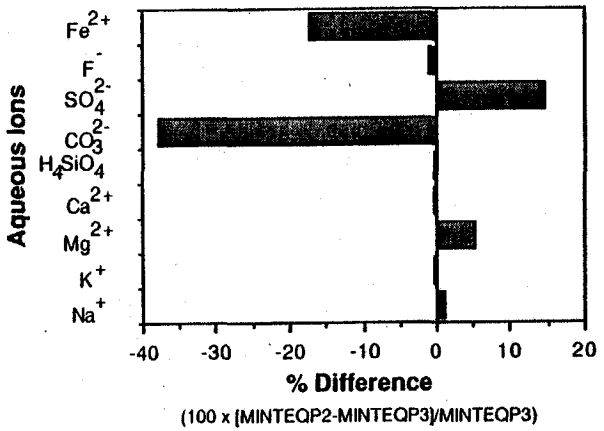


Figure 1. Difference in Ion Activities Calculated with (MINTEQP3) and without (MINTEQP2) Increased Temperature Competence.

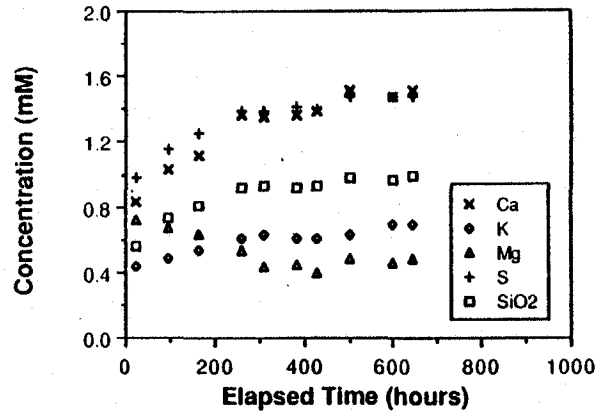


Figure 2. Temporal Variation in Dissolved Concentrations of Key Constituents at 120°C.

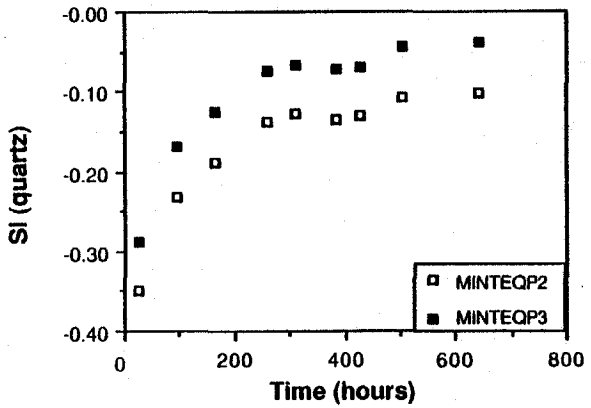


Figure 3. Saturation Index for Quartz at 120°C with and without Increased Temperature Competence.

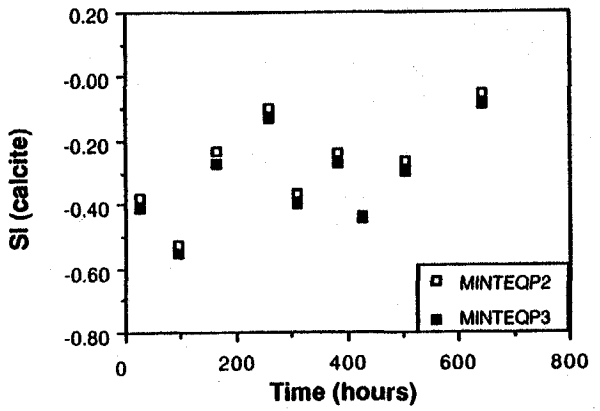


Figure 4. Saturation Index for Calcite at 120°C with and without Increased Temperature Competence.

# PERFORMANCE OF A CHILL ATES SYSTEM

**K. Clark Midkiff, Yeong K. Song, and Walter J. Schaetzle**
Department of Mechanical Engineering
The University of Alabama
Tuscaloosa, AL 35487

**C. Everett Brett**
Natural Resources Center
School of Mines and Energy Development
The University of Alabama

## *Abstract*

*An aquifer air-conditioning system has been installed to cool the Student Recreation Center on the University of Alabama Campus. This research program encompasses the monitoring of the operation of the aquifer system and provision of emplacements to the system. The monitoring includes establishing the instrumentation, acquiring data, and analyzing the results.*

*The instrumentation allows the measurement of water flow rates and corresponding temperatures, electrical energy input, aquifer temperatures at nineteen monitoring wells, and aquifer levels at six monitoring wells.*

*Recent aquifer performance data indicate that 76% of the chill energy stored was recovered for the period Oct/86 - Sep/87 and 70% for the period Oct/87 - Sep/88. This is a substantial improvement over recoveries of 38% for the 1985 season and 55% for 1986. The overall coefficient of performance was 5.4 for Oct/86 - Sep/87 and 4.6 for Oct/87 - Sep/88. The system has supplied 100% of the cooling with only about one-half of the energy input required by a conventional system.*

*Some of the increased recovery of chilled water is a result of modifying the production well operation to reduce the regional flow of water toward the northwest. All warm water is withdrawn from the southeast wells, chilled, and injected in northwest wells. The cold water then withdrawn from the cold wells is used for air-conditioning but not reinjected into the aquifer. Additional flow control is provided by pumping (and discarding) water out of a southeast well, although the complete results of this new strategy are as yet unclear.*

## Background

The University of Alabama has designed, constructed, and is presently monitoring the performance of a seasonal aquifer thermal energy storage (ATES) system that is used to chill and store groundwater in the winter season for later use in air conditioning the Student Recreational Center in the warm months. The

design objective of this system is to provide 100% of the building cooling during the summer months, along with a greatly reduced consumption of electrical energy in comparison with conventional air-conditioning systems. The experimental objectives of this project are to track and analyze the performance of this novel cooling technology, to make minor changes needed to improve the operation and monitoring of the existing system, and to identify design modifications needed to better the performance of a second generation of aquifer chill storage systems. Provided in this introductory section are descriptions of the conceptual design, the system components and the monitoring system for the chill storage system.

**Conceptual Design**

The power requirement for air conditioning, especially in major buildings, is large and peaks during late afternoons. Most large commercial air conditioning systems use evaporative cooling towers to reject heat. In the new systems, more efficient chillers are used along with unique techniques such as "free cooling" in which water from cooling towers is used directly in the cooling coils, by-passing the chiller, any time the tower exit water temperature drops below 50 F (10 C) as a function of external ambient wet-bulb temperature.[3,4]

The system in this study uses direct cooling the year around, not only eliminating the chiller power but also the capital cost for the chiller. The water is chilled during cold periods in cooling towers or ponds, is stored in a water table aquifer, and is recovered as required for air conditioning. The aquifer air-conditioning concept is shown schematically in Figure 1. The system is broken down into three components: heat rejection or water chilling, chilled water storage, and heat absorption. The system is similar to a conventional system except that the chiller has been eliminated. The large energy savings is the elimination of the chiller energy and the chiller energy demand charge.

The largest energy use component, although small compared to a conventional system, is that of chilling water. The water is pumped from the aquifer to the cooling system, shown as a cooling tower in Figure 1. Pumping only occurs during cold weather, normally below 50 F. The water is chilled in the cooling system by the frigid air. Possible cooling systems are cooling towers or spray ponds. With a cooling tower the largest energy input is the tower blower. Nature provides a natural draft for a cooling pond in cold weather, thus eliminating the blower tower. Average wind velocity is higher in the winter, which also makes the cold weather cooling pond more efficient than a conventionally utilized warm weather cooling pond. The water must be pumped into the wells again from either the cooling tower or pond.

The reinjected water is stored underground in the aquifer until required for air-conditioning. At this time, the water is pumped from the cold wells through the building cooling coils. The water removes heat from the air blowing across the coils. The heated water can be returned to the warm wells.

The tower blowers operate any time the wet-bulb temperature goes below the required cooling temperature. Cooling tower or pond operation is related only to weather and is not matched to a corresponding air-conditioning load. The size of the towers is related to chilling hours available. The

more chilling hours available per year, the smaller the cooling tower or pond and the lower the capital cost of the system.

Access to the aquifer is provided by wells drilled between the surface and the base of the aquifer. The casing of the operating wells is perforated throughout the entire thickness of the aquifer and is solid elsewhere. Using the entire thickness of the aquifer is important to minimize the mixing of cold and warm water.

For the Tuscaloosa area, weather conditions average 1200 to 1460 hours below 43 F (6 C) wet-bulb temperature per year. Minimum available temperatures are around 10 F (-6 C). Temperatures rarely have dropped to below 0 F (-18 C). Input water to the aquifer is expected to vary from 35 F to over 45 F with an average temperature of 43 F (6 C).

Water is removed from a warm well, chilled, and is reinjected into a cold well (Figure 2). There is basically zero volume use of water during chilling except for some evaporative losses in the cooling tower.

Water is cooled to 45 F (7 C) in the cooling tower or pond during the winter cycle and injected into the aquifer through the cold wells for thermal storage till required for air-conditioning. Stored cold water is removed from the cold well of the aquifer for air conditioning and is heated to approximately 60 F (15 C) in the cooling coils during the summer cycle, and is either injected into the warm wells, used to water nearby recreational athletic fields, or is discarded to the storm sewers. Water exiting the building air conditioning units may not be reinjected into the aquifer in order to minimize the effect of adverse natural aquifer flow that tends to pull the volume of cold water stored in the winter away from the cold production wells. The system cycles between the wells and water chilling and air conditioning corresponding to outdoor temperatures and cooling loads.

The recovery of chilled water energy from the aquifer can range from 15-90% depending on aquifer thickness, volume of water utilized, and natural water movement. The chilled water recovery efficiency of the system in this project, with a 40 ft plus thick aquifer, was expected to exceed 60% the first year, assuming very little groundwater movement (less than 10 ft/yr), and was expected to approach 80% by the third annual cycle. In reality, an appreciable natural water movement has been detected. Energy recovery efficiency was under 40% in the 1985 season, reached over 50% in the 1986 season, and has averaged about 70% over the two-year period of Jul/86 - Jun/88. Chill recovery efficiency has been improved by the implementation of active measures to reduce chilled water loss from natural aquifer flow.

**System Components**

The Student Recreation Center utilizes a water table aquifer in its cooling system. Construction on the building started in July 1981 and was completed in November 1982. Some chilling of water took place during the winter of 1982-83. The aquifer system was included on a 20 year life cycle cost evaluation.

The system has supplied essentially 100% of the air conditioning since 1983. The facility consists of 62,000 $ft^2$ of conditioned floor space with 14 handball courts, five basketball courts, a running track, weight room, locker rooms, and offices.

The HVAC system is a 4-pipe system employing a total of 30 air handling units with hot water and chilled water coils, a natural gas jet-fired hot water boiler, and a 100 ton standby air-cooled backup chiller. An economizer cycle provides air conditioning during the corresponding weather conditions. The total heating load, including heating the ventilation air, is 1.6 MMBtu/hr; and the maximum cooling load is 148 tons. The standby chiller capacity is 100 tons (the chiller will not carry the maximum load in the gym and the remainder of the building simultaneously).[1] Air conditioning the gym was made possible by the decision to install the aquifer chill storage system.

The Recreation Center aquifer system (Figure 2) consists of three "warm" wells and three "cold" wells, each containing a submersible three-stage pump and return riser, and a cooling tower with a circulating pump. Warm well pump design capacity is 150 gpm at 140 ft head, cold well pump design capacity is 120 gpm at 200 ft head, and the cooling tower water chilling capacity is rated at 450 gpm of water for a water temperature decrease from 56 F to 45 F at a 40 F wet-bulb ambient temperature.

The warm well pumps are started by an outdoor thermostat set at 45 F. The pumps are cycled by a level controller in the first stage cooling tower cold water basin. A three-way diverting valve in the cooling tower pump discharge is modulated by a thermostat in the cooling tower cold water basin to divert water from the cooling tower through the sand filter to the cold wells at water temperatures of 45 F or below. The cooling tower fans are controlled by an outdoor thermostat. Each well pump is equipped with a low level cut-off control in the well casing. The well pump control panel includes a plug-and-jack arrangement to permit manual selection of well pumps. The cold well pumps start when any one of the chilled water coil valves open on temperature demand.

The HVAC System cost was $485,000 including $190,000 for the wells, well pumps, tower, sand filter, and other items related to the aquifer system.[1,6] Designed thermal storage capacity is 139,000 ton hours per year.

**System Monitoring**

The system is monitored by acquiring data on aquifer operation and performance, water chilling system operation and performance, and the air-conditioning system operation and performance. To evaluate and monitor the aquifer, 21 monitoring wells have been drilled, six of which have been added in the past year.

The well locations are shown in Figures 2 and 3. The aquifer has six operating wells, three cold wells, and three warm wells in two rows as shown in both Figures 2 and 3. The wells are 90 to 100 ft deep, use 10 inch PVC sand screen, are packed with gravel in the saturation zone, cased with solid PVC casing, and are grouted with concrete to the surface. The 21 monitoring well locations are shown in Figure 4. These consist of three background head monitoring wells, three additional head monitoring wells in or near the operating well field, and fifteen temperature monitoring wells. The head wells and temperature

monitoring wells use 2 inch PVC casing. The monitoring wells are not ground packed. The head monitoring wells (six) have a section of sand screen near the bottom of the wells.

The data acquired and being acquired to physically define the aquifer and aquifer performance consist of:

1. Drilling samples from the monitoring wells.
2. Water head data to determine the natural water level.flow, and water draw down during pumping.
3. Temperature sensors in monitoring wells to determine the temperature profiles, both static and transient, in the aquifer.
4. Water flow injection and withdrawal rates with temperatures to determine thermal energy storage efficiency.
5. Power input to evaluate performance of the overall cooling system. The data to evaluate the water chilling system include:

    - Water temperature into and out of the cooling tower.
    - Water flow rate into the cooling tower.
    - Power input to the cooling tower; this includes the pumping power to reinject the water into the wells.

The data to evaluate the building air conditioning system include:

1. Water temperature into and out of the building.
2. Water flow rate into the building.
3. Power input for pumping water.

**Summary of Past Research Completed**

Research completed prior to the past year consists primarily of the accumulation of an extensive database of measurements of the pertinent physical variables, and their analysis to determine the performance of the aquifer chill storage system. These measurements are described in the previous subsection. Extensive compilations of earlier data are available, e.g., in Refs. 2 and 7. These references also provide a detailed discussion of the geology of the aquifer site. This information is partially summarized in Figures 4 and 5, which present generalized cross-sectional views of the aquifer site. The past performance of the aquifer system itself is best characterized by the coefficients of performance (COP) of the system components, as shown in Table 1. The overall system COP, which is the ratio of air conditioning provided to electrical energy required to produce the cooling, has generally increased since the system went into operation; although the most recent year shows an apparent decline, as will be discussed in the following section. Comparisons of recent to past system performance are made at several points in the following section.

## Results and Discussion

A summary and analysis of the current research efforts are presented in this section. The aquifer chill storage and cooling system performance can be characterized by the cooling tower performance, the building

performance, the aquifer performance, and the overall system performance. Following a brief overview of the performance statistics of these components, a more detailed look at the individual components is presented.

**Performance Overview**

The aquifer chill storage system has performed well over the past several years, providing 100% of building air conditioning. System performance has been gradually improving, as illustrated by Table 1. There have been few maintenance problems with the system, but an operational problem in the most recent water chilling season resulted in a significant loss of chilled water. Through an inadvertent student error, valves had been left in a position where cold water from the cooling tower could not be injected into two (Wells #4 and #5) of the three cold wells. Chilled water that overflowed from Well #6 ran out onto the ground and was lost. It is estimated that at least 1.5 million and as much as 4 million gallons of chilled water were lost before the problem was discovered in January, 1988. Much of the data presented below in tables and charts does not reflect this chilled water loss; but, at points in the text where appropriate, the effect of the water loss on the data being presented will be discussed.

Cooling tower operation resulted in the removal of 2170 MMBtu from aquifer water for the period Oct/86 - Sep/87, and the removal of 2430 MMBtu in the period Oct/87 - Sep/88. This represents a chill storage of 181,000 ton hours and 203,000 ton hours for the two periods, respectively. Note that if the chilled water loss mentioned above is taken into account, as much as 670 MMBtu were lost and as little as 1760 MMBtu were stored (as much as a 25% loss of chill) for the period Oct/87 - Sep/88. Considering the total power input required to produce this heat rejection, which is the sum of the cooling tower blower power and the warm well production pump power, the cooling tower coefficients of performance for Oct/86 - Sep/87 and Oct/87 - Sep/88 were 9.0 and 9.7, respectively. The cooling tower COP drops significantly for Oct/87 - Sep/88, if the cold water loss is taken into account and the total electric power consumption for the annual period is charged against the COP.

A total of 2040 MMBtu (170,000 ton hours) of air conditioning was provided to the Recreation Center for the period Oct/86 - Sep/87, and 1960 MMBtu (163,000 ton hours) were provided from Oct/87 - Sep/88. These figures may be compared to the total air conditioning provided in the 1986 season (October 1, 1985 - September 30, 1986), which was 1300 MMBtu (108,000 ton hours). Considering the total power required to produce this air conditioning, which is the sum of the cold well pumping power and the warm well pumping power for water pumped from the aquifer for the purpose of reducing aquifer flow losses, the building coefficients of performance for the above two time periods were 14.6 and 11.0, respectively. These numbers are unaffected by the above-mentioned chilled water loss.

The chill recovery from the aquifer for the period Oct/86 - Sep/87 was 76% of the chill stored over the period; and the chill recovery for the Oct/87 - Sep/88 period was 70% of that stored, although this latter figure would be significantly higher if the water loss that occurred over the period is taken into account). These recovery efficiencies are improvements over recovery efficiencies of 59% for the 1986 season and 38%

for the 1985 season. The increase is due both to the larger quantity of water returned and utilized for air conditioning over the period and to the increased efforts to minimize the adverse effects of natural aquifer flow. The aquifer data still indicate a large natural flow to the west northwest at a fairly constant 60 degrees west of north. Modifications have been made in the system operation to minimize the natural flow, although there is thusfar insufficient experience with the control options available to have realized an optimum strategy.

The overall performance of the aquifer chill storage and air-conditioning system is best characterized by an overall coefficient of performance, defined as the ratio of the total air conditioning provided to the total energy input required to produce the air conditioning, which is the sum of the cold and hot well pumps and the cooling tower blower electrical consumption. The measured average COP of the overall system was about 5.4 over the period Oct/86 - Sep/87 and about 4.6 over the period of Oct/87 - Sep/88, compared to a 1986 season COP of 4.7. This operating performance is at least twice the rated conventional air-conditioning system performance, and somewhat better performance in the future is anticipated as we improve our ability to minimize chill losses due to natural aquifer flow. The low system COP for the most recent season results in large part from the waste of electrical power to chill water that was not stored. The sections that follow present more detailed information on aquifer behavior and on the performance of the air-conditioning system components.

**Aquifer Characteristics and Performance**

The water levels from the six head monitoring wells are given for Jan/87 - Dec/87 in Appendix Table A1 and for Jan/88 - Dec/88 in Table A2. In general, the water levels remain stable and are affected little by either the weather or season of the year. Well #H4E shows some major variation in water level over the period 06/01/87 through 02/24/88. In February of 1988, compressed air was used to remove an apparent plug-up at the well bottom that had hydraulically isolated the well from the aquifer. This procedure was performed on 25 February and resulted in an immediate 9 ft head drop that can be seen by comparing the 02/24/88 head data to the 02/29/88 data. The plugging problem was likely caused by an influx of sediment-laden rainwater into the top of the well. The well cover and casing were apparently damaged by the tires of a University vehicle. The well cover and casing were replaced in March; but not before the well had again partially clogged because of rainwater inflow, as evidenced by comparing the 03/07/88 water level measurement from Well #H4E to the measurements from the other head monitoring wells. The water level in Well #H4E returned to that of the aquifer later in March and has not deviated significantly since that time.

The natural aquifer flow and gradient were calculated from water levels in the three head monitoring wells most distant from the primary aquifer chill storage activity, Wells #H4W, #H4S and #H6E. Consider the triangle defined with the above well locations as the vertices. Using the middle water level for these three wells, the identical water level location is determined on the side opposite this well in the triangle by linear interpolation. A line from the middle water level well to this point is a line of constant water

level, and therefore no flow passes along this line. The actual flow is perpendicular to this line and the water level gradient is determined along this perpendicular line. The results of this aquifer flow angle and slope analysis are presented on an approximately weekly basis for the period Jan/87 - Dec/87 in Table A3 and for the period Jan/88 - Dec/88 in Table A4. The flow gradient (proportional to flow velocity) varies somewhat; it is typically about 3 to 4 ft/1000 ft. The aquifer flow direction is quite constant at about 60 to 65 degrees west of north.

A considerable effort has been made in the past year to develop computer-generated isotherm contour plots for planes at various depths in the aquifer. The contour plots provide a more easily visualized representation of thermal conditions in the ground at the ATES site. The isotherm contour plots are interpolated from the three-dimensional set of temperature measurements made from the various monitoring wells in the aquifer. Because of the extent of temperature information required by the contouring routine, our temperature data base was insufficient to generate contour plots prior to the installation of the 6 additional temperature monitoring wells (Wells #H1N, #H2N, #H3N, #H0W, #H1NW and #H2NW), a task which was not completed until mid-February, 1988.

Figures 6-10 are contour plots in a plane roughly parallel to and 10 ft above the Pottsville Formation (which is the aquiclude for the Recreational Center ATES aquifer). The six large open circles on the plots show the locations of the production wells, as indicated by the numbers inside the circles. The heavy rectangular shape indicates the location of the outer walls of the Recreational Center, and the three arrows at the lower right of the figures indicate the undisturbed, normal aquifer flow direction. The contour plots were generated from data taken on the date appearing at the top of each plot. Figure 5 shows the temperature distribution near the end of the winter cooling season, with a large bubble of sub-45 F water located almost due west of Well #4. Figures 6, 7 and 8 show the gradual depletion of the chilled water through the air-conditioning season. Figure 9 shows the isotherms at about midway into the present chilling period. The general appearance of these plots is a product of the seasonal variation in well usage, the fact that Wells #4 and #5 are the primary cold production wells and Wells #2 and #3 are the primary hot production and back-pumping wells (for aquifer flow control), and the overall flow of the undisturbed aquifer in a west-by-northwest direction.

**Cooling Tower Performance**

The aquifer system has operated for the last five years, providing 100% of the air-conditioning except for backup system checkouts and special tests on the aquifer such as pumping tests. The monthly flows for the cooling tower for Jul/86 - Dec/88 are given in Figure 11. Due to some uncertainty as to their magnitude, losses of chilled water that occurred the past winter have not been deducted from this tabulated information. Average cooling tower water inlet and outlet temperatures, as well as volume of water throughput, are presented on a monthly basis in Table A5. Table A6 presents the monthly heat rejection data for the cooling tower. The monthly electrical energy consumption for the cooling tower blower and for the hot well pumps is shown in Table A7. Finally, Table A8 presents the tower heat rejection, electrical power usage

of tower blower plus hot well pumps, and the tower COP on an approximately weekly basis. The data provided for a particular date are cumulative values for the period beginning with the previous listed date.

**Building Performance**

The monthly water flows for building air conditioning are given in Figure 12. The recovery gallons are almost 2.5 times the injection flow for the Oct/86 - Sep/87 period and are 1.8 times the injection flow for the Oct/87 - Sep/88 period. Average water inlet and outlet temperatures for the building, as well as volume of water throughput, are presented on a monthly basis in Table A5. The total monthly air conditioning provided for the building (heat removed from the building) is presented in Table A6. The monthly electrical energy consumption for the cold well pumps is shown in Table A7. It should be noted, again, that electrical power used to operate the hot well pumps during the cooling season for the purpose of minimizing aquifer flow (e.g., May and June, 1988) is charged against the building COP as energy input required to produce air conditioning. Table A8 presents the electrical power usage of the cold well pumps and the building coefficient performance on an approximately weekly basis.

**Overall System Performance**

The overall system performance is best characterized by the overall COP, the aquifer recovery efficiency, and the overall system recovery efficiency. Using the annual air-conditioning data presented in Table A6 and the total electrical power usage presented in Table A7, the overall system COP for several one-year periods was calculated. The results are presented in Table 1.

The annual aquifer recovery efficiency is defined as the fraction of the chill stored during cooling tower operation that is recovered during building air conditioning over an annual period. Energy rejection from the building accomplished by heating the building chiller water to temperatures exceeding the undisturbed aquifer water temperature of 65 F is not included as recovered chill energy. The recovery efficiency for the aquifer system was 76% for Oct/86 - Sep/87 and 70% for Oct/87 - Sep/88 (reported at the bottom of Table A6). The recovery efficiency for Oct/87 - Sep/88 is significantly higher if the loss of chilled water that occurred the past winter is deducted. Aquifer recovery efficiencies of 38% for the 1985 cycle (October 1, 1984-September 30, 1985) and of 59% for the 1986 cycle were measured, thus the most recent results are an improvement over past performance.

The overall system recovery efficiency is defined as the ratio of air conditioning provided to the building to the total heat rejected by the cooling tower over a one-year period. Note that the overall system recovery "efficiency" can be greater than 100%, if enough of the building cooling is provided by heating the water passing through to a temperature higher than the aquifer ambient temperature of 65 F. The computed overall system recovery efficiency, shown in parentheses at the bottom of Table A6, was 94% for Oct/86 - Sep/87 and 81% for Oct/87 - Sep/88. By comparing the aquifer recovery efficiencies to the overall system recovery efficiencies, we see that a substantial percentage of the air conditioning provided (typically about 12%) results from the recovery of "free" chill available in the uncooled aquifer water.

**System Electrical Energy Consumption**

Monthly electrical energy usage data for the cooling tower blower and the hot and cold production well pumps are presented in Table A7. The annual electrical power distribution among the various components is shown in Figures 13 and 14 for the past two seasons. A separate category is included to distinguish hot well pump operation to feed the cooling tower and hot well pumping to reduce the natural aquifer flow velocity during the cooling season. These figures show clearly that the cooling tower blower motor is the largest user of electrical energy in the system. The substitution of a cooling pond for the cooling tower would result in considerable savings of electrical power and would elevate the system COP.

**Benefits of the ATES System**

It is important to note that even with some of the flaws typical of a prototype design, the Recreational Center ATES system is providing 100% of the building air conditioning at only one-half of the electric energy consumption. At energy charges of $0.05/kWh, this represents an annual savings of $6,000 to $8,000 in comparison to conventional air-conditioning costs. Even greater savings result from the avoidance of summer peak demand charges, because the peak power consumption of the aquifer chill energy system occurs in the winter chilling season, as illustrated in Figure 15. With the Tuscaloosa area demand charge of about $5/kW per month (low compared to many locations), demand charge avoidance is estimated to result in a savings of about $9,000 annually.

In addition to these economic benefits offered, the use of an ATES system eliminates the possibility of chlorinated fluorocarbon (CFC) release, as no CFC's are required for an ATES system. CFC's are both greenhouse gases and are responsible for the chemical destruction of the stratospheric ozone layer. The reduction in electrical energy consumption reduces the combustion of coal (in the Tuscaloosa area), thus resulting in the abatement of air pollution problems and the release of greenhouse gases ($CO_2$) associated with fossil fuel combustion. Utilities benefit from the reduced peak capacity requirements as load is shifted from summer to winter.

An additional benefit of the aquifer chill energy storage system is that the resulting low cost of air conditioning opens new areas of application, one example of which is industrial building cooling. Presently, few factories are air-conditioned. Summertime temperatures on the floors of such factories, especially those where heat is generated as a result of the manufacturing process, can reach 110 F and higher. Such extreme heat results in the deterioration of manufacturing materials, the loss of worker productivity, and may lead to severe worker health problems. In a recent incident in an automotive assembly plant in St. Louis, factory floor temperatures of 110 F resulted in the collapse and death of an employee, an event which precipitated the walkout of several hundred other workers.[8] The temperature in such buildings can often be reduced to 85 F by the application of an economical aquifer system. Retrofit projects are often made more feasible by using existing cooling towers that are normally unused in the winter. In general, factory areas where conventional air-conditioning is now economically marginal have a potential to be air-conditioned with an aquifer cooling system. This system offers the possibility of raising U.S. productivity by improving the working environment.

**System Improvements and Future Work**

The University aquifer system has been operating well, providing 100% building air conditioning with operating costs less than one-half those of a similar-sized conventional system. Nevertheless, there is considerable room for improvement and optimization of the current system and those to follow it. Compared to conventional systems, which have limited scope for improvement after many years of development, numerous improvements to aquifer systems remain to be made to further reduce projected system capital costs and operating costs.

One area of improvement for aquifer systems is the location and operation of production wells to minimize adverse effects of natural aquifer flow. The operation of wells to minimize the natural flow is expected to increase performance. Not only is energy recovery increased, but pumping time for air-conditioning will be decreased due to lower average recovery temperatures for air conditioning. The natural movement of water is large at our site but, in our opinion, can be controlled. A major thrust of the Alabama project will be in the area of aquifer flow control. We hope to quantify aquifer and thermal front movement, to measure the effect of various control strategies, and to determine an optimum operating procedure for our present production well configuration. Furthermore, we hope to develop a procedure by which production wells can be optimally sited at new installations.

The largest energy user in the aquifer system is the cooling tower. Substituting a cooling pond could save 50% of the aquifer system energy. In cold weather and with a larger temperature change, cooling ponds are much more efficient because a stable natural draft occurs. Wind velocities are also generally higher in the winter, so the pond is more efficient. The pond could possibly use only 20% as much energy as a cooling tower, thus cutting aquifer system electrical energy usage in half.

Another problem with the aquifer air-conditioning system is that it often does not do as good a job at dehumidification as a conventional system. This is because the air chiller coils of a conventional system are operated at a lower temperature than the aquifer system building chiller. This differential is greatest late in the air-conditioning season when the water entering the building is at its highest temperature. Improved (economical) methods of dehumidification would certainly extend the range of applicability of the aquifer air-conditioning systems. The present aquifer system does offer an economical and reliable air-conditioning alternative in applications where dehumidification is not critical.

A final area of improvement for our current system is the standardization of operating procedures. The aquifer air-conditioning system is novel, and service personnel are as yet somewhat unfamiliar with the operation and maintenance of the system. The lack of a standardized set of operating procedures brought about the previously described loss of chilled water last winter. Steps are being taken to avoid such operational failures in the future.

## Conclusions

An aquifer air-conditioning system has been installed and successfully operated to provide 100% of the building air conditioning at the Recreation Center on the University of Alabama campus. Data for water flow rates and corresponding temperatures, electrical energy input, aquifer temperatures at nineteen monitoring wells, and aquifer levels at six monitoring wells have been collected and analyzed. Aquifer chill recovery efficiencies continue to improve; about 76% of the chill stored was recovered for the period Oct/86 - Sep/87 and about 70% for the period Oct/87 - Sep/88. The overall system coefficient of performance was 5.4 for Oct/86 - Sep/87 and 4.6 for Oct/87 - Sep/88, thus the aquifer system is supplying air conditioning with only about one-half of the energy input required by a conventional system.

Future work will focus on better system performance through improved operation. The main thrust will be to measure the effects of various pumping options for minimizing the loss of chill by natural aquifer flow and to determine and apply the optimum strategy. Also, more attention will be paid to standardizing operational procedures to maximize chill storage and recovery.

## References


1. Brett, C. E., and W. J. Schaetzle, "Experience with Chilled Water Storage in a Water Table Aquifer," Proceedings of Third International Conference on Energy Storage for Building Heating and Cooling, Toronto, Canada, Public Works Canada, 1985.

2. Midkiff, K. C., W. J. Schaetzle and C. E. Brett, 1987 Annual Report, Subcontract No. 8-H5383-A-O, Battelle Pacific Northwest Labs., Richland, WA, 1988.

3. Schaetzle, W. J., C. E. Brett and D. M. Grubbs, "Direct Cooling Utilizing Aquifer Thermal Energy Storage," ASHRAE Transactions, Vol. 86, Pt. 2, 1980.

4. Schaetzle, W. J., C. E. Brett, D. M. Grubbs, and M. S. Seppanen, Thermal Energy Storage in Aquifers: The Design and Applications, Pergamon Press, 1980.

5. Schaetzle, W. J., C. E. Brett, G. Jackins and E. Miller, 'Free Cooling' Applications Using Annual Aquifer Thermal Energy Storage," Proceedings of International Conference on Seasonal Thermal Energy Storage and Compressed Air Storage, Seattle, WA, 1981.

6. Schaetzle, W. J., C. E. Brett and L. Richey, "Experience With Two 'Free Cooling' Systems Using Aquifer Thermal Energy Storage," Proceedings of International Conference on Subsurface Heat Storage in Theory and Practice, Stockholm, Sweden, June 1983.

7. Schaetzle, W. J. and C. E. Brett, 1986 Annual Report, Subcontract No.8-H5383-A-O, Battelle Pacific Northwest Labs., Richland, WA, 1987.

8. Articles appearing in the St. Louis Post-Dispatch, June 22 and June 23, 1988.

Table 1. Summary of aquifer system performance.

| | 1,000 Btu WATER CHILLING | kWh* COOLING TOWER | COP TOWER | 1,000 Btu AIR-COND BUILDING | kWh** WELL PUMP | COP BLDG | 1,000 Btu RECOVERED AQUIFER | kWh TOTAL | COP OVERALL |
|---|---|---|---|---|---|---|---|---|---|
| (OCT/85-SEP/86): | 2892985 | 53188 | 15.9 | 1288897 | 26517 | 14.2 | 1088997 | 79705 | 4.7 |
| (OCT/86-SEP/87): | 2168798 | 70551 | 9.0 | 2037943 | 40874 | 14.6 | 1649802 | 111425 | 5.4 |
| (OCT/87-SEP/88): | 2433504 | 73231 | 9.7 | 1963079 | 52200 | 11.0 | 1701983 | 125431 | 4.6 |
| (JAN/87-DEC/87): | 2054409 | 61527 | 9.8 | 2054683 | 37565 | 16.0 | 1679724 | 99092 | 6.1 |
| (JAN/88-DEC/88): | 2617771 | 80603 | 9.5 | 1889977 | 51992 | 10.7 | 1641835 | 132595 | 4.2 |

* : The column includes kWh of the Tower Blower and the H Well Pumps.
**: The column includes kWh of the C Well Pumps and Back Pumping

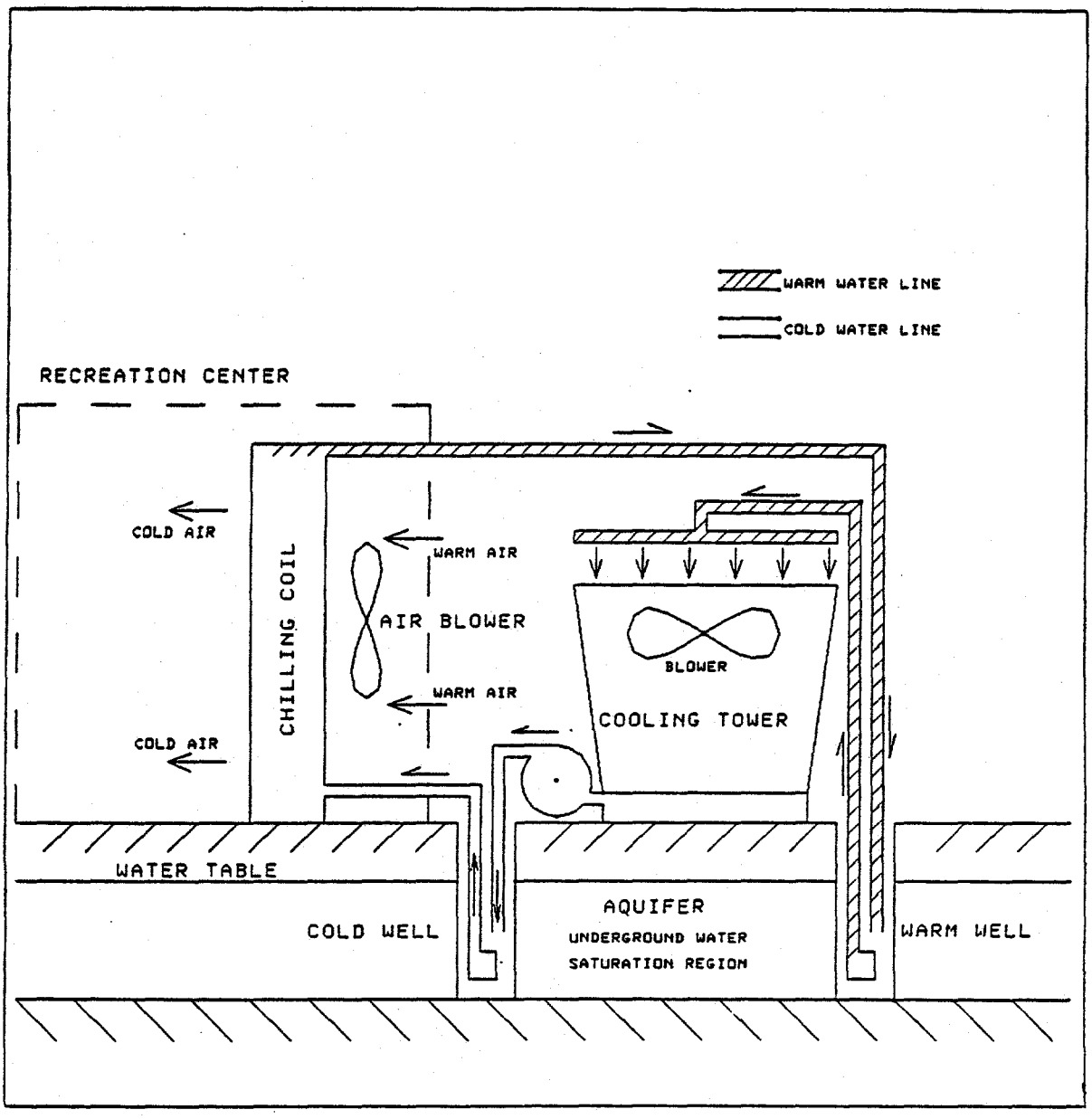


Figure 1. Aquifer air-conditioning system.

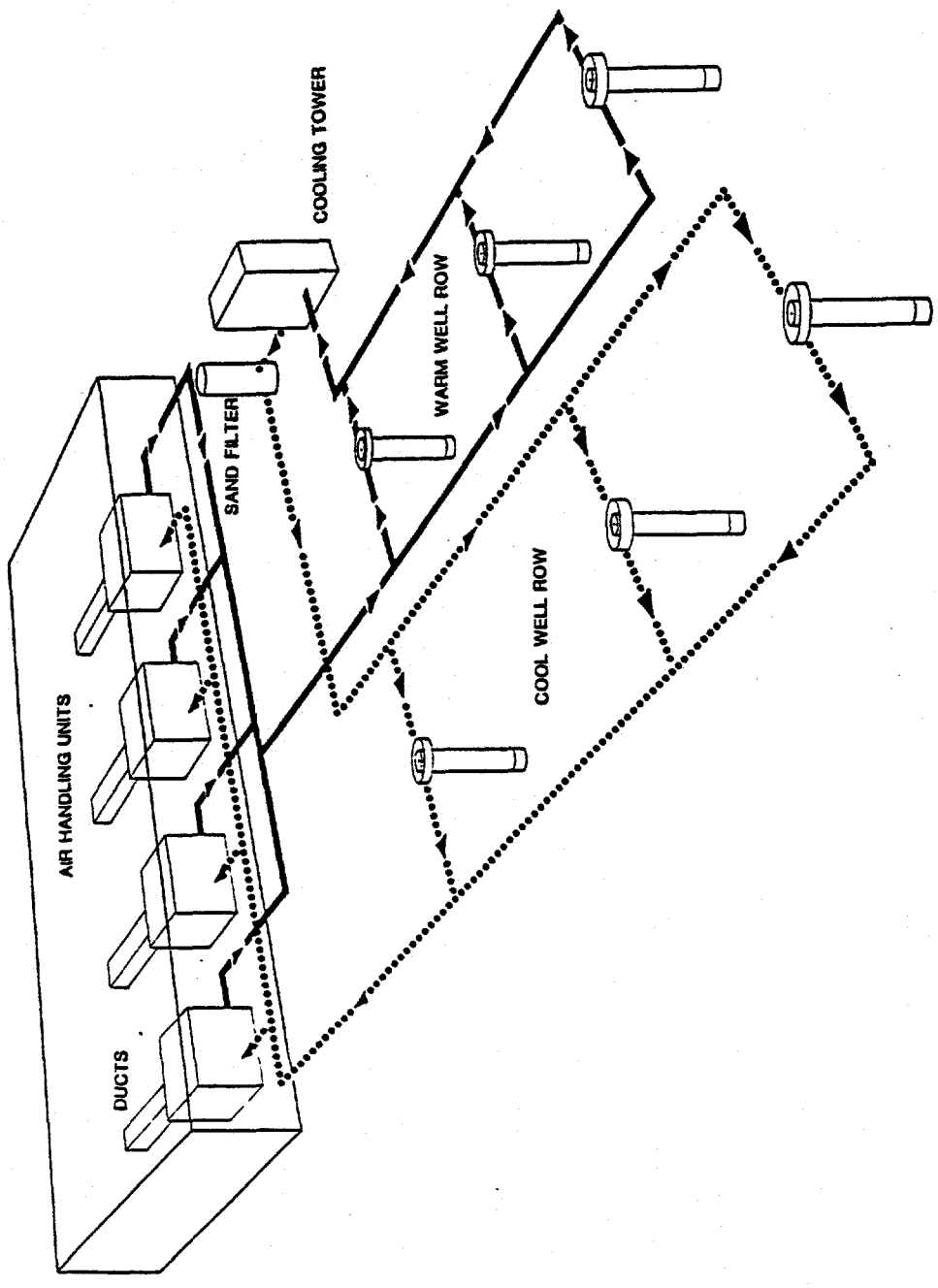


Figure 2. University of Alabama Student Recreation Center; aquifer source heating/cooling flow schematic.

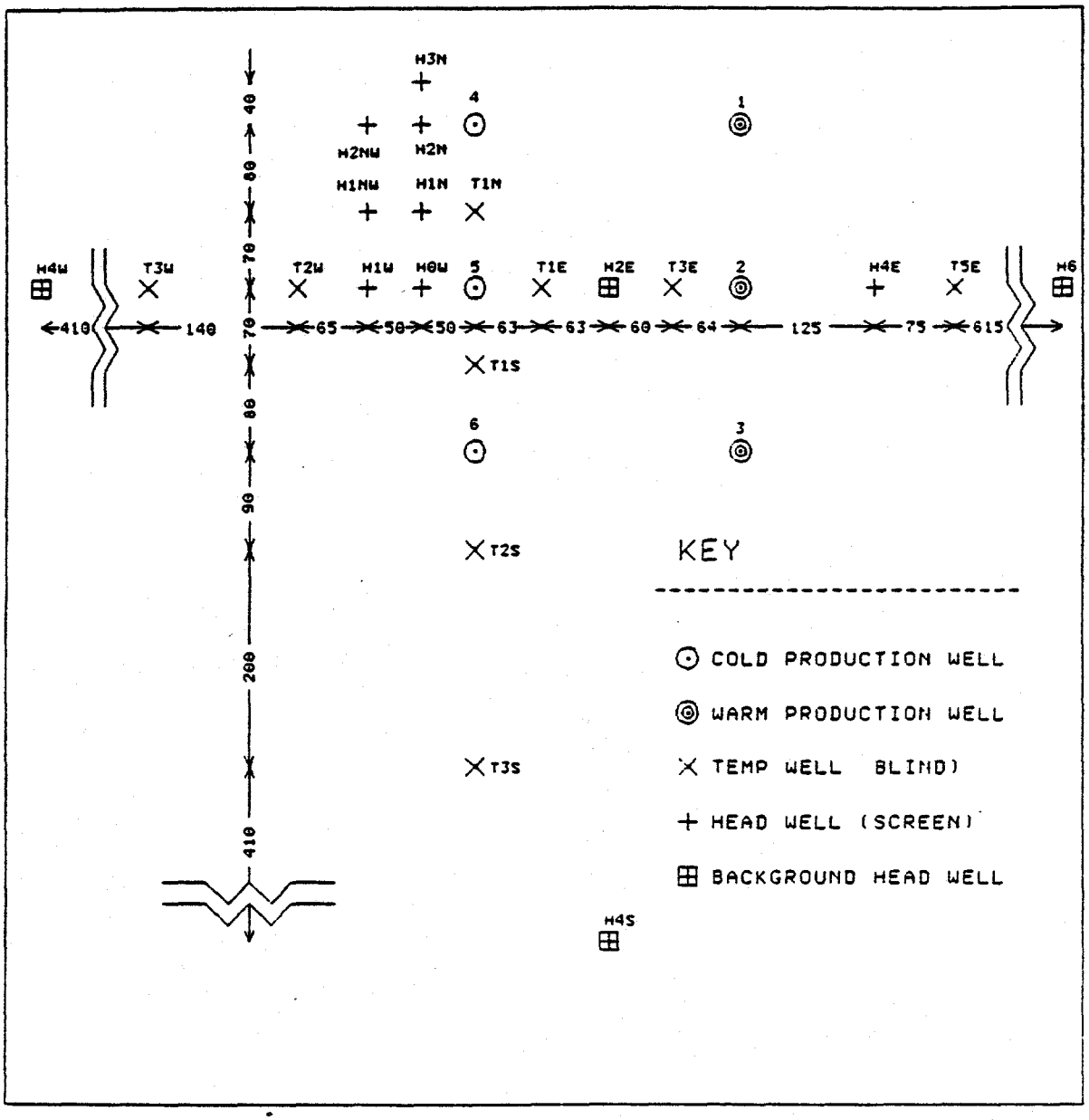


Figure 3. Aquifer system well layout.

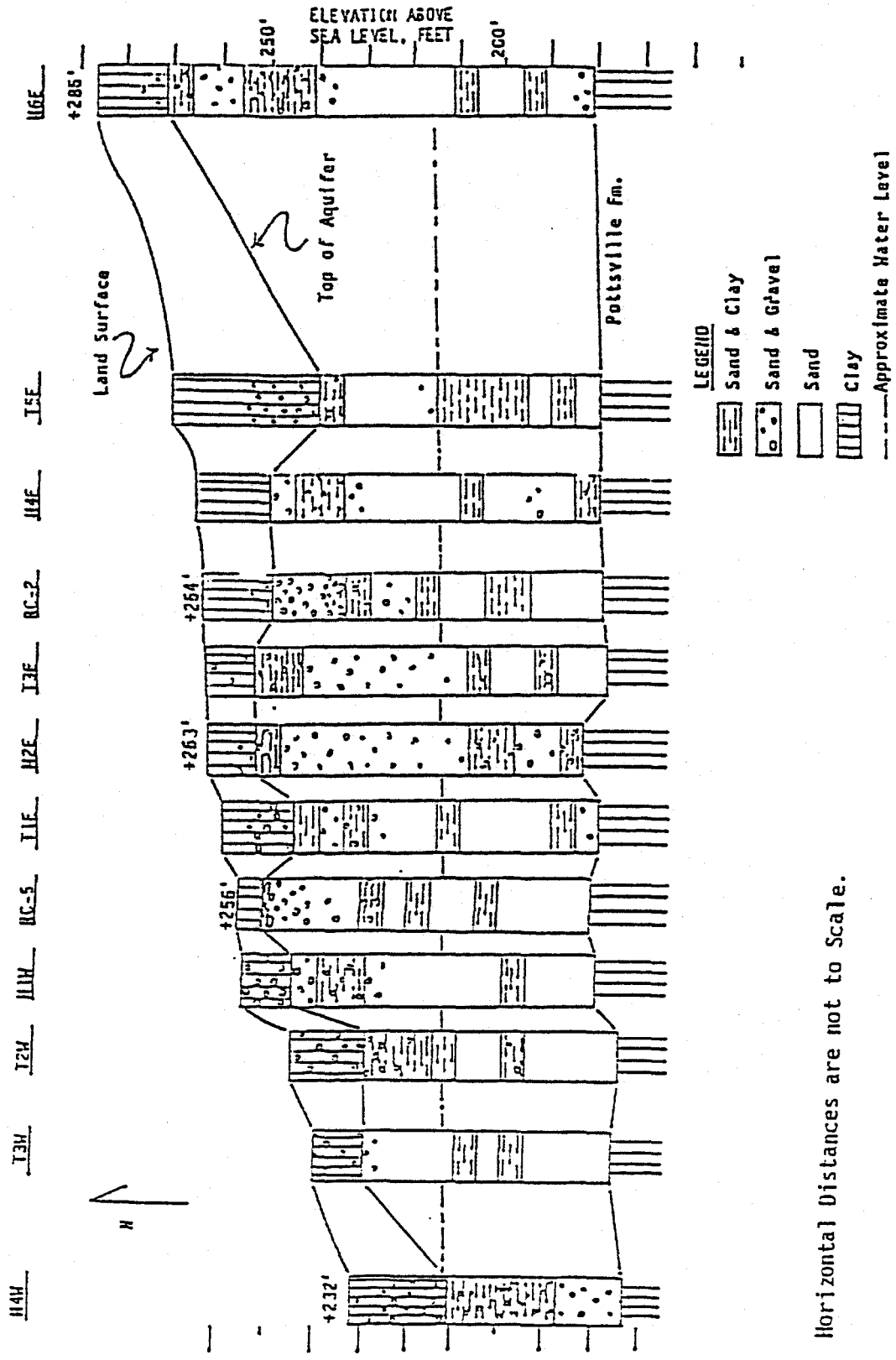


Figure 4. Cross section view of aquifer site showing geology.

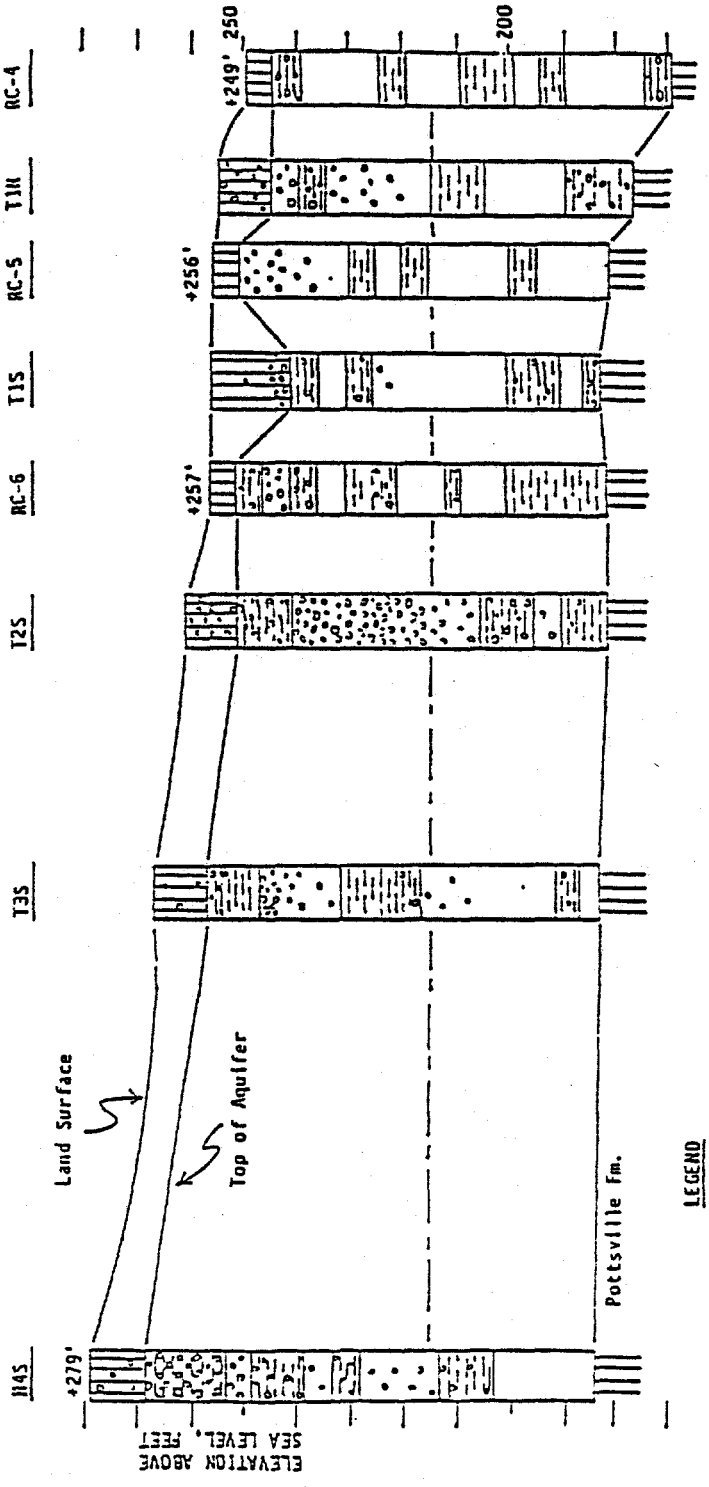


NOTE: Horizontal Distances are not to Scale.

Figure 5. Generalized south to north cross section of aquifer field showing geology.

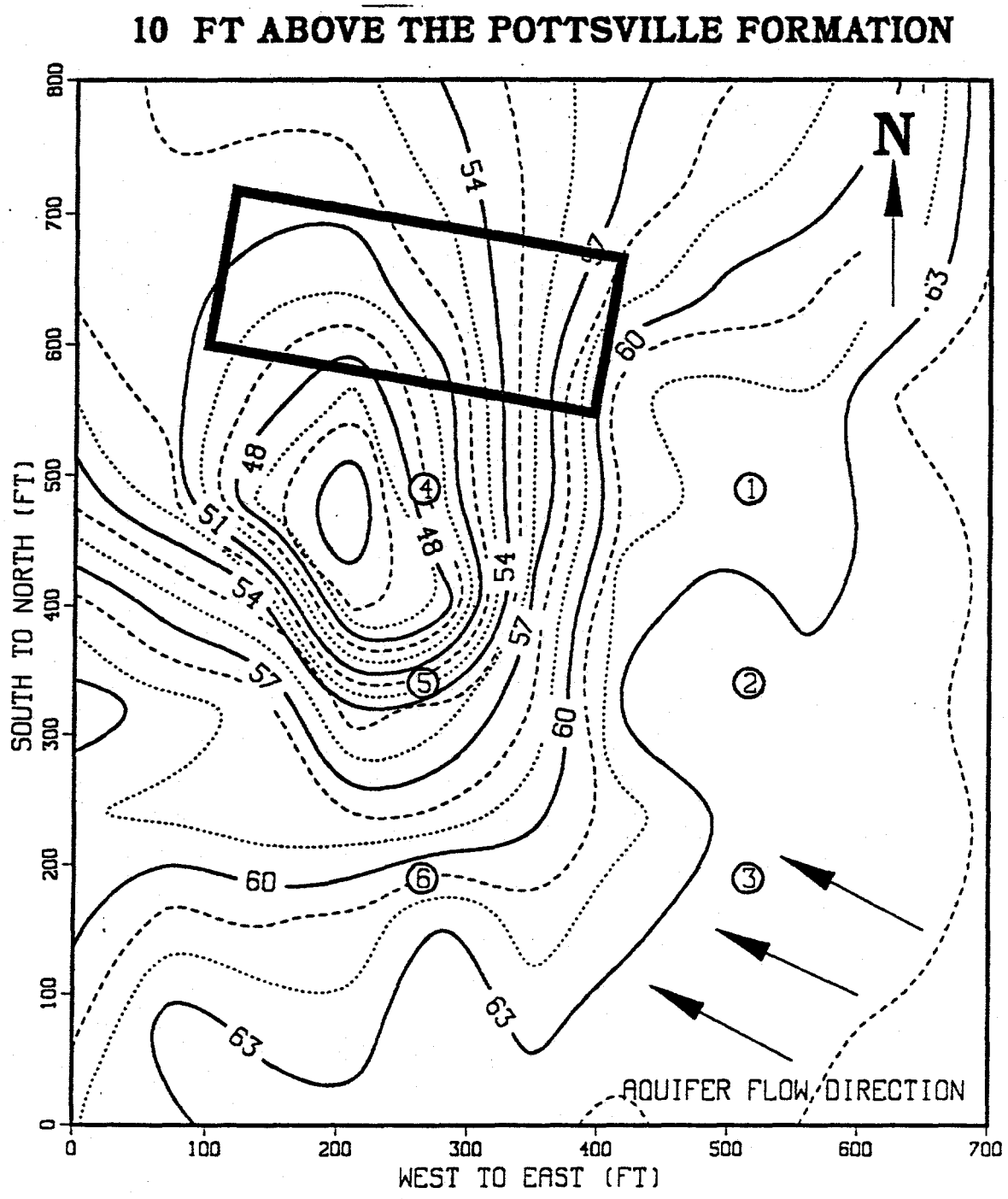


Figure 6. Isotherm contour plot; February 17, 1988.

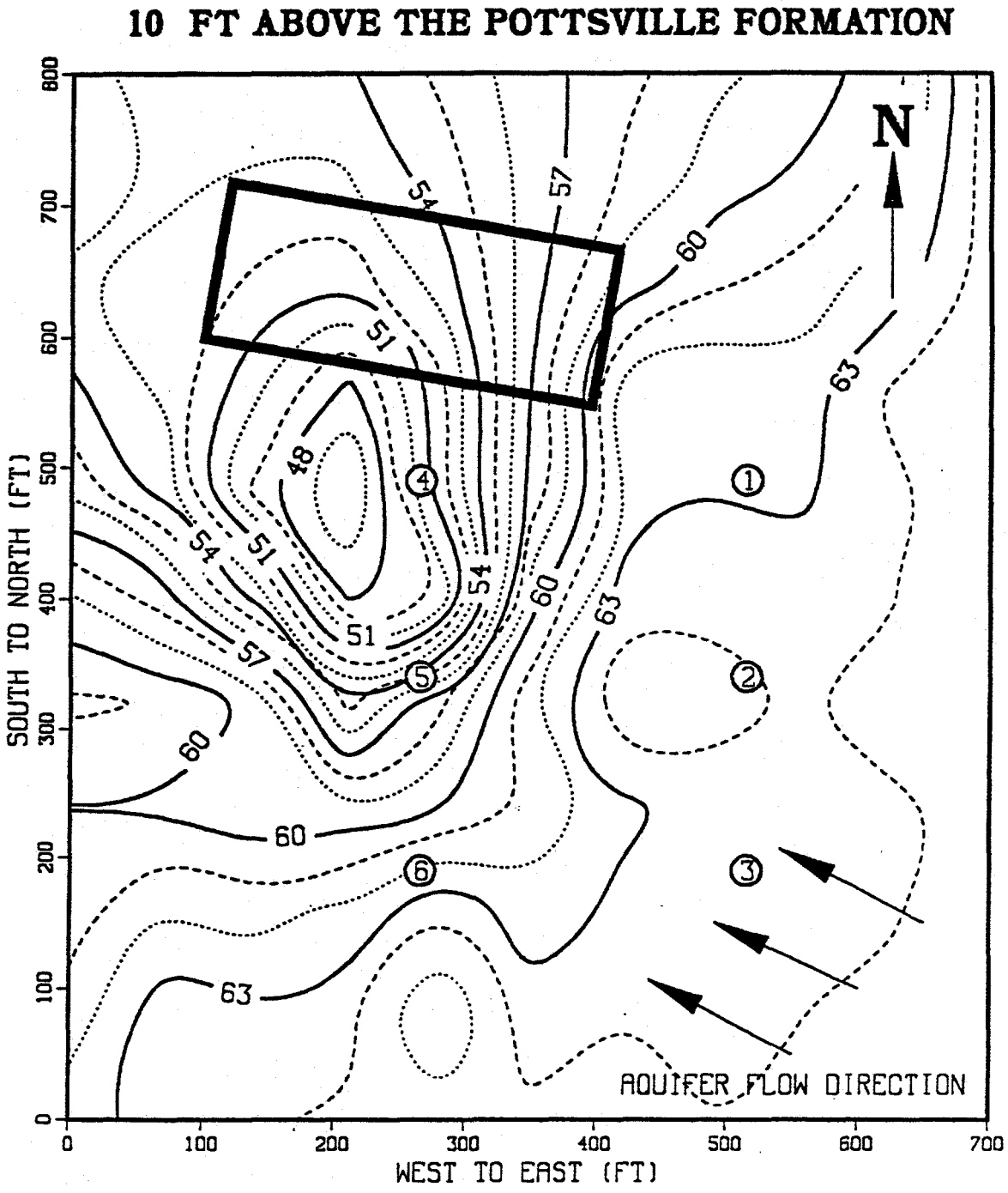


Figure 7. Isotherm contour plot; April 6, 1988.

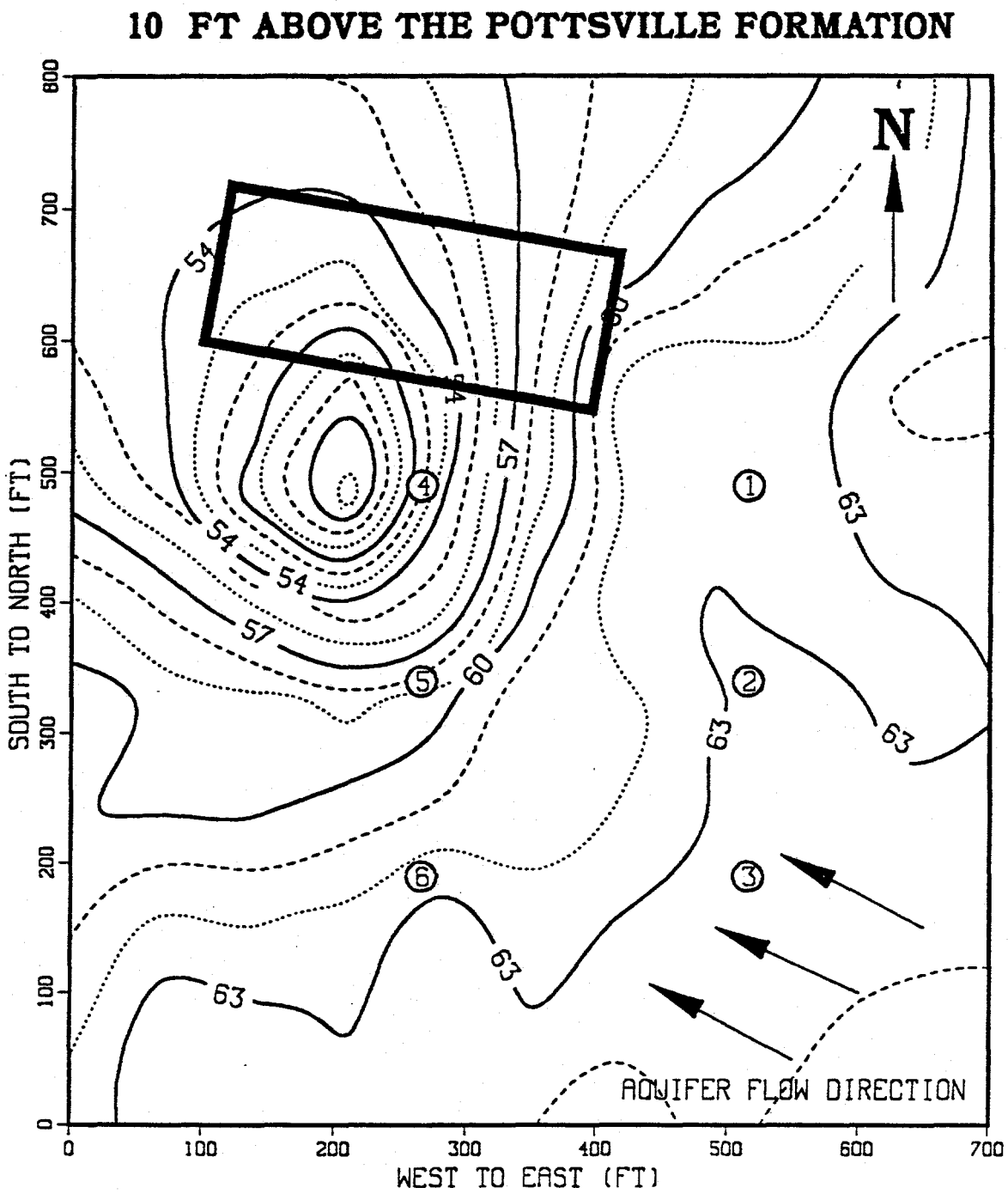


Figure 8. Isotherm contour plot; July 1, 1988.

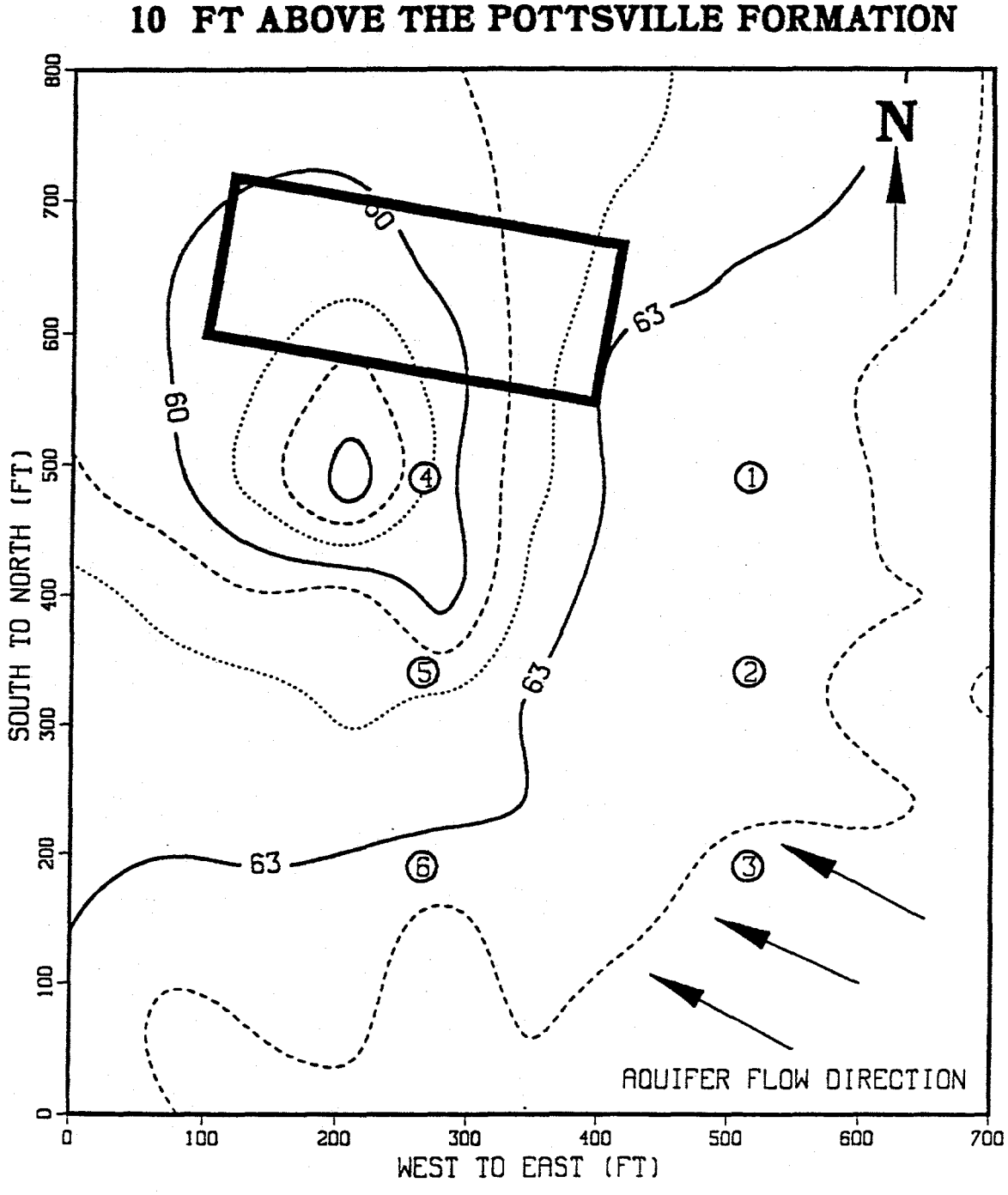


Figure 9. Isotherm contour plot; October 7, 1988.

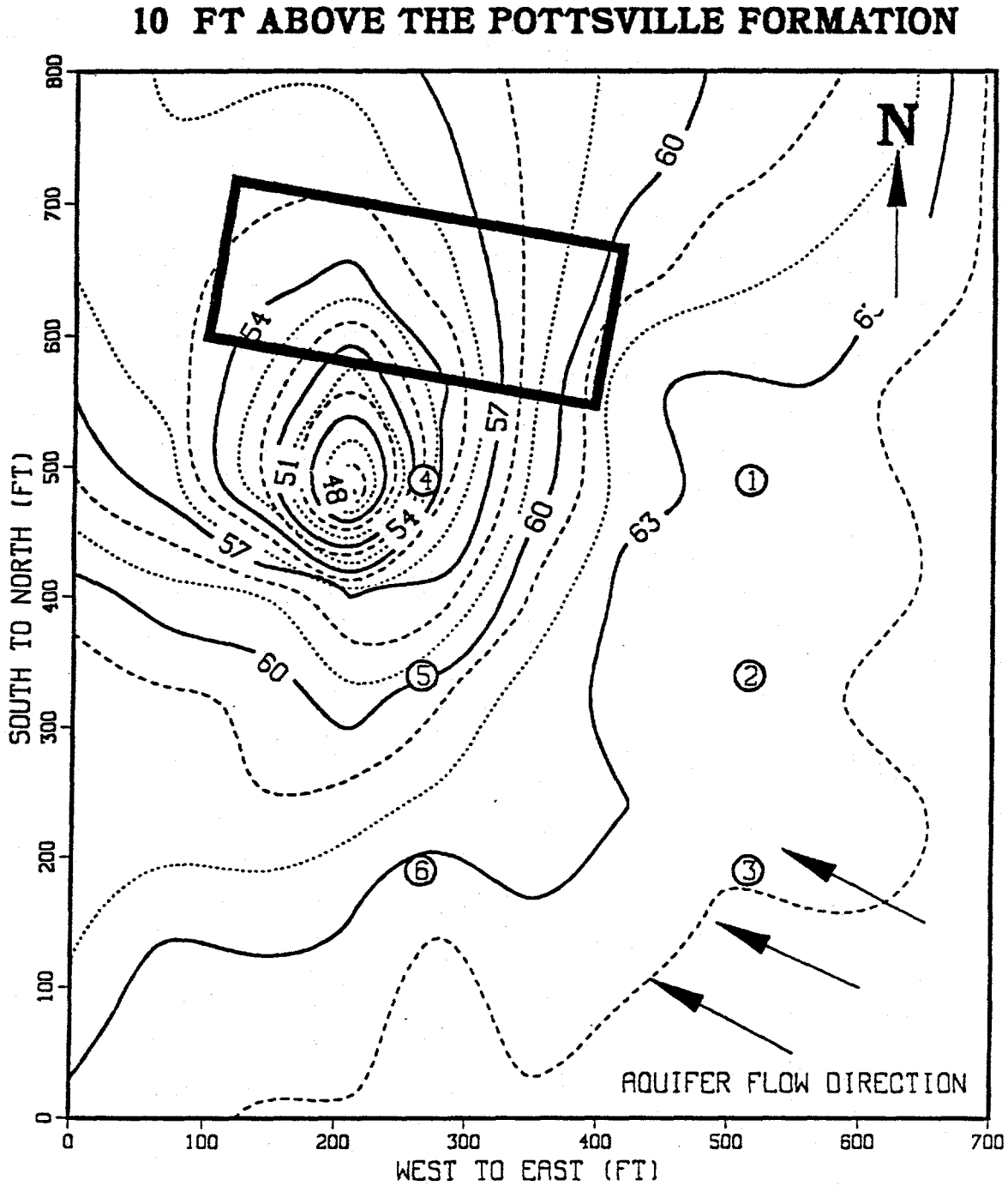


Figure 10. Isotherm contour plot; January 8, 1989.

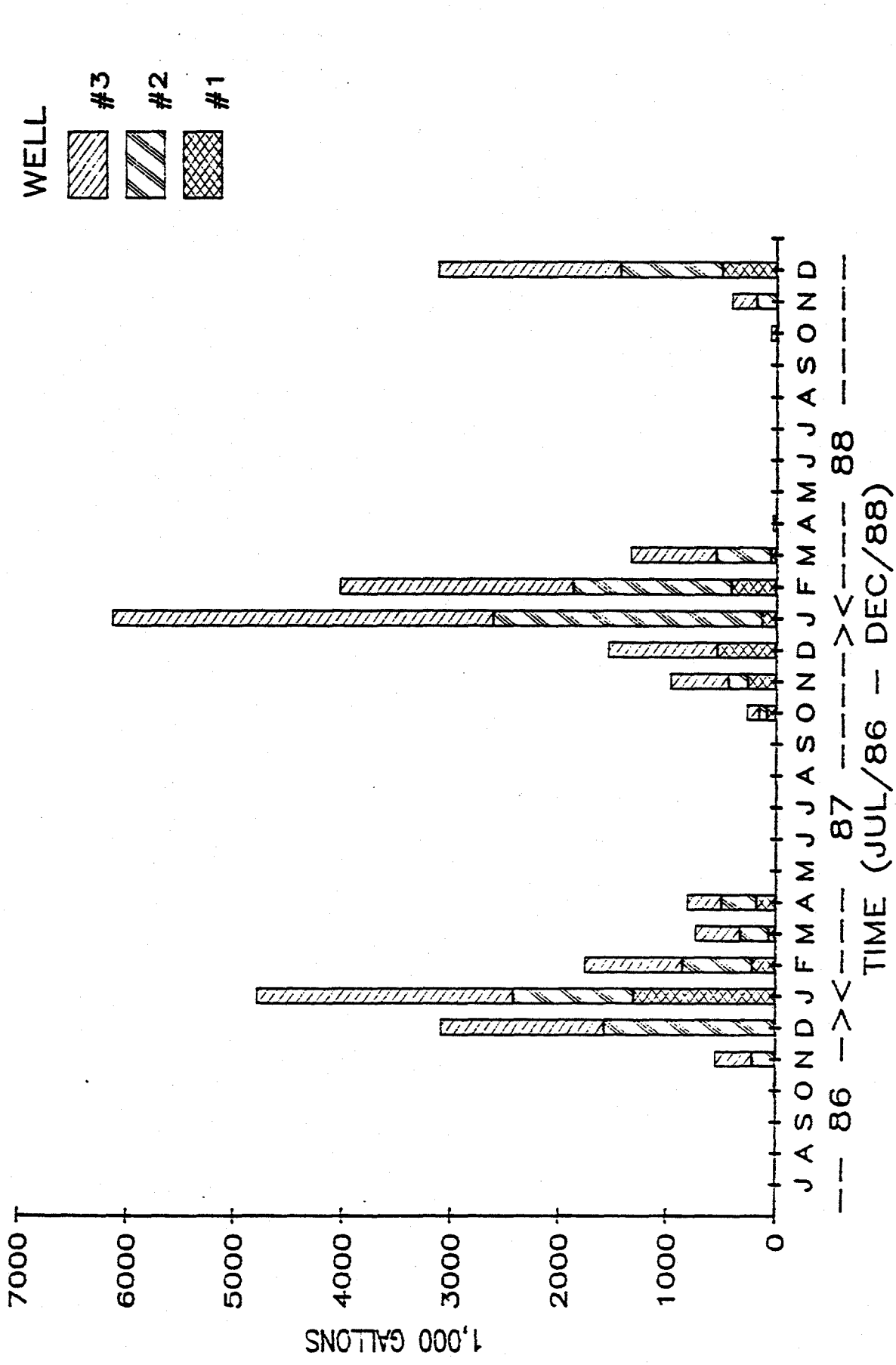


Figure 11. Cooling tower water cooling; monthly record.

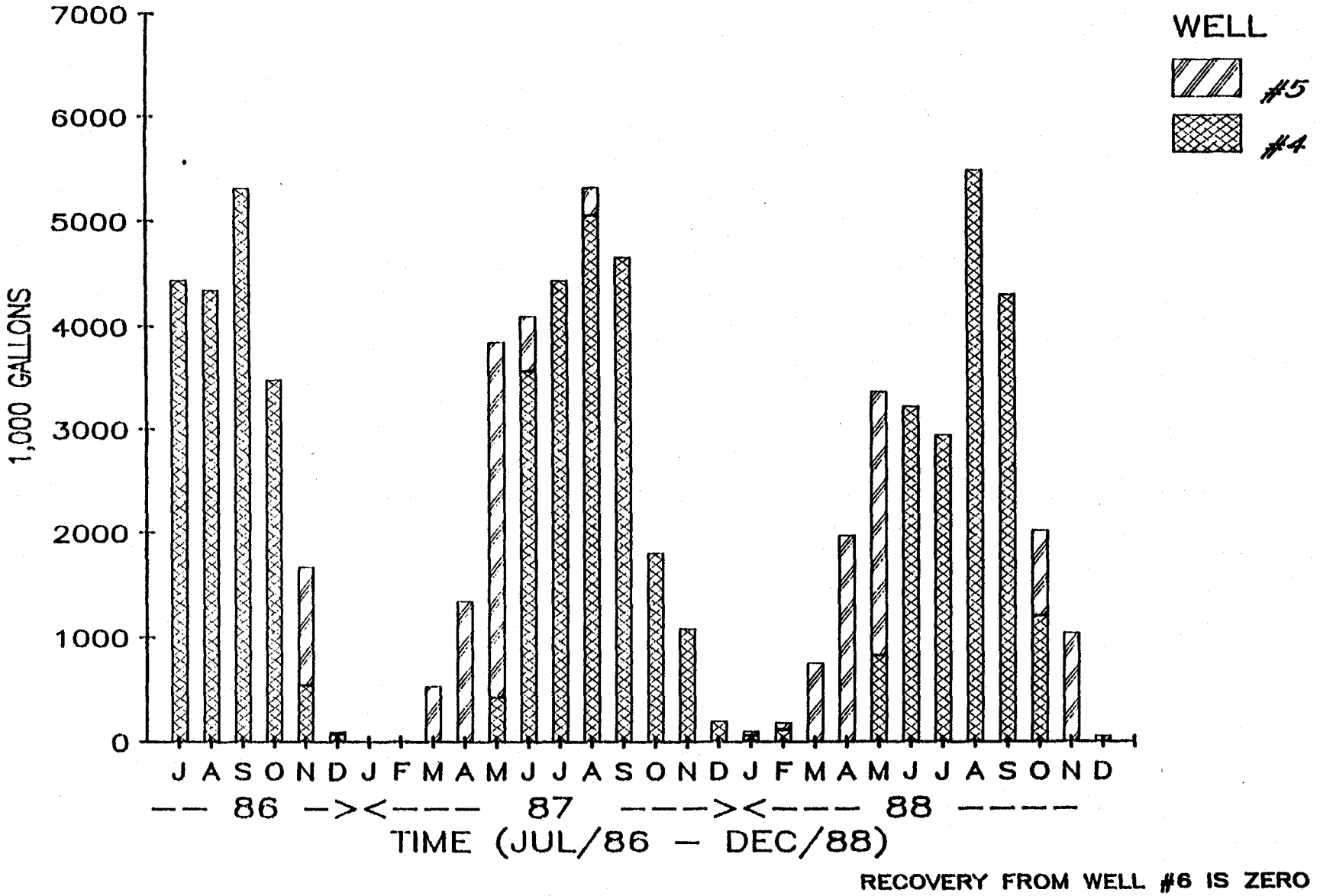


Figure 12. Water use for air-conditioning; monthly record.

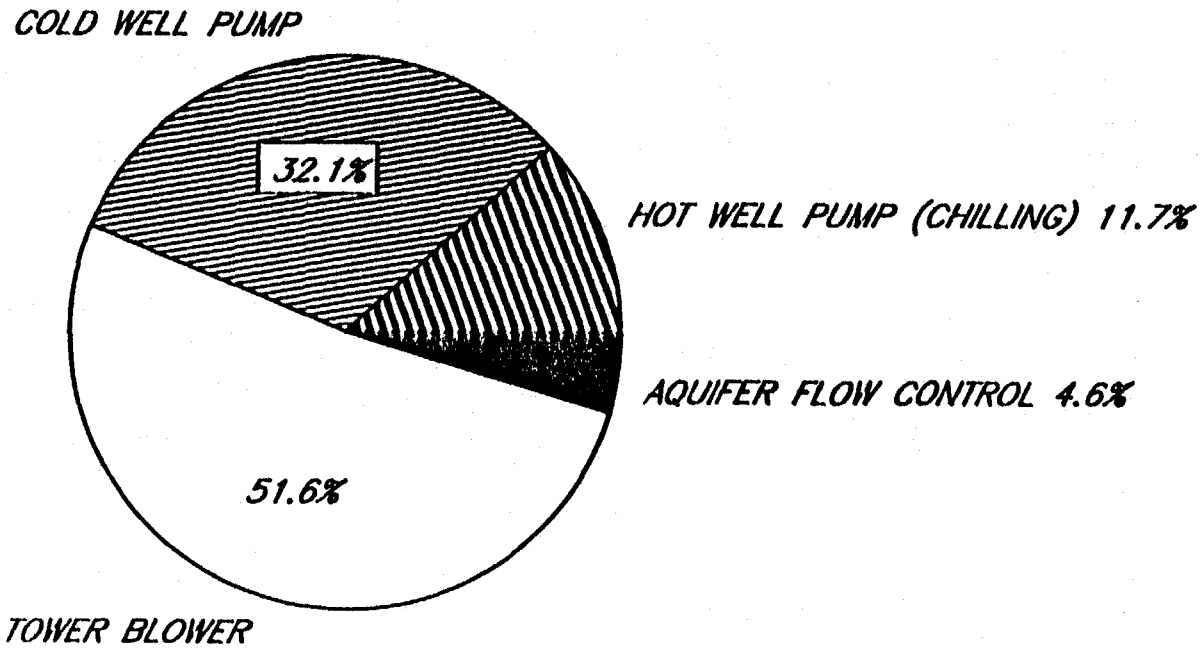


Figure 13. Electrical energy distribution between aquifer system components; October 1986 - September 1987 (total = 111,245 kWh).

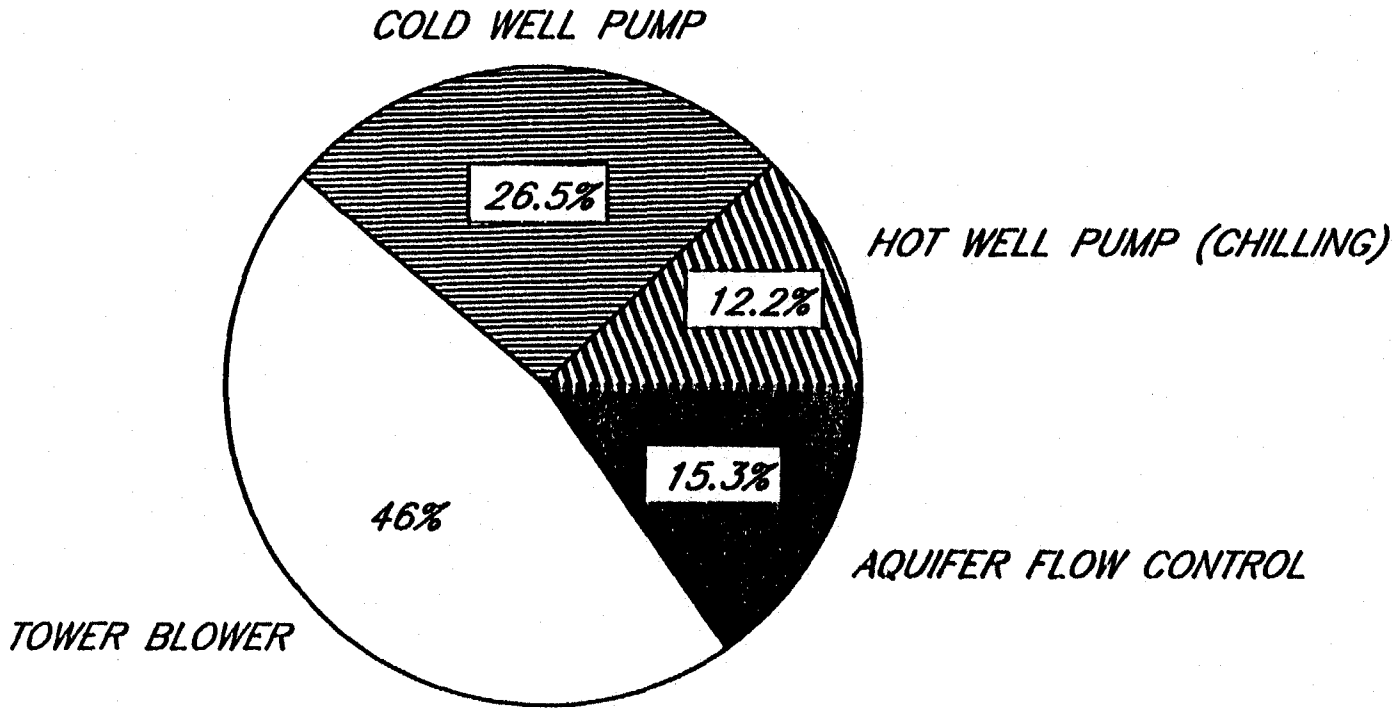


Figure 14. Electrical energy distribution between aquifer system components; October 1987 - September 1988 (total = 125,430 kWh).

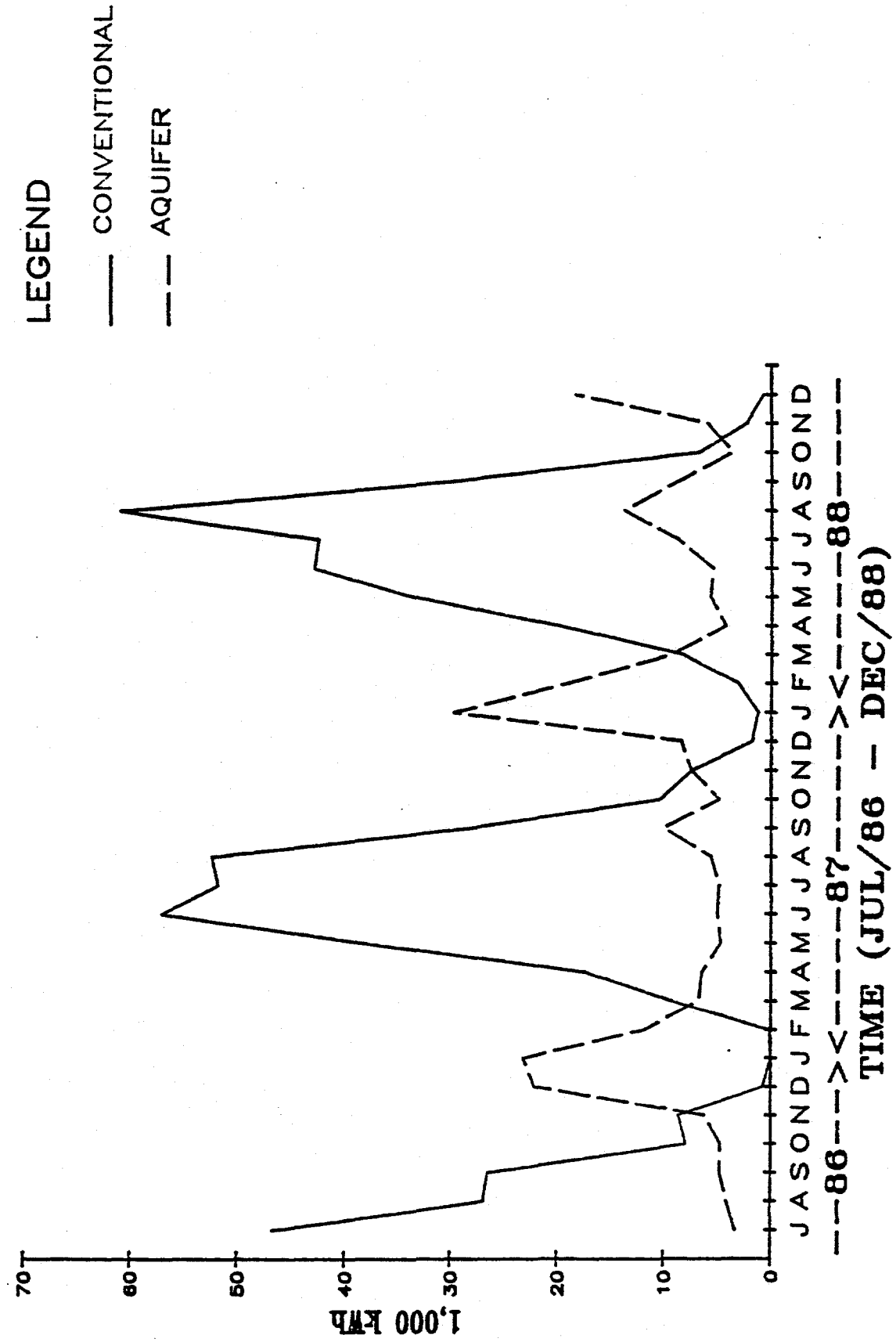


Figure 15. Monthly energy usage comparison between conventional and aquifer systems.

TABLE A1

JAN/87 - DEC/87 MONITOR WELL WATER LEVELS
at UA REC. CENTER ( [ft] above Sea Level )

| DATE | H4W | H1W | H2E | H4E | H6E | H4S |
|---|---|---|---|---|---|---|
| 01/07/87 | 210.61 | 211.90 | 211.71 | 211.80 | 214.16 | 212.88 |
| 01/14/87 | 210.67 | 211.97 | 211.88 | 211.86 | 214.06 | 213.00 |
| 01/19/87 | 210.66 | 211.95 | 211.85 | 211.83 | 213.77 | 213.02 |
| 01/26/87 | 211.68 | 212.81 | 212.29 | 210.98 | 214.10 | 213.05 |
| 02/02/87 | 210.38 | 212.33 | 212.42 | 212.62 | 214.14 | 213.09 |
| 02/09/87 | 210.37 | 213.22 | 212.76 | 212.54 | 214.12 | 213.07 |
| 02/18/87 | 212.03 | 213.59 | 212.95 | 212.47 | 214.11 | 213.62 |
| 02/27/87 | 212.68 | 213.73 | 213.11 | 212.53 | 214.17 | 213.76 |
| 03/04/87 | 211.59 | 213.18 | 213.36 | 213.32 | 214.81 | 213.95 |
| 03/09/87 | 211.50 | 213.37 | 214.73 | 214.10 | 215.07 | 214.16 |
| 03/16/87 | 211.18 | 213.60 | 213.98 | 214.11 | 215.38 | 214.47 |
| 03/23/87 | 211.14 | 213.23 | 213.97 | 214.98 | 215.59 | 214.71 |
| 03/31/87 | 210.61 | 214.03 | 214.10 | 215.03 | 215.74 | 215.13 |
| 04/09/87 | 211.27 | 213.13 | 214.31 | 215.23 | 215.96 | 215.13 |
| 04/13/87 | 210.99 | 212.90 | 214.12 | 215.40 | 215.93 | 215.15 |
| 04/20/87 | 211.13 | 212.80 | 213.95 | 215.10 | 216.02 | 215.21 |
| 04/27/87 | 210.59 | 212.40 | 214.12 | 215.64 | 216.13 | 215.20 |
| 05/08/87 | 210.38 | 211.73 | 213.80 | 215.95 | 216.22 | 215.11 |
| 06/01/87 | 210.51 | 210.70 | 211.74 | 220.71 | 216.02 | 215.03 |
| 06/08/87 | 210.35 | 210.88 | 211.72 | 226.61 | 215.93 | 214.83 |
| 06/18/87 | 210.80 | 211.02 | 212.42 | 251.32 | 215.72 | 214.75 |
| 06/25/87 | 210.67 | 210.82 | 211.55 | 248.01 | 215.87 | 214.77 |
| 07/07/87 | 210.43 | 211.38 | 211.53 | 243.37 | 215.77 | 214.72 |
| 07/14/87 | 210.25 | 210.52 | 211.64 | 241.61 | 215.69 | 214.65 |
| 07/23/87 | 209.82 | 210.33 | 211.07 | 240.85 | 215.69 | 214.58 |
| 08/04/87 | 209.60 | 210.04 | 210.74 | 240.85 | 215.50 | 214.42 |
| 08/17/87 | 209.33 | 209.65 | 210.36 | 238.64 | 215.46 | 214.24 |
| 08/24/87 | 209.27 | 209.45 | 210.26 | 238.14 | 215.36 | 214.11 |
| 08/31/87 | 209.08 | 208.95 | 209.86 | 237.71 | 215.21 | 214.00 |
| 09/10/87 | 208.98 | 208.57 | 208.36 | 236.81 | 214.97 | 213.83 |
| 09/14/87 | 208.77 | 208.02 | 207.72 | 233.09 | 214.71 | 213.60 |
| 09/21/87 | 208.49 | 207.33 | 206.90 | 227.61 | 214.45 | 213.30 |
| 09/30/87 | 208.28 | 207.64 | 208.44 | 225.94 | 214.46 | 213.00 |
| 10/07/87 | 208.32 | 208.96 | 209.85 | 225.63 | 214.48 | 212.90 |
| 10/14/87 | 208.39 | 209.70 | 210.71 | 225.34 | 214.57 | 212.89 |
| 10/21/87 | 208.37 | 209.70 | 211.06 | 225.14 | 214.55 | 212.94 |
| 10/29/87 | 208.47 | 210.46 | 211.15 | 224.92 | 214.66 | 213.00 |
| 11/05/87 | 208.36 | 210.27 | 211.36 | 224.74 | 214.70 | 213.07 |
| 11/12/87 | 208.44 | 210.84 | 211.29 | 224.56 | 214.65 | 213.11 |
| 11/19/87 | 208.54 | 210.56 | 211.27 | 224.40 | 214.60 | 213.11 |
| 11/25/87 | 208.43 | 211.01 | 211.43 | 224.20 | 214.61 | 213.09 |
| 12/03/87 | 208.50 | 211.23 | 211.32 | 225.46 | 214.56 | 213.04 |
| 12/10/87 | 208.45 | 211.20 | 211.42 | 225.26 | 215.48 | 213.02 |
| 12/18/87 | 208.52 | 211.78 | 211.26 | 225.05 | 214.43 | 212.98 |
| 12/24/87 | 208.40 | 211.25 | 211.21 | 225.05 | 214.32 | 212.92 |

# TABLE A2

JAN/88 - DEC/88 MONITOR WELL WATER LEVELS
at UA REC. CENTER ( [ft] above Sea Level )

| DATE | H4W | H1W | H2E | H4E | H6E | H4S |
|---|---|---|---|---|---|---|
| 01/11/88 | 208.88 | 212.57 | 211.18 | 225.33 | 214.21 | 212.83 |
| 01/21/88 | 209.03 | 211.37 | 210.96 | 230.79 | 214.04 | 212.52 |
| 01/27/88 | 209.46 | 213.18 | 211.17 | 225.57 | 214.06 | 212.64 |
| 02/08/88 | 209.56 | 212.95 | 211.65 | 219.44 | 214.11 | 212.76 |
| 02/17/88 | 209.68 | 212.52 | 211.61 | 219.95 | 214.05 | 212.87 |
| 02/24/88 | 209.44 | 211.66 | 211.58 | 219.86 | 214.14 | 212.92 |
| 02/29/88 | 209.46 | 211.53 | 211.18 | 211.93 | 214.15 | 212.96 |
| 03/07/88 | 209.35 | 211.29 | 211.82 | 218.51 | 214.26 | 212.96 |
| 03/21/88 | 209.31 | 211.36 | 211.73 | 213.28 | 214.30 | 213.04 |
| 03/28/88 | 209.27 | 210.92 | 211.71 | 212.94 | 214.32 | 213.04 |
| 03/31/88 | 209.23 | 210.66 | 211.81 | 213.02 | 214.41 | 213.08 |
| 04/06/88 | 209.14 | 210.52 | 211.80 | 213.43 | 214.39 | 213.09 |
| 04/14/88 | 209.07 | 210.87 | 211.70 | 212.65 | 214.46 | 213.10 |
| 04/20/88 | 209.10 | 210.57 | 211.65 | 212.70 | 214.35 | 213.10 |
| 04/26/88 | 209.11 | 210.34 | 211.74 | 213.49 | 214.39 | 213.11 |
| 05/06/88 | 208.95 | 210.25 | 211.62 | 213.47 | 214.41 | 213.10 |
| 05/13/88 | 208.86 | 209.89 | 211.59 | 212.20 | 214.38 | 213.06 |
| 05/23/88 | 208.63 | 209.22 | 210.07 | 211.69 | 214.42 | 212.91 |
| 05/29/88 | 208.54 | 209.42 | 209.75 | 210.12 | 213.99 | 212.81 |
| 06/04/88 | 208.35 | 208.58 | 208.19 | 209.34 | 213.69 | 212.65 |
| 06/10/88 | 208.19 | 208.57 | 209.48 | 210.88 | 213.68 | 212.46 |
| 06/17/88 | 208.17 | 208.86 | 209.78 | 211.33 | 213.75 | 212.38 |
| 06/24/88 | 208.08 | 208.52 | 209.76 | 211.41 | 213.70 | 212.34 |
| 07/01/88 | 208.02 | 208.31 | 209.61 | 211.33 | 213.66 | 212.29 |
| 07/08/88 | 208.11 | 208.68 | 209.83 | 211.40 | 213.65 | 212.26 |
| 07/15/88 | 208.02 | 207.36 | 207.40 | 208.45 | 213.42 | 212.20 |
| 07/21/88 | 207.87 | 206.46 | 206.34 | 207.39 | 213.31 | 212.10 |
| 07/29/88 | 207.61 | 205.87 | 206.31 | 206.82 | 213.01 | 211.80 |
| 08/05/88 | 207.42 | 205.72 | 204.69 | 206.09 | 213.06 | 211.54 |
| 08/12/88 | 207.25 | 205.70 | 205.29 | 206.91 | 213.04 | 211.40 |
| 08/19/88 | 207.07 | 205.67 | 204.68 | 206.11 | 213.08 | 211.18 |
| 08/26/88 | 206.86 | 204.66 | 204.17 | 205.74 | 212.45 | 210.92 |
| 09/05/88 | 206.68 | 205.71 | 205.80 | 207.19 | 212.25 | 210.57 |
| 09/09/88 | 206.67 | 205.79 | 206.30 | 208.20 | 212.36 | 210.50 |
| 09/19/88 | 206.57 | 204.34 | 204.31 | 205.81 | 212.14 | 210.40 |
| 09/23/88 | 206.49 | 203.86 | 203.80 | 205.42 | 212.12 | 210.36 |
| 09/30/88 | 206.37 | 204.31 | 205.11 | 207.10 | 212.10 | 210.18 |
| 10/07/88 | 206.59 | 206.36 | 207.00 | 208.46 | 212.18 | 210.17 |
| 10/14/88 | 206.67 | 206.99 | 207.64 | 208.68 | 212.29 | 210.29 |
| 10/21/88 | 206.73 | 207.34 | 208.02 | 209.19 | 212.32 | 210.43 |
| 10/28/88 | 206.84 | 206.84 | 207.70 | 209.49 | 212.47 | 210.57 |
| 11/05/88 | 206.84 | 206.98 | 208.07 | 209.63 | 212.42 | 210.70 |
| 11/12/88 | 207.01 | 208.02 | 208.84 | 209.97 | 212.59 | 210.79 |
| 11/19/88 | 207.20 | 208.46 | 209.21 | 210.14 | 212.72 | 210.83 |
| 11/28/88 | 207.78 | 208.97 | 209.44 | 210.03 | 212.64 | 210.97 |
| 12/03/88 | 207.86 | 209.91 | 210.09 | 209.65 | 212.62 | 211.05 |
| 12/12/88 | 207.97 | 210.66 | 210.59 | 210.12 | 212.62 | 211.10 |

TABLE A3

AQUIFER FLOW ANGLE AND SLOPE (JAN/87 - DEC/87)

| DATE | FLOW ANGLE (CLOCKWISE FROM N) | FLOW SLOPE |
|---|---|---|
| 01/07/87 | 285.3 | 2.1912E-03 |
| 01/14/87 | 290.3 | 2.1509E-03 |
| 01/19/87 | 297.0 | 2.0784E-03 |
| 01/26/87 | 277.4 | 1.4525E-03 |
| 02/02/87 | 293.5 | 2.4408E-03 |
| 02/09/87 | 293.4 | 2.4330E-03 |
| 02/18/87 | 297.5 | 1.3963E-03 |
| 02/27/87 | 293.9 | 9.7011E-04 |
| 03/04/87 | 294.7 | 2.1091E-03 |
| 03/09/87 | 295.8 | 2.3601E-03 |
| 03/16/87 | 299.2 | 2.8639E-03 |
| 03/23/87 | 300.8 | 3.0839E-03 |
| 03/31/87 | 306.9 | 3.8207E-03 |
| 04/09/87 | 302.5 | 3.3104E-03 |
| 04/13/87 | 304.0 | 3.5476E-03 |
| 04/20/87 | 303.4 | 3.4870E-03 |
| 04/27/87 | 303.2 | 3.9425E-03 |
| 05/08/87 | 301.4 | 4.0744E-03 |
| 06/01/87 | 302.3 | 3.8798E-03 |
| 06/08/87 | 300.9 | 3.8690E-03 |
| 06/18/87 | 300.9 | 3.4113E-03 |
| 06/25/87 | 299.6 | 3.5612E-03 |
| 07/07/87 | 300.9 | 3.7043E-03 |
| 07/14/87 | 301.3 | 3.7917E-03 |
| 07/23/87 | 301.5 | 4.0988E-03 |
| 08/04/87 | 302.0 | 4.1419E-03 |
| 08/17/87 | 300.7 | 4.2434E-03 |
| 08/24/87 | 300.2 | 4.1931E-03 |
| 08/31/87 | 300.8 | 4.2494E-03 |
| 09/10/87 | 301.4 | 4.1782E-03 |
| 09/14/87 | 301.7 | 4.1559E-03 |
| 09/21/87 | 301.2 | 4.1476E-03 |
| 09/30/87 | 297.5 | 4.1464E-03 |
| 10/07/87 | 295.6 | 4.0674E-03 |
| 10/14/87 | 294.2 | 4.0335E-03 |
| 10/21/87 | 295.3 | 4.0680E-03 |
| 10/29/87 | 294.6 | 4.0511E-03 |
| 11/05/87 | 295.6 | 4.1843E-03 |
| 11/12/87 | 296.4 | 4.1276E-03 |
| 11/19/87 | 296.6 | 4.0347E-03 |
| 11/25/87 | 296.6 | 4.1143E-03 |
| 12/03/87 | 296.2 | 4.0190E-03 |
| 12/10/87 | 286.5 | 4.3633E-03 |
| 12/18/87 | 296.7 | 3.9364E-03 |
| 12/24/87 | 297.5 | 3.9712E-03 |

TABLE A4

AQUIFER FLOW ANGLE AND SLOPE (JAN/88 - DEC/88)

| DATE | FLOW ANGLE (CLOCKWISE FROM N) | FLOW SLOPE |
|---|---|---|
| 01/11/88 | 295.4 | 3.5128E-03 |
| 01/21/88 | 291.2 | 3.1981E-03 |
| 01/27/88 | 290.7 | 2.9261E-03 |
| 02/08/88 | 291.8 | 2.9176E-03 |
| 02/17/88 | 294.4 | 2.8560E-03 |
| 02/24/88 | 295.4 | 3.0960E-03 |
| 02/29/88 | 295.9 | 3.1034E-03 |
| 03/07/88 | 294.9 | 3.2216E-03 |
| 03/21/88 | 296.0 | 3.3050E-03 |
| 03/28/88 | 295.9 | 3.3423E-03 |
| 03/31/88 | 295.6 | 3.4196E-03 |
| 04/06/88 | 296.5 | 3.4906E-03 |
| 04/14/88 | 296.0 | 3.5705E-03 |
| 04/20/88 | 297.3 | 3.5172E-03 |
| 04/26/88 | 296.9 | 3.5250E-03 |
| 05/06/88 | 297.2 | 3.6525E-03 |
| 05/13/88 | 297.2 | 3.6950E-03 |
| 05/23/88 | 295.2 | 3.8105E-03 |
| 05/27/88 | 298.1 | 3.6587E-03 |
| 05/29/88 | 299.2 | 3.7167E-03 |
| 06/04/88 | 301.1 | 3.7103E-03 |
| 06/10/88 | 298.7 | 3.7261E-03 |
| 06/17/88 | 296.6 | 3.7161E-03 |
| 06/24/88 | 297.0 | 3.7533E-03 |
| 07/01/88 | 296.9 | 3.7639E-03 |
| 07/08/88 | 296.2 | 3.6739E-03 |
| 07/15/88 | 298.4 | 3.6538E-03 |
| 07/21/88 | 298.7 | 3.6916E-03 |
| 07/29/88 | 298.6 | 3.6594E-03 |
| 08/05/88 | 294.4 | 3.6875E-03 |
| 08/12/88 | 293.1 | 3.7478E-03 |
| 08/19/88 | 289.9 | 3.8048E-03 |
| 08/26/88 | 294.0 | 3.6434E-03 |
| 09/05/88 | 291.4 | 3.5598E-03 |
| 09/09/88 | 288.8 | 3.5784E-03 |
| 09/19/88 | 290.3 | 3.5347E-03 |
| 09/23/88 | 290.3 | 3.5723E-03 |
| 09/30/88 | 288.0 | 3.5861E-03 |
| 10/07/88 | 285.4 | 3.4521E-03 |
| 10/14/88 | 285.8 | 3.4772E-03 |
| 10/21/88 | 287.7 | 3.4924E-03 |
| 10/28/88 | 287.7 | 3.5186E-03 |
| 11/05/88 | 290.7 | 3.5506E-03 |
| 11/12/88 | 289.3 | 3.5184E-03 |
| 11/19/88 | 287.2 | 3.4403E-03 |
| 11/28/88 | 287.1 | 3.0269E-03 |
| 12/03/88 | 288.5 | 2.9882E-03 |
| 12/12/88 | 288.8 | 2.9243E-03 |

TABLE A5

COOLING TOWER AND TEMPERATURE DATA

| MONTH | TOWER FLOW 1,000 Gallons | TOWER TEMPERATURE F T in | T out | BUILDING FLOW 1,000 Gallons | BUILDING TEMPERATUR F T in | T out |
|---|---|---|---|---|---|---|
| OCT/86 | 1 | 62.0 | 47.0 | 3482 | 63.4 | 65.5 |
| NOV/86 | 556 | 62.0 | 43.3 | 1670 | 59.5 | 64.1 |
| DEC/86 | 3093 | 62.6 | 43.6 | 96 | 45.0 | 52.0 |
| JAN/87 | 4785 | 66.7 | 42.2 | 0 | 0.0 | 0.0 |
| FEB/87 | 1763 | 66.0 | 42.9 | 11 | 46.0 | 55.0 |
| MAR/87 | 737 | 65.6 | 42.8 | 529 | 46.0 | 61.7 |
| APR/87 | 811 | 64.0 | 43.5 | 1347 | 48.3 | 59.9 |
| MAY/87 | 0 | 0.0 | 0.0 | 3849 | 56.4 | 65.3 |
| JUN/87 | 0 | 0.0 | 0.0 | 4099 | 51.9 | 64.5 |
| JUL/87 | 0 | 0.0 | 0.0 | 4442 | 57.1 | 67.6 |
| AUG/87 | 0 | 0.0 | 0.0 | 5327 | 60.4 | 69.2 |
| SEP/87 | 0 | 0.0 | 0.0 | 4665 | 61.7 | 67.1 |
| OCT/87 | 273 | 65.0 | 44.0 | 1802 | 53.9 | 59.1 |
| NOV/87 | 973 | 63.2 | 42.6 | 1087 | 54.0 | 60.1 |
| DEC/87 | 1553 | 61.8 | 42.7 | 200 | 46.0 | 54.0 |
| JAN/88 | 6142 | 62.2 | 41.2 | 98 | 44.0 | 55.0 |
| FEB/88 | 4035 | 62.9 | 42.6 | 185 | 43.0 | 58.0 |
| MAR/88 | 1343 | 63.0 | 44.0 | 752 | 45.0 | 56.0 |
| APR/88 | 41 | 61.0 | 45.0 | 1975 | 51.0 | 60.0 |
| MAY/88 | 0 | 0.0 | 0.0 | 3364 | 55.0 | 64.0 |
| JUN/88 | 0 | 0.0 | 0.0 | 3220 | 50.0 | 62.0 |
| JUL/88 | 0 | 0.0 | 0.0 | 2946 | 54.0 | 67.0 |
| AUG/88 | 0 | 0.0 | 0.0 | 5494 | 58.0 | 68.0 |
| SEP/88 | 0 | 0.0 | 0.0 | 4485 | 61.0 | 67.0 |
| OCT/88 | 62 | 63.0 | 44.0 | 2020 | 62.0 | 65.0 |
| NOV/88 | 422 | 62.0 | 44.0 | 1042 | 62.0 | 64.0 |
| DEC/88 | 3126 | 62.0 | 40.0 | 57 | 45.0 | 56.0 |
| TOTALS | | | | | | |
| (OCT/86-SEP/87): | 11746 | 64 | 44 | 29516 | 54 | 63 |
| (OCT/87-SEP/88): | 14359 | 63 | 43 | 25606 | 51 | 61 |
| (JAN/87-DEC/87): | 10895 | 65 | 43 | 27356 | 53 | 62 |
| (JAN/88-DEC/88): | 15171 | 62 | 43 | 25637 | 53 | 62 |

TABLE A6

AQUIFER SYSTEM THERMAL ENERGY FLOWS

| MONTH | TOTAL WATER FLOW THROUGH COOLING TOWER (1,000 Gal) | TOTAL REJECTED ENERGY COOLING TOWER (1,000 Btu) | TOTAL WATER FLOW THROUGH RECREATION CENTER (1,000 Gal) | TOTAL AIR-COND PROVIDED RECREATION CENTER (1,000 Btu) | STORED CHILL RECOVERED FROM AQUIFER (1,000 Btu) |
|---|---|---|---|---|---|
| JUL/86 | 0 | 0 | 4837 | 350542 | 282045 |
| AUG/86 | 0 | 0 | 4345 | 201656 | 182697 |
| SEP/86 | 0 | 0 | 5318 | 198272 | 113901 |
| OCT/86 | 1 | 112 | 3482 | 59322 | 46139 |
| NOV/86 | 556 | 86454 | 1670 | 64505 | 64505 |
| DEC/86 | 3093 | 489513 | 96 | 5598 | 5598 |
| JAN/87 | 4785 | 975259 | 0 | 0 | 0 |
| FEB/87 | 1763 | 338939 | 11 | 847 | 847 |
| MAR/87 | 737 | 140012 | 529 | 68997 | 68997 |
| APR/87 | 811 | 138507 | 1347 | 130935 | 130935 |
| MAY/87 | 0 | 0 | 3849 | 286927 | 277309 |
| JUN/87 | 0 | 0 | 4099 | 428350 | 428350 |
| JUL/87 | 0 | 0 | 4442 | 388493 | 292631 |
| AUG/87 | 0 | 0 | 5327 | 393041 | 204973 |
| SEP/87 | 0 | 0 | 4665 | 210929 | 129518 |
| OCT/87 | 273 | 47773 | 1802 | 77534 | 77534 |
| NOV/87 | 973 | 166879 | 1087 | 55329 | 55329 |
| DEC/87 | 1553 | 247039 | 200 | 13301 | 13301 |
| JAN/88 | 6142 | 1074333 | 98 | 8943 | 8943 |
| FEB/88 | 4035 | 679417 | 185 | 23066 | 23066 |
| MAR/88 | 1343 | 212572 | 752 | 61942 | 61942 |
| APR/88 | 41 | 5491 | 1975 | 148036 | 148036 |
| MAY/88 | 0 | 0 | 3364 | 252214 | 252214 |
| JUN/88 | 0 | 0 | 3220 | 321881 | 321881 |
| JUL/88 | 0 | 0 | 2946 | 319022 | 269942 |
| AUG/88 | 0 | 0 | 5494 | 457650 | 320355 |
| SEP/88 | 0 | 0 | 4485 | 224160 | 149440 |
| OCT/88 | 62 | 9813 | 2020 | 50480 | 50480 |
| NOV/88 | 422 | 63275 | 1042 | 17360 | 26040 |
| DEC/88 | 3126 | 572871 | 57 | 5223 | 9496 |
| TOTALS | | | | | |
| (OCT/86-SEP/87): | 11746 | 2168798 | 29516 | 2037943 | 1649802 |
| % STORED Btu | | | | (94%) | (76%) |
| (OCT/87-SEP/88): | 14359 | 2433504 | 25606 | 1963079 | 1701983 |
| % STORED Btu | | | | (81%) | (70%) |
| (JAN/87-DEC/87): | 10895 | 2054409 | 27356 | 2054683 | 1679724 |
| % STORED Btu | | | | (100%) | (82%) |
| (JAN/88-DEC/88): | 15171 | 2617771 | 25637 | 1889977 | 1641835 |
| % STORED Btu | | | | (72%) | (63%) |

TABLE A7

AQUIFER SYSTEM ELECTRICAL POWER USAGE

| DATE | HOT WELL PUMPS kWh | COLD WELL PUMPS kWh | TOWER BLOWER kWh | TOTAL kWh |
|---|---|---|---|---|
| JUL/86 | 0 | 3342 | 0 | 3342 |
| AUG/86 | 0 | 4114 | 0 | 4114 |
| SEP/86 | 0 | 4780 | 0 | 4780 |
| OCT/86 | 1 | 4468 | 248 | 4716 |
| NOV/86 | 431 | 2605 | 3178 | 6214 |
| DEC/86 | 3346 | 402 | 18370 | 22117 |
| JAN/87 | 4960 | 0 | 18228 | 23187 |
| FEB/87 | 2409 | 16 | 9406 | 11831 |
| MAR/87 | 864 | 1040 | 4803 | 6706 |
| APR/87 | 1004 | 2143 | 3306 | 6453 |
| MAY/87 | 0 | 4679 | 0 | 4679 |
| JUN/87 | 0 | 5030 | 0 | 5030 |
| JUL/87 | 0 | 4840 | 0 | 4840 |
| AUG/87 | 0 | 5611 | 0 | 5611 |
| SEP/87 | 5104 | 4936 | 0 | 10040 |
| OCT/87 | 683 | 1913 | 2250 | 4845 |
| NOV/87 | 908 | 1707 | 4824 | 7439 |
| DEC/87 | 1308 | 546 | 6576 | 8430 |
| JAN/88 | 6797 | 377 | 22548 | 29722 |
| FEB/88 | 4338 | 451 | 14229 | 19018 |
| MAR/88 | 1259 | 1526 | 6556 | 9342 |
| APR/88 | 25 | 3302 | 930 | 4257 |
| MAY/88 | 1073 | 4618 | 0 | 5691 |
| JUN/88 | 958 | 4483 | 0 | 5441 |
| JUL/88 | 4279 | 4439 | 0 | 8718 |
| AUG/88 | 7970 | 5820 | 0 | 13790 |
| SEP/88 | 4487 | 4250 | 0 | 8737 |
| OCT/88 | 65 | 2520 | 1024 | 3609 |
| NOV/88 | 520 | 1344 | 4139 | 6003 |
| DEC/88 | 3654 | 94 | 14519 | 18267 |
| TOTALS | | | | |
| (OCT/86-SEP/87): | 18117 | 35770 | 57538 | 111425 |
| % TOT kWh | (16%) | (32%) | (52%) | |
| (OCT/87-SEP/88): | 34085 | 33433 | 57913 | 125430 |
| % TOT kWh | (27%) | (27%) | (46%) | |
| (JAN/87-DEC/87): | 17238 | 32461 | 49393 | 99092 |
| % TOT kWh | (17%) | (33%) | (50%) | |
| (JAN/88-DEC/88): | 35425 | 33225 | 63945 | 132595 |
| % TOT kWh | (27%) | (25%) | (48%) | |

# TABLE A8

## WEEKLY AQUIFER SYSTEM PERFORMANCE DATA

| DATE | 1,000 Btu Chilling | kWh* Tower | C.O.P. Tower | 1,000 Btu A/C | kWh C Pumps | kWh Back PMP | C.O.P. Building |
|---|---|---|---|---|---|---|---|
| 07/08/86 | 0 | 0 | 0.0 | 63246 | 809 | 0 | 22.9 |
| 07/15/86 | 0 | 0 | 0.0 | 60573 | 750 | 0 | 23.7 |
| 07/23/86 | 0 | 0 | 0.0 | 90254 | 914 | 0 | 28.9 |
| 07/30/86 | 0 | 0 | 0.0 | 65394 | 869 | 0 | 22.1 |
| 08/07/86 | 0 | 0 | 0.0 | 63968 | 995 | 0 | 18.9 |
| 08/15/86 | 0 | 0 | 0.0 | 58322 | 1027 | 0 | 16.6 |
| 08/22/86 | 0 | 0 | 0.0 | 44096 | 959 | 0 | 13.5 |
| 08/29/86 | 0 | 0 | 0.0 | 48495 | 1133 | 0 | 12.5 |
| 09/08/86 | 0 | 0 | 0.0 | 59627 | 1430 | 0 | 12.2 |
| 09/15/86 | 0 | 0 | 0.0 | 41291 | 1079 | 0 | 11.2 |
| 09/22/86 | 0 | 0 | 0.0 | 38634 | 1027 | 0 | 11.0 |
| 09/30/96 | 0 | 0 | 0.0 | 59148 | 1244 | 0 | 13.9 |
| 10/10/86 | 0 | 0 | 0.0 | 23595 | 1934 | 0 | 3.6 |
| 10/17/86 | 112 | 243 | 0.1 | 8224 | 931 | 0 | 2.6 |
| 10/24/86 | 0 | 4 | 0.0 | 4128 | 762 | 0 | 1.6 |
| 10/31/86 | 0 | 0 | 0.0 | 4727 | 842 | 0 | 1.6 |
| 11/07/86 | 0 | 0 | 0.0 | 18583 | 1072 | 0 | 5.1 |
| 11/14/86 | 4732 | 1546 | 0.9 | 12915 | 883 | 0 | 4.3 |
| 11/21/86 | 64639 | 1337 | 14.2 | 12816 | 335 | 0 | 11.2 |
| 11/26/86 | 14258 | 741 | 5.6 | 9575 | 298 | 0 | 9.4 |
| 12/05/86 | 39536 | 1670 | 6.9 | 1281 | 98 | 0 | 3.8 |
| 12/12/86 | 80119 | 4373 | 5.4 | 4321 | 619 | 0 | 2.0 |
| 12/19/86 | 93194 | 3554 | 7.7 | 0 | 0 | 0 | 0.0 |
| 12/23/87 | 46108 | 1149 | 11.8 | 0 | 0 | 0 | 0.0 |
| 12/31/87 | 276829 | 10653 | 7.6 | 0 | 0 | 0 | 0.0 |
| 01/09/87 | 262825 | 7789 | 9.9 | 0 | 0 | 0 | 0.0 |
| 01/14/87 | 179852 | 4296 | 12.3 | 0 | 0 | 0 | 0.0 |
| 01/23/87 | 229426 | 5447 | 12.3 | 0 | 0 | 0 | 0.0 |
| 01/29/87 | 306813 | 5655 | 15.9 | 0 | 0 | 0 | 0.0 |
| 02/06/87 | 31228 | 1360 | 6.7 | 0 | 0 | 0 | 0.0 |
| 02/13/87 | 148532 | 3975 | 11.0 | 0 | 0 | 0 | 0.0 |
| 02/20/87 | 122158 | 4124 | 8.7 | 850 | 16 | 0 | 15.5 |
| 02/25/87 | 40207 | 2356 | 5.0 | 0 | 0 | 0 | 0.0 |
| 03/06/87 | 32955 | 1876 | 5.2 | 800 | 24 | 0 | 10.0 |
| 03/23/87 | 69370 | 2783 | 7.3 | 16718 | 451 | 0 | 10.9 |
| 03/27/87 | 0 | 0 | 0.0 | 18834 | 170 | 0 | 32.4 |
| 04/03/87 | 101444 | 4070 | 7.3 | 40253 | 505 | 0 | 23.4 |
| 04/17/87 | 0 | 0 | 0.0 | 32778 | 581 | 0 | 16.5 |
| 04/24/87 | 0 | 0 | 0.0 | 60106 | 912 | 0 | 19.3 |
| 05/01/87 | 0 | 0 | 0.0 | 46484 | 631 | 0 | 21.6 |
| 05/11/87 | 0 | 0 | 0.0 | 81016 | 1613 | 0 | 14.7 |
| 05/15/87 | 0 | 0 | 0.0 | 34774 | 701 | 0 | 14.5 |
| 05/22/87 | 0 | 0 | 0.0 | 102568 | 1102 | 0 | 27.3 |
| 05/29/87 | 0 | 0 | 0.0 | 75327 | 1102 | 0 | 20.0 |
| 06/05/87 | 0 | 0 | 0.0 | 91483 | 1112 | 0 | 24.1 |
| 06/12/87 | 0 | 0 | 0.0 | 90151 | 1102 | 0 | 24.0 |

| DATE | 1,000 Btu Chilling | kWh* Tower | C.O.P. Tower | 1,000 Btu A/C | kWh C Pumps | kWh Back PMP | C.O.P. Building |
|---|---|---|---|---|---|---|---|
| 06/19/87 | 0 | 0 | 0.0 | 85480 | 1012 | 0 | 24.8 |
| 06/26/87 | 0 | 0 | 0.0 | 101953 | 1072 | 0 | 27.9 |
| 07/02/87 | 0 | 0 | 0.0 | 83930 | 1042 | 0 | 23.6 |
| 07/10/87 | 0 | 0 | 0.0 | 90927 | 1242 | 0 | 21.5 |
| 07/17/87 | 0 | 0 | 0.0 | 90929 | 1092 | 0 | 24.4 |
| 07/24/87 | 0 | 0 | 0.0 | 90769 | 1112 | 0 | 23.9 |
| 07/31/87 | 0 | 0 | 0.0 | 85482 | 1082 | 0 | 23.2 |
| 08/07/87 | 0 | 0 | 0.0 | 93136 | 1132 | 0 | 24.1 |
| 08/14/87 | 0 | 1 | 0.0 | 96705 | 1212 | 0 | 23.4 |
| 08/21/87 | 0 | 0 | 0.0 | 80231 | 1132 | 0 | 20.8 |
| 08/28/87 | 0 | 0 | 0.0 | 82902 | 1443 | 0 | 16.8 |
| 09/04/87 | 0 | 0 | 0.0 | 63834 | 1423 | 0 | 13.2 |
| 09/11/87 | 0 | 0 | 0.0 | 46146 | 2766 | 0 | 4.9 |
| 09/18/87 | 0 | 0 | 0.0 | 61980 | 3166 | 0 | 5.7 |
| 09/25/87 | 0 | 0 | 0.0 | 34971 | 2525 | 0 | 4.1 |
| 10/02/87 | 0 | 0 | 0.0 | 37932 | 767 | 0 | 14.5 |
| 10/09/87 | 4478 | 417 | 3.2 | 26584 | 625 | 0 | 12.5 |
| 10/16/87 | 6000 | 484 | 3.6 | 13720 | 418 | 0 | 9.6 |
| 10/23/87 | 19994 | 805 | 7.3 | 59971 | 1121 | 0 | 15.7 |
| 10/30/87 | 17777 | 812 | 6.4 | 7511 | 264 | 0 | 8.3 |
| 11/06/87 | 1755 | 69 | 7.5 | 27359 | 942 | 0 | 8.5 |
| 11/13/87 | 77912 | 2443 | 9.3 | 7782 | 184 | 0 | 12.4 |
| 11/20/87 | 23124 | 1103 | 6.1 | 9805 | 267 | 0 | 10.8 |
| 11/25/87 | 61494 | 1733 | 10.4 | 4577 | 210 | 0 | 6.4 |
| 12/04/87 | 53439 | 2305 | 6.8 | 989 | 40 | 0 | 7.2 |
| 12/11/87 | 52884 | 1840 | 8.4 | 3435 | 91 | 0 | 11.0 |
| 12/18/87 | 138105 | 3616 | 11.2 | 9876 | 437 | 0 | 6.6 |
| 12/23/87 | 13345 | 589 | 6.6 | 0 | 0 | 0 | 0.0 |
| 01/09/88 | 433366 | 12176 | 10.4 | 0 | 0 | 0 | 0.0 |
| 01/15/88 | 278687 | 6620 | 12.3 | 0 | 0 | 0 | 0.0 |
| 01/22/88 | 80042 | 2625 | 8.9 | 8943 | 325 | 0 | 8.1 |
| 01/29/88 | 283142 | 7976 | 10.4 | 0 | 0 | 0 | 0.0 |
| 02/05/88 | 31796 | 1094 | 8.5 | 15313 | 205 | 0 | 21.9 |
| 02/12/88 | 338262 | 7559 | 13.1 | 0 | 0 | 0 | 0.0 |
| 02/19/88 | 190457 | 5456 | 10.2 | 0 | 0 | 0 | 0.0 |
| 02/29/88 | 157666 | 4490 | 10.3 | 7797 | 213 | 0 | 10.7 |
| 03/04/88 | 23693 | 832 | 8.3 | 14952 | 366 | 0 | 12.0 |
| 03/11/88 | 42828 | 2514 | 5.0 | 10541 | 324 | 0 | 9.6 |
| 03/25/88 | 146052 | 4578 | 9.4 | 9011 | 197 | 0 | 13.4 |
| 04/01/88 | 0 | 0 | 0.0 | 31779 | 641 | 0 | 14.5 |
| 04/08/88 | 0 | 0 | 0.0 | 30382 | 802 | 0 | 11.1 |
| 04/15/88 | 4120.9 | 746 | 1.6 | 16975 | 532 | 0 | 9.4 |
| 04/22/88 | 1612.7 | 192 | 2.5 | 41747 | 785 | 0 | 15.6 |
| 04/29/88 | 0 | 0 | 0.0 | 74654 | 1072 | 0 | 20.4 |
| 05/06/88 | 0 | 0 | 0.0 | 49930 | 992 | 0 | 14.8 |
| 05/13/88 | 0 | 0 | 0.0 | 62765 | 1102 | 0 | 16.7 |

| DATE | 1,000 Btu Chilling | kWh* Tower | C.O.P. Tower | 1,000 Btu A/C | kWh C Pumps | kWh Back PMP | C.O.P. Building |
|---|---|---|---|---|---|---|---|
| 05/20/88 | 0 | 0 | 0.0 | 61256 | 1002 | 0 | 17.9 |
| 05/27/88 | 0 | 0 | 0.0 | 65173 | 982 | 0 | 19.5 |
| 06/03/88 | 0 | 0 | 0.0 | 69890 | 1147 | 1789 | 7.0 |
| 06/10/88 | 0 | 0 | 0.0 | 67862 | 1122 | 0 | 17.7 |
| 06/17/88 | 0 | 0 | 0.0 | 71298 | 972 | 0 | 21.5 |
| 06/24/88 | 0 | 0 | 0.0 | 82207 | 1022 | 0 | 23.6 |
| 07/01/88 | 0 | 0 | 0.0 | 110879 | 1212 | 0 | 26.8 |
| 07/08/88 | 0 | 0 | 0.0 | 49603 | 611 | 0 | 23.9 |
| 07/15/88 | 0 | 0 | 0.0 | 116650 | 883 | 1361 | 15.3 |
| 07/22/88 | 0 | 0 | 0.0 | 98662 | 1048 | 1638 | 10.8 |
| 07/29/88 | 0 | 0 | 0.0 | 82380 | 1149 | 1827 | 8.1 |
| 08/05/88 | 0 | 0 | 0.0 | 84832 | 1129 | 1807 | 8.5 |
| 08/12/88 | 0 | 0 | 0.0 | 86729 | 1192 | 1633 | 9.0 |
| 08/19/88 | 0 | 0 | 0.0 | 80087 | 1143 | 1773 | 8.1 |
| 08/26/88 | 0 | 0 | 0.0 | 94918 | 1240 | 1746 | 9.3 |
| 09/02/88 | 0 | 0 | 0.0 | 88765 | 1292 | 1704 | 8.7 |
| 09/09/88 | 0 | 0 | 0.0 | 23910 | 701 | 0 | 10.0 |
| 09/16/88 | 0 | 0 | 0.0 | 74291 | 1567 | 1319 | 7.6 |
| 09/23/88 | 0 | 0 | 0.0 | 72274 | 1011 | 1394 | 8.8 |
| 09/30/88 | 0 | 0 | 0.0 | 57464 | 752 | 1122 | 9.0 |
| 10/07/88 | 14 | 30 | 0.1 | 27846 | 851 | 0 | 9.6 |
| 10/14/88 | 5619 | 470 | 3.5 | 6960 | 625 | 0 | 3.3 |
| 10/20/88 | 2960 | 303 | 2.9 | 9480 | 471 | 0 | 5.9 |
| 10/28/88 | 1304 | 239 | 1.6 | 3239 | 160 | 0 | 5.9 |
| 11/04/88 | 345 | 66 | 1.5 | 9654 | 701 | 0 | 4.0 |
| 11/11/88 | 7152 | 470 | 4.5 | 4816 | 650 | 0 | 2.2 |
| 11/18/88 | 10481 | 826 | 3.7 | 3813 | 426 | 0 | 2.6 |
| 11/23/88 | 8367 | 568 | 4.3 | 0 | 0 | 0 | 0.0 |
| 12/02/88 | 86196 | 3431 | 7.4 | 0 | 0 | 0 | 0.0 |
| 12/09/88 | 111617 | 4427 | 7.4 | 4490 | 85 | 0 | 15.6 |
| 12/20/88 | 368189 | 10024 | 10.8 | 770 | 21 | 0 | 10.5 |
| 01/02/88 | 72256 | 2851 | 7.5 | 0 | 0 | 0 | 0.0 |

* : The column includes kWh of the Tower Blower and the Hot Well Pumps.

# FIELD TESTING OF A HIGH-TEMPERATURE AQUIFER THERMAL ENERGY STORAGE SYSTEM

**R.L. Sterling and M.C. Hoyer**
Underground Space Center
Department of Civil and Mineral Engineering
University of Minnesota
Minneapolis, MN 55455

## *ABSTRACT*

*The University of Minnesota Aquifer Thermal Energy Storage (ATES) System has been operated as a field test facility for the past six years. Four short-term and two long-term cycles have been completed to date providing a greatly increased understanding of the efficiency and geochemical effects of high-temperature aquifer thermal energy storage. A third long-term cycle is currently being planned to operate the ATES system in conjunction with a real heating load and to further study the geochemical impact on the aquifer from heated water storage cycles. The most critical activities in the preparation for the next cycle have proved to be the applications for the various permits and variances necessary to conduct the third cycle and the matching of the characteristics of the ATES system during heat recovery with a suitable adjacent building thermal load.*

## Introduction

The objectives in creating the University of Minnesota Aquifer Thermal Energy Storage (ATES) System were to design, construct, and operate a field test facility (FTF) to study the feasibility of moderately high-temperature [up to 150 C (302 F)] thermal energy storage system in a confined aquifer. The FTF is located at the St. Paul Campus of the University of Minnesota. It was designed to inject and recover heat at a rate of 5 MW (thermal) using a well doublet spaced at 255 m, operating at 18.9 L/sec (300 GPM) injection/recovery rate and maximum water temperature of 150 C (302 F). Figure 1 shows an artists conceptual drawing of the FTF. Figure 2 shows the surface locations of the injection/supply wells, the core boring and the monitoring wells.

The facility was designed to utilize the highly stratified Franconia-Ironton-Galesville (FIG) confined aquifer which lies at a depth of approximately 180 m, has a thickness of approximately 60 m, and is under a static head of approximately 125 m. The aquifer consists of sandstone interbedded with shale and dolomite beds.

The site is located near the center of the Twin Cities artesian basin containing four Paleozoic aquifers which are used for water supply. Being near the center of the basin, the regional water velocity in the FIG aquifer is extremely low (less than 0.01 m/day). The FIG aquifer is not used as a source of water in the central part of the basin, because of the higher yields obtainable from either the overlying Prairie du Chien-Jordan aquifer or the underlying Mt. Simon-Hinckley aquifer. Preliminary pumping tests, injection tests, packer tests, and laboratory tests established that the overlying and underlying aquifers are hydraulically well separated from the FIG. All of the above characteristics are desirable for an ATES system.

The FIG confined aquifer is an anisotropic highly stratified aquifer. Testing revealed that only the upper part of the Franconia (UF) and the Ironton-Galesville (IG) portions of the aquifer can provide significant amounts of water. In the experimentation completed to date, the source and storage wells were screened only at the UF and IG horizons (allowing the lower Franconia (LF) to act as a reasonably good confining bed). The IG portion of the aquifer contains many thin shale interbeds which inhibit thermal convection of the heated storage water.

The ambient FIG ground water is a calcium-magnesium bicarbonate water having about 12 grains of hardness. To prevent scaling in and around the storage well during injection of heated aquifer water, the hardness of the aquifer water has to be reduced prior to reinjection.

## Completed Storage Test Cycles

Four short-term cycles (ST1-ST4) and two long-term cycles have been conducted at the facility to date. The four short-term cycles were completed prior to December 1983. The first long-term cycle was conducted from November 1984 to May 1985. The second long-term cycle was conducted from October 1986 to April 1987. Summary data for all the cycles completed to date is included in Table 1.

The short term cycles were all scheduled for consecutive 8 day periods of injecting heated water into the aquifer, storing the heated water in the aquifer and recovering the heated water from the storage well. Each short-term cycle was conducted using a progressively higher water temperature for injection rising from 89.4 C in the first cycle to 114.8 C in the fourth cycle.

A precipitator was used during the short term cycles to reduce the hardness of the injected water, but recharging the precipitator proved necessary after each day or two of injection thus interrupting the injection cycle.

Despite the interruptions, the short-term cycles demonstrated that ATES at temperatures above 100 C in an aquifer was feasible and that the thermal behavior and energy performance of the storage could be modeled successfully. Recovery of the energy stored was 59, 46, 62 and 58 percent, respectively, for each of the short-term cycles. Cycle ST2 had a significantly lower recovery because of an extended storage period of 90 days compared to 10 to 13 days for the other cycles.

The two long-term cycles were each scheduled for consecutive 60 day periods of injection, storage, and recovery. Before the long-term cycles began, a permit modification was requested and granted which allowed the use of an ion-exchange water softener to replace the precipitator. This permitted nearly continuous

operation during the water heating and injection phase with interruptions only due to scheduled maintenance, power outages, or system malfunctions. The total durations for the injection phase to obtain 59 days of injection for the long-term cycles were 74.7 and 65.0 days, respectively.

Injected water temperatures for the two long-term cycles averaged 108.5 C and 117.7 C, respectively. Water temperatures during recovery increased slightly during the first 1-2 days and then declined steadily during the withdrawal period (see Figure 3). When adjusted for the difference in injection temperatures of 9 C the temperature recovery curves correspond very closely. There was evidence that in the UF portion of the aquifer significant thermal convection took place during the storage period. This convection was effectively prevented in the IG portion of the aquifer by the shale interbeds.

The modeled and field experimental energy recovery values are in close agreement (Table 2). Chemistry of the recovered water was at, or very close to, equilibrium throughout recovery. The results of the long-term cycles suggested that some mixing of the injected, stored water with 'ambient' surrounding water may explain some of the composition of recovered water.

The responses of the aquifer during the short-term cycles suggested that some changes of aquifer properties may have been taking place; however, because the cycles were so short and operational parameters and changes in attributes (temperature, composition, and flow rates) of injected water changed so rapidly, interpretation of the response within the aquifer was complicated. The responses of the aquifer during both long-term cycles were consistent, suggesting that no significant aquifer property changes were taking place.

## Recent and Planned Activities

As a follow on to the successful long-term cycles, two particular areas for research and development were seen as critical to enable commercialization and adoption of hot water ATES technology:

1. The ability to better understand and predict geochemical changes in the aquifer resulting from continued use of the ATES system.

2. The demonstration of an ATES system interfaced with a real thermal load so that the efficiencies and difficulties that occur in a commercial system operation could be studied.

During 1987 and early 1988, refinements were made in the longstanding plan for the operation of a third long-term cycle using the ATES system connected to the heating system of a campus building adjacent to the site. The plan comprised the following major components:

1. Submission of the necessary permit and variance applications.

2. Modification of the supply and storage wells to limit injection to the Ironton-Galesville portion of the aquifer.

3. Design and construction of the necessary piping, heat exchangers and controls to permit the use of aquifer-stored heat in an adjacent campus building.

4. Operation of a third long-term test cycle integrated with the heating demand characteristics of a real building.

5. Economic analysis of the continued use of the current ATES configuration by the University of Minnesota beyond the planned test cycle.

6. Economic analysis of the potential of a new ATES system developed in conjunction with anticipated future changes in the University physical plant system.

7. Drill post-mortem corehole to examine the effects of hot water injection and withdrawal cycles on the fabric, mineralogy, and geochemistry of the affected rock formations.

8. Computer simulation of the hydraulic, thermal and geochemical activity in the aquifer during the third long-term cycle.

9. Necessary monitoring and analysis to support the above activities and to satisfy permit requirements.

As part of the shift of project emphasis to the utilization of the ATES system, the principal responsibility for the project was shifted within the University of Minnesota from the Minnesota Geological Survey to the Underground Space Center, a division of the Department of Civil and Mineral Engineering.

Each of the planned activities will be described below in more detail together with the current status of the activity and observations or results in connection with the activity to date.

**Required Permits and Variances**

Four permits and/or variances from State rules or regulations issued by three State departments or agencies are required for the operation of the ATES system in Minnesota.

The most critical variance requested is from Minnesota Rules Chapter 7060, which prohibits discharge into the zone of saturation by injection wells and prohibits the long-term storage of pollutants (including heat) underground. The original variance was issued by the Minnesota Pollution Control Agency (MPCA) in 1980 after a contested case hearing. The variance was reissued by the Agency in 1984 after a public informational meeting was held. The expiration date for the reissued variance was July 31, 1988.

The new variance request was received by the agency on February 5, 1988, but the variance was not approved until September 27, 1988. Several meetings were held between MPCA staff and project staff to review the proposed variance request and to request further information. Principal concerns were the increased injection period proposed (120 days versus 60 days in prior long-term cycles) and that not all the heat or volume of water injected would necessarily be recovered in between cycles leading to a gradual spread of the areal influence of the ATES system on the aquifer. A further concern was that limiting the injection and retrieval zone to the Ironton-Galesville portion of the aquifer would also increase the zone of influence of the ATES system. The agency considered requiring a further monitoring well at a greater distance from the injection well to monitor these effects, but this requirement was dropped for the third cycle when the injection period proposed was limited to 90 days. Other injection limitations were 0.39 MGD (17.3 L/sec av.) as a maximum flow rate, 150 C as a maximum injection temperature, and 180 mg/L as a maximum concentration of dissolved sodium (from the water softener). The possibility for two

complete cycles was approved under this variance, but a requirement was added that an equal volume of water to that injected in the first cycle be pumped out before a second cycle could commence. The new variance request was uncontested and is valid until July 31, 1993.

The MPCA also has approval authority for the "National Pollutant Discharge Elimination System And State Disposal System Permit" (NPDES/SDS). The existing NPDES/SDS permit MN 0051632 was reissued by the agency in conjunction with the variance discussed above.

A variance from the Minnesota Well Construction Code is required for the ATES system. An extension of the existing variance was requested from the Minnesota Department of Health on October 5, 1988 (after the MPCA permit approval) and was granted on October 25, 1988.

The final permit required is that authorizing the appropriation of the ground water used in the ATES cycle. An extension permit (#80-6201) was requested from the Minnesota Department of Natural Resources on August 12, 1988 and was issued on December 20, 1988.

As of December 20, 1988 all the necessary permits for the operation of the third long-term cycle have been approved.

**Well Modification and Pump Inspection**

Following the prior cycles, it was felt that the inclusion of the upper Franconia portion of the aquifer as a zone in which injection and retrieval took place had two principal negative impacts on the operation and understanding of the ATES system. These were a loss of efficiency due to thermal convection in the upper Franconia and more complicated geochemical conditions when injection, storage, and retrieval were occurring in portions of the FIG aquifer having substantially different mineralogy.

In June 1988, work on modifying the storage and source wells was begun. Both wells had the 13.7 m of screen removed from the upper Franconia portion of the aquifer and replaced with riser pipe grouted into place.

The pumps in the wells were removed in order to remove the wellscreen, allowing inspection of the pumps following the six ATES cycles and the pumpout. The pumps were inspected by representatives of the manufacturer's servicing agent and by personnel from the St. Anthony Falls Hydraulic Laboratory at the University of Minnesota. The bowls, impellers, and bearings of the storage well pump (well A) showed significant wear. Cost to repair the pump would have exceeded the cost for a replacement pump. Inspection of the source well pump (well B) revealed minor wear, and the pump was considered to be in suitable condition for continued use. The wear in the storage well pump was due in part to the very large temperature range at which the pump operated during its life. The pump has extra adjustment capability, because of the anticipated changes in shaft and column length due to changes in temperature. However, it is probable that the frequency of impeller adjustment as water temperature changed during recovery phases of the cycles and pumpout was not sufficient. This may have contributed to the excessive pump wear. This will be considered a critical item for maintenance in future cycles.

A replacement pump for well A has not yet been ordered, because it may be possible to downsize the pump requirements for the retrieval phase of the cycle which utilizes the pump in well A. The pump specifications will result from the system design for heat utilization in the campus building.

The well modification work was completed in January 1989 with the exception of the reinstallation of the pump in well A and the testing of the wells.

**ATES/Building Interface**

The original concept for interfacing the ATES system with a real building load was to connect the system to Peters Hall, a campus building immediately to the east of the site at well A. The building already had a heating system designed to operate from a hot water supply rather than steam which is the norm for the campus system. In addition, the size of the load at Peters Hall would enable the ATES system to meet the full heating demand of the building. From a readiness standpoint coupled with the low cost of piping to connect the building to the ATES system and the potential demonstration that ATES could handle the full heating load for a campus building, the choice appeared a suitable one. The design of the piping and controls for connection to Peters Hall was initiated early in 1988; but as the design progressed, several major drawbacks to Peters Hall as an end use for the heat became apparent and several significant limitations on how ATES heat could be withdrawn from the current well and pump configuration also became clear.

The most obvious problem was that, while the peak load of Peters Hall was a reasonable match for the thermal withdrawal rate of the ATES system, the load was too small during warmer weather to make effective use of ATES heat as it would be withdrawn. The flow rate of the ATES system during withdrawal is controlled on the high side by the capacity of the pump in well A pumping against the head of water represented by the elevation difference from the aquifer to the highest point in the system plus the head loss in the piping, heat exchangers, etc. On the low flow side, the system is controlled by the need to return water to the aquifer via well B without aeration (ie. sufficient flow must be maintained to keep the drop pipe in well B flowing full) and by a minimum flow requirement for pump cooling. A further condition resulting from system design was that the pump bearings in well B had not been designed to handle water temperatures as high as those in well A. The maximum return temperature to well B is thus limited to 85 C to remain within specifications.

During preliminary design, the change to a variable speed pump was considered but not pursued due to concerns about reliability, control and cost. A dual speed pump coupled with a bypass pipe was considered more reliable and easier to control when trying to match the heating demand in the building. The use of a pair of smaller drop pipes in well B was planned to allow a minimum flow rate of 4.7 L/sec (75 GPM). Flow rates below this level were not considered practical with the current ATES system configuration. Back pressure in the piping system can be used to control flow rates within certain limits but will increase the power requirements for pumping.

The initial water temperature recovered from the aquifer was expected to be potentially as high as 105 C, requiring that the heat exchanger in the building effect a minimum temperature drop of 20 C to permit reinjection at 85 C or below. The other alternative would be to pass the water through an additional heat exchanger to reduce the temperature prior to injection.

The temperature of the hot water heating system in Peters Hall is reset progressively from 82 C at -29 C exterior temperature to 43 C at 10 C. Thus, the minimum useable temperature is higher than 82 C when the exterior temperature is less than -29 C. During warmer weather, the ATES water is useable down to 43 C at 10 C outside temperature.

Because of the progressively falling temperature of recovered water from the ATES system during recovery (see Figure 3) and the need to drop the temperature of the ATES water by the greatest amount early in the recovery period (to permit reinjection), the recovery period for the heat stored is best initiated at the beginning of the period of maximum heat demand. At this time, the recovered water temperature is above the set point value for the coldest weather; and the load is sufficient to drop the ATES water temperature to below 85 C. This scenario does however limit the total amount of ATES-stored energy that can be utilized in the building over the winter season, because the system is not operational during the early portion of the winter. Furthermore, this mode of operation either extends the storage period before heat is recovered (when heat is injected during the summer months) or encourages injection during the late fall and early winter to limit the storage period. Neither of these options is particularly desirable.

As the preliminary design for the interface to Peters Hall progressed, it became increasingly clear that the relatively small peak load of the building and its major dependence on outdoor temperature exacerbated the limitations on ATES operation described above. The delay in permit approval essentially precluded the third long-term cycle from being conducted for the winter of 1988-89, and it was decided to reexamine other options for the utilization of ATES heat on the St. Paul campus.

At the time of writing, a final decision has not been made on the heating load(s) to be utilized for the third long-term cycle. A major problem in making such a determination is that, although the total thermal load history for a particular building is generally available from University records, the individual systems which would be utilized for connection to ATES-supplied heat are not separately monitored. Furthermore, the design capacity of the equipment may be very misleading as to the magnitude and variation of the thermal load especially when process water heat is involved.

Although the investigation of the optimum utilization of the University of Minnesota ATES system heat has proved difficult, it has suggested some general design guidelines for systems intended for commercial operation. The characteristics of an ATES system similar to that at the University of Minnesota FTF are:

1. A high-temperature ATES system is simpler to operate at a relatively constant pumping rate.

2. An ATES system has a falling energy recovery rate during the recovery period when the pumping rate is constant.

3. An ATES system has both a minimum and maximum pumping rate depending on drop pipe arrangements and pumping head.

The above characteristics imply that an ideal use of an ATES system may not be as a system designed to operate to meet peak loads or rapidly changing load variations. A preferable scenario is the use of the ATES system at a constant pumping rate throughout the period when such operation would allow full utilization of the recovered heat, ie. as a base load. Figure 4 illustrates such an operation. The ATES is still being utilized to reduce peak load demand on the rest of the energy plant and load demand matching is left to systems that can already accommodate this requirement. If a larger peak load reduction is desired, a larger ATES system with a dual-speed pump could greatly improve load matching even if switched on a calendar schedule (see Figure 4 also).

The further implication of such a system is that the energy stored on an annual basis in the system should not exceed the amount which can be effectively utilized as a base load in the system to which it is connected. This means that the power capacity of the ATES system can be significantly smaller than the peak power demand of the system to which it is connected. The relative magnitudes of the ideal power capacities of the systems will depend on nature of the load curve in the connected system and its own ratio of base load to peak load.

Due to the limitations of the building loads available in the vicinity of the St. Paul campus ATES site, an ideal interaction for the third long-term cycle will not be found; but it is felt that the investigation, design, and operation of such an applied cycle will prove very valuable to the design of future commercial systems.

**Operation of third long-term cycle**

The third long-term cycle is now planned for late summer 1989 to late winter 1990. The previous long-term cycles had equal 60 day periods for injection, storage, and retrieval and had a approximately constant pumping rate. The third cycle will have 90 days of injection and an undetermined length and rate of withdrawal. Completion of the pumpout of an equal volume of water to that injected is required within 90 days of the end of the operational cycle.

The exact operation of the cycle will depend on the results of the building interface characteristics as discussed above.

**Economic Analyses**

The University of Minnesota is currently in the process of a major review of its physical plant equipment and operation. The analysis is being conducted by a consultant to the University. The economic analyses planned specifically for this project have been phased to allow the data gathered in the above review to be used in the analysis of the economic return of the continued operation of an ATES system on campus.

Two specific economic analyses will be conducted. The first will look at possibilities for the continued operation of the existing ATES system on the St. Paul campus. The second will examine possibilities for a new ATES system located on either the Minneapolis or the St. Paul campus. A location close to the

main University heating plant and cogeneration facility will offer a source of waste heat for storage. It would also increase the opportunity to interface the ATES system with appropriate campus wide loads rather than individual building loads.

**Post-mortem Corehole**

A post-mortem corehole has been planned to examine the effects of hot water injection and withdrawal cycles on the fabric, mineralogy, and geochemistry of the affected rock formations. The data gathered from the post-mortem can be compared directly with data from a similar corehole drilled prior to the start of ATES operation. Geophysical logging and packer tests are planned for this corehole. The core will be examined petrologically and selected intervals will have permeability tests conducted. Particular attention will be paid to rock fabric, grain surfaces, and grain composition.

It has not yet been determined whether the post-mortem corehole will be drilled prior to the third long-term cycle or after it. There are programmatic advantages in allowing the analysis of the corehole data to proceed during the period of cycle operation.

**Computer Simulation**

The cooperative research program with the United States Geological Survey (USGS) active on previous stages of the project has been continued. The USGS is responsible for simulation of the injection, storage, and retrieval of the heated water in the aquifer. Simulation results and methodology are being compared with the geochemical and system simulation work underway at Battelle Pacific Northwest Laboratories (BPNL) - described in the papers by E. Jenne and by L. Vail at this meeting. The USGS is also participating in the site data acquisition and analysis process.

The HST3D code supported by the USGS was chosen for the three-dimensional modeling of the new cycle over the SWIP code used for previous cycles because of changes in the personnel involved in modeling the ATES system within USGS and the discontinued software support of the SWIP code by the USGS. The HST3D code and the SWIP code are both run on the University of Minnesota's Cray 2 Supercomputer.

The BPNL-developed ATESSS code has also been used in project planning and discussions with state regulatory personnel on the impact of the third long-term cycle on the FIG aquifer.

Significant problems in using the HST3D code for the University of Minnesota ATES system simulation have been encountered. In building the grid and conducting preliminary two-dimensional testing, software problems have emerged which have proved time consuming to identify and resolve. At the time of writing, consideration is being given to reverting to the use of the SWIP code.

**Monitoring and Analysis**

Monitoring of aquifer conditions is a continuing process even when the system is not operating. Monitoring wells are sampled quarterly; temperatures are recorded daily; water levels are measured weekly.

During the cycles, the frequency of observation is significantly increased. Temperatures are recorded every 15 minutes; water levels are measured daily; aquifer water is sampled no less than twice weekly. Temperatures are recorded on a datalogger. The existing system datalogger is in the process of being

replaced by a microcomputer-based data acquisition system. Pressures (water levels) may be recorded on the computer, if a suitable pressure transducer arrangement can be incorporated into the system. Building heat exchange systems will also have to be incorporated into the data recorded during the recovery phase of the cycle.

Major-ion chemistry of the water samples is analyzed. For long-term cycle 3, aluminum has been added to the suite of analyses because of its importance in understanding potential geochemical changes within the aquifer.

## Conclusions

The high-temperature storage of water in an ATES system has been successfully demonstrated over six storage cycles to date. These cycles have enabled a considerable improvement in the understanding and the ability to simulate the operation and geochemical effects of such cycles.

The current planned cycle and associated activities are intended to further develop our understanding of the geochemistry of ATES and to demonstrate the use of ATES interfaced with a real heating application.

Conclusions from the preparatory work for the third long-term cycle are principally that:

- Permit approval for ATES systems is a major hurdle for the potential commercial operation of such systems. At present, Minnesota has more restrictive ground water controls than many States; but with the growing national concern over ground water pollution, restrictive regulations are expected to grow. Even benign, localized, and extensively monitored systems, such as the University of Minnesota FTF, are affected by these concerns.

- The characteristic curves for available thermal loads and desired ATES operation should be compared carefully when selecting sites for high-temperature ATES applications. ATES systems similar to the University of Minnesota FTF are best suited to provide a baseload thermal input during the winter rather than to match the varying total thermal load. This has a significant impact on the thermal sizing of the ATES system.

## References

1. Blair, S.C., and W.J. Deutsch, 1983, Determination of important physicochemical processes at an aquifer thermal storage site in Minnesota using both laboratory and field techniques. In International Conference on Subsurface Heat Storage Research, Proceedings, Stockholm, Sweden, p. 800-804.

2. Blair, S.C., W.J. Deutsch, and L.D. Kannberg, 1984. Laboratory permeability measurements in support of an aquifer thermal energy storage site in Minnesota. In Proceedings of the 25th U.S. Symposium on Rock Mechanics, Society of Mining Engineers, New York, p. 296-303.

3. Czarnecki, J.B., 1983, FORTRAN computer programs to plot and process aquifer pressure and temperature data: U.S. Geological Survey, Water-Resources Investigations Report 83-4051, 50 p.

4. Holm, T.R., S.J. Eisenreich, H.L. Rosenberg, and N.P. Holm, 1987, Groundwater geochemistry of short-term aquifer thermal energy storage test cycles: Water Resources Research, v. 23, p. 1005-1019.

5. Hoyer, M.C., and J.F. Splettstoesser, 1987, Results of short- and long-term aquifer thermal energy thermal experimental cycles at the University of Minnesota, St. Paul, Minnesota, U.S.A. In 22nd Intersociety Energy Conversion Engineering Conference, Philadelphia, Proceedings: American Institute of Aeronautics and Astronautics, Washington, D.C., p. 1283-1287.

6. Hoyer, M.C., M. Walton, R. Kanivetsky, T.R. Holm, 1985, Short-term aquifer thermal energy storage (ATES) test cycles, St. Paul, Minnesota U.S.A. In ENERSTOCK 85 - International Conference on Energy Storage for Building Heating and Cooling, 3rd, Toronto, Proceedings: Ottawa, Public Works Canada, p. 75-79.

7. Hoyer, M.C., and Walton, Matt, 1986, Aquifer thermal energy storage experiments at the University of Minnesota, St. Paul, Minnesota U.S.A. In 21st Intersociety Energy Conversion Engineering Conference, San Diego, California, 1986, Proceedings: Washington, D.C., American Chemical Society, v. 2, p. 708-713.

8. Kanivetsky, R. and M.C. Hoyer, 1985, Determination of hydraulic parameters of a confined aquifer by the response method: Hydrological Science and Technology, v. 1, no. 2, p. 15-19.

9. Kannberg, L.D. 1988. Seasonal thermal Energy Storage Program: Progress Summary for the Period April 1986, through March 1988. Battelle Pacific Northwest Laboratory, Richland WA, PNL-6705-UC-204, October 1988, pp. 3.1-3.10.

10. Miller, R.T., 1983, Thermal-energy storage in a deep sandstone aquifer in Minnesota: Field observations and preliminary modeling. In International Conference on Subsurface Heat Storage, Proceedings, Stockholm, Sweden, p. 812-816.

11. Miller, R.T., 1984, Anisotropy in the Ironton and Galesville Sandstones near a thermal-energy-storage well: Ground Water, v. 22, p. 532-538.

12. Miller, R.T., 1985, Preliminary modeling of an aquifer thermal-energy-storage well: U.S. Geological Survey, Water Supply Paper 2270, p. 1-19.

13. Miller, R.T., 1986, Thermal-energy storage in a deep sandstone aquifer in Minnesota: field observations and thermal energy-transport modeling. In 21st Intersociety Energy Conversion Engineering Conference, San Diego, California, 1986, Proceedings: Washington, D.C., American Chemical Society, v. 2, p. 682-685.

14. Miller, R.T. and C.I. Voss, 1986, Finite-difference grid for a doublet well in an anisotropic aquifer: Ground Water, v. 24, p. 490-496.

15. Perlinger, J.A., J.E. Almendinger, N.R. Urban, and S.J. Eisenreich, 1987, Groundwater geochemistry of an aquifer thermal energy storage: Long test cycle: Water Resources Research, v. 23, p. 2215-2226.

Table 1 Summary of ATES test cycle conducted at the University of Minnesota Field Test Facility

| | Short-Term | | | | Long-Term | |
|---|---|---|---|---|---|---|
| | 1 | 2 | 3 | 4 | 1 | 2 |
| Duration (days) | | | | | | |
| Injection - Pumping | 5.2 | 8 | 7.7 | 7.7 | 59.1 | 59.3 |
| Injection - Total | 17 | 10 | 10.4 | 12 | 74.7 | 65.0 |
| Storage | 13 | 90 | 9.7 | 10.1 | 64 | 59.1 |
| Recovery - Pumping | 5.2 | 8 | 7.7 | 7.7 | 58 | 59.7 |
| Recovery - Total | 5.2 | 8 | 8 | 7.7 | 58.8 | 59.8 |
| Temperature (°C) | | | | | | |
| Source Water | 11.0 | 20.5 | 36.1 | 52.6 | 19.7 | 33.1 |
| Injected Water | 89.4 | 97.4 | 106.1 | 114.8 | 108.5 | 117.7 |
| Recovered Water | 59.2 | 55.2 | 81.1 | 89.1 | 74.7 | 85.1 |
| Returned Water | 59.0 | 54.4 | 76.6 | 75.7 | 68.0 | 60.4 |
| Flow Rate (L/s) | | | | | | |
| Injection | 18.4 | 17.6 | 18.3 | 17.9 | 18.0 | 18.3 |
| Recovery | 18.1 | 17.8 | 17.3 | 17.8 | 18.4 | 17.9 |
| Volume ($10^4$ $m^3$) | | | | | | |
| Injection | 0.83 | 1.22 | 1.22 | 1.19 | 9.21 | 9.39 |
| Recovery | 0.81 | 1.23 | 1.18 | 1.19 | 9.22 | 9.21 |
| Energy Recovery Factor | | | | | | |
| (using source temperature) | 0.59 | 0.46 | 0.62 | 0.58 | 0.62 | 0.62 |
| (using ambient temperature) | 0.59 | 0.52 | 0.71 | 0.75 | 0.65 | 0.69 |

Table 2 Comparison of modeled and observed final recovery temperature and energy recovery

| | Final Temperature (°C) | | Energy Recovery | |
|---|---|---|---|---|
| Cycle | Observed | Modeled | Observed | Modeled |
| ST1 | 39.4 | 39.4 | 0.59 | 0.60 |
| ST2 | 39.4 | 43.8 | 0.46 | 0.49 |
| ST3 | 56.7 | 58.3 | 0.62 | 0.58 |
| ST4 | 63.9 | 64.4 | 0.59 | 0.62 |
| LT1 | 45.6 | 45.6 | 0.62 | 0.61 |
| LT2 | 55.4 | 59.5 | 0.62 | 0.62 |

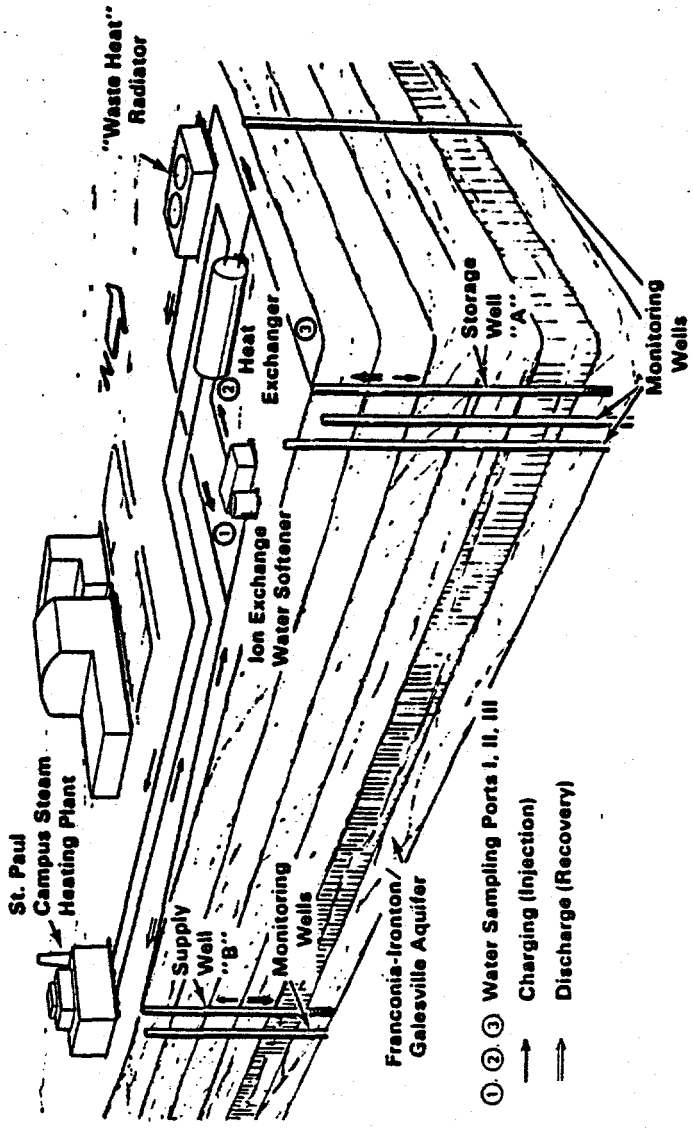


Figure 1. Conceptual drawing of University of Minnesota ATES Field Test Facility

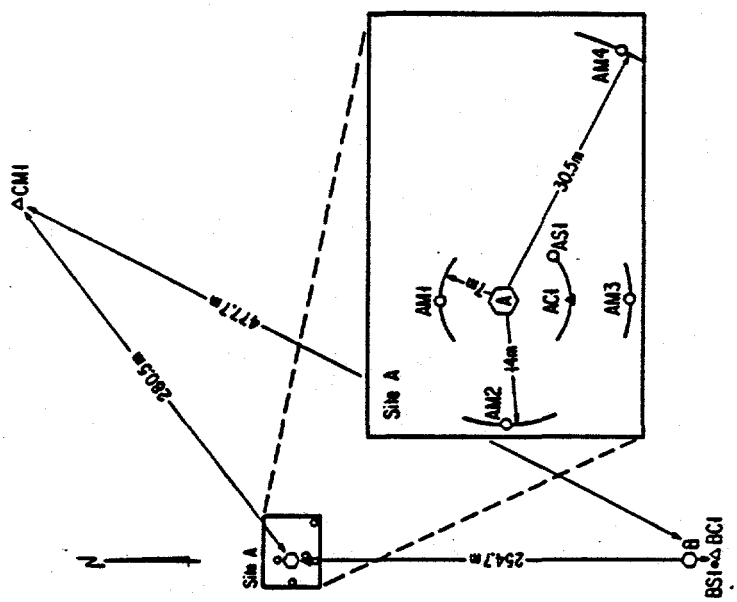


Figure 2. Surface layout of ATES Field Test Facility

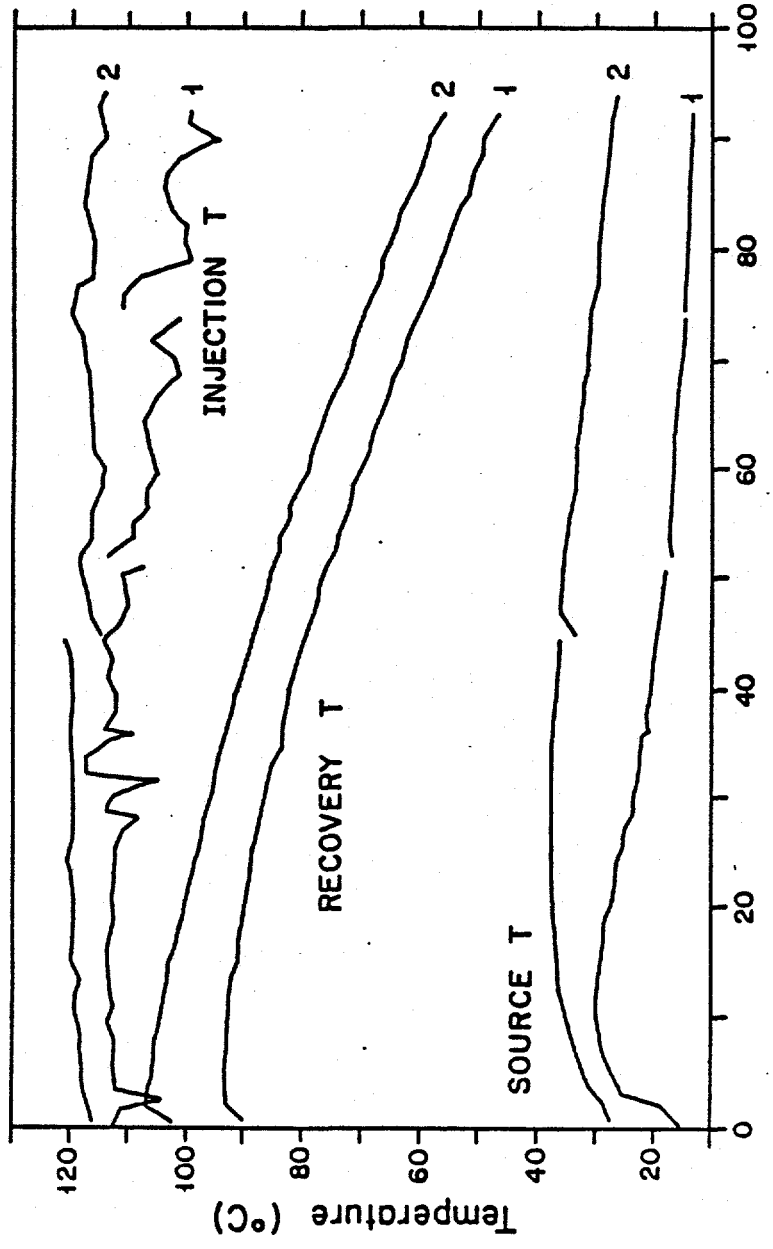


Figure 3. Temperature of source, injected and recovered water for long-term cycles 1 and 2

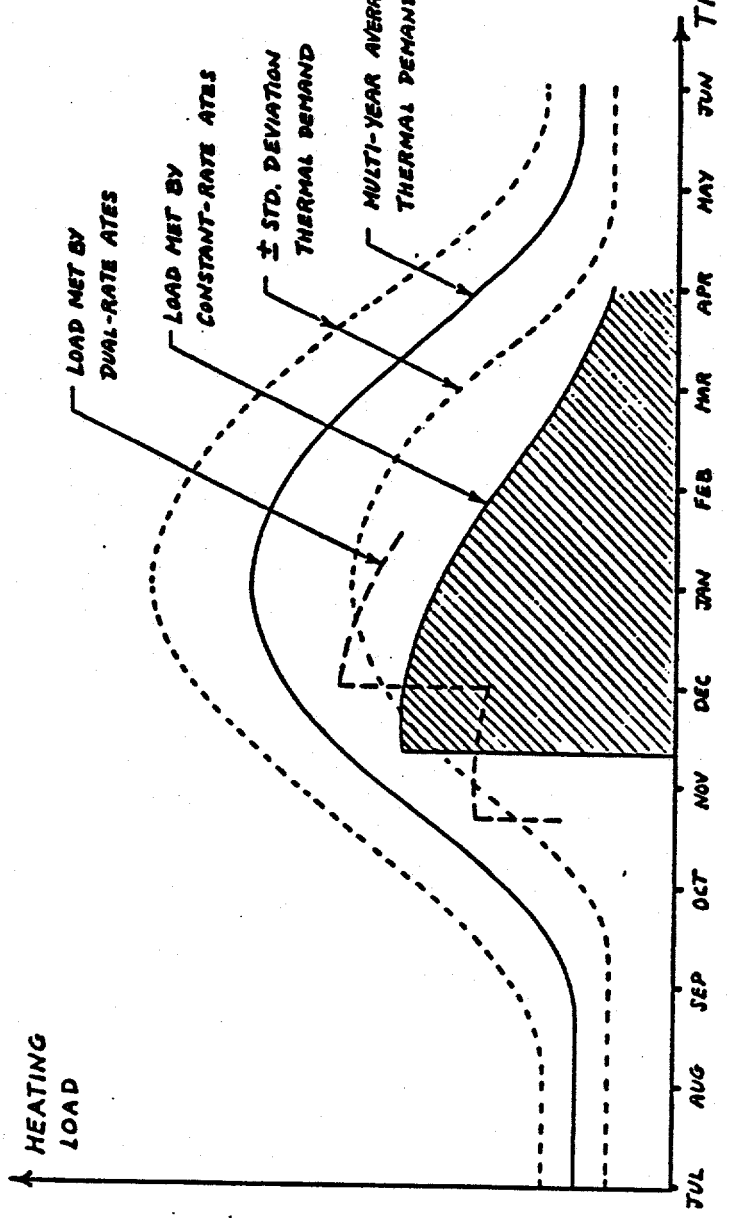


Figure 4. Conceptual utilization of an ATES system with a seasonal thermal load

# STATUS OF NUMERICAL MODELS FOR ATES

**L. W. Vail**
Pacific Northwest Laboratory[a]
Richland, Washington 99352

## *Abstract*

*Research is under way to develop a suite of codes suitable for simulation of geohydrothermal behavior and geochemical behavior of Aquifer Thermal Energy Storage (ATES) Systems. Once developed, these tools will be applied to assist research and will be modified, if necessary, for use by architect/engineer firms. Special attention is being given to geohydrothermal tools focused on assessing ATES feasibility and on preliminary design. In addition, an expert system is being developed to provide geotechnical ATES expertise to groups unfamiliar with the technology.*

## Introduction

In the past, the Underground Energy Storage (UES) Program has supported the development and enhancement of state-of-the-art three-dimensional computer codes to extend our basic understanding of the processes of fluid, energy, and solute transport in aquifers to the unique conditions that occur in ATES. The PT (Pressure/ Temperature) code developed at Lawrence Berkeley Laboratory (Tsang and Doughty 1985) has been used successfully to predict the results of field experiments at Mobile, Alabama (Tsang et al. 1981), and Dorigny, Switzerland. These simulations provided data that showed how the design of wells can mitigate thermal losses resulting from buoyancy. Enhancements to the SWIP (Survey Waste Injection Program) code (Intercomp Resource Development and Engineering, Inc. 1976) by the U.S. Geological Survey allowed SWIP to simulate the field experiments conducted at St. Paul, Minnesota (Miller 1985). More recently, HST3D (Heat and Solute Transport) (Kipp 1987), a significantly improved version of the SWIP code, has been applied to the St. Paul site by researchers at the Pacific Northwest Laboratory (PNL). The CFEST (Coupled Fluid, Energy, and Solute Transport) code developed at PNL (Gupta et al. 1982) has also been used to simulate the Mobile, Alabama, field experiment. These codes provide a sophisticated predictive capability for understanding the basic processes of fluid, energy, and solute transport in aquifers. However, the sophistication of these codes requires that highly-trained professionals apply them.

---

[a] Operated for the U.S. Department of Energy by Battelle Memorial Institute under Contract No. DE-AC06-76-RLO 830.

## Current Activities

Recently, the UES Program has focused on the development of codes that could be used by a broad audience of design engineers whose technical backgrounds in the fields of groundwater hydrology, subsurface heat transfer, and computer-based modeling are limited. Such codes will improve the chances of success of attempts to apply ATES technology, by providing preliminary evaluations of a site's suitability for ATES at minimal cost to design engineers. The projected users of the codes are the design engineers responsible for evaluating the preliminary designs of energy storage systems. The codes will allow a preliminary evaluation to be performed before groundwater hydrology and geochemistry specialists must become involved.

The ATESSS (Aquifer Thermal Energy Storage System Simulator) code takes into account transport and storage of energy in stratified aquifers with multiple wells (Vail, Kannberg, and Kincaid 1985). Additionally, ATESSS includes heat pump, solar array, cooling tower, and counterflow heat exchanger algorithms to accurately quantify the tradeoffs between flow and temperature (Vail 1989). ATESSS is user-friendly and runs on an IBM PC or compatible hardware, so that it is available to a large number of design engineers.

The ATESSS code was used to quantify the impact of vertical stratigraphy on an ATES system's thermal efficiency (Kannberg and Vail 1987). Most aquifers were formed by the gradual deposition of many layers of different geologic materials. Each of these layers or strata may have a different hydraulic conductivity. Therefore, when water is injected through a well into a stratified aquifer, the water will move at a different rate in each of the layers. The number and thickness of the strata have a significant impact on the potential for conductive losses. For instance, an aquifer composed of many alternating layers of permeable and impermeable media may have first-cycle thermal recovery efficiencies of 93% for layers 0.25-m thick, 62% for layers 5.0-m thick, and 85% for layers 25.0-m thick. Representative layer thicknesses estimated from preliminary geologic data can help the design engineer quickly identify those aquifers most suitable for ATES.

The ATESSS code has been evaluated by both PNL and external reviewers. In response to their comments, several modifications have been made in ATESSS. These code modifications allow simulation of aquifers being used simultaneously for both heat and chill storage.

The WELL FIELD DESIGNER (WFD) code was developed to provide a numerical tool that could be used by design engineers with a limited understanding of well-field design to assess the opportunity to mitigate the potentially adverse impact of regional groundwater flow with gradient control wells. This code augments the user's limited design experience with ATES facilities by allowing rapid and reliable evaluation of how various well-field design options affect overall system performance. WFD was developed for use on an IBM PC or compatible machine to allow the program to be transferred to the largest possible number of interested users.

WFD combines numerical optimization methods with a simple groundwater flow model to assist the user in identifying which well-field pumping rates will reduce the regional flow in a region to be used for storage. This combination provides the design engineer with the ability to estimate the costs of the pumping required to counteract regional flow.

The development of an expert system for ATES (called ATES EXPERT) has been initiated to augment "textbook knowledge" with specific knowledge relevant to ATES. The expert system will advise a design engineer as to the suitability of a site and confirm the existence of an energy need suitable for an ATES facility. If additional data are required for evaluating a site, the expert system will list the kinds of data needed and potential sources for them. This knowledge resource will allow design engineers to make initial assessments of ATES at minimal cost without involving specialists in other fields, such as geohydrology and geochemistry. ATES EXPERT incorporates the "rules-of-thumb" employed by geohydrologists, geochemists, and energy systems analysts with the experience gained to date with actual ATES systems in a single set of IF-THEN rules. ATES EXPERT combines its knowledge base with a commercial expert system development package for use on the IBM PC or compatible computers.

The ATES EXPERT's knowledge base was divided into three topic areas:

- geohydrology
- geochemistry
- energy systems.

For each of the three topic areas, a "domain expert" was selected from staff at PNL. All three staff members had experience in ATES research.

I was designated the "knowledge engineer." In that capacity, it is my responsibility to extract and codify the domain experts' knowledge into an expert system. I have initially concentrated on the geohydrology topic area, since that is my technical specialty. A brainstorming session with the geohydrology domain expert developed a list of key concepts. The linkages between the various concepts were defined. These linkages and concepts formed the initial geohydrologic knowledge base of the expert system.

The next step was to begin codifying the knowledge base into an expert system shell. An inexpensive, PC-based shell was selected. This shell requires that the knowledge base be translated into IF-THEN rules. Rule-based expert systems constitute the best means currently available for codifying the problem-solving knowledge and ability of technical experts. Experts often express most of their problem-solving techniques in terms of a set of situation-action rules. These rules can be translated into conditional, IF-THEN rules used by the expert system. The expert system is responsible for solving complex problems by selecting relevant rules and then combining the results in appropriate ways. Additionally, most rule-based expert systems can explain their conclusions by retracing their actual lines of reasoning and translating the logic of each rule into natural language.

The current suite of codes for analysis of ATES systems covers a broad range of potential ATES design issues. Table 1 lists the principal computer codes for analyzing ATES systems.

## Conclusion

A suite of computer codes is being developed to assist in the design of ATES systems. These codes are being developed or modified to allow them to be used by design engineers who lack extensive backgrounds in geohydrology or geochemistry.

## References


1. Gupta, S. K., C. t. Kincaid, P. R. Meyer, C. A. Newbill, and C. R. Cole. 1982. A Multi-Dimensional Finite Element for the Analysis of Coupled Fluid, Energy and Solute Transport (CFEST). PNL-4206, Pacific Northwest Laboratory, Richland, Washington.

2. Intercomp Resource Development and Engineering, Inc. 1976. A Model for Calculating Effects of Liquid Waste Disposal in Deep Saline Aquifers, Part I -- Development, 76-61. U.S. Geologic Survey Water Resources Investigations.

3. Kannberg, L. D., and L. W. Vail. 1987. "Effects of Stratification on Thermal Energy Storage." In Proceedings of 22nd Intersociety Energy Conversion Engineering Conference (IECEC), pp. 1288-1292. American Institute of Aeronautics and Astronautics, New York, New York.

4. Kipp, K. L., Jr. 1987. "HST3D: A Computer Code for Simulation of Heat and Solute Transport in 3-Dimensional Ground-Water Flow Systems." Water Resources Investigations 86-4095, U.S. Geological Survey, Denver, Colorado.

5. Miller, R. T. 1985. Preliminary Modeling of an Aquifer Thermal Energy Storage System. U.S. Geological Survey Water Supply Paper 2270, pp. 1-19, U.S. Geological Survey, Minneapolis, Minnesota.

6. Tsang, C. F., and C. Doughty. 1985. Detailed Validation of a Liquid and Heat Flow Code Against Field Performance. LBL-18833, Lawrence Berkeley Laboratory, Berkeley, California.

7. Tsang, C. F., et al. 1981. "Aquifer Thermal Energy Storage: A Numerical Simulation of Auburn University Field Experiments." Water Resources Research 17:647-658.

8. Vail, L. W., L. D. Kannberg, and C. T. Kincaid. 1985. "A Computer Code for Analyzing the Performance of Aquifer Thermal Energy Storage Systems." In Proceedings of the International Conference on Energy Storage for Building Heating and Cooling, ENERSTOCK 85, pp. 144-148. Public Works Canada, Toronto, Canada.

9. Vail, L. W. 1989. "ATES/Heat Pump Simulations Performed with ATESSS Code". Presented at the Third Workshop on Solar-Assisted Heat Pumps with Ground-Coupled Storage, Gothenburg, Sweden, January 16-18, 1989.

Table 1. Current suite of computer codes for ATES purpose.

| Code | |
|---|---|
| ATESSS | Assists well-field design (placement of wells to mitigate the impact of regional flow). Estimates thermal recovery for ATES systems with single or multiple wells, with or without a heat pump or heat exchanger being used for heating and/or cooling. |
| HST3D | Estimates an aquifer's thermal recovery efficiency and the effects of buoyancy and viscosity changes on thermal recovery. |
| WELL FIELD DESIGNER | Defines the well-field layout that will minimize regional flow in the zone around an ATES facility with minimal total pumpage. |
| CHARM[a] | Evaluates the potential for geochemical problems (precipitation and dissolution) of aquifer minerals in the aquifer and surface heat transfer apparatus. Aids in the design and sizing of precipitators and/or water softeners for ATES systems. |
| ATES EXPERT | Recommends whether a specific site and energy need are suitable for ATES. If available data are insufficient to assess the suitability of a site, provides a list of additional data required and likely sources of such data. |

[a] This code is currently under development by Dutch participants in International Energy Agency Annex VI of the Energy Conservation through Energy Storage Programme. The suitability of the code for U.S. application will be assessed when the final version of CHARM is released